

**Late Mesozoic to Cenozoic erosion and  
sediment dispersal in the Dinaride orogen:  
a sedimentary provenance approach**

**DISSERTATION**

zur Erlangung des Doktorgrades  
der Mathematisch-Naturwissenschaftlichen Fakultäten  
der Georg-August-Universität zu Göttingen

vorgelegt von

**TAMÁS MIKES**

aus Budapest

Göttingen  
2008

D7

Referent:  
*Prof. Dr. Hilmar von Eynatten*

Korreferent:  
*Prof. Dr. Gerhard Wörner*

Tag der mündlichen Prüfung:

Hiermit erkläre ich an Eides statt, die vorliegende Arbeit selbstständig angefertigt zu haben und dabei keine anderen als die von mir angegebenen Quellen und Hilfsmittel benutzt zu haben. Ferner erkläre ich, dass ich nicht anderweitig versucht habe, eine Dissertation einzureichen.

Göttingen, den 25. November 2008

Tamás Mikes

# Table of contents

<b>1. Introduction</b>	1
<b>1.1. Scope</b>	1
<b>1.2. The Dinarides</b>	1
1.2.1. <i>Introduction</i>	1
1.2.2. <i>Overall tectonic architecture</i>	2
1.2.3. <i>Tectonic significance of the ophiolites and the Adriatic continental basement</i>	3
1.2.3.1. <i>Dinaride ophiolite thrust sheets</i>	3
1.2.3.2. <i>Inner Dinaride continental thrust sheets</i>	4
1.2.3.3. <i>Sava Zone</i>	5
1.2.3.4. <i>Outer Dinarides</i>	6
<b>1.3. Recent advances in sedimentary provenance analysis</b>	7
<b>1.4. Structure of the Thesis</b>	10
<b>2. Provenance of the Bosnian Flysch</b>	15
<b>Abstract</b>	15
<b>2.1. Introduction</b>	16
<b>2.2. Tectonic framework</b>	17
<b>2.3. Geological setting of the Bosnian Flysch</b>	20
<b>2.4. Sampling procedure and analytical methods</b>	22
2.4.1. <i>Calcareous nannofossils</i>	23
2.4.2. <i>Accessory mineral separation</i>	23
2.4.3. <i>Whole rock chemistry</i>	24
2.4.4. <i>Clay mineralogy</i>	24
2.4.5. <i>Mineral chemistry</i>	24
2.4.6. <i>U/Pb geochronology</i>	25
2.4.7. <i>Zircon fission-track analysis</i>	25
<b>2.5. Results</b>	25
2.5.1. <i>New constraints on depositional age</i>	25
2.5.2. <i>Petrography</i>	28
2.5.3. <i>Whole-rock geochemistry</i>	30
2.5.4. <i>Clay mineralogy</i>	32
2.5.5. <i>Heavy mineral analysis</i>	33
2.5.6. <i>Geochronology</i>	37
2.5.6.1. <i>Zircon U/Pb dating</i>	37
2.5.6.2. <i>Zircon fission track analysis</i>	37
<b>2.6. Discussion</b>	39
2.6.1. <i>Provenance of sandstones incorporated in the DOZ mélange</i>	40
2.6.2. <i>Provenance of the Vranduk Formation</i>	40
2.6.3. <i>Provenance of the Ugar Formation</i>	42

2.6.4. <i>Do the Vranduk and Ugar formations share a common provenance?</i>	45
2.6.5. <i>Acid intraoceanic magmatism in the Jurassic</i>	47
<b>2.7. Summary: source area evolution of the Bosnian Flysch</b>	48
2.7.1. <i>Middle to Late Jurassic: intraoceanic subduction</i>	48
2.7.2. <i>Jurassic–Cretaceous transition:</i>	
<i>obduction and metamorphism at the continental margin of Adria</i>	48
2.7.3. <i>Early Cretaceous sedimentation: Vranduk Formation</i>	49
2.7.4. <i>Late Cretaceous Ugar sedimentation:</i>	
<i>increasing carbonate contribution and changes in the hinterland</i>	51
<b>3. Insights into Neotethyan ophiolite petrology at the Dinaride–Alpine–Pannonian triple junction: geochemistry of detrital Cr-spinel from Cretaceous synorogenic sediments</b>	55
<b>Abstract</b>	55
<b>3.1. Introduction</b>	56
<b>3.2. Geological setting</b>	57
<b>3.3. Sampling and analytical procedures</b>	62
<b>3.4. Chemical characteristics of Cr-spinels in the studied Cretaceous formations</b>	62
3.4.1. <i>Oštrc Formation</i>	63
3.4.2. <i>Bistra Formation</i>	64
3.4.3. <i>Kravljak Formation</i>	64
3.4.4. <i>Vivodina Formation</i>	65
3.4.5. <i>Glog Formation</i>	66
<b>3.5. Provenance and paleogeographic relations</b>	67
<b>3.6. Conclusions</b>	71
<b>4. Jurassic granitoid magmatism in the Dinaride Neotethys: geochronological constraints from detrital minerals</b>	75
<b>Abstract</b>	75
<b>4.1. Introduction</b>	76
<b>4.2. Geological setting of the sampled units</b>	80
<b>4.3. Analytical methods</b>	81
<b>4.4. Results</b>	81
4.4.1. <i>Monazite dating</i>	81
4.4.2. <i>Zircon U/Pb geochronology</i>	85
4.4.3. <i>Apatite fission track dating</i>	86
<b>4.5. Discussion</b>	87
4.5.1. <i>Magmatic origin of the Jurassic apatite, monazite and zircon crystals</i>	87
4.5.2. <i>Regional comparisons</i>	87
<b>4.6. Conclusions</b>	88

<b>5. Calcareous nannofossil age constraints on Miocene flysch sedimentation in the Outer Dinarides</b>	93
<b>Abstract</b>	93
<b>5.1. Introduction</b>	94
<b>5.2. Geological setting and sedimentology</b>	95
<b>5.3. Present status of flysch biostratigraphy</b>	97
<b>5.4. Methods</b>	101
<b>5.5. Results of nannofossil analyses</b>	102
5.5.1. <i>Istrian Peninsula: Trieste-Koper and Pazin Basin</i>	105
5.5.2. <i>Northern Kvarner</i>	106
5.5.3. <i>Pag Island</i>	108
5.5.4. <i>Northern Dalmatia (Ravni-Kotari)</i>	108
5.5.5. <i>Central Dalmatia</i>	109
5.5.6. <i>Dalmatian-Herzegovinian Zone</i>	110
5.5.7. <i>Southern Adriatic Zone</i>	111
<b>5.6. Nannofossil preservation</b>	112
<b>5.7. Cretaceous to Palaeogene nannofloral elements</b>	113
<b>5.8. Distribution of nannofossil age ranges and sediment recycling</b>	114
<b>5.9. Miocene nannofossils</b>	117
<b>5.10. Implications for palaeoenvironment</b>	119
5.10.1. <i>Pelagic environment with neritic influence</i>	119
5.10.2. <i>Neogene: Absence of planktonic foraminifera, presence of nannofossils</i>	120
5.10.3. <i>Heterochronous redeposition</i>	121
5.10.4. <i>Weak early-stage diagenesis</i>	122
<b>5.11. Implications for palaeogeography</b>	122
<b>5.12. Implications for Cenozoic deformation history</b>	125
<b>5.13. Conclusions</b>	126

<b>6. Double dating of detrital zircon from the Dinarides by fission-track and LA–ICPMS U/Pb analysis</b>	131
<b>Abstract</b>	131
<b>6.1. Introduction</b>	132
<b>6.2. Geologic background</b>	135
6.2.1. <i>Tectonic outline of the Dinarides</i>	135
6.2.2. <i>Sava Zone</i>	135
6.2.3. <i>Outer Dinaride foreland basin</i>	137
<b>6.3. Sampling, analytical techniques and data treatment</b>	138
6.3.1. <i>Sample preparation</i>	139
6.3.2. <i>Fission track analysis</i>	139
6.3.3. <i>Grain referencing</i>	140

6.3.4. Cathodoluminescence (CL) imaging	140
6.3.5. LA-ICPMS U/Pb geochronology	140
6.3.6. Integrated processing of U/Pb and FT age data	142
<b>6.4. Results</b>	142
6.4.1. Fission track analysis	142
6.4.1.1. Sava Zone	142
6.4.1.2. Outer Dinaride foreland basin	143
6.4.2. U/Pb geochronology – assessment of data quality	143
<b>6.5. Discussion</b>	148
6.5.1. Capability of quadrupole LA-ICPMS for zircon U/Pb geochronology	148
6.5.2. Double dating: implications for sedimentary provenance	149
6.5.3. Implications for U concentration determination	154
<b>6.6. Conclusions</b>	157
<b>7. Conclusions</b>	161
<b>References</b>	164
<b>Appendix</b>	



# *Chapter 1*

## Introduction



## **Introduction**

### **1.1. Scope**

The present Thesis is devoted to a detailed analysis of sedimentary provenance indicators from Late Mesozoic to Tertiary synorogenic, mixed siliciclastic-carbonate deposits in the Dinarides. Generally, such sedimentary sequences retain a wealth of information about the past geologic buildup, tectonothermal events and palaeogeographic connections of the orogen, furthermore about the pathways of sediment dispersal and their tectonic control.

Section 1.3 below outlines in more detail the approaches adopted or developed in this study, and Section 1.4. presents the structuration of the Thesis. These are preceded by an overview on the tectonic setting of the Dinarides and the geological framework of the investigated areas in Section 1.2.

I have prepared the Thesis under the supervision of Prof. Dr. Hilmar von Eynatten and Dr. István Dunkl at the Department of Sedimentology/Environmental Geology of the Geoscience Center Göttingen, in the period from October 2004 to November 2008. I most sincerely thank them for their guidance and the ever-stimulating, friendly working atmosphere at the Department. The research was funded by the Deutsche Forschungsgemeinschaft, with additional support coming from the Synthesys Programme.

### **1.2. The Dinarides**

#### *1.2.1. Introduction*

The Dinaride-Hellenide system of the Alpine orogen consists of a highly impressive edifice of orogen-parallel tectonostratigraphic units, extending for over 1500 km from the Southern Alps in the NW to the Aegean region in the SE (Fig. 1, see also Fig.1 of Chapter 2). Its development has been governed by the convergence of the African and European plates since the Jurassic.

The Dinaride-Hellenide tectonic units are currently divided among ten countries speaking six major languages. Some of the political borders run parallel to the orogenic strike infavourably separating internal and external orogenic domains; currently, the level of knowledge on the geodynamic significance of the tectonic units varies from region to region.

*"Namentlich infolge der unermüdlichen Studien von C. Renz, dann aber auch infolge jener der deutschen, österreichischen und ungarischen Geologen, die den Balkan [...] untersuchten, hat sich unsere Kenntnis des Baues der Dinariden wieder wesentlich erweitert und so kann denn eine Synthese der Dinariden versucht werden."*

– begins Franz Baron Nopcsa in 1921 with his lucid synthesis of the Dinaride-Hellenide tectonostratigraphy. Understanding the architecture and evolution of the Dinarides reached further landmark stages owing to the work of, among others, Cvijić (1924), Kossmat (1924), Petković (1961), Aubouin (1973), Dimitrijević (1982, 1997), Pamić *et al.* (1998, 2002) and Karamata (2006). The latest tectonic map and interpretation of the units have been elaborated by Schmid *et al.* (2006, 2008) and we have mostly followed the tectonic subdivision proposed by these authors.

### *1.2.2. Overall tectonic architecture*

As an integral part of the European Alpine chain, the Dinarides are located between the Southern Alps and the Hellenides, forming a SW-vergent pile of Alpine tectonostratigraphic units. They essentially consist of Jurassic ophiolites thrust onto the distal passive margin of the Adriatic plate (Dimitrijević, 1982; Pamić *et al.*, 2002; Karamata, 2006; Schmid *et al.*, 2008). The latter is built up of sedimentary to low-grade metamorphic Lower Palaeozoic basement and its Permo-Mesozoic cover. Large-scale Early Cretaceous thrusting involved several Adria-derived units passively carrying the ophiolites previously thrust onto them, and gave rise to the formation of a vast clastic wedge in front of the continental-ophiolite thrust sheet complex (Aubouin, 1973; Schmid *et al.*, 2008; Chapters 2 and 3 of this Thesis). The Outer Dinaride structural units are dominated by the elements of the large Mesozoic Adriatic Carbonate Platform (Vlahović *et al.*, 2005). Individual tectonic units of the platform are often separated by imbricated slices of Tertiary flysch which shows mixed carbonate–siliciclastic composition (Chorowicz, 1977; Chapter 5 of this Thesis), hinting at a major sediment

source outside the platform. Thrusting in the Outer Dinarides was accompanied by the formation of a retrowedge at the NE margin of the Dinarides – the Sava Zone – that formed the collisional zone of the Dinarides with the Tisza Unit in the Tertiary (e.g. Pamić 1993, Tari, 2002; Schmid *et al.*, 2008).

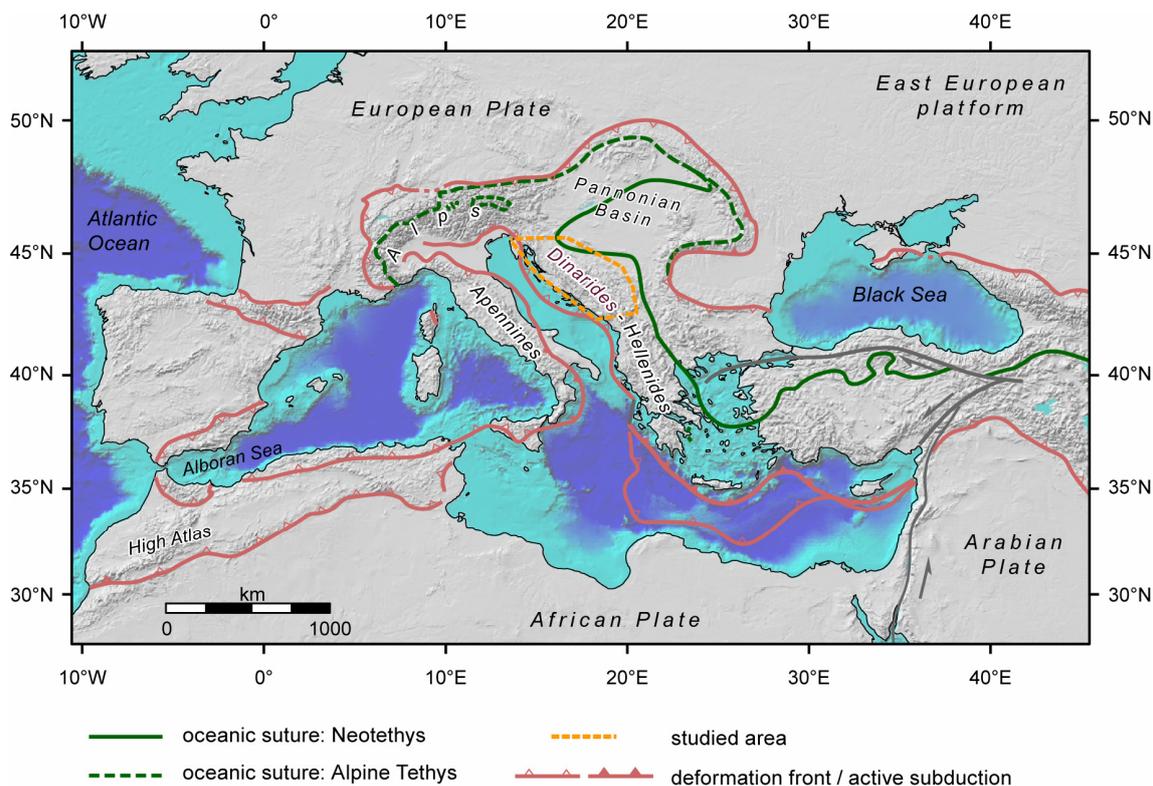


**Fig.1.** Position of the Dinarides within the European Alpine system, with the suture zones of the Alpine Tethys and Neotethys and the major deformation fronts also shown. Map courtesy of K. Ustaszewski

### 1.2.3. Tectonic significance of the ophiolites and the Adriatic continental basement

#### 1.2.3.1. Dinaride ophiolite thrust sheets

The Dinaride ophiolites appear in two distinct belts which gave rise to a vigorous debate on their relation. Several models were proposed; the existence of two oceanic basins, either separated by an intraoceanic "microcontinent" (Robertson and Karamata, 1994; Karamata *et al.*, 2006), or opened consecutively in an arc/back-arc system (Pamić *et al.*, 2002). Alternatively, the ophiolites originated from a single

oceanic basin the fragments of which were emplaced to different distances onto the overridden continental plate (Kober, 1912; Bernoulli and Laubscher, 1972; Schmid *et al.*, 2008). Although there is a consensus in earlier models that oceanic convergence was not associated with a significant island arc igneous activity (Ivanov *et al.*, 1987; Pamić *et al.*, 2002; Dimitrijević *et al.*, 2003), an increasing number of petrological and geochemical data point to island arc affinity in the Dinaride ophiolites, and also in other equivalent, displaced ophiolite sequences in Albania, in the Hellenides and in the Bükk Mts. in NE Hungary and the Apuseni Mts. in Transylvania. The island arc signatures are explained by the development of an intra-oceanic supra-subduction-zone (e.g. Aigner-Torres and Koller 1999; Robertson, 2004; Beccaluva *et al.*, 2005; Bortolotti and Principi 2005; Bazylev *et al.*, 2006; Lugović *et al.*, 2006, 2007; Rassios and Moores 2006; Smith 2006; Dilek *et al.*, 2008). K/Ar, Ar/Ar and Sm/Nd age data of sub-ophiolitic metamorphic soles from Dinaride and Albanian ophiolites range between 178 and 161 Ma, indicating Middle Jurassic intraoceanic thrusting (e.g. Okrusch *et al.* 1978; Parlak and Delaloye 1999; Dimo-Lahitte *et al.* 2001; Olker *et al.* 2001; Smith 2006 and references therein). Ophiolite obduction onto the Adriatic margin was completed by Late Jurassic and involved HP/LT metamorphism in deep crustal levels of both the oceanic and Adriatic plate margins (see discussion in Chapter 2). Stratigraphic constraints on the timing of obduction are provided by the Tithonian-Berriasian age of the oldest sedimentary deposits sealing the ophiolites, consisting of alluvial coarse-grained siliciclastic strata and shallow marine carbonates interfingering with them (Blanchet *et al.* 1970; Bortolotti *et al.*, 1971; Charvet and Termier 1971; Charvet 1973, 1978; Neubauer *et al.* 2003).

### 1.2.3.2. Inner Dinaride continental thrust sheets

The continental units in the Inner Dinarides represent major, Adria-derived thrust sheets exposed in large, orogen-parallel tectonic windows (Bernoulli and Laubscher, 1972; Schmid *et al.*, 2008), and dominated by Palaeozoic to Triassic siliciclastic and carbonate sediments as well as acid igneous suites (Podubsky, 1970; Rampnoux, 1970; Djoković, 1985; Dimitrijević, 1997; Pamić and Jurković, 2002). They underwent regional thermal overprint ranging up to anchi- to epizonal conditions; a latest Jurassic to Early Cretaceous cooling is widely demonstrated by several Ar/Ar, K/Ar and zircon

FT age data from a number of basement units (Milovanović, 1984; Árkai *et al.*, 1995; Belak *et al.*, 1995; Pamić *et al.*, 2004; Ilić *et al.*, 2005; Judik *et al.*, 2006; Muceku *et al.*, 2006; – see discussion in Chapter 2).

### 1.2.3.3. Sava Zone

The Sava Zone is an elongated, highly complex tectonic zone located at the northern margin of the Inner Dinarides (Fig. 1 of Chapter 6). It separates them from the Tisza Unit further in the north, which is a basement unit in a rather exotic position; it was detached from the European margin in the Jurassic, with its subsequent tectonic evolution involving thrusting and large amounts of strike-slip displacement (e.g. Csontos and Vörös, 2004). The Sava Zone comprises Late Cretaceous ophiolites, representing a remnant basin of the Neotethys Ocean subducting below the Tisza Unit, which are overlain by Late Cretaceous to Eocene mixed siliciclastic–carbonatic flysch-like deposits. Sediments of the Sava Zone and their ophiolitic or continental basement underwent deformation and Alpine regional metamorphism due to the collision of the Tisza Unit with the Inner Dinaride continental margin. The degree of metamorphism exhibits a large regional variation, ranging up to amphibolite facies, and dated mostly as Late Cretaceous to Early Paleogene. The sedimentary–metamorphic sequence is intruded by Late Cretaceous to Oligocene granitoids and bimodal volcanic series (Pamić and Šparica 1983; Pamić 1993, 1998, 2002; Pamić *et al.*, 2000; Balen *et al.*, 2003; Starijaš *et al.*, 2005, 2006; Krenn *et al.*, 2008; Ustaszewski *et al.*, in press).

Siliciclastic components of the flysch were sourced from a composite source area made up of ophiolites, granitoids and metamorphic units (Jelaska *et al.*, 1970; Mikes *et al.*, 2006b; Ustaszewski *et al.*, in press). Palaeocurrent indicators suggest sediment transport from NE to E relative to the Sava Zone at present directions (Jelaska *et al.*, 1970, Babić and Zupanić 1976; Jelaska 1978), or from E to SE if the Tertiary counter-clockwise rotation in the Sava Zone that exceeds 30° is also taken into account (Márton *et al.*, 2005).

#### 1.2.3.4. Outer Dinarides

The Outer Dinaride thrust sheets are dominated by Mesozoic carbonate sequences of several km thickness, constituting the vast Adriatic Carbonate Platform (AdCP; Vlahović *et al.*, 2005). The thrust fronts are associated by flysch-like sediments, deposited in a large foreland basin system on top of the SW-directed Dinaride thrust wedge (Fig. 1 of Chapter 5). Basin remnants can be traced along the orogenic strike from the Southern Alps to the Hellenides, occurring mostly as thin imbricate slices (OGK – Basic Geologic Map of former Yugoslavia, 1:100.000 sheets). Stratigraphic position of the flysch has traditionally been described in terms of a Palaeogene marine sequence overstepping the Mesozoic AdCP. The flysch is underlain by well-dated Lower to Upper Eocene Globigerina marls; their contact is conformable at places, but angular or erosional unconformities have been often reported (e.g. Marinčić, 1981; Marjanac, *et al.*, 1998; Marjanac, 2000). Due to imbricate thrusting, the flysch slices are tilted, truncated, and less than 100-400 m thick. Turbidite beds are dominantly composed of siliciclastics, with a highly variable amount of carbonate admixture. Based mostly on paleocurrent indicators and heavy mineral analyses, two different hypotheses exist for the provenance of the siliciclastic material in the NW part of the basin system; a dual, Alpine-Dinaride source (Magdalenić, 1972) and an exclusive sediment supply from Dinaride units in the NE (Marinčić, 1981; Marinčić *et al.*, 1996) were both proposed. In the central and SE parts of the basin, the use of palaeocurrent indicators for deciphering the ultimate source location of siliciclastic input is limited, due to complex basin floor topography and flow reflection (e.g. Marjanac, 1990; 1996), and the origin of the siliciclastic detritus is not well understood.

The flysch sandstones are lithic wackes to calcilithites, with their main framework components averaging at  $Q_{60-85}F_{5-15}L_{10-25}$ , corresponding to a recycled orogenic provenance (Mikes *et al.*, 2006a). Major and trace element geochemistry and heavy mineral analysis indicate provenance mixing of mature, quartzose sedimentary rocks and ophiolitic units. Cr-spinel, garnet, rutile, zircon, tourmaline and apatite as well as minor amounts of staurolite and glaucophane characterize most of the heavy mineral assemblages in the entire basin system (Woletz, 1962; Pavičić *et al.*, 2003; Mikes, 2003; Mikes *et al.*, 2005). Locally however, especially in the central and SE part of the basin, the heavy mineral spectra comprise higher amounts of unstable metamorphic species (hornblende, tremolite, epidote, chloritoid). Regional distribution of new

calcareous nannofossil depositional ages reveals an increasing preservation for the Neogene part of the sequence towards the SE (Chapter 5). This pattern is well in line with a recent kinematic reconstruction by Ustaszewski *et al.* (2008), proposing that the amount of post-Early Miocene shortening increases in this direction. The above data suggest increased relief and exhumation in the SE Dinarides in the Late Tertiary, and westerly-directed drainage into the foreland basin system.

### **1.3. Recent advances in sedimentary provenance analysis**

The composition of siliciclastic sediments yields crucial information for deciphering the lithology, thermal history, kinematic evolution and several other aspects of the rock associations in the sedimentary source area. However, a number of other processes do also operate during the evolution of sediments, which exert a fundamental control on their composition and will modify the original source area signal to varying degrees. The most important processes include chemical weathering, grain breakage and abrasion, provenance mixing, sediment recycling, hydraulic sorting, authigenesis and intrastratal solution. Several techniques are available to describe a particular aspect of sediment composition, the most powerful being petrography, heavy mineral analysis and whole-rock geochemical analysis. In all cases, data interpretation must take the above processes into account in order to reasonably assess source area composition (e.g. Zuffa *et al.*, 1984; Pettijohn *et al.*, 1987; Ibbeken and Schleyer, 1991; Morton *et al.*, 1991; Johnsson and Basu, 1993; Morton and Hallsworth, 1999; von Eynatten and Weltje, 2004).

Heavy minerals – accessory constituents of arenites, with their densities typically higher than that of quartz – are particularly useful indicators of sedimentary provenance. They are rock-forming to accessory minerals of metamorphic and igneous source rocks liberated and released by source area weathering, and they can be introduced to the sedimentary cycle by reworking from older sediments, as well. More than 50 heavy mineral species have been described (Parfenoff *et al.*, 1970; Boenigk, 1983; Mange and Maurer, 1992). Many of them have very specific and restricted paragenesis, providing source rock information which cannot be acquired by other techniques. Principles and procedures of heavy mineral analyses were extensively

discussed by Morton (1985a), Mange and Maurer (1992) and Mange and Wright (2007).

Conventional heavy mineral data can usually not directly mirror the source rock mineralogy for the reasons noted above, and a reliable comparison of samples in terms of source area signatures becomes difficult. However, data directly connected to the sediment source, essentially unbiased by weathering, hydraulic sorting and intrastratal solution can be obtained. Examination of the optical (e.g. Lihou and Mange-Rajetzky, 1996), chemical (e.g. Mange and Morton, 2007), geochronological (e.g. Fedo *et al.*, 2003) and thermochronological (e.g. Carter, 1999) signatures of single grains for a given heavy mineral species are probably the most powerful. In principle, many techniques already well established in igneous and metamorphic petrology can be adopted for the study of heavy minerals whenever a textural context (such as in garnet-biotite Fe-Mg exchange thermometry, for instance) is not required for the target mineral. Source area characterization can be made with an even higher confidence if two or more of the single-grain attributes are combined (Basu *et al.*, 1998; Dunkl *et al.*, 2001). In the following we briefly review the most important single-grain techniques, many of which have been extensively applied in the present Thesis.

*External zircon morphology:* there is a relationship between the external morphology (relative arrangement of prism and pyramid faces) of zircon crystals and the principal chemical magma type in which they were formed (Pupin, 1980; Benisek and Finger, 1993). Recently, the method has been successfully applied to detrital zircon crystals (Caironi *et al.*, 1996; Schäfer and Dörr, 1997; Dunkl *et al.*, 2001).

*Single-grain geochemistry:* numerous heavy mineral species exhibit a wide range of chemical composition, representing end-member solid solutions. The actual composition and chemical zoning patterns of a detrital grain can depend on the metamorphic grade and/or bulk geochemical composition of the parent rock (e.g. Morton, 1991). Measurements performed with an electron microprobe allow rapid and highly reproducible geochemical analyses and a large throughput of detrital grains. The most rewarding detrital minerals are *garnet* (Morton, 1985b; Haughton and Farrow, 1989), *tourmaline* (Henry and Dutrow, 1992; von Eynatten and Gaupp, 1999), *pyroxene* (Cawood, 1983; Krawinkel *et al.*, 1999) and *blue sodic amphibole* (Mange-Rajetzky and Oberhänsli, 1982; Faupl *et al.*, 2002). Of special importance is *chrome spinel*, the composition of which sensitively indicates parental melt or host peridotite compositions (Irvine, 1965 *et* 1967; Dick and Bullen, 1984; Arai, 1992; Barnes and

Roeder, 2001; Kamenetsky *et al.*, 2001). It provides a clue to the plate tectonic setting of mafic-ultramafic source rocks and can in turn give rise to paleogeographic reconstructions (Poher and Faupl, 1988; Arai and Okada, 1991; Hisada and Arai, 1993; Cookenboo *et al.*, 1997). Trace element data of *rutile*, its growth generally restricted to medium-to-high-grade metamorphic rocks (Force, 1980), have been recently shown to be useful in constraining protolith chemistry and metamorphic grade (Zack *et al.*, 2004a,b; Triebold *et al.*, 2007).

*Zircon fission track thermochronology*: determination of single crystal ages of zircon by fission track (FT) dating (e.g. Naeser, 1979) reflects the cooling ages of the source rocks. The obtained zircon age spectra thus provide a guide to possible source areas, by revealing their different thermal evolution (Hurford *et al.*, 1984; Hurford and Carter, 1991; Brandon and Vance, 1992; Dunkl, 1992; Carter, 1999; Dunkl *et al.*, 2001; Trautwein *et al.*, 2001). Combined with morphological analyses, episodes of volcanic activity can also be identified, in addition to the refinement of the petrology of inferred plutonic rocks (Dunkl, 1992; Dunkl and Nagymarosy, 1992; Trautwein *et al.*, 2001; Dunkl *et al.*, 2001).

*White mica  $^{40}\text{Ar}/^{39}\text{Ar}$  chronology*: Ar/Ar single-grain geochronology of detrital white mica is a potential tool for deciphering orogenic processes in both modern and ancient orogens (e.g., Copeland and Harrison, 1990; Stuart *et al.*, 2001). In combination with FT thermochronology of zircon and apatite, the cooling of source rocks in the temperature interval of approx. 400°C down to ~100°C can be precisely traced. Geochemical analysis of the dated minerals provide further petrogenetic information on the source rocks (von Eynatten and Wijbrans, 2003; Grimmer *et al.*, 2003).

*Zircon U/Pb geochronology*: U/Pb single-grain geochronology of detrital zircon reveals the magmatic and/or high-grade metamorphic age structure of the source units and, with expanding instrument capacities and improving precision, its application has been rapidly increasing in the past years (e.g. Košler *et al.*, 2002; Fedo *et al.*, 2003, Jeffries *et al.*, 2003, Frei and Gerdes, 2008).

*Monazite (Th-U)/Pb geochronology*: Since its advent ca. 20 years ago (Suzuki *et al.*, 1991 and references therein), analytical progress made in the electron microprobe (Th-U)/Pb total chemical dating methodology (Montel *et al.* 1996; Williams *et al.*, 2006, Jercinovic *et al.*, 2008) enables it to become a routine procedure also in sedimentary provenance analysis (e.g. Kusiak *et al.*, 2006). Limitations include the

thermal instability of the epoxy resin used for embedding the detrital grains; this requires using a lower beam current than for polished thin-sections, potentially reducing the precision of the Pb concentration determination.

#### **1.4. Structure of the Thesis**

In the following Chapters 2 to 6, we present the results of a detailed sedimentary provenance study undertaken in Cretaceous to Tertiary basins of the Dinarides. The major objective will be to put new constraints on the orogenic evolution of this integral segment of the European Alpine chain. We follow the approach of in-depth characterizing the detritus derived from major tectonostratigraphic units, focusing on information extracted via the geochemistry, geochronology and fission-track thermochronology of single detrital grains. We will use these results to describe the paleogeology and understand sediment dispersal patterns which are all dependent on the large-scale crustal and surface processes involved in the Alpine orogeny.

Chapter 2 deals with the Latest Jurassic to Cretaceous evolution of the distal continental margin of the Adriatic plate, through the provenance analysis of the Bosnian Flysch. We trace the palaeogeology of obducted ophiolite sequences and their continental basement units which were exhumed and eroded, shedding detritus into a foredeep developed in front of the thrust complex. We address the problem by petrography, whole-rock geochemistry, clay mineralogy, single-grain geochemistry of detrital tourmaline, garnet, rutile and Cr-spinel as well as U/Pb geochronology and FT thermochronology of detrital zircon. New constraints on the depositional age come from carbonate microfacies analysis and calcareous nannoplankton determination.

Chapter 3 focuses on the geochemistry of detrital Cr-spinel from Early Cretaceous clastic basins in the NW Dinarides, characterized by a rather comparable tectonic setting to that of the Bosnian Flysch. The results are discussed together with previous data on heavy mineral assemblages and a model is proposed for the evolution of the basins.

Chapter 4 presents the results from three different geochronometers in detrital minerals, from sediments genetically related to the convergent Neotethyan margin in the Dinarides. Apatite FT, monazite electron microprobe (Th-U)/Pb and zircon LA-

ICPMS U/Pb single-grain ages are consistent and provide evidence for Late Jurassic acid magmatism and explosive volcanism at the Neotethyan supra-subduction zone.

In Chapter 5, we provide new constraints on the Miocene depositional age of flysch deposits in the Outer Dinaride foreland basin, based on calcareous nannofossil age determinations. Non-overlapping taxon ranges suggest extensive sediment reworking in the Outer Dinaride wedge-top basins from Late Cretaceous to Neogene times. Discovery of Neogene nannofossil species suggest that the Middle Eocene planktonic foraminifera, on which the earlier age assignment was based, are most probably in an allochthonous position. The results are in agreement with tectonic data from the region and with previous nannofossil age results, and are hoped to provide a new framework for interpreting heavy mineral data from the dated flysch units.

Chapter 6 is devoted to U/Pb–FT double-dating experiments performed on detrital zircon from the Dinarides. We extract a high-temperature geochronological and a low-temperature thermochronological datum from the same detrital grains. They are integrated using a two-dimensional statistical approach which accounts for the contrasting amounts of single-grain age uncertainties yielded by the both techniques, in order to identify geologically meaningful age clusters. Double dating of zircon yields valuable insights into the underlying U/Pb age structure of the sedimentary source area of the Dinaride sediments and into their subsequent thermal evolution. Source identification is possible with a confidence that can not be achieved by using the two dating techniques separately.

Finally, Chapter 7 summarizes the most important conclusions drawn in the Thesis.



## *Chapter 2*

# Provenance of the Bosnian Flysch

---

This chapter is largely identical to the manuscript entitled "Provenance of the Bosnian Flysch"

that is currently in press with the *Swiss Journal of Geosciences*

published OnlineFirst in Nov. 2008, doi:10.1007/s00015-008-1291-z

authored by:

Tamás Mikes, Dominik Christ, Rüdiger Petri, István Dunkl, Dirk Frei, Mária Báldi-Beke, Joachim Reitner, Klaus Wemmer, Hazim Hrvatović and Hilmar von Eynatten



## Provenance of the Bosnian Flysch

*Tamás Mikes, Dominik Christ, Rüdiger Petri, István Dunkl, Dirk Frei, Mária Báldi-Beke, Joachim Reitner, Klaus Wemmer, Hazim Hrvatović and Hilmar von Eynatten*

### Abstract

Sandwiched between the Adriatic Carbonate Platform and the Dinaride Ophiolite Zone, the Bosnian Flysch forms a c. 3000 m thick, intensely folded stack of Upper Jurassic to Cretaceous mixed carbonate and siliciclastic sediments in the Dinarides. New petrographic, heavy mineral, zircon U/Pb and fission-track data as well as biostratigraphic evidence allow us to reconstruct the palaeogeology of the source areas of the Bosnian Flysch basin in late Mesozoic times. Middle Jurassic intraoceanic subduction of the Neotethys was shortly followed by exhumation of the overriding oceanic plate. Trench sedimentation was controlled by a dual sediment supply from the sub-ophiolitic high-grade metamorphic soles and from the distal continental margin of the Adriatic plate. Following obduction onto Adria, from the Jurassic–Cretaceous transition onwards a vast clastic wedge (Vranduk Formation) was developed in front of the leading edge, fed by continental basement units of Adria that experienced Early Cretaceous synsedimentary cooling, by the overlying ophiolitic thrust sheets and by redeposited elements of coeval Urgonian facies reefs grown on the thrust wedge complex. Following mid-Cretaceous deformation and thermal overprint of the Vranduk Formation, the depozone migrated further towards SW and received increasing amounts of redeposited carbonate detritus released from the Adriatic Carbonate Platform margin (Ugar Formation). Subordinate siliciclastic source components indicate changing source rocks on the upper plate, with ophiolites becoming subordinate. The zone of the continental basement previously affected by the Late Jurassic–Early Cretaceous thermal imprint has been removed; instead, the basement mostly supplied detritus with a wide range of pre-Jurassic cooling ages. However, a c. 80 Ma, largely synsedimentary cooling event is also recorded by the Ugar Formation, that contrasts the predominantly Early Cretaceous cooling of the Adriatic basement and suggests, at least locally, a fast exhumation.

## **2.1. Introduction**

One of the most peculiar tectonostratigraphic units of the Dinaride orogen within the SE European Alpine system is the 'Zone Bosniaque', defined by Aubouin *et al.*, (1970). It is tectonically sandwiched between the most external belt of Dinaride ophiolites in the NE that are floored by continental basement nappes (Aubouin 1973) derived from the Adriatic plate (Schmid *et al.*, 2008), and units of the vast Mesozoic carbonate platform of the Adriatic plate in the SW. The Bosnian Zone mainly comprises thick Late Jurassic to Cretaceous flysch successions and other gravity flow deposits. We will collectively refer to them as Bosnian Flysch hereafter.

The presence of ophiolitic detritus in the Bosnian Flysch had been recognized early on (Blanchet 1966; Blanchet *et al.*, 1969; Charvet 1970; Olujić *et al.*, 1978), yet subsequent tectonic models assessed its importance diversely. Aubouin (1973) suggested that, as a result of Late Jurassic obduction, a foredeep was formed in front of the ophiolite nappes and demonstrated that the lower part of the Bosnian Flysch represents a synorogenic sequence. This view was largely contended by Lawrence *et al.*, (1995), Tari & Pamić (1998), Tari (2002) and Schmid *et al.*, (2008). As a marked contrast, Pamić (1993) and Pamić *et al.*, (1998) interpreted the Bosnian Flysch in terms of a sequence that was deposited on the NE passive margin of Adria; a genetic relationship of the sediments to the Dinaride ophiolites was not part of their models.

In this study a wide range of sedimentary provenance information was acquired to decipher the Late Mesozoic evolution of the source area geology of the Bosnian Flysch. The data were used to assess existing models addressing the geodynamic setting of the flysch. Arenitic samples were analysed for a detailed description of the lithology and age of the source rocks, using heavy mineral signatures and zircon chronology. Clay mineralogical and whole-rock geochemical methods were employed to characterize the provenance of the fine-grained sediments. Our investigations were completed by calcareous nannofossil and carbonate microfacies data, which put additional constraints on the biostratigraphic range.

## 2.2. Tectonic framework

The Bosnian Flysch is a 500 km long belt of Late Jurassic to Cretaceous, mixed siliciclastic-carbonate sequences incorporated into the Dinaride nappe pile (Fig. 1). In the NE, the flysch is tectonically overlain by the East Bosnian–Durmitor thrust sheet

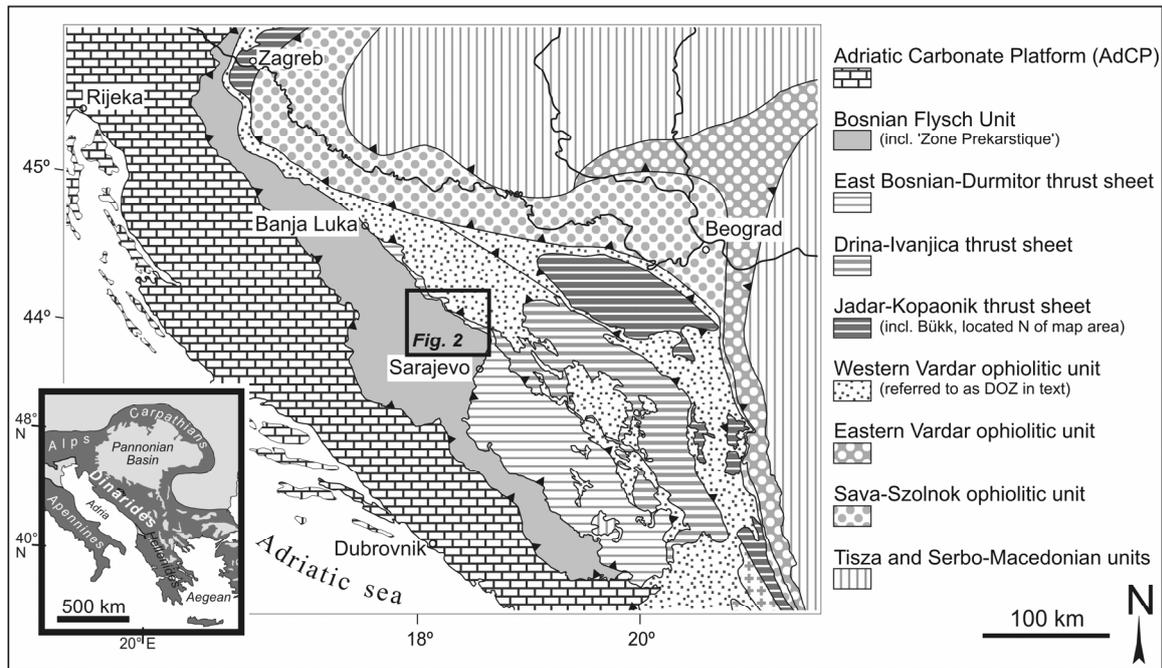


**Fig. 1.** Map showing the major structural units of the Dinarides (after Schmid *et al.*, 2008, slightly modified).

which passively carries Dinaride ophiolite units previously thrust onto it (Schmid *et al.*, 2008; cf. 'Zone Serbe' of Aubouin 1973). The East Bosnian–Durmitor unit wedges out towards the NW, where the Dinaride Ophiolite Zone appears to directly overlie the Bosnian Flysch.

To the SW, the Bosnian Flysch is structurally underlain by the Pre-Karst Subzone and in turn by the Main Karst Zone (Aubouin *et al.*, 1970). The latter largely corresponds to the Adriatic Carbonate Platform (AdCP; defined by Vlahović *et al.*, 2005), the former representing the heteropic, distal slope and basin facies bordering the platform. Overall facies distribution suggests that the AdCP, the largest Mesozoic platform of the Adriatic plate, acted as a palaeotopographic entity during the evolution of the Bosnian Flysch basin (Charvet 1980; Vlahović *et al.*, 2005). It was converted into the tectonic footwall of the Outer Dinaride thrust pile during Tertiary compression (Aubouin *et al.*,

1970; Chorowicz 1977; Charvet 1980; Tari 2002; Mikes *et al.*, 2008a; Schmid *et al.*, 2008).

With respect to the tectonic setting of the ophiolites and other Inner Dinaride structural elements (Fig. 1), we will largely follow the interpretation of a recent kinematic reconstruction made by Schmid *et al.*, (2008). These authors suggest that both belts of Dinaride Triassic-Jurassic oceanic units represent displaced fragments of an initially single zone of Neotethyan ophiolites, which were obducted westwards onto the Adria passive margin in the Late Jurassic. Cretaceous and Tertiary thrusting gave rise to far-travelled thrust sheets composed of continental and ophiolitic series. The orogen-parallel, allochthonous Palaeozoic to Triassic units represent continental basement nappes derived from the distal Adriatic plate, exposed mostly in elongated tectonic windows. This interpretation of Schmid *et al.*, (2008), which is in line with ideas already put forward by, for example, Bernoulli & Laubscher (1972), Charvet (1980), and Gawlick *et al.*, (2008), fundamentally differs from most other models which either propose two Mesozoic oceanic branches separated by a continental microplate (e.g. Dimitrijević & Dimitrijević 1973; Robertson & Karamata 1994; Karamata 2006), or assume that the basement nappes were derived from the European margin by out-of-sequence thrusting (Pamić *et al.*, 1998; Hrvatović & Pamić 2005).

The Jurassic ophiolites structurally above the Bosnian Flysch were described as the Dinaride Ophiolite Zone (DOZ; Dimitrijević & Dimitrijević 1973; Babić *et al.*, 2002; Pamić *et al.*, 2002), Central Dinaride Ophiolite Belt (CDOB; Lugović *et al.*, 1991) or as the zone constituting the most externally transported thrust sheets of the Western Vardar ophiolites (Schmid *et al.*, 2008), or as forming part of the Serb, Golija and Drinjača Zones according to Charvet (1978, 1980). These ophiolites, from now on referred to as Dinaride Ophiolite Zone (DOZ) in this paper, were recently argued to have been formed in an intraoceanic supra-subduction zone setting (Bazylev *et al.*, 2006; Smith 2006; Lugović *et al.*, 2006, 2007). K/Ar, Ar/Ar and Sm/Nd age data of sub-ophiolitic metamorphic soles from Dinaride and Albanian ophiolites range between 178 and 161 Ma, indicating Middle Jurassic intraoceanic thrusting (e.g. Okrusch *et al.*, 1978; Parlak & Delaloye 1999; Dimo-Lahitte *et al.*, 2001; Olker *et al.*, 2001; Smith 2006 and references therein). Petrology of these soles indicates both basaltic (e.g. Pamić *et al.*, 1973; Majer *et al.*, 2003; Operta *et al.*, 2003; Schuster *et al.*, 2007) and sedimentary protoliths (e.g. Karamata *et al.*, 1970; Schreyer & Abraham 1977; Okrusch *et al.*, 1978; Carosi *et al.*, 1996).

Ophiolite obduction onto the Adriatic margin was completed by Late Jurassic. Deep crustal levels of both the oceanic plate and the Adriatic margin suffered largely coeval (Okrusch *et al.*, 1978; Majer & Lugović 1991; Milovanović *et al.*, 1995; Most 2003) HP/LT metamorphic overprint as is indicated by blueschist facies rocks occasionally found among the metapelitic to metabasic rocks on both the upper and lower plates (Majer 1956; Charvet 1978; Djoković 1985; Majer & Lugović 1991; Mutić & Dmitrović 1991; Milovanović *et al.*, 1995; Belak & Tibljaš 1998; Most 2003). Stratigraphic constraints on the timing of obduction are provided by the Tithonian-Berriasian age of the oldest sedimentary deposits sealing the ophiolites, consisting of alluvial coarse-grained siliciclastic strata and shallow marine carbonates interfingering with them (Blanchet *et al.*, 1970; Charvet & Termier 1971; Charvet 1973, 1978; Neubauer *et al.*, 2003). This unconformity is, however, a diachronous surface; the overlying sediments become progressively younger towards the more internal domains of the DOZ, attaining Cenomanian age at the NE border of the DOZ. These observations indicate an overall transgressive trend from the Tithonian/Berriasian to the Cenomanian, perpendicular to the strike of the orogen (Charvet 1978, 1980).

The continental units in the Dinarides are considered to represent major, Adriatic-derived thrust sheets (see discussion in Schmid *et al.*, 2008). The East Bosnian–Durmitor Unit, together with the Drina–Ivanjica, Jadar, Kopaonik, Medvednica and the displaced Bükk units, are dominated by Palaeozoic to Triassic (meta-) sediments (Podubsky 1970; Rampoux 1970; Djoković 1985; Dimitrijević 1997; Pamić & Jurković 2002), which underwent regional thermal overprint ranging up to anchi- to epizonal conditions. Early Cretaceous cooling is widely demonstrated by K/Ar age data yielding  $135 \pm 11$  Ma in the Drina–Ivanjica Unit (Milovanović 1984),  $118 \pm 4$  Ma (Belak *et al.*, 1995) as well as  $107 \pm 8$  Ma (Judik *et al.*, 2006) in the metapelites of the Medvednica Unit, as well as various ages from 133 to 98 Ma in the Bükk Unit, in agreement with zircon FT age data in this latter tectonic unit (see details in Árkai *et al.*, 1995). Ar/Ar age spectra of detrital white mica from the Ljig Flysch (in the External Vardar Subzone *sensu* Dimitrijević 1997; covering the Jadar–Kopaonik thrust sheet according to Schmid *et al.*, 2008) contain a 110 Ma age component (Ilić *et al.*, 2005). Finally, the Palaeozoic of the Bosnian Schist Mts., considered to represent the basement of the Pre-Karst Subzone (Aubouin *et al.*, 1970; Schmid *et al.*, 2008) also records this thermal event (K/Ar ages from 121 to 92 Ma) prior to its main phase of Paleogene cooling (Pamić *et al.*, 2004).

### **2.3. Geological setting of the Bosnian Flysch**

The Bosnian Flysch forms a rather uniform belt (Figs. 1 & 2): formations comparable to those investigated by this study crop out to the NW of Central Bosnia, in the Zrinska Gora and in the Slovenian Trough (Aubouin *et al.*, 1970; Cousin 1972; Babić & upanič 1976; Bušer 1987; Hrvatović 1999; Rožič 2005), and in form of the so-called Durmitor Flysch in the SE (Dimitrijević & Dimitrijević 1968; Blanchet *et al.*, 1969; Rampnoux 1969; Aubouin *et al.*, 1970). Two distinct lithostratigraphic units characterize the Bosnian Flysch (Olujić 1978; Hrvatović 1999). The lower, turbiditic to monotonous pelagic series is more than 1000 m thick, and is dominantly composed of siliciclastic sandstones, marls, shales, cherty micritic limestones, and grey radiolarites (Vranduk Formation). It stretches along the NE side of the flysch zone (Fig. 2), i.e. nearer to the overriding nappes and hence more proximal to the source.

The upper succession (Ugar Formation; Fig. 2) occurs SW of the Vranduk Formation and is carbonate-dominated, comprising thin-bedded marly to micritic limestones and red or grey shales, intercalated with calcareous turbidites, and finally, coarse catastrophic carbonate mass flow deposits, several tens of metres thick, in the upper part of the sequence. These carbonate debrites contain large Scaglia Rossa clasts up to several metres across, exhibiting internal slump folds. Stratigraphic thickness of the Ugar Formation exceeds 2000 m (Hrvatović 1999). Palaeotransport indicators suggest S- to SE-directed shedding for the Vranduk Formation and SE to NE-directed transport for the Ugar Formation (Dimitrijević & Dimitrijević 1968; Hrvatović 1999). The described formations largely correspond to the sediments of the 'flysch bosniaque interne' of Charvet (1978). Calpionellids and foraminifera suggest that the age of the Vranduk Formation in Central Bosnia ranges mostly from the Tithonian to the Berriasian-Valanginian, whereas that of the Ugar Formation ranges from Late Albian to Maastichtian, and locally, into the Paleocene (Cadet 1968; Dimitrijević & Dimitrijević 1968; Charvet 1978; Olujić *et al.*, 1978). To the N (near Banja Luka), and to the S of Central Bosnia (in the Durmitor Flysch), more complete profiles have been observed in the Vranduk Formation, ranging from the Berriasian up to the Cenomanian (Cadet 1968; Cadet & Sigal 1969; Rampnoux 1969; Blanchet 1970; Charvet 1978). It was suggested that the two formations are separated by an angular unconformity (Dimitrijević 1982 p.14; Csontos *et al.*, 2003; Schmid *et al.*, 2008 p.25); however continuous Cretaceous successions are also preserved in parts of the basin (Dimitrijević 1982 p.14; Barremian

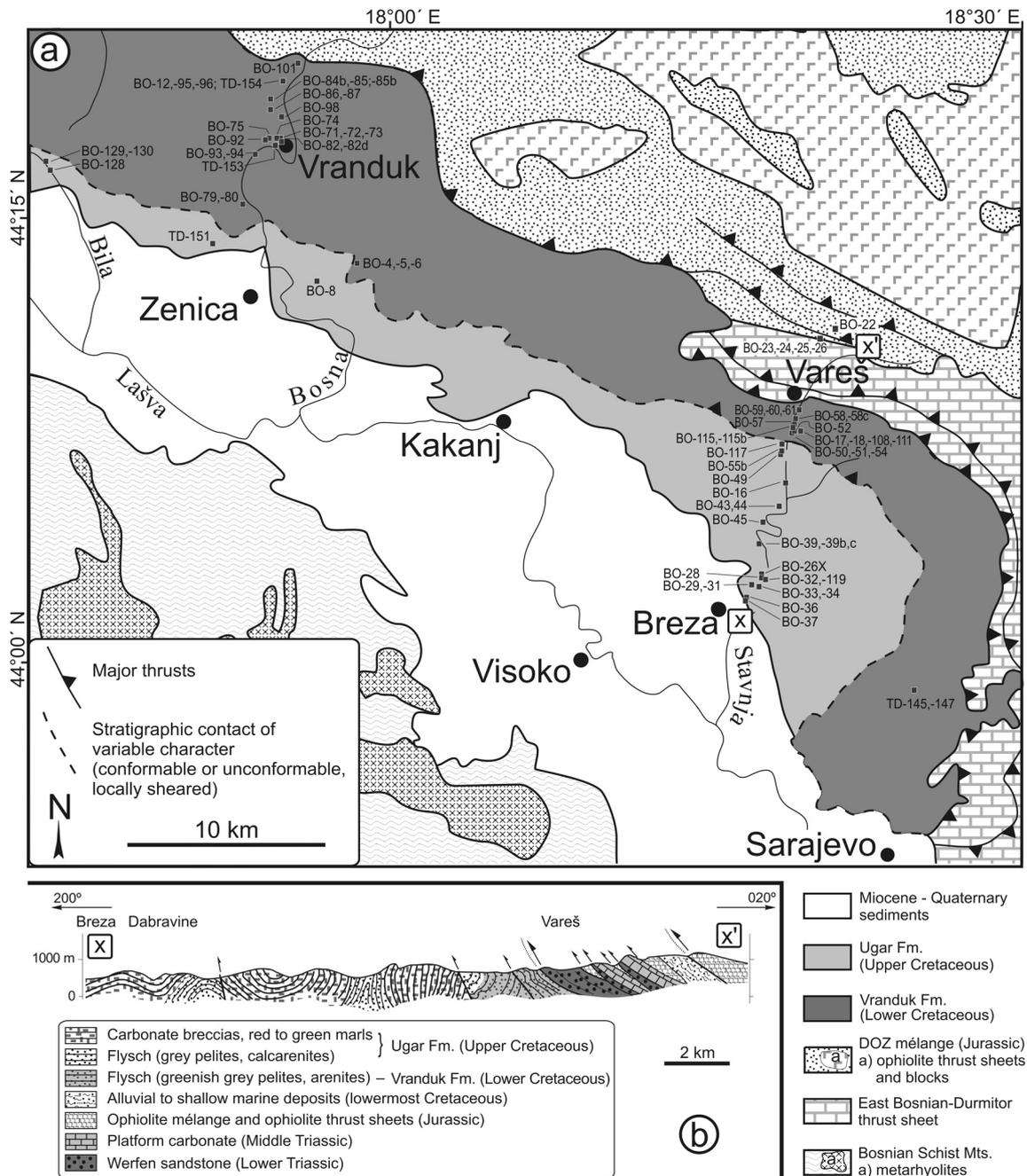


**Fig. 2.** (a) Geological sketch map of Central Bosnia showing sampling locations in the Stavnja Valley (x-x'), in the Bosna Valley and other localities. Map compiled using the 1:100,000 sheets of the Basic Geological Map of Yugoslavia and after Charvet (1978). Refer to Appendix 2-1 for sampling locations off the map. (b) Schematic profile across the Bosnian Unit and the East Bosnian-Durmitor thrust sheet in the Stavnja Valley (after Charvet 1978) illustrating the major tectonostratigraphy of the studied area.

to Campanian succession of Blanchet 1970). The onset of flysch deposition is usually not well constrained because the Vranduk Formation may be either sheared off its basement, or may consist of debrites at its base, lacking direct evidence regarding their sedimentation age. However, most such fragments are Tithonian to lowermost Cretaceous carbonate lithoclasts, and Blanchet *et al.*, (1969) described a profile in which a clastic succession overlies a condensed Upper Triassic to Jurassic sequence. In this profile, red radiolarites are capped by a debrite horizon containing clasts of radiolarite, mafic volcanics and Upper Jurassic marl, in turn overlain by pelagic calcareous marl with Berriasian calpionellids. Recently, Djerić *et al.*, (2007) reported an Oxfordian radiolarite intercalation from the Vranduk Formation. In summary, a transition from pelagic to clastic-dominated deposition in the internal domains of the 'Zone Bosniaque' most likely occurred during the latest Jurassic.

The style of tectonic deformation is different in both units. The Vranduk Formation exhibits tight to isoclinal, metre- to map-scale SW-vergent folds, whereas overprinting box-, mushroom- and kink folds are often observed at outcrop scale. The Ugar Formation, in contrast, is only gently folded. These strata typically exhibit open, map-scale SW-vergent folds. Observed differences in deformation style between the two units may result from the combination of a polyphase folding history (L. Csontos and S. M. Schmid, pers. comm.) and the high competence contrast between the massive Ugar carbonate debrite beds and the siliciclastic-dominated, thinner-bedded Vranduk strata.

#### **2.4. Sampling procedure and analytical methods**

Sampling of the flysch lithologies was performed in two sections cutting perpendicularly across the strike of the nappe pile along the Bosna and Stavnja river valleys (Fig. 2). Additional samples were taken from other parts of the basin (Appendix T2-1). Sampling was completed by sandstone blocks included in the DOZ mélange in the Stavnja Valley profile and further to the NW in the Borja Mountains. For the purpose of this provenance study, the first of its kind performed in the Bosnian Flysch basin, single outcrops were chosen with suitable and representative lithologies. We are aware that this does not replace future detailed sectionwise work.

For petrography, whole-rock geochemistry and accessory mineral separation, fine- to medium-grained sandstones were selected. Coarse-grained sandstones and breccias

were selected for microfacies analysis. For clay mineral analysis and calcareous nannofossil biostratigraphy, pelitic sediments (shale, marl) were sampled, and their aliquots were also used for whole-rock geochemistry. Weathered parts were removed prior to further sample preparation.

#### *2.4.1. Calcareous nannofossils*

Standard smear slides were prepared from 4 suitable pelite samples in the Vranduk Formation and 12 in the Ugar Formation, without chemical treatment or centrifugation. Slides were examined under the microscope in normal and cross-polarized lights at  $\times 1250$  magnification. Stratigraphic evaluation was performed individually for each sample, without using any additional geological information. Cretaceous species ranges were taken from Perch-Nielsen (1985) and Burnett (1998). Taxonomic work followed Bown & Young (1997), Burnett (1998) and Bown *et al.*, (1998). For the list of identified taxa, along with their stratigraphic ranges, refer to Appendix 2-2.

#### *2.4.2. Accessory mineral separation*

About 4-5 kg of fine- to medium-grained sandstone were crushed, dry sieved (0.250 mm), then both fractions were treated individually. For single-crystal geochemistry and chronology, the heavy mineral fraction in the  $<0.250$  mm share was pre-concentrated using a Wilfley-table. Carbonate was removed using a 5% cold acetic acid treatment. Heavy minerals were separated with a hot LST Fastfloat<sup>®</sup> heavy liquid ( $\rho=2.85$  gcm<sup>-3</sup>), then embedded in epoxy, polished and carbon-coated for microprobe analysis. For light microscopy and quantitative heavy mineral analysis, the  $>0.250$  mm share was first disintegrated using 5% acetic acid until carbonate was removed, and then wet sieved to 0.063-0.125 mm. The heavy mineral fraction was separated in the same way as described above, embedded in optical resin and examined under a polarisation microscope.

### *2.4.3. Whole rock chemistry*

Whole rock geochemistry was performed on the same sample set also used for heavy mineral analysis, and was completed with additional coarse-grained sandstone and pelitic samples. About 100 g of rock chips, devoid of cracks and calcite veins, were crushed in polyethylene bags to avoid metal contamination, and powdered in an agate ball mill. Powders were dried at 105 °C, and fused to glass discs using Merck Spectromelt A12 fluxant. Major and trace element concentrations were determined by X-ray fluorescence spectrometry (XRF) using a PANalytical Axios-Advanced instrument at the Geoscience Center Göttingen. Trace element concentrations have 1-2% relative precision. Loss on ignition values (LOI) were determined after overnight heating of two aliquots per sample at 1100 °C. Whole-rock geochemical results are summarized in Appendix 2-4.

### *2.4.4. Clay mineralogy*

The <2 µm and <0.2 µm grain size fractions from gently crushed shale and marl samples were separated by gravity settling using Atterberg cylinder, centrifugation and filtration. X-ray diffraction analyses were performed on oriented and non-oriented samples; each sample was analysed in duplicate. Both glycolated and air-dried samples were scanned from 4° 2θ to 70° 2θ for phase identification using the peak heights as a semi-quantitative estimate of phase abundance, and from 7° 2θ to 10° 2θ for illite crystallinity (=Kübler Index: Kübler 1967; Frey 1987). Appendix 2-1 lists the analysed samples. Refer to Petri (2007) for further details.

### *2.4.5. Mineral chemistry*

Chemical compositions of detrital Cr-spinel, tourmaline, garnet and rutile were determined by a JEOL 8900RL electron microprobe, operated in WDS mode at the Geoscience Center Göttingen. Analytical conditions are given in Appendix 2-3; the results of single-grain analyses are listed in Appendices 2-5 to 2-8.

#### 2.4.6. U/Pb geochronology

U/Pb ages on single zircon grains were obtained by laser ablation ICP-MS from polished mineral mounts, employing a Thermo Element 2 sector-field instrument attached to a Nd:YAG ultraviolet laser system ( $\lambda=213\text{nm}$ ; New Wave Research) at GEUS, Copenhagen (Frei & Gerdes, submitted). 90 to 120 crystals were analysed per sample. Off-line reduction of raw data was performed using PEPITA software (Dunkl *et al.*, 2007). Single-crystal ages were calculated by Isoplot 3.50 (Ludwig 2003) and age population distributions were obtained using AGEDISPLAY (Sircombe 2004) considering analyses with their propagated  $2\sigma$  standard errors only within  $\pm 14\%$  of concordance. For the analytical parameters and the single-crystal U/Pb results, refer to Appendices 2-3 & 2-9, respectively.

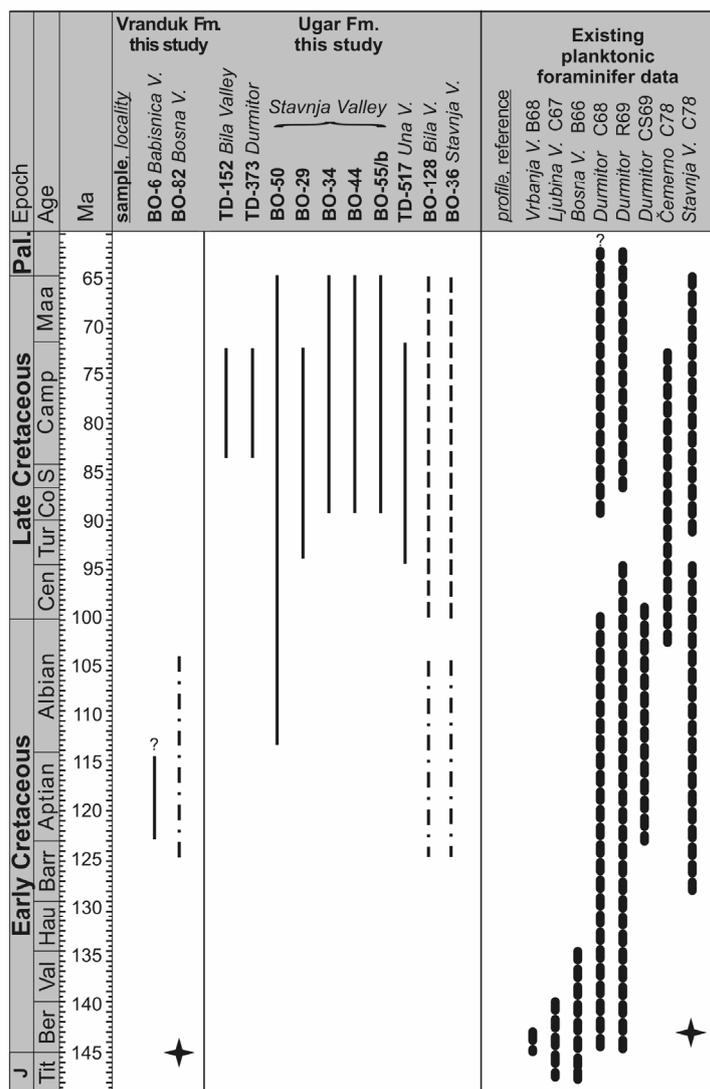
#### 2.4.7. Zircon fission-track analysis

The concentrated zircon crystals were embedded in PFA teflon with two mounts made from each sample. Spontaneous tracks were revealed by etching in NaOH-KOH eutectic melt at  $225^\circ\text{C}$  (Gleadow *et al.*, 1976) for 23 to 74 hours. Neutron irradiations were performed at the research reactor of Oregon State University. The external detector method was used (Gleadow 1981) and, after irradiation, the induced fission tracks in the mica detectors were revealed by etching in 40% HF for 30 min. Track counts were made with a Zeiss Axioskop microscope at  $\times 1000$  magnification combined with a computer-controlled stage system (Dumitru 1993). The FT ages were determined by the zeta method (Hurford & Green 1983) using the age standards listed in Hurford (1998), and visualized using Trackkey (Dunkl 2002). The results will be discussed using Fig. 12, details are given in Appendix 2-10.

## 2.5. Results

### 2.5.1. New constraints on depositional age

Nannofossil assemblages from the Bosnian Flysch, described in this paper for the first time, are scarce; dissolution and over-calcification are rather common. However, their preservation proved sufficient for the age determination. Fig. 3 illustrates the most probable nannofossil ages obtained for each sample, and Appendix 2-2 contains the distribution of the nannofossil species in all Bosnian Flysch samples from this study.



Sample BO-6, taken in the Vranduk Formation, adjacent to the Bosna River profile, contains a diverse Early Cretaceous assemblage with *Braarudosphaera africana* (Aptian to Cenomanian), suggesting that the age of this sample cannot be older than Aptian (Fig. 3; Appendix 2-2). Two more samples from the Vranduk Formation show only unspecific Late Jurassic to Late Cretaceous taxa.

Most samples from the Ugar Formation in the Stavnja River profile and in other localities (Bila Valley, Una Valley and the Durmitor Flysch near Mokro) contain Late Cretaceous nannofossils (Fig. 3). In the Stavnja River

**Fig. 3.** New fossil age data from the Vranduk and Ugar Fm samples (left) and comparison with published biostratigraphic ranges of other profiles (right). Solid black lines: stratigraphic position of zonal marker nannofossil species. Dot-dashed lines: probable age range of derived Urgonian facies fossils and lithoclasts in the sampled sediment. Dashed lines: Stratigraphic range of planktonic foraminifera. Star indicates age of calpionellid-bearing lithoclasts. Individual samples are arranged in columns, and the bars in each column represent the ranges of zonal markers found in that sample. Samples containing exclusively persistent taxa living through several epochs were not plotted. Refer to Table T2 (electronic supplement) for more details. Upper age limit of sample BO-6 is constrained by the mid-Cretaceous thermal overprint affecting the Vranduk Formation (Petri 2007). Thick dotted lines on the right: total, continuous stratigraphic interval in a profile established mostly using planktonic foraminifera by earlier workers. Literature source abbreviations: B68 – Blanchet (1968); C67 – Charvet (1967); B66 – Blanchet (1966); C68 – Cadet (1968); R69 – Rampnoux (1969); CS69 – Cadet and Sigal (1969); C78 – Charvet (1978).

profile, they suggest depositional ages ranging from the Coniacian to the Maastrichtian, which agrees well with the Albian/Cenomanian to Maastrichtian age range established by means of planktonic foraminifera (Charvet 1978). Individual samples collected in the Bila Valley and in the Durmitor Flysch yield Campanian age, and a Turonian to Campanian age was obtained in the Una Valley (N Bosnia). The latter nannofossil ages likewise support results based on planktonic foraminifera in the Durmitor Flysch (e.g. Cadet 1968; Rampnoux 1970) and in N Bosnia (Blanchet 1970). Additional constraints on the maximum depositional age are provided by benthic fossils and datable carbonate clasts. They occur in calcilithites and polymict breccias throughout the Vranduk Formation, and include isolated tests of orbitolinids (*Iraqia simplex*, *Textularia* sp., *Mesorbitolina* sp.) and rudist fragments (hippuritids, requinids, radiolitids). Peloidal biomicrite intraclasts with nebulous texture are also common. These bio- and intraclasts originate from different habitats in a typical Urganian facies carbonate platform, which existed only from the Late Barremian onwards. Figs. 4i-j illustrate the most frequent types of clasts with Urganian facies. Calpionellid-bearing lithoclasts also occur in the Vranduk Formation and are Late Tithonian to Early Berriasian in age based on *Calpionella alpina* (J. Haas, pers. comm.). This may indicate intrabasinal redeposition of latest Jurassic to earliest Cretaceous pelagic sediments. In the Ugar Formation, redeposited Urganian platform members are also common. However, orbitolinids are more abundant and, as a distinctive feature, there is a lack of quartz in their agglutinated tests (Figs. 4b & 4f). Instead, carbonate particles or Rhaxella spicules are incorporated. These contrasting types of orbitolinid tests may indicate that the Urganian facies clasts in the Ugar and Vranduk formations were derived from different carbonate platform habitats; their sea floor sediments being either "clean" lime mud or slightly contaminated by siliciclastics.

In the Ugar Formation, the dark, brown matrix around the Early Cretaceous fragments contains planktonic foraminifera (*Rotalipora appenninica*, Heterohelicidae, Globotruncanidae, Hedbergellidae and Pitonellidae; Fig. 4c shows an example), which collectively indicate that the Cenomanian most probably represents a maximum depositional age for the Ugar Formation in the Stavnja Valley (Fig. 3).

### 2.5.2. Petrography

The most common rock types among the sandstone blocks found in the DOZ mélange are litharenites. In contrast, the Vranduk and Ugar formations are built up of litharenites (including calcilithites), shales and marls. The coarse-grained lithologies greatly differ within the two flysch formations: poorly sorted polymict breccias occur in the Vranduk Formation, whereas in the Ugar Formation breccias are dominated by carbonate clasts. The main petrographic characteristics of sandstones and breccias in the DOZ mélange and the two Bosnian flysch formations are briefly described below.

*DOZ mélange:* The samples comprise poorly sorted litharenites to sublitharenites with angular mono- and polycrystalline quartz grains, plagioclase and K-feldspar, and lithoclasts of mafic volcanic rocks and serpentinite, as well as quartz arenite, quartzose siltstone, shale and phyllite. Carbonate framework grains were not observed.

*Vranduk Formation:* Litharenites to lithic wackes are occasionally composed of up to 40% carbonate grains. Sublitharenites, greywackes, calcarenites and pelagic biomicrites are less frequent. Major framework components include angular monocrystalline quartz, plagioclase (often with dense lamellae of polysynthetic twinning), chert, mafic volcanic lithoclasts (of variolitic to subophitic texture) and serpentinite. In addition, chlorite flakes and Cr-spinel grains often occur. Carbonate grains include litho- or intraclasts (mainly lime mudstones), peloids, rudist fragments and orbitolinids. In the Bosna Valley profile, reddish radiolarite fragments commonly occur, the radiolaria occasionally being calcified. Other framework grains, such as potassium feldspar, polycrystalline quartz, both foliated and non-foliated quartz-mica aggregates, amphibolite, "granitoid" lithoclasts (quartz-feldspar aggregates), quartz arenite, quartzose siltstone and shale, are subordinate.

*Ugar Formation:* Calcarenites and carbonate breccias with variable amounts (0 to 50%) of siliciclastic grains are the typical lithologies; greywackes are rare. Framework components commonly include carbonate clasts (lime mudstone/wackestone litho- or intraclasts, peloids), rudist fragments and orbitolinids as well as angular monocrystalline quartz. Less frequent is polycrystalline quartz, whereas feldspar, quartz-mica aggregates, mafic volcanic lithoclasts and Cr-spinel grains were observed in a few samples in subordinate amounts only.

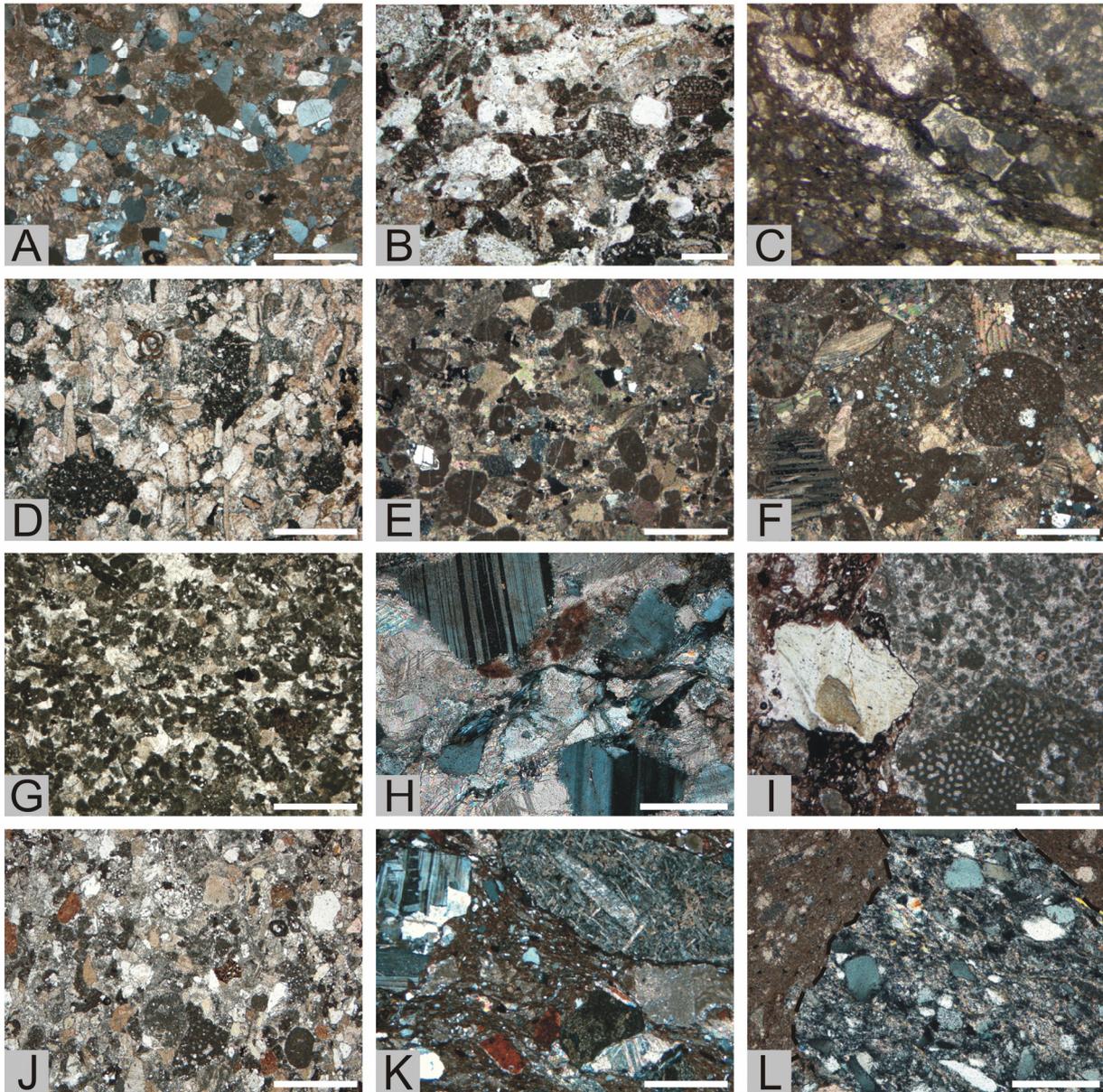


**Fig. 4.** Microphotographs of characteristic sandstone and breccia varieties in the Ugar Formation (a-f) and Vranduk Formation (g-l) of the Bosnian Flysch. +N: crossed polarizers. Scale bar is usually 1 mm; for (c), (h) and (l) it is 250  $\mu\text{m}$ . (a) Calcareous litharenite with mono- and polycrystalline quartz, chert, micritic carbonate rock fragments and bioclasts, +N, sample BO-31, (b) calcarenite with orbitolinids, BO-18, (c) bicarinate *Globotruncana* sp. indicative of a Senonian age, in the red pelitic matrix of a matrix-supported carbonate breccia, BO-36, (d) calcarenite with bioclasts and red biomicrite rock fragments, BO-129, (e) calcarenite with peloids, bioclasts, chert and monocrystalline quartz, +N, BO-5, (f) calcarenite with orbitolinid and rudistid bioclasts, +N, BO-51, (g) calcarenite (pelsparite) with chert and Cr-spinel grains, BO-85/b, (h) grains of plagioclase feldspar and quartz in calcareous litharenite, +N, BO-75, (i) carbonate rock fragment (pelbiosparite) and chlorite flake in polymict breccia, BO-82/2, (j) calcareous litharenite with quartz, chert, radiolarite, carbonate rock fragments, orbitolinid and rudistid bioclasts, TD-153, (k) plagioclase, mafic volcanic lithoclast of intersertal texture, serpentinite and radiolarite in polymict breccia +N, BO-82/6, (l), sublitharenite rock fragment in red finer-grained matrix, +N, TD-145.

Many samples in the Vranduk and Ugar formations show characteristic diagenetic features. Replacement of chert and radiolarite lithoclasts and plagioclase by calcite patches or rhombohedra is common. Calcite often replaces clayey sandstone matrix, in addition to abundant calcite veinlets crosscutting the texture. Small (80-160  $\mu\text{m}$ ), euhedral albite crystals may occur in carbonate-dominated arenites. There, they replace micritic carbonate, especially peloids and ooids.

### 2.5.3. Whole-rock geochemistry

The concentrations of major and several trace elements of pelites and arenites from both flysch formations are summarized in Appendix 2-4. In the sample set a strong negative correlation appears between  $\text{SiO}_2$  and  $\text{CaO}$ , with  $\text{SiO}_2$  concentrations varying between 1.6 and 77.0 wt% and  $\text{CaO}$  ranging from 0.5 to 54.1 wt% (Fig. 5a). This trend is accompanied by a likewise strong positive correlation between  $\text{CaO}$  and LOI, indicating that  $\text{CaO}$  is almost entirely carbonate-bound. Therefore, a continuous mixing trend can be established from the Vranduk to the Ugar formations, where the siliclastic proportions are diluted by additional carbonate to various degrees. A slight deviation from this trend is mostly related to pelitic samples having higher Al-proportions in the silicate fraction.

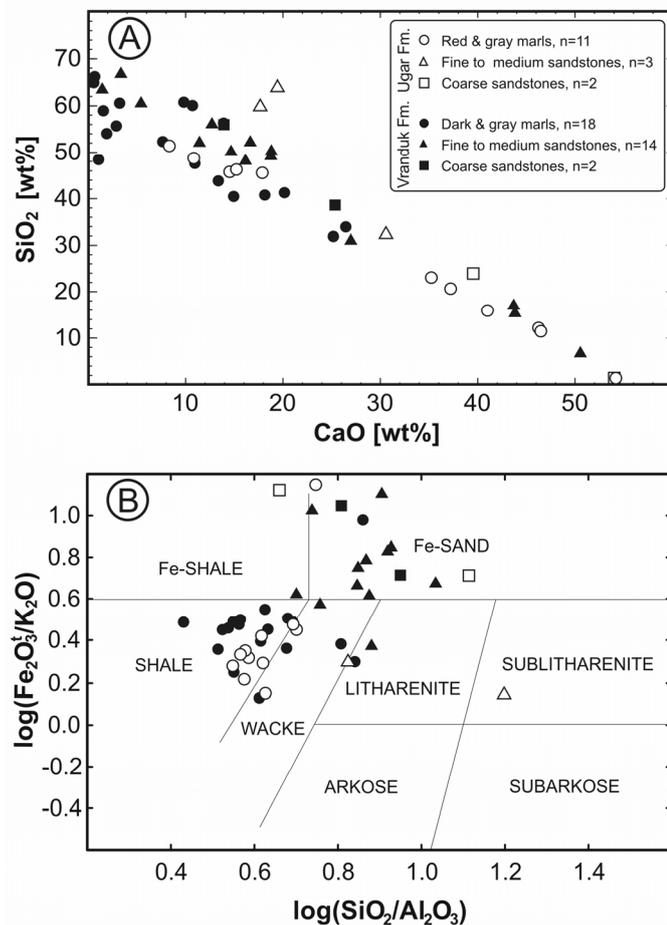


**Fig. 5.** Major element geochemistry of the Bosnian Flysch sediments. (a)  $\text{CaO}$ – $\text{SiO}_2$  plot showing the generally higher carbonate contents of the Ugar Formation samples in comparison to the Vranduk Formation (b) Classification of the flysch sandstones based on the ratios of  $\text{SiO}_2/\text{Al}_2\text{O}_3$  vs.  $\text{Fe}_2\text{O}_3^t/\text{K}_2\text{O}$  (Herron 1988).

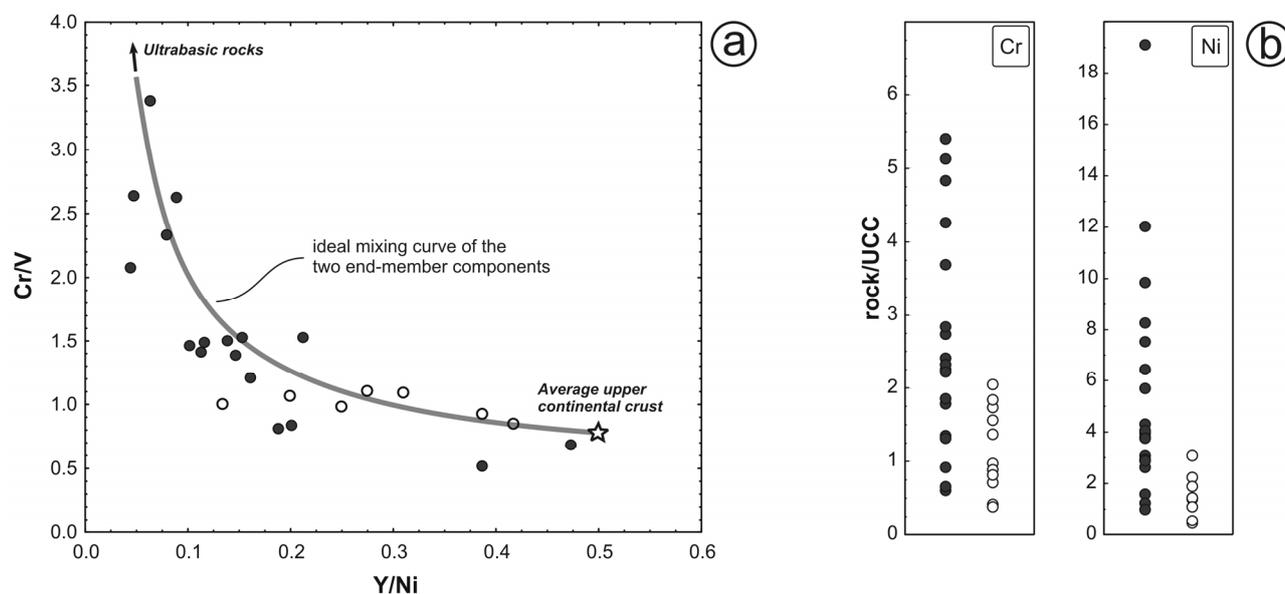
Our data show a conspicuous stratigraphic control on this mixing trend, with the Vranduk Formation being richer in siliciclastic material, whereas in the Ugar Formation the carbonate proportion increases up to almost those of pure calcarenites. However, as is evident from Fig. 5a, the transition is continuous with minor overlap, and shows no abrupt jump in carbonate content between the Vranduk and Ugar formations.

Fig. 5b shows the results of the major element discrimination procedure based on Herron (1988). Most pelites fall into the field of shale, with no pelite sample reaching the Fe-shale field. By contrast, both the coarse and the fine- to medium-grained sandstones have mostly Fe-sand compositions. The reason for this behaviour is probably not only related to Fe, as most variation in analyses of carbonate-corrected  $\text{Fe}_2\text{O}_3$  occurs in a limited range of 4 to 8 wt%; this is only slightly above the normal range for lithic arenites and greywackes from active continental margin settings (Pettijohn *et al.*, 1987) and seems largely unrelated to grain-size. Rather, the tendency of  $\text{K}_2\text{O}$  to be enriched in pelites (2 to 3.5 wt%) relative to the sandstones, which show low concentrations (0.2 to 1.5 wt%) when compared to average lithic arenites and greywackes (Fig. 5b), could account for the high  $\text{Fe}_2\text{O}_3/\text{K}_2\text{O}$  ratios of the sandstones.

Selected provenance-sensitive trace elements of the pelitic samples are displayed in the Cr/V vs. Y/Ni plot (Fig. 6a; McLennan *et al.*, 1993) in order to reveal the nature of the source lithologies. Cr/V ratios range from ~0.5 to 3.4 and thus largely exceed average upper continental crust (UCC; according to McLennan 2001), whereas Y/Ni ratios are lower compared to UCC. For the sake of comparison, a mixing curve was also constructed, using the composition of the UCC and that of ultramafic rocks as end-members (Fig. 6a). The majority of the samples plots close to this mixing curve, which provides evidence for the simultaneous erosion of ultramafic lithologies and felsic rocks. The proportion of mafic and/or ultramafic source rocks in most Vranduk samples is distinctly higher compared to the Ugar Formation. UCC-normalized, carbonate-corrected concentrations of Cr and Ni in shales and marls are in agreement with this observation (Fig. 6b). Ni, for example, is up to 10 times enriched in the Vranduk Formation (two more samples have even higher enrichment factors of 12 and 19). Contrary to this, the Ugar samples scatter around the UCC values, with the enrichment factors of Ni ranging between 0.4 and 3 only.

Cr/Ni ratios of the arenitic samples do not exceed (with one exception in Ugar Formation) the Cr/Ni values for ultramafic (2.0) and mafic rocks (5.2) of the Dinarides (Lugović *et al.*, 1991; Robertson & Karamata 1994; Pamić *et al.*, 2002). This indicates

that sediment recycling and, consequently, Cr-spinel concentration is not a significant process in forming these sandstones (von Eynatten 2003). Similarly, Zr/Sc ratios (McLennan *et al.*, 1993) give no evidence for significant zircon concentration.



**Fig. 6.** Trace element geochemistry of the Vranduk and Ugar formations. Only pelitic samples are plotted. Filled and open circles indicate Vranduk and Ugar samples, respectively. (a) Cr/V vs. Y/Ni ratio-ratio plot (McLennan *et al.*, 1993). Calculated mixing line uses ultrabasic (Cr/V=40; Y/Ni~0.0003 – Turekian and Wedepohl 1961) and average upper continental crust (UCC) compositions (Cr/V=0.775; Y/Ni=0.5 – McLennan 2001) as end-members. Star refers to UCC composition. Four Ugar Formation samples had Y and/or Ni concentrations below instrumental detection limit and are excluded from the plot. (b) Carbonate-corrected, UCC-normalized values of Cr and Ni.

#### 2.5.4. Clay mineralogy

Chlorite and illite are the dominant clay-sized minerals in pelites from all units examined. In addition, kaolinite in the Ugar Formation, and serpentine in the DOZ mélange matrix, amount to *c.* 10% of the entire clay mineral assemblages. Kaolinite and serpentine were not detected in the Vranduk Formation pelites. Smectite was detected in several Vranduk samples (refer to Petri 2007 for details); the proportion of smectite in the illite/smectite mixed layer structures is usually below 10% in both the <2 $\mu$ m and <0.2 $\mu$ m size fractions.

In the Vranduk Formation, the Kübler Index (KI) of the  $<0.2\mu\text{m}$  size fractions ranges between  $0.40 \Delta^{\circ}2\Theta$  and  $0.98 \Delta^{\circ}2\Theta$ . In the  $<2\mu\text{m}$  size fractions of the same samples the KI values are consistently lower, varying between  $0.24 \Delta^{\circ}2\Theta$  and  $0.63 \Delta^{\circ}2\Theta$ . These inconsistencies probably indicate the disturbing effects of detrital micas in the  $<2\mu\text{m}$  fraction. The KI data, along with the presence of kaolinite, suggest that both the Vranduk and the Ugar formations experienced only diagenetic overprint. No obvious trend was revealed by the regional distribution of these data.

#### 2.5.5. Heavy mineral analysis

The heavy mineral spectra of the Bosnian Flysch are overall dominated by Cr-spinel, especially in the Vranduk Formation. Further species include zircon, rutile, garnet, tourmaline, and lesser amounts of apatite, titanite and monazite (Table 1). In the DOZ mélange, however, Cr-spinel is not predominant, tourmaline and monazite are even absent. The main constituents of the heavy mineral spectra in the DOZ mélange are garnet and zircon, chloritoid, kyanite, clinozoisite, and epidote. Epidote is locally also found in the Vranduk Formation (Table 1). The Ugar Formation differs from the Vranduk Formation by its subordinate garnet content, lower average Cr-spinel concentrations, and the absence of epidote (Table 1). Whereas a significant proportion of zircon in the Vranduk Formation is euhedral with sharp crystal edges, zircons of the Ugar Formation are typically subhedral to rounded, indicating a metapelitic or a mature sedimentary source. Chemical compositions of selected heavy mineral species were determined by electron microprobe to characterize their source in more detail.

*Tourmaline:* Nearly all crystals are derived from metapelitic sources and have largely similar compositions in the Vranduk and Ugar formations (Fig. 7). The proportion of magmatic-derived tourmaline crystals is rather small. Well-preserved growth zoning and compositional polarity, as revealed by back-scattered electron images, correspond mainly to a Barrovian type, lower-grade metamorphic source (cf. Henry & Dutrow 1996). If outer and inner metamorphic zone compositions are plotted separately (Fig. 7), a general enrichment in Fe is observed towards the rims. The predominance of tourmaline of metamorphic origin is also supported by their high Ti and low Zn contents (up to 0.2 and 0.015 atoms per formula unit, respectively; see Viator 2003).

**Table 1.** Semi-quantitative heavy mineral composition of arenites in the DOZ mélangé, and the Vranduk and Ugar formations. Symbols refer to species abundances: *triangles* predominant, *x*'s common, *circles* subordinate, *dots* very rare.

profile	unit	sample	spl	zrn	rt	grt	tur	ap	others
Stavnya Valley	Ugar Fm.	BO-17	X	○	○				mnz
		BO-117	○	○	•	○	○		ep, mnz
		BO-16	X	○	X	○	○	•	ttn
	Vranduk Fm.	BO-61	▲	X	○		X		ttn
		BO-59	▲	○	X		X		
		BO-115/b	▲	○	○		•		
		BO-52	▲	○	○		○	•	ttn, mnz
	DOZ mél.	BO-25	○	○	X	X		•	ep, ttn, zo, ky
		BO-23	○	X	○	X		•	cld, ttn, ep, zo, ky
BO-22		○	X	○	X		•	ttn, ep, zo, czo, ky	
Bosna Valley	Vranduk Fm.	BO-12	X	○	○	X		•	mnz
		BO-87	▲	○	X	X	X		
		BO-95	X	○	○	○	•	•	mnz, ttn
		BO-72	▲	X	○	○	•	•	mnz, xnt, ttn, aug
		BO-73	X	X	○			•	ttn
		BO-75	▲	X	○	•	•	•	ttn
		BO-92	X	○	X				
		BO-4	▲	X	X	○	•		ep

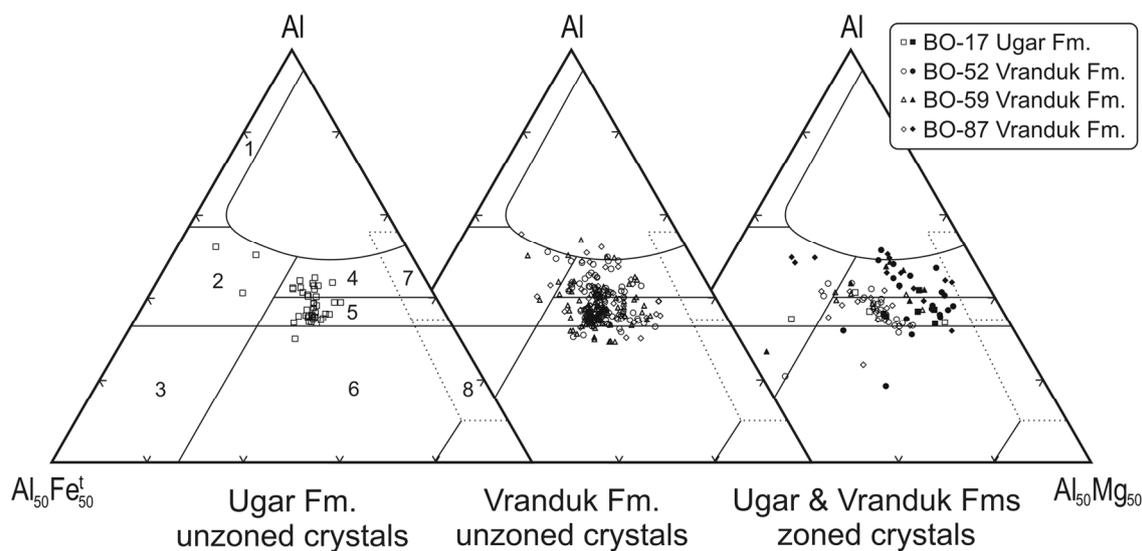


**Fig. 7.** Ternary plots of tourmaline chemistry in the Fe-Mg-Al system and assignment to probable source lithologies (Henry and Guidotti, 1985). Numbered fields: tourmaline compositions dominantly in (1) Li-rich or (2) Li-poor granitoids, (3) hydrothermally altered granites; (4-5): metapelites (4) coexisting or (5) not coexisting with an Al-saturating phase, (6) skarns, (7) metamorphosed ultramafic rocks, (8) metacarbonates. Filled symbols: cores or inner zones, open symbols: outer zones or unzoned crystals.

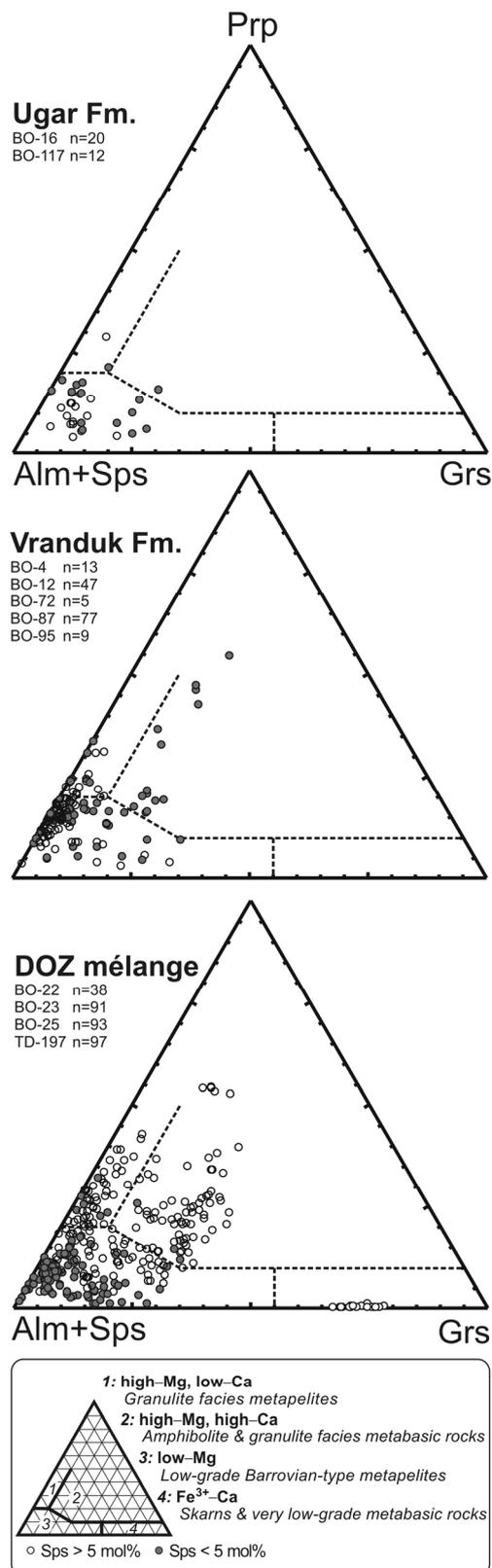


**Fig. 8.** Comparison of detrital garnet compositions from the DOZ mélange and the Vranduk and Ugar formations, according to the classification scheme of Morton *et al.*, (2003). Alm: almandine, Sps: spessartite, Prp: pyrope, Grs: grossular.

Garnet chemistry indicates a variety of source lithologies, the most dominant being greenschist facies metamorphic rocks. Additional garnet populations are also observed: one is derived, according to the classification scheme of Morton *et al.*, (2003), from amphibolite to granulite facies metapelites (along the almandine-pyrope join) and another one from amphibolite to eclogite facies metabasic rocks (pyrope- and grossular-rich almandines; Fig. 8). The share of the contribution from these high-grade sources is the highest in the DOZ mélange (in total ~45%). It then decreases significantly in the Vranduk Formation (~21%) and probably disappears in the Ugar Fm (only a few grains that plot close to the boundaries; Fig. 8). A small proportion of garnets (c. 4%) derived from skarns or low-grade metabasic rocks also occurs in the DOZ mélange.

Rutile crystals are mostly (60 to 80% throughout the samples) of metapelitic origin, as deduced from their Cr/Nb ratio (Zack *et al.*, 2004a, Triebold *et al.*, 2007), with the remaining portion derived from metamafic lithologies (Appendix 2-6). Zr-in-rutile thermometry was performed on the metapelitic crystals in order to assess source rock metamorphic conditions following Zack *et al.*, (2004b) and Watson *et al.*, (2006). The results yield a broad dis-

tribution of calculated metamorphic temperatures between c. 500 and 900°C (Fig. 9). The distribution of inferred temperatures in the detritus of the DOZ mélange most likely consists of two components:

one ranging from 650-700 to ~850 °C, and one between 500 and 650-700 °C. This is different from the both flysch formations which appear to be dominated by a single population with a mode between 550 and 700 °C (Fig. 9).

*Cr-spinel* chemical data from the DOZ mélange and from the Vranduk and Ugar formations indicate abundant (65 to 87%) mantle-derived spinels and a subordinate magmatic-derived spinel population, based on the criterion by Lenaz *et al.*, (2000), taking 0.20 wt% TiO<sub>2</sub> as a "threshold" value (Fig. 10). The Cr number [Cr# = Cr/(Cr+Al)] of mantle-derived spinels range from 0.20 to 0.75, with more than 50% of the analyses lying between 0.45 and 0.65. This is explained by the dominance of harzburgitic lithologies in a mixed lherzolitic-harzburgitic ophiolite zone, or simply by abundant mantle rocks of transitional harzburgitic character. Occasional across-sample variations in the range of Cr# in the Vranduk and Ugar formations do not affect the overall picture, but reveal local variations in ophiolite petrology.

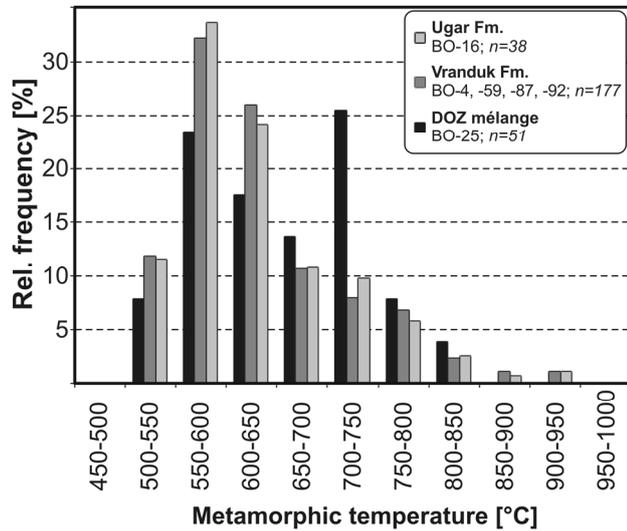


**Fig. 9.** Thermometry of detrital rutile from the DOZ mélange and the Vranduk and Ugar formations. Histograms show the distribution of metamorphic temperatures recorded by single rutile crystals of metapelitic origin (Cr<Nb) as calculated from their Zr content according to Watson *et al.*, (2006).

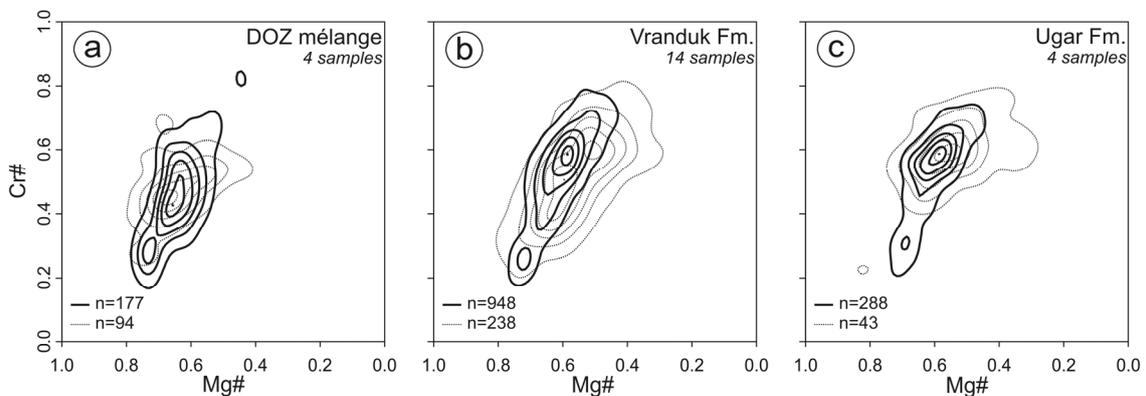


**Fig. 10 (previous page, bottom):** Geochemistry of detrital Cr-spinel from (a) the DOZ mélange and (b) the Vranduk and (c) Ugar formations, presented by data density contouring of all data points. Contours were derived by two-dimensional kernel density estimation using the *kde2d* function of the software package *MASS* in *R* environment. Contouring covers 90, 70, 50, 30 and 10% of the entire dataset. Ellipses in bold lines refer to Cr-spinel crystals with TiO<sub>2</sub> values <0.2 wt% (peridotitic origin), those in dotted lines account for TiO<sub>2</sub> values >0.2 wt% (magmatic origin).

### 2.5.6. Geochronology

#### 2.5.6.1. Zircon U/Pb dating

Detrital zircon U/Pb age data show a marked contrast among the three formations studied, apart from the ubiquitous Permo-Triassic ages (Fig. 11). A Permo-Triassic population, with a minor admixture of Variscan, Caledonian and Pan-African ages, dominates zircon age spectra from the ophiolite mélange. Age spectra of Vranduk zircons display Caledonian, Variscan, Permo-Triassic, and in 3 out of 4 samples, a characteristic Middle/Late Jurassic population with a mode at around 150 Ma. In the Ugar Formation, Permo-Triassic, Variscan and several pre-Variscan populations prevail, with no signs of Jurassic or Cretaceous contribution. The U/Pb ages clearly indicate changing source rocks from the Jurassic mélange formation to Late Jurassic and finally Cretaceous flysch sedimentation.

#### 2.5.6.2. Zircon fission track analysis

Single grain zircon fission track geochronology was performed on selected, zircon-rich arenitic samples, one each from the Ugar and the Vranduk formations. The results are given in Fig. 12. In the Vranduk sample around half of the dated crystals are euhedral, whereas euhedral crystals make up only some 20% in the Ugar sandstone. The majority of the single crystal ages range between 80 and 200 Ma in case of the Vranduk sample. The single grain age distributions (Appendix 2-10) were tested by PopShare computer software (Dunkl & Székely 2002) in order to identify the FT age populations. The youngest and dominant FT age population within the Vranduk Formation lies at  $121 \pm 21$  Ma; an older, more diffuse age group is also present.

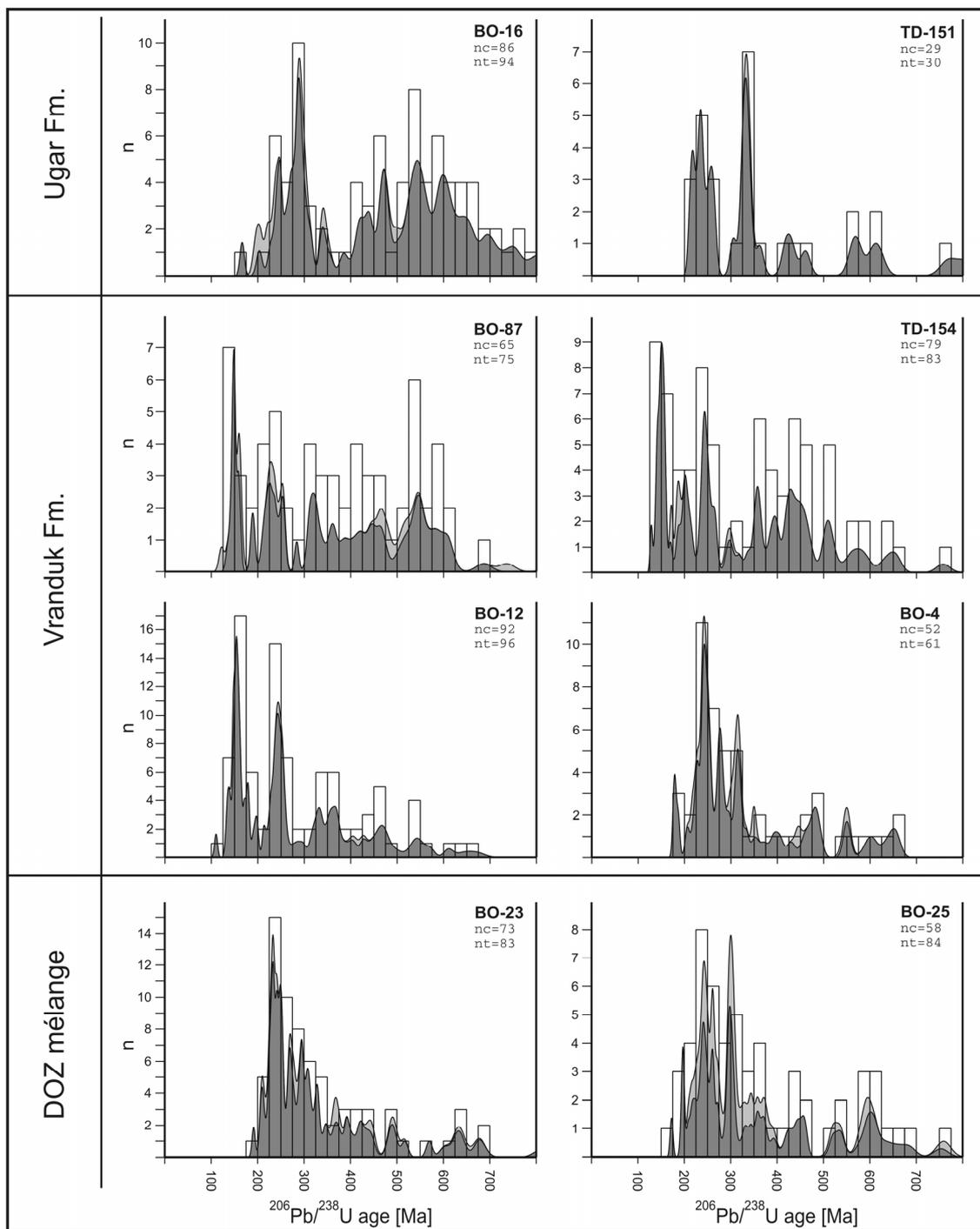


**Fig. 11.** Zircon U/Pb age distribution in the DOZ mélange, and the Vranduk and Ugar formations. Dark grey area indicates probability density distribution of single-grain age data concordant at the 86-114% level. Histogram also shows the filtered data. Light grey area represents all data. Grains older than 800 Ma are very subordinate and were excluded from the plot. nt: number of all accepted age analyses; nc: number of concordant age data. Calculations according to Sircombe (2004).

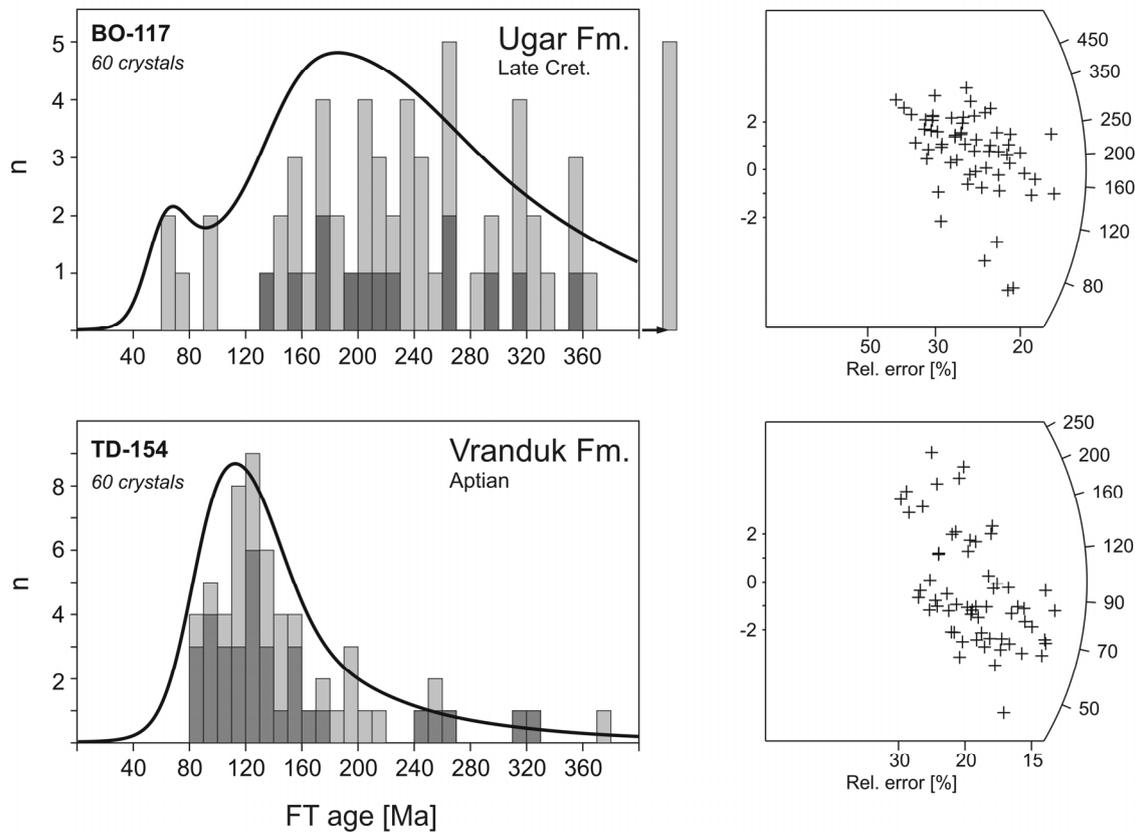


**Fig. 12.** Zircon single grain fission track age distributions in the Vranduk and Ugar formations. Dark grey bars express the frequency of euhedral zircons, while light grey bars show all grains. The grey lines represent age spectra (probability density plots) and they were computed for all crystals according to Hurford *et al.*, (1984). Radial plots are according to Galbraith (1990).

The age distribution in the Ugar sample is wider compared to the Vranduk sandstone. Here a small and young age component is present at around 80 Ma, while some 90% of the single grain ages form a very diffuse distribution covering an age range between the Early Palaeozoic and the Jurassic. The frequency maximum in the age distribution of the Vranduk sample coincides with a frequency low in the Ugar sample.

## 2.6. Discussion

A large number of new single-grain mineral chemical data (over 3000 electron microprobe analyses), together with clay mineralogical, whole-rock geochemical and geochronological data gathered in this study, allows for a comprehensive characterization

of the source area of the two Bosnian Flysch units, as well as that of the sandstone blocks in the DOZ mélange. In the following, we evaluate the biostratigraphic and sedimentary provenance data to assess existing views (e.g. Charvet 1980; Pamić *et al.*, 1998) on the Cretaceous erosion history of the Central Dinaride segment of the Alpine orogen.

#### *2.6.1. Provenance of sandstones incorporated in the DOZ mélange*

In addition to low-grade metamorphic (typically Fe- and Mn-rich garnet) and small amounts of ophiolitic (mainly Cr-spinel) detritus, also specific heavy mineral species are identified in the sandstone blocks of the DOZ mélange which proved largely absent in the Vranduk and Ugar formations (Table 1). They include kyanite, two chemical populations of garnet indicating amphibolite facies metabasic and amphibolite to granulite facies metapelitic source lithologies (Fig. 8) and finally, a rutile population revealing higher-temperature (650-700 to 850 °C, i.e. amphibolite to granulite facies) metamorphic conditions of their source rocks (Fig. 9). These mineral signatures can most probably be attributed to the sub-ophiolitic metamorphic soles in the DOZ. On the other hand, zircon U/Pb age spectra (Fig. 11) clearly demonstrate that the detritus was also sourced from the continental margin of Adria exposing Palaeozoic basement rocks and their Permo-Triassic cover. The high proportion of sedimentary lithic fragments among the framework components, and possibly also the presence of "unstable" heavy mineral species (Table 1), hint at relatively short transport distances.

The composition of the sandstone blocks is interpreted in terms of a combined sediment supply into a trench environment both from the basal parts of the overriding ophiolitic slab and from the Adriatic margin, followed by local sediment recycling in the trench.

#### *2.6.2. Provenance of the Vranduk Formation*

Apart from abundant quartz and subordinate feldspar, the framework components of the Vranduk sandstones and breccias indicate derivation from a composite source dominated by ophiolitic lithologies, but also comprising carbonates and metamorphic

rocks. Lithic fragments mainly include serpentinised mafic/ultramafic rocks, altered basalt fragments, chert, red radiolarite, greywacke and shale (Figs. 4g & 4j-l). Limestone fragments are also common and yield, among other components, Urgonian facies benthic fauna of a Late Barremian or younger age. One sample from the hemipelagic strata close to the Bosna Valley section yields calcareous nannofossils indicative of an Aptian maximum age (Fig. 3; Appendix 2-2). As supported by petrographic observations, the relatively low carbonate content (mostly <20 wt% CaO) of the Vranduk Formation is partly related to carbonate lithoclasts, and possibly also to intrabasinal carbonate particles.

Throughout the Vranduk Formation, clay mineral assemblages of the pelitic lithologies are dominated by illite/smectite mixed-layer structures. Kaolinite and serpentine were not detected in these samples. This composition conforms to weathering in a mafic-dominated source area, where smectitic soils tend to develop and where lateritic weathering is absent (Thiry 2000). The source rocks of the detrital component of illite were anchi- to epizonal metapelites (e.g. slates, phyllites), eroded together with the ophiolites. Proximity of the exposed ophiolite slices is also shown by trace element systematics (Fig. 6). Pelite Cr/V ratios and carbonate-corrected Cr and Ni concentrations are elevated with respect to the UCC composition and suggest direct input from ophiolitic sources. The Cr/Ni ratios of arenites are within the range of the Dinaride mafic to ultramafic rocks and, thus, preclude significant mineral concentration due to reworking. Finally, a well-represented population of Middle to Late Jurassic ages appears in the zircon U/Pb spectra (Fig. 11), which can likely also be connected to the exhumed ophiolitic sequence and will be discussed later.

In addition to the ophiolites, subordinate amounts of metamorphic source components were also admixed to the Vranduk Formation detritus. This is indicated by: (1) the detrital component of illite, (2) the presence of quartz framework grains, (3) the intermediate position of most samples on the Cr/V–Y/Ni mixing curve which links ultrabasic and UCC composition (Fig. 6a), and (4) heavy mineral occurrences and chemistry.

Zircon, metamorphic tourmaline, the majority of garnet showing Fe- and Mn-rich compositions and accessory amounts of monazite and titanite document the erosion of a diverse suite of low-grade metamorphic lithologies. Zircon U/Pb geochronology shows a predominance of Permo-Triassic, Variscan and pre-Variscan crystallization ages (Fig. 11). These data indicate that the major source of the continental detritus of

the Vranduk Formation were Palaeozoic to Permo-Triassic low- to very low-grade metapelitic sequences, probably located on the Adriatic plate. A minor garnet population from amphibolite-facies metabasic source rocks (Fig. 8) may indicate continued erosion of the sub-ophiolitic metamorphic soles, but contribution from the rare amphibolite facies basement units of the Adriatic plate (Pamić & Jurković 2002; Pamić *et al.*, 2004) can not be entirely ruled out.

The comparatively uniform population of zircon fission track ages at around 120 Ma indicates Early Cretaceous, nearly synsedimentary cooling of the source area below mid-crustal temperatures (Fig. 12) which agrees well with the major phase of cooling of the Adriatic basement (Milovanović 1984, Árkai *et al.*, 1995; Belak *et al.*, 1995; Judik *et al.*, 2006).

In summary, our results suggest that the Vranduk Formation records Early Cretaceous exhumation of the Adriatic plate occurring relatively shortly (in less than 20 Ma) after ophiolite obduction. The catchment area included both continental basement and ophiolitic units, capped by short-lived Urgon facies reefs that were immediately redeposited onto the clastic fan.

### *2.6.3. Provenance of the Ugar Formation*

The Ugar Formation is distinguished from the Vranduk Formation by its overall dominance of carbonate clasts, inferred to have been largely derived from the Adriatic Carbonate Platform (AdCP) by many previous workers (e.g. Aubouin 1973). With respect to its rather subordinate siliciclastic source components, several lines of evidence point to a sediment source, which neither entirely matches the eroding DOZ (at least with its structure and composition being as it is known today), nor can it be completely credited to the recycling of the Vranduk Formation. These siliciclastic source components thus also require direct erosion of continental basement units. The signatures of carbonate and siliciclastic detritus are further discussed below.

The high carbonate concentration of the Ugar Formation arenites is distinct from most arenites found in the Vranduk Formation (Fig. 5). The pelites also reveal a similar difference, although Ugar Formation pelites may have been influenced by a higher flux of pelagic carbonate sedimentation beyond their detrital carbonate component. Carbonate-corrected, UCC-normalized concentrations of elements typical for ma-

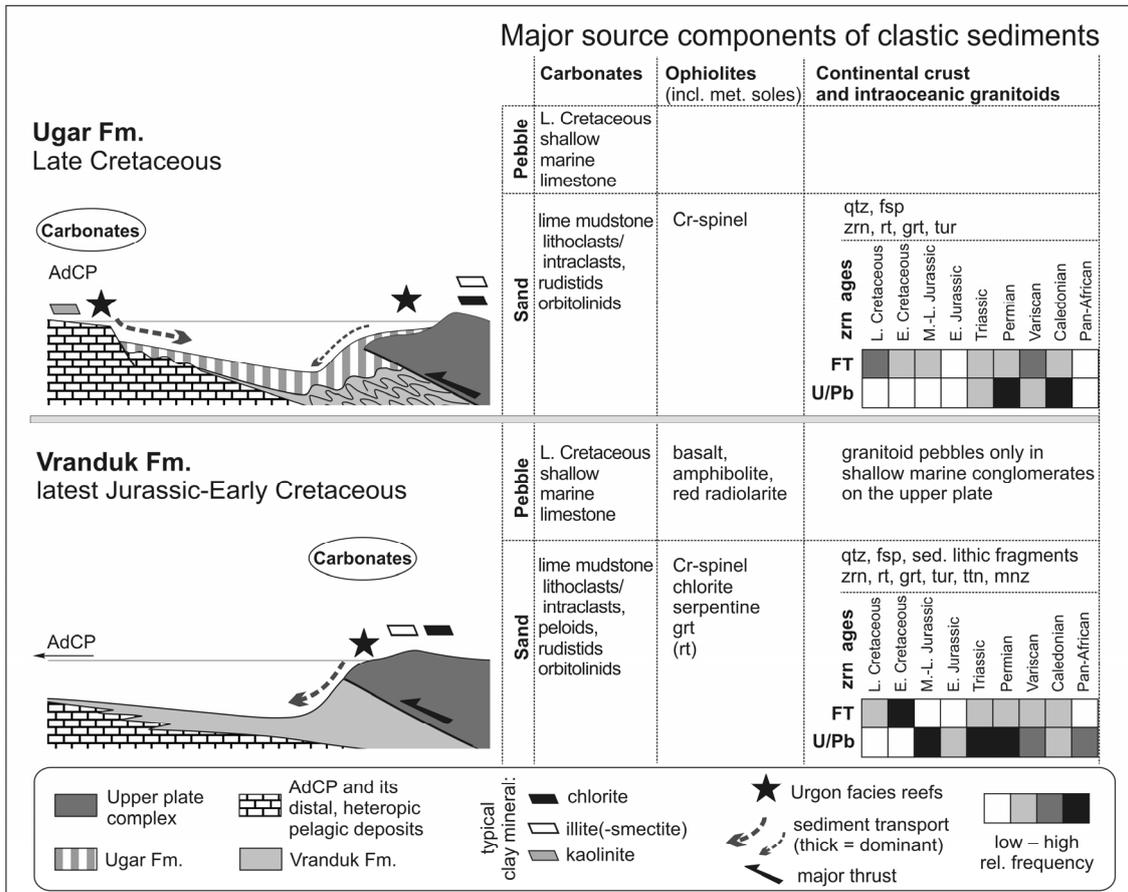


**Fig. 13.** Sketch summarizing the new provenance data for the Vranduk and Ugar formations. The ophiolitic, continental and carbonate detritus of the Vranduk formation was eroded exclusively from the upper plate, while the sediments of Ugar formation were derived from both sides of the basin (the carbonate gravity flows and the lateritic clay from AdCP, the siliciclastic material from the upper plate).

fic/ultramafic lithologies, such as Cr and Ni, show no marked anomaly for the pelites of the Ugar Formation, and scatter around UCC composition (Fig. 6). These values are 2 to 3 times lower than those of the Vranduk Formation. Combined with low Cr/V ratios and elevated Y/Ni ratios in the Ugar Formation, the trace element data suggest that dilution by carbonate alone is not responsible for the relative scarcity of detrital ophiolitic components. In fact, there is a predominance of felsic components in the siliciclastic portion of the Ugar Formation pelites in comparison with the Vranduk Formation.

Although carbonate debris (orbitolinids, rudist fragments, lithoclasts) are similar in both formations, the following observations suggest that the Ugar Formation was sourced from a carbonate platform with a different setting from that previously supplying the Vranduk Formation with Urgonian facies clasts: (1) orbitolinids agglutinate carbonate particles and *Rhaxella* spicules instead of quartz, and (2) there is a salient age

gap of at least 15 Ma between the bioclasts and the Upper Cretaceous pelagic matrix (Fig. 3). These features, along with the predominance of carbonate detritus in the Ugar Formation, suggest the erosion of a relatively thick carbonate succession, previously deposited on a platform where no siliciclastics were shed to. These data confirm that the AdCP, a thick and isolated carbonate platform located to the SW of the flysch basin and comprising a thick Cretaceous carbonate sequence (Vlahović *et al.*, 2005), represents the source area of the carbonate detritus, in line with earlier models (e.g. Aubouin 1973).

The clay minerals of red marl intercalations in the thin-layered carbonate sequences of the Ugar Formation are dominated by illite/smectite and, contrary to the Vranduk Formation, they contain kaolinite as well. In general, kaolinite in fine-grained hemipelagic sediments indicates highly matured, lateritic soils developed in the source area, although lateritic weathering in tectonically active areas characterized by high erosion rates is not typical (Bárdossy & Aleva 1990; Thiry 2000). However, the Mesozoic sequence of the AdCP, located in a more external paleogeographical position with respect to the site of the deposition of the Ugar Formation, is punctuated by several bauxite and palaeosol horizons (Vlahović *et al.*, 2005), the clay mineral fraction of which is dominantly kaolinite (e.g. Šćavničar 1978). It is thus probable that also the kaolinite in the red shale was derived from the AdCP, as a result of the erosion of its weathering products.

A change in the character of the source area in respect of the felsic detritus is well constrained by the chemistry of detrital garnet and by zircon age data. The Ugar Formation is characterized mostly by a single, almandine-rich garnet population, exclusively derived from low-grade metamorphic sources (Fig. 8). Permo-Triassic zircon crystals and variable amounts of Variscan to pre-Variscan grains are the prominent U/Pb age components in the Ugar Formation (Fig. 11). Although the Vranduk Formation also contains a marked Permo-Triassic group and a rather heterogeneous distribution of pre-Permian age components as well, it comprises a significant Middle to Late Jurassic population (Fig. 11) which is absent in the Ugar Formation.

The zircon FT age data (Fig. 12) are well in line with the U/Pb age data: they also call for contrasting source areas for the two formations. Zircon FT age spectrum of the Ugar Formation contains a 80 Ma group (Fig. 12), which could indicate rapid Late Cretaceous exhumation of the Adriatic basement (Fig. 14). This age group could however, from a geochronological point of view, fit well also with other events: (1) the early stage

of the Late Cretaceous to Palaeogene acid to intermediate igneous activity in the Sava Zone (Pamić 1993, 1998; Starijaš *et al.*, 2005), (2) connected with HT/LP metamorphism (Pamić 1993, 1998; Balen *et al.*, 2003; Starijaš *et al.*, 2006; Krenn *et al.*, 2008) and in the (3) 'banatite belt' of the Southern Carpathians and Apuseni Mts. (Kräutner *et al.*, 1984; Wiesinger *et al.*, 2005), as well as (4) with the characteristic Late Cretaceous thermal event recorded in the SE part of the Tisza-Dacia Unit basement rocks (Pamić 1998; Tari *et al.*, 1999; Árkai *et al.*, 2000; Balen *et al.*, 2003; Lelkes-Felvári *et al.*, 2003; Schuller 2004; Starijaš *et al.*, 2005, 2006; Krenn *et al.*, 2008). However, as the detrital zircon U/Pb age spectra record no contribution from Upper Cretaceous igneous rocks, the 80 Ma FT age group of the Ugar Formation more probably reflects a metapelitic rather than magmatic source. Because such a thermal event is not typical for the Adriatic basement, we can not exclude that this minor detrital component is connected to the exhumation of the Sava Zone and/or SE Tisza-Dacia basement units in the Late Cretaceous.

Derivation of the low-grade metamorphic detritus in the Late Cretaceous Ugar Formation from the Bosnian Schist Mountains (BSM) is possible on petrologic grounds, but is contradicted by the structural position of the BSM, which forms the basement of the Pre-Karst (and Bosnian) units (Aubouin *et al.*, 1970; Schmid *et al.*, 2008). Also, the Palaeogene K/Ar and Ar/Ar ages that are frequent in the BSM (Pamić *et al.*, 2004) preclude its erosion in the Late Cretaceous.

In summary, our data suggest that the clastic material of the Ugar Formation was derived from at least three principal sources; (1) dismembered elements of the AdCP, and subordinately (2) ophiolitic units and (3) Variscan low-grade metamorphic basement units (including their Permo-Mesozoic cover), parts of which were affected by a thermal overprint of Late Cretaceous age (Fig. 14). The data also demonstrate that recycled Vranduk Formation sediments did not represent a significant source for the clastic components in the Ugar Formation.

#### *2.6.4. Do the Vranduk and Ugar formations share a common provenance?*

The contrasting palaeocurrent directions and lithofacies, as well as the discrepancies reflected by the heavy mineral and geochronological signatures of the Vranduk and Ugar formations suggest that contrasting source rock associations exerted a strong con-

trol on the composition of the basin fill. Yet, the provenance signatures with respect to the siliciclastic source components share some comparable aspects, and this is briefly discussed below.

The heavy mineral spectra of both formations include Cr-spinel, a mineral that is characteristic for obducted ophiolites (e.g. Zimmerle 1984). The chemical composition of the spinels indicates a mixed source area exposing lherzolite- and harzburgite-dominated ophiolites, although a single source of "transitional harzburgites", or Type-II peridotites (Dick & Bullen 1984), is equally possible. As shown in Fig. 10, a great part of the spinel compositions exhibit Cr# values between 0.40 and 0.65, and their distribution in the field of Cr# and Mg# is comparable. The proportion of spinels of magmatic origin is similarly low in both formations: about 20% in the Vranduk Formation and 13% in the Ugar Formation (Figs. 10b & 10c). Thus, there is little difference in the ophiolitic source lithologies in time, although the ratio of ophiolitic to continental source rock volumes was smaller during the Late Cretaceous on the basis of whole-rock trace element data (Figs. 6a-b).

The petrology of the felsic crystalline source rock assemblages could also have been, in part, comparable, as can be deduced from the chemical compositions of tourmaline. In both formations, chemical composition and internal texture of tourmaline crystals identify low-grade metamorphic source rocks, similar to those constituting the metapelitic basement of the East-Bosnian–Durmitor (e.g. Rampnoux 1970) and Drina-Ivanjica (e.g. Podubsky 1970; Djoković 1985) units. In addition, the occurrence of a prominent rimward zoning with increasing Fe and decreasing Mg is also a common feature in tourmaline from both formations.

Distribution of calculated metamorphic temperatures using detrital rutile covers a broad range with most data ranging between 500 and 850 °C. This large range of high temperatures may correspond to a uniform contribution from the sub-ophiolitic metamorphic soles, but garnet from such rocks is not detected in the Ugar Formation and is rather subordinate in the Vranduk Formation. Alternatively, and more probably, in both formations most of these rutile crystals were derived from older sediments and low-grade metapelites of the Adriatic plate, which did not experience the temperature conditions necessary for Zr re-equilibration in the rutile lattice, resulting in "inherited" temperatures (Zack *et al.*, 2004a; Triebold *et al.*, 2007).

The above data indicate that the major source of the sand-sized siliciclastic components in both the Vranduk and the carbonate-dominated Ugar formations included

comparable rock associations with ophiolites and low- to very low-grade metamorphic continental basement units. The heterogeneity, and contrasting thermal histories of these lithological units on the upper plate, possibly combined with drainage evolution (e.g. the NE-ward shift of the coastline upon the DOZ; Charvet 1980), are reflected by changes in the chemistry of detrital garnet and spinel, and in zircon chronology.

#### 2.6.5. Acid intraoceanic magmatism in the Jurassic

Zircon U/Pb age spectra of the Vranduk Formation (Fig. 11) suggest a pulse of acid to intermediate magmatism in the Middle-Late Jurassic in the Neotethys Ocean. Melt generation was largely contemporaneous with, or closely followed intraoceanic subduction, as reflected by the ages of metamorphic sole formation (about 180 to 160 Ma – Okrusch *et al.* 1978; Parlak & Delaloye 1999; Dimo-Lahitte *et al.*, 2001; Olker *et al.*, 2001; Smith 2006 and references therein) and the age ranges of zircon crystallization (about 165 to 140 Ma). Obvious mechanisms for generation of acid to intermediate magmatic rocks in an intra-oceanic setting can be explained by (1) plagiogranite formation at the spreading ridge; (2) island-arc magmatism; and (3) anatexis of metasediments below the ophiolite thrust sheet.

Hitherto there has been no evidence for any voluminous, acid to intermediate Jurassic magmatism that is related to island-arc development in the Dinaride segment of the Neotethys (e.g. Pamić *et al.*, 2002, Dimitrijević *et al.*, 2003) in spite of ample evidence for the existence of intra-oceanic subduction in the Neotethys (see Smith 2006, for a review). Recently however, mafic dykes were reported which intersect the DOZ ophiolites and display island arc geochemical signatures (Lugović *et al.*, 2006).

Plagiogranitic differentiates may be voluminous (e.g. Pamić & Tojerkauf 1970, Bébien *et al.*, 1997) and thus, in principle, capable of producing detritus in such amount that would be sufficiently represented in the turbiditic Vranduk Formation. In this case, an active oceanic ridge would be required at the time of subduction, as melt generation appears to slightly post-date intra-oceanic subduction. Such a scenario has recently been documented in the Vourinos ophiolite (Hellenides) by precise zircon U/Pb geochronology (Liati *et al.*, 2004).

An alternative explanation for the observed age patterns is offered by the anatexis of HT metamorphic rocks at the base of the overriding ophiolite sheets. Jurassic S-type

granites are known to have intruded many ophiolitic units and their metamorphic soles in the Dinarides–Hellenides (e.g. Borsi *et al.*, 1966, Anders *et al.*, 2005, Resimić-Šarić *et al.*, 2005), that will be discussed elsewhere (Mikes *et al.*, submitted).

## **2.7. Summary: source area evolution of the Bosnian Flysch**

In this chapter we outline several steps that played a major role in the evolution of the Bosnian Flysch basin and its surrounding source areas. Fig. 13 summarizes the most important provenance data for the situation in Early Cretaceous (Vranduk Formation) and Late Cretaceous (Ugar Formation) times. Fig. 14. provides a tentative tectono-thermal synthesis of the zircon-supplying source areas based on thermochronological data published previously and obtained in this study.

### *2.7.1. Middle to Late Jurassic: intraoceanic subduction*

Intraoceanic subduction within the Neotethys resulted in vast amounts of ophiolite bodies exposed at the overriding oceanic plate. Sandstone blocks within the Jurassic DOZ mélange record erosional events linked to the plate convergence. Sandstone composition indicates a dual source with ophiolites and their high-grade metamorphic soles at the upper plate and with detritus derived from the more distally-located continental margin of Adria. The sediments underwent local reworking, consistent with an erosional-depositional scenario in a highly active trench setting. If the oceanic ridge was located continentward of the subduction zone as depicted in Fig 14, then the trench sedimentation could be controlled by detritus from the Adriatic basement only after the oceanic ridge was subducted, that had previously posed a barrier for trenchward sediment transport.

### *2.7.2. Jurassic–Cretaceous transition: obduction and metamorphism at the continental margin of Adria*

Inverse heat transfer from the obducted hot ophiolites caused a regionally widespread, epizonal thermal overprint in the upper part of the Adriatic plate (Fig. 14). Deep crustal levels of both the oceanic plate and the continental margin suffered largely coeval HP/LT metamorphic overprint (Okrusch *et al.*, 1978; Milovanović *et al.*, 1995; Most 2003) related to both intraoceanic subduction and the subsequent obduction onto Adria. The main phase of cooling took place already in the Early Cretaceous (Milovanović 1984, Árkai *et al.*, 1995; Belak *et al.*, 1995; Judik *et al.*, 2006). However, basal detachments related to the ophiolite emplacement and nappe advancement possibly gave rise to exhumation of small continental crustal slices and to their incorporation into the thrust wedge already from the latest Jurassic onwards as shown by earliest Cretaceous coarse-grained continental crustal detritus in sediments sealing the DOZ mélange (Charvet 1978; Neubauer *et al.*, 2003).

### 2.7.3. Early Cretaceous sedimentation: Vranduk Formation

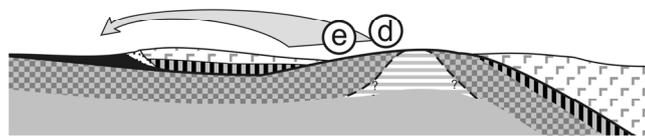
Sediments formed in front of the leading edge of the ophiolite–continental basement thrust wedge complex were subsequently accreted to the base of the thrust wedge, parts of which were exposed to erosion again. Clastic wedge development commenced already at the Jurassic–Cretaceous transition, with the submarine fan deposits prograding SW-ward onto the pelagic sequence of the 'Zone Bosniaque'. Tips of the growing imbricate slices that achieved shallow bathymetry were rapidly colonised by Urgonian facies reefs. These build-ups and their ophiolitic substrate were immediately redeposited onto the clastic fan (Fig. 13).

Erosion, drainage evolution and nappe emplacement could all result in slight changes in source rock composition between incipient obduction and Early Cretaceous flysch deposition. The ophiolitic detritus records an increasing volume of harzburgites exposed to erosion. The obducted oceanic thrust pile contained Jurassic acid to intermediate magmatic bodies as well, interpreted as plagiogranites formed at the ridge, or as S-type granitoids produced by anatexis of subducted oceanic sediment (Fig. 14). Granulite facies metapelitic rocks of the sub-ophiolitic metamorphic soles were no longer eroded, likely due to their extremely small volume relative to the ophiolitic sheet (cf. Karamata *et al.*, 1970, their Fig. 1).

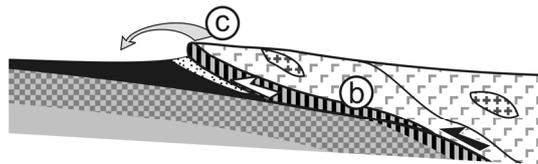
The relatively rapid exhumation and erosion of Adria-derived continental crustal units in the late Early Cretaceous is indicated by a largely synsedimentary age component around 120 Ma in the detrital zircon FT age spectrum of the Vranduk strata (Fig. 14). Parts of the clastic wedge underwent burial and folding in the mid-Cretaceous as suggested by a locally developed erosional unconformity on top of the Vranduk Formation (Figs. 3 & 13; Dimitrijević 1982 p.14; Csontos *et al.*, 2003; Schmid *et al.*, 2008 p.25), and by K/Ar age dating of illite from Vranduk Formation shales (Petri 2007).

**Fig. 14.** Cartoon summarizing the development of the zircon FT ages in tectonic units providing *siliciclastic* detritus to the Vranduk and Ugar formations. (a) Zone of zircon FT reset in the Adriatic basement due to the inverse heat transfer from the overriding hot ophiolites and tectonic load. (b) Obduction is followed by thrusting of the overprinted continental slices that were detached from the topmost level of the lower plate. (c) Early Cretaceous erosion of Adria-derived basement slices is documented by synsedimentary zircon FT ages in the Vranduk Formation. (d) In the Late Cretaceous, the lower plate experienced fast exhumation: the thin upper layer of the Adriatic margin with completely reset zircon FT ages was removed, and a wide range of Jurassic and pre-Jurassic zircon FT ages were supplied. Although these ages are predominant in the Ugar formation, (e) a minor age component with Late Cretaceous zircon FT ages is also present. This can be interpreted by exhumation of deeper-seated, hitherto undated crustal levels of the Adriatic plate, whereas temporally it also agrees with the early stages of collision of Adria with Tisza-Dacia (not shown) implying that the Late Cretaceous catchment already included the docking upper plate. See text for discussion.

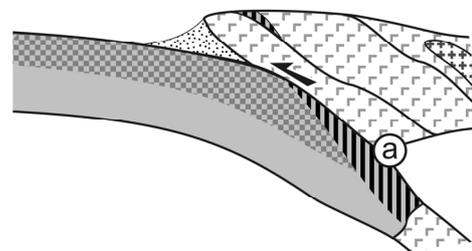
Sedimentation of Ugar Fm. (from ca. 100 Ma)



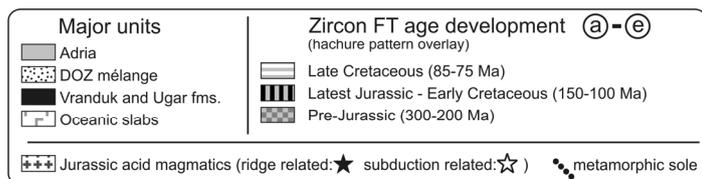
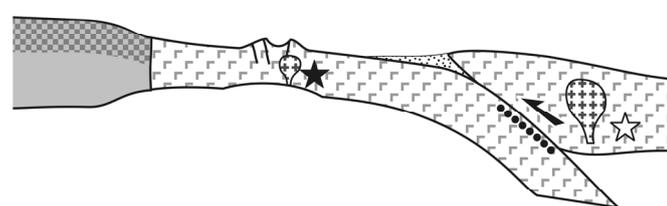
Sedimentation of Vranduk Fm. (from ca. 145 Ma)



Onset of obduction onto Adria (ca. 150 Ma)



Intra-oceanic subduction (ca. 180-160 Ma)



*2.7.4. Late Cretaceous Ugar sedimentation: increasing carbonate contribution and changes in the hinterland*

Propagation of the folded imbricate wedge towards the SW led to a platformward migration of the actual depozone. Vast carbonate mass flows released from the AdCP margin were intercalated with Scaglia Rossa-type Upper Cretaceous basin sediments. The origin of the suspended matter can be located on both basin margins, most likely representing a mixture from both areas. Sand-sized siliciclastic components were derived from the DOZ and the underlying, continental crustal thrust sheets of Adria, parts of which experienced fast exhumation. Notably, this c. 80 Ma cooling event has been largely unknown in the Adriatic basement so far.

In the light of the largely E-directed palaeocurrent indicators the site and mechanism of intermingling of the carbonate and sand-sized siliciclastic components prior to the final deposition of the Ugar Formation remains ambiguous. Signs of continued convergence during the Cenozoic, such as fault propagation, basin migration and cannibalistic sediment reworking further toward SW, are seen in the imbricate wedges of Cenozoic flysch of the AdCP (Chorowicz 1977; Mikes *et al.*, 2008a and references therein).

\* \* \*

The data presented in this paper reinforce previously published tectonic models inasmuch as they relate the deposition of the Vranduk Formation to the adjacent and exhumed ophiolite units (e.g. Aubouin 1973; Charvet 1980; Tari 2002; Schmid *et al.*, 2008). However, although the Vranduk Formation is underlain by pelagic Jurassic strata of the distal Adriatic plate, it represents a SW-ward propagating clastic wedge at the front of the leading edge of the DOZ and a continental thrust sheet complex. Our results thus do not support the model put forward by Pamić (1993) and Pamić *et al.*, (1998) describing the entire Bosnian Flysch in terms of a passive margin sequence of the distal Adriatic plate.



## *Chapter 3*

# Insights into Neotethyan ophiolite petrology at the Dinaride–Alpine– Pannonian triple junction: geochemistry of detrital Cr-spinel from Cretaceous synorogenic sediments

---

This chapter is largely identical to the manuscript entitled:  
"Ophiolitic detritus in Cretaceous clastic formations of the Dinarides (NW Croatia): evidence from Cr-spinel  
chemistry" that is currently in press with the *International Journal of Earth Sciences*  
published OnlineFirst in March 2008, doi:10.1007/s00531-008-0306-3  
authored by:  
Borna Lužar-Oberiter, Tamás Mikes, Hilmar von Eynatten and Ljubomir Babić



# **Insights into Neotethyan ophiolite petrology at the Dinaride–Alpine–Pannonian triple junction: geochemistry of detrital Cr-spinel from Cretaceous synorogenic sediments**

*Borna Lužar-Oberiter, Tamás Mikes, Hilmar von Eynatten and Ljubomir Babić*

## **Abstract**

Cr-spinel is a common heavy mineral in the sandstones of Cretaceous synorogenic sedimentary formations of the NW Dinarides. The rocks occur in isolated exposures in the uplifted basement units of Medvednica, Ivanščica, Žumberak and Samobor Mountains near Zagreb. In this area evidence of the early Alpine evolution of the Dinarides is obscured due to strong dismemberment of pre-Tertiary tectonostratigraphic units resulting from an intense tectonic history, as well as due to the widespread sedimentary cover of the Pannonian Basin. Electron microprobe analyses of detrital Cr-spinels from the Oštrc Formation reveal that in the Early Cretaceous the ophiolitic source area was predominantly composed of harzburgite peridotites and associated cumulate rocks which developed in a supra-subduction zone setting. The supply of Cr-spinels with the same chemical signature remained dominant until the end of the Cretaceous, suggesting that exposed remnants of the same ophiolite belt persisted through the Cretaceous and/or that recycling was significant. Similarities with data reported from the Northern Calcareous Alps and the Transdanubian Central Range imply that a rather extensive harzburgitic ophiolite belt probably extended along the Adriatic margin during the Early Cretaceous. A slight trend of increasing variation in the Cr# is observed from the Early to the latest Cretaceous, suggesting that the source areas became more heterogeneous with the ongoing Cretaceous tectonic evolution. Differences in Cr-spinel compositions in two contemporaneous latest Cretaceous formations are well in line with existing data on heavy mineral proportions, which together identify contrasting hinterland geology for these formations and strongly suggest the coeval existence of two separate basins.

### 3.1. Introduction

Cr-spinel is an important accessory mineral in mafic and ultramafic rocks, though its considerable chemical and mechanical stability make it a common accessory constituent of sedimentary rocks as well (Zimmerle 1984; Morton and Hallsworth 1999). Its potential to survive the sedimentary cycle, unlike other mafic and ultramafic rock components, often leaves Cr-spinel as the only remaining evidence of a once existing source of detritus, making it a promising target of investigation for provenance studies (Morton 1991). Detrital Cr-spinel chemistry has received considerable attention in studies of clastic sediments, particularly those associated with orogenic suture zones where large masses of mafic and ultramafic rocks tend to be obducted onto the upper plate to form extensive ophiolite sequences (Pober and Faupl 1988; Árgyelán 1996; Cookenboo *et al.*, 1997; Arai and Okada 1991; Hisada and Arai 1993; Lenaz *et al.*, 2000, 2003; von Eynatten 2003; Zhu *et al.*, 2004; Faupl *et al.*, 2006).

During processes of partial melting of mantle rocks and fractional crystallization of magmas the partitioning of elements between solid and melt has a profound effect on the composition of Cr-spinel (Irvine 1965, 1967; Kamenetsky *et al.*, 2001). Studies of mafic and ultramafic rocks have identified the degree of partial melting of mantle peridotites, magma chemistry, temperature of crystallization, cooling rate, pressure and oxygen fugacity as influential factors (Dick and Bullen 1984; Sack and Ghiorso 1991; Arai 1992; Kamenetsky *et al.*, 2001). The variable chemistry of Cr-spinel can provide useful information on the petrogenesis of ophiolite members exposed and eroded during the evolution of an orogen, allowing a better understanding of the tectonic history and nature of sediment dispersal.

This study presents single grain chemical data of detrital Cr-spinels from the sandstones of five Cretaceous clastic formations in the NW Dinarides, Croatia (Fig. 1 and 2). The studied formations range in age from Early to latest Cretaceous, and consist of synorogenic deep-marine and shallow-marine sediments. They record important events in the early evolution of the northern Dinarides, including the Dinaride-Alpine transitional area. To date, a considerable amount of single grain Cr-spinel chemical data has been published from sedimentary formations of the Alpine-Carpathian region (e.g. Pober and Faupl 1988; Árgyelán 1996; Lenaz *et al.*, 2000, 2003; Jablonský *et al.*, 2001;

von Eynatten 2003; Sciunnach and Tremolada 2004; Oszczytko and Salata 2005). However, hitherto no data have been available from Cretaceous sediments of the NW Dinarides. Our new data allow comparison to be made with sedimentary formations and potential source ophiolites exposed today in neighboring areas. By means of Cr-spinel chemistry our aim is to better constrain the composition and tectonic history of the obducted ophiolites supplying detritus into sedimentary basins of the NW Dinarides during the Cretaceous.

### 3.2. Geological setting

The Dinarides represent a major segment of the Alpine orogenic belt in SE Europe (Fig. 1). The Outer Dinarides are dominated by thick Mesozoic platform carbonates forming part of the Adriatic plate, while the Inner Dinarides are on the other hand represented by various lithologies, which occur in NW-SE trending tectonic zones (Aubouin *et al.*, 1970; Pamić *et al.*, 1998; Dimitrijević 1982, 2001; Tomljenović *et al.*, in press). Prominent features of the Dinaride nappe stack are extensive ophiolite units. These represent the remnants of the Neotethys Ocean which existed between Eurasian and African continental elements during the Mesozoic, and may have consisted of several ocean branches or marginal basins (e.g. Dimitrijević and Dimitrijević 1973; Robertson and Karamata 1994; Channell and Kozur 1997, Schmid *et al.*, 2008). In the central and SE Dinarides ophiolites occur in two zones: the Central Dinaride Ophiolite Zone (CDOZ) in the SW and the Vardar Zone to the NE. Separating them is the Drina-Ivanjica intermediate unit which has been interpreted as a continental fragment (Aubouin *et al.*, 1970; Dimitrijević and Dimitrijević 1973; Robertson and Karamata 1994), as an out-of-sequence nappe derived from the northern Tethyan margin (Pamić *et al.*, 1998) or as a basement nappe derived from the Adriatic plate (Schmid *et al.*, 2008). These major Dinaride tectonostratigraphic units extend southwards into the Hellenides. Towards the NW, at the Dinaride-Alpine junction in which the study area is located, the Dinaride structural pattern is obscured by Tertiary lateral displacements and considerable clockwise rotation (Haas *et al.*, 2000; Tomljenović *et al.*, 2008), as well as by the Neogene sedimentary cover. The evolution of the Inner Dinaride zones, as well as their northerly continuation is still a matter of debate. In the Alpine-Carpathian region ophiolite occurrences of the western Tethys have been ascribed to

the Meliata domain, while for others, such as those included in the Bükk Mts., a Dinaride affinity has long been recognized (Haas and Kovács 2001, and references therein). The connection of the Meliata domain itself with the southerly Dinaride ophiolite zones has been both advocated (e.g. Kovács 1982; Dal Piaz *et al.*, 1995; Halamić and Goričan 1995; Gawlick *et al.*, 1999) and contradicted (e.g. Kozur 1991; Channell and Kozur 1997). In the NW Dinarides, ophiolite fragments occur within a mélangé complex collectively termed as Repno Complex (Babić and Zupanić 1978). Results obtained from dating both the matrix and the tectonized blocks of the mélangé suggest a Triassic onset of ocean spreading, subduction beginning in the Middle Jurassic, and a Late Jurassic to Early Cretaceous closure of the oceanic basin (Halamić and Goričan 1995; Halamić *et al.*, 1999; Babić *et al.*, 2002).

The Cretaceous clastic formations considered in this Chapter are situated in a tectonically complex region between the Alps, Dinarides and Tisza (Fig. 1). The area bound by the Periadriatic-Balaton and Zagreb-Zemplén Lineaments, the Sava Composite Unit, comprises several juxtaposed structural units of different affinity. The intense dismemberment of this pre-Tertiary unit results from a severe and long-lasting Mesozoic to Cenozoic deformational history (Vörös 1993; Pamić *et al.*, 1998, 2002; Haas *et al.*, 2000; Tomljenović and Csontos 2001; Haas and Péro 2002; Babić *et al.*, 2002; Csontos and Vörös 2004). The studied strata, together with other pre-Tertiary units are exposed only in uplifted basement

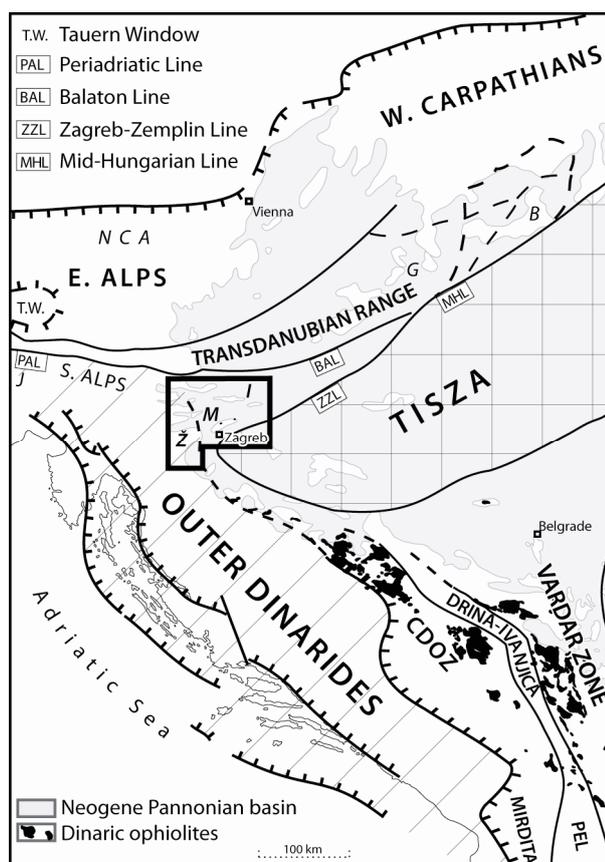


**Fig. 1.** Tectonic situation of the Alpine-Dinaric-Pannonian region with the main structural units outlined. Map compiled from different sources, mainly Haas *et al.*, (2000), Haas and Kovács (2001), Aubouin *et al.*, (1970) and Geological Map of Yugoslavia, 1:500000 (F.Y.I., 1970). B = Bükk Mts., G = Gerecse Mts., I = Ivanščica Mt., J = Julian Basin, M = Medvednica Mt., Ž = Žumberak Mts., CDOZ = Central Dinaride Ophiolite Zone, NCA = Northern Calcareous Alps, PEL = Pelagonian unit. Framed area is shown in Fig. 2

units, or "inselbergs", on the Ivanščica, Medvednica, Žumberak and Samobor Mountains (Fig. 2).

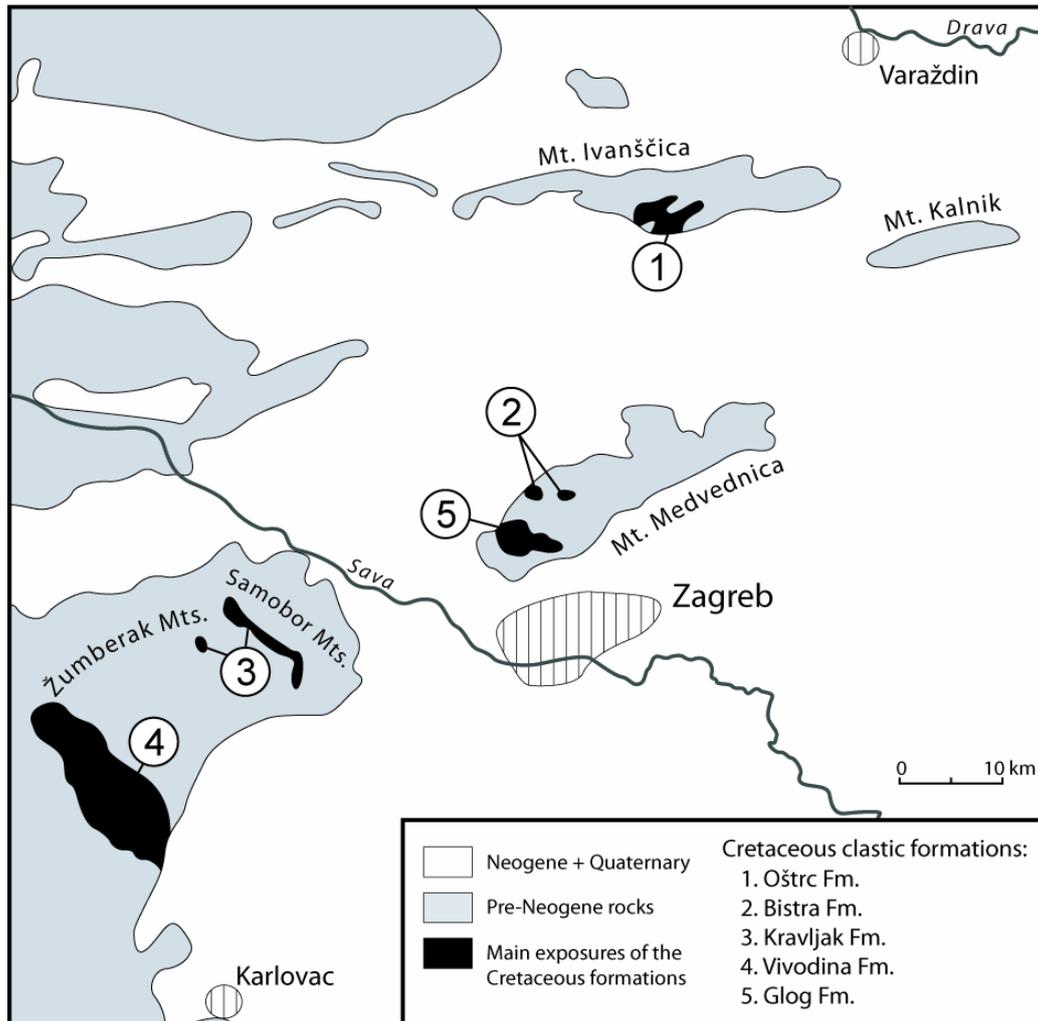


**Fig. 2.** Simplified geological map showing the distribution of the studied formations

The Mesozoic sediments of Mt. Ivanščica consist of deposits of the Adriatic platform and its NE margin which occur in tectonic contact with a Jurassic ophiolitic mélangé (Repno Complex, Babić *et al.*, 2002). These are Late Triassic shallow marine carbonates, Jurassic pelagic limestones and cherts, and Tithonian-Valanginian “Aptychus Limestones” which are overlain by the *Oštrc Formation* (Fig 2.). The Oštrc Fm. is Barremian to Albian in age and dominated by siliciclastic turbidites (Fig. 3; Babić and Zupanić 1973; Babić 1975; Babić and Gušić 1978). Babić *et al.*, (2002) suggested that these sediments were deposited on the subsided carbonate platform margin of the Adriatic plate. Facies and composition records a dramatic change in sedimentation due to the

influx of high amounts of siliciclastic material. Heavy mineral spectra from sandstones of the Oštrc Fm. show a very high proportion of chrome spinel (>90%), indicating, together with abundant mafic and ultramafic lithic fragments, a dominantly ophiolitic provenance with minor continental contribution (Zupanič *et al.*, 1981).

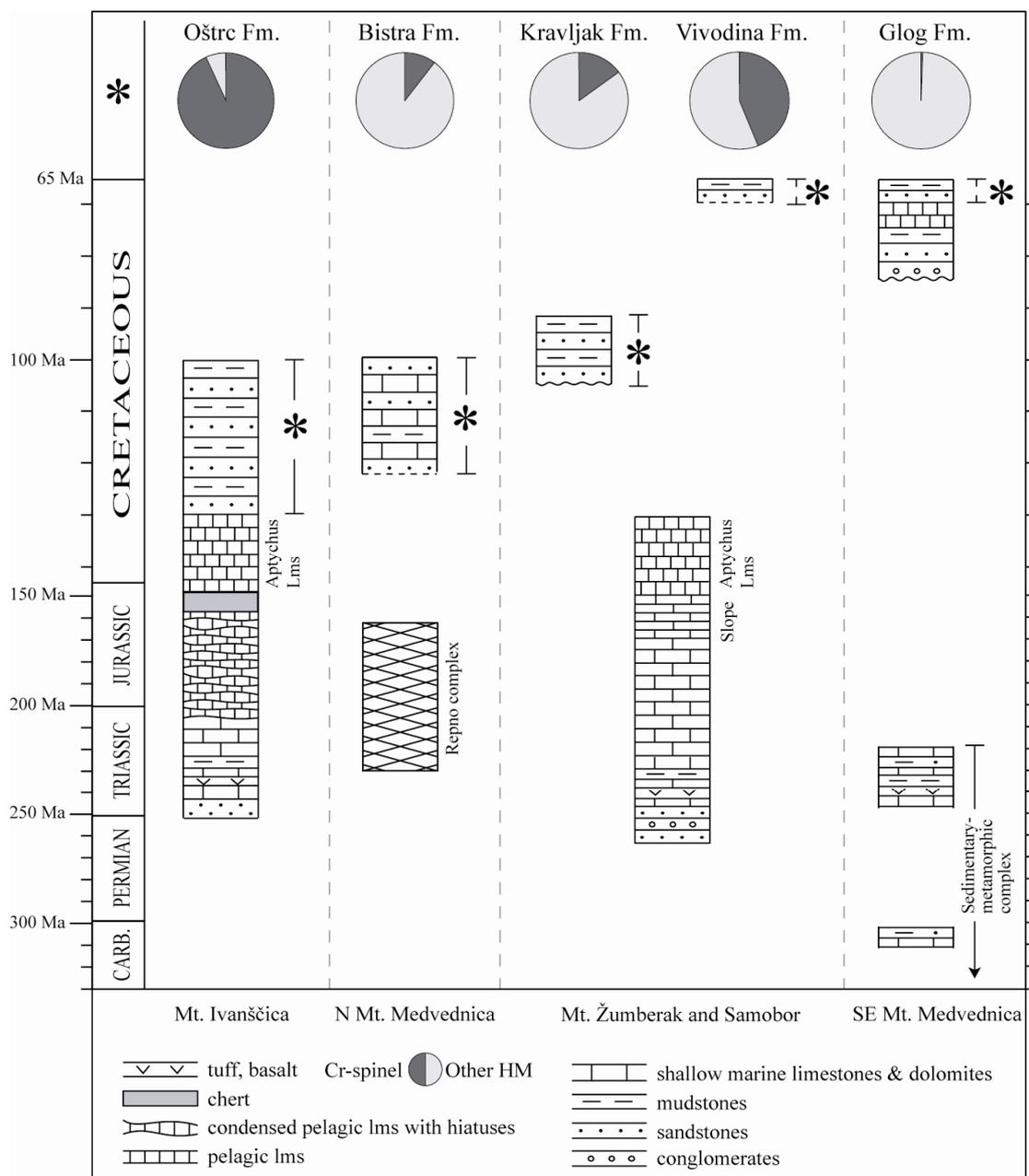


**Fig. 3.** Simplified chronostratigraphic logs of the studied formations and their basement. Average Cr-spinel abundances are presented at the top with pie diagrams (Crnjaković 1981; 1989; Crnjaković *et al.*, 2000; Zupanič *et al.*, 1981; Zupanič 1981). Note that the vertical time scale is not linear.

Two Cretaceous clastic formations were investigated on Mt. Medvednica (Fig. 2). The Aptian-Albian *Bistra Formation* consists of shallow-marine to coastal carbonates and clastic sediments (Gušić 1975; Crnjaković 1989). The shallow-marine environment probably developed on top of the exhumed Jurassic ophiolitic mélangé complex, which also occurs in Mt. Medvednica (Babić *et al.*, 2002). The heavy mineral associations of the sandstones contain ultrastable minerals (zircon, tourmaline and rutile = ZTR), Cr-spinel, and only minor proportions of other minerals (e.g. apatite, garnet, amphibole and epidote). The heavy minerals and framework composition reflect a mixed continental-ophiolitic provenance (Crnjaković 1989). The Maastrichtian *Glog Formation* consists of deep-water sandstone and marl deposits which represent the youngest part of a Senonian alluvial to deep-water succession overlying low-grade metamorphic rocks, as well as the ophiolitic mélangé (Babić *et al.*, 1973; Crnjaković 1981, 1987). This sedimentary-metamorphic complex builds up the “core” of Mt. Medvednica and underwent Early Cretaceous low-grade metamorphism (Belak *et al.*, 1995; Belak 2005). Opinion is divided as to whether it is of Dinaride affinity (Haas *et al.*, 2000), or does it rather derive from an easterly continental block (Tisza or Drina-Ivanjica Unit – Babić *et al.*, 2002). The heavy mineral associations in the sandstones of the Glog Fm. are heavily dominated by ZTR, with only minor proportion of other heavy minerals (Crnjaković 1981). It is important to note that in the studied Glog samples, Cr-spinel occurs only in trace amounts, which is considerably less than in any of the other formations.

The Albian-Cenomanian *Kravljak Formation* and the Maastrichtian *Vivodina Formation* are both deep-water turbiditic deposits and occur in the Žumberak and Samobor Mts. (Fig.2), located in the SW edge of the Sava Composite Unit (Babić 1974; Zupanič 1981; Devidé-Nedéla *et al.*, 1982). Probably, these formations record deposition on the distal Adriatic margin in the Late Cretaceous, and are laterally equivalent to the “Zone Prekarstique” (Babić 1974) described further to the SE in Bosnia-Herzegovina by Blanchet *et al.*, (1970). The onset of clastic deposition in this area thus occurred earlier than elsewhere on the carbonate platform (Babić 1974; Čosović *et al.*, 2008; Mikes *et al.*, 2008a). Heavy mineral associations from the sandstones of these formations contain ZTR, Cr-spinel, and garnet as well as a minor proportion of other mineral species (e. g. epidote, amphibole, chloritoid), indicating derivation from both ophiolitic and continental sources (Zupanič 1981; Crnjaković *et al.*, 2000).

### 3.3. Sampling and analytical procedures

Samples were taken from fine to medium grained sandstone beds, taking care to avoid sampling of weathered rock. Cr-spinel grains were obtained using standard heavy mineral separation procedures. Sandstone samples were crushed, dry sieved down to <0.250 mm, and the heavy fraction pre-concentrated using a Wilfley-table. Carbonate was removed by 5% cold acetic acid treatment. Heavy minerals were separated by hot LST Fastfloat ( $\rho=2.85 \text{ gcm}^{-3}$ ), embedded in epoxy and polished for microprobe analysis. Most sprinkled mounts contained sufficient amount of Cr-spinel grains, whereas Glog Formation spinels were separated by hand-picking due to their low abundance in the samples. Measured grains range in size from coarse silt to very fine sand.

In total we have analyzed Cr-spinels from 17 sandstone samples taken from 5 different formations (Oštrc=7, Bistra=3, Kravljak=2, Vivodina=3, Glog=2). Chemical data of 773 detrital Cr-spinel grains were obtained using a JEOL electron microprobe (JXA-8900RL) equipped with five wavelength dispersive spectrometers at the Geoscience Center Göttingen. Analyses were performed using an accelerating voltage of 20 kV, a beam current of 20 nA and a 3  $\mu\text{m}$  beam diameter. Mg, Al, Cr, Fe, V, Si, Ti, Mn, Ni and Zn were analyzed. One spot analysis was performed in the center of each grain. Measured grains range in size from coarse silt to very fine sand. No zoning was evident based on back-scattered electron images, neither were ferrian chromite rims encountered. Ferric iron content was calculated based on charge balance assuming stoichiometry, following the procedure of Barnes and Roeder (2001). All data are listed in Appendix 3-1.

### 3.4. Chemical characteristics of Cr-spinels in the studied Cretaceous formations

The chemical composition of Cr-spinel is commonly presented by values which display considerable variation, such as Cr# ( $\text{Cr}/(\text{Cr}+\text{Al})$ ), Mg# ( $\text{Mg}/(\text{Mg}+\text{Fe}^{2+})$ ),  $\text{TiO}_2$  and  $\text{Fe}^{3+\#}$  ( $\text{Fe}^{3+}/(\text{Cr}+\text{Al}+\text{Fe}^{3+})$ ). During processes of partial melting in the mantle Cr is strongly partitioned into the solid as compared to Al which preferentially partitions into the melt. This makes the Cr# of Cr-spinel an excellent indicator of the degree of partial melting which its host peridotite underwent, since the degree of depletion is often sug-

gestive of the tectonic setting (e.g. mid-oceanic ridge or supra-subduction zone). The causes for the variation of Mg# are more complex. The partitioning of Mg and Fe<sup>2+</sup> is affected by the relative activities of Cr and Al in spinel, causing a shift towards lower Mg# with increasing Cr# (Dick and Bullen 1984). Furthermore, Mg# is dependent on temperature and cooling rate, as well as magma chemistry during crystallization and re-equilibration processes. The TiO<sub>2</sub> content and Fe<sup>3+</sup># differ between Cr-spinels from residual mantle peridotites ('residual' or 'mantle' spinels) and those formed by crystallization of the extracted melt ('magmatic' spinels). Residual spinels have low TiO<sub>2</sub> (<0.2%), while those originating from cumulate and extrusive volcanic rocks tend to have higher TiO<sub>2</sub> (>0.2%) (e.g. Kamenetsky *et al.*, 2001).

#### 3.4.1. Oštrc Formation

In the Cr-spinels from the sandstones of the Oštrc Formation Cr# values range from 0.39 up to 0.81, mostly (88%) between 0.50 and 0.70. Only 2% of the analysis fall below 0.45 (all of these coming from only one of the seven Oštrc samples). The Mg# displays a relatively wide range, from 0.37 to 0.76. Of the analyzed grains, 28% display TiO<sub>2</sub> concentrations above 0.2%. It is interesting to note that a few of the grains display high TiO<sub>2</sub> concentrations, up to 2.17%. When the residual spinels alone (<0.2 % TiO<sub>2</sub>) are plotted on the Cr# vs. Mg# diagram (Fig. 4), most of the data fall within the harzburgite field defined by Pober and Faupl (1988). Following the classification of Dick and Bullen (1984), they resemble Type II alpine-type peridotites which are thought to evolve through a complex multistage melting history as may be encountered in a subduction zone. The high Ti magmatic spinels (>0.2 % TiO<sub>2</sub>) display a shift towards lower Mg#, as in the Fe-Ti trend of Barnes and Roeder (2001). Their similar range of Cr# values to the residual spinels (with a tendency towards higher Cr#), high Fe<sup>3+</sup> and TiO<sub>2</sub>, along with lower Mg# suggests that these spinels could be the products of fractional crystallization and re-equilibration at lower temperatures due to slow cooling (Arai 1992; Kamenetsky *et al.*, 2001), and thus probably derived from cumulate members containing disseminated Cr-spinel of the same ophiolite source (Dick and Bullen 1984; Pober and Faupl 1988; Barnes and Roeder 2001). On the Al<sub>2</sub>O<sub>3</sub> vs. TiO<sub>2</sub> discrimination diagram (Fig. 5) proposed by Kamenetsky *et al.*, (2001), the residual spinels concentrate in the middle of the field of suprasubduction zone peridotites. Meanwhile, the

magmatic spinels fall within fields defining volcanic rocks from different settings, but mostly group in the border region between MORB and arc basalts. The same can be observed on the  $\text{TiO}_2$  vs.  $\text{Fe}^{3+\#}$  diagram when comparing the data with compositional fields proposed by Arai (1992). Several grains display compositions such as those found in ocean island basalts (i.e. intra-plate basalts).

### *3.4.2. Bistra Formation*

Generally, high-Cr harzburgitic spinels predominate in the Early Cretaceous Bistra Fm. (Fig. 4), although the Cr# ranges differ noticeably between the three studied samples. Sample 05-H/B-201 contains spinels with Cr# above 0.50. A single outlier is a relatively high-Al spinel with a Cr# as low as 0.30. Similar to the spinels of the Oštrc Fm., the residual spinels of sample 05-H/B-201 fall predominantly within the harzburgite field, while the magmatic spinels display higher Cr# and shift towards lower Mg# values. Spinel from sample 05-H/B-216 have Cr# values above 0.40. Unlike in the two previous samples, in sample 05-H/B-207 Cr# values spread in a wider range, from 0.26 to 0.87. The proportion of magmatic spinels is also variable among the three studied samples (24%, 13% and 19%). Overall, the variability between the samples suggests that the source area was rather heterogeneous and included small exposures of less depleted residual peridotites and magmatic rocks.

### *3.4.3. Kravljak Formation*

The Cr-spinels from sandstones of the Albian-Cenomanian Kravljak formation display a range of Cr# values from 0.36 to 0.79, with only 2% of the data falling below 0.40. Most of the grains (83%) cluster within the 0.50-0.70 Cr# range, falling predominantly within the harzburgite field (Fig. 4). 24% of the spinels can be classified as magmatic, the maximum recorded  $\text{TiO}_2$  being 1%. On the  $\text{Al}_2\text{O}_3$  vs.  $\text{TiO}_2$  diagram most of the spinels fall within the field of suprasubduction peridotites, while the magmatic grains fall predominantly in the MORB field (Fig. 5).

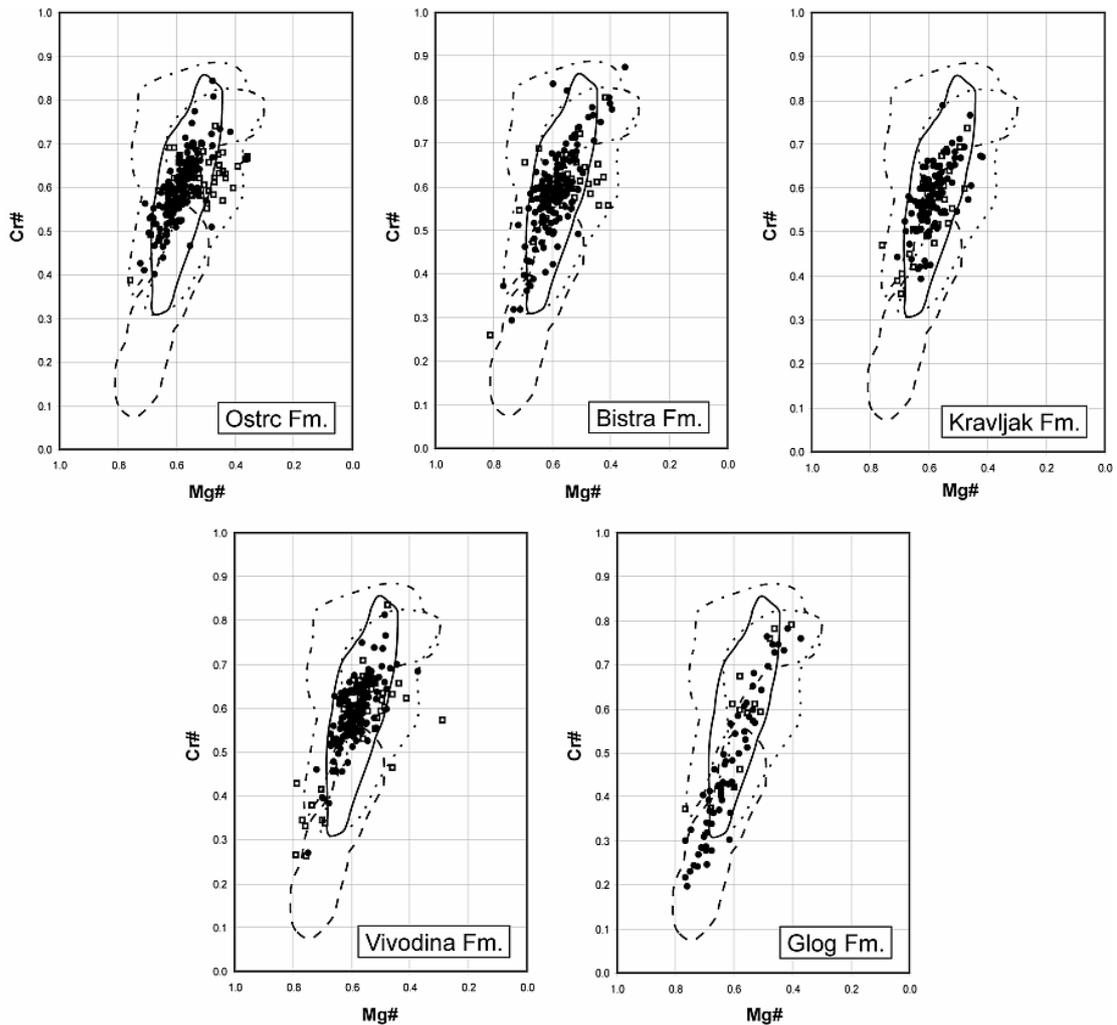


**Fig. 4.** Cr# vs. Mg# diagrams of Cr-spinels from each formation. Fields after Pober and Faupl (1988). *full line* harzburgites, *dashed line* lherzolites, *dotted line* cumulates, *dash-dot* podiform chromites, *full circles* spinels with  $<0.2\%$   $\text{TiO}_2$ , *open squares* spinels with  $>0.2\%$   $\text{TiO}_2$ .

#### 3.4.4. Vivodina Formation

In the Maastrichtian Vivodina Formation Cr-spinels display a wide range of Cr# and Mg# values (0.26-0.84 and 0.29-0.79, respectively), but concentrate (85%) within the 0.5-0.7 Cr# range like in the other formations. 20% of the spinels classify as magmatic. These high  $\text{TiO}_2$  spinels concentrate in two groups on the Cr#-Mg# diagram (Fig. 4). The first group is characterized by high Cr# and low Mg#, very similar to those identified as cumulate spinels in the older formations (Ostrc, Bistra and Kravljak Fms.). The second group, however, displays low Cr# and higher Mg#, which is a characteristic

of Cr-spinels identified in abyssal basalts (Dick and Bullen 1984). On the  $\text{Al}_2\text{O}_3$  vs.  $\text{TiO}_2$  diagram, these tend to fall within the MORB field (Fig. 5). The residual spinels group in the middle of the suprasubduction zone field of the same diagram, as in the samples from the older three studied formations.

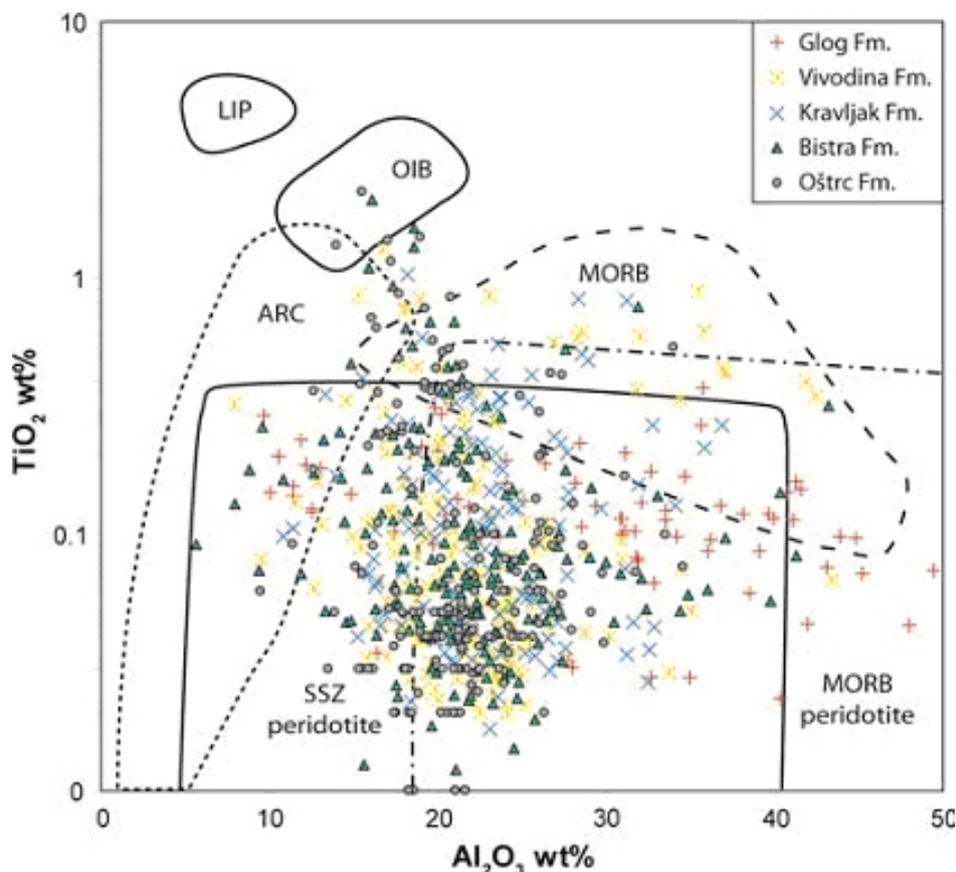


**Fig. 5.**  $\text{TiO}_2$  vs.  $\text{Al}_2\text{O}_3$  diagram with Cr-spinel data from all five formations. Fields after Kamenetsky *et al.*, (2001). MORB mid-ocean ridge basalt, OIB ocean-island basalt, LIP large igneous province, ARC island-arc magmas, SSZ supra-subduction zone.

### 3.4.5. Glog Formation

Of all the studied samples, the Cr-spinels from the Glog Fm. display the greatest range of Cr# values (0.2-0.79). The Cr# values spread continuously across the entire range (Fig. 4), lacking the predominance of high-Cr spinels identified in the other formations. The proportion of grains with  $\text{TiO}_2$  content above 0.2% is 16%. The highest recorded  $\text{TiO}_2$  content is 0.36%, much lower than in the other formations.

### 3.5. Provenance and paleogeographic relations

Following the Tithonian-Hauterivian period, which was marked by widespread deposition of deep marine *Aptychus* limestones and marls, the closure of the western Tethys Ocean triggered a strong influx of siliciclastic material onto the passive margin of the Adriatic plate. This change in sedimentary regime is evident on Mt. Ivanščica, where from the Barremian up to the Albian deep marine clastic sediments rich in ophiolitic detritus (Oštrc Fm.) were deposited on top of pelagic limestones (Fig. 6a). Considering the ubiquity of ophiolitic lithoclasts and Cr-spinel, a source area consisting primarily of obducted ophiolites must have come into close proximity of the Oštrc Basin (Zupanič *et al.*, 1981; Babić *et al.*, 2002). The chemical compositions of the Cr-spinels (Fig. 4) indicate that these exposed ophiolites consisted mostly of harzburgitic peridotites and associated cumulate rocks, i.e. oceanic mantle and lower crustal rocks. The eroded mantle peridotites underwent a considerable degree of partial melting prior to their obduction, above the limit normally achieved at mid-oceanic ridges (Dick and Bullen 1984), and instead likely evolved in a supra-subduction zone setting. These characteristics of the source area apparently did not change significantly during continuous erosion and deposition of the Oštrc Fm., as no systematic change in Cr-spinel composition is detected among the seven studied samples.

In addition to Mt. Ivanščica, Early Cretaceous formations containing abundant ophiolitic detritus are well known in the Northern Calcareous Alps (NCA; Rossfeld Fm.) and the Transdanubian Central Range (Gerecse Mts.). Facies and petrologic similarities among these sedimentary successions have been recognized by previous authors (e.g. Decker *et al.*, 1987; Faupl and Wagreich 1992; Császár and Árgyelán 1994), and a common provenance, the suture zone of the Tethys Ocean has been suggested (Poher and Faupl 1988; Árgyelán 1996; Babić *et al.*, 2002). A comparison of Cr-spinel data from all three areas (Fig. 7) lends support for a common provenance of the ophiolitic material. Although they are today separated by hundreds of kilometers due to Tertiary tectonic displacement, during the Mesozoic the NCA and the Transdanubian Central Range sat adjacent to one another along the Tethyan passive margin (Kázmér and Kovács 1985; Schmidt *et al.*, 1991; Vörös and Galács 1998). During this time Mt. Ivanščica probably held a more southerly position and may represent an important link to the Inner Dinaride realms. A rather extensive ophiolite belt containing large harzburgite bodies, capable of providing large quantities of detritus over a regional scale, may have ex-

tended during the Early Cretaceous along the Adriatic margin, from the area of the NCA in the north to the Dinarides (Fig. 8). Today, in the surroundings of the northernmost Dinarides and in the East Alpine-Carpathian region there are no major exposures of mantle rocks. They are restricted to smaller dismembered occurrences mostly within mélangé complexes of the Sava Zone (Pamić 1997; Slovenec and Pamić 2002), the Alps and the Western Carpatians (Kozur 1991). Large ultramafic bodies are exposed in the CDOZ, in places occurring as several kilometers thick slices of oceanic lithosphere (e.g. Pamić *et al.*, 2002). From the peridotites of the two major zones in the Inner Dinarides, Maksimović and Majer (1981) reported both high-Cr (common to the Vardar Zone) and low-Cr spinels (common to the CDOZ), but in fact there is likely to be a gradual transition in the degree of depletion of the mantle rocks within these zones (Pamić 1983). The northwesternmost peridotites of the CDOZ, such as those occurring in the Banija region, south of the study area, are lherzolitic with low-Cr spinels (Maksimović and Majer 1981), ruling them out as potential remnants of the obducted ophiolites which supplied the Oštrc Fm. Although the ophiolites of the CDOZ were already obducted in the Early Cretaceous (Pamić *et al.*, 2002; Robertson and Karamata 1994), detritus produced by their erosion was not transported into the Oštrc Basin. Rather, a connection to the Vardar Zone, where harzburgites predominate, is more conceivable (Fig. 8). The unusual spread in the Al content of the high-Ti spinels in some of the studied formations (Fig. 5) may be suggestive of a back-arc basin origin of the magmatic rocks from which some of these grains are derived from (Arai 1992; Kamenetsky *et al.*, 2001).

The ophiolite source supplying most of the detritus of the Early Cretaceous Bistra Fm., exposed on Mt. Medvednica, was mostly similar in composition to that supplying the Oštrc Fm. in that high-Cr spinels dominate. Babić *et al.*, (2002) suggested that the Bistra Fm. developed as a shallow basin on top of the ophiolitic mélangé (Repno complex) whose remnants occur in the N part of Mt. Medvednica. Serpentinized harzburgites as well as cumulate ultramafics with relatively high-Cr spinels are present as smaller tectonized blocks within this mélangé (Šimunić and Pamić 1989; Slovenec and Lugović 2000) and may have presented a potential source (Fig. 6a). The variability encountered among the individual samples of the Bistra Fm. may reflect the smaller catchment area of the shallow marine environment and the heterogeneous nature of the mélangé, which incorporated ophiolite fragments of slightly varying composition.

The supply of Cr-spinels from ophiolites with the same chemical signature as those supplying the Oštrc Fm. continued at least until the latest Cretaceous along the NE margin of the Outer Dinarides, as evident from the data obtained from the Kravljak and Vivodina Fms. Recycled Cr-spinels from older sedimentary formations being incorporated into propagating nappes (e.g. the Oštrc) may have represented an important source (Fig. 6b and 6c). However, the presence of ophiolite-derived lithoclasts and a relatively high proportion of Cr-spinels in the heavy mineral fraction of the Vivodina sandstones (up to 70%; Zupanič *et al.*, 1981) suggest that exposed remnants of the above mentioned ophiolite belt persisted along the margin of the Adriatic plate at least until the end of the Cretaceous (Fig. 6b and 6c).

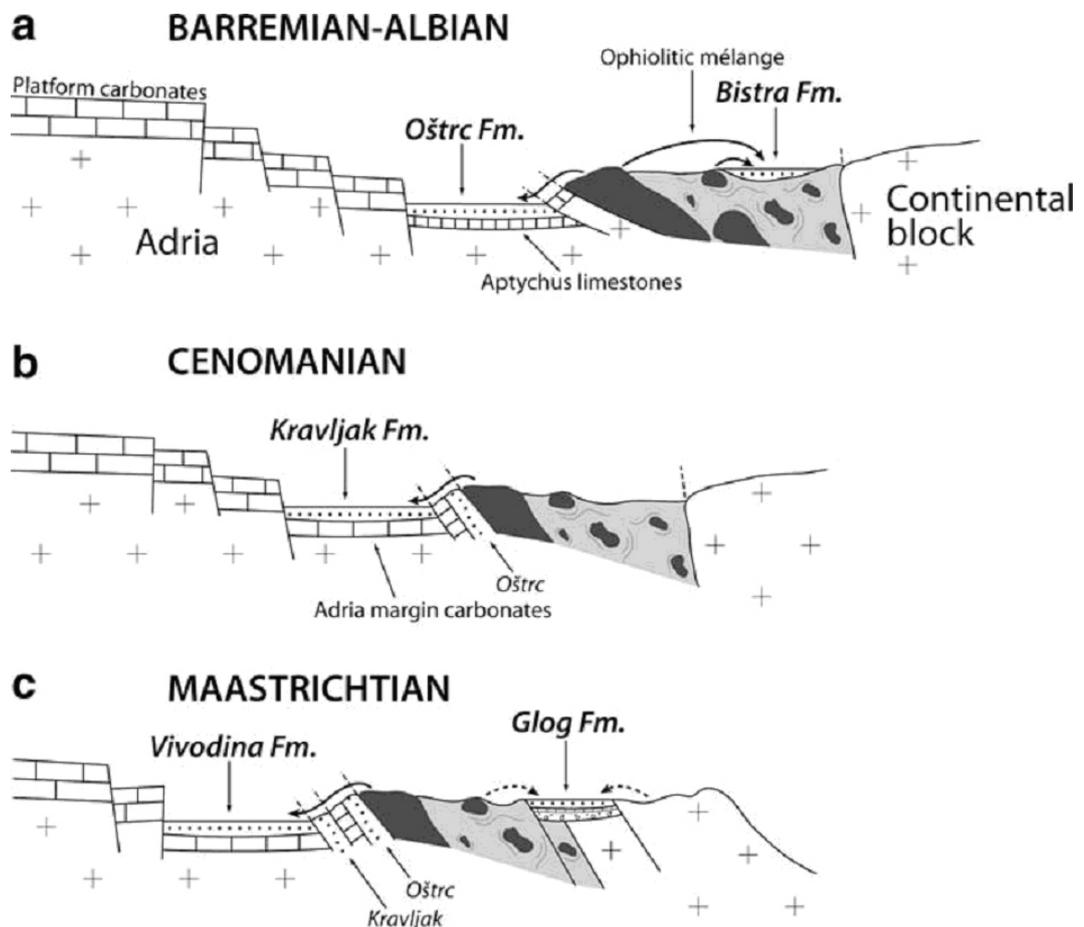


**Fig. 6.** Schematic cross-sections portraying the Cretaceous tectonic evolution of the study area and the major sources of Cr-spinels (thick black arrows) for the five studied formations. See text for details.

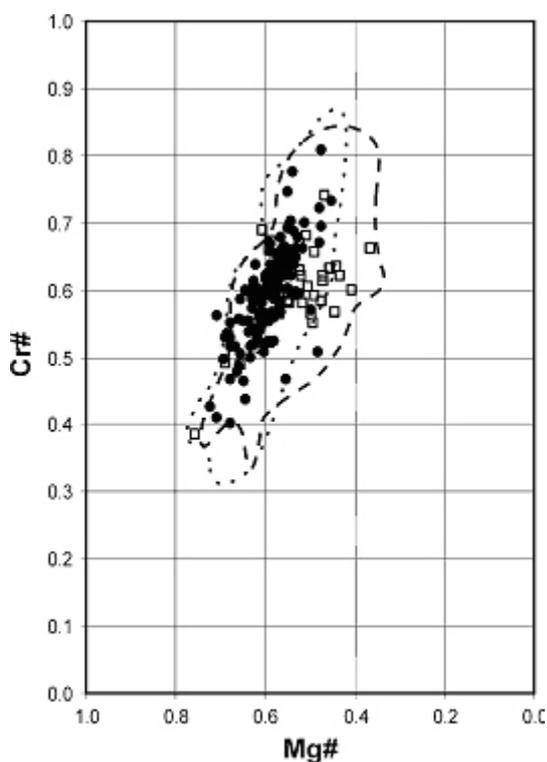


**Fig. 7.** A comparison of the data from the Oštrc Fm. with those published for the Rossfeld Fm., Northern Calcareous Alps (dashed line) and Gerecse Mts., Transdanubian Central Range (dotted line). Full circles = spinels with  $<0.2\%$   $\text{TiO}_2$ ; open squares = spinels with  $>0.2\%$   $\text{TiO}_2$ .

detritus in the Glog sandstones originated from an entirely continental hinterland probably composed of the sedimentary-metamorphic complex of Mt. Medvednica (Crnjaković 1979). The dominant availability of felsic continental lithologies for erosion in the source area likely accounts for the small proportion of Cr-spinel in the HM spectra of Glog sandstones. The differences in Cr-spinel chemistry of the coeval Vivodina and Glog formations can be reconciled by the erosion of a heterogeneous ophiolite mélange source containing peridotite blocks of different degrees of depletion (Fig. 6c). Together with contrasting heavy mineral data and differences in the underlying lithology, these results suggest the coeval existence of two separate basins.

Although the supply of high-Cr spinels prevailed in general, a slight trend of increasing variation in the Cr# (among both residual and magmatic spinels) is noticeable from the Early to the latest Cretaceous, suggesting that the source areas became more heterogeneous with the ongoing Cretaceous tectonic evolution of the Dinaride-Alpine

An additional source of Cr-spinels is recorded in the Maastrichtian. A number of grains in the Maastrichtian Vivodina sandstones (Fig. 4 and 5) have compositions similar to those reported for abyssal/MORB basalts (Dick and Bullen 1984; Kamenetsky *et al.*, 2001). Lenaz *et al.*, (2000) obtained very similar results from Cr-spinels in the Maastrichtian to Middle Eocene sediments of the Julian Basin in the Southern Alps (Fig. 1), which imply a possible common provenance and a paleogeographic connection between the Julian and Vivodina basins.

The presence of many low-Cr# spinels in the Glog Fm. requires a separate source from that which supplied the other formations examined. The Glog Fm. belongs to a Senonian succession lying on a tectonized basement (Fig. 6c), presumably deposited in a piggy-back basin (Babić *et al.*, 2002). The

region. Pober and Faupl (1988) and von Eynatten (1996) identified a trend of increasing lherzolitic component from Early to Late Cretaceous among sedimentary formations of the NCA and the Drauzug which had a “southern provenance”, i.e. sourced by the Tethys suture (Rossfeld Fm., Lavant Fm. and parts of the Gosau-type sediments).

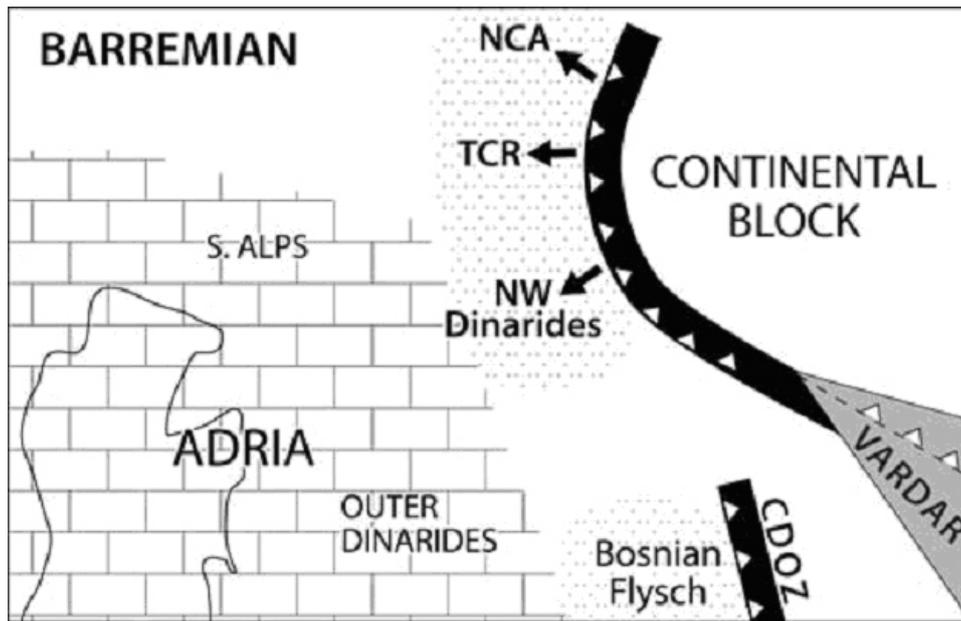


**Fig. 8.** Paleogeographic sketch map of the Dinaride-Alpine region during the Barremian. NCA = Northern Calcareous Alps; TCR = Transdanubian Central Range; CDOZ = Central Dinaride Ophiolite Zone.

### 3.6. Conclusions

1. Detrital Cr-spinel grains in the Early Cretaceous Oštrc Formation on Mt. Ivanščica display relatively high Cr#. The ophiolite source consisted of harzburgitic mantle peridotites and associated cumulate rocks which developed in a supra-subduction zone setting.

2. There is a similarity in detrital Cr-spinel compositions between the Oštrc Fm. and those reported from contemporaneous formation in the NCA and the Transdanubian Central Range. A rather extensive harzburgitic ophiolite belt, capable of providing large quantities of detritus over a regional scale, probably extended along the Adriatic margin during the Early Cretaceous, from the area of the NCA in the north to the northernmost Dinarides.

3. The supply of Cr-spinels high in Cr# remained dominant throughout the Cretaceous. A likely source were exposed remnants of the W Tethyan ophiolite belt, while recycling from Early Cretaceous sediments also played an important role.

4. The Cr-spinels from the Maastrichtian Glog Fm. on Mt. Medvednica were derived from a source of different composition as compared to the contemporaneous Vivodina Fm. in the Žumberak Mts. Together with contrasting heavy mineral data and differences in the underlying lithologies, these results imply the coeval existence of two separate basins.

5. The source areas became more heterogeneous with the ongoing Cretaceous tectonic evolution, which is suggested by the increasing variation in the Cr# of Cr-spinels from the Early to the latest Cretaceous.

## *Chapter 4*

# Jurassic granitoid magmatism in the Dinaride Neotethys: geochronological constraints from detrital minerals

---

This chapter is largely identical to the manuscript entitled:  
"Jurassic granitoid magmatism in the Dinaride Neotethys: geochronological constraints from detrital minerals"  
that is currently in review with *Terra Nova*, submitted Nov. 2008  
authored by:  
Tamás Mikes, Björn Baresel, Andreas Kronz, Dirk Frei, István Dunkl,  
Raimon Tolosana-Delgado and Hilmar von Eynatten



# **Jurassic granitoid magmatism in the Dinaride Neotethys: geochronological constraints from detrital minerals**

*Tamás Mikes, Björn Baresel, Andreas Kronz, Dirk Frei, István Dunkl, Raimon Tolosana-Delgado and Hilmar von Eynatten*

## **Abstract**

Three independent single-grain geochronometers applied to detrital minerals from Central Dinaride sediments constrain the timing of felsic magmatism that associated the Jurassic evolution of the Neotethys. The Lower Cretaceous clastic wedge of the Bosnian Flysch, sourced from the Dinaride ophiolitic thrust complex, yields magmatic monazite and zircon grains with dominant age components of  $164 \pm 3$  Ma and  $152 \pm 10$  Ma, respectively. A unique tephra horizon within the Mesozoic Adriatic Carbonate Platform was dated at  $148 \pm 11$  Ma by apatite fission track analysis. These consistent results suggest that leucocratic melt generation in the Central Dinaride segment of the Neotethys culminated in Middle to Late Jurassic times, coeval with and slightly post-dating sub-ophiolitic sole metamorphism. Monazite growth and explosive volcanism call for supra-subduction zone processes at the convergent Neotethyan plate margin. New compilation of geochronological data demonstrates that such Jurassic felsic rocks are widespread in the entire Dinaride-Hellenide orogen.

#### 4.1. Introduction

A characteristic element of the Dinaride-Hellenide orogen of SE Europe is an extensive, complex belt of Jurassic ophiolites, representing the obducted remnants of the Neotethys ocean (Fig. 1). The parallel map appearance of two belts of ophiolitic units (Dimitrijević and Dimitrijević, 1973) gave rise to a vigorous debate on their relation. Models include the existence of two oceanic basins, either separated by an intraoceanic "microcontinent" (Robertson and Karamata, 1994; Karamata *et al.*, 2006), or opened consecutively in an arc/back-arc system (Pamić *et al.*, 2002). Alternatively, a single oceanic basin is proposed, the fragments of which were emplaced as ophiolite thrust sheets to different distances onto the overridden continental plate (Kober, 1912; Bernoulli and Laubscher, 1972; Schmid *et al.*, 2008). Although now there is consensus that oceanic convergence was not associated with significant island arc igneous activity (Ivanov *et al.*, 1987; Pamić *et al.*, 2002; Dimitrijević *et al.*, 2003), an increasing number of petrological and geochemical data point to island arc affinity in the Dinaride ophiolites, and also in other equivalent ophiolite sequences in Albania, in the Hellenides and in the Bükk and Apuseni Mts. The island arc signatures are explained by the development of an intra-oceanic supra-subduction-zone (SSZ), the remains of which now preferentially occur as the "eastern" ophiolites (e.g. Aigner-Torres and Koller 1999; Robertson, 2004; Beccaluva *et al.*, 2005; Bortolotti and Principi 2005; Bazylev *et al.*, 2006; Lugović *et al.*, 2006; Rassios and Moores 2006; Smith 2006; Dilek *et al.*, 2008).

Felsic magmatic rocks invariably associate the ophiolite sequences. Although small in volume, they are widespread in the Dinarides-Hellenides and their tectonically displaced units, such as the Apuseni Mts. and the Gemer-Bükk Unit (Fig. 1). They can be subdivided into three major genetic groups; (1) oceanic plagiogranites, generated at the region of mid-ocean spreading and at the SSZ (Majer and Garašić, 2001; Beccaluva *et al.*, 2005; Dilek *et al.*, 2008); (2) calc-alkaline magmatic suites at an immature island arc (Máthé and Szakmány, 1990; Bortolotti *et al.*, 2004; Dilek *et al.*, 2008); and (3) anatexis of gabbro, amphibolite and sediments of the subducted slab beneath the overriding hot oceanic plate (Pearce, 1989; Koepke *et al.*, 2007). K/Ar, Ar/Ar and Sm/Nd geochronological data of sub-ophiolitic metamorphic soles range between 178 and 161 Ma, marking the Middle Jurassic onset of intra-oceanic subduction (e.g. Okrusch *et al.*,

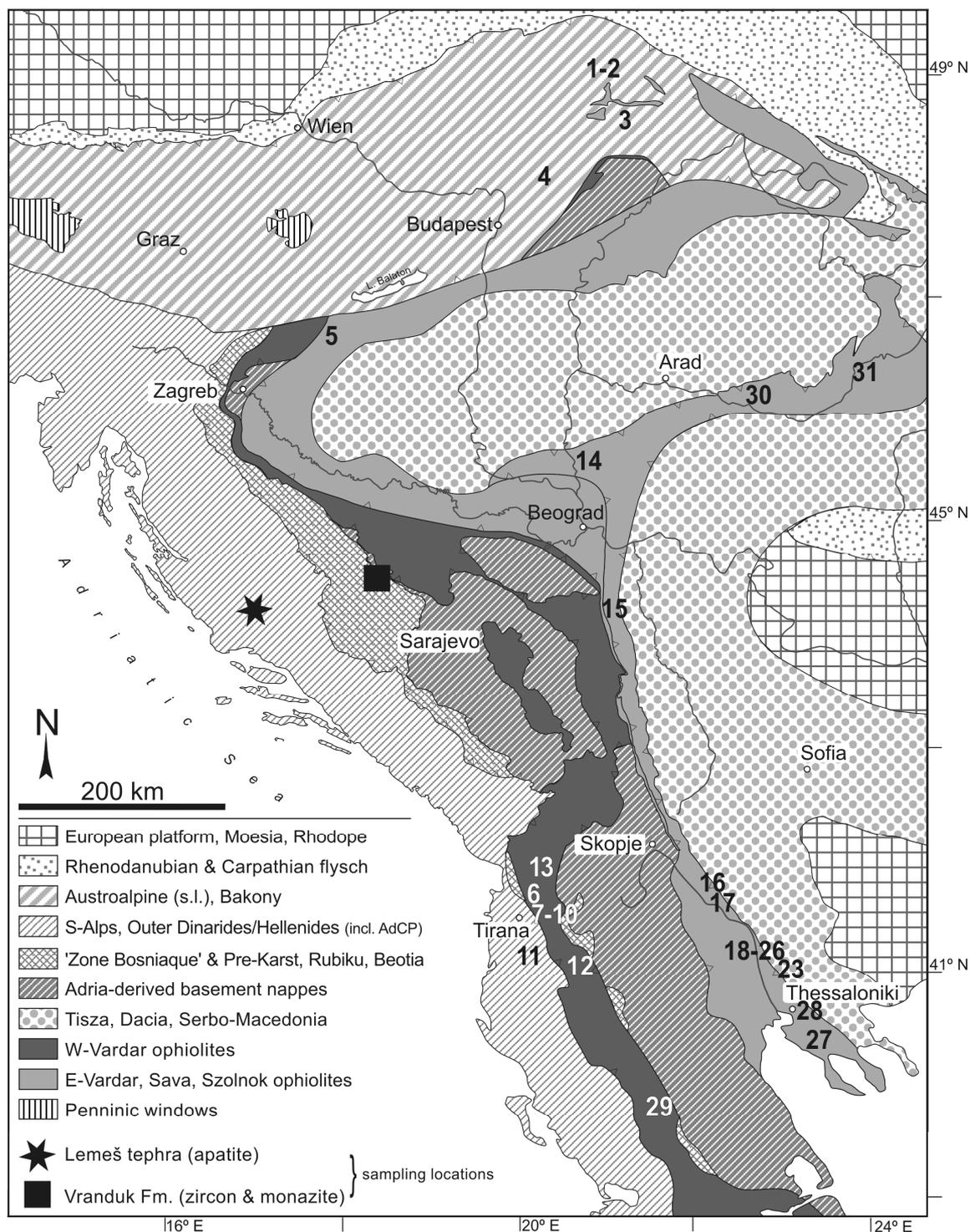


**Fig. 1.** Tectonic framework of the the Carpatho-Pannonian-Dinaride-Hellenide area showing the distribution of Jurassic Neotethyan ophiolites and other major tectonic units. Position of felsic magmatic bodies associating the ophiolites is indicated by numbers, as referred to in Table 1 and Fig. 8. Only dated occurrences were included. Map compiled after Jacobshagen, 1986; Papanikolaou, 1997; Csontos and Vörös, 2004; and Schmid *et al.*, 2008.

**Table 1.** Published radiometric age data from felsic magmatic rocks associating Neotethyan ophiolites of the Carpatho-Pannonian-Dinaride-Hellenide orogen. Early Cretaceous apparent ages are also included whenever local geologic context suggests a slightly older crystallization age. Refer to Fig. 8 for a graphical overview of the these data. n.s.: not specified in the cited work; wr: whole-rock; plag: plagioclase, cel: celadonite, CL: cathodoluminescence-controlled in-situ dating; ŽOC: Ždraljica Ophiolite Complex; DGC: Demir Kapija–Gevelija Ophiolite Complex. Numbered comments: (1) 11.4 ± 4.5 Ma whole-rock K/Ar age (Arva-Sós *et al.*, 1987); (2) 92.9 ± 3.7 < 2 μm sericite K/Ar age (*ibid*); (3) single-grain, step heating experiment; (4) single-grain, multiple spot fusion experiment; (5) multigrain, step heating experiment; (6)–(9) corrected from 156 ± 3 Ma, 168 ± 7 Ma, 150 ± 2 Ma and 150 Ma respectively, by Spray *et al.*, (1984), using the decay constant by Steiger and Jäger (1977).

Tectonic unit	Occurrence	Rock type	Age ± Method	Component dated	Reference	comment	locality code (Fig. 8)
Gemer-Bükk, S Slovakia	Podšľovák-1 well	anatectic granite	142 6 Rb/Sr	wr	Kováč <i>et al.</i> (1986)		1
Gemer-Bükk, S Slovakia	Dlhá dolina (G. Poloma)	metasomatized granite	151 14 Rb/Sr	wr	Kováč <i>et al.</i> (1986)		2
Gemer-Bükk, S Slovakia	Dlhá dolina (G. Poloma)	metasomatized granite	146 6 Rb/Sr	wr	Kováč <i>et al.</i> (1986)		2
Gemer-Bükk, Meliaticum, NE Hungary	Szalonna	rhyolite	154 38 Rb/Sr	wr	Á. Kovách unpubl. in Kovács (1988)	1	3
Gemer-Bükk, ?Melaticum, N Hungary	Nagybátony-324 well	andesite	154 3 K/Ar	wr, plag, cel	Árva-Sós <i>et al.</i> (1988)		4
Sava Composite Unit, SW Hungary	Inke-1 well, sample I.11	metarhyolite	184 52 Rb/Sr	wr	Árkai <i>et al.</i> (1991)	2	5
Mirdita Zone, Albania	Fierzë	granite	168 4 K/Ar	n.s.	Castorina <i>et al.</i> (1995)		6
Mirdita Zone, Albania	Fierzë	granite	186 9 Rb/Sr	n.s.	Castorina <i>et al.</i> (1995)		6
Mirdita Zone, Albania	Fierzë	granite	174 15 FT	zircon	Muceku <i>et al.</i> (2006)		6
Mirdita Zone, Albania	Shëmri	plagiogranite	165 3.1 ID-TIMS U/Pb	zircon	Dilek <i>et al.</i> (2001, 2007)		7
Mirdita Zone, Albania	Shëmri	plagiogranite	164 3.9 Ar/Ar	amphibole	Vergély <i>et al.</i> (1998), Dimo-Lahitte <i>et al.</i> (2001)	3	7
Mirdita Zone, Albania	Paluçë	plagiogranite	162 0.4 ID-TIMS U/Pb	zircon	Dilek <i>et al.</i> (2001, 2007)		8
Mirdita Zone, Albania	Tuç/Lumbardhë	plagiogranite	166 0.6 ID-TIMS U/Pb	zircon	Dilek <i>et al.</i> (2001, 2007)		9
Mirdita Zone, Albania	Kimëz	plagiogranite	163 0.6 ID-TIMS U/Pb	zircon	Dilek <i>et al.</i> (2001, 2007)		10
Mirdita Zone, Albania	Rubik	plagiogranite	160 0.4 ID-TIMS U/Pb	zircon	Dilek <i>et al.</i> (2001, 2007)		11
Mirdita Zone, Albania	Bulqiza	leucocratic dike	173 1.7 Ar/Ar	biotite	Vergély <i>et al.</i> (1998), Dimo-Lahitte <i>et al.</i> (2001)	4	12
Mirdita Zone, Albania	Tropoja massif	"vein"	160 2.6 Ar/Ar	phlogopite	Vergély <i>et al.</i> (1998), Dimo-Lahitte <i>et al.</i> (2001)	5	13
Vardar Zone, Vojvodina, N Serbia	Miloševo	granite	130 n.s. K/Ar	n.s.	A. Lovrić unpubl. in Čanović and Kemenci (1988)		14
Vardar Zone, Central Serbia	ŽOC	quartz diorite	168 7 K/Ar	amphibole	Resimić-Šarić <i>et al.</i> (2005)		15
Vardar Zone, Central Serbia	ŽOC	quartz monzodiorite	145 6 K/Ar	amphibole	Resimić-Šarić <i>et al.</i> (2005)		15
Vardar Zone, FYR Macedonia	DGC, Štip	granite	161 3 K/Ar	biotite	G. Soptrajanova unpubl. in Spray <i>et al.</i> (1984)	6	16
Vardar Zone, FYR Macedonia	DGC, Madenska Reka	biotite granite	143 7 K/Ar	n.s.	Stojanov and Svešnikova (1984)		17
Vardar Zone, FYR Macedonia	DGC, Madenska Reka	granite	136 6 K/Ar	n.s.	Stojanov and Svešnikova (1984)		17
Vardar Zone, FYR Macedonia	DGC, Madenska Reka	"granosyenite"	113 5 K/Ar	n.s.	Stojanov and Svešnikova (1984)		17

(continued)

Tectonic unit	Occurrence	Rock type	Age ± Method	Component dated	Reference	comment	locality code (Fig. 8)
Vardar Zone, FYR Macedonia	DGC, Furka	granite	173 7 K/Ar	biotite	G. Soptrajanova unpubl. in Spray <i>et al.</i> (1984)	7	18
Vardar Zone, FYR Macedonia	DGC, Furka	granitoid n.s.	161 5 K/Ar	n.s.	Boev and Lepitkova (2002)		19
Vardar Zone, FYR Macedonia	DGC, Gurničet	granitoid n.s.	152 2 K/Ar	n.s.	Boev and Lepitkova (2002)		20
Vardar Zone, FYR Macedonia	DGC, Smokvica	syenite porphyry	155 6 Ar/Ar	n.s.	Boev and Lepitkova (2002)		21
Vardar Zone, Greece	DGC, Fanos	granite	153 2 K/Ar	biotite	Borsi <i>et al.</i> (1966)	8	22
Vardar Zone, Greece	DGC, Fanos	granite	153 n.s. Rb/Sr	biotite	Borsi <i>et al.</i> (1966)		22
Vardar Zone, Greece	DGC, Fanos	granite	148 3 K/Ar	biotite	Spray <i>et al.</i> (1984)	9	22
Vardar Zone, Greece	DGC, Fanos	granite	148 4 K/Ar	biotite	Marakis (1970)		22
Vardar Zone, Greece	DGC, Fanos	granite	158 1 SHRIMP U/Pb	zircon (CL)	Anders <i>et al.</i> (2005)		22
Vardar Zone, Greece	DGC, Lahanas	granite	140 4 K/Ar	biotite	Marakis (1970)		23
Vardar Zone, Greece	DGC, Skra	mylonitized granite	155 2 SIMS U/Pb	zircon (CL)	Anders <i>et al.</i> (2005)		24
Vardar Zone, Greece	DGC, Skra	mylonitized granite	155 2 SIMS U/Pb	zircon (CL)	Anders <i>et al.</i> (2005)		24
Vardar Zone, Greece	DGC, Mikro Dassos	rhyolite	164 2 SIMS U/Pb	zircon (CL)	Anders <i>et al.</i> (2005)		25
Vardar Zone, Greece	DGC, Pigi	orthoigneiss	158 4 EPMA (U-Th)/Pb	monazite	Anders <i>et al.</i> (2005)		26
Vardar Zone, Greece	Monopigadon	granodiorite	142 3 K/Ar	biotite	Michard <i>et al.</i> (1998)		27
Vardar Zone, Greece	Monopigadon	granite	149 n.s. n.s.	n.s.	unpubl. in Mussallam and Jung (1986)		27
Vardar Zone, Greece	Monopigadon	granite	161 n.s. ID-TIMS U/Pb	zircon	Koroneos <i>et al.</i> unpubl. in Koroneos <i>et al.</i> , (2001)		27
Vardar Zone, Greece	Thessaloniki	granitic pegmatite	156 n.s. K/Ar	n.s.	Kreuzer, unpubl. in Mussallam and Jung (1986)		28
Vourinos Ophiolite, Greece	Mikroklissoura	plagiogranite	173 3 SHRIMP U/Pb	zircon (CL)	Liati <i>et al.</i> (2004)		29
Southern Apuseni Mts., Romania	Săvărsin	granite	153 0.6 ID-TIMS U/Pb	zircon	Pană <i>et al.</i> (2002)		30
Southern Apuseni Mts., Romania	Ighiel Valley	keratophyre	160 5 K/Ar	wr	Nicolae <i>et al.</i> (1987)		31

1978; Spray *et al.*, 1984; Dimo-Lahitte *et al.*, 2001; Olker *et al.*, 2001; Chiari *et al.*, 2003; Smith 2006).

Here we present the results of detrital monazite and zircon geochronology and apatite fission track (FT) thermochronology from Central Dinaride Mesozoic sediments genetically linked to Neotethyan evolution, and use these data to further constrain the existence and timing of Jurassic subduction. We also review complementary geochronological data from other segments of the Neotethyan ophiolites.

#### **4.2. Geological setting of the sampled units**

Intensely folded, the Mesozoic '*Zone Bosniaque*' sediments (Aubouin *et al.*, 1970) are tectonically sandwiched into the SW-vergent Dinaride thrust system (Fig. 1). They are overlain by Neotethyan ophiolite thrust sheets floored by continental basement nappes of the Adriatic plate (Aubouin, 1973; Schmid *et al.*, 2008), and overlie the large Adriatic Carbonate Platform (AdCP – Vlahović *et al.*, 2005). The '*Zone Bosniaque*' includes a thick Late Jurassic to Cretaceous flysch sequence sourced from the upper plate complex (Aubouin 1973; Mikes *et al.*, 2008b). Recently, its Early Cretaceous part (Vranduk Formation) revealed heavy mineral associations including zircon and minor monazite. The zircon U/Pb age spectra comprise a Late Jurassic age population (Mikes *et al.*, 2008b).

The AdCP is a Late Palaeozoic to Paleogene carbonate-dominated platform attaining 8-10 km in thickness (Vlahović *et al.*, 2005). It formed the SW basin margin during the Mesozoic evolution of the '*Zone Bosniaque*', and was converted into the tectonic footwall of the Outer Dinaride thrust pile during Tertiary compression (Fig. 1; Aubouin *et al.*, 1970; Chorowicz, 1977; Charvet, 1980; Tari, 2002; Mikes *et al.*, 2008a; Schmid *et al.*, 2008). Late Jurassic sequence of the AdCP is distinguished by its felsic tephra intercalations ('*Lemeš-Schichten*', Furlani, 1910; Šćavničar and Nikler, 1976). Pelagic fossils indicate a Kimmeridgian to Lower Tithonian age for this horizon (Ziegler, 1963; Chorowicz and Geysant, 1972; Vlahović *et al.*, 2005).

### 4.3. Analytical methods

Accessory minerals were separated from three medium-grained sandstone samples in the Vranduk Fm. and from a fresh, friable felsic tephra sample of Lemeš. Sampling localities are shown in Fig. 1 and listed in Appendix 4-4. Methods of preparation, analysis and data processing for in-situ zircon U/Pb geochronology were outlined in detail by Frei and Gerdes (2008) and Mikes *et al.* (2008b). Procedures of apatite FT analysis followed Dunkl *et al.* (2001). Total (Th-U)/Pb geochronology of monazite was carried out in-situ by electron microprobe analysis (Montel *et al.* 1996; Jercinovic *et al.*, 2008). Five to ten spots were placed on homogeneous internal domains in each monazite grain, to reduce age uncertainty (Williams *et al.*, 2006). In the absence of age mapping (Williams *et al.*, 1999; Goncalves *et al.*, 2005), this approach helped reducing the risk of analyzing volumes that consist of different age domains. Details of the analytical procedure, age calculation, error treatment and age deconvolution are provided in Appendix 4-5. Elemental detection limits (d.l.) are quoted at the 3 $\sigma$  level throughout.

### 4.4. Results

#### 4.4.1. Monazite dating

A total of 496 single-spot total (Th-U)/Pb age datum was acquired on 79 grains from three samples. Analytical results are listed in Appendix 4-2. Only little inter-sample difference was noticed in chemistry and texture, thus the results are discussed together.

ThO<sub>2</sub> concentrations are typically in the range between 3 and 7 wt%, with UO<sub>2</sub> generally not exceeding 0.8 wt%. About 95% of the measured Pb contents range from 186 to 835 ppm, significantly above the d.l. of ca. 90 ppm. Most Eu concentrations do not exceed 800 ppm (d.l.: 270 ppm), Sr was below d.l. (120 ppm). Chondrite-normalized rare earth element (REE) concentrations show a slight decrease from light REE to middle REE. All grains with Eu above d.l. display a strong negative Eu-anomaly with Eu/Eu\* mostly around 0.02 and invariably <0.3 (Fig. 2). Y<sub>2</sub>O<sub>3</sub> concentrations vary in a wide range from 0.14 to 5.3 wt%, although they are more restricted in the Permian grains (Fig. 3).

The analyses define two well-separated age populations (Fig. 4, Table 2): a predominant Middle/Late Jurassic group with a total (Th-U)/Pb age of  $164 \pm 3$  Ma; and a minor Early/Middle Permian group with a total (Th-U)/Pb age of  $274 \pm 13$  Ma.

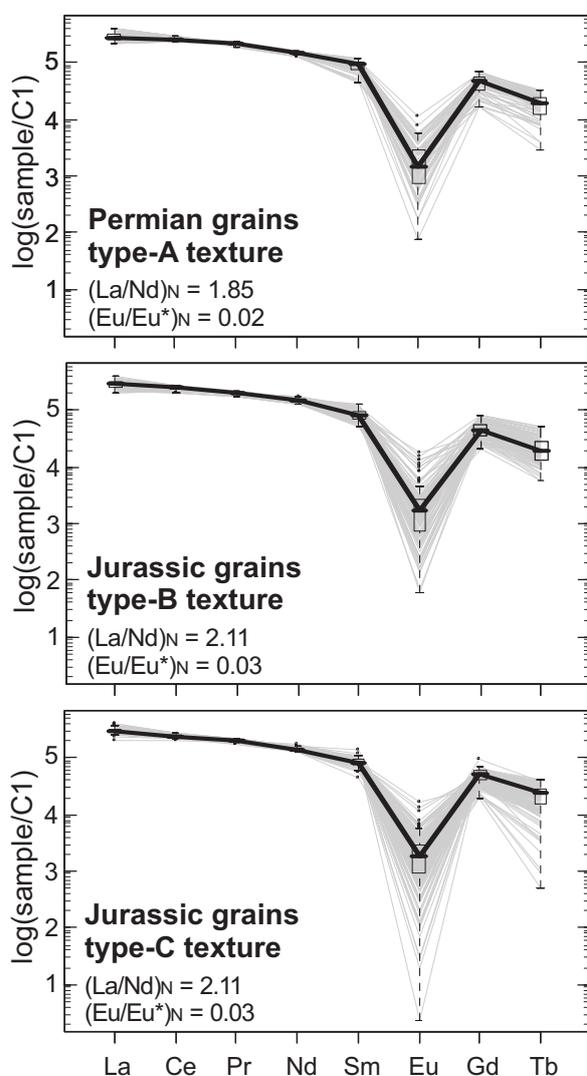


**Fig. 2.** Chondrite-normalized REE patterns of the detrital monazite grains. Plots subdivided on the basis of grain age and textural assignment (see Fig. 5). Grey lines connect all single spots, black line represents their median. Boxes and whiskers comprise the central 50% and 95% of the data, respectively. Note that in ca. two-thirds of the analyses, Eu was below the d.l. (ca. 270 ppm). This implies that the actual overall range of the Eu anomaly in these detrital grains can be a few orders of magnitude larger than displayed. La/Nd and Eu/Eu\* are median values. Chondrite composition taken from Taylor and McLennan, 1985.

The BSE images reveal several distinct texture types, mainly controlled by Th and Y distribution (Fig. 5). Type A is distinguished by slightly rounded crystals, with very fine oscillatory zoning combined with sector growth, the sector boundaries often being slightly diffuse. Type B grains are euhedral and exhibiting a composite zoning of large internal domains with homogeneous intensity distribution and sharp boundaries, surrounded by simple, oscillatory zoned rims. Type C also comprises euhedral grains but with a complex patchwork of irregular, curvilinear to flame-like domains in grain interiors. This latter texture is suggestive of fluid-controlled dissolution-precipitation processes following monazite growth (Putnis, 2002; Harlov *et al.*, 2007). BSE images allow to examine a possible relationship between age data and textural patterns.

Type A grains typically yielded Permian dates, whereas most Type B and C grains gave Jurassic dates. The ages neither show an obvious interrelation with the degree of textural disturbance, nor with spot position in the grain. This suggests either the interaction of monazite with fluids of low (epidote-amphibolite facies) maximum tempera-

tures, leaving its Th-U-Pb element systematics largely undisturbed after crystallization (Teufel and Heinrich, 1997; Seydoux-Guillaume *et al.*, 2002, 2004), or points to a higher-temperature, high-pH autometasomatic overprint that resulted in (Th-U)/Pb ages indistinguishable from those of the undisturbed crystals (Harlov *et al.*, 2007; Koepke *et al.*, 2007).

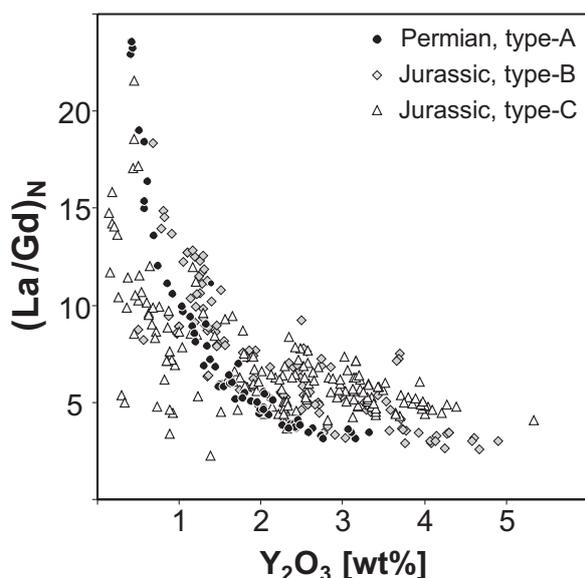


**Fig. 3.** Chondrite-normalized La/Gd ratios as a measure of light REE fractionation, plotted against  $Y_2O_3$  concentrations. Symbols subdivided on the basis of grain age and textural assignment (see Fig. 5). Note the difference in REE behaviour between the age populations. Chondrite composition taken from Taylor and McLennan, 1985.

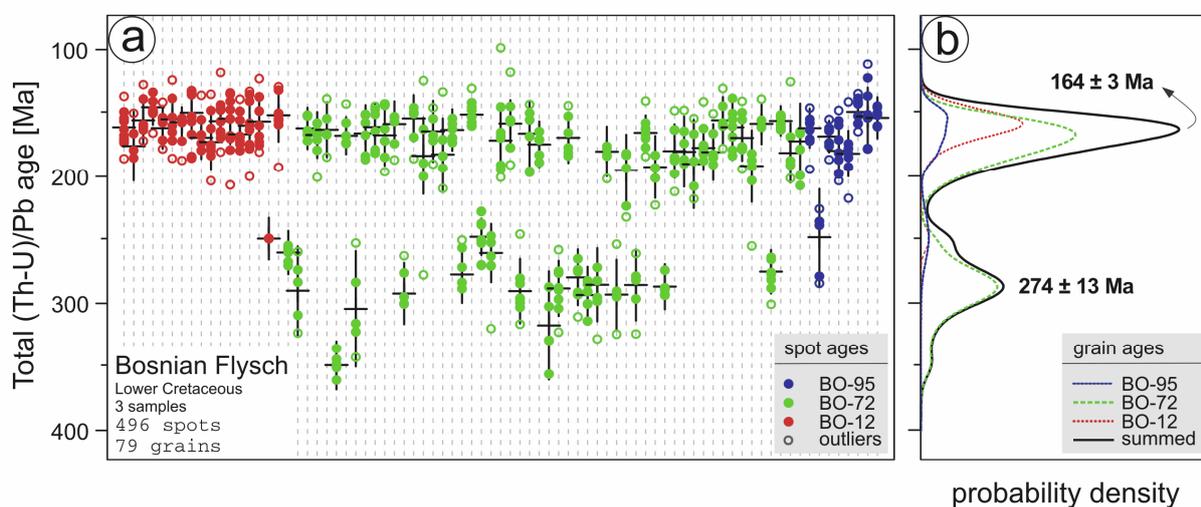


**Fig. 4.** EPMA (Th-U)/Pb chemical age distribution of detrital monazite grains from the Lower Cretaceous Vranduk Formation of the Bosnian Flysch. **(a)** Dot-chart showing individual spot ages, arranged vertically for each grain. Single grain ages were calculated by the weighted average of all spot ages passing the Grubbs-test (see electronic supplement for details). Thin vertical bars:  $2\sigma$  confidence interval around the mean grain ages (horizontal marks). **(b)** Single-grain age distribution and the most probable ages ( $\pm 2\sigma$  s.e.) for both the Jurassic and Permian populations. Refer to Table 2 and Appendix 4-6 for details of age deconvolution.

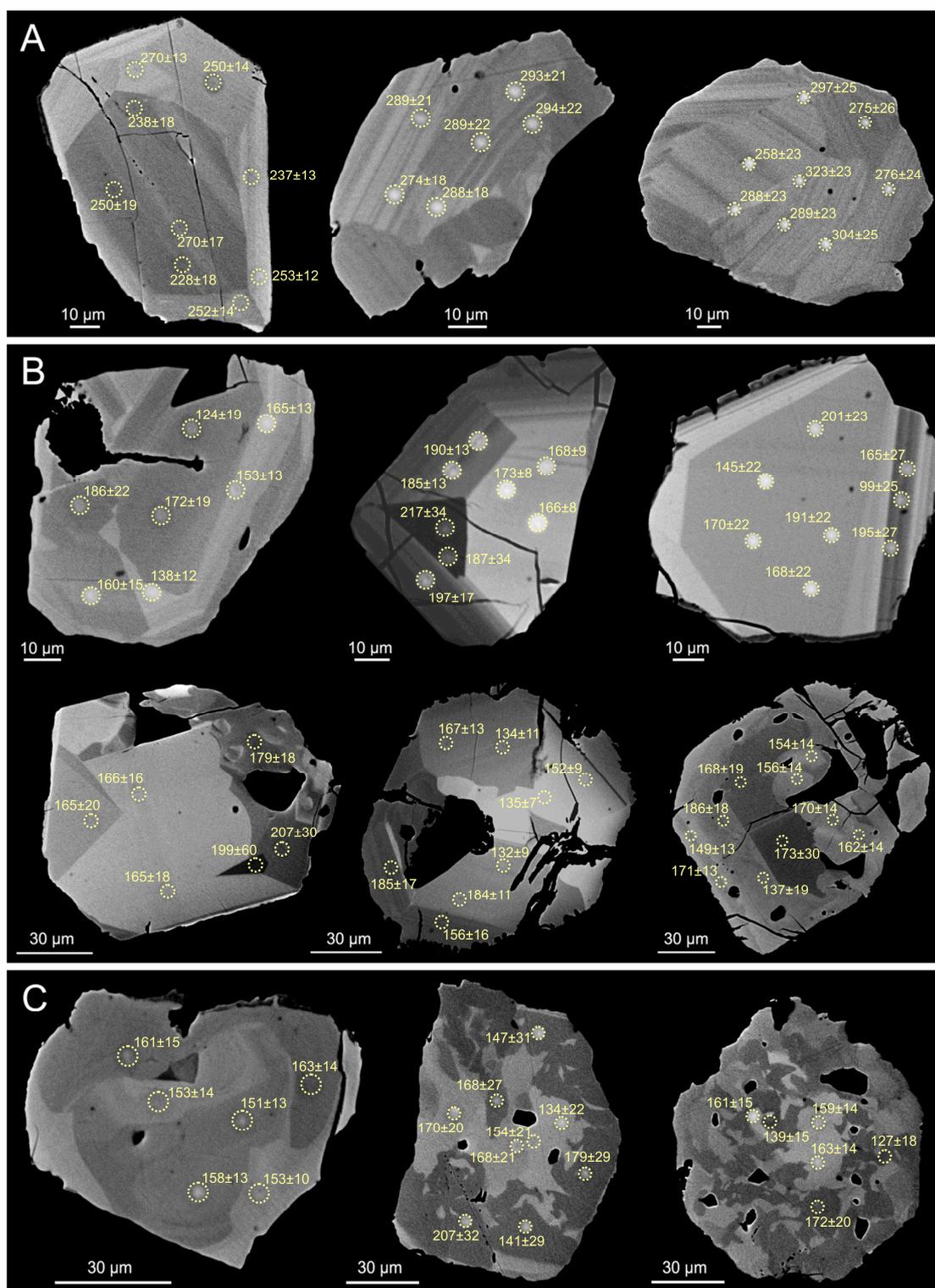


**Fig. 5.** Characteristic textural patterns of the detrital monazite grains as revealed by back-scattered electron imaging. Spot ages (in Ma,  $\pm 2\sigma$  s.e.) are also shown. **Type A:** subangular grains with fine oscillatory zoning locally combined with sector growth. Sector boundaries are usually slightly diffuse. This texture type is typical for most grains dated as Permian. **Type B:** mostly euhedral grains exhibiting a composite zoning of large internal domains with homogeneous intensity distribution and mostly sharp boundaries, surrounded by simple, oscillatory zoned rims. **Type C:** mostly euhedral grains with complex patchwork of irregular, rounded to flame-like domains, suggestive of fluid-controlled dissolution-precipitation processes after monazite growth. Grains of texture types (B) and (C) typically yielded Jurassic ages. No correlation was found between the intensity of textural disturbance and the variance of spot ages.

#### 4.4.2. Zircon U/Pb geochronology

Oscillatory zoning and euhedral crystal shape was indicated by a BSE survey prior to the dating procedure. Age results from the Vranduk Fm. sample are listed in Appendix 4-3. In the following, we evaluate these data together with another detrital zircon U/Pb dataset from the same stratigraphic unit (Mikes *et al.*, 2008b). 89% of the single-grain ages are within  $\pm 14\%$  of concordance with their propagated  $2\sigma$  standard errors, with the summed  $^{206}\text{Pb}/^{238}\text{U}$  age spectrum of 361 grains from five samples revealing a broad scatter in zircon age distribution (Fig. 6). At least two age clusters characterize the dataset; a Late Jurassic and a Permo-Triassic group with their modi around 152 and 245 Ma, respectively. Each of them accounts for about 20% of all dated crystals. A minor but probably distinct Early/Middle Jurassic population around 185 Ma partly overlaps the Late Jurassic population (Fig. 6, Table 2). Age distributions of individual samples are comparable, although one out of five samples does not contain a significant Jurassic population (Mikes *et al.*, 2008b).

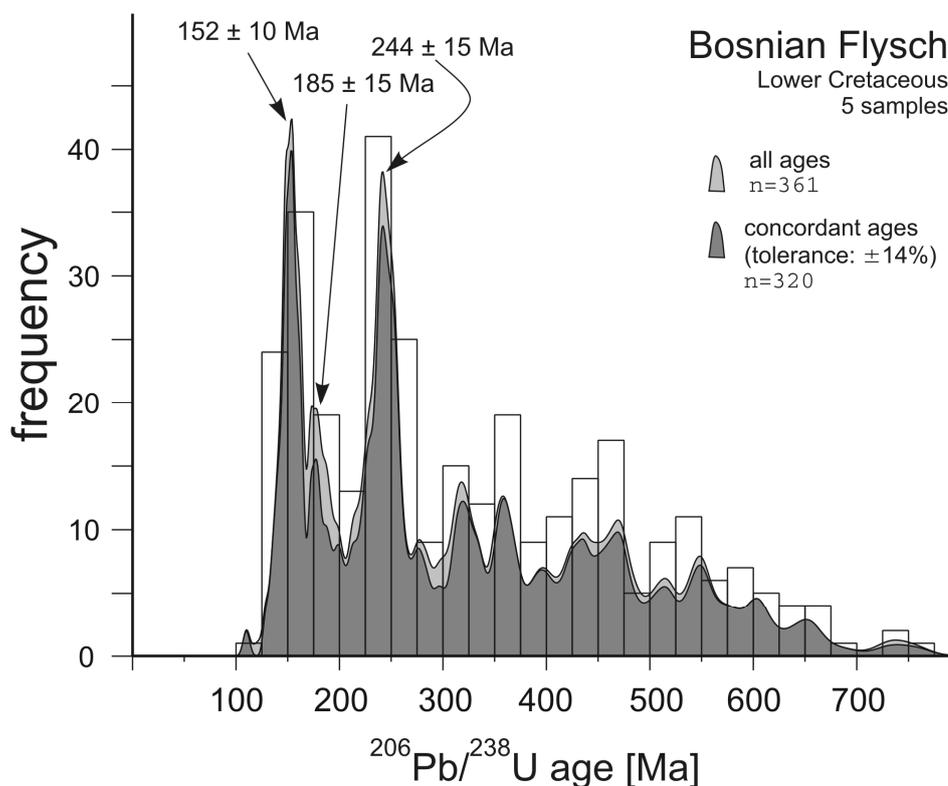
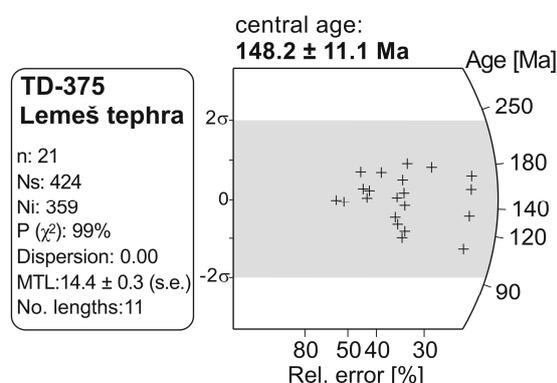


**Fig. 6.** Summed distribution of detrital zircon single-grain U/Pb ages from five sandstone samples of the Lower Cretaceous Vranduk Formation of the Bosnian Flysch. Data partly taken from Mikes *et al.*, (2008). Subordinate grains older than 800 Ma (14% of the dataset) are not shown. Age distribution calculation according to Sircombe (2004). Arrows indicate the most probable population ages in the <290 Ma portion (see also Table 2).

## 4.4.3. Apatite fission track dating

Analytical results of the Lemeš tephra sample are shown in Fig. 7. The age distribution is unimodal, with a central age of  $148 \pm 11$  Ma, consistent with the Kimmeridgian–Lower Tithonian biostratigraphic age assignment of the host strata (see above). Track-length distribution ( $14.4 \pm 0.3$   $\mu\text{m}$ ;  $n=11$ ) gives no evidence for track annealing and significant post-depositional heating. The obtained low FT age dispersion suggests a single-component population with no detrital admixture. The apatite FT age is interpreted as indicating Late Jurassic volcanic activity.

**Fig. 7.** Results of apatite FT dating of the Lemeš tephra sample. Radial plot according to Galbraith (1990). The largely unannealed tracks (mean track length:  $14.4 \pm 0.3$   $\mu\text{m}$ ) suggest that Late Jurassic and younger horizons of the AdCP did not experience significant post-depositional heating. Low age dispersion points to a single age component in the Lemeš tephra, i.e. no contribution from detrital grains. Central age calculated according to Galbraith and Laslett (1993).



mineral dating method	apatite FT analysis	monazite EPMA (Th-U)/Pb		zircon LA-ICPMS U/Pb	
		Popshare	Isoplot	Popshare	Isoplot
software used for age deconvolution	-	2	2	3	3
age components	1	2	2	3	3
grains (n)	21	79	79	191	191
<i>age comp. I (Ma)</i>	148.2	163.8	163.3	151.6	151.1
s.e. (2 $\sigma$ , Ma)	11.1	3.0	2.3	9.6	10.8
s.d. (1 $\sigma$ , Ma)	-	11.2	8.9	37.9	42.8
fraction (%)	-	70	75	32.6 (17.2)	33.0 (17.5)
<i>age comp. II (Ma)</i>	-	274.1	278.5	184.8	183.5
s.e. (2 $\sigma$ , Ma)	-	13.2	4.9	14.8	19.3
s.d. (1 $\sigma$ , Ma)	-	32.1	10.9	46.6	59.8
fraction (%)	-	30	25	20.8 (11)	20.0 (10.6)
<i>age comp. III (Ma)</i>	-	-	-	244.3	245.5
s.e. (2 $\sigma$ , Ma)	-	-	-	15.0	15.2
s.d. (1 $\sigma$ , Ma)	-	-	-	70.8	72.0
fraction (%)	-	-	-	46.6 (24.7)	47.0 (24.9)

**Table 2.** Summary of the geochronological results, showing the major age populations. Deconvolution of composite age spectra of monazite and zircon was performed independently by Popshare (Dunkl and Székely, 2002) and Isoplot (Ludwig, 2003) softwares, which yielded consistent results. A most probable age along with its 2 $\sigma$ ( $\pm$ ) standard error is assigned for each separated age component. The 1 $\sigma$ ( $\pm$ ) standard deviations indicate the age range produced by ca. 68% of all grain ages within that component. The zircon dataset was truncated at 290 Ma to facilitate a meaningful deconvolution in the discussed age range. Values in parantheses express the fractions as related to the whole (not truncated) zircon dataset ( $n=361$ ). See Appendix 4-6 for statistical details.

## 4.5. Discussion

### 4.5.1. Magmatic origin of the Jurassic apatite, monazite and zircon crystals

The significance of the Late Jurassic tephra layer preserved in the AdCP sequence is that it records explosive volcanism coeval to Neotethyan convergence, an event for which no geochronological record has been previously available in the Dinarides.

Monazite growth from melt is evidenced by the sharp oscillatory zoning of the grains. This is corroborated by the marked negative Eu anomaly (e.g. Nagy *et al.*, 2002; Buick *et al.*, 2006), and by the elevated  $Y_2O_3$  concentrations (up to 5.3 wt%), as Y would preferentially be fractionated into garnet during metamorphism (Gibson *et al.*, 2004). The texturally disturbed grains are likely of the same generation as those exhibiting a normal oscillatory growth: the two texture types yield comparable ages, and intact textural domains are occasionally preserved in some grains. Magmatic monazite is common to felsic, Ca-poor peraluminous melts but is rare in peralkaline environment where light REE are fractionated into apatite and allanite (Watt and Harley 1993). The textural and REE variations (Figs. 3 & 5) can be explained in terms of coeval growth from separate melts each with slightly distinct element budget and degree of differentiation.

As for zircon, 96-98% of the Jurassic age population exhibits a Th/U ratio  $>0.1$  (typically 0.05-1.1; Appendix 4-3), characteristic of magmatic growth (Rubatto, 2002), although the validity of this approach was questioned (Harley *et al.*, 2007). A metamorphic origin however, is unlikely also for zircon because the evolution of the Dinaride passive margin during Late Jurassic obduction did not involve any high-temperature metamorphic event (Schmid *et al.*, 2008; Mikes *et al.*, 2008b).

### 4.5.2. Regional comparisons

Felsic igneous rocks associate Jurassic Neotethyan ophiolites in the Carpathian-Pannonian-Dinaride-Hellenide region at several locations, either intruding mafic/ultramafic lithologies or interfingering with *mélange* deposits. Several radiometric age determinations are published for these rocks and are compiled in Table 1 and Fig. 8. Combining these geochronological results with the geochemical

characteristics of the ophiolites (Pamić *et al.*, 2002; Bortolotti *et al.*, 2004; Dilek *et al.*, 2008), source assignment of the dated zircon and monazite crystals becomes ambiguous. From the Middle Jurassic on, oceanic felsic magmatism likely occurred coevally at several settings: at the site of late-stage mid-oceanic spreading, at the SSZ and/or island arc, and via sub-ophiolitic anatexis of underplated oceanic sediments. Analytical uncertainty renders the separation of the various magmatic events and the sole metamorphism difficult (Dimo-Lahitte *et al.*, 2001; Liati *et al.*, 2004).

Our results show that felsic magmatism in the Dinarides was coeval to and also shortly followed the sole metamorphism of the intraoceanic subduction zone (Fig. 8). The geochemical diversity of the plagiogranite bodies investigated so far suggests the addition of crustal components (especially Th, LREE, Zr, Hf) to their source magmas (e.g. Bébien *et al.*, 1997; Aigner-Torres and Koller, 1999), which is a viable scenario above SSZ's (Flagler and Spray, 1991; Pearce, 2003; Metcalf and Shervais, 2008). Explosive volcanism, generation of peraluminous to metaluminous melts from which monazite was crystallized, and previous data showing significant crustal component in the Jurassic plagiogranites and granitoid complexes (Pearce 1989; Aigner-Torres and Koller, 1999; Resimić-Šarić *et al.*, 2005; Anders *et al.*, 2005) all suggest that Dinaride SSZ magmatism played a more important role than considered in previous tectonic reconstructions (Pamić *et al.*, 2002; Dimitrijević *et al.*, 2003). Duration of these processes was constrained to a <30 Ma period by the early Mid-Jurassic onset of subduction and the latest Jurassic completion of ophiolite obduction (Fig. 8).

#### 4.6. Conclusions

Three independent geochronometers applied to detrital minerals from Central Dinaride sediments constrain the timing of Jurassic felsic magmatism in the Neotethys Ocean. Magmatic monazite from synorogenic Vranduk Formation sandstones reveals a dominant  $164 \pm 3$  Ma age component. Zircon U/Pb age spectra contain an age population at  $152 \pm 10$  Ma. Additionally, a tephra horizon in the Adriatic Carbonate Platform bordering the clastic basin is dated at  $148 \pm 11$  Ma, yielding the first Dinaride geochronological datum for explosive volcanism related to Neotethyan convergence. The major period of leucocratic melt generation was restricted to Middle to Late Jurassic times, coeval to and slightly post-dating sub-ophiolitic sole metamorphism. Crystallization of

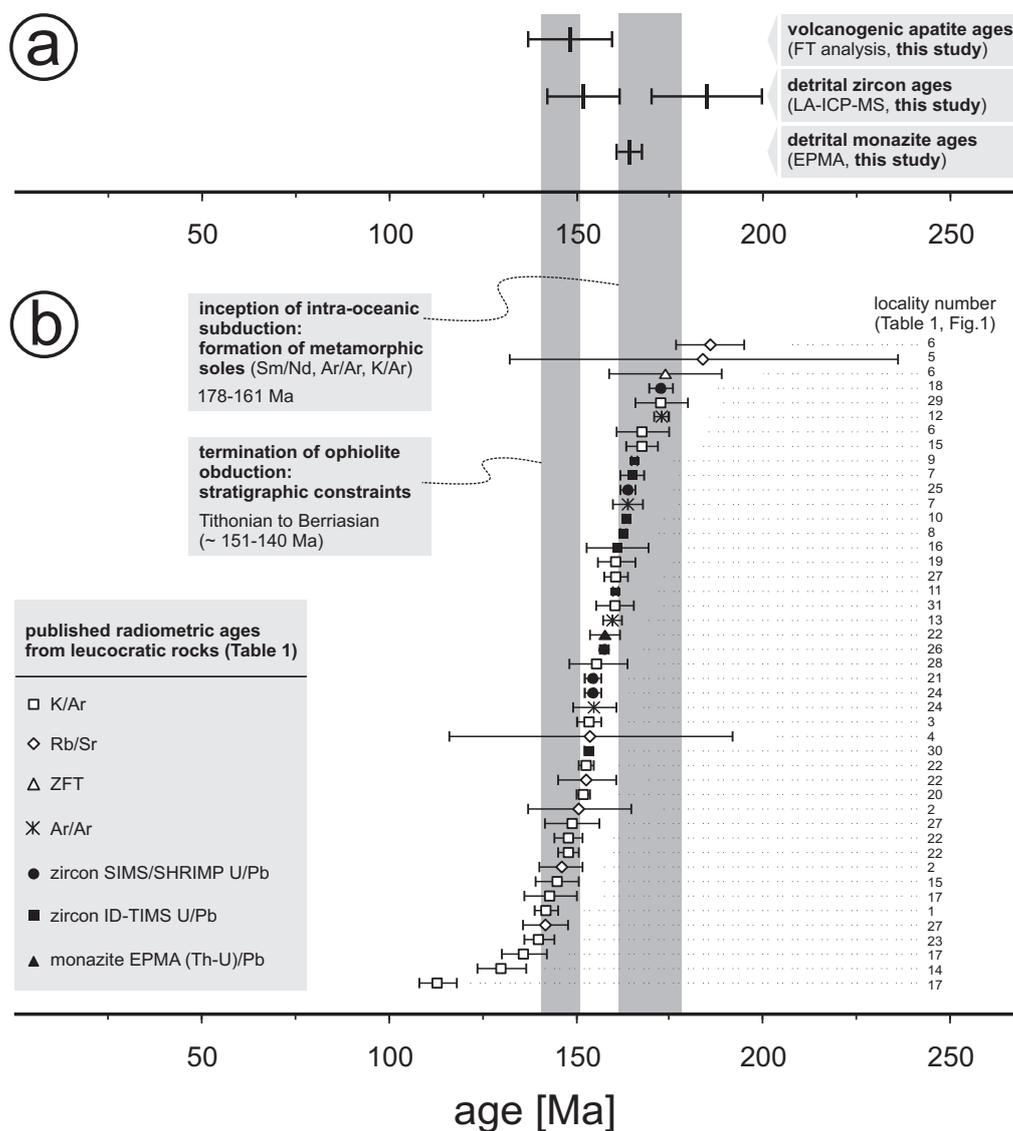


**Fig. 8.** Comparison of the new geochronological data to published radiometric ages from felsic magmatic rocks associating Neotethyan ophiolites of the Carpatho-Pannonian-Dinaride-Hellenide orogen, as compiled in Table 1. (a) Apatite FT (central age  $\pm 2\sigma$  s.e. – Fig. 7), and detrital monazite and zircon geochronological results (population ages  $\pm 2\sigma$  s.e. – see full age spectra in Figs. 4 and 6, resp.). (b) Distribution of the published ages. Legend symbols are arranged in an upward increasing approximate order of thermal sensitivity of the geochronometer used. An estimated error of 5% is assigned to age data for which no error range was specified in the cited work. Note that higher-temperature chronometers (filled symbols) yield older dates than lower-temperature chronometers (empty symbols), and plot closer to the well-constrained age range of the sub-ophiolitic metamorphic soles (right vertical grey bar, 178-161 Ma, see text for references). Within the limit of analytical uncertainties and regional age scatter, felsic magmatism appears to have started coeval with intraoceanic subduction in the early Middle Jurassic (reflected by the sole Ar/Ar ages, that remained largely unaffected by Eoalpine overprint reaching subgreenschist facies) and continued until the at least the Kimmeridgian (reflected by the youngest "high-temperature" geochronologic datum at c. 153 Ma). Note that only lower-temperature chronometers yield post-obduction dates. Biostratigraphic age of the oldest unconformable deposits overlying the obducted Dinaride ophiolites is Tithonian to Berriasian (Mercier, 1966; Bortolotti *et al.*, 1971; Charvet and Termier, 1971; Charvet, 1973).

zircon and especially monazite is consistent with crustal geochemical signatures (elevated Th, LREE, Zr, Hf) reported from both SSZ plagiogranites and calc-alkaline, felsic metaluminous to peraluminous granitoid rocks over the entire Dinaride-Hellenide orogen. Introduction of crustal components into the magmatic source region of these felsic suites was likely controlled by intraoceanic subduction commencing in early Middle Jurassic times.

## *Chapter 5*

# Calcareous nannofossil age constraints on Miocene flysch sedimentation in the Outer Dinarides

---

This chapter is largely identical to the manuscript entitled:  
"Calcareous nannofossil age constraints on Miocene flysch sedimentation in the Outer Dinarides (Slovenia, Croatia, Bosnia-Herzegovina and Montenegro)"  
that has been published in July 2008 in:  
Tectonic Aspects of the Alpine-Dinaride-Carpathian System (Siegesmund, S., Fügenschuh, B. & Froitzheim, N., eds). *Geological Society of London, Special Publications* 298: 335-363, doi:10.1144/SP298.16  
authored by:  
Tamás Mikes, Mária Báldi-Beke, Miklós Kázmér, István Dunkl and Hilmar von Eynatten



# **Calcareous nannofossil age constraints on Miocene flysch sedimentation in the Outer Dinarides**

*Tamás Mikes, Mária Báldi-Beke, Miklós Kázmér, István Dunkl and Hilmar von Eynatten*

## **Abstract**

Flysch deposits are associated with the Outer Dinaride nappe front. They overlie Eocene platform carbonate to bathyal marl successions that subsequently cover Cretaceous platform carbonates of Apulia and the Dinaride nappes. Planktonic foraminifer biostratigraphy indicates Eocene age of flysch sedimentation. New calcareous nannofossil data reveal that several assemblages are present; besides the dominant Mid-Eocene species, Cretaceous, Palaeocene, Oligocene and Miocene taxa were also identified throughout the entire flysch belt. Widespread occurrence of nannofossil species of zone NN4-6 indicate that flysch deposition lasted up to at least Mid-Miocene. Ubiquitous occurrence of various pre-Miocene taxa demonstrate that extensive, possibly submarine sediment recycling has occurred in the Cenozoic.

As flysch remnants are typically sandwiched between thrust sheets, these new stratigraphic ages give a lower bracket on deformation age of the coastal range. The data provide a link between Cretaceous compression in the Bosnian Flysch and recent deformation in the Adriatic offshore area.

## **5.1. Introduction**

Cenozoic synorogenic clastic rocks overlie an upward-deepening Eocene carbonate platform to bathyal marl succession of the Apulian foreland and of the outermost parts of the SW-vergent Outer Dinaride thrust belt (Fig. 1). Established mostly on the basis of planktonic foraminifera, and locally by calcareous nannofossils, the stratigraphic age of the deposits has been traditionally placed into the Mid- or Late Eocene (Table 1). A SE-directed orogen-parallel younging of Palaeogene sedimentation has been inferred by Piccoli and Proto Decima (1969).

Recent calcareous nannofossil studies indicate, however, that at several locations in the central and SE part of the basin system clastic deposition lasted up to the Middle Miocene (review in de Capoa and Radoičić 2002). In addition, tectonic slices of older flysch series dated or inferred to be of Late Cretaceous and Palaeogene age are found in the inner part of the Dinaride imbricate thrust belt occupying structurally higher positions.

These contradictory data pose a series of important questions that need to be addressed in detail:

- (1) Can ages younger than Eocene be demonstrated in the NW parts of the coastal flysch zone, too?
- (2) Why do the age data from planktonic foraminifera and calcareous nannofossil studies seem to mismatch?
- (3) Where and when did flysch deposition start? Are the deposits in the main belt and those preserved in narrow thrust slices related?
- (4) Does revised biostratigraphy support the idea of diachronic onset of deposition along the orogenic front?
- (5) What is the bearing of such young stratigraphic ages on the understanding of the Outer Dinaride geodynamic evolution?

In the present paper, new results of a calcareous nannofossil study are reported, obtained from several flysch localities throughout the Outer Dinaride region. Areas of large-scale regional sampling included the Trieste-Koper and Pazin Basins at Istrian Peninsula, the Northern Kvarner Islands (Krk and Rab), Pag Island, Šopot section near Benkovac in Northern Dalmatia, Central Dalmatia, Southern Dalmatia, Montenegro

coast as well as the “Dalmatian-Herzegovinian Zone” of Southern Bosnia-Herzegovina and Montenegro inland (Fig. 1, Appendix 5-2).

## 5.2. Geological setting and sedimentology

The Outer Dinarides and their foreland are dominated by the thick deposits of the Adriatic Carbonate Platform (AdCP – Vlahović *et al.*, 2005) that existed throughout the entire Mesozoic until its final drowning in the Mid-Eocene. Structurally, it consists of two parts: the lower plate corresponds to autochthonous Apulia, while the upper plate forms a broad, ca. 100 km wide zone made up of the Dinaride nappes and imbricate thrust sheets. These units are built up mainly of Cretaceous rudistid limestones and Eocene foraminiferal limestones and marls and are covered by Tertiary flysch that inter-fingers with and underlies shallow marine to continental clastic sediments. For extensive reviews of the Cenozoic stratigraphy the reader is referred to Drobne (1977); Marjanac and Čosović (2000) and Čosović *et al.*, (2008). The carbonate nappes are thrust by the folded, Mesozoic units of the Bosnian Flysch and its low-grade metamorphic, Palaeozoic basement, the Bosnian Schist Mountains (BSM). They underwent Early Cretaceous metamorphism and the BSM was exhumed during the Eocene-Oligocene (Pamić *et al.*, 2004; Petri, 2007).

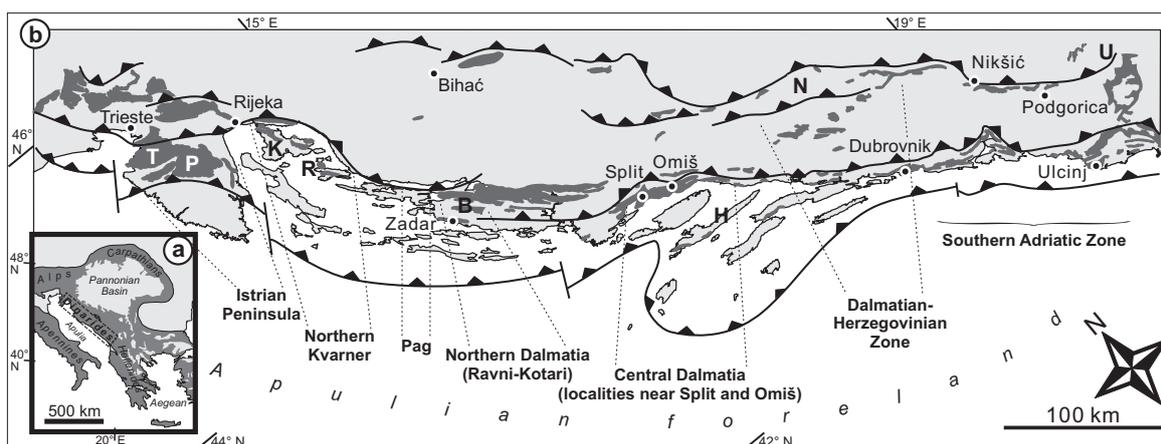


**Fig. 1.** (a) Position of the Dinarides within the European Alpine chain. Dark grey: Alpine orogen; light grey: postorogenic basins. (b) Schematic geological setting of the Outer Dinarides with locations of the major sampling areas. Light grey: substrate of the flysch – mainly Palaeozoic to Mesozoic formations, dominantly platform carbonates. Dark grey: Cenozoic flysch and associated shallow marine sediments in the Outer Dinaride foreland basin system. T, Trieste-Koper Basin; P, Pazin Basin; K, Krk Island; R, Rab Island; B, Benkovac town; H, Hvar Island; U, Kuči Thrust; N, Nevesinjsko Polje. Position of thrusts after the Geological Map of Yugoslavia (F.G.I. 1970), Tari (2002) and Schmid *et al.* (2006).

The Outer Dinaride flysch is part of the fill of a large foreland basin system at the front of the thrust wedges (Fig. 1). Sub-basins stretch from the Southern Alps along the Adriatic Sea coastline as far to the SE as the Hellenides. Stratigraphic position of the flysch is described in terms of a Palaeogene marine sequence overstepping the Cretaceous platform. The underlying foraminiferal ramp covers a regionally widespread unconformity and started to develop in the Palaeocene with paralic deposits. Facies development indicates transgression throughout the Early to Middle Eocene but the sequence is punctuated with a number of short-lived subaerial exposure events probably due to the interplay of eustatic oscillations in a shallow marine environment and the effects of ongoing compressional tectonics affecting the Adriatic area already since the Cretaceous (Channell *et al.*, 1979; Mindszenty *et al.*, 1995; Pamić *et al.*, 1998). The Eocene carbonate unit is rarely thicker than 200 m and is overlain by the "Transitional Beds" – a deepening-upward shelf to shallow bathyal sequence several tens of metres thick, characterized by increasing amount of pelagic biota, glauconite and silt upsection. Its thin lower part is referred to as "Marl with crabs", passing upwards into the thick "*Globigerina* Marl" (e.g. Juračić 1979; Čosović *et al.*, 2004).

The flysch rests upon the "*Globigerina* Marl". Their contact is conformable at places but angular or erosional unconformities have been often reported (e.g. Marinčić 1981; Marjanac *et al.*, 1998; Marjanac 2000). Due to repetitive thrusting, flysch profiles are usually truncated and less than 100-400 m thick. The offshore succession resting on the Apulian plate is gently folded, reaches up to the Neogene, and may exceed 1000 m in thickness (e.g. Tari-Kovačić 1998).

Turbidite beds are dominantly composed of siliciclastics with variable (0-50%) amounts of carbonate admixture. In the N part of the basin, palaeocurrent data were interpreted as resulting from largely SW-directed primary, and SE-directed deflected (longitudinal) flows (e.g. Magdalenić 1972; Babić and Zupanić 1983; Orehek 1991). Radial current directions are commonly found in Central Dalmatia, resulting from complex basin floor topography and multiple flow reflection (Marjanac 1990).

A clear NE-directed flow direction can be observed in the N part of the basin on carbonate debrites and calciturbidites that intercalate into the siliciclastic succession (Engel 1974; Babić and Zupanić 1996). The coarser-grained debrites range in composition from breccia consisting exclusively of well-cemented Eocene foraminiferal limestone lithoclasts, through mixed ones having much isolated larger foraminifer tests and rhodoliths beside the lithoclasts, to pure grain- or matrix-supported debrites made

up of *Nummulites* tests. Marl and Upper Cretaceous limestone clasts are subordinate (Skaberne 1987; Magdalenić 1972; Hagn *et al.*, 1979; Marjanac and Marjanac 1991; Radoičić *et al.*, 1991; Tunis and Venturini 1992; Babić *et al.*, 1995; Marjanac 1996; Tomljenović 2000; Bergant *et al.*, 2003; Pavlovec 2003).

Based on its narrow appearance in map view and the – largely scattered – uniform, longitudinal, SE-directed palaeoflow indicators, the flysch basin has been interpreted as a single major elongated trough (e.g. Marinčić 1981). However, flysch deposits at places rapidly grade upsection into thick sandstone beds deposited in shallow shelf environments, pointing to a complex, dissected basin floor topography with different subsidence histories in the individual domains (Zupanič and Babić 1991; Babić *et al.*, 1993; Babić and Zupanič 1998). Rapid upward decrease of water-depth in the upper part of the thin flysch sequences have also been observed in other localities at the Island of Pag and in Northern Dalmatia (Lj. Babić, pers. comm. 2005).

### 5.3. Present status of flysch biostratigraphy

Traditionally, Cenozoic clastic strata stretching along the Adriatic coast have been regarded as Middle to Late Eocene in age. Ages based on planktonic foraminifera and partly on nannofossil range from Early Eocene to Early Oligocene, mostly Bartonian to Priabonian, as summarized in Table 1. Piccoli and Proto Decima (1969) recognized that the ages become progressively younger towards the SE. Since then, deposition of the flysch in the coastal zone has been commonly explained in terms of a SE-directed diachroneity (Marjanac and Čosović 2000; Čosović *et al.*, 2008, and references therein).

Upper Eocene to Lower Oligocene planktonic foraminifera described from Pazin and Motovun localities in Istria and from Hvar Island by Marinčić (1981), and from sites near Split by Grubić and Komatina (1963) received little attention in subsequent works. Recently, Šparica *et al.* (2005) reported Upper Oligocene larger foraminiferal, calcareous nannofossil and pollen assemblages from the Pićan profile in Istria.

The first notion of onshore Neogene is from Puškarić (1987) who proved distinct biozones in two nearby profiles on Hvar Island by means of calcareous nannofossils: NP17 (Bartonian) and NN1 (Uppermost Chattian to Lower Aquitanian). Nannofossil studies of de Capoa revealed Early to Middle Miocene ages up to Serravallian from a considerable number of localities in the central and SE part of the flysch basin (Radoičić *et al.*, 1989, 1991; de Capoa and Radoičić 1994a, b; de Capoa *et al.*, 1995; de Ca-

**Table 1.** Overview of published age data from the Outer Dinaride flysch. Offshore and sporadic mainland data are not included. Whenever available, standard planktonic foraminifer or calcareous nannoplankton biozones are also indicated. Results yielding Neogene age are marked bold for clarity. Abbreviations: np - nannofossils, pf - planktonic foraminifera, lf - larger foraminifera, po - palynomorphs, mo - mollusc macrofauna

Area	Age	Locality	Source	Age based on	Biozone	Notes
<b>Istria</b>	Upper Oligocene	Piñan	Sparica <i>et al.</i> (2005)	lf, np, po		
	Priabonian	Oprtalj	Benić (1991)	np	NP18	
	Upper Eocene/Lower Oligocene	Pazin, Motovun	Marinčić (1981)	pf		
	Upper Eocene	Piñan	Drobne <i>et al.</i> (1979)	pf, np		1
	Middle Lutetian to Lower Priabonian	several localities, review	Ćosović <i>et al.</i> (in press)	pf, np	P11-P15	
	Bartonian	Pričejak (Učka)	Benić (1991)	np	NP17	
	Bartonian	Piñan	Benić (1991)	np	NP17	
	Upper Lutetian-Bartonian	Piñan	Hagn <i>et al.</i> (1979)	np, lf, pf	NP16	
	Upper Middle Eocene	several localities	Krašeninnikov <i>et al.</i> (1968)	pf		
	Middle Eocene	Vranja, Velanov brijeg	Stradner (1962)	np		2
	Middle Lutetian	Piñan	Pavlovec <i>et al.</i> (1991)	pf, np		3
	Middle Lutetian	Buzet, Paz, Vranje, Kotle, Draguč	Muldini-Mamužić (1965)	pf		4
	Upper Lutetian-Bartonian	Izola, Piran	Pavšić (1981)	np	NP16	
	Upper Lutetian-Bartonian	Piran	Pavšić & Peckmann (1996)	np	NP16-?NP17	
	Middle Eocene	several localities	Piccoli & Proto Decima (1969)	pf		
	Middle Lutetian to Lower Bartonian	Piñan-Gračiče	Živković & Babić (2003)	pf	P11-P13	
	Cuisian to Middle/Late Lutetian	several localities	Živković (2004)	pf		
<b>Northern Kvarner:</b>	Upper Mid-Eocene	several localities	Šikić (1963)	mo		
<b>Krk</b>	Upper Mid-Eocene	Murvenica	Schubert (1905)	mo		
	Lower Eocene	Omišalj, Baška, Dobrinj	Piccoli & Proto Decima (1969)	pf		
<b>Northern Kvarner:</b>	Upper Mid-Eocene to Upper Eocene	Lopar	Muldini-Mamužić (1962)	pf		
<b>Rab</b>						

(continued)

Area	Age	Locality	Source	Age based on	Biozone	Notes
<b>Pag</b>	Middle Lutetian-Bartonian	Dinjiška	Benić (1975)	np	NP15-17	5
	Middle Eocene	Gorica, Vrčići	Piccoli & Proto Decima (1969)	pf		
<b>Northern Dalmatia (Ravni-Kotari)</b>	Upper Eocene	Šopot	Krašeninnikov <i>et al.</i> (1968)	pf		
	Bartonian to Priabonian	Šopot	Drobne <i>et al.</i> (1991)	pf	P13-P16/17 NP16-17	
	Uppermost Lutetian to Bartonian	Šopot	Benić (1983, <i>fide</i> Marjanac <i>et al.</i> 1998)	np		
	Middle Eocene	Zadar, Zemunik	Piccoli & Proto Decima (1969)	pf		
<b>Central Dalmatia</b>	<b>Lower Tortonian</b>	"Split E"	de Capoa <i>et al.</i> (1995)	np	NN9	
	<b>Middle Miocene</b>	Mravince	de Capoa <i>et al.</i> (1995)	np	NN1	
	<b>Lower Aquitanian</b>	Hvar Island	Puškaric (1987)	np	NP25-NN2	
	<b>Upper Oligocene to Lower Miocene</b>	Jadro quarry	de Capoa <i>et al.</i> (1995)	np		
	Upper Rupelian	Gornje Sitno	de Capoa <i>et al.</i> (1995)	np	NP23	
	Bartonian	Hvar Island	Puškaric (1987)	np	NP17	
	Upper Eocene/Lower Oligocene	Split-Omiš	Grubić & Komatina (1963)	pf		
	Upper Eocene/Lower Oligocene	Hvar Island	Marinčić (1981)	pf		
	Upper Eocene	Marjan Peninsula in Split	Piccoli & Proto Decima (1969)	pf		6
	Priabonian	Hvar Island	Krašeninnikov <i>et al.</i> (1968)	pf		
	Upper Eocene	Hvar Island	Herak <i>et al.</i> (1976)	pf		
	Upper Priabonian	Split	Jerković & Martini (1976)	np		
Bartonian to Upper Priabonian	Hvar Island	Marjanac <i>et al.</i> (1998)	pf		NP19/20 NP17-NP19	
Bartonian	Orebić (Pelješac Peninsula)	Benić (1983, <i>fide</i> Marjanac <i>et al.</i> 1998)	np		NP17	7
<b>Dalm.-Herz. Zone</b>	<b>Lower Tortonian</b>	Vukov Klanac	Radoičić <i>et al.</i> (1991)	np	NN9	
	<b>Lower Tortonian</b>	Badula	Radoičić <i>et al.</i> (1991)	np	NN9	
	<b>Lower Tortonian</b>	Moševčići	Radoičić <i>et al.</i> (1991)	np	NN9	
	<b>Lower Serravallian</b>	Žitomislčići	Radoičić <i>et al.</i> (1991)	np	NN5 top	
	<b>Lower Serravallian</b>	Gradnčići	Radoičić <i>et al.</i> (1991)	np	NN5 (?NN7)	
	<b>Lower Serravallian (?Upper Serravallian)</b>	Dabarsko-Fatničko Polje	Radoičić <i>et al.</i> (1991)	np		

(continued)

Area	Age	Locality	Source	Age based on	Biozone	Notes		
<b>Dalm.-Herz. Zone</b> (cont.)	<b>Upper Burdigalian</b> Middle Eocene Middle Eocene Middle Eocene	Glavatovići	de Capoa & Radoičić (1994b)	np	NN4			
		Ljubuški	Krašennikov <i>et al.</i> (1968)	pf				
		Gornji Studenci	Krašennikov <i>et al.</i> (1968)	pf				
		Lukavačko polje	Krašennikov <i>et al.</i> (1968)	pf				
	<b>S-Adriatic Zone</b>	<b>Lower Tortonian</b> <b>Upper Serravallian</b> (?Lower Tortonian)	Možura North	de Capoa <i>et al.</i> (1995)	np	NN9b		
			Možura-Šaško Brdo	Radoičić <i>et al.</i> (1989)	np			
		<b>Serravallian</b> <b>Lower Serravallian</b>	W of Grbalj	de Capoa <i>et al.</i> (1995)	np			
			Konavle	de Capoa <i>et al.</i> (1995)	np			
		<b>(?Upper Serravallian)</b> <b>Lower Serravallian</b>	Kotor-Trojica	de Capoa & Radoičić (1994a)	np	NN5 top		
			Trojica-Grbalj	de Capoa & Radoičić (1994a)	np		NN5	
<b>Lower Serravallian</b> <b>Lower Serravallian</b>		Tivat	de Capoa & Radoičić (1994a)	np	NN5			
		Petrovac	de Capoa & Radoičić (1994a)	np	NN5			
<b>Lower Serravallian</b> <b>Langhian</b>		Kruševica	de Capoa & Radoičić (1994a)	np	NN5			
		Grbalj	de Capoa <i>et al.</i> (1995)	np	NN5			
<b>?Miocene</b> Oligocene	Kotor-Vrtnac	de Capoa & Radoičić (1994a)	np					
	Ulcinj	Čanović & Džodžo-Tomić (1958)	pf					
Upper Bartonian to Lower Oligocene	Ulcinj	Luković & Petković (1952)	lf					
	Cavtat	Krašennikov <i>et al.</i> (1968)	pf					
Middle to Upper Eocene Bartonian	several localities	Pavić (1970)	pf, lf					
	Izvor Česma	de Capoa & Radoičić (1994a)	np		NP17			

## Notes:

- (1) Drobne *et al.* (1979) report Lower, Middle and Upper Lutetian as well as Upper Eocene planktonic foraminifera and Middle Lutetian nannoplankton from the Pićan flysch. They conclude that age of the strata is Middle Lutetian.
- (2) Age younger than the LO of *Discosaster lodoensis* and *D. kuepperi*, but older than the FO of *Isthmolithus recurvus* and may correspond to the zones NP12-15 as re-interpreted by Jerković & Martini (1976).
- (3) Pelagic foraminifera with different biozonal ranges within Middle Lutetian.
- (4) Flysch contains arenaceous species of Foraminifera, which markedly contrast the *Globigerina* in the "Transitional Beds". The change appears just above the "Nummulite breccia" and was observed at several localities in Istria (Buzet, Kotle, Draguč).
- (5) Summarizing description of 20 samples. Reworked Palaeocene and Lower Eocene forms are also reported.
- (6) reworked Middle Eocene forms are also reported.
- (7) "similarly as in Split region" (Marjanac *et al.* 1998).

poa and Radoičić 2002). Their results are summarized in Table 1. Quantitative test data from nanofossil counting by Radoičić *et al.* (1989) suggest that Miocene forms constitute only a few percent of the dominantly reworked nanofossil assemblage at any locality.

#### 5.4. Methods

Pelitic rocks were collected for nanofossil analysis throughout the flysch belt (Appendix 5-2). This study does not replace detailed sectionwise biostratigraphic work, yet it represents an exemplary sampling of the most suitable outcrops in the entire basin, as such performed for the first time. Rocks were sampled in five various facies: (1) laminated hemipelagic pelite, (2) pelite rip-up clasts found within sandstone turbidite beds, as well as (3) plastically deformed pelite fragments included in clast-supported carbonate breccia or in (4) *Nummulites* debrite, finally, (5) the pelite matrix of matrix-supported debrites made up of limestone clasts and *Nummulites* tests. The small sampled volume of the clasts (few mm<sup>3</sup>) required extreme clean conditions during preparation to avoid contamination.

Standard smear slides were prepared from a total of 69 crushed samples using no chemical treatment or centrifugation. Slides were examined under the microscope in normal and cross-polarized lights at 1250× magnification.

Stratigraphic evaluation was performed for each sample individually, since correlated or thick continuous profiles were not sampled. Evaluation was based on stratigraphic ranges of the taxa alone [from the first (FO) to the last (LO) occurrences, see Appendix 5-1], without using any additional geological information. Species older than the youngest assemblage were also determined and registered, so as to gain information on recycling. In flysch deposits where recycled forms are typically the most abundant, species LO-s are only relevant to the age of the „original” assemblage in the sediment they were eroded from. Sedimentation ages were always established by forms having the youngest FO. In cases where a narrow biozone was proven (e.g. the most frequent NP16), it does not necessarily follow that a „peak sedimentation event” occurred within that zone.

As many long-lived Cenozoic taxa reach into the Neogene, the identified specimens could be either autochthonous or allochthonous, but both types may also occur together in

the sample and cannot be distinguished from each other. This is crucial insofar as abundance of the youngest zonal markers was often found to be extremely low.

Calcareous nannofossil classification in this paper follows Bown and Young (1997) for the Mesozoic and Young and Bown (1997) for the Cenozoic. Ranges of Cretaceous species are from Burnett (1998) and Perch-Nielsen (1985a), while Palaeogene species ranges are from Perch-Nielsen (1985b) and Báldi-Beke (1977; 1984). With respect to Neogene, the latest summary of Young (1998) was used, a work taking also results from the Mediterranean into consideration (Fornaciari *et al.*, 1996; Fornaciari and Rio 1996). The applied nannoplankton zonation is from Martini (1971).

The nannofossil assemblages examined are mostly of poor preservation and allowed the estimation of abundances only, without exact counting. Our experience has shown that this procedure is good enough for stratigraphic evaluation if flysch samples are dealt with (e.g. Nagymarosy and Báldi-Beke 1993). Species abundances were variable but generally low, which may depend on their preservation upon long-lasting depositional, diagenetic and weathering processes. Special care was taken to search and identify forms smaller than 10  $\mu\text{m}$ , too, as most Neogene taxa occur in this size range.

### **5.5. Results of nannofossil analyses**

A total of 69 samples were analyzed along the Outer Dinaride coastal range from various tectonostratigraphic units. Four of them were barren of calcareous nannofossils. Estimated taxon abundances are summarized in Table 2. Established stratigraphic ranges for each sample are shown in Fig. 2.

The youngest nannofossil assemblages correspond to the zones NN4-6, placing most of the flysch into the Lower to Middle Miocene, most probably the upper part of this interval, i.e. Langhian to Early Serravallian. In addition, there are many reworked specimens from the Upper Cretaceous, and from the Middle and Upper Eocene – many of them having non-overlapping stratigraphic ranges. The obtained Miocene ages of deposition are rather uniform throughout the flysch zone.





### 5.5.1. Istrian Peninsula: Trieste-Koper and Pazin Basins

Fourteen samples were analyzed from the Istrian Peninsula; seven each from the Trieste-Koper Basin (localities Izola, Dekani, Babiči and two nearby sites each at Korte and Momjan) and from the Pazin Basin (Baredine, Kaščerga, Žlepčari, Pićan and Lukačići). Most of them are dominated by Bartonian nannoflora.

At Dekani village (sample TD11) *Pemma* sp. ind., *Chiasmolithus* cf. *modestus* and *Sphenolithus spiniger* indicate Middle Eocene, whereas at the coastal cliffs of Izola (TD13) the co-occurrence of *Chiasmolithus grandis* and *Reticulofenestra placomorpha* correspond to zones NP16-17, Uppermost Lutetian to Bartonian. The same age was proven at Lukačići (TD171), together with a variable Middle Eocene assemblage. At Pićan (PIC-2) a Bartonian to Priabonian age can be established. Few older Eocene species also occur whose ranges do not reach into zone NP16 (*Tribrachiatus orthostylus*: NP11-12, middle part of the Ypresian; *Discoaster septemradiatus*: NP12-14, Upper Ypresian to Lowermost Lutetian).

Scarce but ubiquitous reworked Cretaceous forms include Lower and Upper Cretaceous markers as well.

In subordinate quantity, Miocene forms were also discovered throughout Istria, in all but one sample. The assemblage *Calcidiscus leptoporus*, *C. premacintyreii*, *Coccolithus miopelagicus*, *Reticulofenestra pseudoumbilicus* (partly >7 µm) and, possibly also six-rayed *Discoaster* spp., hint a Miocene age. In the Pićan (PIC-2), Korte (TD15), Babiči (TD16) and Baštini (TD178) localities, specimens of *Helicosphaera carteri* were also identified. *Helicosphaera carteri* has its FO at the base of Miocene worldwide and is a very characteristic form (Photos 13-14 in Fig. 4). Overall, the identified Neogene species define the zones NN4-6 which correspond to Late Burdigalian to Serravallian age. However, at Izola (TD13), Korte (TD15, TD18), Momjan (TD22) and Babiči (TD16) *Reticulofenestra pseudoumbilicus* is dominated by specimens larger than 7 µm, such occur first in the Langhian, close to base NN5. Neogene nannofossils found near Dekani (TD11) is somewhat poorer than at Pićan, indicating either similar or slightly older, Early Miocene age. At Lukačići (TD171), the Neogene is only represented by few and small specimens of *Reticulofenestra pseudoumbilicus*. Of all, the most diverse Miocene assemblage is identified in the Pićan sample (PIC-2), within a rather fresh pelite rip-up clast from the base of a sandstone turbidite bed. *Sphenolithus conicus*, identified in Istria only in sample MOM-3, ranges

from NP25 to NN3 (Upper Chattian to Middle Burdigalian) and is probably reworked due to the presence of *Coccolithus miopelagicus*, *Reticulofenestra haqii* and *R. pseudoumbilicus* in MOM-3.

#### 5.5.2. Northern Kvarner

Sampling sites are located on Krk and Rab Islands and on the mainland near Crikvenica. Three out of nine samples are barren of nannofossils, the rest being rather poor. They always contain reworked Cretaceous nannofloral elements.

On Krk, near Draga Bašćanska (TD28) only a poor assemblage was found with *Arkhangelskiella* sp. and abundant *Watznaueria barnesae* suggesting a Late Cretaceous age, together with rare Eocene forms. In the slide only two specimens of *Reticulofenestra pseudoumbilicus* >7 µm were found, pointing to zone NN4 or younger, i.e. not older than Burdigalian. A poorly preserved but rather rich Middle Eocene assemblage is found near Bribir (TD29). Although in this sample most species range from Early to Middle Eocene and *Sphenolithus radians* is rather rare from the NP17 upwards, the FO of the larger forms of *Reticulofenestra placomorpha* is in NP16. The nannoflora of Bribir likely indicates the zones NP15-17 of Mid-Lutetian to Bartonian age. Another sample from Štale near Bribir (TD30) also contains a very poor assemblage, with the identified Upper Cretaceous, Eocene and Miocene taxa being represented with only one specimen each.

Three samples are from the clastic sediments of Rab Island. Near the town of Rab (TD32) a scarce but diverse Palaeogene nannoflora was established. The characteristic forms of *Reticulofenestra placomorpha* (FO in NP16), together with *Sphenolithus furcatolithoides* (LO in NP16) indicate the zone NP16, Uppermost Lutetian to Bartonian. A single specimen of Miocene *Reticulofenestra pseudoumbilicus* was also found here. Similarly, in a poor nannoflora at the port of Lopar (TD35) which contains mostly Senonian and Lower to Middle Eocene nannofloral elements, only one specimen is encountered which resembles *Reticulofenestra pseudoumbilicus*. A likewise poor assemblage was obtained from sample TD37 from Dumići, 1 km NW of Supetarska Draga. Among its Eocene species, *Discoaster lodoensis* has the shortest range, and indicates Late Ypresian to Early Lutetian age (NP12-14). Alternatively, based on

*Reticulofenestra cf. placomorpha*, the Dumići (TD37) assemblage can be evaluated as a younger one (Bartonian), with *Discoaster lodoensis* then being in reworked position.

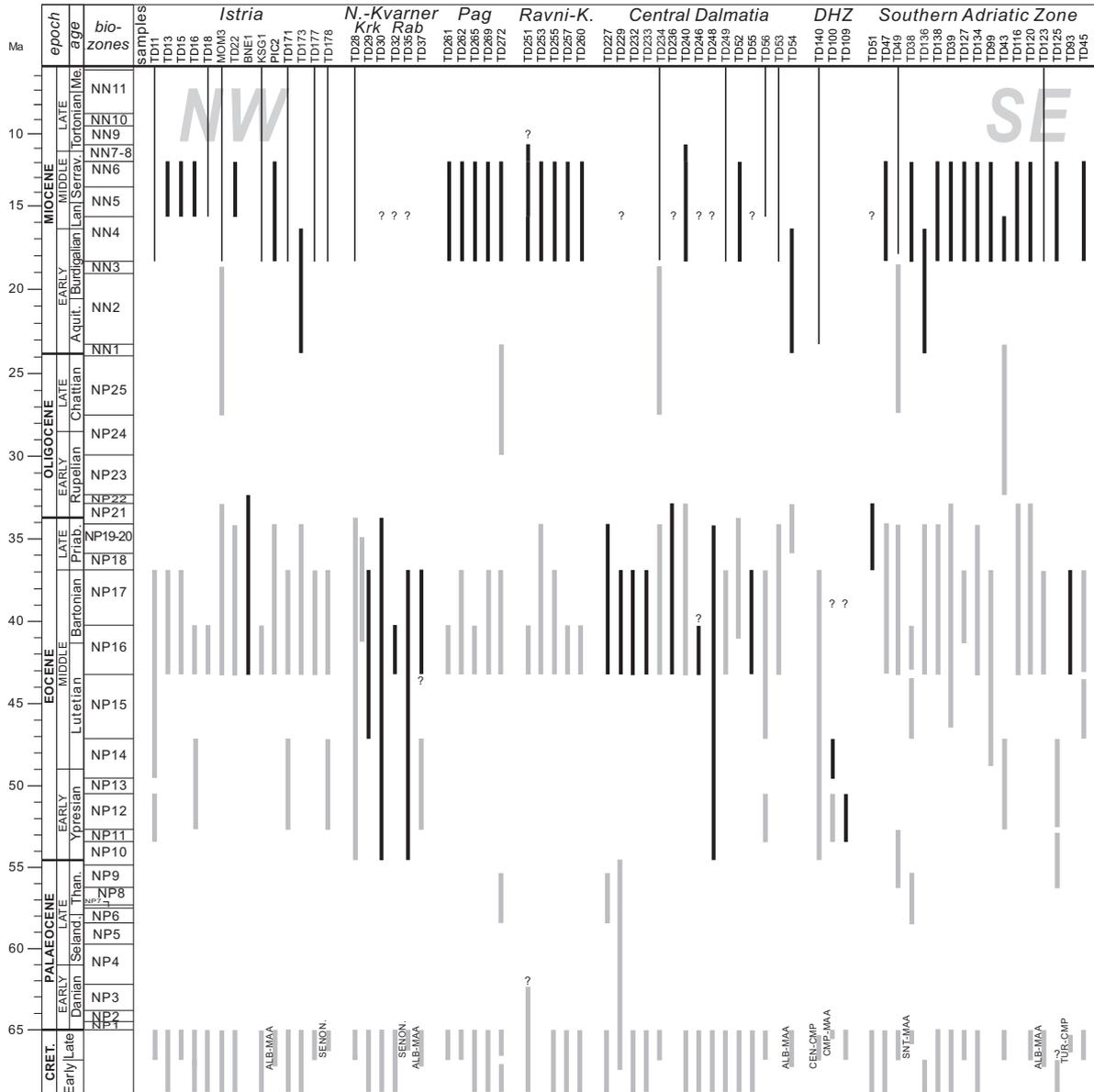


**Fig. 2.** Stratigraphic position of zonal marker nannoplankton species in the Outer Dinarides. Samples are arranged in columns, bars in each column represent the ranges of zonal markers found in that single sample. N.B.: only species with short zonal ranges are displayed, persistent species living through several epochs are omitted. Black bars mark the youngest assemblages indicating the most probable age of sedimentation. Narrow black lines: Neogene assemblages only comprising species that range beyond the Miocene. Grey bars represent reworked nannoflora. Abbreviations: Ravni-K.: Northern Dalmatia (Ravni-Kotari area), DHZ: Dalmatian-Herzegovinian Zone.

### 5.5.3. Pag Island

Two profiles of the undisturbed, SW-dipping subvertical flysch succession were sampled on Pag Island. At Stara Vas, 10 km SE of Pag town, three samples were taken 9, 45 and 92 m above the foraminiferal limestone (TD261, TD262 and TD265, respectively). Two samples stem from the coastal profile at Vlašići, collected 17 and 34 m above the limestone top (TD269 and TD272, respectively).

In all samples the nannoflora is very diverse, and a particular abundance was observed in the middle portion of the Stara Vas profile (TD262). Overall, the observed Cretaceous elements are rare, but indicate reworking of Upper Cretaceous assemblages (*Arkhangelskiella* sp., *Microrhabdulus* sp.). Majority of the nannofossils are Middle Eocene and most probably belong to zones NP16-17, i.e. Uppermost Lutetian to Bartonian. In the upper sample from Vlašići (TD272), the dominant Middle Eocene assemblage and the isolated Lower and Upper Cretaceous forms are accompanied by single specimens of *Heliolithus kleinPELLI* from the Late Palaeocene (NP6-9) and *Cyclicargolithus abisectus* most probably from the Chattian (NP24-NN1).

The Neogene part of the assemblages consists of three to five species which are identical in all samples throughout. Of these, *Calcidiscus premacintyreii* is characterized by the shortest range, i.e. Late Burdigalian and Early Serravallian (zones NN4-6). The remaining Neogene species have their FO mainly in the Early Miocene but FO of *Reticulofenestra pseudoumbilicus* >7 µm is close to the base of zone NN5, in the Langhian. Although Neogene taxa make up only a very small part of the whole of the assemblages, in sample TD262 they appear to be more abundant than elsewhere in Pag together with a similarly higher abundance of Palaeogene forms.

### 5.5.4. Northern Dalmatia (Ravni-Kotari)

The nearly complete profile exposed by the Šopot railway cut was sampled at four sites (28, 116, 130 and 383 m above the foraminiferal limestone) and an additional sample is from a road cut of the recently constructed Zagreb-Split motorway near Islam Latinski, beneath the Suhovare bridge. Except the section top, all Šopot samples were extracted from fresh rip-up pelite clasts at the base of graded turbidite beds.

The observed nannofossil assemblages bear close resemblance to each other. Reworked Cretaceous coccoliths are rare compared to other parts of the basin system, being represented by *Watznaueria barnesae*. The Palaeogene nannoflora is rather diverse, yet uniform between samples. It is not older than latest Lutetian (zone NP16), as proven by samples bracketing the Šopot section at its base and top (TD251, TD257) and by the Suhovare outcrop (TD260). Although in none of the two intermediate samples in the Šopot section can the Eocene nannoflora be narrowed to NP16, a younger Palaeogene age for these assemblages is unlikely.

Neogene species identified in this unit are similar to those appearing in the Istrian Peninsula and Pag Island. *Calcidiscus premacintyreii*, *Coccolithus miopelagicus* and *Reticulofenestra pseudoumbilicus* occur in each sample in low yet meaningful amounts. Six-rayed *Discoaster* spp. occur in both profiles, while *Calcidiscus leptoporus* and *Helicosphaera carteri* were identified in the Šopot section only. The Neogene assemblage is assigned to the NN4-6 zones, indicating Late Burdigalian to Early Serravallian age.

#### 5.5.5. Central Dalmatia

In Central Dalmatia, near the cities of Split and Omiš, fifteen samples were analyzed. The very scarce reworked Cretaceous nannofossils are represented mostly by *Watznaueria barnesae*, and Eocene nannofossils constitute the vast majority of the diverse and mostly rich assemblages.

Four sites near Mravince (TD227, TD232, TD233 and TD234) reveal a rather similar Palaeogene nannoflora, composed of very abundant but poorly preserved Uppermost Lutetian to Priabonian forms. In addition, older index species also appear in Mravince: *Heliolithus kleinPELLI* (NP6-9, Upper Palaeocene) and *Cyclagelosphaera reinhardtii*, Albian to Palaeocene. In the marl quarry at Mravince (TD229) recrystallized coccoliths dominate the sample and indicate Middle to Late Eocene age (NP16-21). The three most frequent species (*Reticulofenestra bisecta*, *Coccolithus pelagicus* and *Cyclococcolithus formosus*) share a common size and shape, strongly suggesting hydrodynamic control on species composition. Only a few specimens of *Calcidiscus premacintyreii* were found in the sample from the Mravince quarry (TD229) which may place the marl to the zones NN4-6.

We established Miocene ages with more confidence only in a part of the localities. In Jadro Valley, at Vrilo Jadro (TD240), besides Eocene species which define only a broad range of zones NP16-21 (Bartonian to Priabonian) also five Neogene taxa occur. Of these, *Calcidiscus premacintyreii* and *Reticulofenestra pseudoumbilicus* define the zones NN4-6, placing the age of these beds between Late Burdigalian and Early Serravallian.

Of the samples taken at Mravince, a pelite lithoclast extracted from a grain-supported *Nummulites* debrite (TD234) yielded comparatively abundant Neogene nannoflora: *Sphenolithus conicus* (Upper Chattian to Middle Burdigalian; probably reworked), as well as *Coccolithus miopelagicus*, *Reticulofenestra haqii* and *R. pseudoumbilicus*, corresponding to an age not older than Late Burdigalian.

Another pelite lithoclast (TD56) from a limestone breccia exposed by the large abandoned quarry of Omiš also yielded rather diverse Neogene nannofossils; *Helicosphaera carteri*, *Coccolithus miopelagicus*, *Reticulofenestra haqii*, *R. pseudoumbilicus* and *Umbilicosphaera rotula*, which suggest biozone NN5 or younger, i.e. at least Langhian age.

In other Central Dalmatian localities examined, either an abundant but monotonous and poorly preserved nannoflora occurs displaying Middle to Late Eocene age (the larger pit of the Jadro quarry, TD236), or solely a poor Eocene assemblage is encountered. Such extremely scarce nannoflora was found at several localities over larger along-strike distances (80 km): in the town of Solin in the Voljaka Street section (TD248), a laminated pelite sample in the large abandoned quarry of Omiš (TD55), road cut at Porat near Živogošće (TD52) and in a metre-sized, grey, angular marl block included in thick limestone debrite at Gizdići near Klis (TD246).

#### *5.5.6. Dalmatian-Herzegovinian Zone*

In the densely imbricated thrust belt of the Dinaride carbonate platform in Southern Herzegovina, a single sample was analyzed from Crnići village near the Neretva valley (TD140). The diverse, reworked Cretaceous nannofossil association hints at an Upper Cretaceous source older than Maastrichtian. A scarce Lower to Middle Eocene nannoflora is also present. Indication for the Neogene age of the rocks is

provided by several specimens of *Calcidiscus leptoporus* ranging from the Early Miocene to recent (NN2-21).

Further to the SE, a narrow flysch zone is exposed in front of the Kuči Thrust that stretches NW-SE from the Nevesinjsko Polje to Podgorica. Two samples were taken close to Podgorica; from a fault-bounded block standing out from the Zeta Valley 3 km NW of Spuž village (TD100), and in Medun village, 2 km ENE of Podgorica (TD109).

Both profiles contain reworked Upper Cretaceous taxa; age ranges can be probably narrowed to Campanian-Maastrichtian at Spuž. Here the relatively rich nannoflora is Lower to Middle Eocene and consists of several taxa with overlapping stratigraphic ranges (Table 2). *Discoaster lodoensis* and *Discoaster septemradiatus* are markers of zones NP12-14 indicating Late Ypresian to Early Lutetian age. Important is a single specimen of *Discoaster* cf. *sublodoensis*, which marks the base NP14, the base of the Lutetian. The Ypresian *Tribrachiatulus orthostylus* (NP11-12) is also part of the assemblage. Such a complexity is best explained by a multiple reworking history and will be discussed later.

In Medun profile (TD109) the Palaeogene assemblage is scarce but *Tribrachiatulus orthostylus* occurs here as well, the Ypresian index species of the zones NP11-12.

#### 5.5.7. Southern Adriatic Zone

A common feature of the seventeen flysch samples taken in the Southern Adriatic Zone is their paucity of Cretaceous forms. In two samples they are entirely absent (Ulcinj, TD99; Stari Bar, TD116). Nevertheless, reworked Upper Cretaceous index forms are identified in some cases and they preferentially occur in the southern part of the zone. *Eiffellithus eximius* and *Uniplanarius gothicus* are characterized by the shortest range of all, and indicate reworking from Turonian-Campanian and Santonian-Maastrichtian strata, respectively. Two samples bear *Nannoconus steinmanni* hinting at reworking from Lower Cretaceous sediments (TD125, TD136).

In all samples Eocene forms are predominant, albeit different in origin. Often the zones NP16-17 were registered (Uppermost Lutetian and Bartonian) but in other cases merely a longer interval could be given (NP16-20 or NP16-21).

Three, partly overlapping biozones can be proven at the base of the Klezna profile (TD125) from the Upper Palaeocene to the Lutetian (range of *Discoaster multiradiatus*

is NP9-11, that of *Tribrahiatus orthostylus* is NP11-12 and that of *Discoaster lodoensis* and *Discoaster septemradiatus* is NP12-14). This peculiar overlap offers a wide range of interpretations with respect to the age and recycling history of the sediment and will be discussed in the subsequent part.

A variety of reworked Palaeogene zone markers have been encountered throughout the Southern Adriatic Zone. Specimens of *Discoaster multiradiatus* (NP9-11; Palaeocene) occur in sample TD49 (Dubravka). The NP12-14 zones are proven from the Zaljevo profile (TD43) corresponding to Upper Ypresian and earliest Lutetian. In addition, sample TD45 yielded *Nannotetrina* sp., a marker for NP15 (Mid-Lutetian). In TD51 an Upper Eocene zonal marker was encountered, *Chiasmolithus oamaruensis* (NP18-22). Oligocene marker taxa are extremely rare in the entire flysch belt, thus the finding of *Reticulofenestra lockeri* (NP23-NN1; Middle Rupelian to Lower Aquitanian) in sample TD43 and *Sphenolithus conicus* (NP25-NN3; Chattian to Middle Burdigalian) in sample TD49 is of particular importance.

Thirteen out of seventeen samples Miocene forms are sufficiently represented, whereas in TD93 they are missing, in TD51 there is one specimen and in TD45 and TD136 there are two specimens. Miocene species characteristic of zones NN4-6 indicate depositional ages not older than Late Burdigalian. In Zaljevo (TD43), occurrence of two specimens of *Helicosphaera ampliapertura* (range NN2-4) are of particular importance as together with other Neogene species (*Calcidiscus leptoporus*, *C. premacintyreii* and possibly also six-rayed *Discoaster* spp.) the stratigraphic position can be ascertained to the zone NN4 (Upper Burdigalian to Lower Langhian).

## **5.6. Nannofossil preservation**

Our results reveal that the Neogene calcareous nannofossil assemblages are surprisingly low both in abundance and diversity. Accurate dating of the Outer Dinaride Neogene successions awaits further bio- and chronostratigraphic control.

Physical and chemical processes operating during flysch formation and diagenesis influence the composition of the nannoflora (disintegration, dissolution, recrystallisation) and likely account for the observed overall scarcity of the nannoflora (e.g. Thierstein 1980; de Kaenel and Villa 1996). High degree of reworking of older species, together with evidence for diagenetic processes as indicated by carbonate-cemented tur-

bidite beds, carbonate veinlets dissecting the turbidites, bent mica plates and severely etched surfaces of susceptible heavy mineral grains (amphibole, staurolite, garnet) are in accordance with the poor preservation of the nannoflora. Indeed, samples from pelite clasts, embedded in breccias or well-cemented sandstones and presumably preserved from corrosive solutions, proved to yield more diverse Neogene assemblages than those found in laminated pelites (e.g. samples MOM-3, KSG-1, PIC-2, TD253, TD255, TD234, TD56; see Table 2).

### 5.7. Cretaceous to Palaeogene nannofloral elements

Most nannofossil assemblages are mixed, with evidence for recycling of specimens from pre-existing sediments. Cretaceous forms commonly occur together with the Cenozoic ones. Common long-lived Cretaceous species, e.g. *Watznaueria barnesae* are ubiquitous. Among the shorter-range taxa *Nannoconus steinmanni* indicates Lower Cretaceous, and several Upper Cretaceous markers occur as well (*Arkhangelskiella* sp., *Microrhabdulus* sp., *Eiffelithus turriseiffelii*). A limited number of characteristic taxa prove the availability of Lower Palaeogene sediments to erosion: *Heliolithus kleinPELLI*, *Discoaster multiradiatus*, *Discoaster lenticularis* (Palaeocene), *Tribachiatus orthostylus* (Lower Eocene), *Discoaster lodoensis* (Ypresian to lowermost Lutetian). All these Lower Palaeogene species are large in size and, according to our experience, fairly resistant against dissolution.

In spite of reworking, an attempt was made to identify characteristic Palaeogene assemblages preserved in the entire sample material. The most frequent Middle Eocene forms can, in several localities, be placed into the NP16 zone. Often, NP16 zone was recognized using the FO of *Reticulofenestra placomorpha* and the LO-s of *Sphenolithus furcatolithoides* and *Chiasmolithus solitus*. Whenever the latter species were not registered, the possible age of that assemblage could only be bracketed with lower precision, which might then extend from the NP16 upward into NP17 or even longer to the Late Eocene or Early Oligocene. We used the LO of *Chiasmolithus grandis* for the end of NP17, that of *Discoaster saipanensis* and/or *Discoaster barbadiensis* for the NP20/NP21 boundary (close to the Eocene/Oligocene boundary), and that of *Cyclococcolithus formosus* and *Reticulofenestra placomorpha* for the end of NP 21 and NP 22 zones, respectively, in the Early Oligocene. As for Late Eocene, a single, poorly pre-

served specimen of *Chiasmolithus oamaruensis* occurred in the entire studied material, as previously reported from Oprtalj, Istria (Benić 1991), Split (Jerković and Martini 1976) and Hvar (Marinčić 1981) in Central Dalmatia, and the North Mozura section in the Southern Adriatic Zone as well (de Capoa *et al.*, 1995). *Isthmolithus recurvus* (NP20-22), which indicates Late Priabonian to Middle Rupelian, was found at Omiš (sample TD54).

Species of even longer ranges spanning from the Middle Eocene to various levels in the Miocene include the ubiquitous and highly abundant *Cyclicargolithus floridanus* and *Coccolithus pelagicus*. Also *Sphenolithus moriformis*, *Helicosphaera euphratis*, *H. intermedia*, *Discolithina* div. sp., and *Transversopontis* sp. appear in a number of samples. It is evident that among them there may exist specimens indistinguishably that lived in a given part of the Eocene, Oligocene or Miocene.

In the Oligocene nannofossil zonation there are only a few markers to appear, due to the global cooling trend following the terminal Eocene events (e.g. Pomerol 1985). These few FO-s are typically represented by the low latitude forms of *Sphenolithus*. Of them, *Sphenolithus conicus*, ranging from NP25 to NN3 have been found in Istria, Central Dalmatia and the Southern Adriatic Zone. Further short-range index species include *Cyclicargolithus abisectus* and *Reticulofenestra lockeri*, and in this study both species have been encountered on Pag Island and in the Southern Adriatic Zone.

The scarcity of Palaeocene nannofloral elements is probably due to the unavailability of Palaeocene sediments for the reworking processes. Normally, both the diversity of Palaeocene zonal markers and their resistance would permit them to be well-represented in Cenozoic flysch sediments.

### **5.8. Distribution of nannofossil age ranges and sediment recycling**

Apart from significant Upper Cretaceous and Middle Eocene nannofloral components, and the presence of Lower to Middle Miocene nannoflora, there are index species of Palaeocene, Lower and Upper Eocene and Oligocene present, too (Fig. 3). Unusual composition of some assemblages depicts characteristic age distribution patterns, whether or not Neogene forms are recognized in that sample (Fig. 2). We can discern two types.

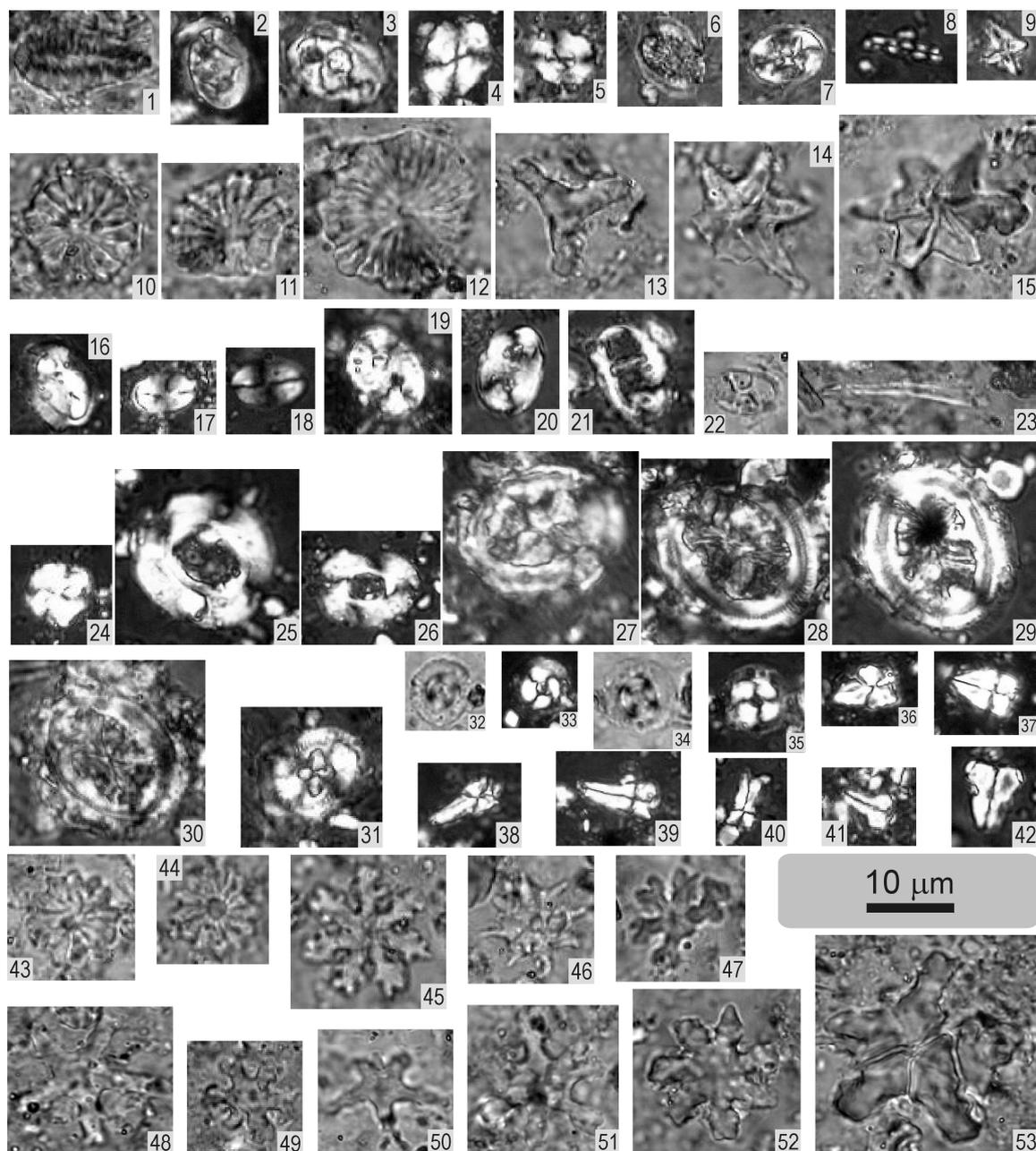


**Fig. 3.** Cretaceous (1-9), Palaeocene (10-12), Lower Eocene (13-15) and diverse Palaeogene (15-53) nannoplankton in the Outer Dinaride flysch. Abbreviations refer to light types used: PP, plane-polarized; SX, slightly cross-polarized; XP: cross-polarized. **1**, *Nannoconus steinmanni* (Sample TD43, SX); **2-3**, *Zeugrhabdotus embergeri* (2: TD16, XP; 3: TD123, XP); **4-5**, *Watznaueria barnesae* (4: TD16, XP; 5: TD262, XP); **6**, *Cribrosphaerella ehrenbergii* (TD123, SX); **7**, *Eiffellithus turriseiffelii* (TD43, XP); **8**, *Microrhabdulus* sp. (TD18, XP); **9**, *Micula* sp. (TD123, XP); **10-11**, *Discoaster multiradiatus* (10: TD262, PP; 11: TD123, PP); **12**, *Discoaster lenticularis* (TD43, PP); **13**, *Tribrachiatus orthostylus* (TD262, PP); **14-15**, *Discoaster lodoensis* (14: TD16, PP; 15: TD43, PP); **16**, *Helicosphaera compacta* (TD43, XP); **17-18**, *Discolithina plana* (17: TD261, XP; 18: TD16, XP); **19**, *Transversopontis pulcher* (TD262, XP); **20**, *Transversopontis* sp. (TD15, XP); **21**, *Lophodolithus nascens* (TD262, XP); **22**, *Neococcolithes dubius* (TD253, PP); **23**, *Blackites* sp. (TD123, PP); **24**, *Reticulofenestra bisecta* (PIC-2, XP); **25-26** *Reticulofenestra placomorpha* (25: TD16, XP; 26: TD18, XP); **27-30**, *Chiasmolithus grandis* (27: TD16, XP; 28: TD16, XP; 29: TD15, XP; 30: TD262, SX); **31**: *Chiasmolithus* sp. (TD43, XP); **32-35** *Cyclococcolithus formosus* (32-33: TD43, PP and XP resp.; 34-35: TD16, PP and XP resp.); **36-39**, *Sphenolithus radians* (36: TD123, XP; 37: TD123, XP; 38: TD16, XP; 39: TD16, XP); **40**, *Sphenolithus furcatolithoides* (TD16, XP); **41-42** *Zygrhablithus bijugatus* (41: TD261, XP; 42: TD16, XP); **43-44**, *Discoaster barbadiensis* (43: TD262, PP; 44: TD262, PP); **45**, *Discoaster mirus* (TD262, PP); **46**, *Discoaster saipanensis* (TD262, PP); **47** and **49**, *Discoaster deflandrei* (both TD262, PP); **48** and **50-51**: *Discoaster tanii* (48: TD123, PP; 50: TD123, PP; 51: TD123, PP); **52-53**, *Discoaster nodifer* (52: TD262, PP; 53: TD18, PP).

(1) Joint occurrence of Palaeogene species with no overlapping age ranges. We observe this in Istria (TD11, TD171), Northern Kvarner area (TD37), Pag Island (TD272) at Mravince in Central Dalmatia (TD227), and in the Southern Adriatic Zone (TD38, TD43, TD45).

(2) A blurred, consecutive overlap pattern of several index species: *Discoaster multiradiatus* (NP9-11), *Tribrachiatus orthostylus* (NP11-12), *Discoaster lodoensis* and *D. septemradiatus* (NP12-14) and *Discoaster* cf. *sublodoensis* (NP14-15) occur together, in addition to Lower and Upper Cretaceous markers. Such mixed assemblages were encountered both in the Zeta Valley in the Dalmatian-Herzegovinian Zone (TD100) and in the Southern Adriatic Zone (TD125). Evidently, the partly overlapping ranges of these species can be combined to a number of species coexistence patterns, but recycling remains necessary to explain overall species composition. The resulting maximum time span for the Early Palaeogene „cascade” alone may cover ca. 9 Ma, but presence of further non-overlapping taxa suggests a more or less continuous and by all means cannibalistic sedimentation. Both types of age distribution provide an insight into the progressive Cretaceous to Cenozoic sediment reworking history. Actual sedimentation ages of the flysch likely become younger towards the foreland, along with the increasing number of reworked “fossil” biozones. During thrusting, the deposited flysch was off-scraped, reworked, its material acting as a source for the yet younger flysch deposits.

We need to stress that the few, comparatively thick flysch profiles available (e.g. Brkini, Šopot, Skradin, Split, Petrovac) all display a limited thickness (ca. 300-500 m), which is not enough to accommodate the time represented by the full nannofossil age spectrum assuming typical flysch sedimentation rates (50-2000 m/Ma; Einsele 1992, p. 389). De Capoa *et al.*, (1995) documented the nannofossils of the 140 metres thick Petrovac profile in the Southern Adriatic. With nearly equidistant sampling they obtained successively younger assemblages upsection from the Upper Thanetian to the Langhian, which spans ca. 40 Ma implying a sedimentation rate of only ca. 3.5 m/Ma, which is not realistic for submarine fan depositional setting. Judging from their data, at Petrovac there are either undiscovered, short-lived unconformities or, more likely, most of the older ages come from reworked nannofossils due to extensive dilution.

### 5.9. Miocene nannofossils

The majority of samples contains nannofossils suggesting Miocene age. In the NW portion of the Dinaride foreland basin, this paper reports such fossils for the first time from onshore outcrops. Unfortunately, these crucial forms are small, very rare, often poorly preserved and tend to comprise morphologically variable species.

In our experience however, most standard flysch nannofossil stratigraphic studies typically ignore or overlook such “inconvenient” forms. As they have outstanding importance in Dinaride flysch stratigraphy, they have to be discussed in more detail.

The most common placolith species encountered in the Outer Dinarides are species of the *Calcidiscus* group, *Reticulofenestra pseudoumbilicus*, *Reticulofenestra haqii* and *Coccolithus miopelagicus*. As demonstrated by Young (1998), however, these often exhibit a wide variety in shape and size, hampering exact taxonomic identification. In fact, morphologically related forms do occur in the Palaeogene, albeit a very rare phenomenon, e.g. *Reticulofenestra dictyoda* (Deflandre in Deflandre and Fert) Stradner in Stradner and Edwards (see Varol 1998). The comparatively high frequency of this type of placoliths met in the Dinaride samples strongly argues for their Miocene rather than Eocene age. Among these species, *Reticulofenestra pseudoumbilicus* >7 µm is the most common one. Regarding the *Calcidiscus* species, *C. leptoporus* and *C. macintyreii* are of very low frequency, only a few specimens were found in the entire material. On the contrary, *Calcidiscus premacintyreii* has been often registered, even though it occurs in its less typical varieties. The occurrence of *Coccolithus miopelagicus* is well demonstrated (Fig. 4).

The genus *Helicosphaera* is represented by several species, two of them have a Miocene FO; *Helicosphaera carteri* and *Helicosphaera ampliapertura*. Unfortunately, *Helicosphaera* is just moderately resistant to dissolution and overcalcification, resulting in poor preservation. This makes *H. carteri* difficult to identify, but the flange and the central area with the two pores are visible (Fig. 4). A third species of *Helicosphaera* is characterized by prominent central openings and a conjunct central bar which suggests Neogene age despite the poorly preserved flange at the rim of the coccolith (Photo 12 in Fig. 4).

Among the *Discoaster* species a rather frequent type occurs with five or six narrow rays. Their preservation is always very poor, with heavily overcalcified specimens, and ends of their arms mostly broken off. Although this type exists also in the Eocene, *Dis-*

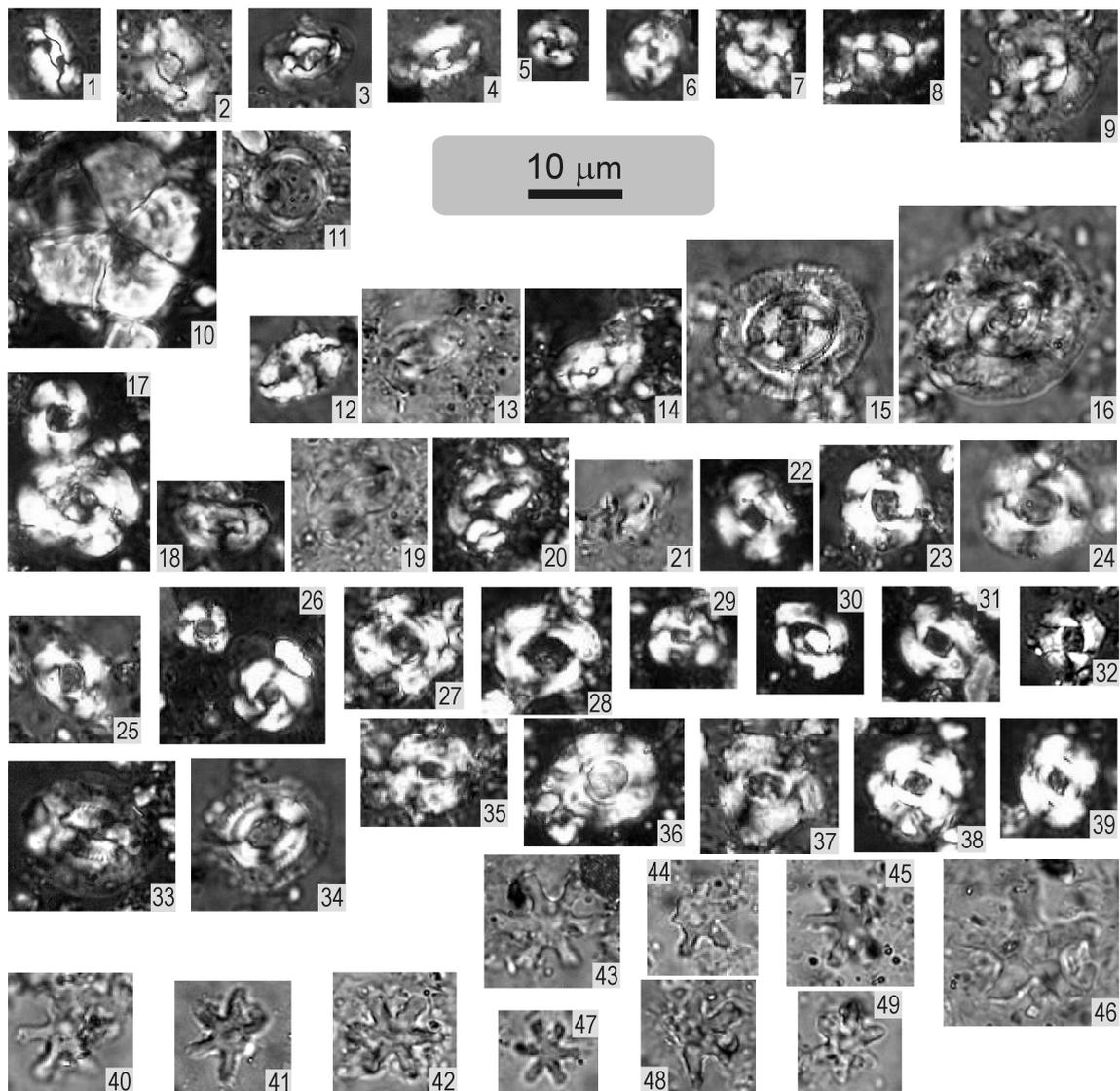


**Fig. 4.** Palaeogene to Neogene (1-11) and Neogene (12-46) nannoplankton of the Outer Dinaride flysch. Designations as in Fig. 3. **1-2**, *Helicosphaera euphratis* (1: Sample TD43, XP; 2: Sample TD262, XP); **3-4**, *Helicosphaera intermedia* (3: TD127, XP; 4: TD43, XP); **5-7**, *Cyclicargolithus floridanus* (5-6: PIC-2, XP; 7: TD261, XP); **8-9**, *Coccolithus pelagicus* (8: TD261, XP; 9: TD262, SX); **10**, *Braarudosphaera bigelowi* (TD127, XP); **11**, *Coronocyclus nitescens* (TD262, SX); **12**, *Helicosphaera* sp. (flange poorly preserved but note prominent central openings and the conjunct central bar, TD127, XP); **13-14**, *Helicosphaera carteri* (13: TD15, PP; 14: TD15, XP); **15-16**, *Coccolithus miopelagicus* (15: TD262, PP; 16: TD16, XP); **17**, *Reticulofenestra pseudoumbilicus* >7 $\mu$ m (above; together with the Palaeogene *Reticulofenestra placomorpha*, below, TD15, XP); **18-20**, *Helicosphaera carteri* (18: TD16, XP; 19: TD262, PP; 20: TD262, XP); **21**, *Helicosphaera obliqua* (TD262, SX); **22-26**, *Reticulofenestra haqii* (22: TD16, XP; 23: TD18, XP; 24: TD262, XP; 25: TD123, XP; 26: TD43, XP, 2 specimens); **27-32**, *Reticulofenestra pseudoumbilicus* >7 $\mu$ m (27: TD261, XP; 28: TD261, XP; 29: TD261, XP; 30: TD251, XP; 31: TD16, XP; 32: TD15, XP); **33-34**, *Coccolithus miopelagicus* (33: TD16, SX; 34: TD16, SX); **35-37**, *Calcidiscus premacintyreii* (35: TD261, XP; 36: TD262, XP; 37: TD261, XP); **38-39**, *Calcidiscus* sp. (38: TD15, XP; 39: TD261, XP); **40-44** and **48-49** *Discoaster* spp. 6-ray (40: PIC-2, PP; 41: TD15, PP; 42: TD18, PP; 43: TD123, PP; 44: TD253, PP; 48 and 49: TD18, PP); **45-46**, *Discoaster* spp. 5-ray (45: TD15, PP; 46: TD123, PP); **47**, *Discoaster* sp. 7 $\mu$ m, 6-ray (TD261, PP).

*coaster tani* and similar forms are generally very rare. In fact, in the Miocene the most frequent *Discoaster* spp. are 5- or 6-rayed with bifurcations at the end of their arms, represented by a wide variety of species. Among them the *Discoaster exilis* group is the most probable candidate (e.g. with *Discoaster aulakos* Gartner 1967 in Young 1998, p. 257), but they bear close resemblance to *Discoaster variabilis* Martini and Bramlette 1963 as well. If bifurcation is not visible it is either broken off or it is a primary characteristic (such as that of *Discoaster bellus* Bukry and Percival 1971, for example). With respect to decisive specific characteristics, the central area (with or without knob), the inter-ray area (rounded or rather V-shaped), the arms (with the sides tapering, parallel or curving) and the ending of the arms (bifurcating or not) were considered. In spite of poor preservation of the *Discoaster* spp. under discussion, their characteristics suggest Miocene age.

Overall, the identified Miocene nannofossil species correspond to the zones NN4-6 (based on *Calcidiscus premacintyre*), but they are probably not older than NN5 as *Reticulofenestra pseudoumbilicus* >7 µm occurs first in this zone. Consequently, whenever Neogene taxa are present, the age of clastic sedimentation in the Adriatic onshore area is likely not older than Langhian.

As a result of the surprisingly rare occurrence and poor preservation of the nannofossils and occasionally wide specific morphological variability, the Neogene age of deposition cannot be unambiguously confirmed. Noticeably, the observed problematic forms are unknown in the Bakony Eocene Basin in Hungary although it exhibits rather comparable Middle Eocene nannofossil assemblages to those in the Outer Dinarides (Báldi-Beke 1984; Báldi-Beke and Báldi 1991).

Research is in progress to further address this stratigraphic problem by looking at the roles of hydraulic, diagenetic and weathering processes being suspect to exert a fundamental control on the assemblage compositions.

## **5.10. Implications for palaeoenvironment**

### *5.10.1. Pelagic environment with neritic influence*

Despite sediment mixing and reworking, it is evident that the most frequent forms pertain to a Middle Eocene assemblage. The species composition is rather complex and

exhibits common placoliths. Some species possess a specific habitat and are thus of ecologic importance, such as the nearshore taxa *Neococcolithes dubius*, *Pemma* sp., *Discolithina*, *Transversopontis* and holococcoliths, e.g. *Zygrhablithus bijugatus* (e.g. Perch-Nielsen 1985b). Although abundance of these nearshore taxa is low in all samples, as many of them are at the same time particularly susceptible to dissolution, it can be assumed that their initial abundance was higher in the sediment, which in turn calls for a remarkable neritic influence on sedimentation in the Eocene. The scarce Neogene assemblage does not provide useful environmental information.

#### *5.10.2. Neogene: Absence of planktonic foraminifera, presence of nannofossils*

Preliminary examination of our samples containing Miocene nannofossils did not yield any planktonic foraminifera younger than Middle Eocene in Istria and Kvarner or younger than Early Oligocene in the Southern Adriatic (V. Čosović, pers. comm. 2006; F. Rögl, pers. comm. 2007). To our knowledge, no such data have been published from onshore localities, either (Table 1).

The characteristic depth habitat of several planktonic foraminifer species can preclude their survival in relatively shallow waters. Most species require oceanic salinities near 35-36 ‰, a few of them can tolerate salinities down to 30.5 ‰ and can thus only penetrate coastal waters if sufficiently clear and lacking in turbidity (Haynes 1981, p. 330). Nannoplankton, in contrast, tolerates reduced salinity although diversity can be reduced in brackish water under elevated freshwater input (e.g. Olszewska and Garecka 1996; Schulz *et al.*, 2005).

In places, the Outer Dinaride flysch deposits rapidly grade into shallow marine deposits. Sand-rich shallow shelf environments influenced by nearby river mouths have been described from the Islands of Rab and Pag and from Northern Dalmatia (Zupanič and Babić 1991; Babić *et al.*, 1993; Babić and Zupanič 1998). Facies architecture of clastic deposits in Northern and Central Dalmatia is also well documented (e.g. Postma *et al.*, 1988; Mrinjek 1993; Marjanac 1996), and show fan deltas prograding on the flysch succession. The increasing proximity of the alluvial environments implies significant freshwater input which could have a profound effect on salinity and thus adversely influenced foraminifer distribution.

### 5.10.3. Heterochronous redeposition

As a prominent feature, debrites of several metres of thickness that intercalate the turbiditic flysch successions of the Outer Dinarides often contain isolated tests of Eocene larger foraminifera. In spite of attempts to date the depositional age by means of such fossils (Pavić 1970) they are evidently allochthonous in submarine fan setting. Pavlovec (2003) noted that *Nummulites* assemblages found in flysch deposits Dinarides-wide were in fact no true biocoenoses but rather mixed in composition with unusual species proportion as compared to those in the limestones. Indeed, derived fossils may occur in a state of preservation as good as or better than that of the original rock, and the reworked fauna may be more diverse and contains a much higher proportion of planktonics than that of the source rock (Curry 1982).

Ample examples from the Outer Dinarides and from comparable settings in the surrounding areas show that larger, smaller and also pelagic foraminifer tests can survive diagenesis in unconsolidated sediment and be reworked into younger strata: (i) Lower Eocene (Upper “Cuisian”) flysch of Trnovo, SW Slovenia contains Lower to Middle Cuisian larger foraminifera: *Nummulites subdistans* (Pavlovec 2006); (ii) Planktonic foraminifera in the flysch of Pićan are uniformly Middle Lutetian in age but if examined in detail, they belong to various biozones (Pavlovec *et al.*, 1991); (iii) Lower Oligocene (NP21-22) calcareous turbidites in Budapest, Hungary contain Upper Eocene (Priabonian) larger foraminifera: *Chapmanina gassinensis* and *Nummulites fabianii* (Varga 1982, 1985; Nagymarosy 1987); (iv) Lower Oligocene flysch in the Carpathians yielded Eocene *Nummulites* (Kulka 1985). (v) The Frazzanò Flysch of the Calabria-Peloritani arc previously dated by Upper Eocene foraminifera yielded Upper Oligocene calcareous nannofossils (de Capoa *et al.*, 1997); (vi) Similarly, flysch of the Sicilian Maghrebids containing Lower Oligocene planktonic foraminifera were dated by means of calcareous nannofossils to be at least Aquitanian (de Capoa *et al.*, 2000); (vii) Microfossils of Lower Miocene strata of the Zawada Formation in the Carpathians are dominated by reworked Middle Eocene planktonic foraminifera and calcareous nannoplankton (Oszczypko *et al.*, 1999); (viii) Flysch of the Ionian Zone in the Hellenides, to the SE of the Outer Dinaride flysch basins, is Early Miocene in age and contains abundant reworked Cretaceous and Eocene nannofossils (Piper *et al.*, 1978; Bellas 1997). Evidence for a considerable time gap between foraminifer and nannofossil ages arises also from our new results. For instance, isolated Lower to Middle Eocene *Nummulites* tests from

various biozones occur together with older, massive Palaeogene and Cretaceous carbonate lithoclasts (Hagn *et al.*, 1979) as well as with Middle to Upper Eocene planktonic foraminifera and Cretaceous to Palaeogene nannofossils from a number of biozones (Drobne *et al.*, 1979) and with Upper Oligocene palynomorphs, nannofossils and larger foraminifera (Šparica *et al.*, 2005) in the Pićan flysch profile on Istria. These strata have been dated herein to be not older than Late Burdigalian. Table 1 and Fig. 2 illustrate the contradiction of microfossil age data from the entire Outer Dinaride flysch.

#### *5.10.4. Weak early-stage diagenesis*

Redeposition of micro- and macrofossils such as larger, smaller and planktonic foraminifera without intense signal of wearing or abrasion can be attributed to subaqueous mud volcanoes linked to dewatering, in what might be a dynamic, accretionary wedge-type environment (e.g. Kohl and Roberts 1994). Probably, high water content of sediment prevented diagenesis initially, and allowed easy removal of carbonate particles from the siliciclastic matrix downslope the submarine fans, over a longer time span. Such a mechanism for a continuous redeposition and accumulation of Eocene foraminifera until at least Middle Miocene is very likely to have taken place in the imbricated frontal thrust belt of the Dinarides, interpreted as an accretionary wedge (Tari-Kovačić 1998).

### **5.11. Implications for palaeogeography**

We have demonstrated that our new calcareous nannofossil data from the Outer Dinaride Cenozoic prove the presence of a wide range of Lower Cretaceous, Upper Cretaceous, Palaeocene, several non-overlapping Eocene, Oligocene and Miocene species in these strata.

The significance of our results is twofold. On the one hand, they indicate that the Cretaceous platform carbonate nappes have been covered by pelitic sediments, connected with progressive sediment reworking during the Cenozoic. It is essential to assume that before, during, and after the deposition of the Eocene foraminiferal lime-

stones in the present-day Outer Dinaride coastal range, there existed widespread marine environments, covering the Cretaceous platform carbonates in the inner imbricate belt, where the nannofossils can be derived from.

On the other hand, the data strongly suggest a considerably younger, at least Burdigalian sedimentation age throughout the onshore flysch deposits, with clear implications on Outer Dinaride tectonics. Overall, this picture is best explained by a series of wedge-top basins (see DeCelles and Giles 1996) progressively migrating towards the Apulian foreland.

The flysch develops from the underlying "*Globigerina* Marl" (Marjanac and Ćosović 2000). These shelf to shallow bathyal deposits are dated by means of micro- and macrofauna and by calcareous nannofossils (Muldini-Mamužić 1965; Benić 1991; Drobne and Pavlovec 1991; Pavšič and Premec-Fuček 2000; Schweitzer *et al.*, 2005) ranging in age from Palaeocene in the NW to Upper Eocene in the SE.

Biostratigraphic results obtained in our study for Central Dalmatia and the Southern Adriatic Zone agree well with the findings of Puškarić (1987), Radoičić *et al.*, (1989, 1991), de Capoa *et al.*, (1995), and de Capoa and Radoičić (1994*a, b*, 2002) who first demonstrated Neogene nannofossil age in a number of flysch localities of the SE part of the basin system. Further to SE, flysch in the Ionian Zone in the Hellenides is likewise dated to be Lower Miocene (Piper *et al.*, 1978; Bellas 1997). Our new data, however, lead us to extend the Miocene sedimentation ages to other portions of the coastal onshore localities as well, from Northern Dalmatia through Pag Island till the Istrian Peninsula. As a consequence, proposing SE-directed diachroneity along the Outer Dinaride front (Piccoli and Proto Decima 1969) is no longer reasonable. Furthermore, superposition of Neogene flysch onto the Eocene "Marl with crabs" or *Globigerina* marl implies a widespread, basin-scale regional unconformity, but hitherto this issue has not received much attention. In fact, the thickness of the *Globigerina* marl varies extremely from 10 to 150 m (Marjanac and Ćosović 2000), and contacts with angular (Marjanac 2000) or erosional (Marjanac *et al.*, 1998) unconformity to the overlying flysch both exist. Šikić (1963; 1968) also argued that deposition of the both units was interrupted by a deformational event and suggested the existence of a basin-wide unconformity. An abrupt change in the composition of the planktonic foraminifer fauna above a carbonate debrite horizon separating the *Globigerina* marl and the flysch was noted by Muldini-Mamužić (1965). De Capoa *et al.*, (1995) noted that a hardground is developed on top of the "Marl with crabs", directly overlain by flysch. All these data suggest a

break in sedimentation and possibly slight submarine erosion as well, in spite of the classical view dealing with the progressive transition of the *Globigerina* marl to the flysch (see review in Marjanac and Ćosović 2000). Although remnants of Palaeogene flysch can exist in the coastal range, our data clearly imply that, at most localities in the basin, the flysch is of Neogene age and separated from the *Globigerina* marl or from older flysch strata by unconformity (Fig. 5).

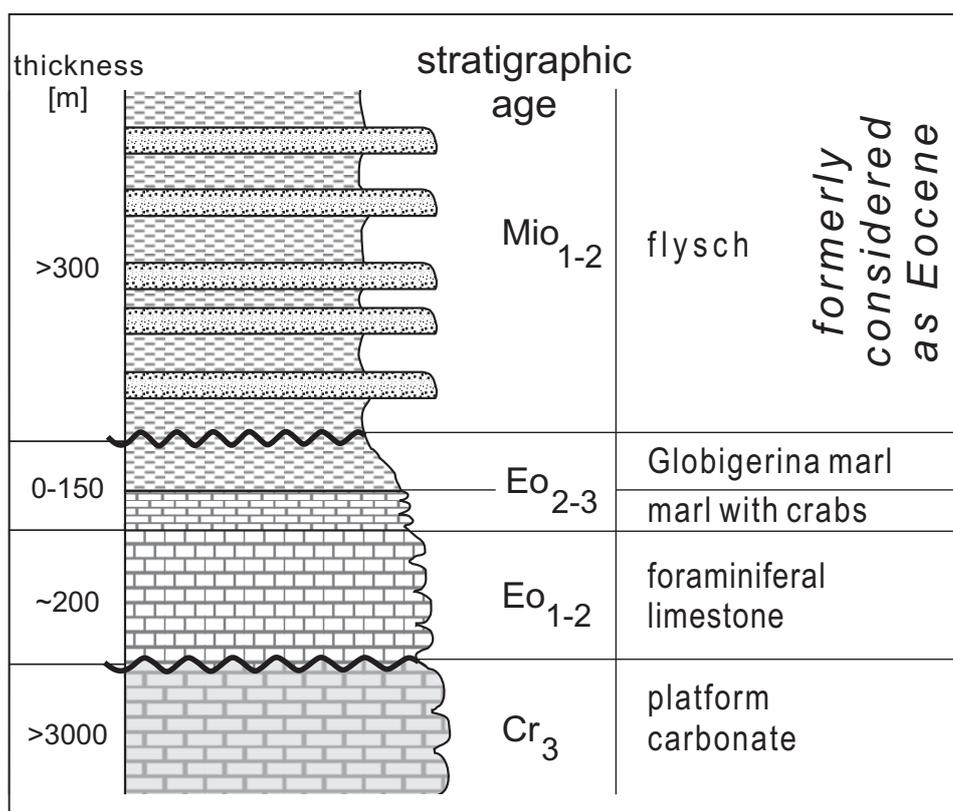


**Fig. 5.** Schematic stratigraphic setting of the Outer Dinaride flysch in the coastal range according to the new nannofossil age data. As it directly overlies well-dated Eocene *Globigerina* marls, their relationship requires the presence of a major, basin-wide unconformity separating them. At places however, also small erosional remnants of older, Palaeogene flysch may still exist in the same orogenic strike.

The heavy mineral composition of the flysch (Magdalenić 1972; Mikes *et al.*, 2004, 2005) and especially the nannofossil "age spectra" both exhibit a remarkable degree of basinwide homogenization. In the course of wedge-top deposition, a series of small, relatively shallow basins could have been developed on and in front of the advancing thrust sheets. The "smoothing" is interpreted as a result of multiple reworking from the

precursor flysch slices and sediment dispersal that occurred within the westward-propagating, complex thrust wedge (Fig. 6).

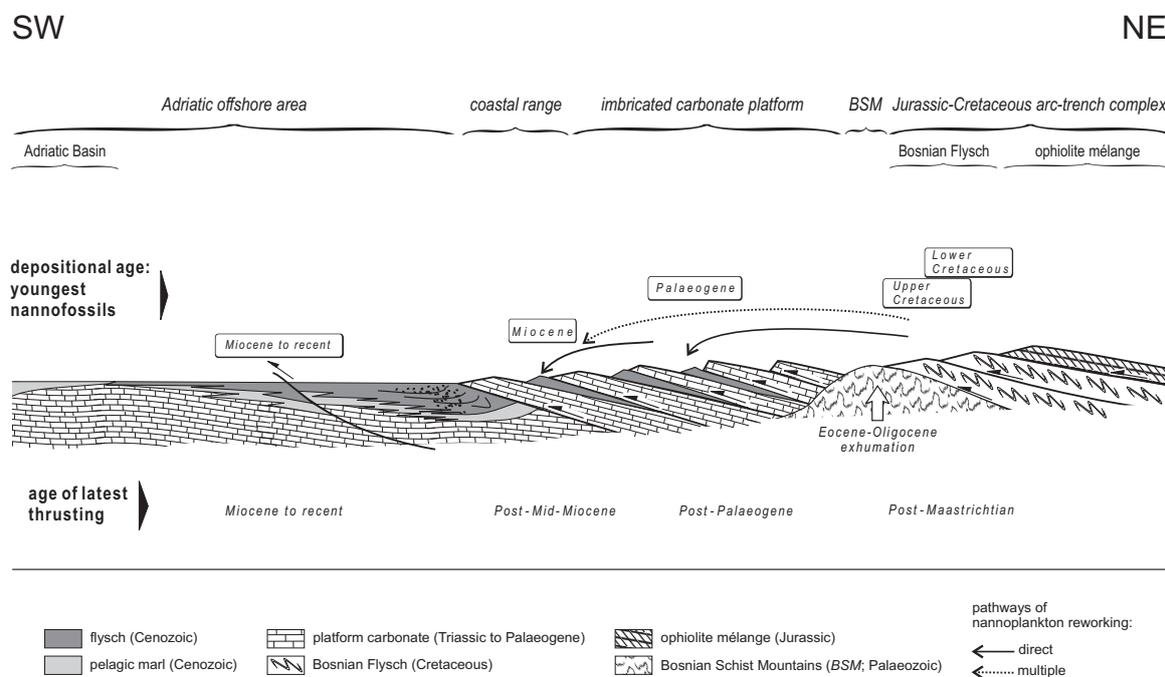


**Fig. 6.** Schematic sketch showing the implications of biostratigraphic data. With progressive nappe propagation towards Apulia, shallow foredeeps develop at the actual nappe front. Continuous thrusting and associated sediment off-scraping result in consecutive reworking of planktonic fossils into younger strata. Flysch remnants preserved at the base of thrust sheets become progressively younger towards Apulia. This process lasted until at least late Early Miocene in the present-day Outer Dinaride coastal range, as indicated by deformed flysch sediments yielding Neogene calcareous nannoplankton. In the offshore Adriatic basin, clastic sedimentation has lasted until recent time. Age of the Bosnian Flysch taken from Hrvatović (1999) and Christ (2007). In the upper nappe unit of the Bosnian Flysch, an Albian deformation phase is also supposed (Petri 2007). Thermal history of the Bosnian Schist Mountains after Pamić *et al.* (2004).

## 5.12. Implications for Cenozoic deformation history

Flysch remnants are typically sandwiched between thrust sheets, and occur in different structural position in the Outer Dinaride nappe pile. The Bosnian Flysch is in uppermost position, and ranges in age up to Turonian to Palaeocene (Dimitrijević 1997 p. 38, Hrvatović 1999; Christ 2007). Turbiditic sequences of comparable age are found in the same structural position along orogenic strike in isolated outcrops near Zagreb, Bosanski Novi and Bihać (Jelaska *et al.*, 1969; Babić 1974; Babić and Zupanić 1976;

Crnjaković 1981) and in the Slovenian Trough (e.g. Buser 1987). These units are thrust on the AdCP, an imbricated pile of Mesozoic carbonates, the detachment surfaces being marked by a series of extremely narrow slices of Cenozoic flysch. Here, limited evidence suggests Early Eocene age of deposition (samples TD100 and TD109; planktonic foraminifer data of Krašeninnikov *et al.*, 1968). In the thrust slices below, available biostratigraphic and sedimentological data suggest a foreland-directed migration of clastic facies zones in the Palaeogene (e.g. Bignot 1972; Engel 1974; Chorowicz 1977; Drobne 1977; Cadet 1978; Marinčić 1981; Košir 1997).

Our new biostratigraphic data imply post-Mid-Miocene deformation in the Outer Dinaride coastal range. Older thrusting events to the NE are recorded by the Lower and Upper Cretaceous units of the folded Bosnian Flysch (Dimitrijević 1997; Hrvatović 1999; Christ 2007; Petri 2007) and by Lower Eocene flysch slices thrust by Mesozoic carbonates (Krašeninnikov *et al.*, 1968). On the other hand, to the SW of our sample sites, deformed Pliocene sediments and GPS measurements indicate ongoing shortening along the coastal range (Tari-Kovačić 1998; Pribičević *et al.*, 2002; Picha 2002; Tari 2002; Prelogović *et al.*, 2003; Altiner *et al.*, 2006; Mantovani *et al.*, 2006; Vrabc and Fodor 2006). Therefore, the new Miocene nannofossil depositional age of most flysch units and their structural position indicate that both sedimentation and deformation have been a long-lived continuous process in the Dinarides. The formation, subsidence and inversion of the subbasins and thus sediment cannibalization are well-documented by the high proportion of recycled nannofossils.

### **5.13. Conclusions**

Sixty-nine samples taken along the 700-km onshore sector of the Outer Dinaride flysch belt were analyzed for calcareous nannofossils. Most of them yielded mixed nannoflora with Cretaceous, Palaeogene and Neogene species.

In the light of the new nannofossil data presented herein, we suggest that the flysch sedimentation lasted at least up to Mid-Miocene all along the Dinaride coastal range. In spite of disagreement with existing planktonic foraminifer biostratigraphic data, our results are well in line with recently published nannofossil data from a number of localities within the flysch basin.

Majority of the nannoflora consists of Middle Eocene taxa, together with less abundant Cretaceous, Palaeocene and Oligocene nannofossils. Wherever Neogene species have been discovered, all these older floras are implied to be recycled from older flysch units of the Outer Dinaride accretionary wedge.

Cretaceous platform carbonate nappes of the Outer Dinarides were extensively covered by Cenozoic marine sediments. Remnants are preserved at the base of thrust sheets while the reworked microfossils also testify to the existence of Cenozoic basins on top of the accretionary wedge.

The stratigraphic relation of well-dated Eocene *Globigerina* marls lacking evidence for reworked fossil content and the Neogene flysch allows us to propose a working hypothesis on a major, widespread, hitherto largely ignored unconformity along the entire Dinaride coastal range, which requires further field evidence.

The Miocene onshore Outer Dinaride flysch suffered severe compressional deformation and is typically preserved below the imbricate thrust sheets of the Dinaride carbonate platform. Along the coastal zone, the deformation postdates Middle Miocene. This compressional phase provides evidence for the continuity of deformational events between the more internal, older Late Cretaceous to Palaeogene compressional phases and the ongoing thrusting at the Adriatic front.



## *Chapter 6*

# Double dating of detrital zircon from the Dinarides by fission-track and LA-ICPMS U/Pb analysis

---

This chapter contains a manuscript that is currently under preparation:  
"Double dating of detrital zircon from the Dinarides by fission-track and LA-ICPMS U/Pb analysis"  
for publication in *Chemical Geology*.  
authored by:  
Tamás Mikes, Teresa E. Jeffries, István Dunkl, Raimon Tolosana-Delgado and Hilmar von Eynatten



# **Double dating of detrital zircon from the Dinarides by fission-track and LA–ICPMS U/Pb analysis**

Tamás Mikes, Teresa E. Jeffries, István Dunkl, Raimon Tolosana-Delgado and Hilmar von Eynatten

## **Abstract**

In sedimentary provenance analysis, a fundamental question is the age of a crystalline source rock and the timing of subsequent thermotectonic events that affected crystalline terrains prior to exhumation and erosion. Zircon is a useful detrital mineral which carries a wealth of information about the petrogenesis, geochronology, alteration, and cooling history of its source rocks, but only few attempts were made so far to combine such data from single grains. We present an approach combining fission track (FT) and in-situ LA–ICPMS U/Pb isotopic analyses from the same grain. Detrital zircons were dated by the FT method, and grain interiors were imaged by SEM-CL to avoid ablation of inherited or other unsuitable domains. Precise and accurate U/Pb isotopic compositions were determined by a simple setup consisting of a 213 nm Nd:YAG laser source, coupled to a quadrupole ICPMS instrument. Our results are significant for at least two reasons: (1) The U/Pb analytical protocols provide an excellent trade-off between analysis quality and a high, cost-effective sample throughput (70–100 zircon grains per day). Figures of merit include a sensitivity of >2100 cps/ppm for  $^{207}\text{Pb}$  in case of a 55  $\mu\text{m}$  nominal pit diameter. Within-run U/Pb elemental fractionation remains below 1%, rendering correction for it unnecessary. CL-control and a good spatial resolution aid in reducing age bias, as judged from the notably high proportion (>90%) of concordant ( $\pm 5\%$ ) grain ages. (2) The double dating approach yields valuable insights into the thermal history of source terrains of Dinaride synorogenic sediments. Several clusters of age-pairs can be isolated that identify Alpine tectonostratigraphic units. The results can be effectively used for building a more realistic model of hinterland erosion and sediment dispersal patterns than normally achieved by using the two dating techniques separately.

## 6.1. Introduction

Zircon is a prime U/Pb geochronometer for igneous and high-grade metamorphic rocks, due to its broad occurrence, high stability and retentivity for radiogenic Pb. It remains rather stable in the sedimentary cycle and, hence, is extensively used in detrital U/Pb geochronology as a tool for provenance analysis, in constraining maximum depositional ages, and in stratigraphic correlation. The U/Pb single grain ages are used to constrain high-temperature events such as magmatic crystallization and high-grade metamorphism (Davis *et al.*, 2003; Fedo *et al.*, 2003)

Zircon also retains a diverse range of further chronological, petrogenetical and thermal information about its metamorphic, igneous and sedimentary host rocks. Many single-grain techniques have been implemented to examine zircon genetical aspects, such as crystal structure (Nasdala *et al.*, 2005), external and internal morphology (Dunkl *et al.*, 2001; Vavra, 1990) trace element signatures (e.g. Hoskin and Schaltegger, 2003), O isotope composition (Valley, 2003), Hf isotopic systematics (Gerdes and Zeh, 2006), Li isotopic signature (Ushikubo *et al.*, 2008) and cooling ages both by fission track (FT) analysis (Hurford *et al.*, 1984; Carter, 1999) and (U-Th)/He analysis (Reiners, 2005).

In sedimentary provenance studies, a fundamental question is the age and petrogenesis of a crystalline source rock and the timing of subsequent thermotectonic events that affected crystalline terrains prior to exhumation and erosion (e.g. Weltje and von Eynatten, 2004). Single detrital grains lend themselves favourably to address this question, although attempts to combine the above techniques in the same grain have been limited so far.

Carter and Moss (1999) were the first to couple U/Pb and FT ages of detrital zircon. They used aliquots of the same detrital sample sets, and compared the principal U/Pb and FT age components from them using the statistical method of Sambridge and Compston (1994), in order to constrain the age signature of the source units of Mesozoic sediments in Thailand. For the first time, however, these authors also attempted to perform the U/Pb analyses on the same grains previously dated by the FT method, although the approach they followed was rather time-consuming; it consisted of identifying and removing the FT-dated grains from the Teflon mount, remounting them in epoxy and repolishing for in-situ U/Pb analysis. The U/Pb ages were derived in both types of experiments by sensitive high-resolution ion microprobe (SHRIMP). Recently,

Bernet *et al.* (2006) presented a combined U/Pb–FT study of detrital zircon from Neogene (Siwalik Group) to recent sediments from the Himalayan foreland basin. They also used ion microprobe techniques (secondary ion mass spectrometry – SIMS) to derive the U/Pb ages. However, in the lack of direct textural control, and due to the prevalence of old polymetamorphic rocks in the source area, their U/Pb ages potentially represent mixtures from zircon domains of different isotopic composition, revealing only limited geological information.

Whereas ion-probe techniques yield precise and accurate results (SIMS and especially SHRIMP), measurement times and analytical costs per isotopic datum are rather high. Furthermore, there is a risk of obtaining a biased isotope ratio due to contamination by recent common Pb at the sample surface, which even increases by the etching of fission tracks. Finally, these techniques require a high quality of the analyzed surface; this is difficult to realize in the case of etched zircon grains that have been embedded in a low-adhesion material such as PFA Teflon. Such grains exhibit an irregular, rugged surface if the density of the etched tracks is high and, in our experience, repolishing such FT mounts can not be accomplished without losing a significant proportion of grains. For the reasons above, we consider the ion-probe techniques to be of limited use in zircon U/Pb–FT double dating studies.

Recent advances in laser ablation–inductively coupled plasma mass spectrometry (LA–ICPMS) have made it a tool now challenging SIMS and SHRIMP in accuracy, precision and also spatial resolution (Günther *et al.*, 1999; Horn *et al.*, 2000; Horstwood *et al.*, 2003; Jeffries *et al.*, 1998, 2003; Košler *et al.*, 2002). Moreover it can offer a high throughput, capable of providing as many as 1000 single-grain U/Pb isotopic analyses per day (Frei and Gerdes, 2008). Laser ablation would typically remove a 10 to 30  $\mu\text{m}$  thick layer within the analyzed area and, hence, it does not require a particularly high quality for the polished sample surface. Time-resolved analysis of the laser ablation signal allows to isolate the signal portion that is no longer affected by potential surface contamination.

In double dating studies (less than 10 publications so far), LA–ICPMS U/Pb analysis has been already utilized in conjunction with (U-Th)/He thermochronology of the grains (Rahl *et al.*, 2003; Reiners *et al.*, 2005; Campbell *et al.*, 2005).

Here we present the results of a study combining FT and cathodoluminescence-controlled LA–ICPMS U/Pb geochronology from the same detrital zircon grains, from synorogenic sedimentary deposits in the Dinarides; one of the most complex and least

understood part of the European Alps. We use the data to develop a scheme for constraining major tectonic units in the sedimentary source area, many of them possessing a characteristic age-signature.

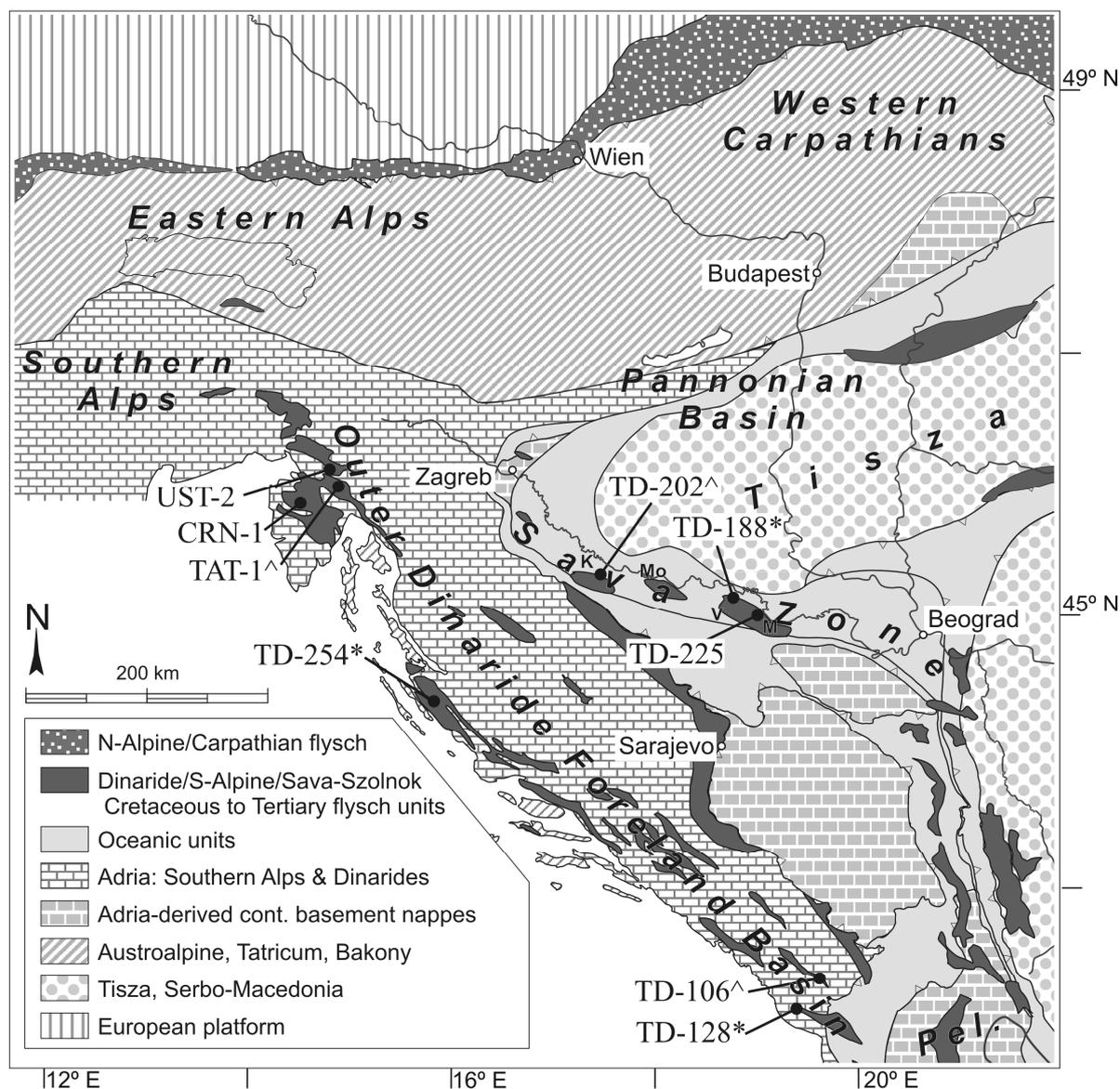


**Fig. 1.** Tectonic setting of the Dinarides with sampling locations shown. Map compiled after FGI, (1970), Aubouin (1973) and Schmid *et al.* (2008). *Star*, U/Pb dating was performed also on a handpicked zircon aliquot from that sample; *circumflex*, FT analysis alone, without U/Pb geochronology on the same grains. *Pel.*: Pelagonian Unit. Letters refer to isolated outcrops in the Sava Zone: *K*, Kozara Mts.; *Mo*, Motajica Mts.; *V*, Vučjak Mts.; *M*, Majejica Mts.

## 6.2. Geologic background

The samples chosen for this study were collected in two Tertiary basins of the Dinarides, each characterized by an entirely different geodynamic setting. Our previous work (Mikes *et al.*, 2005, 2006b) has revealed that these sedimentary sequences share many similarities in terms of their heavy mineral spectra, which are dominated by Cr-spinel, garnet and the very stable zircon + tourmaline + rutile assemblage.

### 6.2.1. Tectonic outline of the Dinarides

The Dinarides are an integral part of the European Alpine chain, located between the Southern Alps and the Hellenides (Fig. 1). An impressive SW-vergent pile of Alpine tectonostratigraphic units, they are characterized by Jurassic ophiolites thrust onto the distal passive margin of the Adriatic plate (Dimitrijević, 1982; Pamić *et al.*, 2002, Karamata, 2006; Schmid *et al.*, 2008). The latter is built up of sedimentary to low-grade metamorphic Lower Palaeozoic basement and its Permo-Mesozoic cover. The Early Cretaceous thrusting involved several Adria-derived units passively carrying the ophiolites previously thrust onto them, and gave rise to the formation of a vast clastic wedge in front of the continental-ophiolite thrust sheet complex (Aubouin 1973; Schmid *et al.*, 2008; Chapter 2 of this Thesis). The Outer Dinaride structural units are dominated by the elements of the large Mesozoic Adriatic Carbonate Platform (Vlahović *et al.*, 2005). Individual tectonic units of the platform are often separated by imbricated slices of Tertiary flysch which shows mixed carbonate–siliciclastic composition (Chorowicz, 1977; Chapter 5 of this Thesis), hinting at a major sediment source outside the platform. Thrusting in the Outer Dinarides was accompanied by the formation of a retrowedge at the NE margin of the Dinarides – the Sava Zone – that formed the collisional zone of the Dinarides with the Tisza Unit in the Tertiary (Pamić 1993, 1998, 2002; Tari, 2002; Schmid *et al.*, 2008).

### 6.2.2. Sava Zone

The Sava Zone is an elongated, highly complex tectonic zone located at the northern margin of the Inner Dinarides, separating them from the Tisza Unit further in the north (Fig. 1). It forms isolated outcrops, while a great part of the zone is covered by

Neogene sediments of the Pannonian Basin. The Sava Zone consists of Late Cretaceous ophiolites overlain by Late Cretaceous to Eocene mixed siliciclastic–carbonatic flysch-like sediments. Their deposition started in a forearc basin setting, created by the Late Cretaceous to Early Paleogene northward-directed subduction of remnant oceanic lithosphere – off the distal margin of the Adriatic plate – beneath the Tisza Unit (Pamić 1993; Pamić *et al.*, 2002, Schmid *et al.*, 2008). Whereas obduction of the Neotethys onto the Adriatic margin went to completion in the latest Jurassic already, (see Chapters 2–4 of this Thesis for details) biostratigraphic and geochronologic results revealed the existence of Campanian to Early Maastrichtian oceanic crust as well, which was thrust southwards onto the Jurassic ophiolites (Pamić and Šparica 1983; Karamata *et al.*, 2005, Ustaszewski *et al.*, in press). Geochemical data from the Cretaceous ophiolites in the Sava Zone are most consistent with an active back-arc extension behind the – already obducted – leading edge of the Neotethyan oceanic slab, with this back-arc magmatism thus considerably post-dating the onset of the obduction (Pamić *et al.*, 2002; Ustaszewski *et al.*, in press). Meanwhile, according to the interpretation of Tari (2002), around the Cretaceous/Tertiary transition the Sava Zone was converted to a retrowedge, developing behind the main thrust-wedge complex of the SW-vergent Dinaride orogen.

Siliciclastic flysch is underlain by Upper Cretaceous pelagic sediments ranging in age up to Late Campanian–Early Maastrichtian (Babić and Zupanić 1976; Bulić *et al.*, 1978; Jelaska 1978). Siliciclastic components found in the very rare intercalations of the pelagic sequence of the Banija–Kordun area (the westernmost part of the Sava Zone) comprise quartz, feldspar, chlorite, muscovite, tourmaline and rounded quartz grains and indicate a mature continental source area to the NE of the basin (Babić and Zupanić, 1976). In many occurrences a Maastrichtian age seems likely for the onset of flysch deposition, probably lasting until the Middle Eocene (Motajica Mts.: Pantić and Jovanović, 1970; Majevisa Mts.: Bulić *et al.*, 1978; Trebovac Mts.: Jelaska, 1978). In the Kozara Mts., the age of flysch deposition can be bracketed by the Campanian age of the underlying ophiolites (Karamata *et al.*, 2005; Ustaszewski *et al.*, in press) and the age of overprinting of the flysch at anchizonal conditions, based on K/Ar data from the shale sample TD207;  $63.2 \pm 1.4$  Ma and  $55.6 \pm 0.8$  Ma from the  $<2 \mu\text{m}$  and  $<0.2 \mu\text{m}$  fractions, respectively (K. Wemmer, pers. comm. 2007). These data are consistent with a Paleocene calcareous nannofossil assemblage identified in the same sample (M. Báldi-Beke, pers. comm. 2007), with the Late Paleocene age of intercalated shallow

marine limestone debris (Ustaszewski *et al.*, in press), and with Middle Eocene planktonic foraminifera from marls unconformably overlying the deformed and overprinted flysch (V. Čosović, pers. comm. 2006).

Siliciclastic components of the flysch were sourced from a composite source area made up of ophiolites, granitoids and metamorphic units (Jelaska *et al.*, 1970; Mikes *et al.*, 2006b; Ustaszewski *et al.*, in press). The geochemistry, textural patterns and (Th-U)/Pb geochronology of detrital monazite suggest that these rock suites included Late Permian A-type granitoids and Jurassic to Early Cretaceous metamorphic rocks (Krenn *et al.*, 2008). Palaeocurrent indicators suggest sediment transport from NE to E relative to the Sava Zone at present directions (Jelaska *et al.*, 1970, Babić and Zupanić 1976; Jelaska 1978), or from E to SE if the Tertiary counter-clockwise rotation in the Sava Zone that exceeds 30° is also taken into account (Márton *et al.*, 2005).

Sediments of the Sava Zone and their ophiolitic or continental basement underwent deformation and Alpine regional metamorphism due to the collision of the Tisza Unit with the Inner Dinaride continental margin (Pamić, 1993). The degree of metamorphism shows large regional variations, ranging up to amphibolite facies, and is dated mostly as Late Cretaceous to Early Paleogene (Pamić 1993, 1998; Balen *et al.*, 2003; Starijaš *et al.*, 2006; Krenn *et al.*, 2008). The sedimentary–metamorphic sequence is intruded by Late Cretaceous to Oligocene granitoids and bimodal volcanic series (Pamić and Šparica 1983; Pamić 1997, 2002; Pamić *et al.*, 2000; Starijaš *et al.*, 2005; Ustaszewski *et al.*, in press).

### 6.2.3. Outer Dinaride foreland basin

Flysch-like sediments in the Outer Dinarides form part of a large foreland basin system at the front of the SE-directed Dinaride thrust wedges (Fig. 1). Basin remnants can be traced along the orogenic strike from the Southern Alps to the Hellenides. Stratigraphic position of the flysch is described in terms of a Palaeogene to Neogene marine sequence overstepping Cretaceous platform carbonates, that are locally overlain by coarse-grained delta deposits draining Outer Dinaride carbonate nappes. The flysch overlies well-dated Lower to Upper Eocene *Globigerina* marls; their contact is conformable at places, but angular or erosional unconformities have been often reported (e.g. Marinčić, 1981; Marjanac, *et al.*, 1998; Marjanac, 2000). Due to repetitive thrusting, flysch profiles are tilted, usually truncated at their base and less than 100-

400 m thick. Turbidite beds are dominantly composed of siliciclastics, with a highly variable amount of carbonate admixture. In the NW part of the basin system, palaeocurrent data indicate largely SW-directed primary, and SE-directed deflected (longitudinal) flows (Magdalenić, 1972; Babić and Zupanić, 1983; Orehek, 1991). Radial current directions are commonly found in Central Dalmatia, resulting from complex basin floor topography and multiple flow reflection (Marjanac 1990). Based mostly on paleocurrent indicators and heavy mineral analyses in the NW, two different hypotheses exist for the provenance of the siliciclastic material. Magdalenić (1972) suggested a dual, Alpine-Dinaride source, whereas Marinčić (1981) and Marinčić *et al.* (1996) proposed derivation from the Dinaride units to the NE of the basin.

The flysch sandstones are lithic wackes to calcilithites, with their main framework components averaging at  $Q_{60-85}F_{5-15}L_{10-25}$ , corresponding to a recycled orogenic provenance (Mikes *et al.*, 2006a). Major and trace element geochemistry as well as heavy mineral analysis indicate provenance mixing of mature, quartzose sedimentary rocks and ophiolitic sequences. Locally however, especially in the central and SE part of the basin, the heavy mineral spectra comprise higher amounts of unstable metamorphic species (hornblende, tremolite, epidote, chloritoid), whereas Cr-spinel, garnet, rutile, zircon, tourmaline and apatite as well as minor amounts of staurolite and glaucophane characterize most of the heavy mineral assemblages elsewhere in the entire basin system (Woletz, 1962; Pavičić *et al.*, 2003; Mikes, 2003; Mikes *et al.*, 2005). Regional distribution of new calcareous nannofossil depositional ages reveals an increasing preservation for the Neogene part of the sequence towards the SE (Chapter 5). This pattern is well in line with a recent kinematic reconstruction by Ustaszewski *et al.* (2008), proposing that the amount of post-Early Miocene shortening increases in this direction. The above data suggest increased relief and exhumation in the SE Dinarides in the Late Tertiary, and westerly-directed drainage towards the foreland basin system.

### 6.3. Sampling, analytical techniques and data treatment

Fresh, medium-grained sandstones were selected for this study; three from the Sava Zone and six from the Outer Dinaride foreland basin. Of them, double dating was performed on two and four samples, respectively (Table 1). Samples TD-188, TD-254 and TD-128 were chosen for preparing a second, handpicked zircon aliquot to perform

a systematic comparison of the U/Pb ages obtained on fission-track etched and unetched aliquots.

**Table 1.** Sample set used in this study for zircon FT and U/Pb analyses. The lower number of U/Pb analyses from fission track dated grains is mostly due to a loss of some crystals from the FT mount during the steps of transfer to the LA cell; only less than 2 % of all analyses were rejected due to a severe age bias. From sample UST-2, only one out of the two FT mounts (n=30) was used for U/Pb dating. *SZ*, Sava Zone; *ODFB*, Outer Dinaride foreland basin. Stratigraphic ages are as compiled in Ustaszewski *et al.* (in press) and from V. Čosović (pers. comm), M. Bálđi-Beke (pers. comm), and Chapter 5; chronostratigraphic assignment according to Gradstein *et al.* (2004).

sample	locality	depositional age (Ma)	ZFT analysis		U/Pb geochronology			
				<i>n</i>	<i>grain-matched with ZFTA</i>	<i>n</i>	<i>on unetched aliquot</i>	<i>n</i>
TD-188	SZ, Vucjak Mt.	<70.6	x	60	x	48	x	10
TD-225	SZ, Majevisa Mt.	<65.5	x	55	x	46		
TD-202	SZ, Kozara Mt.	65.5–48.6	x	60				
UST-2	ODFB, NW	<55.8	x	60	x	30		
TAT-1	ODFB, NW	<55.8	x	60				
CRN-1	ODFB, NW	<33.9	x	60	x	46		
TD-30	ODFB, NW	<55.8					x	58
TD-254	ODFB, central	<18.2	x	60	x	53	x	131
TD-128	ODFB, SE	<18.2	x	60	x	53	x	142
TD-106	ODFB, SE	<53.6	x	50			x	71

### 6.3.1. Sample preparation

Zircon grains were recovered from about 2 to 5 kg samples of sandstones, following dry sieving (<0.250 mm), hydraulic pre-concentration using a Wilfley-table, dissolution of the carbonate component by cold 5% acetic acid, gravity separation by hot LST heavy liquid ( $\rho=2.88 \text{ gcm}^{-3}$ ), and electromagnetic separation.

### 6.3.2. Fission track analysis

Crystals were embedded in PFA Teflon with two mounts made from each sample. Spontaneous tracks were revealed by etching in NaOH-KOH eutectic melt at 225°C (Gleadow *et al.*, 1976) for 23 to 74 hours. Neutron irradiations were performed at the research reactor of Oregon State University. The external detector method was used (Gleadow, 1981) and, after irradiation, the induced fission tracks in the mica detectors were revealed by etching in 40% HF for 30 min. Track counts were made with a Zeiss

Axioskop microscope at  $\times 1000$  magnification combined with a computer-controlled stage system (Dumitru, 1993). The FT ages were determined by the zeta method (Hurford and Green 1983) using the age standards listed in Hurford (1998). See Dunkl *et al.* (2001) for further details.

### 6.3.3. Grain referencing

Following FT analyses, grains were documented by reflected light photomicrographs in all samples selected for the double dating. Grain co-ordinates were exported from the FT stage system and transferred to the stage control softwares of both the scanning electron microscope and the laser ablation instrument. This facilitated a rapid and easy re-identification of the grains.

### 6.3.4. Cathodoluminescence (CL) imaging

The FT-dated grains were imaged by CL prior to laser ablation. An Oxford Instruments CL system was used, interfaced to a JEOL 8900 RL electron microprobe operated at 15 kV accelerating voltage and 30 nA beam current. Images were less contrasty than those normally acquired by routine zircon imaging. We attribute this to the combined effects of the (1) rather uneven surfaces of the sectioned crystals resulting from the etching procedure (cf. Fig. 13), and (2) the unusually low beam current (chosen to reduce evaporation of the thermally unstable PFA teflon surrounding the grain in the rastered area) was not sufficient for the CL detector to produce a more brilliant image of the CL intensity contrasts.

### 6.3.5. LA-ICPMS U/Pb geochronology

U/Pb isotopic composition was determined on carefully selected crystal domains by laser ablation – inductively coupled plasma mass spectrometry (LA-ICPMS). The instrumental setup used consists of a single-collector Agilent 7500cs ICPMS equipped with a quadrupole mass filter, and a New Wave UP213 Nd:YAG UV laser system ( $\lambda = 213$  nm) operated in dynamic ablation mode. Analytical parameters are listed in Table 2. Off-line reduction of raw data was made by LAMTRACE (Jackson, 2008) and PapiAGE (Dunkl *et al.*, in prep.), with no correction for any common Pb present. Age

calculations were made using Isoplot 3.0 (Ludwig, 2003). Results of analysis and age calculation are listed in Appendices 6-1 and 6-2.

**Table 2.** LA-ICPMS instrumental parameters and measurement protocol used in this study.

<i>ICP-MS instrument operating conditions</i>	
Instrument	Agilent 7500 cs
Forward power	1500 W
Coolant gas flow	13 lmin <sup>-1</sup> Ar
Auxiliary gas flow	0.8 lmin <sup>-1</sup> Ar
Carrier gas flow	0.9 lmin <sup>-1</sup> He
Sampling depth	6.9 mm
<i>ICP-MS data acquisition parameters</i>	
Analyzed masses	201; 204; 206; 207; 208; 235; 232; 238
Dwell time	10 ms (20 ms for masses 207 and 235)
Sweeps	1000
Background acquisition time	60 s
Total ablation time	75 s
Washout time	90–120 s
Ablation time taken for age calculation	10–40 s
<i>Laser ablation operating conditions</i>	
Instrument	New Wave Research UP213 Q-switched Nd:YAG
Wavelength	213 nm
Pulse width	3 ns
Fluence at surface	2.5–3.5 Jcm <sup>-2</sup>
Pulse energy at surface	0.01–0.1 mJ per pulse
Energy distribution	Homogenized flat beam, aperture imaged
Repetition rate	10 Hz
Laser focus	fixed to target surface
Sampling scheme	ablation along short line rasters
Raster scan speed	5 μm <sup>s</sup> -2
Nominal pit diameter	55 μm (standard); 30–55 μm (unknowns)
Ablation cell	New Wave's standard circular design (V~9 cm <sup>3</sup> )
Length of tubing	1.5 m
<i>Standardization and data reduction</i>	
External standard used	Nancy 91500 zircon
Standard-sample bracketing sequence	...-[4-12-4]-[4-12-4]-...
Reference used for quality control	Plešovice zircon
Data reduction software used	LAMTRACE (primary) / PepiAGE (test phase)

### 6.3.6. Integrated processing of U/Pb and FT age data

The fact that contrasting amounts of error associate single-grain U/Pb and FT ages requires a rigorous statistical treatment of the data, in order to identify geologically meaningful age clusters. First, marginal age distributions were constructed using a variable bandwidth kernel density estimation, where a so-called normal kernel was attributed to each grain age; the standard deviation of the kernel was set equal to the standard error of that particular analysis (see details in Sircombe and Hazelton, 2004). For creating the age-pair plots presented in Fig. 10, a two-dimensional version of the same variable bandwidth kernel density estimation was used, assuming no correlation between the two standard errors. Clusters on the age-pair plots were defined by iso-density levels of the 2D variable bandwidth kernel density estimate. A higher density, i.e. a more probable grain clustering, is achieved whenever more grains plot together and/or if they have low analytical error.

## 6.4. Results

### 6.4.1. Fission track analysis

The track counting results are listed in Appendix 1. The  $\chi^2$ -test (Green, 1981) and the dispersion (Galbraith and Laslett, 1993) indicate that most samples represent mixtures from multiple sources having different cooling ages. The PopShare software (Dunkl and Székely, 2002) was used to deconvolute the age spectrum in up to 3 age components. Table 3 contains the best fitting results.

#### 6.4.1.1. Sava Zone

Three samples from the Sava Zone are all dominated by a Late Cretaceous age component (Fig. 2; Table 3). In the Kozara (TD-202) and Vučjak Mts. (TD-188), the age distribution is dominated by a Late Cretaceous mode around 75 Ma, and in the latter a less significant age component of 90 Ma is also present. The majority of single-grain ages is connected to glass-clear, euhedral crystals with intact crystal edges and

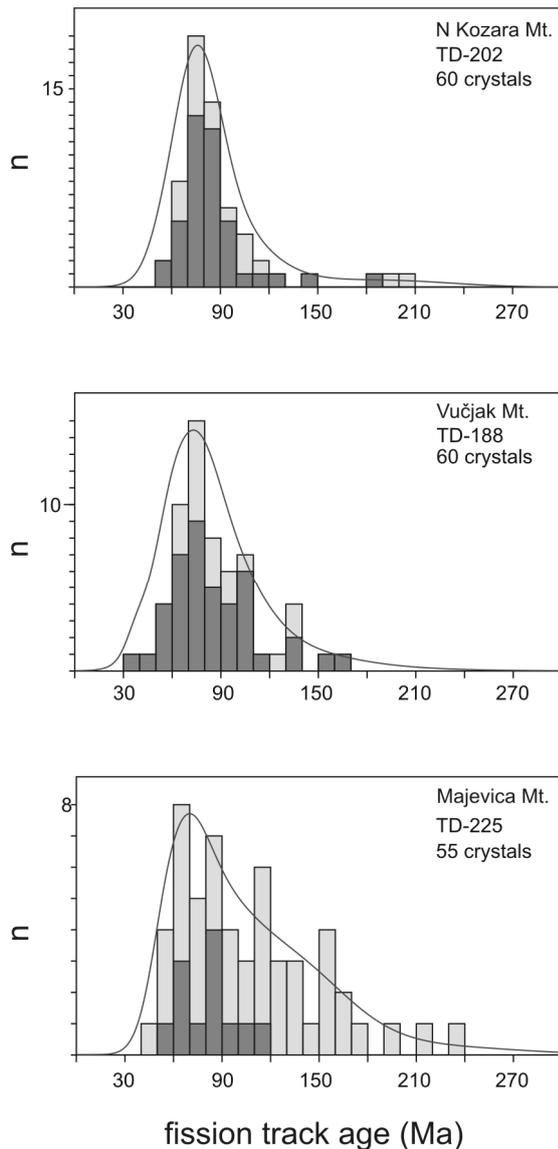


**Fig. 2.** Distribution of single grain zircon fission track ages in three flysch sandstone samples of the Sava Zone. *Dark grey bars*, glass-clear, euhedral zircon crystals; *light grey bars*, all crystals. Composite age spectra (continuous lines) were computed according to Hurford *et al.* (1984).

#### 6.4.2. U/Pb geochronology – assessment of data quality

We performed 276 U/Pb age determinations by LA-ICPMS on zircon single grains that were previously dated by FT analysis. In order to test the possible effects of (1) the etching on the U-Pb isotopic systematics of the grains and (2) the FT operator bias on the underlying U/Pb age structure of the FT dated grains, we also analyzed an unetched aliquot from three samples (see details in Table 1).

faces, suggesting a direct derivation from a magmatic and/or volcanic source in the Cretaceous. Sample TD-225 (Majevisa Mts.) shows the broadest age distribution; about one half of the grains is derived from a different source that experienced a last cooling event in the Jurassic-Early Cretaceous (Fig. 2; Table 3).

#### 6.4.1.2. Outer Dinaride foreland basin

FT age distributions in six samples are invariably dominated by a Late Cretaceous age population, with their modes ranging between 69 and 88 Ma, comparable to the results in the Sava Zone. They all emerge from a broad distribution of older single-grain ages (except for sample TD-106). There, a Jurassic-Early Cretaceous group with a mode around 143 Ma and a Permo-Triassic group with a mode around 247 Ma can additionally be isolated (Fig. 3; Table 3).

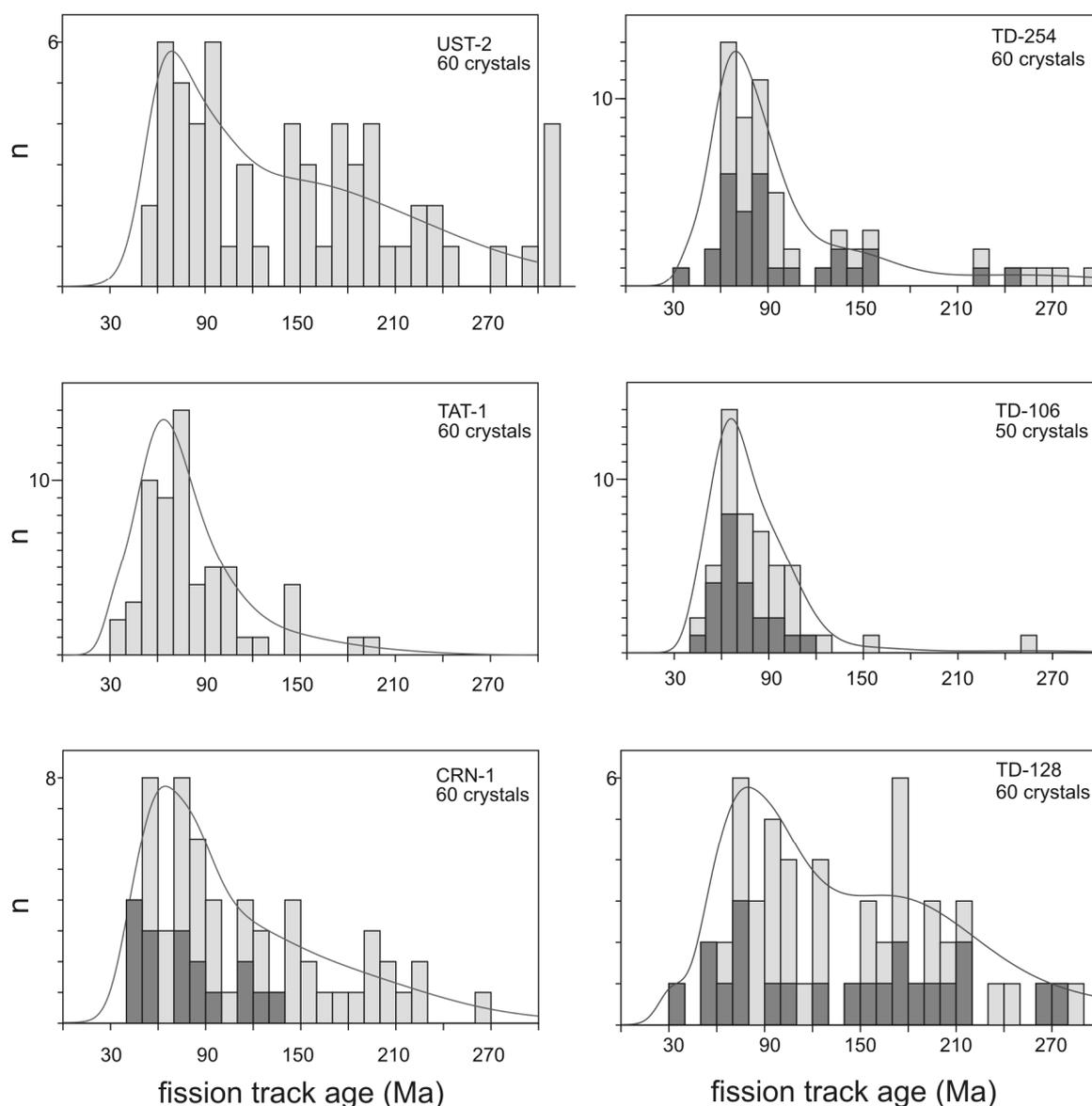


**Fig. 3.** Distribution of single grain zircon fission track ages in six flysch sandstone samples of the Outer Dinaride foreland basin. *Dark grey bars*, glass-clear, euhedral zircon crystals; *light grey bars*, all crystals (morphology was not registered in samples UST-2 and TAT-1). Composite age spectra (continuous lines) were computed according to Hurford *et al.* (1984).

Due to our unusual sample material (i.e. etched surfaces) we briefly assess data quality to ensure a meaningful geological interpretation of the U/Pb geochronologic results.

The amount of isotope ratio drift encountered during the laser ablation was minimal. This phenomenon is partly attributed to chemical fractionation caused by non-stoichiometric sampling by the laser pulses (e.g. Hergenröder, 2006), and necessitates several labour-intensive correction steps, e.g. the use of a thallium tracer solution aspirated into the plasma and employing a fractionation law that relates laser fluence and

crater aspect ratio to the rate of Pb/U fractionation during ablation (Horn *et al.*, 2000) or an off-line mathematical correction of the drifted dataset (Sylvester and Ghaderi, 1997). These additional measures are both a source of additional error that (1) needs to be propagated into the uncertainties of the final isotope ratio results, and (2) adversely affects the accuracy. We used the ratio of the y-intercept of the linear regression of the  $^{206}\text{Pb}/^{238}\text{U}$  signal to the median of the individual, time-resolved  $^{206}\text{Pb}/^{238}\text{U}$  ratios in order to quantify the ablation-induced within-run drift. In most cases this value remained below 1%, which enabled us to take the median isotope ratios for the age calculation without performing a drift correction additionally (Fig.4).

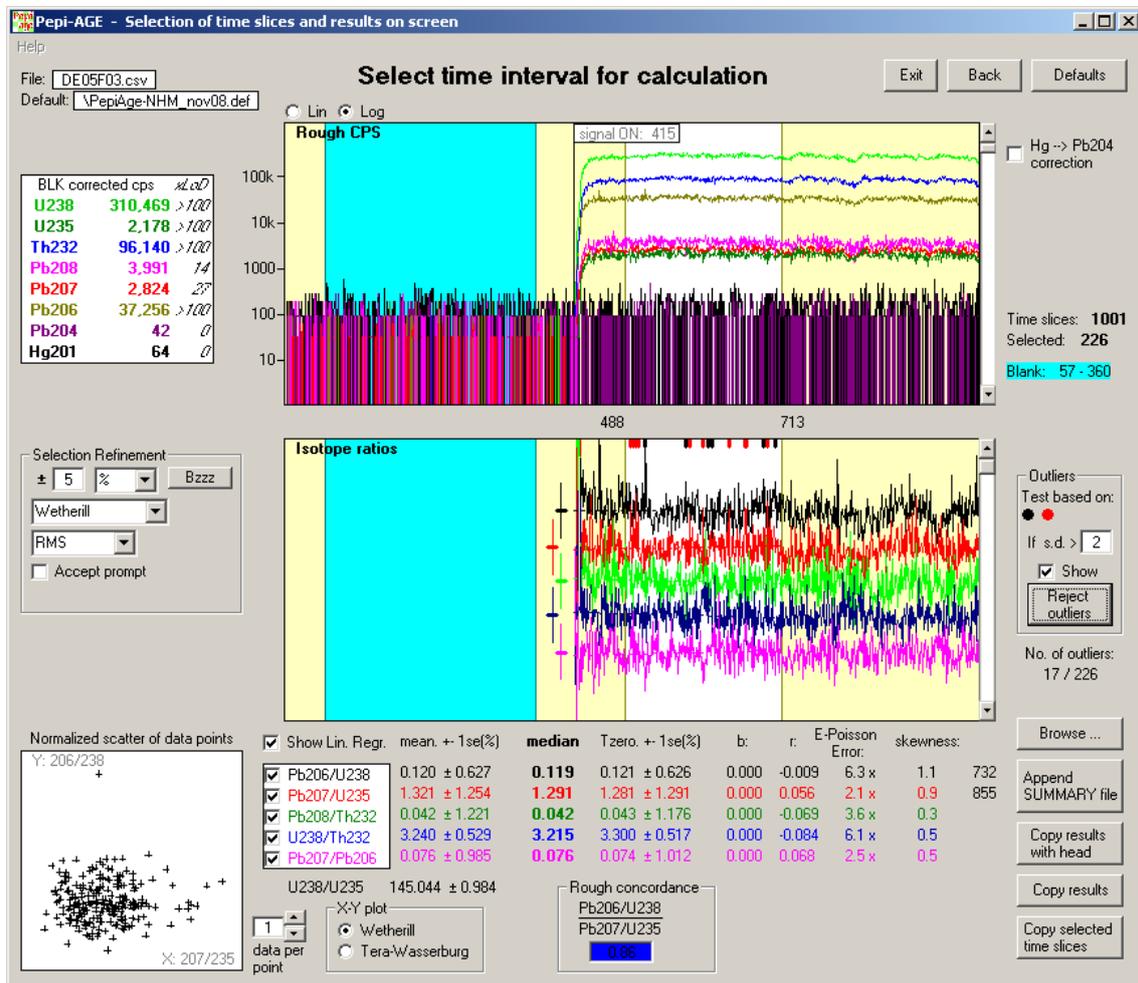


**Fig. 4.** Time-resolved isotope ratio analysis by laser-ablation ICPMS of the 91500 zircon reference material. The background-corrected analyte intensity ratios  $^{207}\text{Pb}/^{235}\text{U}$  and  $^{206}\text{Pb}/^{238}\text{U}$  show no significant time-dependent drift away from the initial value at the begin of the experiment, which rendered any correction for within-run drift unnecessary.

Preliminary assessment of the possible incorporation of the common Pb component was made using Tera-Wasserburg concordia plots (Figs. 5 & 6; Tera and Wasserburg, 1972). For the majority of the analyses, the  $2\sigma$  error ellipses are within the concordia, pointing to no significant amounts of common Pb component in the analyzed zircon volumes. This is corroborated by the conventional Wetherill concordia plots, showing a good agreement of the  $^{207}\text{Pb}/^{235}\text{U}$  and  $^{206}\text{Pb}/^{238}\text{U}$  ages (Figs. 7 & 8). On the basis of this pattern, no common Pb correction procedure was applied to our detrital datasets.

The data show several major cluster of concordant U/Pb age data at: 630 to 610, 460, 270 and 80 Ma in the Sava Zone, and at 500, 470 to 450, 370, 270, 240 and 80 Ma in the Outer Dinaride foreland basin. Most of the ages can reflect magmatic or volcanic crystallization events, based on the prevalence of grains with a euhedral to subhedral character and a well-defined oscillatory zoning pattern throughout the imaged surface.

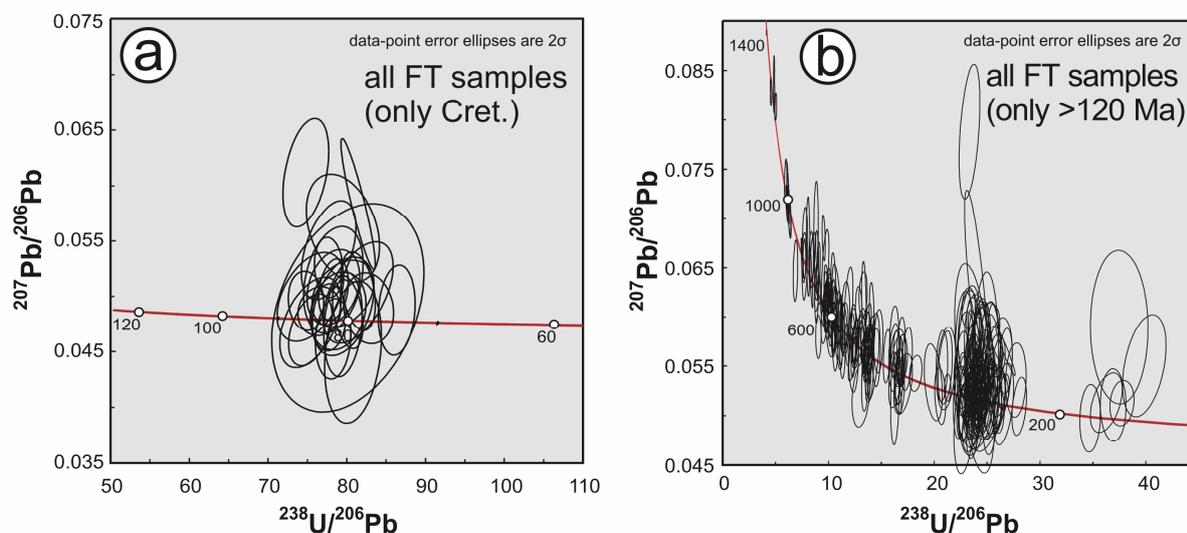


**Fig. 5.** Tera-Wasserburg concordia for all double dated grains. **a:** ages around 80 Ma; **b:** ages older than ca. 120 Ma.

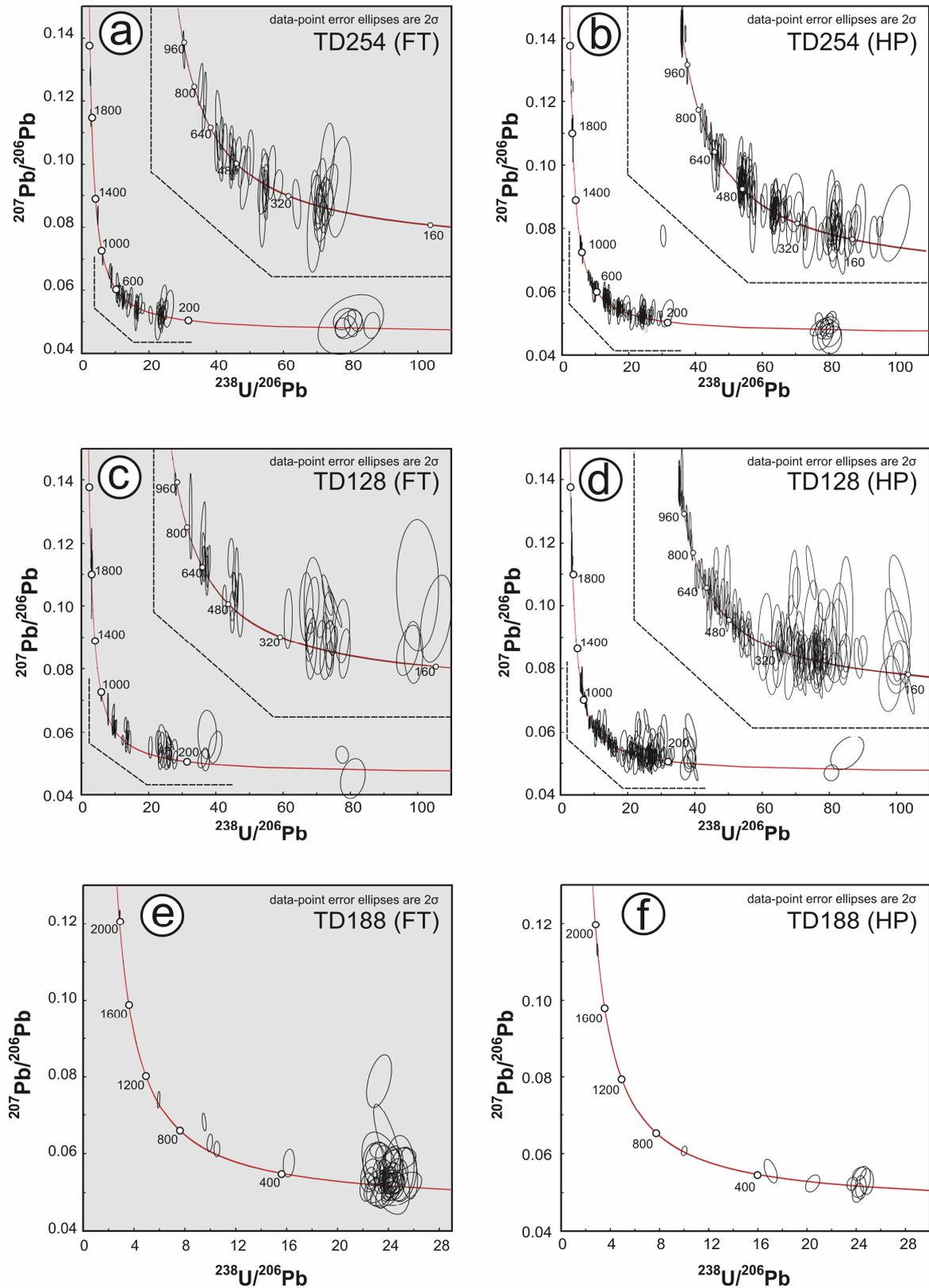


**Fig. 6.** Tera-Wasserburg concordia of three double dated zircon samples (left) for which additional U/Pb analyses were performed on their unetched aliquots (right). Both the overall age distributions and the common Pb levels of crystals in the FT mounts are fairly comparable to those in the epoxy mounts.

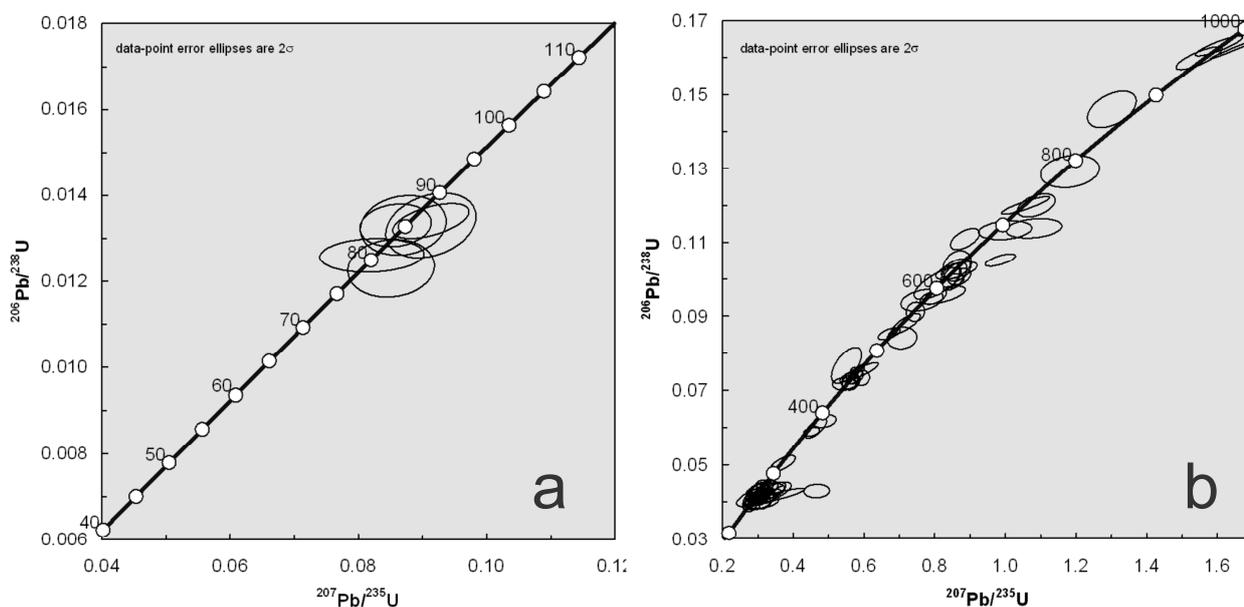


**Fig. 7.** Wetherill concordia of the double dated zircon grains in the Sava Zone. **a:** Cretaceous age group; **b:** older, Phanerozoic to Late Proterozoic grains. A few, largely concordant grains >1000 Ma plot outside the diagram.

## 6.5. Discussion

### 6.5.1. Capability of quadrupole LA-ICPMS for zircon U/Pb geochronology

The analytical setup and parameters used in this study (Table 2) enabled us to acquire precise and accurate isotopic ratios for zircon U/Pb geochronology. In concordant Phanerozoic zircons,  $^{207}\text{Pb}$  is the least abundant isotope of the U-Pb system, thus the success of the analyses largely depends on the ability to detect this analyte. Table 4 shows the typical performance of the Agilent 7500cs ICPMS instrument in terms of sensitivity for the 207 and other masses. We used the  $^{207}\text{Pb}$  sensitivity values to determine the instrumental limits of U/Pb dating at the laser beam diameters employed, taking the typical range of U concentrations encountered in the Dinaride zircon grains (Fig. 9). The calculations show that the intersection of the age-intensity function with the ca. 90 cps limit of detection (grey band) yields an estimate for the actual instrumental "limit of dating". Knowing the U concentrations in advance – derived from the fission track chronology – is helpful to decide if an adjustment of ablation parameters is necessary prior to analysis of that particular grain.

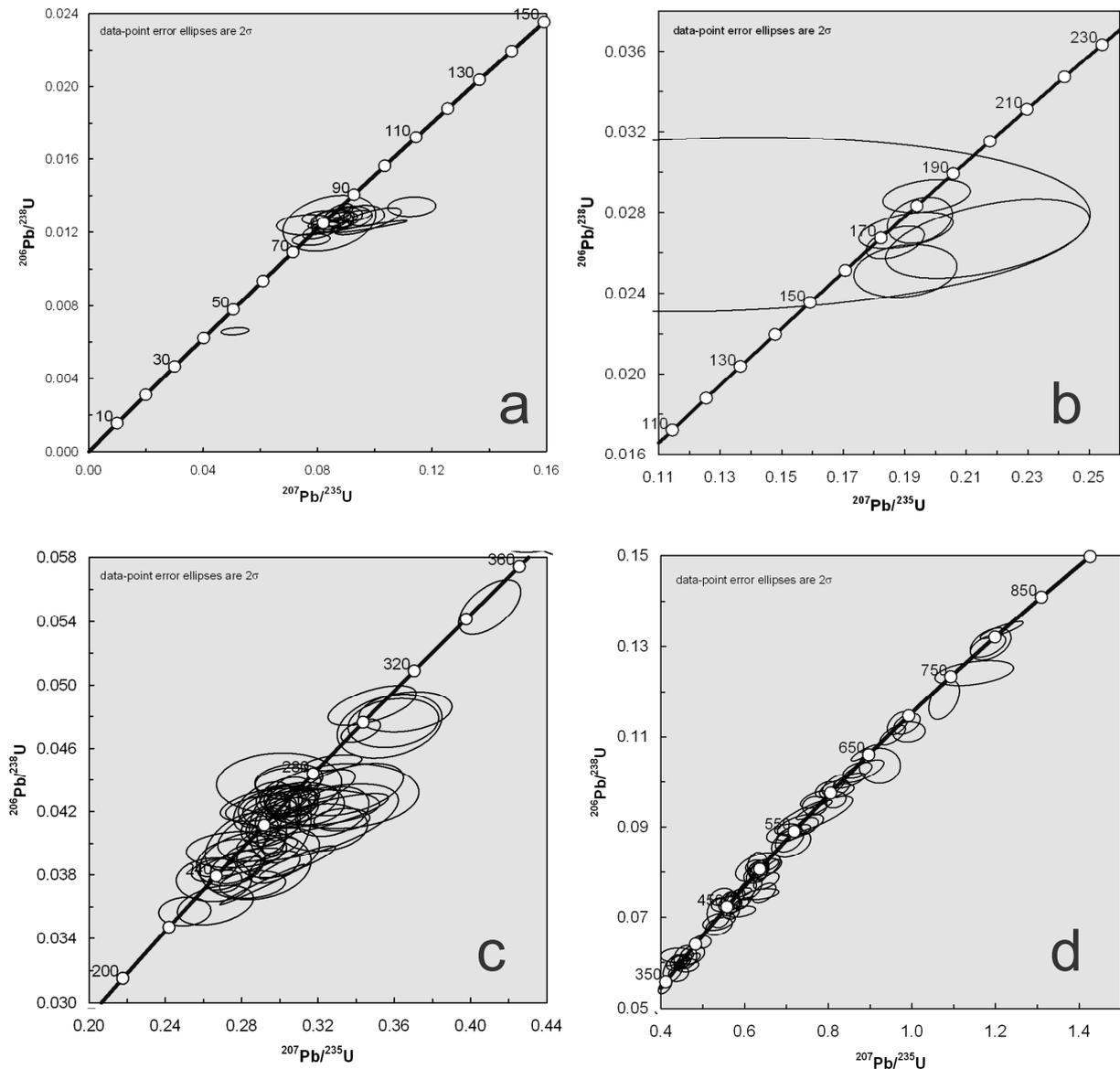


**Fig. 8.** Wetherill concordia of the double dated zircon grains in the Outer Dinaride foreland basin. **a:** Cretaceous age group; **b:** Jurassic age group; **c:** Permo-Triassic age group; **d:** Phanerozoic to Late Proterozoic grains. A few, largely concordant grains >1000 Ma plot outside the diagram.

### 6.5.2. Double dating: implications for sedimentary provenance

We combined the  $^{206}\text{Pb}/^{238}\text{U}$  geochronological and FT thermochronological results for each grain in order to obtain a two-dimensional distribution of ages, which highlights several important provenance characteristics.

**Table 3.** Deconvolution of composite zircon FT age spectra for all samples that failed the  $\chi^2$ -test, i.e. shows a broad age distribution suggesting a composite source. Calculations were based on the Simplex algorithm (Cserepes, 1989) implemented by Popshare software (Dunkl and Székely, 2002); fittings were performed by iteratively minimizing the root mean square. Tect: tectonic unit (S – Sava Zone; D – Outer Dinarides); M1, M2, M3: mean of the isolated age components; SD1, SD2, SD3: standard deviations of the components (Ma); %C1: proportion of the youngest component (%); RMS: root mean square.

sample	tect	comp.	n	M1	SD1	%C1	M2	SD2	M3	SD3	RMS
TD-188	S	2	60	74	9	39	91	29	-	-	0.023
TD-225	S	3	55	72	16	44	118	24	187	24	0.021
UST-2	D	3	60	80	20	43	177	34	301	44	0.017
TAT-1	D	2	60	69	13	59	95	43	-	-	0.018
CRN-1	D	3	60	72	19	57	133	23	201	19	0.012
TD-254	D	3	60	76	15	73	143	13	265	25	0.028
TD-128	D	3	60	88	24	46	179	23	295	55	0.008
all "D"	D	3	300	75.2	16.9	45.7	143	47.1	247.3	77.8	0.016

**Table 4.** Typical instrument sensitivities for selected analytes as determined here on the Nancy 91500 zircon reference material, using background corrected count rates from experiment #no30b18. Recommended isotope concentrations are as reported in the GeoRem database (Jochum *et al.*, 2005). Sensitivities in case of pit diameters other than 55  $\mu\text{m}$  are calculated from the ratios of the different ablated volumes. All sensitivities are corrected for the difference between the nominal and the measured pit diameter which is usually around 10%.

**Instrument sensitivity**

Agilent 7500 cs & New Wave UP213 Nd:YAG laser  
 experiment # no30b18, 91500 zircon  
 Date: 30/11/2007

nominal dia [um]	real dia [um]	volume ratio	conc. [ppm]						sensitivity [cps/ppm]						
			14.9	1.19	1.76	29.9	0.58	80.6	206Pb	207Pb	208Pb	232Th	235U	238U	
15	11.7	13.507							calculated	169	159	151	222	270	273
30	22	3.820							calculated	596	564	533	784	956	966
40	34	1.599							calculated	1423	1347	1273	1873	2282	2307
55	43	1.000	33912	2563	3583	89590	2134	297436	measured	2276	2154	2036	2996	3651	3690
65	62	0.480							calculated	4741	4486	4241	6241	7604	7687
100	78	0.304							calculated	7489	7087	6699	9859	12012	12143
120	93.6	0.211							calculated	10784	10205	9646	14197	17297	17485

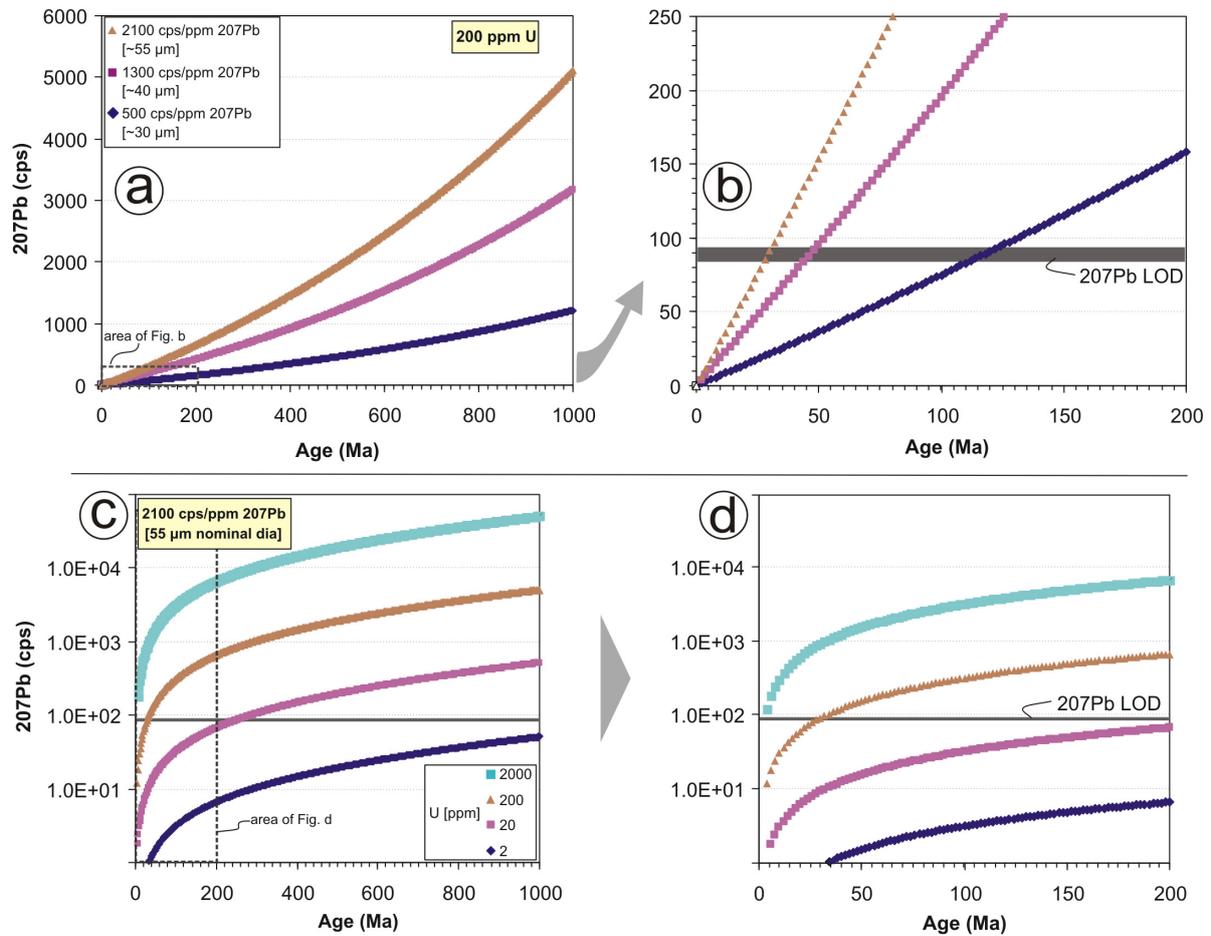


**Fig. 9.** Modelled ICPMS instrument response on mass 207 in the laser ablation experiments, as a function of various parameters. **a** and **b** (blow-up of framed area in **a**): a zircon with a typical U concentration of 200 ppm, as a function of the geological age, assuming only single-component radiogenic Pb in the lattice. Three cases are shown; for 500, 1300 and 2100 cps/ppm sensitivities, which correspond to nominal pit diameters of 30, 40 and 55 μm, respectively, most frequently chosen in this work. **c** and **d** (blow-up of framed area in **c**): instrument response on mass 207 at a sensitivity of 2100 cps/ppm as a function of geological age, for zircons with four different U concentrations. These calculations show the limits (and capabilities) of the instrumental setup for the purposes of U/Pb age dating. Intersection of any curve with the ca. 90 cps limit of detection (grey line) would yield an estimate for the actual "limit of dating". Knowing the U concentrations in advance – derived from the neutron irradiations – is helpful to decide if an adjustment of ablation parameters is necessary prior to analysis of that particular grain.

In the Sava Zone (Fig. 10a), well isolated groups of Late Cretaceous (86 to 79 Ma), late Early to Late Permian and Ordovician to Early Silurian crystallization ages occur. Probably, a Late Proterozoic group of ages between 640 to 600 Ma also forms a less pronounced cluster. The Ordovician to Early Silurian group and a minor fraction of the Permian group were derived from source units experiencing no major thermal event after Jurassic to Early Cretaceous times. However, the majority of the Permian crystals

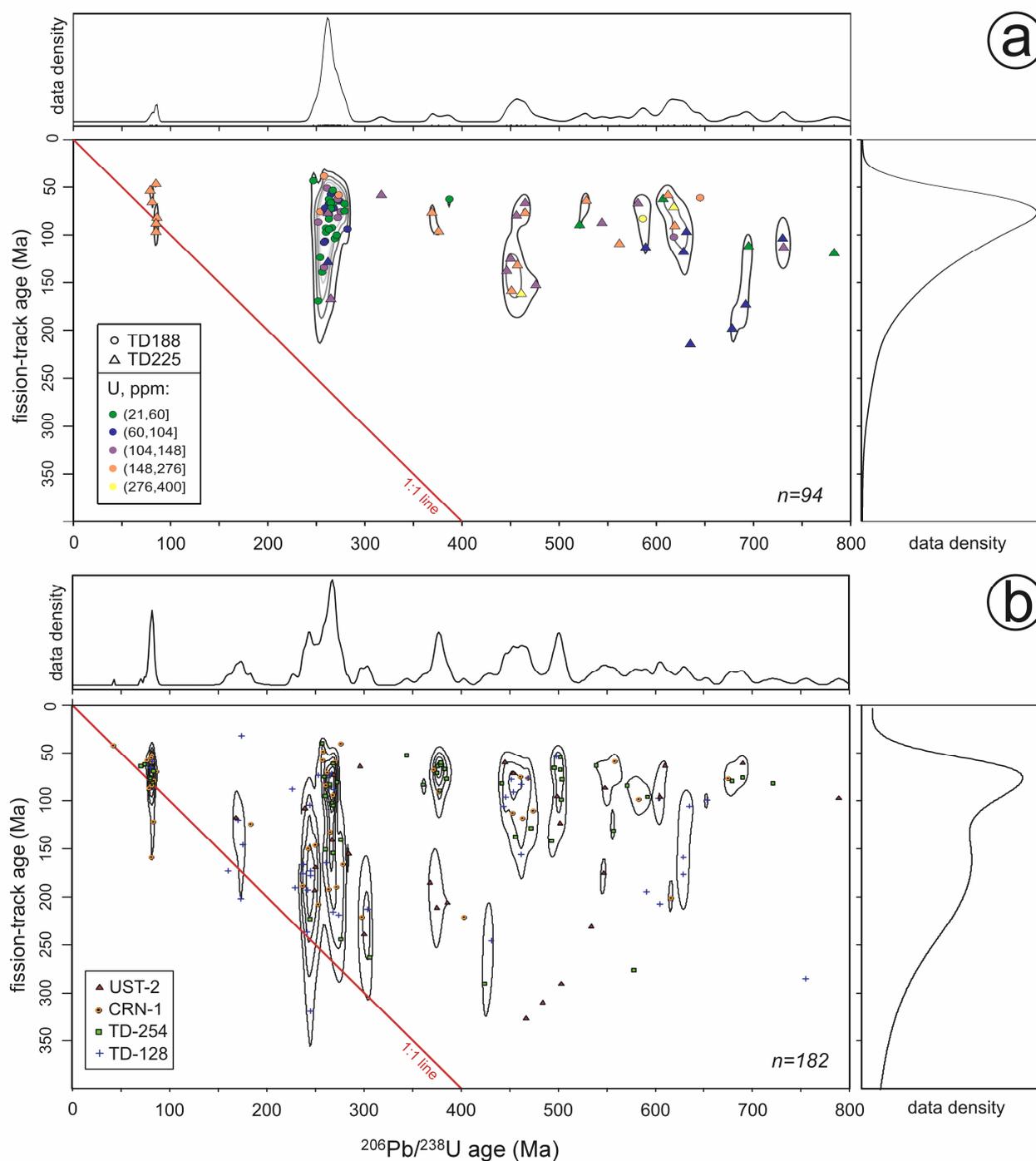


**Fig 10.** Age-pair plots portraying the relationship of U/Pb and FT ages on a single-grain level, reflecting the ages of crystallization and of cooling below mid-crustal levels, respectively. **a:** Sava Zone; **b:** Outer Dinaride foreland basin. Individual kernel density estimates for the marginal distribution of both sorts of ages are displayed as well. Characteristically, standard error is low with the U/Pb ages ( $1\sigma$ : 0.5-1.5%), and high with the FT ages ( $1\sigma$ : 15-30%), which explains the contrasting age distribution types. In this two-dimensional combination of the age distributions, the clusters are defined by isodensity levels of a variable bandwidth 2D kernel density estimate (as described in Section 6.3.6.). See text for discussion.

is derived from units that cooled below the thermal zone of zircon track instability only in the Late Cretaceous. The youngest cluster of identical U/Pb and FT ages of ca. 80 Ma clearly represent a first-cycle source. Their magmatic (probably volcanic), rather than metamorphic origin is supported by oscillatory zoning with faint but straight zone boundaries, and their rather uniform U concentration (colour coding in Fig. 10a). It is possible that grains of this group represent a single source.

Age distributions in the Outer Dinaride foreland basin reveal essentially the same clusters, but several additional ones occur here as well (Fig. 10b). These include a Late Cambrian (c. 500 Ma), a Late Devonian (c. 380 Ma) and a Triassic (c. 240 Ma) component; however only the two former are characterized by Late Cretaceous cooling ages. Small but coherent groups of further Late Devonian to Early Carboniferous (380 to 340 Ma) as well as Late Carboniferous to Early Permian ages (310-290 Ma) may reflect a Triassic thermal event affecting their source rocks. As in the Sava Zone, a fraction of the Permian grains shows no effective thermal reset in the source units after their Jurassic/Early Cretaceous cooling. A striking feature is that none of the Triassic grains indicates dominant Late Cretaceous cooling event, but they belong to the same Late Mesozoic FT age population as the Permian grains noted above. Finally, a small age cluster of Jurassic crystals documenting an Early Cretaceous cooling event also occurs. A part of these peculiar crystals exhibits an unusually large size (up to 200  $\mu\text{m}$ ), typically low U contents, and large regular and homogeneous CL domains indicative of magmatic zoning, altogether suggesting a gabbroid origin (Vavra, 1990; Grimes *et al.*, 2007).

The age clusters isolated herein match typical Alpine tectonostratigraphic units. Given that basement geochronology is known in detail, several source terranes can be pinpointed with such a confidence that is normally not achieved by using the two dating techniques separately. We preliminarily conclude that a majority of the grains indicating Late Cretaceous overprint is derived from the Austroalpine and/or Tisza Units as this thermal event is not recorded in the Central and Northern Dinarides (see discussion in Chapter 2 of this Thesis). Our results clearly demonstrate the mixing of sediments derived from exhumed source areas that previously underwent fundamentally different thermal histories (Fig. 11). In summary, the double dating technique has the potential to discriminate among detrital grains (1) derived from several sources characterized by different thermal evolution but an identical U/Pb age signature, or (2)

derived from units sharing a uniform cooling history but comprising rocks with a variety of zircon U/Pb ages.

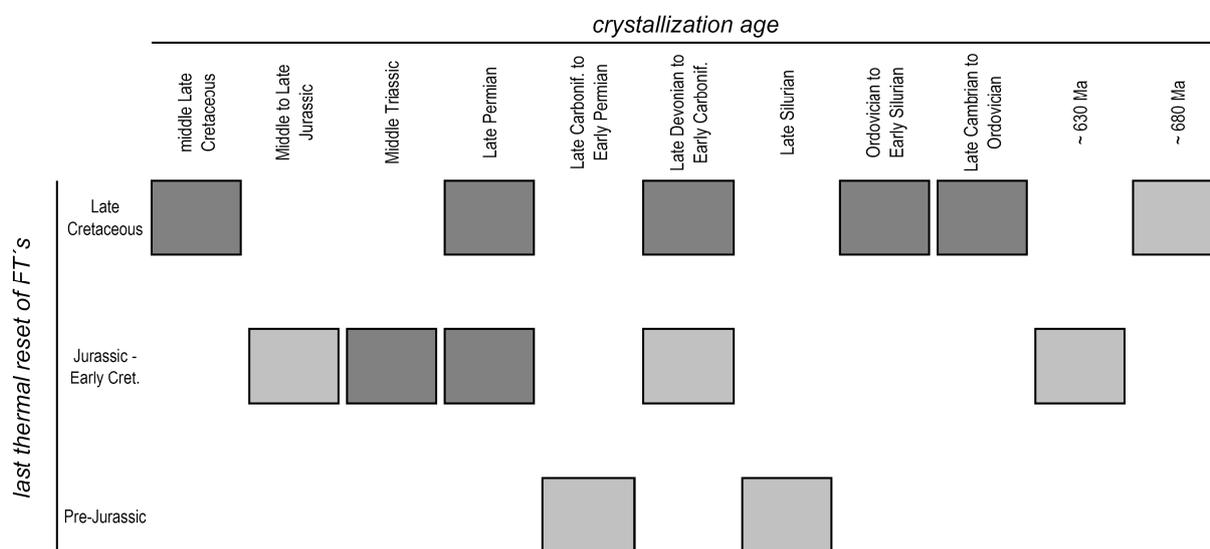


**Fig. 11.** Schematic representation of the zircon double-datum clusters which have been isolated by the two-dimensional statistical treatment, for the case of the Outer Dinaride foreland basin (Fig. 10b). The double dating technique has the potential to discriminate detrital grains from sources with an identical U/Pb age signature if the tectonic units comprising these rocks underwent different thermal histories; this is normally not achieved by using the two dating techniques separately. The remarkable mixed FT age character of the Permian grains along with the lack of a Late Cretaceous thermal imprint on the Middle Triassic age population strongly suggest the mixing of Dinaride and Austroalpine/Tisza-derived detritus in the sediment dispersal system; a Late Cretaceous regional thermal overprint is not typical for the Dinaride basement as its last main cooling occurred in the Jurassic-Early Cretaceous (see discussion in Chapter 2 of this Thesis).

### 6.5.3. Implications for U concentration determination

With conventional FT analysis, the U concentration is determined by irradiating the sample with thermal neutrons. This will induce a fission of the  $^{235}\text{U}$  atoms, which is then recorded by an external detector placed directly onto the crystals. The induced tracks are used to derive the U concentration distribution in the crystal, exactly on those areas where the spontaneous tracks were counted (e.g. Hurford and Green, 1982; Tagami and O'Sullivan, 2005). Although unparalleled in spatial resolution, still a number of limitations remain with this technique that are related both to the quality of irradiation (affecting U concentration data quality), and also to the serious hindrance of the need to ship the samples to a suitable research reactor (resulting in long turn-

around times, serious safety issues related to the treatment of low-activity materials, and the ever-decreasing number of suitable reactors).

Recent efforts focused on overcoming these issues by utilizing LA-ICPMS to derive the U concentration of zircon for FT age calculation (Cox *et al.*, 2000; Svojtka and Košler, 2002; see also Hasebe *et al.*, 2004, for apatite).

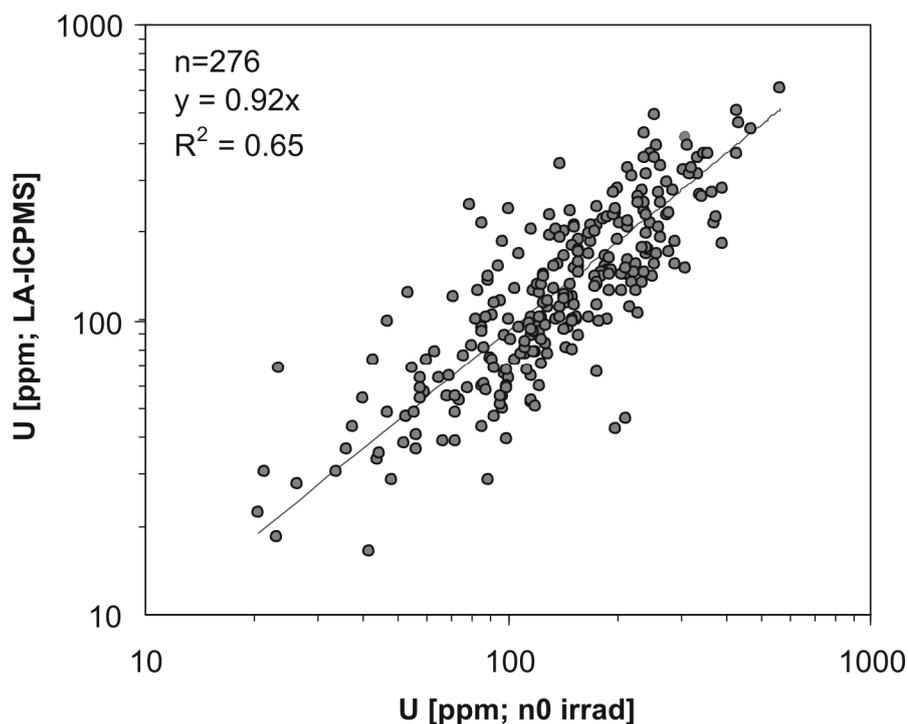
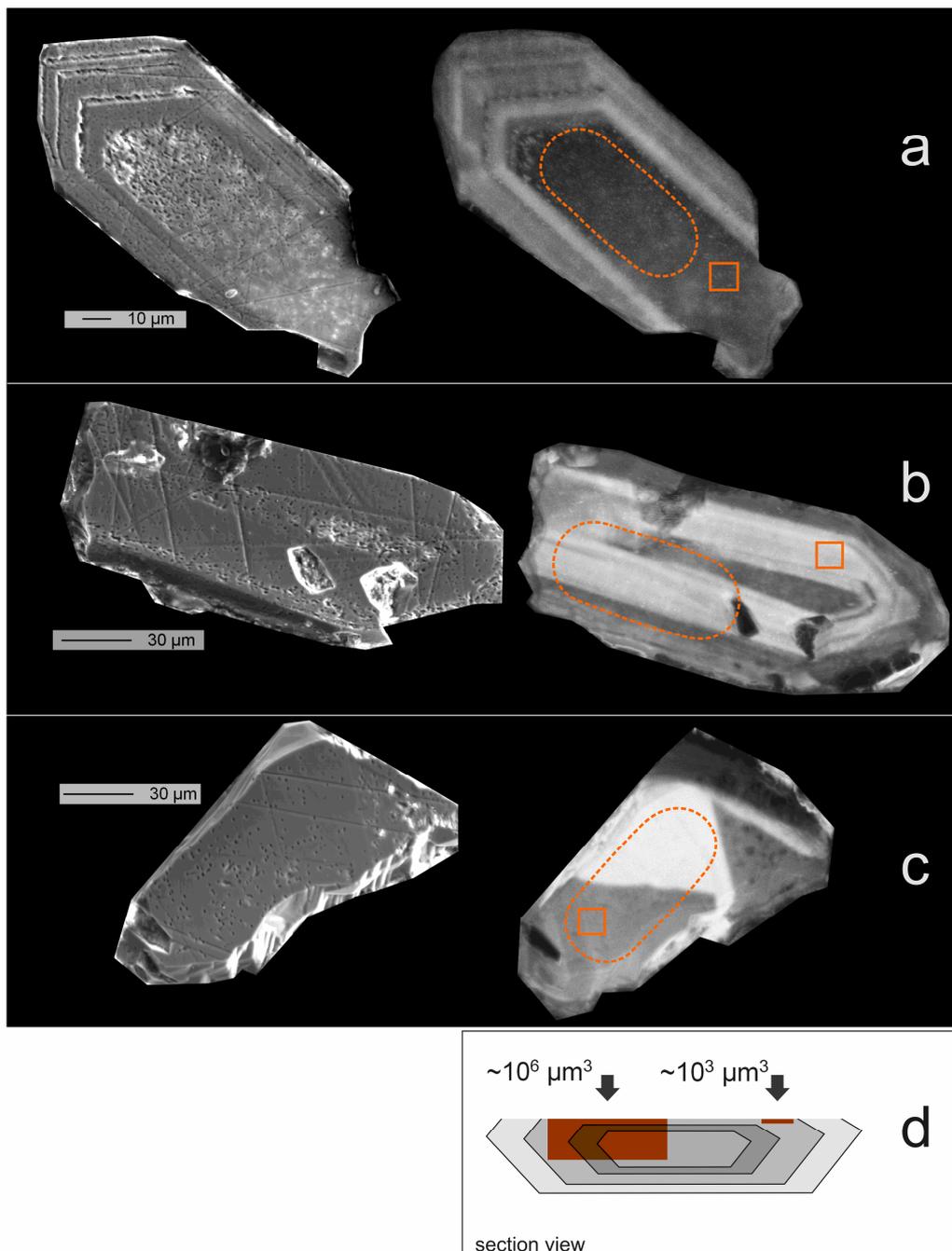


**Fig. 12.** Cross-plot of zircon U concentrations determined by neutron irradiation and subsequently by LA-ICPMS. The data are only moderately correlated, accounted for by the different sampling area and depth of the techniques used, together with the three-dimensional extension of U heterogeneity in zircon (see also Fig. 13).

Although LA-ICPMS instrument tuning parameters and the analytical protocol were optimized for U/Pb age determination (Table 2), we made an attempt in this study to determine the U concentrations. Comparing the results to the U concentrations derived from the neutron irradiations (Fig. 12), a moderate correlation is obtained. We attribute the deviation to four possible factors; (1) the considerable difference in the spatial resolution of the two techniques clearly shows that U concentrations integrated over different volumes (Fig. 13) pose a serious source of inconsistency in case of U heterogeneity; (2) the geometry of the ablation cell used features a large (ca. 10 mm) distance between the sample grains and the 91500 zircon

standard, which is unfavourable due to different efficiency in aerosol transport in these regions of the cell (Bleiner and Bogaerts, 2007); (3) the heterogeneous distribution of U in the 91500 standard ( $\pm 17\%$ ; Belousova *et al.*, 2002); (4) the uncertainty inherent to the neutron irradiation. We consider (1) to be the most dominant factor and future work should focus on developing ablation protocols that converge the ablated volume to that used in the FT analysis.



---

**Fig. 13 (previous page):** SEM (left) and CL (right) images of zircon grains illustrating U zoning. Zones rich in U are characterized by a higher track density and darker CL than U-poor zones. Note the inherent volume difference of the dating approaches, which at the same time provide the U concentrations as well. Track counting is performed in the square area; the induced tracks counted in the external detector reflect the average U concentration in the topmost 7  $\mu\text{m}$  thick layer of the zircon grain, whereas laser ablation integrates U concentration from a ca. three orders of magnitude larger volume. The examples are arranged in a downward increasing order of expected disagreement between the both concentration values.

## 6.6. Conclusions

The zircon FT–U/Pb double dating approach as developed and described in this study yields valuable insights into the thermal history of source terrains of Alpine synorogenic sediments, demonstrated by case studies from the peripheral and rethrow-edge foreland basins of the Dinarides. The "age-pairs" clearly match typical Alpine tectonostratigraphic units and the results can be effectively used for building a more realistic model of hinterland erosion and sediment dispersal patterns than normally achieved by using the two dating techniques separately. In the Tertiary basins of the Dinarides, a major sediment contribution from the adjacent Tisza, Austroalpine and Pelagonian Units is highly probable.



## *Chapter 7*

### Conclusions



## Conclusions

This work presents the results of a sedimentary provenance study undertaken in Cretaceous to Tertiary basins of the Dinarides. The major objective has been to put new constraints on the orogenic evolution of this integral, yet one of the least known segment of the European Alpine chain. We have taken on the approach of in-depth characterizing the detritus derived from major tectonostratigraphic units, focusing on information extracted via the geochemistry, geochronology and fission-track thermochronology of single detrital grains. We used these results to describe the paleogeology and understand sediment dispersal patterns which are all dependent on the large-scale crustal and surface processes involved in the Alpine orogeny.

The Bosnian Flysch forms a *c.* 3000 m thick, intensely folded stack of Upper Jurassic to Cretaceous mixed carbonate and siliciclastic sediments in the Central Dinarides, sandwiched between the Adriatic Carbonate Platform and the Dinaride Ophiolite Zone. Rich in ophiolite- and continental-derived detritus, its detailed study revealed important tectonic events related to the closure and obduction history of the Neotethys Ocean. Middle Jurassic intraoceanic subduction was shortly followed by exhumation of the overriding oceanic plate. Trench sedimentation was controlled by a dual sediment supply from the sub-ophiolitic high-grade metamorphic soles and from the distal continental margin of the Adriatic plate. Following the obduction onto Adria, from the Jurassic–Cretaceous transition onwards a vast clastic wedge (Vranduk Formation) was developed in front of the leading edge, fed by continental basement units of Adria that experienced Early Cretaceous synsedimentary cooling, by the overlying ophiolitic thrust sheets and by redeposited elements of coeval Urganian facies reefs grown on the thrust wedge complex.

Erosion of the ophiolitic thrust sheets provides important evidence for Late Jurassic acid magmatism at the intraoceanic convergent margin, inferred from detrital monazite (Th-U)/Pb and zircon U/Pb geochronology in the Vranduk Fm., as well as from apatite fission-track (FT) analysis of a unique tephra horizon preserved at the basin margin. The dominant monazite and zircon age components of  $164 \pm 3$  Ma and  $152 \pm 10$  Ma, respectively, as well as the apatite FT age of  $148 \pm 11$  Ma consistently indicate that leucocratic melt generation culminated in Middle to Late Jurassic times, coeval with and slightly post-dating sub-ophiolitic sole metamorphism. Monazite

growth and explosive volcanism call for supra-subduction zone processes at the convergent intraoceanic plate margin of the Neotethys. Extensive compilation of geochronological data demonstrates that such Jurassic felsic rocks are widespread also in the entire Dinaride-Hellenide orogen.

To characterize the eroded ophiolitic lithologies in more detail, we determined the chemical composition of detrital Cr-spinel grains by electron microprobe in several further Cretaceous sedimentary units in the same orogenic strike. These rocks occur in isolated exposures in the uplifted basement units of Medvednica, Ivanščica, Žumberak and Samobor Mountains near Zagreb. Evidence of the early Alpine evolution of the Dinarides in this area is less clear due to intense Tertiary strike-slip tectonics and the Neogene sedimentary cover of the Pannonian Basin. Cr-spinel geochemistry from the Oštrc Formation reveals that in the Early Cretaceous the ophiolitic source area was predominantly composed of harzburgite peridotites and associated cumulate rocks, probably developed in a supra-subduction zone setting. The supply of Cr-spinel with comparable chemical signatures remained dominant until the end of the Cretaceous, suggesting that exposed remnants of the same ophiolite belt persisted through the Cretaceous and/or that recycling was significant. Similarities with the Bosnian Flysch and data reported from the Northern Calcareous Alps and the Transdanubian Central Range imply a rather extensive harzburgitic ophiolite belt extending along the Adriatic margin during the Early Cretaceous.

Following mid-Cretaceous deformation and thermal overprint of the Vranduk Formation and the Adria-derived basement nappes, the depozone migrated further towards SW and received increasing amounts of redeposited carbonate detritus released from the Adriatic Carbonate Platform margin (Ugar Formation). Subordinate siliciclastic source components indicate changing source rocks on the upper plate, with ophiolites becoming subordinate. The zone of the continental basement previously affected by the Late Jurassic–Early Cretaceous thermal imprint has been removed; instead, the basement mostly supplied detritus with a wide range of pre-Jurassic cooling ages. However, a c. 80 Ma, largely synsedimentary cooling event is also recorded by the Ugar Formation, that contrasts the predominantly Early Cretaceous cooling of the Adriatic basement and suggests, at least locally, a fast exhumation.

In the Outer Dinarides, the Cenozoic thrust fronts are associated with flysch deposits. They overlie Eocene platform carbonate to bathyal marl successions that subsequently cover the Adriatic Carbonate Platform. Planktonic foraminifer

biostratigraphy indicates Eocene age of flysch sedimentation. New calcareous nanofossil data reveal that several assemblages are present; besides the dominant Mid-Eocene species, Cretaceous, Palaeocene, Oligocene and Miocene taxa were also identified throughout the entire flysch belt. Widespread occurrence of nanofossil species of zone NN4-6 indicate that flysch deposition lasted up to at least Mid-Miocene. Ubiquitous occurrence of various pre-Miocene taxa demonstrate that extensive, possibly submarine sediment recycling has occurred in the Cenozoic. As flysch remnants are typically sandwiched between thrust sheets, these new stratigraphic ages give a lower bracket on deformation age of the coastal range. The data provide a link between Cretaceous compression in the Bosnian Flysch and recent deformation in the Adriatic offshore area.

Using detrital zircon grains from the Outer Dinaride flysch and from the Sava Zone, we developed an approach to combine fission track (FT) and in-situ LA-ICPMS U/Pb isotopic analyses from the same grain. Detrital zircons were dated by the FT method, and grain interiors were imaged by cathodoluminescence (CL) to avoid ablation of inherited or other unsuitable domains. Precise and accurate U/Pb isotopic compositions were determined by a simple setup consisting of a 213 nm Nd:YAG laser source, coupled to a quadrupole ICPMS instrument. Our double dating study of detrital zircon shows that: (1) The U/Pb analytical protocols provide an excellent trade-off between analysis quality and a high, cost-effective sample throughput (70-100 zircon grains per day). Figures of merit include a sensitivity of >2100 cps/ppm for  $^{207}\text{Pb}$  in case of a 55  $\mu\text{m}$  nominal pit diameter. Within-run U/Pb elemental fractionation remains below 1%, rendering correction for it unnecessary. CL-control and a good spatial resolution aid in reducing age bias, as judged from the notably high proportion (>90%) of concordant ( $\pm 5\%$ ) grain ages; (2) The double dating approach allows several clusters of age-pairs to be isolated, that identify Alpine tectonostratigraphic units. In the Outer Dinaride flysch basin, a remarkably mixed FT age character of the Permian grains is observed, with a dominant Late Cretaceous FT age component. This, along with the lack of the same Late Cretaceous thermal imprint on the Middle Triassic age population strongly suggest the mixing of Dinaride and Austroalpine/Tisza-derived detritus in the sediment dispersal system. Zircon double dating can be effectively used for building a more realistic model of hinterland erosion and sediment dispersal patterns than normally achieved by using the two dating techniques separately.

## References

- Aigner-Torres, M. and Koller, F. 1999. Nature of the magma source of the Szarvaskő Complex, NE Hungary: Petrological and geochemical constraints. *Ophioliti*, 24: 1–12.
- Altiner, Y., Marjanović, M., Medved, M. and Rasić, L. 2006. Active deformation of the Northern Adriatic region: Results from the CRODYN geodynamical experiment. In: Pinter, N., Grenczy, G., Weber, J., Stein, S. and Medak, D. (eds) *The Adria Microplate: GPS Geodesy, Tectonics and Hazards*. NATO Science Series IV, 61, Springer, 257–267.
- Anders, B., Reischmann, T., Poller, U. and Kostopoulos, D. 2005. Age and origin of granitic rocks of the eastern Vardar Zone, Greece: new constraints on the evolution of the Internal Hellenides. *Journal of the Geological Society* 162: 857–870.
- Arai, S. 1992. Chemistry of chromian spinel in volcanic rocks as a potential guide to magma chemistry. *Mineralogical Magazine* 56: 173–184.
- Arai, S. and Okada, H. 1991. Petrology of serpentine sandstone as a key to tectonic development of serpentine belts. *Tectonophysics* 195: 65–81.
- Árgyelán, G.B. 1996. Geochemical investigations of detrital chrome spinels as a tool to detect an ophiolitic source area (Gerecse Mountains, Hungary). *Acta Geologica Hungarica* 39: 341–368.
- Árkai, P., Balogh, K. and Dunkl, I. 1995. Timing of low-temperature metamorphism and cooling of the Paleozoic and Mesozoic formations of the Bükkium, Innermost Western Carpathians, Hungary. *Geologische Rundschau* 84: 334–344.
- Árkai, P., Bérczi-Makk, A. and Balogh, K. 2000. Alpine low-T prograde metamorphism in the post-Variscan basement of the Great Plain, Tisza Unit (Pannonian Basin, Hungary). *Acta Geologica Hungarica* 43, 43–63.
- Árkai, P., Lantai, Cs., Főrizs, I. and Lelkes-Felvári, Gy. 1991. Diagenesis and low-temperature metamorphism in a tectonic link between the Dinarides and the Western Carpathians: the basement of the Igal (Central Hungarian) Unit. *Acta Geologica Hungarica*, 34: 81–100.
- Árva-Sós, E., Balogh, K. and Ravasz-Baranyai, L. 1988. Mesozoic andesite in borehole Nagybatony 324 (In Hungarian with English summary). *Magyar Állami Földtani Intézet Évi Jelentése az 1986. évről*: 117–120.
- Árva-Sós, E., Balogh, K., Ravasz-Baranyai, L. and Ravasz, Cs. 1987. K/Ar dates of Mesozoic igneous rocks in some areas of Hungary (In Hungarian with English summary). *Magyar Állami Földtani Intézet Évi Jelentése az 1985. évről*, 268–307.
- Aubouin, J. 1973. Des tectoniques superposées et de leur signification par rapport aux modèles géophysiques: l'exemple des Dinarides; paléotectonique, tectonique tarditectonique, néotectonique. *Bulletin de la Société géologique de France* (7), 15: 428–460.
- Aubouin, J., Blanchet, R., Cadet, J.-P., Celet, P., Charvet, J., Chorowicz, J., Cousin, M. and Rampoux, J.-P. 1970. Essai sur la géologie des Dinarides. *Bulletin de la Société géologique de France* (7)12: 1060–1095.
- Babić, Lj. 1974. Hauterivian to Cenomanian time in the region of Žumberak, Northwestern Croatia: stratigraphy, sediments, paleogeographic and paleotectonic evolution [In Croatian with English summary]. *Geološki vjesnik* 27: 11–33.
- Babić, Lj. 1975. Condensed Liassic sedimentation on Mt. Medvednica and Mt. Ivanščica (Northern Croatia) and its significance for the interpretation of the paleogeographic evolution of the Inner Dinaric Belt [In Croatian with English summary]. *Geološki vjesnik* 28: 11–28.
- Babić, Lj. and Gušić, I. 1978. Review of fossils from the clastic complex with “ophiolites” of Mt. Ivanščica and their stratigraphic importance [In Croatian with English summary]. *Geološki vjesnik* 30: 1–19.

- Babić Lj., Gušić, I., Devidé-Nedéla, D. 1973. Senonian breccias and overlying deposits on Mt. Medvednica (northern Croatia) [In Croatian with English summary]. *Geološki vjesnik* 25: 11–27.
- Babić, Lj., Hochuli, P.A. and Zupanić, J. 2002. The Jurassic ophiolitic mélange in the NE Dinarides: Dating, internal structure and geotectonic implications. *Eclogae geologicae Helvetiae* 95: 263–275.
- Babić, Lj. and Zupanić, J. 1973. Uppermost Jurassic and Early Cretaceous deposits on Mt. Ivanščica (Northern Croatia) [In Croatian with English summary]. *Geološki vjesnik* 26: 267–272.
- Babić, Lj. and Zupanić, J. 1976. Sediments and paleogeography of the Globotruncana calcarata zone (Upper Cretaceous) in Banija and Kordun (Central Croatia) [In Croatian with English summary]. *Geološki vjesnik*, 29: 49–73.
- Babić Lj. and Zupanić, J. 1978. The younger Mesozoic of Ivanščica [In Croatian]. In: Babić, Lj. and Jelaska, V. (eds.) Vodič ekskurzije 3. Skupa sedimentologa Jugoslavije. Croatian Geological Society, Zagreb, 11–23.
- Babić, Lj. and Zupanić, J. 1983. Paleogene clastic formations in Northern Dalmatia: Excursion A2. *Contributions to sedimentology of some carbonate and clastic units of the coastal Dinarides. Excursion Guide-book, 4th IAS Regional Meeting, Split 1983*, 37–61.
- Babić, Lj. and Zupanić, J. 1996. Coastal Dinaric flysch belt: paleotransport model for the Pazin Basin, and the role of a foreland uplift (Istria, Croatia). *Natura Croatica*, 5: 317–327.
- Babić, Lj. and Zupanić, J. 1998. Nearshore deposits in the Middle Eocene clastic succession in Northern Dalmatia (Dinarides, Croatia). *Geologia Croatica*, 51: 175–193.
- Babić, Lj., Zupanić, J. and Crnjaković, M. 1993. An association of marine tractive and gravity flow sandy deposits in the Eocene of the Island of Pag (Outer Dinarides, Croatia). *Geologia Croatica*, 46: 107–123.
- Babić, Lj., Zupanić, J. and Juračić, M. 1995. Supply from an Outer Carbonate Platform to the Foreland Basin of the Coastal Dinarides: the Pazin Flysch Basin (Eocene, Croatia). 1. Hrvatski geološki kongres Opatija, 1: 43–45.
- Báldi-Beke M. 1977. Stratigraphical and faciological subdivisions of the Oligocene as based on nannoplankton. *Földtani Közlöny* 107: 59–89.
- Báldi-Beke M. 1984. The nannoplankton of the Transdanubian Palaeogene formations. *Geologica Hungarica, Series Palaeontologica* 43.
- Báldi-Beke, M. and Báldi, T. 1991. Palaeobathymetry and palaeogeography of the Bakony Eocene Basin in western Hungary. *Palaeogeography, Palaeoclimatology, Palaeoecology*, 88: 25–52.
- Balen, D., Schuster, R., Garašić, V. and Majer, V. 2003. The Kamenjača olivine gabbro from Moslavačka Gora (South Tisia, Croatia). *RAD Hrvatske akademije znanosti i umjetnosti*, 486: 27: 57–76.
- Bárdossy, Gy. and Aleva, G. J. J. 1990. Lateritic Bauxites. *Developments in Economic Geology* No. 27, Elsevier, Amsterdam, 624 pp.
- Barnes, S.J. and Roeder, P.L. 2001. The Range of Spinel Compositions in Terrestrial Mafic and Ultramafic Rocks. *Journal of Petrology* 42: 2279–2302.
- Basu, A., Molinaroli, E. and Andersson, S., 1998. Diversity of physical and chemical properties of detrital zircons and garnets in Cenozoic sediments of southwestern Montana. *The Mountain Geologist*, 35: 23–39.
- Bazylev, B., Popević, A., Karamata, S., Kononkova, N. and Simakin, S. 2006: Spinel peridotites from Zlatibor Massif (Dinaric Ophiolite Belt): Petrological evidences for a supra-subduction origin. In: Mesozoic ophiolite belts of northern part of the Balkan Peninsula. International Symposium, Belgrade-Banja Luka, May 31 – June 6: 2006, Belgrade, 1–4.
- Bébién, J., Dautaj, N., Shallo, M., Turku, I. and Barbarin, B. 1997. Diversité des plagiogranites ophiolitiques: l'exemple albanais. *Comptes Rendus de l'Académie des Sciences, sér. IIA*, 324: 875–882.
- Beccaluva, L., Coltorti, M., Saccani, E. and Siena, F. 2005. Magma generation and crustal accretion as evidenced by supra-subduction ophiolites of the Albanide-Hellenide Subpelagonian Zone. *The Island Arc*, 14: 551–563.

- Belak, M. 2005. Metamorphic rocks of the blueschist and greenschist facies on the Medvednica Mt. PhD Thesis, University of Zagreb.
- Belak, M., Pamić, J., Kolar-Jurkovšek, T., Pécskay, Z. and Karan, D. 1995. Alpinski regionalno metamorfni kompleks Medvednice (sjeverozapadna Hrvatska) [In Croatian with English summary]. Abstracts, 1st Croatian Geological Congress, Opatija, 67–70.
- Belak, M. and Tibljaš, D. 1998. Discovery of blueschists in the Medvednica Mountain (Northern Croatia) and their significance for the interpretation of geotectonic evolution of the area. *Geološki vjesnik* 51: 27–32.
- Bellas, S. M. 1997. Calcareous nanofossils of the Tertiary Flysch (Post Eocene to Early Miocene) of the Ionian Zone in Epirus, NW-Greece: Taxonomy and biostratigraphical correlations. *Berliner Geowissenschaftliche Abhandlungen*, E(22), 1–173.
- Belousova, E.A., Griffin, W.L., O'Reilly, S.Y. and Fisher, N.I. 2002. Igneous zircon: trace element composition as an indicator of source rock type. *Contributions to Mineralogy and Petrology*, 143, 602–622.
- Benić, J. 1975. Calcareous nannoplankton from the Eocene flysch on Pag Island. *Geološki vjesnik*, 28: 19–23.
- Benić, J. 1991. The age of the Istria flysch deposits based on calcareous nanofossils. In: Introduction to the Paleogene SW Slovenia and Istria Field-Trip Guidebook IGCP Project 286 "Early Paleogene Benthos", 2nd Meeting, Postojna, 25.
- Benisek, A. and Finger, F., 1993. Factors controlling the development of prism faces in granite zircons: a microprobe study. *Contributions to Mineralogy and Petrology*, 114, 441–451.
- Bergant, S., Tišljar, J. and Šparica, M. 2003. Istrian flysch and its relationship with flysch from NE Italy, SW Slovenia and the Adriatic coastal region in Croatia (Ravni Kotari area and Dalmatia). In: Evolution of Depositional Environments from the Palaeozoic to the Quaternary in the Karst Dinarides and the Pannonian Basin. 22nd IAS Meeting of Sedimentology, Opatija - September 17-19: 2003, Field Trip Guidebook, 57–63.
- Bernet, M., van der Beek, P., Pirk, R., Huyghe, P., Mugnier, J.L., Labrin, E. and Szulc, A. 2006. Miocene to Recent exhumation of the central Himalaya determined from combined detrital zircon fission-track and U/Pb analysis of Siwalik sediments, western Nepal. *Basin Research*, 18: 393–412.
- Bernoulli, D. and Laubscher, H. 1972. The palinspastic problem of the Hellenides. *Eclogae geologicae Helveticae* 65: 107–118.
- Bignot, G. 1972. Recherches stratigraphiques sur les calcaires du Crétacé supérieur et de l'Eocène d'Istrie et des régions voisines. Essai de révision du Liburnien. *Travaux du Laboratoire de Micropaléontologie* 2: 1–353.
- Blanchet, R. 1966. Sur l'âge tithonique-éocrétacé d'un flysch des Dinarides internes en Bosnie: le flysch de Vranduk (Yougoslavie). *Compte rendu sommaire des séances de la Société géologique de France* 10: 401–403.
- Blanchet, R. 1968. Sur l'extension du flysch tithonique-éocrétacé en Bosnie centrale (Yougoslavie). *Compte rendu sommaire des séances de la Société géologique de France* 3, 97–98.
- Blanchet, R. 1970. Données nouvelles sur le flysch bosniaque: la région de Banja Luka, Bosnie septentrionale, Yougoslavie. *Bulletin de la Société géologique de France* (7) 12: 659–663.
- Blanchet, R., Cadet, J.-P. and Charvet, J. 1970. Sur l'existence d'unités intermédiaires entre la zone du Haut-Karst et l'unité du Flysch Bosniaque, en Yougoslavie: la sous-zone Prékarstique. *Bulletin de la Société géologique de France* (7)12: 227–236.
- Blanchet, R., Cadet, J.-P., Charvet, J. and Rampoux, J.-P. 1969. Sur l'existence d'un important domaine de flysch tithonique-crétacé inférieur en Yougoslavie: l'unité du flysch bosniaque. *Bulletin de la Société géologique de France* (7) 11: 871–880.
- Blanchet, R., Durand Delga, M., Moullade, M. and Sigal, J. 1970. Contribution à l'étude du Crétacé des Dinarides internes: la région de Maglaj, Bosnie (Yougoslavie). *Bulletin de la Société géologique de France* (7) 12: 1003–1009.
- Blainer, D. and Bogaerts, A. 2007. Computer simulations of sample chambers for laser ablation-inductively coupled plasma spectrometry. *Spectrochimica Acta Part B - Atomic Spectroscopy*, 62: 155–168.
- Boenigk, W., 1983. Schwermineralanalyse. Enke, Stuttgart, 158 pp.

- Boev, B. and Lepitkova, S. 2002. The age of ophiolite rocks in the territory of the Republic of Macedonia. In: Proceedings of XVII. Congress of Carpathian-Balkan Geological Association, Bratislava, September 1st-4th 2002 (Michalík, J., Šimon, L. and Vozár, J., eds). *Geologica Carpathica, Special Publications*, 2.
- Borsi, S., Ferrara, G., Mercier, J. and Tongiorgi, E. 1966. Age stratigraphique et radiométrique jurassique supérieur d'un granite des zones internes des Hellénides (granite de Fanos, Macédoine, Grèce). *Revue de Géographie physique et de Géologie dynamique*, 8: 279–287.
- Bortolotti, V., Ficarelli, G., Manetti, P., Passerini, P., Pirini Radrizzani, C. and Torre, D. 1971. A Jurassic sequence on top of the Zlatibor ultramafic massif (Yugoslavia). *Bolletino Società Geologica Italiana*, 90: 415–428.
- Bortolotti, V., Marroni, M., Nicolae, I., Pandolfi, L., Principi, G. and Saccani, E. 2004. An update of the Jurassic ophiolites and associated calc-alkaline rocks in the South Apuseni Mountains (western Romania). *Ofioliti*, 29: 5–18.
- Bortolotti, V. and Principi, G. 2005. Tethyan ophiolites and Pangea break-up. *The Island Arc*, 14: 442–470.
- Bown, P. R., Rutledge, D. C., Cruy, J. A. and Gallagher, L. T. 1998. Lower Cretaceous. In: Brown, P. R. (Ed.): *Calcareous Nannofossil Biostratigraphy*. Chapman and Hall, London, 86–131.
- Bown, P. R. and Young, J. R. 1997. Mesozoic calcareous nannoplankton classification. *Journal of Nannoplankton Research* 19: 21–36.
- Bown, P. R. and Young, J. R. 1998. Techniques. In: Bown, P. R. (ed) *Calcareous Nannofossil Biostratigraphy*. Chapman and Hall, London, 16–28.
- Brandon, M.T. and Vance, J.A. 1992. Tectonic evolution of the Cenozoic Olympic Subduction complex, Washington state, as deduced from fission track ages for detrital zircons. *American Journal of Science*, 292: 565–636.
- Buick, I.S., Hermann, J., Williams, I.S., Gibson, R.L. and Rubatto, D. 2006. A SHRIMP U-Pb and LA-ICP-MS trace element study of the petrogenesis of garnet-cordierite-orthoamphibole gneisses from the Central Zone of the Limpopo Belt, South Africa. *Lithos*, 88: 150–172.
- Bulić, J., Bauer, V. and Jelaska, V. 1978. Paleocene deposits of the north-eastern part of Mt. Majejica (north Bosnia, Yugoslavia). *Geološki vjesnik*, 30: 453–458.
- Burnett, J. A. 1998. Upper Cretaceous. In: Bown, P. R. (Ed.): *Calcareous Nannofossil Biostratigraphy*. Chapman and Hall, London, 133–199.
- Bušer, S. 1987. Development of the Dinaric and the Julian carbonate platforms and of the intermediate Slovenian basin (NW Yugoslavia). *Memorie della Società Geologica Italiana* 40: 313–320.
- Cadet, J.-P. 1968. Sur l'âge de flyschs de la haute vallée de la Neretva (région de Ulog, Bosnie Yougoslavie). *Compte rendu sommaire des séances de la Société géologique de France* 4: 118–120.
- Cadet, J.-P. 1978. Essai sur l'évolution alpine d'une paléomarge continentale. *Mémoires de la Société géologique de France*, 57: 1–83.
- Cadet, J.-P. and Sigal, J. 1969. Sur la stratigraphie et l'extension du flysch éocétacé en Bosnie Hercegovine méridionale. *Compte rendu sommaire des séances de la Société géologique de France* 2: 52–53.
- Caironi, V., Garzanti, E. and Sciunnach, D., 1996. Typology of detrital zircon as a key to unravelling provenance in rift siliciclastic sequences (Permo-Carboniferous of Spiti, N India). *Geodinamica Acta*, 9: 101–113.
- Campbell, I.H., Reiners, P.W., Allen, C.M., Nicolescu, S. and Upadhyay, R. 2005. He–Pb double dating of detrital zircons from the Ganges and Indus Rivers: Implication for quantifying sediment recycling and provenance studies. *Earth and Planetary Science Letters*, 237: 402–432.
- Čanović, M. and Džodžo-Tomić, R. 1958. Vorläufige Mitteilung über die Oligozäne Mikrofauna aus der Bohrung Us-6 bei Ulcinj (Montenegro). *Geološki Glasnik (Titograd)*, 2: 203–213.
- Čanović, M. and Kemenci, R. 1988. Mezozoik podine Panonskog Basena u Vojvodini; stratigrafija i facije, magmatizam, paleogeografija. Matica Srpska, Belgrade, 337 pp.

- Carosi, R., Cortesogno, L., Gaggero, L. and Marroni, M. 1996. Geological and petrological features of the metamorphic sole from the Mirdita Nappe, northern Albania. *Ophioliti* 21: 21–40.
- Carter, A. 1999. Present status and future avenues of source region discrimination and characterization using fission track analysis. *Sedimentary Geology*, 124: 31–45.
- Carter, A. and Moss, S.J. 1999. Combined detrital zircon fission-track and U-Pb dating: A new approach to understanding hinterland evolution. *Geology*, 27: 235–238.
- Castorina, F., Garbarino, C., Masi, U., Mignardi, S., Nicoletti, M. and Beqirai, A. 1995. The granitic rocks from Fierza (North-Eastern Albania): geochemical evidence of the Jurassic margin of the Balcan continent. *Geological Society of Greece, Special Publication*, 4: 436–442.
- Cawood, P.A., 1983. Modal composition and detrital clinopyroxene geochemistry of lithic sandstones from the New England Fold Belt (east Australia): Paleozoic forearc terrane. *Bulletin of the Geological Society of America*, 94: 1199–1214.
- Channell, J. E. T., D'Argenio, B. and Horváth, F. 1979. Adria, the African Promontory, in Mesozoic Mediterranean Palaeogeography. *Earth Science Reviews*, 15: 213–292.
- Channell, J.E.T. and Kozur, H.W. 1997. How many oceans? Meliata, Vardar, and Pindos oceans in Mesozoic Alpine palaeogeography. *Geology* 25: 183–186.
- Charvet, J. 1967. Sur un jalon de flysch tithonique-éocétacé au nord de Sarajevo (Bosnie-Herzégovine, Yougoslavie). *Compte rendu sommaire des séances de la Société géologique de France* 8: 371–373.
- Charvet, J. 1970. Aperçu géologique des Dinarides aux environs du méridien de Sarajevo. *Bulletin de la Société géologique de France* (7) 12: 986–1002.
- Charvet, J. 1973. Sur les mouvements orogéniques du Jurassique-Crétacé dans les Dinarides de Bosnie orientale. *Comptes rendus de l'Académie des Sciences Paris, Série D* 276: 257–259.
- Charvet, J. 1978. Essai sur un orogène alpin: Géologie des Dinarides au niveau de la transversale de Sarajevo (Yougoslavie). *Publications de la Société géologique du Nord* 2: 1–554.
- Charvet, J. 1980. Développement de l'orogène dinarique d'après l'étude du secteur transversal de Sarajevo (Yougoslavie). *Revue de Géologie Dynamique et de Géographie Physique* 22: 29–50.
- Charvet, J. and Termier, G. 1971. Les Nérinéacés de la limite Jurassique-Crétacé de Bjeliš (Nord de Sarajévo, Yougoslavie). *Annales – Société Géologique du Nord* 91: 187–191.
- Chiari, M., Bortolotti, V., Marcucci, M., Photiades, A. and Principi, G. 2003. The Middle Jurassic siliceous sedimentary cover at the top of the Vourinos Ophiolite. *Ophioliti*, 28: 95–103.
- Chorowicz, J. 1977. Étude géologique des Dinarides le long de la structure transversale Split-Karlovac (Yougoslavie). *Publications de la Société géologique du Nord* 1: 1–331.
- Chorowicz, J. and Geysant, J.R. 1972. Presence des couches de Lemes (calcaires à Ammonites subméditerranéennes du Malm) dans la Lika (Croatie, Yougoslavie). *Comptes Rendus Hebdomadaires des Séances de l'Académie des Sciences, Série D: Sciences Naturelles*, 275: 731–734.
- Christ, M. D. 2007. Sedimentologie und Liefergebietsanalyse an ausgewählten Profilen des Bosnischen Flysches. M.Sc. Thesis, University of Göttingen, 89 pp. + Appendix.
- Cocherie, A., Legendre, O., Peucat, J.J. and Kouamelan, A.N. 1998. Geochronology of polygenetic monazites constrained by in situ electron microprobe Th-U total lead determination: Implications for lead behaviour in monazite. *Geochimica et Cosmochimica Acta*, 62: 2475–2497.
- Cookinboo, H.O., Bustin, R.M. and Wilks, K.R. 1997. Detrital chrome spinel compositions used to reconstruct the tectonic setting of provenance: implication for orogeny in the Canadian cordillera. *Journal of Sedimentary Research* 67: 116–123.
- Copeland, P. and Harrison, T. M. 1990. Episodic uplift in the Himalaya revealed by  $^{40}\text{Ar}/^{39}\text{Ar}$  analysis of detrital K-feldspar and muscovite, Bengal fan. *Geology*, 18: 354–357.

- Corfu, F., Hanchar, J.M., Hoskin, P.W.O. and Kinny, P. 2003. Atlas of zircon textures. In: *Zircon (Hanchar, J.M. and Hoskin, P.W.O., eds). Reviews in Mineralogy and Geochemistry*, 53, 469–500.
- Ćosović, V., Drobne, K. and Moro, A. 2004. Paleoenvironmental model for Eocene foraminiferal limestones of the Adriatic carbonate platform (Istrian Peninsula). *Facies*, 50: 61–75.
- Ćosović, V., Marjanac, T., Drobne, K. and Moro, A. 2008. Eastern Adriatic Coast – External Dinarids. In: McCann, T. (ed) *Geology of Central Europe*. Geological Society London, Special Publications, Vol. 2.
- Cousin, M. 1972. Équisse géologique des confins italo-yougoslaves; leur place dans les Dinarides et les Alpes méridionales. *Bulletin de la Société géologique de France (7)* 12: 1034–1047.
- Cox, R., Košler, J., Sylvester, P. and Hodych, J. 2000. Apatite fission-track (FT) dating by LAM–ICP–MS analysis. *Journal of Conference Abstracts*, 5: 322.
- Crnjaković, M. 1979. Sedimentation of transgressive Senonian in Southern Mt. Medvednica [In Croatian with English summary]. *Geološki vjesnik* 32: 81–95.
- Crnjaković, M. 1981. Maastrichtian flysch sediments in the south-west part of Mt. Medvednica [In Croatian with English summary]. *Geološki vjesnik* 34: 47–61.
- Crnjaković, M. 1987. Sedimentology of Cretaceous and Paleogene clastics of Mt. Medvednica, Ivanščica, and Žumberak. PhD Thesis, University of Zagreb.
- Crnjaković, M. 1989. Lower Cretaceous shallow marine deposits in Mt. Medvednica [In Croatian with English summary]. *Acta Geologica (Zagreb)* 19: 61–93.
- Crnjaković, M., Babić, Lj., Zupanič, J. 2000. Albian–Cenomanian arenites overlying Dinaric platform carbonates contain detritus derived from continental and ophiolitic rocks. *Vijesti Hrvatskog geološkog društva* 37: Special Issue PAN-CARDI 2000, Dubrovnik
- Császár, G. and Árgyelán, G.B. 1994. Stratigraphic and micromineralogical investigations on Cretaceous Formations of the Gerecse Mountains, Hungary and their palaeogeographic implications. *Cretaceous Research* 15: 417–434.
- Cserepes, L. 1989. Numerical mathematics – for geophysicist students. Tankönyvkiadó, Budapest, 358 pp.
- Csontos, L. and Vörös, A. 2004. Mesozoic plate tectonic reconstruction of the Carpathian region. *Palaeogeography, Palaeoclimatology, Palaeoecology* 210: 1–56.
- Csontos, L., Gerzina, N., Hrvatović, H., Schmid, S. and Tomljenović, B. 2003. Structure of the Dinarides: a working model. *Annales Universitatis Budapestinensis, Sectio Geologica* 35: 143–144.
- Curry, D. 1982. Differential preservation of foraminiferids in the English Upper Cretaceous – consequential observations. In: Banner, F. T. and Lord, A. R. (eds) *Aspects of Micropalaeontology*. Papers presented to Professor Tom Barnard. George Allen and Unwin, London, 240–261.
- Cvijić, J. 1924. *Geomorfologija I*. Državna štamparija Kraljevine Srba Hrvata i Slovenaca, Belgrade, 588 p.
- Dal Piaz, G.V., Martin, S., Villa, M.I., Gosso, G. and Marschalko, R. 1995. Late Jurassic blueschist facies pebbles from the Western Carpathian orogenic wedge and paleostructural implications for Western Tethys evolution. *Tectonics* 14: 874–885.
- Davis, D.W., Williams, I.S. and Krogh, T.E. 2003. Historical developments in zircon geochronology. *Reviews in Mineralogy and Geochemistry*, 53, 145–181.
- de Capoa, P., Guerrera, F., Perrone, V. and Serrano, F. 1997. New biostratigraphic data on the Frazzanò Formation (Longi-Taormina Unit): consequences on defining the deformation age of the Calabria-Peloritani arc southern sector. *Rivista Italiana di Paleontologia e Stratigrafia*, 103, 343–356.
- de Capoa, P., Guerrera, F., Perrone, V., Serrano, F. and Tramontana, M. 2000. The onset of the syn-orogenic sedimentation in the flysch basin of the Sicilian Maghrebids; state of the art and new biostratigraphic constraints. *Eclogae geologicae Helvetiae*, 93, 65–79.

- de Capoa, P. and Radoičić, R. 1994a. Calcareous nannoplankton biostratigraphy of Tertiary sequences of the Cukali-Budva Basin (Montenegro, External Dinarides, Yugoslavia). *Rivista Española de Micropaleontología*, 26: 101–116.
- de Capoa, P. and Radoičić, R. 1994b. Tertiary nannoplankton biostratigraphy of the Zeta Intraplatform Furrow (Montenegro). *Palaeopelagos*, 4: 289–294.
- de Capoa, P. and Radoičić, R. 2002. Geological implications of biostratigraphic studies in the external and internal domains of the Central-Southern Dinarides. *Memorie della Società Geologica Italiana*, 57: 185–191.
- de Capoa, P., Radoičić, R. and D'Argenio, B. 1995. Late Miocene deformation of the External Dinarides (Montenegro and Dalmatia): New biostratigraphic evidence. *Memorie di Scienze Geologiche*, 47: 157–172.
- de Kaenel, E. and Villa, G. 1996. Oligocene-Miocene calcareous nanofossil biostratigraphy and paleoecology from the Iberia abyssal plain. *Proceedings of the Ocean Drilling Program, Scientific Results*, 149: 79–145.
- DeCelles, P. G. and Giles, K. A. 1996. Foreland basin systems. *Basin Research*, 8: 105–123.
- Decker, K., Faupl, P. and Müller, A. 1987. Synorogenic Sedimentation on the North Calcareous Alps During the Early Cretaceous. In: Flügel, H.W. and Faupl, P. (eds) *Geodynamics of the Eastern Alps*. Deuticke, Vienna: 126–141.
- Devidé-Nedéla, D., Babić, Lj. and Zupanić, J. 1982. Maastrichtian age of Vivodina Flysch in Žumberak and Ozalj region (western Croatia), determined by planktonic foraminifera [In Croatian with French summary]. *Acta Geologica (Zagreb)* 35: 21–36.
- Dick, H.J.B. and Bullen, T. 1984. Chromian spinel as a petrogenetic indicator in abyssal and Alpine-type peridotites and spatially associated lavas. *Contributions to Mineralogy and Petrology* 86: 54–76.
- Dilek, Y., Furnes, H. and Shallo, M. 2007. Suprasubduction zone ophiolite formation along the periphery of Mesozoic Gondwana. *Gondwana Research*, 11: 453–475.
- Dilek, Y., Furnes, H. and Shallo, M. 2008. Geochemistry of the Jurassic Mirdita Ophiolite (Albania) and the MORB to SSZ evolution of a marginal basin oceanic crust. *Lithos*, 100: 174–209.
- Dilek, Y., Furnes, H., Shallo, M. and Mortensen, J.K. 2001. Structure, petrology and geochronology of the Albanian ophiolites and their tectonic evolution within the Neotethyan orogenic belt. EUG XI Meeting Strasbourg, 8-12 April 2001, Abstracts, 320–321
- Dimitrijević, M. D. 1982. Dinarides: An outline of the tectonics. *Earth Evolution Sciences* 1: 4–23.
- Dimitrijević, M. D. 1997. *Geology of Yugoslavia*. Geological Institute GEMINI, Belgrade, 187 pp.
- Dimitrijević, M.D. 2001. Dinarides and the Vardar Zone: a short review of the geology. *Acta Vulcanologica* 13: 1–8.
- Dimitrijević, M. D. and Dimitrijević, M. N. 1973. Olistostrome mélange in the Yugoslavian Dinarides and late Mesozoic plate tectonics. *Journal of Geology* 81: 328–340.
- Dimitrijević, M. N. and Dimitrijević, M. D. 1968. The multilateral paleotransport on the example of the Durmitor Flysch, Yugoslavia. XXXIII International Geological Congress 3, 249–256.
- Dimitrijević, M. N., Dimitrijević, M. D., Karamata, S., Sudar, M., Gerzina, N., Kovács, S., Dosztály, L., Gulácsi, Z., Less, Gy. and Pelikán, P. 2003. Olistostrome/mélanges – an overview of the problems and preliminary comparison of such formations in Yugoslavia and NE Hungary. *Slovak Geological Magazine* 9: 2–21.
- Dimo-Lahitte, A., Monié, P. and Vergély, P. 2001. Metamorphic soles from the Albanian ophiolites: Petrology, <sup>40</sup>Ar/<sup>39</sup>Ar geochronology, and geodynamic evolution. *Tectonics*, 20: 78–96.
- Djerić, N., Vishnevskaya, V. S. and Schmid, S. M. 2007. New data on radiolarians from the Dinarides (Bosnia and Serbia). In: Froitzheim, N., Bousquet, R., Fügenschuh, B., Schmid, S. and Tomljenović, B. (Eds.): Abstract Volume, 8th Workshop on Alpine Geological Studies, Davos/Switzerland, 10.-12. October 2007, Bonn, 17–18.
- Djoković, I. 1985. The use of structural analysis in determining the fabric of Palaeozoic formations in the Drina-Ivanjica region [in Serbian with English summary]. *Geološki anali Balkanskoga poluostrva* 49: 11–160.
- Drobne, K. 1977. Alvéolines paléogènes de la Slovénie et de l'Istrie. *Schweizerische Paläontologische Abhandlungen* 99.

- Drobne, K. and Pavlovec, R. 1991. Paleocene and Eocene beds in Slovenia and Istria. In: Introduction to the Paleogene SW Slovenia and Istria Field-Trip Guidebook IGCP Project 286 "Early Paleogene Benthos", 2nd Meeting, Postojna, 19–21.
- Drobne, K., Pavlovec, R., Šikić, L. and Benić, J. 1979. Pićan, Istria – Cuisian, Lutetian. In: Drobne, K. (ed) 16th European Micropaleontological Colloquium, Guidebook, Ljubljana, F177–F182.
- Dumitru, T. 1993. A new computer-automated microscope stage system for fission-track analysis. *Nuclear Tracks and Radiation Measurement*, 21: 575–580.
- Dunkl, I., 1992. Origin of Eocene-covered karst bauxites of the Transdanubian Central Range (Hungary): evidence for early Eocene volcanism. *European Journal of Mineralogy*, 4: 581–595.
- Dunkl, I. 2002. Trackkey: a Windows program for calculation and graphical presentation of fission track data. *Computers and Geosciences* 28: 3–12. Available online at: [www.sediment.uni-goettingen.de/staff/dunkl/software/](http://www.sediment.uni-goettingen.de/staff/dunkl/software/)
- Dunkl, I., Di Giulio, A. and Kuhlemann, J. 2001. Combination of single-grain fission-track chronology and morphological analysis of detrital zircon crystals in provenance studies sources of the Macigno Formation (Apennines, Italy). *Journal of Sedimentary Research*, 71: 516–525.
- Dunkl, I., Józsa, S., Frei, D., Karius, V., Simon, K., Baresel, B., Mikes, T. and von Eynatten, H. 2008. Age-signature of the exotic boulders of the Délegyháza gravel pit. SloVTECO8 Meeting Proceedings and Excursion Guide, April 23–26, 2008: Úpohlav, 26–27
- Dunkl, I., Mikes, T., Frei, D., Gerdes, A. and von Eynatten, H., in prep. PepiAGE: data reduction program for time-resolved U/Pb analyses. Available at: [www.sediment.uni-goettingen.de/staff/dunkl/software](http://www.sediment.uni-goettingen.de/staff/dunkl/software)
- Dunkl, I., Mikes, T., Simon, K. and von Eynatten, H. 2007. Data handling, outlier rejection and calculation of isotope concentrations from laser ICP-MS analyses by PEPITA software. *Geochimica et Cosmochimica Acta* 71: A243–A243.
- Dunkl, I. and Nagymarosy, A. 1992. A new tie-point candidate for the Paleogene timescale calibration: Fission track dating of tuff layers of Lower Oligocene Tard Clay (Hungary). *Neues Jahrbuch für Mineralogie, Abhandlungen* 186: 345–364.
- Dunkl, I. and Székely, B. 2002. Component analysis with visualization of fitting; PopShare, a Windows program for data analysis (abstract). *Geochimica et Cosmochimica Acta* 66: 201. Available online at: [www.sediment.uni-goettingen.de/staff/dunkl/software/](http://www.sediment.uni-goettingen.de/staff/dunkl/software/)
- Einsele, G. 1992. *Sedimentary Basins*. Springer, Berlin, 628 pp.
- Engel, W. 1974. Sedimentologische Untersuchungen im Flysch des Beckens von Ajdovščina (Slowenien). *Göttinger Arbeiten zur Geologie und Paläontologie*, 16: 1–65.
- von Eynatten, H. 1996. Provenanzanalyse kretazischer Siliziklastika aus den Nördlichen Kalkalpen: Petrographie, Mineralchemie und Geochronologie des frühalpidsch umgelagerten Detritus. PhD thesis, University of Mainz, 145 pp. + App.
- von Eynatten, H. 2003. Petrography and chemistry of sandstones from the Swiss Molasse Basin; an archive of the Oligocene to Miocene evolution of the Central Alps. *Sedimentology* 50: 703–724.
- von Eynatten, H. and Gaupp, R., 1999. Provenance of Cretaceous synorogenic sandstones in the Eastern Alps: constraints from framework petrography, heavy mineral analysis and mineral chemistry. *Sedimentary Geology*, 124: 81–111.
- von Eynatten, H. and Wijbrans, J.R. 2003. Precise tracing of exhumation and provenance using Ar/Ar-geochronology of detrital white mica: the example of the Central Alps.- In: *Tracing Tectonic Deformation Using the Sedimentary Record* (ed. by T. McCann and A. Saintot), Geological Society of London, Special Publications, 208: 289–305.
- Faupl P., Pavlopoulos, A., Klötzli, U. and Petrakakis, K. 2006. On the provenance of mid-Cretaceous turbidites of the Pindos zone (Greece): implications from heavy mineral distribution, detrital zircon ages and chrome spinel chemistry. *Geological Magazine* 143: 329–342.

- Faupl, P., Petrakakis, K., Migiros, G. and Pavlopoulos, A., 2002. Detrital blue amphiboles from the western Othrys Mountain and their relationship to the blueschist terrains of the Hellenides (Greece). *International Journal of Earth Sciences (Geologische Rundschau)*, 91: 433–444.
- Faupl, P. and Wagreich, M. 1992. Cretaceous flysch and pelagic sequences of the Eastern Alps; correlations, heavy minerals, and palaeogeographic implications. *Cretaceous Research* 13: 387–403.
- Federal Geological Institute (F.G.I.) 1970. SFR Yugoslavia Geological Map 1:500000. Belgrade.
- Fedo, C.M., Sircombe, K.N. and Rainbird, R.H. 2003. Detrital zircon analysis of the sedimentary record. *Reviews in Mineralogy and Geochemistry*, 53, 277–303.
- Flagler, P.A. and Spray, J.G. 1991. Generation of plagiogranite by amphibolite anatexis in oceanic shear zones. *Geology*, 19: 70–73.
- Force, E., 1980. The provenance of rutile. *Journal of Sedimentary Petrology*, 50: 485–488.
- Fornaciari, E., Di Stefano, A., Rio, D. and Negri, A. 1996. Middle Miocene quantitative calcareous nannofossil biostratigraphy in the Mediterranean region. *Micropaleontology*, 42: 37–63.
- Fornaciari, E. and Rio, D. 1996. Latest Oligocene to early middle Miocene quantitative calcareous nannofossil biostratigraphy in the Mediterranean region. *Micropaleontology*, 42: 1–36.
- Frei, D. and Gerdes, A. 2008. Precise and accurate in situ U-Pb dating of zircon with high sample throughput by automated LA-SF-ICP-MS. *Chemical Geology*, doi:10.1016/j.chemgeo.2008.07.025
- Frey, M. 1987. Low temperature metamorphism. Blackie and Son Ltd., Glasgow, 351 pp.
- Furlani, M. 1910. Die Lemeš-Schichten. Ein Beitrag zur Kenntnis der Juraformation in Mitteldalmatien. *Jahrbuch der geologischen Reichsanstalt Wien*, 60: 67–98.
- Galbraith, R. F. 1990. The radial plot; graphical assessment of spread in ages. *Nuclear Tracks and Radiation Measurements* 17: 207–214.
- Galbraith, R. F. and Laslett, G. M. 1993. Statistical models for mixed fission-track ages. *Nuclear Tracks and Radiation Measurements* 21: 459–470.
- Gawlick, H. J., Frisch, W., Hoxha, L., Dumitrica, P., Krystyn, L., Lein, R., Missoni, S. and Schlagintweit, F. 2008. Mirdita Zone ophiolites and associated sediments in Albania reveal Neotethys Ocean origin. *International Journal of Earth Sciences* 97: 865–881.
- Gawlick, H.-J., Frisch, W., Vecsei, A., Steiger, T. and Böhm, F. 1999. The change from rifting to thrusting in the Northern Calcareous Alps as recorded in Jurassic sediments. *Geologische Rundschau* 87: 644–657.
- Gerdes, A. and Zeh, A. 2006. Combined U-Pb and Hf isotope LA-(MC-)ICP-MS analyses of detrital zircons: Comparison with SHRIMP and new constraints for the provenance and age of an Annorican metasediment in Central Germany. *Earth and Planetary Science Letters*, 249: 47–61.
- Gibson, H.D., Carr, S.D., Brown, R.L. and Hamilton, M.A. 2004. Correlations between chemical and age domains in monazite, and metamorphic reactions involving major pelitic phases: an integration of ID-TIMS and SHRIMP geochronology with Y-Th-U X-ray mapping. *Chemical Geology*, 211: 237–260.
- Gleadow, A. J. W. 1981. Fission-track dating methods: what are the real alternatives? *Nuclear Tracks and Radiation Measurements* 5: 3–14.
- Gleadow, A. J. W., Hurford, A. J. and Quaife, R. D. 1976. Fission-track dating of zircon – Improved etching techniques. *Earth and Planetary Science Letters* 33, 273–276.
- Goncalves, P., Williams, M.L. and Jercinovic, M.J. 2005. Electron-microprobe age mapping of monazite. *American Mineralogist*, 90: 578–585.
- Gradstein, F.M. et al. 2004. A Geologic Time Scale 2004. Cambridge University Press.

- Grimes, C.B., John, B.E., Kelemen, P.B., Mazdab, F.K., Wooden, J.L., Cheadle, M.J., Hanghoj, K. and Schwartz, J.J. 2007. Trace element chemistry of zircons from oceanic crust: A method for distinguishing detrital zircon provenance. *Geology*, 35: 643–646.
- Grimmer, J.C., Ratschbacher, L., McWilliams, M., Franz, L., Gaitzsch, I., Tichomirowa, M., Hacker, B.R. and Zhang, Y., 2003. When did the ultrahigh-pressure rocks reach the surface? A  $^{207}\text{Pb}/^{206}\text{Pb}$  zircon,  $^{40}\text{Ar}/^{39}\text{Ar}$  white mica, Si-in-white mica, single grain provenance study of Dabie Shan synorogenic foreland sediments. *Sedimentary Geology*, 197: 87–110.
- Grubbs, F. 1969. Procedures for detecting outlying observations in samples. *Technometrics*, 11: 1–21.
- Grubić, A. and Komatina, M. 1963. Properties of the Eocene-Oligocene Flysch between Split and Makarska. *Sedimentologija*, 2-3, 21–38.
- Gunther, D., Jackson, S.E. and Longerich, H.P. 1999. Laser ablation and arc/spark solid sample introduction into inductively coupled plasma mass spectrometers. *Spectrochimica Acta Part B – Atomic Spectroscopy*, 54: 381–409.
- Gušić, I. 1975. Lower Cretaceous imperforate Foraminiferida of Mt. Medvednica, Northern Croatia (Families: Litoulidae, Ataxophragmididae, Orbitolinidae). *Paleontologica Jugoslavica* 14: 7–48.
- Haas, J. and Kovács, S. 2001. The Dinaridic-Alpine connection – as seen from Hungary. *Acta Geologica Hungarica* 44: 345–362.
- Haas, J., Mioč, P., Pamić, J., Tomljenović, B., Árkai, P., Bérczi-Makk, A., Koroknai, B., Kovács, S. and Rálišch-Felgenhauer, E. 2000. Complex structural pattern of the Alpine-Dinaridic-Pannonian triple junction. *International Journal of Earth Sciences* 89: 377–389.
- Haas, J. and Péró, Cs. 2002. Mesozoic evolution of the Tisza Mega-unit. *International Journal of Earth Sciences* 93: 297–313.
- Hagn, R., Pavlovec, R. and Pavšič, J. 1979. Gračišće near Pićan, Istria – Eocene. In: Drobne, K. (ed) 16th European Micropaleontological Colloquium, Guidebook, Ljubljana, G185–G189.
- Halamić, J. and Goričan, Š. 1995. Triassic Radiolarites from Mts. Kalnik and Medvednica (Northwestern Croatia). *Geologia Croatica* 48: 129–146.
- Halamić, J., Goričan Š., Slovenec, D. and Kolar-Jurkovšek, T. 1999. A Middle Jurassic Radiolarite-Clastic Succession from the Medvednica Mt. (NW Croatia). *Geologia Croatica* 52: 29–57.
- Harley, S.L., Kelly, N.M. and Möller, A. 2007. Zircon behaviour and the thermal histories of mountain chains. *Elements*, 3, 25–30.
- Harlow, D.E., Wirth, R. and Hetherington, C.J. 2007. The relative stability of monazite and huttonite at 300–900 °C and 200–1000 MPa: Metasomatism and the propagation of metastable mineral phases. *American Mineralogist*, 92: 1652–1664.
- Hasebe, N., Barbarand, J., Jarvis, K., Carter, A. and Hurford, A.J. 2004. Apatite fission-track chronometry using laser ablation ICP–MS. *Chemical Geology*, 207: 135–145.
- Haughton, P.D.W. and Farrow, C.M., 1989. Compositional variation in Lower Old Red Sandstone detrital garnets from the Midland Valley of Scotland and the Anglo-Welsh Basin. *Geological Magazine*, 126: 373–396.
- Haynes, J. R. 1981. Foraminifera. Macmillan, London, 433 p.
- Henry, D. J. and Dutrow, B. L. 1996. Metamorphic tourmaline and its petrologic applications. In: Anovitz, L. and Grew, E. (ed.): Boron: Mineralogy, Petrology and Geochemistry. *Reviews in Mineralogy* 33, 503–557.
- Herak, M., Marinčić, S. and Polšak, A. 1976. Geology of the Island of Hvar. *Prirodoslovna Istraživanja*, 42: 5–14.
- Hergenröder, R. 2006. A model of non-congruent laser ablation as a source of fractionation effects in LA-ICP-MS. *Journal of Analytical Atomic Spectrometry*, 21: 505–516.
- Herron, M. M. 1988. Geochemical classification of terrigenous sands and shales from core or log data. *Journal of Sedimentary Petrology* 58: 820–829.

- Hisada, K. and Arai, S. 1993. Detrital chrome spinels in the Cretaceous Sanchu sandstone, central Japan: indicator of serpentinite protrusion into a fore-arc region. *Palaeogeography, Palaeoclimatology, Palaeoecology* 105: 95–109.
- Horn, I., Rudnick, R.L. and McDonough, W.F. 2000. Precise elemental and isotope ratio determination by simultaneous solution nebulization and laser ablation–ICP–MS: application to U–Pb geochronology. *Chemical Geology*, 164: 281–301.
- Horstwood, M.S.A., Foster, G.L., Parrish, R.R., Noble, S.R. and Nowell, G.M. 2003. Common–Pb corrected in situ U–Pb accessory mineral geochronology by LA–MC–ICP–MS. *Journal of Analytical Atomic Spectrometry*, 18: 837–846.
- Hoskin, P.W.O. and Schaltegger, U. 2003. The composition of zircon and igneous and metamorphic petrogenesis. *Reviews in Mineralogy and Geochemistry*, 53, 27–62.
- Hrvatović, H. 1999. Geološki vodič kroz Bosnu i Hercegovinu. Zavod za Geologiju, Sarajevo, 203 pp.
- Hrvatović, H. and Pamić, J. 2005. Principal thrust-nappe structures of the Dinarides. *Acta Geologica Hungarica* 48: 133–151.
- Hurford, A. J. 1998. ZETA: the ultimate solution to fission-track analysis calibration or just an interim measure. In: Van den Haute, P. and De Corte, F. (Ed.): *Advances in Fission-Track Geochronology*, Kluwer Academic Publishers, pp. 19–32.
- Hurford, A.J. and Carter, A., 1991. The role of fission track dating in discrimination of provenance. In: *Developments in Sedimentary Provenance Studies* (Morton, A.C., Todd, S.P. and Haughton, P.D.W., eds). 57: 67–78.
- Hurford, A. J., Fitch, F. J., and Clarke, A. 1984. Resolution of the age structure of the detrital zircon populations of two Lower Cretaceous sandstones from the Weald of England by fission track dating. *Geological Magazine*, 121: 269–277.
- Hurford, A.J. and Green, P.F. 1983. The zeta age calibration of fission-track dating. *Chemical Geology – Isotope Geoscience*, 41: 285–312.
- Ibbeken, H., Schleyer, R., 1991. *Source and Sediment: A Case Study of Provenance and Mass Balance at an Active Plate Margin* (Calabria, Southern Italy). Springer, Berlin. 286 pp.
- Ilić, A., Neubauer, F. and Handler, R. 2005. Late Paleozoic-Mesozoic tectonics of the Dinarides revisited: Implications from <sup>40</sup>Ar/<sup>39</sup>Ar dating of detrital white micas. *Geology* 33, 233–236.
- Irvine, T.N. 1965. Chromian spinel as a petrogenetic indicator. Part 1. Theory. *Canadian Journal of Earth Sciences* 2: 648–672.
- Irvine, T.N. 1967. Chromian spinel as a petrogenetic indicator. Part 2. Petrologic applications. *Canadian Journal of Earth Sciences* 4: 71–103.
- Ivanov, T., Misař, Z., Bowes, D.R., Dudek, A., Dumurdzanov, N., Jaroš, J., Jelínek, E. and Pačesová, M. 1987. The Demir Kapija-Gevgelija ophiolite massif, Macedonia, Yugoslavia. *Ofioliti*, 12: 457–478.
- Jablonský, J., Sýkora, M. and Aubrecht, R. 2001. Detritic Cr-spinels in Mesozoic sedimentary rocks of the Western Carpathians (overview of the latest knowledge) [In Slovak with English abstract]. *Mineralia Slovaca* 33: 487–498.
- Jackson, S.E. 2008. LAMTRACE data reduction software for LA–ICP–MS. In: *Laser Ablation ICP–MS in the Earth Sciences: Current Practices and Outstanding Issues* (Sylvester, P., ed). *Mineralogical Society of Canada Short Course Series*, 40: 305–306.
- Jacobshagen, V. 1986. *Geologie von Griechenland*. Borntraeger, Berlin, 363 pp.
- Jeffries, T.E., Fernandez-Suarez, J., Corfu, F. and Alonso, G.G. 2003. Advances in U–Pb geochronology using a frequency quintupled Nd : YAG based laser ablation system ( $\lambda = 213$  nm) and quadrupole based ICP–MS. *Journal of Analytical Atomic Spectrometry*, 18: 847–855.
- Jeffries, T.E., Jackson, S.E. and Longerich, H.P. 1998. Application of a frequency quintupled Nd : YAG source ( $\lambda = 213$  nm) for laser ablation inductively coupled plasma mass spectrometric analysis of minerals. *Journal of Analytical Atomic Spectrometry*, 13, 935–940.

- Jelaska, V. 1978. Senonian–Paleogene flysch of the Mt. Trebovac area (north Bosnia): stratigraphy and sedimentology. *Geološki vjesnik*, 30: 95–117.
- Jelaska, V., Amšel, V., Kapović, B. and Vuksanović, B. 1969. Sedimentological characteristics of the clastic Upper Cretaceous of the western part of Bosanska Krajina. *Nafta*, 20: 487–495.
- Jelaska, V., Bulić, J. and Oreški, E. 1970. Stratigraphic model of Eocene flysch sediments in the Banija area [In Croatian with English summary]. *Geološki vjesnik*, 23, 81–94.
- Jercinovic, M.J., Williams, M.L. and Lane, E.D. 2008. In-situ trace element analysis of monazite and other fine-grained accessory minerals by EPMA. *Chemical Geology*, 254: 197–215.
- Jerković, L. and Martini, E. 1976. Upper Eocene calcareous nannoplankton from Split and Dugi Rat (Yugoslavia). *Nafta*, 27: 67–70.
- Jochum, K.P., Nohl, U., Herwig, K., Lammel, E., Stoll, B. and Hofmann, A.W. 2005. GeoReM: A new geochemical database for reference materials and isotopic standards. *Geostandards and Geoanalytical Research*, 29: 333–338.
- Johnsson, M.J. and Basu, A., (eds.) 1993. Processes Controlling the Composition of Clastic Sediments. *Geological Society of America Special Paper*, 284, 342 pp.
- Judik, K., Árkai, P., Horváth, P., Dobosi, G., Tibljaš, D., Balen, D., Tomljenović, B. and Pamić, J. 2004. Diagenesis and low-temperature metamorphism of Mt. Medvednica, Croatia: Mineral assemblages and phyllosilicate characteristics. *Acta Geologica Hungarica* 47: 151–176.
- Judik, K., Balogh, K., Tibljaš, D. and Árkai, P. 2006. New age data on the low-temperature regional metamorphism of Mt. Medvednica (Croatia). *Acta Geologica Hungarica* 49: 207–221.
- Juračić, M. 1979. Sedimentation depth of the “Marls with crabs” based on planktonic to benthic foraminifer ratio. *Geološki vjesnik*, 31: 61–67.
- Kamenetsky, V.S., Crawford, A.J. and Meffre, S. 2001. Factors controlling chemistry of magmatic spinel; an empirical study of associated olivine, Cr-spinel and melt inclusions from primitive rocks. *Journal of Petrology* 42: 655–671.
- Karamata, S. 2006. The geological development of the Balkan Peninsula related to the approach, collision and compression of Gondwanan and Eurasian units. In: Robertson, A. H. F. and Mountrakis, D. (Eds.): Tectonic Development of the Eastern Mediterranean Region. *Geological Society, London, Special Publications* 260: 155–178.
- Karamata, S., Keesmann, I. and Okrusch, M. 1970. Ein Paragonit-führender Granatquarzit im Raum Brezovica, Südserbien. *Neues Jahrbuch für Mineralogie, Monatshefte* 1–18.
- Karamata, S., Sladić-Trifunović, M., Cvetković, V., Milovanović, D., Šarić, K., Olujić, J. and Vujnović, L. 2005. The western belt of the Vardar Zone with special emphasis to the ophiolites of Podkozarje – the youngest ophiolitic rocks of the Balkan Peninsula. *Bulletin l'Académie serbe des sciences et des arts, Classe des Sciences mathématiques et naturelles, T. 130*: 43, 85–96.
- Kázmér, M. and Kovács, S. 1985. Permian–Paleogene paleogeography along the eastern part of the Insubric-Periadriatic Lineament system: evidence for continental escape of the Bakony-Drauzug Unit. *Acta Geologica Hungarica* 28: 71–84.
- Kober, L. 1914. Die Bewegungsrichtung der alpinen Deckengebirge des Mittelmeeres. *Petermann's Geographische Mitteilungen*, 60: 250–256.
- Koepke, J., Berndt, J., Feig, S.T. and Holtz, F. 2007. The formation of SiO<sub>2</sub>-rich melts within the deep oceanic crust by hydrous partial melting of gabbros. *Contributions to Mineralogy and Petrology*, 153, 67–84.
- Kohl, B. and Roberts, H. H. 1994. Fossil Foraminifera from four active mud volcanoes in the Gulf of Mexico. *Geo-Marine Letters*, 14: 126–134.
- Koroneos, A., Christofides, G., Heaman, L. and Krstić, D. 2001. Petrology, geochemistry and evolution of the peraluminous Monopigadon plutonite (Macedonia, Northern Greece). *Mitteilungen der Österreichischen Mineralogischen Gesellschaft*, 146: 148–150.
- Kossmat, F. 1924. Geologie der zentralen Balkanhalbinsel. In: Wilser, J. (ed.) Die Kriegsschauplätze 1914 – 1918 geologisch dargestellt, 12, 1–198, Borntraeger, Berlin.

- Košir, A. 1997. Eocene platform-to-basin depositional sequence, southwestern Slovenia. *Gaea heidelbergensis*, 3, 205.
- Košler, J., Fonneland, H., Sylvester, P., Tubrett, M. and Pedersen, R.B. 2002. U–Pb dating of detrital zircons for sediment provenance studies – a comparison of laser ablation ICPMS and SIMS techniques. *Chemical Geology*, 182: 605–618.
- Kováč, A., Svingor, É. and Grecula, P. 1986. Rb-Sr isotopic ages of granitoid rocks from the Spišsko-gemerské rudohorie Mts., Western Carpathians, Eastern Slovakia. *Mineralia slovaca*, 18: 1–14.
- Kovács, S. 1982. Problems of the "Pannonian Median Massif" and the plate tectonic concept. Contributions based on the distribution of Late Paleozoic – Early Mesozoic isopic zones. *Geologische Rundschau* 71: 617–639.
- Kovács, S. 1988. Olistostromes and other deposits connected to subaqueous mass-gravity transport in the North Hungarian Paleo-Mesozoic. *Acta Geologica Hungarica*, 31: 265–287.
- Kozur, H. 1991. The evolution of the Meliata-Hallstatt ocean and its significance for the early evolution of the Eastern Alps and Western Carpathians. *Palaeogeography, Palaeoclimatology, Palaeoecology* 87: 109–135.
- Krašeninnikov, V., Muldini-Mamužić, S. and Džodžo-Tomić, R. 1968. Signification des foraminifères planctoniques pour la division du paléogène de la Yougoslavie et comparaison avec les autres régions examinées. *Geološki vjesnik*, 21: 117–145.
- Krawinkel, H., Wozacek, S., Krawinkel, J. and Hellmann, W. 1999. Heavy-mineral analysis and clinopyroxene geochemistry applied to provenance analysis of lithic sandstones from the Azuero-Sona Complex (NW Panama). *Sedimentary Geology* 124: 149–168.
- Krätner, H. G., Vajdea, E. and Romanescu, O. 1984. K-Ar dating of the banatitic magmatites from the southern Poiana-Rusca Mountains (Rusca Montana sedimentary basin). *Dări de seamă ale şedinţelor, Institutul de Geologie şi Geofizică 1 – Mineralogie-Petrologie-Geochemie* 70–71: 373–388.
- Krenn, E., Ustaszewski, K. and Finger, F. 2008. Detrital and newly formed metamorphic monazite in amphibolite-facies metapelites from the Motajica Massif, Bosnia. *Chemical Geology*, 254: 164–174.
- Kusiak, M.A., Kedzior, A., Paszkowski, M., Suzuki, K., Gonzalez-Alvarez, I., Wajsprych, B. and Doktor, M., 2006. Provenance implications of Th-U-Pb electron microprobe ages from detrital monazite in the Carboniferous Upper Silesia Coal Basin, Poland. *Lithos*, 88: 56–71.
- Kübler, B. 1967. La cristallinité de l'illite et les zones tout à fait supérieures du métamorphisme. In: Schaer, J.P. (Ed.): *Étages Tectoniques, Colloque de Neuchâtel 1966*. A La Baconnière, Neuchâtel, 105–121.
- Kulka, A. 1985. Nummulites from Poręba near Myślenice (Polish Western Carpathians). *Kwartalnik Geologiczny*, 29: 199–236.
- Lawrence, S. R., Tari-Kovačić, V. and Gjukić, B. 1995. Geological evolution model of the Dinarides. *Nafta* 46: 103–113.
- Lelkes-Felvári, Gy., Frank, W. and Schuster, R. 2003. Geochronological constraints of the Variscan, Permian-Triassic and Eo-Alpine (Cretaceous) evolution of the Great Hungarian Plain basement. *Geologica Carpathica* 54: 299–315.
- Lenaz, D., Kamenetsky, V.S. and Princivalle, F. 2003. Cr-spinel supply in the Brkini, Istrian and Krk Island flysch basins (Slovenia, Italy and Croatia). *Geological Magazine* 140: 335–342.
- Lenaz, D., Kamenetsky, V.S., Crawford, A.J. and Princivalle, F. 2000. Melt inclusions in detrital spinel from the SE Alps (Italy-Slovenia): a new approach to provenance studies of sedimentary basins. *Contributions to Mineralogy and Petrology* 139: 748–758.
- Liat, A., Gebauer, D. and Fanning, C.M. 2004. The age of ophiolitic rocks of the Hellenides (Vourinos, Pindos, Crete): first U-Pb ion microprobe (SHRIMP) zircon ages. *Chemical Geology*, 207: 171–188.
- Lihou, J.C. and Mange-Rajetzky, M.A., 1996. Provenance of the Sardona Flysch, eastern Swiss Alps: example of high-resolution heavy mineral analysis applied to an ultrastable assemblage. *Sedimentary Geology*, 105: 141–157.
- Ludwig, K.R. 2003. Isoplot 3.00 – A geochronological toolkit for Microsoft Excel. *Berkeley Geochronology Center Special Publication*, 4: 1–70.

- Lugović, B., Altherr, R., Raczek, I., Hofmann, A. W. and Majer, V. 1991. Geochemistry of peridotites and mafic igneous rocks from the central Dinaric ophiolite belt, Yugoslavia. *Contributions to Mineralogy and Petrology* 106: 201–216.
- Lugović, B., Šegvić, B., Babajić, E. and Trubelja, F. 2006. Evidence of short-living intraoceanic subduction in the Central Dinarides, Konjuh ophiolite complex (Bosnia-Herzegovina). In: Mesozoic ophiolite belts of northern part of the Balkan Peninsula. International Symposium, Belgrade-Banja Luka, May 31 – June 6, 2006, Belgrade, 72–75.
- Lugović, B., Slovenec, D., Halamić, J. and Altherr, R. 2007. Petrology, geochemistry and tectonic significance of Mesozoic ultramafic rocks from the Zagorje-Mid-Transdanubian Zone in Croatia. *Geologica Carpathica* 58: 511–530.
- Luković, M. and Petković, K. 1952. Geology and tectonics of the area of Ulcinj (littoral of Montenegro); an analysis of previous works and some new contributions. *SANU Posebna izdanja, knjiga 197*: 4: 1–62.
- Magdalenić, Z. 1972. Sedimentology of Central Istria flysch deposits [In Croatian with English summary]. *Acta Geologica (Zagreb)*, 7: 71–100.
- Majer, V. 1956. Petrography and petrogenesis of the ultrabasic rocks of Brezovica on the northern side of Šar Planina mountain (Yugoslavia) [In Croatian with English summary]. *Acta Geologica JAZU* 1: 89–148.
- Majer, V., Ackerman, D., Vrkljan, M. 2003. Garnet pyroxenites and hornblendites associated with iherzolites of Solila region in Borje mountain, central Dinaride ophiolite belt, Bosnia: petrography and petrology. *Rad Hrvatske akademije znanosti i umjetnosti (Razred za prirodne znanosti)* 27: 17–56.
- Majer, V. and Garašić, V. 2001. Plagiogranites from the ophiolite complexes of Dinarides and Vardar Zone. *Rudarsko-geološko-naftni zbornik*, 13, 1–7.
- Majer, V. and Lugović, B. 1991. The blueschists of Yugoslavia [in Croatian with English summary]. *Rad Hrvatske akademije znanosti i umjetnosti (Razred za prirodne znanosti)* 458 (25), 103–129.
- Maksimović, Z. and Majer, V. 1981. Accessory spinels of the main zones of Alpine Ultramafic Rocks in Yugoslavia. *Bulletin of the Serbian Academy of Sciences and Arts, Classis Sci. Nat.* 21: 47–58.
- Mange, M. and Maurer, F., 1992. Schwerminerale in Farbe. Enke, Stuttgart, 148 pp.
- Mange, M.A. and Morton, A.C., 2007. Geochemistry of heavy minerals. In: *Heavy Minerals in Use (Mange, M.A. and Wright, D.T., eds). Developments in Sedimentology* 58: 345–391.
- Mange, M.A. and Wright, D.T., (eds.) 2007 Heavy Minerals in Use. *Developments in Sedimentology*, 58, Elsevier, Amsterdam, 1283 pp.
- Mange-Rajetzky, M.A. and Oberhänsli, R., 1982. Detrital lawsonite and blue amphibole in the Molasse of Savoy, France and their significance in assessing Alpine evolution. *Schweizerische mineralogische und petrographische Mitteilungen*, 62: 415–436.
- Mantovani, E., Babbucci, D., Viti, M., Albarello, D., Mugnaioli, E., Cenni, N. and Casula, G. 2006. Post-Late Miocene kinematics of the Adria microplate: Inferences from geological, geophysical and geodetic data. In: Pinter, N., Grenerezy, G., Weber, J., Stein, S. and Medak, D. (eds) *The Adria Microplate: GPS Geodesy, Tectonics and Hazards*. NATO Science Series IV, 61, Springer, 51–69.
- Marakis, G.I. 1970. Geochronology of some granites from Macedonia (In Greek with English summary). *Annales Géologiques des Pays Helléniques*, 21: 121–152.
- Marinčić, S. 1981. Eocene flysch of Adriatic area [In Croatian with English abstract]. *Geološki vjesnik*, 34: 27–38.
- Marinčić, S., Šparica, M., Tunis, G. and Uchman, A. 1996. The Eocene flysch deposits of the Istrian Peninsula in Croatia and Slovenia: regional, stratigraphic, sedimentological and ichnological analyses. *Annales (Annals for Istrian and Mediterranean Studies)*, 9: 139–156.
- Marjanac, T. 1990. Reflected sediment gravity flows and their deposits in flysch of middle Dalmatia, Yugoslavia. *Sedimentology*, 37: 921–929.
- Marjanac, T. 1996. Deposition of megabeds (megaturbidites) and sea-level change in a proximal part of the Eocene-Miocene Flysch of central Dalmatia (Croatia). *Geology*, 24: 543–546.

- Marjanac, T. 2000. Kaštela-Split flysch region. *Vijesti Hrvatskoga geološkog društva*, 37(2), 109–116.
- Marjanac, T., Babac, D., Benić, J., Čosović, V., Drobne, K., Marjanac, L., Pavlovec, R. and Velimirović, Z. 1998. Eocene carbonate sediments and sea-level changes on the NE part of Adriatic Carbonate Platform (Island of Hvar and Pelješac Peninsula, Croatia). *Dela-Opera SAZU 4. razr.*, 34: 243–254.
- Marjanac, T. and Čosović, V. 2000. Tertiary depositional history of Eastern Adriatic realm. *Vijesti Hrvatskoga geološkog društva*, 37(2), 93–103.
- Marjanac, T. and Marjanac, Lj. 1991. Shallow-marine clastic Paleogene on the Island of Rab (Northern Adriatic). In: Bosellini, A., Brandner, R., Flügel, E., Purser, B., Schlager, W., Tucker, M. and Zenger, D. (eds) Dolomieu Conference on Carbonate Platforms and Dolomitization, Ortisei, 159–160.
- Martini, E. 1971. Standard Tertiary and Quaternary calcareous nannoplankton zonation. In: Farinacci, A. (ed) Proceedings of the Second Planktonic Conference, Roma 1970: 739–785.
- Márton, E., Pavelić, D., Tomljenović, B., Márton, P. and Avanić, R. 2005. Paleomagnetic investigations in the Croatian part of the Pannonian Basin: a review. *Acta Geologica Hungarica*, 48: 225–233.
- Máthé, Z. and Szakmány, Gy. 1990. The genetics (formation) of rhyolite occurring in the Rudabánya Mts. (NE Hungary) on the basis of REE and other trace elements. *Acta Mineralogica-Petrographica, Szeged*, 31: 43–55.
- McLennan, S. M. 2001. Relationships between the trace element composition of sedimentary rocks and upper continental crust. *Geochemistry Geophysics Geosystems* 2: Paper No. 2000GC00109.
- McLennan, S. M., Hemming, S., McDaniel, D. K. and Hanson, G. N. 1993. Geochemical approaches to sedimentation, provenance and tectonics. In: Johnsson, M. J. and Basu, A. (Ed.): Processes Controlling the Composition of Clastic Sediments. *Geological Society of America Special Paper* 284: 21–40.
- Mercier, J. 1966. Mouvements orogéniques et magmatisme d'âge jurassique supérieur-éocène dans les zones internes des Hellénides (Macédoine, Grèce). *Revue de Géographie physique et de Géologie dynamique*, 8: 265–278.
- Metcalf, R.V. and Shervais, J.W. 2008. Suprasubduction-zone ophiolites: Is there really an ophiolite conundrum? In: Ophiolites, Arcs and Batholiths: A Tribute to Cliff Hopson. *The Geological Society of America, Special Paper* (Wright, J.E. and Shervais, J.W., eds). 438: 191–222.
- Michard, A., Feinberg, H. and Montigny, R. 1998. The Chalkidiki supra-ophiolitic formations, and their bearing on the Vardarian obduction process. *Bulletin of the Geological Society of Greece*, 32: 59–64.
- Mikes, T. 2003. Provenance analysis of Eocene flysch sandstones in the Northwestern External Dinarides. M.Sc. Thesis, University of Tübingen, 75 pp. + App.
- Mikes, T., Báldi-Beke, M., Kázmér, M., Dunkl, I. and von Eynatten, H. 2008. Calcareous nannofossil age constraints on Miocene flysch sedimentation in the Outer Dinarides (Slovenia, Croatia, Bosnia-Herzegovina and Montenegro). In: Siegesmund S, Froitzheim N, Fügenschuh B (eds) Tectonic Aspects of the Alpine-Carpathian-Dinaride System. *Geological Society, London, Special Publications*, 298: 335–363.
- Mikes, T., Baresel, B., Kronz, A., Frei, D., Dunkl, I., Tolosana-Delgado, R. and von Eynatten, H.: Jurassic granitoid magmatism in the Dinaride Neotethys: geochronological constraints from detrital minerals. *Terra Nova*, submitted.
- Mikes, T., Christ, D., Petri, R., Dunkl, I., Frei, D., Báldi-Beke, M., Reitner, J., Wemmer, K., Hrvatović, H. and von Eynatten, H. 2008. Provenance of the Bosnian Flysch. *Swiss Journal of Geosciences*, 101. doi:10.1007/s00015-008-1291-z.
- Mikes, T., Dunkl, I. and von Eynatten, H. 2005. Significance of ophiolitic and high-grade metamorphic detritus in the Tertiary External Dinaride flysch belt. Abstracts Book, 7th Workshop on Alpine Geological Studies, Opatija, 61–62.
- Mikes, T., Dunkl, I. and Frisch, W. 2004. Provenance mixing in a foreland basin as revealed by sandstone geochemistry and detrital zircon fission track analysis: the Eocene flysch of the NW Dinarides. In: Pena Dos Reis, R., Callapez, P. and Dinis, P. (eds) 23rd IAS Meeting of Sedimentology, Coimbra - September 15-17: 2004, Abstracts Book, Coimbra, 199.
- Mikes, T., Dunkl, I., Frisch, W. and von Eynatten, H. 2006a. Geochemistry of Eocene flysch sandstones in the NW External Dinarides. *Acta Geologica Hungarica*, 49: 103–124.

- Mikes, T., von Eynatten, H. and Dunkl, I. 2006b. Detrital chrome spinel in Upper Cretaceous to Paleogene synorogenic sediments of the Sava-Vardar Belt. *XVIII Congress of the Carpathian-Balkan Geological Association, Belgrade*, 379–380.
- Milovanović, D. 1984. Petrology of low-grade metamorphic rocks of the middle part of the Drina-Ivanjica Palaeozoic [in Serbian with English summary]. *Glasnik Prirodnjačkog Muzeja u Beogradu (Ser. A)* 39: 13–139.
- Milovanović, D., Marchig, V. and Karamata, S. 1995. Petrology of the crossite schist from Fruška Gora Mts (Yugoslavia), relic of a subducted slab of the Tethyan oceanic crust. *Journal of Geodynamics* 20: 289–304.
- Mindszenty, A., D'Argenio, B. and Aiello, G. 1995. Lithospheric bulges recorded by regional unconformities. The case of Mesozoic-Tertiary Apulia. *Tectonophysics*, 252: 137–161.
- Montel, J.M., Foret, S., Veschambre, M., Nicollet, C. and Provost, A. 1996. Electron microprobe dating of monazite. *Chemical Geology*, 131: 37–53.
- Morton, A.C., 1985a. A new approach to provenance studies: electron microprobe analysis of detrital garnets from Middle Jurassic sandstones of the North Sea. *Sedimentology*, 32: 553–566.
- Morton, A.C., 1985b. Heavy minerals in provenance studies. *Provenance of arenites*, 148: 249–278
- Morton, A.C., 1991. Geochemical studies of detrital heavy minerals and their application to provenance research. In: *Developments in Sedimentary Provenance Studies (Morton, A.C., Todd, S.P. and Haughton, P.D.W., eds)*. Geological Society of London, Special Publication, 57: 31–45.
- Morton, A., Allen, M., Simmons, M., Spathopoulos, F., Still, J., Hinds, D., Ismail-Zadeh, A. and Kroonenberg, S. 2003. Provenance patterns in a neotectonic basin: Pliocene and Quaternary sediment supply to the South Caspian. *Basin Research* 15: 321–337.
- Morton, A.C. and Hallsworth, C.R. 1999. Processes controlling the composition of heavy mineral assemblages in sandstones. *Sedimentary Geology* 124: 3–29.
- Morton, A.C., Todd, S.P. and Haughton, P.D.W., (eds). 1991. Developments in Sedimentary Provenance Studies. *Geological Society of London Special Publication*, 57: 370 pp.
- Most, T. 2003. Geodynamic evolution of the Eastern Pelagonian Zone in northwestern Greece and the Republic of Macedonia. Implications from U/Pb, Rb/Sr, K/Ar, <sup>40</sup>Ar/<sup>39</sup>Ar geochronology and fission track thermochronology. University of Tübingen, 98 p. + App.
- Mrinjek, E. 1993. Sedimentology and depositional setting of alluvial Promina Beds in northern Dalmatia, Croatia. *Geologia Croatica*, 46: 243–261.
- Muceku, B., Mascle, G.H. and Tashko, A. 2006. First results of fission-track thermochronology in the Albanides. *Geological Society, London, Special Publications*, 260: 539–556.
- Muldini-Mamužić, S. 1962. Mikrofaunistische untersuchungen des Eozän-Flysches der Insel Rab. *Geološki vjesnik*, 15: 149–159.
- Muldini-Mamužić, S. 1965. The microfauna of limestones and of the clastic development in the Paleogene of central Istria. *Geološki vjesnik*, 18: 281–289.
- Mussallam, K. and Jung, D. 1986. Petrology and geotectonic significance of salic rocks preceding ophiolites in the Eastern Vardar Zone. *Tschermaks Mineralogische und Petrographische Mitteilungen*, 35: 217–242.
- Mutić, R. and Dmitrović, R. 1991. Accessory glaucophane in Miocene deposits of Hrvatsko Zagorje, Samoborska Gora, Medvednica and Dilj-Gora (Croatia) [In Croatian with English summary]. *Geološki vjesnik* 44: 89–119.
- Naeser, C. W. 1979. Fission-track dating and geologic annealing of fission tracks. in E. Jäger and J. C. Hunziker (eds) *Lectures in isotope Geology*, Springer-Verlag, Heidelberg, 154–169.
- Nagy, G., Draganits, E., Demény, A., Pantó, Gy. and Árkai, P. 2002. Genesis and transformations of monazite, florencite and rhabdophane during medium grade metamorphism: examples from the Sopron Hills, Eastern Alps. *Chemical Geology*, 191: 25–46.

- Nagyvarosy, A. 1987. Geological key profile of Hungary. Buda Hills, Budapest, Róka-hegy, Ibolya Street, quarry. Tard Clay Formation. Hungarian Geological Institute, Budapest, 7 pp.
- Nagyvarosy, A. and Báldi-Beke, M. 1993. The Szolnok Unit and its probable paleogeographic position. *Tectonophysics*, 226: 457–470.
- Nasdala, L., Zhang, M., Kempe, U., Panczer, G., Gaft, M., Andrut, M. and Plötze, M. 2003. Spectroscopic methods applied to zircon. *Reviews in Mineralogy and Geochemistry*, 53, 427–467.
- Neubauer, F., Pamić, J., Dunkl, I., Handler, R. and Majer, V. 2003. Exotic granites in the Cretaceous Pogari Formation overstepping the Dinaric Ophiolite Zone mélange in Bosnia. *Annales Universitatis Scientiarum Budapestinensis de Rolando Eötvös nominatae* 35: 133–134.
- Nicolae, I., Cuna, S. and Soroiu, M. 1987. Preliminary, K-Ar investigations of ophiolites from the South Apuseni Mountains (Romania). *Studii și cercetări de geofizică*, 25: 43–49.
- Nopcsa, F. 1921. Geologische Grundzüge der Dinariden. *Geologische Rundschau* 12 (1-2), 1–19.
- Okrusch, M., Seidel, E., Kreuzer, H. and Harre, W. 1978. Jurassic age of metamorphism at the base of the Brezovica peridotite (Yugoslavia). *Earth and Planetary Science Letters* 39: 291–297.
- Olker, B., Altherr, R. and Lugović, B. 2001. Metamorphic evolution of mafic granulites from the metamorphic sole of Central Dinaric Ophiolites (Bosnia-Herzegovina). EUG XI Meeting Strasbourg, 8-12 April 2001, Abstracts, 320–321.
- Olszewska, B. and Garecka, M. 1996. Foraminifer and nannoplankton biostratigraphy of the lower Miocene of the Carpathian Foredeep. *Przeгляд Geologiczny*, 44: 1049–1053.
- Olujić, J. 1978. Distribution and genesis of Mesozoic flysches in Bosnia and Herzegovina. Unpublished Manuscript, Geological Survey of Bosnia and Herzegovina, Sarajevo.
- Olujić, J., Pamić, O., Pamić, J., Milojević, R., Veljković, D., and Kapeler, I. 1978. Explanatory notes of the Basic Geological Map, Sheet Vareš L34-133, 68 pp. Federal Geological Institute, Belgrade.
- Operta, M., Pamić, J., Balen, D. and Tropper, P. 2003. Corundum-bearing amphibolites from the metamorphic basement of the Krivaja-Konjuh ultramafic massif (Dinaride Ophiolite Zone, Bosnia). *Mineralogy and Petrology* 77: 287–295.
- Orehek, S. 1991. Palaeotransport of SW Slovenian flysch. In: Introduction to the Paleogene SW Slovenia and Istria Field-Trip Guidebook IGCP Project 286 "Early Paleogene Benthos", 2nd Meeting, Postojna, 27–31.
- Oszczypko, N., Andreyeva-Grigorovich, A.S., Malata, E., Oszczypko-Clowes, M.A. 1999. The lower Miocene deposits of the Rača Subunit near Nowy Sącz (Magura Nappe, Polish Outer Carpathians). *Geologica Carpathica*, 50: 419–433
- Oszczypko, N. and Salata, D. 2005. Provenance analyses of the Late Cretaceous - Paleocene deposits of the Magura basin (Polish Western Carpathians) - evidence from a study of the heavy minerals. *Acta Geologica Polonica* 55: 237–267.
- Pamić, J. 1983. Considerations on the boundary between Iherzolite and harzburgite subprovinces in the Dinarides and northern Hellenides. *Ofioliti* 8: 153–164.
- Pamić, J. 1993. Eoalpine to Neoalpine magmatic and metamorphic processes in the northwestern Vardar Zone, the easternmost Periadriatic Zone and the southwestern Pannonian Basin. *Tectonophysics* 226: 503–518.
- Pamić, J. 1997. The northwesternmost outcrops of the Dinaric ophiolites: a case study of Mt. Kalnik (Northern Croatia). *Acta Geologica Hungarica* 40: 37–56.
- Pamić, J. 2002. The Sava–Vardar Zone of the Dinarides and Hellenides versus the Vardar Ocean. *Eclogae geologicae Helveticae*, 95: 99–113.
- Pamić, J., Balogh, K., Hrvatović, H., Balen, D., Jurković, I. and Palinkaš, L. 2004. K-Ar and Ar-Ar dating of the palaeozoic metamorphic complex from the Mid-Bosnian Schist Mts., Central Dinarides, Bosnia and Herzegovina. *Mineralogy and Petrology* 82: 65–79.

- Pamić, J., Belak, M., Bullen, T.D., Lanphere, M.A. and McKee, E.H. 2000. Geochemistry and geodynamics of a Late Cretaceous bimodal volcanic association from the southern part of the Pannonian Basin in Slavonija (Northern Croatia). *Mineralogy and Petrology*, 68: 271–296.
- Pamić, J., Gušić, I. and Jelaska, V. 1998. Geodynamic evolution of the Central Dinarides. *Tectonophysics*, 297: 251–268.
- Pamić, J. and Jurković, I. 2002. Paleozoic tectonostratigraphic units of the northwest and central Dinarides and the adjoining South Tisia. *International Journal of Earth Sciences* 91: 538–554.
- Pamić, J., Ščavničar, S. and Medjimorec, S. 1973. Mineral Assemblages of Amphibolites Associated with Alpine-Type Ultramafics in the Dinaride Ophiolite Zone (Yugoslavia). *Journal of Petrology* 14: 133–157.
- Pamić, J. and Šparica, M. 1983. The age of the volcanic rocks of Požeška Gora (Croatia, Yugoslavia) [In Croatian with English summary]. *RAD Jugoslavenske akademije znanosti i umjetnosti, razred za prirodne znanosti*, 404: 183–198.
- Pamić, J. and Tojerkauf, E. 1970. Granites on the border of the Borje ultramafic massif [In Croatian with English summary]. *Geološki glasnik (Sarajevo)* 14: 149–153.
- Pamić, J., Tomljenović, B. and Balen, D. 2002: Geodynamic and petrogenetic evolution of Alpine ophiolites from central an NW Dinarides: an overview. *Lithos* 65: 113–142.
- Paná, D., Balintoni, I., Heaman, L. and Erdmer, P. 2002. An alternative tectonic model for the Carpathian-Pannonian system. *Studia Universitatis Babeş-Bolyai, Geologia, Special Issue*, 1: 265–277.
- Pantić, N. and Jovanović, O. 1970. On the age of “Azoic” or “Palaeozoic slates” in Motajica Mountain based on microfloristic remnants [in Croatian with English summary]. *Geološki glasnik (Sarajevo)*, 14: 190–214.
- Papanikolaou, D. 1997. The tectonostratigraphic terranes of the Hellenides. *Annales Géologiques des Pays Helléniques*, 37: 495–514.
- Parfenoff, A., Pomerol, C. and Tourenq, J. 1970. Les Minéraux en Grains. Masson et Cie, Éditeurs, Paris, 578 pp.
- Parlak, O. and Delaloye, M. 1999. Precise <sup>40</sup>Ar/<sup>39</sup>Ar ages from the metamorphic sole of the Mersin Ophiolite (southern Turkey). *Tectonophysics* 301: 145–158.
- Pavić, A. 1970. Paléogène marin du Montenegro. Ph.D. Thesis. Zavod za geološka Istraživanja Crne Gore. Titograd, 208 pp.
- Pavičić, L., Zupanić, J. and Babić, Lj. 2003. Changing heavy mineral associations along the Outer Dinaric Eocene flysch belt: evidence for different structures along the rising Dinarides. *22nd IAS Meeting of Sedimentology, Opatija – September 17-19, 2003, Abstracts Book*, 149.
- Pavlovec, R. 2003. The type of nummulitins localities in the Dinarides. *Materials and Geoenvironment*, 50: 777–788.
- Pavlovec, R. 2006. Lower Eocene Nummulits from Trnovo in surroundings of Ilirska Bistrica (SW Slovenia). *Geologija*, 49: 45–52.
- Pavlovec, R., Knez, M., Drobne, K. and Pavšič, J. 1991. Profiles: Košana, Sv. Trojica and Leskovec; the disintegration of the carbonate platform. In: Introduction to the Paleogene SW Slovenia and Istria Field-Trip Guidebook IGCP Project 286 "Early Paleogene Benthos", 2nd Meeting, 69–72.
- Pavšič, J. 1981. Nannoplankton of the flysch in the Slovenian coast. *Radovi Znanstvenog Savjeta za Naftu, Sekcija za Primjenu Geologije, Geofizike i Geokemije, JAZU, Serija A*. 8: 257–266
- Pavšič, J. and Peckmann, J. 1996. Stratigraphy and sedimentology of the Piran Flysch Area (Slovenia). *Annales (Annals for Istrian and Mediterranean Studies)*, 9: 123–138.
- Pavšič, J. and Premec-Fuček, V. 2000. Calcareous nannoplankton and planktonic foraminiferal Zones during the Middle and Upper Eocene of the Transitional Beds on the Adriatic platform. *Annali del Museo Civico di Storia Naturale di Ferrara*, 3, 22–23.
- Pearce, J.A. 1989. High T/P metamorphism and granite genesis beneath ophiolite thrust sheets. *Ofoliti*, 14: 195–211.

- Perch-Nielsen, K. 1985a. Mesozoic calcareous nannofossils. In: Bolli, H. M., Saunders, I. B. and Perch-Nielsen, K. (eds) *Plankton stratigraphy*. Cambridge University Press, Cambridge, 329–425.
- Perch-Nielsen, K. 1985b. Cenozoic calcareous nannofossils. In: Bolli, H. M., Saunders, I. B. and Perch-Nielsen, K. (eds) *Plankton stratigraphy*. Cambridge University Press, Cambridge, 427–554.
- Petković, K. 1961. La carte tectonique de la R.F.P. de Yougoslavie. *Glasnik Srpska Akademija Nauka*, 149, odelj. prir. mat. nauka, 22: 129–144.
- Petri, R. 2007. Grad und Alter der schwachmetamorphen Überprägung an ausgewählten Profilen des Bosnischen Flysches. Unpublished M.Sc. Thesis, University of Göttingen, Göttingen, 111 pp. + Appendix.
- Pettijohn, F. J., Potter, P. E. and Siever, R. 1987. *Sand and Sandstone*. 2nd edition. Springer, New York, Berlin, 553 pp.
- Piccoli, G. and Proto Decima, F. 1969. Ricerche biostratigrafiche sui depositi flyschoidi della regione Adriatica settentrionale e orientale. *Memorie degli Istituti di Geologia e Mineralogia dell' Università di Padova*, 27: 3–21.
- Picha, F. J. 2002. Late orogenic strike-slip faulting and escape tectonics in frontal Dinarides-Hellenides, Croatia, Yugoslavia, Albania and Greece. *AAPG Bulletin*, 86: 1659–1671.
- Piper, D. J. W., Panagos, A. G. and Pe, G. G. 1978. Conglomeratic Miocene flysch of Western Greece. *Journal of Sedimentary Petrology*, 48: 117–126.
- Pober, E. and Faupl, P. 1988. The chemistry of detrital chromian spinels and its implications for the geodynamic evolution of the Eastern Alps. *Geologische Rundschau* 77: 641–670.
- Podubsky, V. 1970. Petrographic characteristics of Palaeozoic series in East Bosnia [In Croatian with English summary]. *Geološki glasnik (Sarajevo)* 14: 155–180.
- Pomerol, C. 1985. La transition Eocène-Oligocène: est-elle un phénomène progressif ou brutal? *Bulletin de la Société géologique de France, série 8*, 1: 263–267.
- Postma, G., Babić, Lj., Zupanić, J. and Røe, S.-L. 1988. Delta-front failure and associated bottomset deformation in a marine, gravelly Gilbert-type fan delta. In: Nemeč, W. and Steel, R. J. (eds) *Fan deltas; sedimentology and tectonic settings*. Blackie and Son, Glasgow, 91–102.
- Prelogović, E., Pribičević, B., Ivković, Ž., Dragičević, I., Buljan, R. and Tomljenović, B. 2003. Recent structural fabric of the Dinarides and tectonically active zones important for petroleum-geological exploration in Croatia. *Nafta*, 55: 155–161.
- Pribičević, B., Medak, D. and Prelogović, E. 2002. Determination of the recent structural fabric in the Alps-Dinarides area by combination of geodetic and geologic methods. *Raziskave s področja geodezije in geofizike, Zbornik predavanja*, 2002: 57–64.
- Puškarčić, S. 1987. Calcareous nannoplankton from clastic sediments of the Island of Hvar. *RAD Jugoslavenske akademije znanosti i umjetnosti*, 431: 7–16.
- Pupin, J.P., 1980. Zircon and granite petrology. *Contributions to Mineralogy and Petrology*, 73: 207–220.
- Putnis, A. 2002. Mineral replacement reactions; from macroscopic observations to microscopic mechanisms. *Mineralogical Magazine*, 66: 689–708.
- Radoičić, R., de Capoa, P. and D'Argenio, B. 1989. Late rather than early Tertiary deformation of External Dinarides. Stratigraphic evidence from Montenegro. *Rendiconto dell' Accademia delle Scienze Fisiche e Matematiche Napoli*, 56: 41–59.
- Radoičić, R., de Capoa, P. and D'Argenio, B. 1991. Middle-Late Miocene age of the preorogenic sedimentation in the Dinaric carbonate platform domain of Herzegovina. *Annales Géologiques de la Péninsule Balkanique*, 55: 1–21.
- Rahl, R.M., Reiners, P.W., Campbell, I.H., Nicolescu, S. and Allen, C.M. 2003. Combined single-grain (U–Th)/He and U/Pb dating of detrital zircons from the Navajo Sandstone, Utah. *Geology*, 31: 761–764.
- Rampoux, J.-P. 1969. A propos du flysch du 'Durmitor' (Monténégro, Yougoslavie). *Compte rendu sommaire des séances de la Société géologique de France* 2: 54–55.

- Rampnoux, J.-P. 1970. Regards sur les Dinarides internes yougoslaves (Serbie-Monténégro oriental): stratigraphie, évolution paléogéographique, magmatisme. *Bulletin de la Société géologique de France* (7) 12: 948–966.
- Rassios, A.H.E. and Moores, E.M. 2006. Heterogeneous mantle complex, crustal processes, and obduction kinematics in a unified Pindos-Vourinos ophiolitic slab. In: Tectonic Development of the Eastern Mediterranean region (Robertson, A.H.F. and Mountrakis, D., eds). *Geological Society, London, Special Publications*, 260: 237–266.
- Reiners, P.W. 2005. Zircon (U–Th)/He thermochronometry. *Reviews in Mineralogy and Geochemistry*, 58: 151–179.
- Reiners, P.W., Campbell, I.H., Nicolescu, S., Allen, C.M., Hourigan, J.K., Garver, J.I., Mattinson, J.M. and Cowan, D.S. 2005. (U–Th)/(He–Pb) double dating of detrital zircons. *American Journal of Science*, 305: 259–311.
- Resimić-Šarić, K., Cvetković, V. and Balogh, K. 2005. Radiometric K/Ar data as evidence of the geodynamic evolution of the Ždraljica Ophiolitic Complex (central Serbia). *Geološki anali Balkanskoga poluostrva*, 66: 73–79.
- Robertson, A. 2004. Development of concepts concerning the genesis and emplacement of Tethyan ophiolites in the Eastern Mediterranean and Oman regions. *Earth-Science Reviews*, 66: 331–387.
- Robertson, A. H. F. and Karamata, S. 1994. The role of subduction-accretion processes in the tectonic evolution of the Mesozoic Tethys in Serbia. *Tectonophysics* 234: 73–94.
- Rožič, B. 2005. Albian – Cenomanian resedimented limestone in the Lower flyschoid Formation of the Mt. Mrzli Vrh Area (Tolmin Region, NW Slovenia). *Geologija* 48: 193–210.
- Rubatto, D. 2002. Zircon trace element geochemistry: partitioning with garnet and the link between U–Pb ages and metamorphism. *Chemical Geology*, 184: 123–138.
- Sack, R.O. and Ghiorsio, M.S. 1991. Chromite as a Petrogenetic Indicator. In: Lindsley DH (ed) Oxide Minerals: Petrologic and Magnetic Significance. *Reviews in Mineralogy* 25: 323–353.
- Sambridge, M.S. and Compston, W. 1994. Mixture modeling of multicomponent data sets with application to ion-probe zircon ages. *Earth and Planetary Science Letters*, 128: 373–390.
- Šćavničar, S. 1978. New data on the insoluble residuum of limestone. In: Augustithis, S.S. (Ed.): Bauxites. 4th International Congress for the Study of Bauxites, Alumina and Aluminum, 2: 765–772.
- Šćavničar, B. and Nikler, L. 1976. Staklasti tuf u Lemeskim naslagama Velike Kapele. *Geološki vjesnik*, 29: 269–275.
- Schäfer, J. and Dörr, W., 1997. Heavy-mineral analysis and typology of detrital zircons: a new approach to provenance study (Saxothuringian Flysch, Germany). *Journal of Sedimentary Research*, 67: 451–461.
- Schmid, S.M., Bernoulli, D., Fügenschuh, B., Matenco, L., Schefer, S., Schuster, R., Tischler, M. and Ustaszewski, K. 2008. The Alpine-Carpathian-Dinaridic orogenic system: correlation and evolution of tectonic units. *Swiss Journal of Geosciences*, 101: 139–183.
- Schmid, S. M., Fügenschuh, B., Matenco, L., Schuster, R., Tischler, M. and Ustaszewski, K. 2006. The Alps-Carpathians-Dinarides-connection: a compilation of tectonic units. In: Sudar, M., Ercegovac, M. and Grubić, A. (eds) XVIII Congress of the Carpathian-Balkan Geological Association, Belgrade, 535–538.
- Schmidt, T., Blau, J. and Kázmér, M. 1991. Large-scale strike-slip displacement of the Drauzug and the Transdanubian Mountains in early Alpine history: evidence from Permo-Mesozoic facies belts. *Tectonophysics* 200: 213–232.
- Schreyer, W. and Abraham, K. 1977. Howieite and other high-pressure indicators from the contact aureole of the Brezovica, Yugoslavia, Peridotite. *Neues Jahrbuch für Mineralogie, Abhandlungen* 130: 114–133.
- Schubert, R. J. 1905. Zur Stratigraphie des istrisch-norddalmatinischen Mitteleocäns. *Jahrbuch der Kaiserlich-Königlichen Geologischen Reichsanstalt*, 55: 153–188.
- Schuller, V. 2004. Evolution and geodynamic significance of the Upper Cretaceous Gosau basin in the Apuseni Mountains (Romania). *Tübinger Geowissenschaftliche Arbeiten* A70: 1–112.
- Schulz, H.-M., Bechtel, A. and Sachsenhofer, R. F. 2005. The birth of the Paratethys during the Early Oligocene: From Tethys to an ancient Black Sea analogue? *Global and Planetary Change* 49: 163–176.

- Schuster, R., Koller, F. and Frank, W. 2007. Pebbles of upper-amphibolite facies amphibolites of the Gosau Group from the Eastern Alps: relics of a metamorphic sole? Abstract Volume, 8th Workshop on Alpine Geological Studies, Davos/Switzerland, 10.-12. October 2007, p. 74.
- Schweitzer, C. E., Čosović, V. and Feldmann, R. M. 2005. Harpactocarcinus from the Eocene of Istria, Croatia, and the paleoecology of the Zanthopsidae Via, 1959 (Crustacea : Decapoda : Brachyura). *Journal of Paleontology*, 79: 663–669.
- Sciunnach, D. and Tremolada, F. 2004. The Lombardian Gonfolite Group in central Brianza (Como and Milano Provinces, Italy): Calcareous nannofossil biostratigraphy and sedimentary record of neo-Alpine tectonics. *Eclogae geologicae Helvetiae* 97: 119–131.
- Seydoux-Guillaume, A.M., Paquette, J.L., Wiedenbeck, M., Montel, J.M. and Heinrich, W. 2002. Experimental resetting of the U-Th-Pb systems in monazite. *Chemical Geology*, 191: 165–181.
- Seydoux-Guillaume, A.M., Wirth, R., Deutsch, A. and Schärer, U. 2004. Microstructure of 24-1928 Ma concordant monazites; implications for geochronology and nuclear waste deposits. *Geochimica et Cosmochimica Acta*, 68: 2517–2527.
- Šikić, D. 1963. Eine vergleichende Darstellung der Entwicklung des jüngeren klastischen Paläogens in Istrien, dem kroatischen Küstenland und Dalmatien. *Geološki vjesnik*, 15: 329–336.
- Šikić, D. 1968. The development of the Paleogene and the Lutetian movements in northern Dalmatia. *Geološki vjesnik*, 22: 309–331.
- Šimunić, A. and Pamić, J. 1989. Ultramafic rocks from the neighbourhood of Gornje Orešje on the northwestern flanks of Mt. Medvednica (northern Croatia) [in Croatian with English summary]. *Geološki vjesnik* 42: 93–101.
- Sircombe, K. N. 2004. AGEDISPLAY; an EXCEL workbook to evaluate and display univariate geochronological data using binned frequency histograms and probability density distributions. *Computers and Geosciences* 30: 21–31.
- Sircombe, K.N. and Hazelton, M.L. 2004. Comparison of detrital zircon age distributions by kernel functional estimation. *Sedimentary Geology*, 171: 91–111.
- Skaberne, D. 1987. Megaturbidites in the Paleogene flysch in the region of Anhovo (W Slovenia, Yugoslavia). *Memorie della Società Geologica Italiana*, 40: 231–239.
- Slovenec, D. and Lugović, B. 2000. Ultramafic Cumulate Rocks from the Medvednica Mts. Ophiolite Complex (Northwestern Croatia) [in Croatian with English summary]. Proceedings, 2nd Croatian Geological Congress, Dubrovnik, 379–385.
- Slovenec, D. and Pamić, J. 2002. Geology of the Vardar Zone ophiolites of the Medvednica Mountain area located along the Zagreb-Zemlin line (NW Croatia). *Geologica Carpathica* 53: 53–59.
- Smith, A.G. 2006. Tethyan ophiolite emplacement, Africa to Europe motions, and Atlantic spreading. In: Tectonic Development of the Eastern Mediterranean region (Robertson, A.H.F. and Mountrakis, D., eds). *Geological Society, London, Special Publications*, 260: 11–34.
- Šparica, M., Koch, G., Ibrahimpašić, H., Galović, I. and Bergant, S. 2005. New data to the Palaeogene stratigraphy of the clastic-carbonate beds in SE Istria, Croatia. In: Velić, I., Vlahović, I. and Biondić, R. (eds) Third Croatian Geological Congress, Abstracts Book, Opatija, 29.09-01.10.2005: Zagreb, 147–148.
- Spray, J.G., Bébien, J., Rex, D.C. and Roddick, J.C. 1984. Age constraints on the igneous and metamorphic evolution of the Hellenic-Dinaric ophiolites. In: The geological evolution of the eastern Mediterranean (Dixon, J.E. and Robertson, A.H.F., eds). *The Geological Society, London, Special Publications*, 17: 619–627.
- Starijaš, B., Balen, D., Tibljaš, D., Humer, B. and Finger, F. 2005. Geochemistry, geochronology and metamorphic evolution of the Moslavačka Gora Massif (Croatia). *Abstracts Book, 7th Workshop on Alpine Geological Studies, Opatija*, 92.
- Starijaš, B., Gerdes, A., Balen, D., Tibljaš, D., Schuster, R., Mazer, A., Humer, B. and Finger, F. 2006. Geochronology, metamorphic evolution and geochemistry of granitoids of the Moslavačka Gora Massif (Croatia). *XVIII Congress of the Carpathian-Balkan Geological Association, Belgrade*, 594–597.

- Steiger, R.H. and Jäger, E. 1977. Subcommittee on Geochronology - Convention on use of decay constants in geochronology and cosmochronology. *Earth and Planetary Science Letters*, 36: 359–362.
- Stojanov, R. and Svešnikova, E.V. 1984. Granites and contact-metamorphic rocks in Madenska Reka on the way Štip-Radoviš (SR Macedonia). *Geologica Macedonica*, 1: 165–181.
- Stradner, H. 1962. Über das fossile Nannoplankton des Eozän-Flysch von Istrien. *Verhandlungen der Geologischen Bundesanstalt, Jg. 1962*: 176–186.
- Stuart, F.M., Bluck, B.J. and Pringle, M.S. 2001. Detrital muscovite  $^{40}\text{Ar}/^{39}\text{Ar}$  ages from Carboniferous sandstones of the British Isles: Provenance and implications for the uplift history of orogenic belts. *Tectonics*, 20: 255–267.
- Suzuki, K., Adachi, M. and Tanaka, T., 1991. Middle Precambrian provenance of Jurassic sandstone in the Mino Terrane, central Japan: Th-U-total Pb evidence from an electron microprobe monazite study. *Sedimentary Geology*, 75: 141–147.
- Svojtka, M. and Košler, J. 2002. Fission-track dating of zircon by laser ablation ICPMS. *Geochimica et Cosmochimica Acta*, 66: A756–A756.
- Sylvester, P.J. and Ghaderi, M. 1997. Trace element analysis of scheelite by excimer laser ablation inductively coupled plasma mass spectrometry (ELA-ICP-MS) using a synthetic silicate glass standard. *Chemical Geology*, 141: 49–65.
- Tagami, T. and O'Sullivan, P.B. 2005. Fundamentals of fission-track thermochronology. *Reviews in Mineralogy and Geochemistry*, 58: 19–47.
- Tari, G., Dövényi, P., Dunkl, I., Horváth, F., Lenkey, L., Stefanescu, M., Szafián, P. and Tóth, T. 1999. Lithospheric structure of the Pannonian basin derived from seismic, gravity and geothermal data. In: Durand, B., Jolivet, L., Horváth, F. and Seranne, M. (Eds.): *The Mediterranean Basins: Tertiary Extension Within The Alpine Orogen*. *Geological Society, London, Special Publications* 156: 215–250.
- Tari, V. 2002. Evolution of the northern and western Dinarides: a tectonostratigraphic approach. *EGS Stephan Mueller Special Publication Series*, 1: 1–21.
- Tari-Kovačić, V. 1998. Geodynamics of the Middle Adriatic offshore area, Croatia, based on stratigraphic and seismic analysis of Paleogene beds. *Acta Geologica Hungarica*, 41: 313–326.
- Tari, V. and Pamić, J. 1998. Geodynamic evolution of the northern Dinarides and the southern part of the Pannonian basin. *Tectonophysics* 297: 269–281.
- Taylor, S.R. and McLennan, S.M. 1985. *The Continental Crust: Its Composition and Evolution*. Blackwell, Oxford, 312 pp.
- Tera, F. and Wasserburg, J. 1972. U-Th-Pb systematics in three Apollo 14 basalts and the problem of initial Pb in lunar rocks. *Earth and Planetary Science Letters*, 14: 281–304.
- Teufel, S. and Heinrich, W. 1997. Partial resetting of the U-Pb isotope system in monazite through hydrothermal experiments: An SEM and U-Pb isotope study. *Chemical Geology*, 137: 273–281.
- Thierstein, H. R. 1980. Selective dissolution of Late Cretaceous and Earliest Tertiary calcareous nannofossils: Experimental evidence. *Cretaceous Research*, 2: 165–176.
- Thiry, M. 2000. Palaeoclimatic interpretation of clay minerals in marine deposits: an outlook from the continental origin. *Earth-Science Reviews* 49: 201–221.
- Tomljenović, B. 2000. Map-scale folding and thrust faulting in Eocene flysch sediments (The Bay of Omiš). *Vijesti Hrvatskoga geološkog društva*, 37(2), 106–108.
- Tomljenović, B. and Csontos, L. 2001. Neogene-Quaternary structures in the border zone between Alps, Dinarides and Pannonian Basin (Hrvatsko zagorje and Karlovac Basins, Croatia). *International Journal of Earth Sciences* 90: 560–578.
- Tomljenović B, Csontos L, Márton E, Márton P 2008. Tectonic evolution of the northwestern Internal Dinarides as constrained by structures and rotation of Medvednica Mts., North Croatia. In: Siegesmund S, Froitzheim N, Fügenschuh B (eds) *Tectonic Aspects of the Alpine-Carpathian-Dinaride System*. *Geological Society, London, Special Publications*, 298: 145–167

- Trautwein, B., Dunkl, I., Kuhlemann, J. and Frisch, W., 2001. Cretaceous-Tertiary Rhenodanubian flysch wedge (Eastern Alps): clues to sediment supply and basin configuration from zircon fission-track data. *Terra Nova*, 13: 382–393.
- Triebold, S., von Eynatten, H., Luvizotto, G. L. and Zack, T. 2007. Deducing source rock lithology from detrital rutile geochemistry: An example from the Erzgebirge, Germany. *Chemical Geology* 244: 421–436.
- Tunis, G. and Venturini, S. 1992. Evolution of the southern margin of the Julian Basin with emphasis on the megabeds and turbidites sequence of the southern Julian Prealps (NE Italy). *Geologia Croatica*, 45: 127–150.
- Turekian, K. K. and Wedepohl, K.-H. 1961. Distribution of the elements in some major units of the Earth's crust. *Geological Society of America Bulletin* 72: 175–191.
- Ushikubo, T., Kita, N.T., Cavosie, A.J., Wilde, S.A., Rudnick, R.L. and Valley, J.W. 2008. Lithium in Jack Hills zircons: Evidence for extensive weathering of Earth's earliest crust. *Earth and Planetary Science Letters*, 272: 666–676.
- Ustaszewski, K., Schmid, S.M., Fügenschuh, B., Tischler, M., Kissling, E. and Spakman, W. 2008. A map-view restoration of the Alpine–Carpathian–Dinaridic system for the Early Miocene. *Swiss Journal of Geosciences*, doi: 10.1007/s00015-008-1288-7.
- Ustaszewski, K., Schmid, S.M., Lugovic, B., Schuster, R., Schaltegger, U., Bernoulli, D., Hottinger, L., Kounov, A., Fügenschuh, B. and Schefer, S., in press. Late Cretaceous intra-oceanic magmatism in the internal Dinarides (northern Bosnia and Herzegovina): Implications for the collision of the Adriatic and European plates. *Lithos*
- Valley, J. 2003. Oxygen isotopes in zircon. *Reviews in Mineralogy and Geochemistry*, 53, 343–385.
- Varga, P. 1982. The lower marine member of the Tard Clay: Its age on the foraminiferal evidence of allodapic limestone beds. *Földtani Közöny*, 112: 177–184.
- Varga, P. 1985. Turbiditic limestone intercalations of the Buda Marl and Tard Clay. *Őslénytani Viták*, 31: 93–99.
- Varol, O. 1998. Palaeogene. In: Bown, P. R. (ed) *Calcareous nannofossil biostratigraphy*. Chapman and Hall, London, 200–224.
- Vavra, G. 1990. On the kinematics of zircon growth and its petrogenetic significance – a cathodoluminescence study. *Contributions to Mineralogy and Petrology*, 106: 90–99.
- Vergély, P., Dimo, A. and Monie, P. 1998.  $^{40}\text{Ar}/^{39}\text{Ar}$  dating of metamorphic soles from the Albanian ophiolites: implications for their emplacement models. *Comptes Rendus de l'Academie des Sciences*, sér. Ila, 326: 717–722.
- Viator, D. B. 2003. Detrital tourmaline as an indicator of provenance: a chemical and sedimentological study of modern sands from the Black Hills, South Dakota. Unpublished MSc Thesis, Louisiana State University, Baton Rouge, 139 pp.
- Vlahović, I., Tišljarić, J., Velić, I. and Matičec, D. 2005. Evolution of the Adriatic carbonate platform: Palaeogeography, main events and depositional dynamics. *Palaeogeography, Palaeoclimatology, Palaeoecology*, 220: 333–360.
- Vörös, A. 1993. Jurassic microplate movements and brachiopod migrations in the western part of the Tethys. *Palaeogeography, Palaeoclimatology, Palaeoecology* 100: 125–145.
- Vörös, A. and Galácz, A. 1998. Jurassic palaeogeography of the Transdanubian Central Range (Hungary). *Rivista Italiana di Paleontologia e Stratigrafia* 104: 69–84.
- Vrabec, M. and Fodor, L. 2006. Late Cenozoic tectonics of Slovenia: Structural styles at the northwestern corner of the Adriatic microplate. In: Pinter, N., Grenerezy, G., Weber, J., Stein, S. and Medak, D. (eds) *The Adria Microplate: GPS Geodesy, Tectonics and Hazards*. NATO Science Series IV, 61, Springer, 151–168.
- Watson, E. B., Wark, D. A. and Thomas, J. B. 2006. Crystallization thermometers for zircon and rutile. *Contributions to Mineralogy and Petrology* 151: 413–433.
- Watt, G.R. and Harley, S.L. 1993. Accessory phase controls on the geochemistry of crustal melts and restites produced during water-undersaturated partial melting. *Contributions to Mineralogy and Petrology*, 114: 550–566.

- Weltje, G.J. and von Eynatten, H. 2004. Quantitative provenance analysis of sediments: review and outlook. *Sedimentary Geology*, 171: 1–11.
- Wiesinger, M., Neubauer, F., Berza, T., Jandler, R. and Genser, J. 2005.  $^{40}\text{Ar}/^{39}\text{Ar}$  amphibole and biotite dating of Romanian banatites. Abstracts Book, 7th Workshop on Alpine Geological Studies Opatija, 105–106.
- Williams, M.L., Jercinovic, M.J., Goncalves, P. and Mahan, K. 2006. Format and philosophy for collecting, compiling, and reporting microprobe monazite ages. *Chemical Geology*, 225: 1–15.
- Williams, M.L., Jercinovic, M.J. and Terry, M.P. 1999. Age mapping and dating of monazite on the electron microprobe; deconvoluting multistage tectonic histories. *Geology*, 27: 1023–1026.
- Woletz, G. 1962. Beobachtungen im Flysch von Istrien (Jugoslawien). – 8. Schwermineralanalysen von Flyschsandsteinen aus Istrien. *Verhandlungen der Geologischen Bundesanstalt*, 239–245.
- Young, J. R. 1998. Neogene. In: Bown, P. R. (ed) Calcareous nannofossil biostratigraphy. Chapman and Hall, London, 225–265.
- Young, J. R. and Bown, P. R. 1997. Cenozoic calcareous nannoplankton classification. *Journal of Nannoplankton Research*, 19: 36–47.
- Zack, T., von Eynatten, H. and Kronz, A. 2004a. Rutile geochemistry and its potential use in quantitative provenance studies. *Sedimentary Geology* 171: 37–58.
- Zack, T., Moraes, R. and Kronz, A. 2004b. Temperature dependence of Zr in rutile: empirical calibration of a rutile thermometer. *Contributions to Mineralogy and Petrology* 148: 471–488.
- Zhu, B., Kidd, W.S.F., Rowley, D.B. and Currie, B.S. 2004. Chemical compositions and tectonic significance of chrome-rich spinels in the Tianba Flysch, Southern Tibet. *Journal of Geology* 112: 417–434.
- Ziegler, B. 1963. Die Fauna der Lemeš-Schichten (Dalmatien) und ihre Bedeutung für den mediterranen Oberjura. *Neues Jahrbuch für Geologie und Paläontologie, Monatshefte*, 405–421.
- Zimmerle, W. 1984. The geotectonic significance of detrital brown spinel in sediments. *Mitteilungen des dem Geologisch-Paläontologischen Institut der Universität Hamburg* 56: 337–360.
- Živković, S. 2004. Smaller benthic foraminifers from the Eocene clastics from western Croatia: Paleoecology of sedimentary basin. Ph.D. Thesis. University of Zagreb, Zagreb, 101 pp.
- Živković, S. and Babić, Lj. 2003. Paleoceanographic implications of smaller benthic and planktonic foraminifera from the Eocene Pazin Basin (coastal Dinarides, Croatia). *Facies*, 49: 49–60.
- Zuffa (ed.) 1984. Provenance of Arenites. Nato ASI Series, Reidel, Dordrecht, 408 pp.
- Zupanić, J. 1981. Non-carbonate detritus from arenite sediments of Maastrichtian Vivodina Flysch (Žumberak, Western Dinarides) [In Croatian with English summary]. *Geološki vjesnik* 34: 109–120.
- Zupanić, J. and Babić, Lj. 1991. Cross-bedded sandstones deposited by tidal currents in the Eocene of the Outer Dinarides (Island of Rab, Croatia). *Geološki vjesnik*, 44: 235–245.
- Zupanić, J., Babić, Lj. and Crnjaković, M. 1981. Lower Cretaceous basinal clastics (Ostrč Formation) in the Mt. Ivansčica (Northwestern Croatia) [In Croatian with English summary]. *Acta Geologica (Zagreb)* 11: 1–44.



# APPENDIX

## **List of Appendices**

### **Appendices of Chapter 2:**

Appendix 2-1: Geographic position of sampling localities and overview of the performed analyses

Appendix 2-2: Stratigraphic range and distribution of calcareous nannofossils in the Bosnian Flysch. See table notes

Appendix 2-3: Instrument setup and measurement conditions of the EMP and LA-ICP-SF-MS analyses

Appendix 2-4: Major and trace element X-ray fluorescence geochemical analyses of the DOZ mélange and the Bosnian Flysch sediments

Appendix 2-5: Microprobe analyses of detrital tourmaline in the Bosnian Flysch sediments

Appendix 2-6: Microprobe analyses of detrital rutile in the DOZ mélange and the Bosnian Flysch sediments

Appendix 2-7: Microprobe analyses of detrital Cr-spinel in the DOZ mélange and the Bosnian Flysch sediments

Appendix 2-8: Microprobe analyses of detrital garnet in the DOZ mélange and the Bosnian Flysch sediments

Appendix 2-9: Results of U/Pb LA-ICP-SF-MS dating of detrital zircon from the DOZ mélange and the Bosnian Flysch sediments

Appendix 2-10: Results of detrital zircon fission track thermochronology from the Bosnian Flysch sediments. Refer to text for the principal age components

### **Appendix of Chapter 3:**

Appendix 3-1. Electron microprobe analyses of Cr-spinel from Cretaceous clastic sediments in the NW Dinarides

#### **Appendices of Chapter 4:**

- Appendix 4-1. Analytical parameters used for electron probe microanalysis of monazite grains in this study
- Appendix 4-2. Chemical composition of detrital monazite grains of the Lower Cretaceous Vranduk Formation, determined in-situ by electron probe microanalysis
- Appendix 4-3. New U/Pb age results of detrital zircon grains of the Lower Cretaceous Vranduk Formation, determined in-situ by laser-ablation ICP-SF-MS
- Appendix 4-4. Geographic position of the sampling localities.
- Appendix 4-5. Description of the electron microprobe total (Th-U)/Pb chemical dating method of detrital monazite
- Appendix 4-6. Details of age spectrum deconvolution of detrital monazite and zircon

#### **Appendices of Chapter 5:**

- Appendix 5-1 List of all calcareous nannofossil taxa cited in the text and figures of Chapter 5
- Appendix 5-2 Geographic position of sampling localities treated in Chapter 5

#### **Appendices of Chapter 6:**

- Appendix 6-1 Analytical results of the detrital zircon FT – LA-ICPMS U/Pb double dating experiments
- Appendix 6-2 Analytical results of detrital zircon LA-ICPMS U/Pb geochronology, performed on unetched aliquots of the double dated samples on conventional polished epoxy mounts

**Geographic position of sampling localities and overview of the performed analyses**

Profile	Unit	Sample	Lithology	calc. microfossils analysis	carb. microfossils analysis	clay mineralogy	KRF geochemistry	semiquant. HM analysis	tourmaline geochemistry	rutile thermometry	Cr-spinel geochemistry	garnet geochemistry	zircon U/Pb dating	zircon FT thermochronology	N [deg]	N [min]	E [deg]	E [min]	elev. [m]
Bila Valley	Ugar Fm.	BO-128	greyish brown limestone	X	X	X	X								44	16.561	17	43.542	615
Bila Valley	Ugar Fm.	BO-129	carbonate breccia with pellicle clasts	X	X	X	X								44	16.862	17	43.341	664
Bila Valley	Ugar Fm.	BO-130	light grey marl	X	X	X	X								44	16.862	17	43.341	664
Bila Valley	Ugar Fm.	TD-151	carbonate breccia	X	X	X	X				X		X		44	14.103	17	51.302	610
Durmitor Mt.	Ugar Fm.	TD-373	sandstone	X	X	X	X				X		X		42	56.798	19	4.629	1073
Stavnja Valley	Ugar Fm.	BO-16	grey sandstone	X	X	X	X				X		X		44	6.032	18	18.671	686
Stavnja Valley	Ugar Fm.	BO-17	grey sandstone	X	X	X	X				X		X		44	7.784	18	19.363	848
Stavnja Valley	Ugar Fm.	BO-18	dark grey sandstone	X	X	X	X				X		X		44	7.784	18	19.363	848
Stavnja Valley	Ugar Fm.	BO-111	pellicle rip-up clasts from carbonate debris	X	X	X	X				X		X		44	7.784	18	19.363	848
Stavnja Valley	Ugar Fm.	BO-117	grey siltstone, with plant debris	X	X	X	X				X		X		44	7.450	18	18.494	730
Stavnja Valley	Ugar Fm.	BO-119	clay sand from Ugar Fm. catchment	X	X	X	X				X		X		44	2.792	18	17.701	556
Stavnja Valley	Ugar Fm.	BO-26-X	red marl (Scaglia)	X	X	X	X				X		X		44	3.015	18	17.539	552
Stavnja Valley	Ugar Fm.	BO-28	carbonate breccia	X	X	X	X				X		X		44	2.863	18	17.540	534
Stavnja Valley	Ugar Fm.	BO-29	red marl (Scaglia)	X	X	X	X				X		X		44	2.647	18	17.012	519
Stavnja Valley	Ugar Fm.	BO-31	calcarene	X	X	X	X				X		X		44	2.647	18	17.012	519
Stavnja Valley	Ugar Fm.	BO-32	carbonate breccia	X	X	X	X				X		X		44	2.792	18	17.701	556
Stavnja Valley	Ugar Fm.	BO-33	grey marl	X	X	X	X				X		X		44	2.577	18	17.385	545
Stavnja Valley	Ugar Fm.	BO-34	red marl (Scaglia)	X	X	X	X				X		X		44	2.577	18	17.385	545
Stavnja Valley	Ugar Fm.	BO-36	carbonate breccia	X	X	X	X				X		X		44	2.224	18	16.787	502
Stavnja Valley	Ugar Fm.	BO-37	calcarene	X	X	X	X				X		X		44	2.084	18	16.724	502
Stavnja Valley	Ugar Fm.	BO-39	dark grey marl	X	X	X	X				X		X		44	4.031	18	17.374	572
Stavnja Valley	Ugar Fm.	BO-39b	carbonate breccia	X	X	X	X				X		X		44	4.031	18	17.374	572
Stavnja Valley	Ugar Fm.	BO-39c	carbonate breccia	X	X	X	X				X		X		44	4.031	18	17.374	572
Stavnja Valley	Ugar Fm.	BO-43	red marl (Scaglia)	X	X	X	X				X		X		44	5.301	18	18.386	621
Stavnja Valley	Ugar Fm.	BO-44	grey marl	X	X	X	X				X		X		44	5.301	18	18.386	621
Stavnja Valley	Ugar Fm.	BO-45	red marl (Scaglia)	X	X	X	X				X		X		44	4.732	18	17.582	609
Stavnja Valley	Ugar Fm.	BO-49	dark grey pellicle, organic-rich	X	X	X	X				X		X		44	6.991	18	18.434	720
Stavnja Valley	Ugar Fm.	BO-50	greenish grey marl	X	X	X	X				X		X		44	7.718	18	18.943	860
Stavnja Valley	Ugar Fm.	BO-51	grey calcarenite	X	X	X	X				X		X		44	7.718	18	18.943	860
Stavnja Valley	Ugar Fm.	BO-54	red marl (Scaglia)	X	X	X	X				X		X		44	7.710	18	18.753	750
Stavnja Valley	Ugar Fm.	BO-55b	grey marl	X	X	X	X				X		X		44	7.131	18	18.451	691
Una Valley	Ugar Fm.	TD-517	sandstone	X	X	X	X				X		X		44	55.813	16	9.438	168

Profile	Unit	Sample	Lithology	calc. microfossils analysis	carb. microfossils analysis	clay mineralogy	KRF geochemistry	Semiquant. HM analysis	tourmaline geochemistry	rutile thermometry	Cr-spinel geochemistry	garnet geochemistry	Zircon U/Pb dating	Zircon FT thermochronology	N [deg]	N [min]	E [deg]	E [min]	elev. [m]
Babišnica Valley	Vranduk Fm.	BO-4	grey sandstone, with plant debris												44	13.453	17	58.201	445
Babišnica Valley	Vranduk Fm.	BO-5	calcarenite												44	13.453	17	58.201	445
Babišnica Valley	Vranduk Fm.	BO-6	grey marl	X											44	13.453	17	58.201	445
Babišnica Valley	Vranduk Fm.	BO-8	greyish brown calcarenite												44	12.868	17	56.288	351
Babišnica Valley	Vranduk Fm.	BO-12	sandstone												44	19.555	17	54.675	280
Bosna Valley	Vranduk Fm.	BO-71	red shale												44	17.653	17	54.518	309
Bosna Valley	Vranduk Fm.	BO-72	grey sandstone, micaceous												44	17.611	17	54.357	312
Bosna Valley	Vranduk Fm.	BO-73	grey sandstone												44	17.611	17	54.357	312
Bosna Valley	Vranduk Fm.	BO-74	dark grey shale												44	17.654	17	53.985	299
Bosna Valley	Vranduk Fm.	BO-75	grey sandstone												44	17.654	17	53.985	299
Bosna Valley	Vranduk Fm.	BO-79	dark grey shale												44	15.444	17	52.717	313
Bosna Valley	Vranduk Fm.	BO-80	grey calcarenite												44	15.444	17	52.717	313
Bosna Valley	Vranduk Fm.	BO-82	breccia, polymictic												44	17.549	17	54.584	297
Bosna Valley	Vranduk Fm.	BO-82d	reddish grey shale												44	17.549	17	54.584	297
Bosna Valley	Vranduk Fm.	BO-84b	grey shale												44	18.955	17	54.053	284
Bosna Valley	Vranduk Fm.	BO-85, -85b	grey calcarenite												44	18.955	17	54.053	284
Bosna Valley	Vranduk Fm.	BO-86	red shale												44	18.602	17	54.067	290
Bosna Valley	Vranduk Fm.	BO-87	grey sandstone												44	18.602	17	54.067	290
Bosna Valley	Vranduk Fm.	BO-92	reddish brown calcarenite												44	17.583	17	53.848	271
Bosna Valley	Vranduk Fm.	BO-93	grey marly shale												44	17.122	17	53.320	258
Bosna Valley	Vranduk Fm.	BO-94	grey calcarenite												44	17.122	17	53.320	258
Bosna Valley	Vranduk Fm.	BO-95	grey calcarenite												44	19.555	17	54.675	280
Bosna Valley	Vranduk Fm.	BO-96	dark grey shale												44	19.555	17	54.675	280
Bosna Valley	Vranduk Fm.	BO-98	red shale												44	18.346	17	54.609	298
Bosna Valley	Vranduk Fm.	BO-101	red shale												44	20.179	17	55.350	286
Bosna Valley	Vranduk Fm.	TD-153	calcarenite												44	17.374	17	54.274	534
Bosna Valley	Vranduk Fm.	TD-154	sandstone												44	19.552	17	54.674	282
Bosna Valley	Vranduk Fm.	TD-145	sandstone												43	59.101	18	24.805	512
Ljubina Valley	Vranduk Fm.	TD-147	sandstone												43	59.101	18	24.805	512
Ljubina Valley	Vranduk Fm.	BO-52	greenish black sandstone												44	7.805	18	19.064	872
Stavnja Valley	Vranduk Fm.	BO-57	dark grey shale												44	8.039	18	19.087	770
Stavnja Valley	Vranduk Fm.	BO-58	dark grey shale												44	8.206	18	19.115	734
Stavnja Valley	Vranduk Fm.	BO-58C	dark grey shale												44	8.206	18	19.115	734
Stavnja Valley	Vranduk Fm.	BO-59	greyish brown sandstone, micaceous												44	8.471	18	19.306	762
Stavnja Valley	Vranduk Fm.	BO-60	dark shale, micaceous												44	8.536	18	19.396	790
Stavnja Valley	Vranduk Fm.	BO-61	grey sandstone												44	8.536	18	19.396	790
Stavnja Valley	Vranduk Fm.	BO-108	dark grey shale												44	7.764	18	19.363	848
Stavnja Valley	Vranduk Fm.	BO-115	greyish green shale												44	7.890	18	19.009	770
Stavnja Valley	Vranduk Fm.	BO-115b	brownish grey sandstone, micaceous												44	7.890	18	19.009	770
Uzloamac Mt.	Vranduk Fm.	TD-315	sandstone	X											44	40.937	17	20.997	212
Borja Mt.	DOZ mélange	TD-197	sandstone												44	35.905	17	35.928	738
Stavnja Valley	DOZ mélange	BO-22	grey sandstone												44	11.208	18	21.014	990
Stavnja Valley	DOZ mélange	BO-23	grey sandstone												44	10.886	18	20.338	932
Stavnja Valley	DOZ mélange	BO-24	dark grey shale												44	10.900	18	20.332	923
Stavnja Valley	DOZ mélange	BO-25	dark grey sandstone												44	10.900	18	20.332	923
Stavnja Valley	DOZ mélange	BO-26	dark grey shale												44	10.900	18	20.332	923

List of calcareous nannofossil taxa identified in the Bosnian Flysch samples. Stratigraphic ranges of each taxon are also indicated

	Vranduk Fm.						Ugar Fm.							
	BO-6	BO-93	TD-315	TD-152	TD-373	BO-33	BO-50	BO-29	BO-34	BO-44	BO-55b	BO-39	BO-111	TD-517
<i>Arkhangelskiella</i> sp.				?	♦									
<i>Arkhangelskiella cymbiformis</i> Vekshina 1959														
<i>Braarodospaera</i> sp.	□													
<i>Braarodospaera africana</i> Stradner 1961	□													
<i>Braarodospaera bigelovi</i> (Gan & Braand 1935) Deflandre 1947														
<i>Braarodospaera parca</i> (Stradner 1963) Buky 1969, ssp. <i>constricta</i> Hattner et al. 1980														
<i>Bronsonia</i> sp.														
<i>Calcutites obscurus</i> (Deflandre 1959) [a: Phins & Sissingh in Sissingh 1977; b: Campanian – Maastrichtian]														
<i>Cribrosphaerella ehrenbergii</i> (Arkhangelsky 1912) Deflandre in Piveteau 1952														
<i>Cruciellipsis cvillieri</i> (Manivit 1966) Thierstein 1971														
<i>Cyclagelosphaera argensis</i> Bown 1992														
<i>Cyclagelosphaera magerelii</i> Noël 1965														
<i>Cyclagelosphaera reinhardtii</i> (Perch-Nielsen 1968) Romein 1977	cf													
<i>Eiffelithus</i> sp.														
<i>Eiffelithus eximius</i> (Stover 1966) Perch-Nielsen 1968														
<i>Eiffelithus turiseiffelii</i> (Deflandre in Deflandre & Fert. 1954) Reinhardt 1965														
<i>Lucianorhabdus cayeuxii</i> Deflandre 1959														
<i>Lucianorhabdus</i> sp.														
<i>Micrantholithus</i> sp.	?													
<i>Microrhabdulus</i> sp.														
<i>Micula steurophora</i> (Gardet 1955) Stradner 1963														
<i>Nannocorus steinmanni</i> Kampher 1931														
<i>Percivalia</i> aff. <i>imperfossa</i> Black 1971														
<i>Uniplanarius gothicus</i> (Deflandre 1959) Hattner & Wise 1980														
<i>Uniplanarius sissinghii</i> Perch-Nielsen 1986														
<i>Uniplanarius trifidus</i> (Stradner in Stradner & Papp 1961) Hattner & Wise 1980														
<i>Watznaueria</i> sp.														
<i>Watznaueria barnesae</i> (Black 1959) Perch-Nielsen 1968	▲	■	□	□	□	□	▲	▲	♦	□	□	♦	▲	
<i>Watznaueria biporta</i> Buky 1969														
<i>Watznaueria britannica</i> (Stradner 1963) Reinhardt 1964	■													
<i>Watznaueria manilivae</i> Buky 1973	□													
<i>Watznaueria ovata</i> Buky 1969														
<i>Zeughabdotus</i> sp.														
<i>Zeughabdotus embergeri</i> (Noel 1958) Perch-Nielsen 1984														

Observed nannofossil abundance per 1000 fields of view

□ present  
 ■ very rare  
 ♦ rare  
 □ frequent  
 ▲ common

1-2 specimens observed  
 <10 specimen  
 10-100  
 >100  
 >>100

?: questionable occurrence. In case of entries "cf" and "?" 1-2 specimens were observed  
 Samples BO127b and TD148 were barren of calcareous nannofossils

**Instrument setup and measurement conditions of (a) EMP and (b) LA-ICP-SF-MS analyses**

**(a) Electron microprobe analyses**

Analyzed mineral	<b>Tourmaline</b>				
Acceleration voltage	20 kV				
Beam current	15 nA				
Probe diameter	7 µm				
Data correction	ZAF (including a fixed value of 10.2 wt% B <sub>2</sub> O <sub>3</sub> to account for boron matrix)				
Element	Spectrometer	X-ray line	Counting time peak (s)   bgd (s)		Standard
Si	1 TAP	Kα	15	5	Wollastonite; Willsboro (NY, USA)
Ti	3 PETJ	Kα	30	15	TiO <sub>2</sub> (synthetic)
Al	1 TAP	Kα	15	5	Al <sub>2</sub> O <sub>3</sub> (synthetic)
Fe	4 LIF	Kα	15	5	Haematite; Elba (Italy)
Mn	4 LIF	Kα	30	15	Rhodonite; Broken Hill (Australia)
Mg	2 TAP	Kα	15	5	MgO (synthetic)
Na	2 TAP	Kα	15	5	Albite; Amelia (VA, USA)
Ca	3 PETJ	Kα	15	5	Wollastonite, Willsboro (NY, USA)
K	3 PETJ	Kα	15	5	Sanidine; Weibern (Germany)
Zn	5 LIFH	Kα	30	15	Gahnite (USNM 145883)
V	5 LIFH	Kα	30	15	metallic V
Analyzed mineral	<b>Garnet</b>				
Acceleration voltage	15 kV				
Beam current	15 nA				
Probe diameter	3 µm				
Data correction	ZAF				
Element	Spectrometer	X-ray line	Counting time peak (s)   bgd (s)		Standard
Si	1 TAP	Kα	15	5	Pyrope; Kakanui (New Zealand)
Ti	3 PETJ	Kα	30	15	TiO <sub>2</sub> (synthetic)
Al	1 TAP	Kα	15	5	Al <sub>2</sub> O <sub>3</sub> (synthetic)
Fe	5 LIFH	Kα	15	5	Haematite; Elba (Italy)
Mn	5 LIFH	Kα	15	5	Rhodonite; Broken Hill (Australia)
Mg	2 TAP	Kα	30	15	MgO (synthetic)
Ca	4 PETJ	Kα	30	15	Wollastonite; Willsboro (NY, USA)
Na	2 TAP	Kα	10	3	Albite; Amelia (VA, USA)
K	4 PETJ	Kα	10	3	Sanidine; Weibern (Germany)
Analyzed mineral	<b>Rutile</b>				
Acceleration voltage	25 kV				
Beam current	80 nA (unknowns), 20 nA (standards)				
Probe diameter	3 µm				
Data correction	Phi-Rho-Z				
Element	Spectrometer	X-ray line	Counting time peak (s)   bgd (s)		Standard
Si	2 TAP	Kα	150	50	ZrSiO <sub>4</sub> (synthetic; provided by J. Hanchar)
Ti	4 LIF	Kβ	30	15	TiO <sub>2</sub> (synthetic)
Al	2 TAP	Kα	150	50	Al <sub>2</sub> O <sub>3</sub> (synthetic)
Fe	3 LIF	Kα	100	50	Haematite; Elba (Italy)
V	4 LIF	Kα	200	100	metallic V
Cr	3 LIF	Kα	200	100	Cr <sub>2</sub> O <sub>3</sub> (synthetic)
Zr	5 PETH	Lα	300	150	ZrSiO <sub>4</sub> (synthetic; provided by J. Hanchar)
Nb	1 PETJ	Lα	300	150	metallic Nb

Refer to Zack et al. (2004a) and Triebold et al. (2007) for further analytical details

Analyzed mineral	<b>Cr-spinel</b>				
Acceleration voltage	20 kV				
Beam current	20 nA				
Probe diameter	3 µm				
Data correction	Phi-Rho-Z				
Element	Spectrometer	X-ray line	Counting time peak (s)   bgd (s)		Standard
Cr	3 PETJ	Kα	30	15	Cr <sub>2</sub> O <sub>3</sub> (synthetic)
Al	2 TAP	Kα	30	15	Al <sub>2</sub> O <sub>3</sub> (synthetic)
Fe	4 LIF	Kα	30	15	Haematite; Elba (Italy)
Mg	1 TAP	Kα	30	15	MgO (synthetic)
Mn	4 LIF	Kα	30	15	Rhodonite; Broken Hill (Australia)
Ti	3 PETJ	Kα	60	30	TiO <sub>2</sub> (synthetic)
Zn	5 LIFH	Kα	30	15	Gahnite (USNM 145883)
V	5 LIFH	Kα	30	15	metallic V
Ni	5 LIFH	Kα	30	15	NiO (synthetic)
Si	2 TAP	Kα	30	15	Wollastonite; Willsboro (NY, USA)

**(b) LA-ICP-SF-MS analyses**

*ICP-SF-MS: instrument operating conditions*

Instrument	Thermo Element 2
Forward power	1100 - 1350 W
Coolant gas flow	16 l min <sup>-1</sup> Ar
Auxiliary gas flow	1 l min <sup>-1</sup> Ar
Carrier gas flow	0.8 l min <sup>-1</sup> He
Make-up gas flow	0.3 l min <sup>-1</sup> Ar

*ICP-SF-MS: data acquisition parameters*

Scan mode	E-scan
Scanned masses	202; 204; 206; 207; 208; 235; 232; 238
Mass resolution	low
Detector dead time	18 ns
Dwell time	4 ms
Settling time	1 ms
Number of scans	1000
Detector mode	analogue for mass 238, pulse for all other masses
Background acquisition time	30 s
Total ablation time	60 s
Ablation time taken for age calculation	15-45 s

*Laser ablation: operating conditions*

Laser type	New Wave UP213 Nd:YAG
Wavelength	213 nm
Laser mode	Q switched
Laser fluency	3.5 Jcm <sup>-2</sup>
Repetition rate	10 Hz
Sampling scheme	single spot static ablation
Nominal pit diameter	30 µm
Ablation cell	teardrop-shaped, low volume (V~3 cm <sup>3</sup> )
Length of tubing	1 m

*Standardization and data reduction*

External standard used	GJ-1 zircon
Reference used for quality control	Plešovice zircon
Data reduction software used	PEPITA















**Electron microprobe analyses of detrital rutile from the Dinaride Ophiolite Zone mélange and the Bosnian Flysch**

Formation	Sample & spot ID	trace element concentrations in ppm								
		TiO <sub>2</sub> [wt%]	Total oxides [wt%]	Nb [n.d.: not detected]	Al	Cr	Zr	Si	Fe	V
DOZ mélange	BO25rt001	99.13	101.46	7207	88	556	74	47	7454	1363
DOZ mélange	BO25rt003	99.97	100.88	684	444	996	1028	366	2054	691
DOZ mélange	BO25rt004	99.33	101.10	6481	418	700	129	56	3774	846
DOZ mélange	BO25rt005	100.49	101.50	2554	100	374	103	47	3003	1077
DOZ mélange	BO25rt007	99.83	101.31	3096	260	194	657	56	4938	1511
DOZ mélange	BO25rt008	100.61	101.53	520	102	2213	133	86	1791	1610
DOZ mélange	BO25rt009	100.83	101.83	2089	239	55	740	47	3070	944
DOZ mélange	BO25rt010	99.99	101.14	1119	111	2258	1102	86	469	2782
DOZ mélange	BO25rt012	101.04	102.28	3539	472	286	668	76	3446	286
DOZ mélange	BO25rt013	99.94	100.93	2900	552	146	449	83	2375	401
DOZ mélange	BO25rt014	100.07	101.22	776	274	n.d.	430	104	6726	307
DOZ mélange	BO25rt015	100.41	101.56	1808	127	343	63	68	5414	666
DOZ mélange	BO25rt016	100.47	101.13	78	204	68	833	151	3269	290
DOZ mélange	BO25rt017	100.37	103.15	243	126	245	193	47	19821	642
DOZ mélange	BO25rt018	101.83	102.63	1218	388	155	128	47	2489	1226
DOZ mélange	BO25rt019	98.86	100.25	2303	444	1935	1101	61	2843	1079
DOZ mélange	BO25rt020	99.68	101.47	2322	69	7063	436	64	819	1533
DOZ mélange	BO25rt021	101.58	102.16	201	160	72	90	n.d.	2669	1043
DOZ mélange	BO25rt023	100.38	100.91	249	204	n.d.	378	47	2066	943
DOZ mélange	BO25rt024	99.43	100.49	2092	376	519	74	177	2955	1240
DOZ mélange	BO25rt025	98.59	99.57	351	174	2115	138	469	2580	939
DOZ mélange	BO25rt026	101.96	102.84	2248	185	345	105	n.d.	2751	655
DOZ mélange	BO25rt027	101.78	102.36	82	238	n.d.	240	99	2223	1179
DOZ mélange	BO25rt028	100.72	102.11	2169	145	2094	802	47	4514	300
DOZ mélange	BO25rt029	100.40	100.86	56	171	211	75	51	1917	800
DOZ mélange	BO25rt030	101.00	101.69	1313	114	277	77	47	1557	1502
DOZ mélange	BO25rt031	98.39	99.42	1427	420	53	518	706	2400	1412
DOZ mélange	BO25rt032	99.79	100.62	1895	129	378	150	47	2616	748
DOZ mélange	BO25rt033	98.62	100.10	1674	270	1399	2268	57	741	3840
DOZ mélange	BO25rt034	100.39	101.00	404	179	966	146	47	1284	1215
DOZ mélange	BO25rt035	98.91	100.46	917	390	83	255	n.d.	7698	2046
DOZ mélange	BO25rt036	101.15	101.93	302	65	715	234	47	3771	690
DOZ mélange	BO25rt037	98.68	99.59	98	281	460	874	n.d.	2459	2272
DOZ mélange	BO25rt038	99.29	99.92	171	136	352	78	47	1838	1816
DOZ mélange	BO25rt039	99.65	100.39	185	108	1112	122	47	2908	927
DOZ mélange	BO25rt040	99.16	100.05	402	315	612	1102	92	2950	895
DOZ mélange	BO25rt041	99.15	99.90	717	147	896	107	78	2103	1261
DOZ mélange	BO25rt042	100.82	101.89	1241	194	463	950	47	3059	1755
DOZ mélange	BO25rt044	101.17	102.36	3154	193	551	235	218	2795	1150
DOZ mélange	BO25rt046	99.92	101.17	192	118	930	306	56	851	6141
DOZ mélange	BO25rt047	100.80	101.55	1652	111	86	814	179	2325	178
DOZ mélange	BO25rt048	100.52	101.30	1521	142	235	137	70	2607	877
DOZ mélange	BO25rt049	100.33	101.14	1416	192	540	110	248	1856	1275
DOZ mélange	BO25rt050	100.90	102.23	2868	164	1218	244	71	3034	1759
DOZ mélange	BO25rt051	100.74	101.61	1214	171	431	309	161	2387	1465
DOZ mélange	BO25rt052	99.29	100.71	4244	157	494	602	47	3021	1547
DOZ mélange	BO25rt053	100.72	101.56	1382	209	1678	187	n.d.	1789	660
DOZ mélange	BO25rt054	99.58	100.61	888	95	969	486	156	1038	3479
DOZ mélange	BO25rt055	101.97	102.72	1194	146	733	133	64	2407	725
DOZ mélange	BO25rt056	100.08	102.06	996	2266	339	427	4213	1923	998
DOZ mélange	BO25rt057	99.24	100.43	3037	256	386	535	99	3440	756
DOZ mélange	BO25rt058	100.04	100.90	1969	229	315	89	104	2102	1275
DOZ mélange	BO25rt059	100.70	101.58	324	265	495	232	47	3527	1415
DOZ mélange	BO25rt060	101.09	102.36	3071	179	808	962	259	2159	1443
DOZ mélange	BO25rt061	100.59	101.37	1597	155	529	125	47	1579	1465
DOZ mélange	BO25rt062	99.99	100.71	235	515	n.d.	141	n.d.	3196	1030
DOZ mélange	BO25rt063	99.94	101.00	1802	185	286	1338	68	2303	1600
DOZ mélange	BO25rt066	99.52	101.63	570	172	1882	175	107	12359	587
DOZ mélange	BO25rt067	99.87	100.82	1941	332	716	730	147	2296	568
DOZ mélange	BO25rt068	100.09	101.41	1664	122	1250	415	63	1107	4476
DOZ mélange	BO25rt069	99.86	101.25	2119	206	997	929	n.d.	5300	630
DOZ mélange	BO25rt070	99.58	100.68	785	205	931	968	76	4389	697
DOZ mélange	BO25rt071	99.96	101.14	2953	276	57	913	n.d.	3506	825
DOZ mélange	BO25rt072	101.46	102.39	1099	180	258	1325	n.d.	3144	790
DOZ mélange	BO25rt073	101.38	102.04	482	141	260	329	120	2306	1120
DOZ mélange	BO25rt074	99.39	100.27	1473	215	499	218	62	2794	1017
DOZ mélange	BO25rt075	100.53	101.99	1506	325	128	229	n.d.	7661	948
DOZ mélange	BO25rt076	99.01	100.45	1211	1476	67	1065	383	2089	3311
DOZ mélange	BO25rt077	99.84	101.44	3333	324	445	1571	84	4876	880
DOZ mélange	BO25rt078	100.28	101.00	961	147	361	286	80	2533	763
DOZ mélange	BO25rt080	100.26	101.09	1328	257	261	888	140	2121	881

Formation	Sample & spot ID	trace element concentrations in ppm							V	
		TiO <sub>2</sub> [wt%]	Total oxides [wt%]	Nb	Al	Cr	Zr	Si		Fe
Ugar Fm.	BO16r001	99.45	100.30	1667	53	1898	399	47	1002	901
Ugar Fm.	BO16r002	99.86	101.08	3630	n.d.	878	76	51	2909	1100
Ugar Fm.	BO16r003	100.26	101.09	1960	82	510	111	47	2391	846
Ugar Fm.	BO16r004	99.45	100.52	2026	n.d.	699	66	83	3289	1509
Ugar Fm.	BO16r005	100.10	101.03	2170	n.d.	614	124	103	2092	1405
Ugar Fm.	BO16r006	99.38	99.96	322	n.d.	926	178	108	1581	1032
Ugar Fm.	BO16r007	99.03	100.25	621	n.d.	1529	276	50	204	5661
Ugar Fm.	BO16r009	99.88	102.09	8311	134	636	439	84	4974	1131
Ugar Fm.	BO16r010	99.41	99.91	248	n.d.	866	424	47	480	1383
Ugar Fm.	BO16r011	101.65	102.53	231	53	2507	304	54	1409	1584
Ugar Fm.	BO16r012	99.28	100.45	960	112	4801	69	302	654	1001
Ugar Fm.	BO16r014	99.66	101.31	2114	n.d.	718	3650	47	1884	3400
Ugar Fm.	BO16r016	100.29	101.14	1911	n.d.	606	164	102	2115	1137
Ugar Fm.	BO16r017	101.47	102.11	58	78	1336	116	66	573	2179
Ugar Fm.	BO16r018	101.61	102.23	73	95	677	128	47	992	2311
Ugar Fm.	BO16r019	102.22	103.25	2625	n.d.	572	125	140	2214	1534
Ugar Fm.	BO16r021	100.73	102.06	4392	n.d.	690	89	58	2456	1685
Ugar Fm.	BO16r022	101.90	102.91	2823	107	551	128	n.d.	2191	1349
Ugar Fm.	BO16r023	101.19	102.21	2321	86	703	147	149	1914	1800
Ugar Fm.	BO16r024	101.27	102.22	2113	n.d.	439	178	89	2676	1266
Ugar Fm.	BO16r025	99.00	100.08	2540	64	1937	204	74	836	1813
Ugar Fm.	BO16r026	100.79	101.78	2747	n.d.	627	95	47	1918	1594
Ugar Fm.	BO16r027	101.70	102.65	2639	53	786	147	47	2194	866
Ugar Fm.	BO16r028	98.67	99.57	1946	n.d.	569	57	134	2559	1145
Ugar Fm.	BO16r029	97.79	99.10	2187	232	1332	406	979	1678	1880
Ugar Fm.	BO16r030	99.01	99.87	1942	53	432	125	113	2395	1050
Ugar Fm.	BO16r031	101.62	102.07	275	52	105	127	69	1384	1249
Ugar Fm.	BO16r032	101.25	102.40	3187	85	829	220	163	1914	1618
Ugar Fm.	BO16r033	101.07	101.62	69	n.d.	511	107	47	642	2490
Ugar Fm.	BO16r034	99.14	100.97	4480	n.d.	1509	2284	73	1630	2883
Ugar Fm.	BO16r036	101.92	102.80	511	53	571	185	142	728	3835
Ugar Fm.	BO16r037	99.12	100.11	2242	n.d.	825	83	71	2624	1180
Ugar Fm.	BO16r038	99.18	100.34	2619	105	1487	130	68	1622	2060
Ugar Fm.	BO16r039	99.88	100.91	2851	76	1037	162	47	1705	1417
Ugar Fm.	BO16r040	98.07	99.11	2210	n.d.	729	271	n.d.	2222	1916
Ugar Fm.	BO16r042	100.30	100.88	1531	53	249	149	n.d.	1015	1107
Ugar Fm.	BO16r043	101.15	101.92	160	n.d.	204	394	47	1513	3096
Ugar Fm.	BO16r044	101.11	102.03	2232	99	284	146	47	2176	1532
Ugar Fm.	BO16r045	100.30	101.18	2499	n.d.	117	147	68	3321	285
Ugar Fm.	BO16r046	96.86	99.23	1295	n.d.	2312	640	93	1357	10605
Ugar Fm.	BO16r047	100.02	100.92	2442	57	207	241	47	2510	926
Ugar Fm.	BO16r048	99.99	102.11	6727	n.d.	1728	100	47	2935	3333
Ugar Fm.	BO16r049	97.98	99.33	2384	n.d.	1481	369	n.d.	260	4787
Ugar Fm.	BO16r050	100.63	101.51	1811	53	681	132	97	1945	1545
Ugar Fm.	BO16r051	101.40	102.04	606	n.d.	505	59	47	1754	1625
Ugar Fm.	BO16r052	98.04	99.05	2305	141	610	79	69	2774	1167
Ugar Fm.	BO16r053	100.01	100.55	115	227	569	475	72	958	1279
Ugar Fm.	BO16r054	98.65	99.33	755	n.d.	898	337	n.d.	837	1961
Ugar Fm.	BO16r055	99.73	100.76	2853	n.d.	607	224	47	2431	1193
Ugar Fm.	BO16r056	98.11	100.38	4440	228	1165	210	279	9049	1118
Ugar Fm.	BO16r057	100.78	101.94	3244	n.d.	701	155	47	1989	1997
Ugar Fm.	BO16r058	100.70	101.43	385	53	1167	196	82	1783	1467
Ugar Fm.	BO16r059	98.88	99.87	2305	n.d.	731	151	47	2352	1494
Ugar Fm.	BO16r060	99.14	100.33	2827	53	496	282	95	3128	1602
Ugar Fm.	BO16r061	99.38	100.47	3124	110	694	192	58	1671	1723
Ugar Fm.	BO16r063	100.86	101.66	1613	103	599	120	142	2654	472
Ugar Fm.	BO16r064	101.02	101.68	56	121	1314	138	52	1727	1270
Ugar Fm.	BO16r065	101.21	102.30	1769	53	2134	138	138	1296	1997
Ugar Fm.	BO16r066	100.05	101.27	3632	53	430	249	n.d.	3547	866
Ugar Fm.	BO16r067	101.65	102.10	184	53	235	257	86	1871	612
Ugar Fm.	BO16r069	101.87	102.51	437	50	390	204	n.d.	1255	2149
Ugar Fm.	BO16r070	98.69	99.70	407	n.d.	68	107	47	6243	763
Ugar Fm.	BO16r071	100.88	101.84	1845	n.d.	1405	197	n.d.	2026	1340
Ugar Fm.	BO16r073	101.33	102.19	1773	n.d.	606	58	150	2105	1399
Ugar Fm.	BO16r074	101.84	102.40	63	n.d.	376	85	47	1692	1720
Ugar Fm.	BO16r074	98.18	99.30	2054	138	766	516	168	1381	2701
Ugar Fm.	BO16r075	98.48	99.28	1755	203	625	121	99	1494	1275
Ugar Fm.	BO16r076	100.44	101.79	3285	n.d.	473	121	47	4717	1161
Vranduk Fm.	BO4r001	99.98	100.76	875	53	574	146	n.d.	3273	753
Vranduk Fm.	BO4r002	99.35	100.05	1024	74	312	56	n.d.	2368	1233
Vranduk Fm.	BO4r003	98.40	99.94	4524	126	721	191	n.d.	4145	1293
Vranduk Fm.	BO4r004	101.00	101.70	326	n.d.	1945	100	47	1101	1421
Vranduk Fm.	BO4r005	101.03	102.32	1762	212	615	2098	n.d.	2873	1748
Vranduk Fm.	BO4r006	100.22	101.39	2794	n.d.	1672	366	n.d.	1052	2241
Vranduk Fm.	BO4r007	100.56	101.83	2715	n.d.	991	507	n.d.	2595	2262
Vranduk Fm.	BO4r008	101.01	102.37	3823	n.d.	300	74	47	5614	192
Vranduk Fm.	BO4r009	101.66	102.56	417	n.d.	1572	195	47	3507	843
Vranduk Fm.	BO4r010	100.43	101.53	1902	n.d.	629	76	60	4549	827
Vranduk Fm.	BO4r012	101.06	101.95	816	245	n.d.	593	277	3389	1012
Vranduk Fm.	BO4r013	101.93	102.82	76	n.d.	666	2777	n.d.	1443	1475
Vranduk Fm.	BO4r014	101.47	102.07	554	53	360	116	n.d.	2641	632
Vranduk Fm.	BO4r015	100.93	101.64	895	n.d.	177	156	n.d.	2023	1750
Vranduk Fm.	BO4r016	99.23	100.58	1938	596	1129	175	782	2883	1603
Vranduk Fm.	BO4r018	100.88	101.70	1894	215	282	107	n.d.	2542	842
Vranduk Fm.	BO4r018	100.92	101.61	334	56	206	264	47	3597	625
Vranduk Fm.	BO4r025	99.42	100.43	2391	112	497	153	47	2746	1232
Vranduk Fm.	BO4r030	101.19	101.89	216	n.d.	92	171	n.d.	4377	445
Vranduk Fm.	BO4r032	99.28	100.33	2019	53	989	231	n.d.	2945	1351
Vranduk Fm.	BO4r033	100.26	101.24	1505	n.d.	212	84	n.d.	4827	658
Vranduk Fm.	BO4r034	98.82	100.00	316	n.d.	68	133	47	7759	749
Vranduk Fm.	BO4r035	99.26	100.03	554	108	68	696	n.d.	2557	1623
Vranduk Fm.	BO4r036	100.47	101.41	683	53	611	1294	76	641	3192
Vranduk Fm.	BO4r038	100.08	102.38	6562	53	2496	1000	n.d.	2648	3403
Vranduk Fm.	BO4r039	100.25	101.68	3679	761	176	53	564	3470	1022
Vranduk Fm.	BO4r040	101.32	102.16	255	n.d.	144	458	n.d.	4707	778
Vranduk Fm.	BO4r041	99.06	99.92	196	53	500	224	n.d.	3863	1522
Vranduk Fm.	BO4r042	99.33	100.45	516	n.d.	209	295	n.d.	6787	637
Vranduk Fm.	BO4r050	99.58	101.41	5209	n.d.	588	227	n.d.	4861	2185
Vranduk Fm.	BO4r051	99.99	101.66	4293	333	605	1158	n.d.	4064	1458
Vranduk Fm.	BO4r052	100.82	101.73	336	n.d.	393	295	n.d.	1649	3786
Vranduk Fm.	BO4r054	100.58	101.57	807	230	1674	251	269	3174	528
Vranduk Fm.	BO4r055	100.18	101.19	2545	53	562	223	n.d.	2525	1303
Vranduk Fm.	BO4r057	100.63	101.69	2028	n.d.	1204	55	n.d.	2211	1954
Vranduk Fm.	BO4r060	100.17	101.79	2492	208	612	3270	47	2389	2534
Vranduk Fm.	BO4r062	99.07	100.17	912	53	473	458	47	4516	1578
Vranduk Fm.	BO4r066	101.46	102.26	65	53	990	624	n.d.	3224	937
Vranduk Fm.	BO4r068	100.94	101.91	1286	n.d.	805	377	n.d.	4322	396

Formation	Sample & spot ID	trace element concentrations in ppm								
		TiO <sub>2</sub> [wt%]	Total oxides [wt%]	Nb	Al	Cr	Zr	Si	Fe	V
Vranduk Fm.	BO4r070	101.22	102.27	1955	n.d.	475	618	n.d.	2072	2233
Vranduk Fm.	BO4r071	101.79	102.71	580	204	707	53	72	3004	1984
Vranduk Fm.	BO4r073	99.19	100.59	4321	53	231	356	n.d.	2891	2148
Vranduk Fm.	BO4r075	101.00	101.89	67	117	1710	723	n.d.	1070	2519
Vranduk Fm.	BO4r076	100.57	101.60	56	56	149	505	65	2594	3872
Vranduk Fm.	BO4r079	100.79	101.55	866	97	616	118	104	2511	1170
Vranduk Fm.	BO4r080	100.13	100.89	1544	109	308	93	47	3033	409
Vranduk Fm.	BO4r081	100.47	101.99	4821	158	785	376	n.d.	2618	1916
Vranduk Fm.	BO4r082	100.24	101.75	4822	170	752	380	n.d.	2630	1877
Vranduk Fm.	BO59rt001	99.20	100.08	812	60	1198	110	n.d.	3552	664
Vranduk Fm.	BO59rt002	99.91	101.03	2611	250	208	78	115	3592	1146
Vranduk Fm.	BO59rt004	102.12	102.85	354	53	2019	135	n.d.	1988	674
Vranduk Fm.	BO59rt006	101.02	102.21	2716	304	311	107	450	2965	1358
Vranduk Fm.	BO59rt007	99.94	100.58	101	71	454	70	n.d.	1274	2592
Vranduk Fm.	BO59rt008	100.78	101.63	1404	85	1171	169	77	1714	1305
Vranduk Fm.	BO59rt009	99.44	100.50	2519	n.d.	816	111	50	2687	1349
Vranduk Fm.	BO59rt010	100.92	102.11	2453	82	339	170	85	4962	608
Vranduk Fm.	BO59rt011	99.77	100.57	190	53	1017	150	47	2473	1815
Vranduk Fm.	BO59rt013	100.45	101.12	449	n.d.	564	189	76	1872	1578
Vranduk Fm.	BO59rt014	100.68	101.54	1526	75	385	178	n.d.	2931	1133
Vranduk Fm.	BO59rt015	98.94	99.77	576	59	818	152	47	3542	915
Vranduk Fm.	BO59rt016	101.38	102.24	1618	53	547	235	n.d.	2421	1296
Vranduk Fm.	BO59rt017	101.10	102.02	1669	162	703	218	n.d.	2841	1003
Vranduk Fm.	BO59rt019	100.38	101.85	3252	53	925	179	56	5321	913
Vranduk Fm.	BO59rt020	102.42	103.06	521	105	185	66	n.d.	2452	1311
Vranduk Fm.	BO59rt021	101.25	102.07	292	53	278	215	113	4350	825
Vranduk Fm.	BO59rt023	100.73	101.57	375	n.d.	78	112	654	3791	918
Vranduk Fm.	BO59rt027	100.40	101.81	1628	145	1353	551	111	1148	4759
Vranduk Fm.	BO59rt028	101.99	102.53	140	53	354	118	47	2241	1023
Vranduk Fm.	BO59rt029	102.54	103.24	970	83	476	566	47	1878	1071
Vranduk Fm.	BO59rt030	102.04	102.89	1289	53	899	130	n.d.	1862	1782
Vranduk Fm.	BO59rt031	100.77	101.65	1676	77	419	212	n.d.	2628	1275
Vranduk Fm.	BO59rt033	99.55	100.50	1951	89	237	128	115	3590	757
Vranduk Fm.	BO59rt034	99.52	101.42	5640	53	n.d.	83	137	7653	249
Vranduk Fm.	BO59rt035	98.83	100.76	3131	53	722	1196	n.d.	6543	2428
Vranduk Fm.	BO59rt036	100.62	102.15	3401	53	1024	219	n.d.	5669	796
Vranduk Fm.	BO59rt037	99.04	99.85	1405	131	693	95	118	1697	1533
Vranduk Fm.	BO59rt038	98.17	99.43	1640	499	92	1489	1033	2925	770
Vranduk Fm.	BO59rt039	101.06	102.19	3346	223	707	321	n.d.	2429	1014
Vranduk Fm.	BO59rt041	100.20	101.13	2116	91	330	466	127	2380	1075
Vranduk Fm.	BO59rt042	100.44	101.98	3223	354	532	3494	n.d.	1494	1766
Vranduk Fm.	BO59rt043	100.24	101.70	3177	85	99	135	n.d.	6708	598
Vranduk Fm.	BO59rt044	100.33	101.07	1733	111	521	151	47	2038	732
Vranduk Fm.	BO59rt045	100.06	100.92	1434	57	407	102	62	2707	1417
Vranduk Fm.	BO59rt046	102.08	102.69	1055	66	624	67	47	1869	693
Vranduk Fm.	BO59rt048	100.94	101.97	265	221	352	115	309	5144	1094
Vranduk Fm.	BO59rt049	99.11	101.00	2640	3733	415	168	192	4123	1012
Vranduk Fm.	BO59rt051	102.03	102.84	1711	125	551	121	47	2196	1071
Vranduk Fm.	BO59rt052	97.67	101.55	16021	330	891	74	47	9181	1179
Vranduk Fm.	BO59rt053	100.98	102.12	3507	176	298	275	n.d.	3267	678
Vranduk Fm.	BO59rt054	99.62	100.51	890	64	568	844	47	2633	1363
Vranduk Fm.	BO59rt057	99.98	100.54	85	53	137	130	47	1630	1968
Vranduk Fm.	BO59rt060	100.54	101.45	1736	171	692	50	177	2267	1281
Vranduk Fm.	BO59rt061	99.77	100.81	1308	96	705	118	327	4785	158
Vranduk Fm.	BO59rt062	101.20	101.89	795	50	958	93	n.d.	2137	898
Vranduk Fm.	BO59rt064	99.14	99.79	406	105	1520	178	n.d.	1468	937
Vranduk Fm.	BO59rt065	98.86	100.19	1826	53	696	120	47	5999	1058
Vranduk Fm.	BO59rt066	100.04	100.82	641	527	447	171	109	2239	1279
Vranduk Fm.	BO59rt067	100.59	101.49	112	53	1145	128	47	4417	754
Vranduk Fm.	BO59rt069	100.88	101.58	296	75	666	144	136	2940	863
Vranduk Fm.	BO59rt071	100.08	100.94	1569	132	675	181	n.d.	2213	1302
Vranduk Fm.	BO59rt073	99.81	101.04	2546	58	926	161	n.d.	2586	2390
Vranduk Fm.	BO59rt074	100.91	101.61	111	56	83	161	50	3173	1542
Vranduk Fm.	BO59rt075	101.01	102.02	2856	60	848	166	50	2089	1011
Vranduk Fm.	BO59rt076	98.63	99.82	2605	103	1508	104	n.d.	2356	1742
Vranduk Fm.	BO59rt077	99.58	100.79	3223	n.d.	686	98	344	3231	962
Vranduk Fm.	BO59rt079	102.05	102.75	1432	95	467	85	n.d.	1865	1015
Vranduk Fm.	BO59rt080	98.51	100.01	4844	161	601	71	47	3768	1192
Vranduk Fm.	BO87r001	99.37	100.35	2059	78	216	229	55	3170	1269
Vranduk Fm.	BO87r002	98.85	100.03	2967	226	719	245	47	2710	1425
Vranduk Fm.	BO87r003	100.96	102.28	731	53	1417	713	47	725	5480
Vranduk Fm.	BO87r005	99.45	100.56	2748	112	910	170	47	2167	1657
Vranduk Fm.	BO87r006	99.87	100.90	1776	188	1173	98	73	1276	2513
Vranduk Fm.	BO87r007	100.72	101.56	290	97	2181	93	n.d.	1486	1746
Vranduk Fm.	BO87r009	100.04	100.70	443	88	582	170	47	2545	991
Vranduk Fm.	BO87r010	100.60	101.51	1643	175	328	90	164	3019	1065
Vranduk Fm.	BO87r011	100.97	101.81	991	168	887	227	47	2634	1024
Vranduk Fm.	BO87r012	100.85	101.96	1011	85	551	739	97	5048	660
Vranduk Fm.	BO87r013	99.05	99.93	1415	191	617	141	100	2543	1238
Vranduk Fm.	BO87r014	100.92	101.84	1766	131	505	124	106	1925	1888
Vranduk Fm.	BO87r015	98.14	100.01	5267	179	697	680	57	3916	2412
Vranduk Fm.	BO87r017	100.88	101.66	219	234	586	230	95	2068	2098
Vranduk Fm.	BO87r018	100.91	101.78	417	294	482	95	78	3580	1317
Vranduk Fm.	BO87r019	98.92	100.22	3456	143	535	175	161	4003	833
Vranduk Fm.	BO87r020	98.94	101.44	4622	327	619	4466	2121	3915	738
Vranduk Fm.	BO87r022	98.58	99.71	2445	177	902	191	59	3313	996
Vranduk Fm.	BO87r023	101.69	102.34	1049	146	336	223	82	1414	1294
Vranduk Fm.	BO87r024	101.68	102.22	639	104	163	198	97	1431	1194
Vranduk Fm.	BO87r025	101.77	102.37	294	75	525	172	n.d.	2312	986
Vranduk Fm.	BO87r026	98.50	99.62	2410	171	882	178	59	3304	1048
Vranduk Fm.	BO87r027	101.06	101.87	1467	109	487	134	165	2371	1049
Vranduk Fm.	BO87r028	101.30	102.29	101	133	1651	81	201	1000	3598
Vranduk Fm.	BO87r031	99.73	100.95	2950	162	729	138	62	2691	1862
Vranduk Fm.	BO87r033	97.93	99.14	2366	101	968	214	n.d.	3321	1658
Vranduk Fm.	BO87r034	97.55	98.77	2378	79	971	234	n.d.	3459	1634
Vranduk Fm.	BO87r036	100.46	101.57	227	82	671	259	47	4864	2014
Vranduk Fm.	BO87r037	101.10	101.85	1300	152	529	244	55	1443	1563
Vranduk Fm.	BO87r038	100.79	101.98	3021	156	209	310	n.d.	3961	959
Vranduk Fm.	BO87r039	101.16	101.83	69	163	564	127	136	3338	539

Formation	Sample & spot ID	trace element concentrations in ppm								
		TiO <sub>2</sub> [wt%]	Total oxides [wt%]	[n.d.: not detected]					Fe	V
				Nb	Al	Cr	Zr	Si		
Vranduk Fm.	BO87rt040	97.88	99.14	963	927	n.d.	1131	1549	2509	918
Vranduk Fm.	BO87rt041	99.30	100.85	4102	109	380	278	108	5257	977
Vranduk Fm.	BO87rt042	100.44	101.48	1900	170	600	133	134	3495	988
Vranduk Fm.	BO87rt044	101.03	101.91	1733	99	907	137	73	2084	1177
Vranduk Fm.	BO87rt046	100.64	101.61	2145	155	622	335	50	2599	1004
Vranduk Fm.	BO87rt048	101.00	101.91	1801	148	57	178	56	2281	1899
Vranduk Fm.	BO87rt049	99.00	99.89	1440	162	780	150	67	2058	1617
Vranduk Fm.	BO87rt050	101.65	102.22	75	70	125	207	47	2581	1129
Vranduk Fm.	BO87rt051	99.71	100.76	267	909	n.d.	240	1579	3436	152
Vranduk Fm.	BO87rt052	100.53	102.10	2353	435	1975	814	47	3555	1908
Vranduk Fm.	BO87rt053	100.89	101.84	2077	88	495	306	137	2030	1503
Vranduk Fm.	BO87rt054	99.85	100.54	948	79	362	113	47	2228	1179
Vranduk Fm.	BO87rt056	99.83	100.84	1609	65	244	170	50	4506	772
Vranduk Fm.	BO87rt057	98.44	100.12	2475	83	540	3742	n.d.	2113	3035
Vranduk Fm.	BO87rt058	100.78	101.90	1632	60	418	148	90	5866	130
Vranduk Fm.	BO87rt059	99.66	100.26	173	188	63	515	58	2216	1281
Vranduk Fm.	BO87rt060	100.17	101.05	1709	148	335	183	147	2689	1046
Vranduk Fm.	BO87rt061	99.68	100.99	1947	53	3359	928	83	829	1880
Vranduk Fm.	BO87rt062	101.24	102.09	203	82	184	275	135	3960	1358
Vranduk Fm.	BO87rt064	99.52	100.66	3203	103	556	88	182	3417	582
Vranduk Fm.	BO87rt065	100.50	101.16	119	114	817	515	141	1576	1562
Vranduk Fm.	BO87rt066	100.28	101.35	2222	200	536	144	114	2794	1347
Vranduk Fm.	BO87rt067	99.59	101.19	2911	560	478	67	1089	5042	790
Vranduk Fm.	BO87rt069	100.07	101.05	653	80	1504	259	69	3722	826
Vranduk Fm.	BO87rt070	100.66	101.78	2467	182	230	536	54	3670	923
Vranduk Fm.	BO87rt071	100.40	100.94	190	239	450	176	47	1855	912
Vranduk Fm.	BO87rt072	100.51	101.33	1316	103	974	191	205	1758	1205
Vranduk Fm.	BO87rt073	99.32	100.39	2292	162	1496	192	104	2498	780
Vranduk Fm.	BO87rt074	100.51	102.02	2735	98	636	318	72	6492	716
Vranduk Fm.	BO87rt075	98.17	100.25	6355	1137	569	2324	71	1674	2150
Vranduk Fm.	BO87rt077	99.04	100.15	2563	156	685	182	n.d.	2532	1728
Vranduk Fm.	BO87rt078	101.41	102.07	1025	99	411	76	79	1642	1296
Vranduk Fm.	BO87rt080	100.51	101.95	3510	243	376	138	443	4775	675
Vranduk Fm.	BO87rt081	100.81	102.17	3115	101	267	132	47	5234	1006
Vranduk Fm.	BO87rt082	100.98	101.71	982	294	2015	235	195	250	880
Vranduk Fm.	BO92rt001	100.57	101.22	921	146	77	157	107	2420	811
Vranduk Fm.	BO92rt002	101.30	102.42	1818	n.d.	831	2239	47	180	2731
Vranduk Fm.	BO92rt003	101.15	101.98	375	53	110	810	n.d.	3677	1146
Vranduk Fm.	BO92rt004	101.43	102.07	543	164	636	1013	n.d.	1964	355
Vranduk Fm.	BO92rt005	100.92	101.44	423	450	1002	56	n.d.	1439	201
Vranduk Fm.	BO92rt006	101.71	102.25	374	100	n.d.	78	n.d.	2473	975
Vranduk Fm.	BO92rt007	102.02	102.91	697	91	306	247	n.d.	4817	523
Vranduk Fm.	BO92rt008	99.57	100.61	1229	492	74	61	320	3270	1740
Vranduk Fm.	BO92rt009	99.97	100.93	96	n.d.	442	77	47	4981	1506
Vranduk Fm.	BO92rt010	101.03	102.05	3071	182	521	481	n.d.	1915	1036
Vranduk Fm.	BO92rt011	100.26	100.99	2442	1226	77	61	n.d.	909	58
Vranduk Fm.	BO92rt012	99.05	100.74	1363	755	n.d.	363	1889	6229	646
Vranduk Fm.	BO92rt013	101.53	102.14	318	n.d.	168	509	55	2926	567
Vranduk Fm.	BO92rt015	100.61	101.84	2385	74	621	1188	n.d.	2902	1655
Vranduk Fm.	BO92rt016	100.66	101.98	3821	439	95	506	n.d.	2986	1467
Vranduk Fm.	BO92rt017	100.81	101.74	1852	n.d.	2443	113	69	1152	865
Vranduk Fm.	BO92rt018	101.49	102.25	443	53	122	1029	n.d.	2892	1066
Vranduk Fm.	BO92rt019	100.61	101.45	1180	56	1739	654	n.d.	2407	n.d.
Vranduk Fm.	BO92rt020	99.75	100.51	101	n.d.	729	424	n.d.	3766	633
Vranduk Fm.	BO92rt021	101.00	101.57	473	59	621	365	n.d.	2176	455
Vranduk Fm.	BO92rt023	98.87	99.64	418	59	393	198	n.d.	3883	797
Vranduk Fm.	BO92rt024	99.32	100.15	1553	n.d.	1709	278	n.d.	873	1366
Vranduk Fm.	BO92rt025	98.35	99.63	4236	275	n.d.	61	495	3559	283
Vranduk Fm.	BO92rt026	98.65	99.38	912	53	523	144	n.d.	2874	852
Vranduk Fm.	BO92rt028	100.63	101.64	1871	82	892	1153	n.d.	2512	777
Vranduk Fm.	BO92rt029	96.97	98.69	1621	113	68	123	62	9486	1440
Vranduk Fm.	BO92rt030	102.21	102.73	251	53	1538	95	n.d.	1248	510
Vranduk Fm.	BO92rt031	101.74	102.46	1188	102	873	480	n.d.	2103	242
Vranduk Fm.	BO92rt032	100.02	101.65	246	n.d.	627	6360	173	2107	2207
Vranduk Fm.	BO92rt033	98.99	99.91	1409	169	1144	840	n.d.	271	2485
Vranduk Fm.	BO92rt034	97.26	99.83	7929	159	2749	1267	n.d.	5104	1060
Vranduk Fm.	BO92rt037	100.21	100.94	292	600	1238	145	1156	687	260
Vranduk Fm.	BO92rt038	99.91	100.93	130	53	450	74	47	5374	1485
Vranduk Fm.	BO92rt039	99.95	100.83	1293	309	68	88	187	2651	1638
Vranduk Fm.	BO92rt040	101.01	102.53	668	n.d.	315	269	47	9748	527
Vranduk Fm.	BO92rt041	99.14	99.96	250	111	253	164	47	4087	1098
Vranduk Fm.	BO92rt042	99.75	100.75	2741	126	72	612	n.d.	1539	1891
Vranduk Fm.	BO92rt043	101.53	102.28	878	110	1552	874	n.d.	1620	310
Vranduk Fm.	BO92rt044	99.78	100.65	106	131	n.d.	1598	684	2588	874
Vranduk Fm.	BO92rt045	99.67	100.33	263	57	100	828	n.d.	2346	1238
Vranduk Fm.	BO92rt046	100.59	101.14	131	149	242	1426	n.d.	1521	534
Vranduk Fm.	BO92rt047	101.95	102.58	503	98	491	298	71	2556	513
Vranduk Fm.	BO92rt049	99.64	101.85	6458	53	2800	1213	58	3492	1556
Vranduk Fm.	BO92rt050	100.30	101.02	378	158	293	657	47	1880	1790
Vranduk Fm.	BO92rt051	98.99	100.81	978	n.d.	1848	4604	n.d.	4927	1079
Vranduk Fm.	BO92rt052	101.16	101.96	972	58	1993	455	73	1358	743
Vranduk Fm.	BO92rt053	100.42	101.36	2220	n.d.	389	128	n.d.	3127	892
Vranduk Fm.	BO92rt054	95.75	99.33	9108	53	n.d.	239	n.d.	17179	n.d.
Vranduk Fm.	BO92rt055	98.70	99.59	584	n.d.	2781	360	n.d.	2164	475
Vranduk Fm.	BO92rt056	101.01	102.54	3050	n.d.	66	93	47	7688	471
Vranduk Fm.	BO92rt058	101.51	102.31	340	82	105	452	47	3578	1282
Vranduk Fm.	BO92rt059	101.03	101.83	338	n.d.	1317	509	n.d.	1172	2289
Vranduk Fm.	BO92rt060	101.32	102.00	97	123	1006	358	n.d.	1975	1318
Vranduk Fm.	BO92rt061	98.11	100.31	4010	180	631	111	n.d.	9360	1833
Vranduk Fm.	BO92rt062	97.44	99.72	4982	176	454	84	n.d.	9227	1759
Vranduk Fm.	BO92rt063	98.04	100.39	4127	980	n.d.	74	2686	6703	789
Vranduk Fm.	BO92rt065	99.50	100.19	456	326	77	953	n.d.	1796	1294
Vranduk Fm.	BO92rt066	100.51	101.13	130	70	1516	58	368	1227	818
Vranduk Fm.	BO92rt067	97.62	99.65	4447	911	n.d.	164	1512	6278	426
Vranduk Fm.	BO92rt068	100.74	101.64	1542	71	455	998	n.d.	1470	1820
Vranduk Fm.	BO92rt069	99.87	100.74	69	n.d.	643	103	n.d.	4707	1043
Vranduk Fm.	BO92rt070	99.92	101.12	5255	466	193	259	123	1726	241
Vranduk Fm.	BO92rt071	98.50	99.29	969	117	707	602	90	1958	1171
Vranduk Fm.	BO92rt072	101.71	102.51	871	n.d.	1639	158	47	2424	621
Vranduk Fm.	BO92rt073	99.59	100.77	155	n.d.	2062	3815	n.d.	897	1512
Vranduk Fm.	BO92rt074	97.12	99.37	5519	n.d.	5616	1495	n.d.	2227	884
Vranduk Fm.	BO92rt075	101.07	102.02	173	53	1269	1285	n.d.	2975	1233
Vranduk Fm.	BO92rt076	101.44	101.98	930	n.d.	804	117	47	1003	857
Vranduk Fm.	BO92rt078	101.74	102.44	714	93	1572	447	47	2018	195

Electron microprobe analyses of detrital Cr-spinel from the Dinaride Ophiolite Zone mélange and the Bosnian Flysch

Formation	Sample & spot ID	Analyses in wt%. Shown are the recalculated FeO and Fe <sub>2</sub> O <sub>3</sub> values and the amended total																		Cations per formula unit on the basis of 3 oxygens									
		SiO <sub>2</sub>	TiO <sub>2</sub>	V <sub>2</sub> O <sub>5</sub>	Al <sub>2</sub> O <sub>3</sub>	Cr <sub>2</sub> O <sub>3</sub>	MnO	MgO	NiO	ZnO	FeO	Fe <sub>2</sub> O <sub>3</sub>	Total	Cr	Ti	V	Al	Fe <sup>3+</sup>	Fe <sup>2+</sup>	Mn	Mg	Ni	Zn						
		n.d.	n.d.	n.d.	n.d.	n.d.	n.d.	n.d.	n.d.	n.d.	n.d.	n.d.	n.d.	n.d.	n.d.	n.d.	n.d.	n.d.	n.d.	n.d.	n.d.	n.d.	n.d.	n.d.	n.d.				
DOZ mélange	BO22sp002	1.20	0.32	25.88	34.01	0.21	13.72	0.19	0.08	15.81	8.47	99.89	0.814	0.027	0.006	0.924	0.133	0.401	0.005	0.619	0.005	0.005	0.002						
DOZ mélange	BO22sp003	0.10	0.19	36.70	29.85	0.13	16.12	0.19	0.14	12.56	2.90	98.88	0.679	0.002	0.004	1.246	0.063	0.303	0.003	0.682	0.004	0.003	0.003						
DOZ mélange	BO22sp004	0.02	0.22	28.18	40.84	0.19	14.20	0.09	0.20	14.37	1.39	99.70	0.965	0.003	0.004	0.993	0.031	0.359	0.005	0.633	0.002	0.005	0.005						
DOZ mélange	BO22sp005	0.15	0.18	34.75	33.50	0.16	16.07	0.17	0.15	12.64	1.96	99.73	0.763	0.003	0.003	1.180	0.043	0.304	0.004	0.690	0.004	0.003	0.003						
DOZ mélange	BO22sp006	0.10	0.24	32.66	34.06	0.20	14.63	0.14	0.13	14.37	2.85	99.38	0.791	0.002	0.005	1.132	0.063	0.363	0.005	0.641	0.003	0.003	0.003						
DOZ mélange	BO22sp007	0.02	0.20	27.96	41.41	0.24	12.74	0.05	0.27	16.52	0.51	99.83	0.988	0.001	0.004	0.991	0.012	0.417	0.006	0.573	0.001	0.006	0.006						
DOZ mélange	BO22sp008	0.03	0.17	35.42	35.42	0.17	15.00	0.18	0.23	13.81	1.81	99.79	0.817	0.001	0.003	1.135	0.040	0.337	0.004	0.652	0.004	0.005	0.005						
DOZ mélange	BO22sp009	0.06	0.16	26.28	42.59	0.21	13.81	0.09	0.15	14.87	2.04	100.26	1.012	0.001	0.003	0.932	0.046	0.374	0.005	0.619	0.002	0.003	0.003						
DOZ mélange	BO22sp010	0.75	0.26	25.35	38.56	0.23	12.74	0.13	0.14	16.94	5.15	100.26	0.927	0.007	0.005	0.909	0.118	0.431	0.006	0.578	0.003	0.003	0.003						
DOZ mélange	BO22sp011	0.43	0.19	40.20	24.80	0.16	18.14	0.26	0.06	10.56	4.98	99.84	0.547	0.009	0.004	1.323	0.105	0.246	0.004	0.754	0.006	0.001	0.001						
DOZ mélange	BO22sp012	0.31	0.27	35.37	33.01	0.14	15.17	0.12	0.23	14.27	0.68	99.58	0.755	0.007	0.005	1.206	0.015	0.345	0.004	0.654	0.003	0.005	0.005						
DOZ mélange	BO22sp013	n.d.	0.16	34.08	34.72	0.15	15.74	0.14	0.25	12.90	1.80	99.93	0.793	0.000	0.003	1.161	0.039	0.312	0.004	0.678	0.003	0.003	0.005						
DOZ mélange	BO22sp014	n.d.	0.01	32.85	34.83	0.20	13.53	0.09	0.41	15.97	1.99	100.05	0.810	0.000	0.003	1.139	0.044	0.393	0.005	0.593	0.002	0.009	0.009						
DOZ mélange	BO22sp015	n.d.	0.23	26.21	41.17	0.23	11.93	0.07	0.31	17.53	2.11	99.17	0.999	0.005	0.007	0.949	0.026	0.450	0.006	0.546	0.002	0.007	0.007						
DOZ mélange	BO22sp016	n.d.	0.06	28.24	44.80	0.19	14.04	0.10	0.10	14.23	2.10	100.05	1.074	0.001	0.006	0.863	0.048	0.361	0.006	0.635	0.002	0.002	0.002						
DOZ mélange	BO22sp017	n.d.	1.14	0.30	24.92	36.66	0.26	12.38	0.17	17.44	5.95	99.35	0.892	0.026	0.006	0.904	0.138	0.449	0.007	0.568	0.004	0.003	0.003						
DOZ mélange	BO22sp018	n.d.	0.08	0.18	33.49	33.14	0.14	15.72	0.19	12.97	4.01	100.10	0.759	0.002	0.003	1.143	0.087	0.314	0.003	0.678	0.005	0.004	0.004						
DOZ mélange	BO22sp019	n.d.	0.17	0.16	34.40	33.36	0.16	15.83	0.15	12.98	2.38	99.71	0.762	0.004	0.003	1.172	0.052	0.314	0.004	0.682	0.003	0.003	0.003						
DOZ mélange	BO22sp020	n.d.	0.44	0.38	25.01	40.15	0.22	13.14	0.15	16.05	4.65	100.40	0.963	0.010	0.008	0.895	0.106	0.407	0.006	0.594	0.004	0.005	0.005						
DOZ mélange	BO22sp021	n.d.	0.01	0.14	33.44	34.71	0.30	15.10	0.13	13.71	2.44	100.26	0.796	0.000	0.003	1.144	0.053	0.333	0.007	0.663	0.003	0.006	0.006						
DOZ mélange	BO22sp022	n.d.	0.17	0.19	26.00	40.55	0.25	12.27	0.10	17.09	3.30	100.19	0.976	0.004	0.004	0.933	0.076	0.435	0.006	0.557	0.002	0.006	0.006						
DOZ mélange	BO22sp023	n.d.	0.08	0.20	34.43	32.69	0.14	16.29	0.18	12.19	3.37	99.69	0.745	0.002	0.004	1.170	0.073	0.294	0.003	0.700	0.004	0.003	0.003						
DOZ mélange	BO22sp024	n.d.	0.47	0.27	32.29	34.44	0.18	15.09	0.16	14.19	2.91	100.18	0.794	0.010	0.005	1.110	0.064	0.346	0.005	0.666	0.004	0.004	0.004						
DOZ mélange	BO22sp025	n.d.	0.11	0.27	30.88	35.29	0.20	13.90	0.13	15.46	3.84	100.28	0.824	0.002	0.002	1.075	0.085	0.382	0.005	0.612	0.003	0.005	0.005						
DOZ mélange	BO22sp026	n.d.	0.03	0.16	31.82	36.37	0.20	14.21	0.13	14.90	1.96	100.03	0.846	0.001	0.003	1.103	0.043	0.367	0.005	0.623	0.003	0.005	0.005						
DOZ mélange	BO22sp027	n.d.	0.14	0.17	33.90	33.71	0.20	14.81	0.10	14.32	1.99	99.56	0.777	0.003	0.003	1.166	0.044	0.349	0.005	0.644	0.002	0.005	0.005						
DOZ mélange	BO22sp028	n.d.	0.09	0.37	32.40	34.80	0.23	13.00	0.06	16.87	1.71	99.98	0.813	0.002	0.007	1.129	0.038	0.417	0.006	0.573	0.001	0.010	0.010						
DOZ mélange	BO22sp029	n.d.	0.02	0.16	33.25	35.45	0.18	15.08	0.13	13.89	1.76	100.13	0.832	0.001	0.003	1.139	0.038	0.338	0.004	0.653	0.003	0.005	0.005						
DOZ mélange	BO22sp030	n.d.	0.04	0.15	32.37	35.92	0.19	14.75	0.13	14.15	1.93	99.82	0.832	0.001	0.003	1.118	0.043	0.347	0.005	0.644	0.003	0.004	0.004						
DOZ mélange	BO22sp031	0.04	0.45	0.19	40.59	0.13	17.37	0.23	0.05	11.65	5.60	99.15	0.509	0.010	0.003	1.347	0.119	0.274	0.003	0.728	0.005	0.001	0.001						
DOZ mélange	BO22sp032	n.d.	0.04	0.31	26.54	40.45	0.28	11.90	0.08	17.50	2.09	99.41	0.979	0.001	0.006	0.958	0.048	0.448	0.007	0.543	0.002	0.005	0.005						
DOZ mélange	BO22sp033	n.d.	0.14	0.18	31.31	35.71	0.20	13.22	0.15	16.24	2.13	99.57	0.840	0.003	0.004	1.099	0.048	0.404	0.005	0.586	0.004	0.007	0.007						
DOZ mélange	BO22sp034	n.d.	0.18	0.23	29.86	35.41	0.22	12.95	0.15	16.49	3.82	99.53	0.840	0.004	0.005	1.056	0.086	0.414	0.005	0.579	0.004	0.005	0.005						
DOZ mélange	BO22sp036	n.d.	0.42	0.25	24.41	41.16	0.25	12.67	0.12	16.53	4.20	100.20	0.994	0.010	0.005	0.879	0.097	0.422	0.007	0.577	0.003	0.004	0.004						
DOZ mélange	BO22sp037	n.d.	0.08	0.21	33.00	33.95	0.22	15.24	0.17	13.58	3.35	99.94	0.782	0.002	0.004	1.133	0.073	0.331	0.005	0.661	0.004	0.003	0.003						
DOZ mélange	BO22sp038	n.d.	0.06	0.21	36.96	29.65	0.17	15.75	0.18	13.38	3.27	99.78	0.671	0.001	0.004	1.248	0.070	0.320	0.004	0.672	0.004	0.003	0.003						
DOZ mélange	BO22sp039	n.d.	0.02	0.15	33.14	35.84	0.17	15.31	0.15	13.36	1.36	99.72	0.825	0.000	0.003	1.138	0.030	0.326	0.004	0.665	0.003	0.005	0.005						
DOZ mélange	BO22sp041	n.d.	0.21	0.33	27.22	37.65	0.23	12.93	0.13	16.33	4.71	99.97	0.900	0.005	0.007	0.970	0.107	0.413	0.006	0.582	0.003	0.005	0.005						
DOZ mélange	BO22sp042	n.d.	0.16	0.24	30.56	38.76	0.18	15.45	0.11	13.10	1.29	100.01	0.898	0.004	0.005	1.056	0.029	0.321	0.004	0.675	0.003	0.003	0.003						
DOZ mélange	BO22sp043	n.d.	0.20	0.26	28.93	37.02	0.22	12.50	0.13	17.30	3.43	100.24	0.879	0.004	0.005	1.024	0.077	0.434	0.006	0.559	0.003	0.006	0.006						
DOZ mélange	BO22sp044	n.d.	0.18	0.34	29.29	36.54	0.25	12.67	0.10	17.05	3.21	99.81	0.868	0.004	0.007	1.037	0.073	0.428	0.006	0.567	0.002	0.004	0.004						
DOZ mélange	BO22sp045	n.d.	0.03	0.24	25.66	44.31	0.22	15.08	0.13	12.88	1.98	100.77	1.043	0.001	0.005	0.901	0.044	0.321	0.006	0.669	0.003	0.005	0.005						
DOZ mélange	BO22sp046	n.d.	0.05	0.24	27.04	40.96	0.24	14.08	0.07	14.39	2.49	99.74	0.973	0.001	0.005	0.958	0.056	0.362	0.006	0.631	0.002	0.004	0.004						
DOZ mélange	BO22sp048	n.d.	0.16	0.34	27.37	38.01	0.20	14.31	0.17	14.27	4.57	99.59	0.903	0.008	0.005	1.024	0.077	0.434	0.006	0.559	0.003	0.006	0.006						
DOZ mélange	BO22sp049	n.d.	0.16	0.21	34.22	33.55	0.16	15.87	0.16	12.91	2.43	99.82	0.766	0.003	0.004	1.166	0.053	0.312	0.004	0.683	0.004	0.003	0.003						
DOZ mélange	BO22sp050	n.d.	0.06	0.24	6.36	59.82	0.88	4.35	0.03	25.32	2.77	100.35	1.651	0.002	0.006	0.282	0.073	0.739	0.026	0.226	0.001	0.013	0.013						
DOZ mélange	BO22sp051	0.02	0.32	0.19	29.74	37.03	0.24	17.02	0.10	10.60	4.56	99.90	0.855	0.007	0.004	1.024	0.100	0.259	0.004	0.741	0.005	0.001	0.001						
DOZ mélange	BO22sp052	n.d.	0.30	0.40	23.62	39.28	0.24	12.33	0.20	17.34	5.54	99.99	0.956	0.021	0.008	1.024	0.128	0.446	0.006	0.566	0.003	0.004	0.004						
DOZ mélange	BO22sp053	n.d.	0.21	0.18	30.93	35.33	0.24	14.41	0.15	14.59	3.68	99.85	0.825	0.005	0.003	1.077	0.082	0.360	0.006	0.634	0.004	0.003	0.003						
DOZ mélange	BO22sp054	0.03	0.61	0.13	41.40	0.15	18.16	0.29	0.07	10.72	6.48	99.60	0																





		analyses in wt%. Shown are the recalculated FeO and Fe <sub>2</sub> O <sub>3</sub> values and the amended total														cations per formula unit on the basis of 3 oxygens									
Formation	Sample & spot ID	SiO <sub>2</sub>	TiO <sub>2</sub>	V <sub>2</sub> O <sub>5</sub>	Al <sub>2</sub> O <sub>3</sub>	Cr <sub>2</sub> O <sub>3</sub>	MnO	MgO	NiO	ZnO	FeO	Fe <sub>2</sub> O <sub>3</sub>	Total	Cr	Ti	V	Al	Fe <sup>3+</sup>	Fe <sup>2+</sup>	Mn	Mg	Ni	Zn		
		n. d.	n. d.	0.05	7.15	58.51	0.34	8.46	0.06	0.15	19.75	5.19	99.82	1.571	0.001	0.004	0.286	0.133	0.561	0.010	0.428	0.002	0.004		
DOZ mélange	B025sp0089	n. d.	1.55	0.37	21.33	36.05	0.31	9.46	0.15	0.22	21.93	9.03	100.40	0.901	0.037	0.008	0.795	0.215	0.579	0.008	0.445	0.004	0.005		
DOZ mélange	B025sp0090	n. d.	0.06	0.19	27.48	41.70	0.18	14.69	0.12	0.15	13.68	1.98	100.18	0.982	0.001	0.003	0.964	0.044	0.341	0.005	0.652	0.003	0.001		
DOZ mélange	B025sp0091	n. d.	0.60	0.17	22.88	40.59	0.21	14.88	0.26	0.06	13.12	7.75	100.53	0.971	0.014	0.004	0.817	0.177	0.444	0.005	0.671	0.006	0.001		
DOZ mélange	B025sp0092	n. d.	1.80	0.45	19.85	38.54	0.31	10.39	0.15	0.15	20.61	8.11	100.36	0.962	0.043	0.009	0.739	0.193	0.544	0.008	0.489	0.004	0.004		
DOZ mélange	B025sp0093	0.01	0.01	0.45	34.75	33.56	0.14	18.24	0.20	0.16	9.20	3.45	99.91	0.754	0.000	0.003	1.164	0.074	0.219	0.003	0.773	0.005	0.003		
DOZ mélange	B025sp0094	n. d.	0.48	0.25	13.01	33.72	0.28	10.81	0.10	0.12	17.23	3.81	100.30	1.376	0.012	0.005	0.497	0.093	0.480	0.008	0.522	0.003	0.003		
DOZ mélange	B025sp0095	n. d.	0.12	0.22	27.68	38.79	0.21	13.30	0.15	0.24	15.83	3.99	100.43	0.920	0.003	0.004	0.975	0.090	0.397	0.005	0.595	0.003	0.005		
DOZ mélange	B025sp0096	n. d.	0.10	0.25	8.23	59.71	0.38	9.05	0.03	0.18	19.23	3.08	100.23	1.581	0.002	0.006	0.325	0.078	0.539	0.011	0.462	0.001	0.004		
DOZ mélange	B025sp0097	n. d.	0.05	0.35	16.11	53.19	0.26	11.14	0.04	0.20	17.42	1.49	100.24	1.341	0.001	0.007	0.606	0.036	0.464	0.007	0.529	0.001	0.005		
DOZ mélange	B025sp0098	n. d.	0.10	0.22	27.68	38.79	0.21	13.30	0.15	0.24	15.83	3.99	100.43	0.920	0.003	0.004	0.975	0.090	0.397	0.005	0.595	0.003	0.005		
DOZ mélange	B025sp0099	n. d.	0.22	0.16	36.01	31.63	0.17	16.37	0.18	0.12	12.41	2.43	99.70	0.716	0.005	0.003	1.216	0.052	0.297	0.004	0.664	0.003	0.005		
DOZ mélange	B025sp0100	n. d.	0.22	0.16	36.01	31.63	0.17	16.37	0.18	0.12	12.41	2.43	99.70	0.716	0.005	0.003	1.216	0.052	0.297	0.004	0.664	0.003	0.005		
DOZ mélange	B025sp0101	n. d.	0.11	0.14	41.90	25.68	0.15	17.63	0.20	0.13	11.12	2.06	99.13	0.567	0.002	0.003	1.379	0.043	0.260	0.004	0.734	0.005	0.003		
DOZ mélange	B025sp0102	n. d.	0.10	0.28	31.53	35.62	0.24	13.99	0.12	0.19	15.37	2.54	99.92	0.831	0.002	0.005	0.927	0.117	0.403	0.006	0.615	0.003	0.004		
DOZ mélange	B025sp0103	0.02	0.47	0.23	25.97	38.63	0.24	13.28	0.13	0.11	15.91	5.13	100.11	0.925	0.011	0.005	1.097	0.056	0.379	0.005	0.599	0.003	0.002		
DOZ mélange	B025sp0104	n. d.	0.23	0.24	26.16	39.53	0.16	13.60	0.14	0.17	15.16	4.42	99.79	0.946	0.005	0.005	0.933	0.101	0.384	0.004	0.613	0.003	0.004		
DOZ mélange	B025sp0105	n. d.	0.30	0.19	30.19	36.41	0.21	16.13	0.16	0.07	11.97	4.09	99.71	0.844	0.007	0.004	1.044	0.090	0.294	0.005	0.705	0.004	0.001		
DOZ mélange	B025sp0106	n. d.	0.27	0.14	32.33	34.28	0.18	16.06	0.21	0.05	12.35	3.82	99.69	0.789	0.006	0.003	1.110	0.084	0.301	0.004	0.697	0.005	0.001		
DOZ mélange	B025sp0107	n. d.	0.07	0.20	41.04	26.84	0.13	17.25	0.21	0.12	11.60	1.71	99.17	0.595	0.001	0.004	1.358	0.036	0.272	0.003	0.721	0.005	0.002		
DOZ mélange	B025sp0108	n. d.	0.03	0.27	33.00	34.63	0.18	14.59	0.12	0.25	14.46	2.05	99.59	0.802	0.001	0.005	1.140	0.045	0.354	0.005	0.637	0.003	0.005		
DOZ mélange	B025sp0109	n. d.	0.04	0.19	40.78	26.54	0.13	17.41	0.24	0.13	11.24	2.50	99.20	0.589	0.001	0.003	1.349	0.053	0.264	0.003	0.728	0.005	0.003		
DOZ mélange	B025sp0110	n. d.	0.13	0.22	29.53	37.15	0.19	14.49	0.13	0.18	14.24	3.63	99.89	0.871	0.003	0.004	1.033	0.081	0.353	0.005	0.641	0.003	0.004		
DOZ mélange	B025sp0111	n. d.	0.02	0.23	25.36	44.44	0.19	14.85	0.11	0.09	13.05	1.46	99.79	1.057	0.007	0.005	0.899	0.033	0.328	0.005	0.666	0.003	0.002		
DOZ mélange	B025sp0112	0.03	0.30	0.19	30.25	36.40	0.20	15.93	0.16	0.06	12.29	3.93	99.74	0.845	0.007	0.004	1.044	0.087	0.302	0.005	0.697	0.004	0.001		
DOZ mélange	B025sp0113	n. d.	0.08	0.19	40.85	27.08	0.16	17.29	0.21	0.16	11.55	1.95	99.52	0.600	0.002	0.004	1.349	0.041	0.270	0.004	0.722	0.003	0.003		
DOZ mélange	B025sp0114	n. d.	0.59	0.27	25.40	39.12	0.25	12.63	0.13	0.15	17.02	4.94	100.49	0.939	0.013	0.005	0.910	0.113	0.432	0.006	0.572	0.003	0.003		
DOZ mélange	B025sp0115	n. d.	0.06	0.29	30.76	36.21	0.20	13.46	0.07	0.31	15.94	2.56	99.87	0.850	0.001	0.006	1.077	0.057	0.396	0.005	0.596	0.002	0.007		
DOZ mélange	B025sp0116	n. d.	0.40	0.28	22.35	41.88	0.25	10.80	0.10	0.24	18.97	4.70	99.98	1.035	0.009	0.006	0.823	0.110	0.496	0.007	0.503	0.003	0.006		
DOZ mélange	B025sp0117	n. d.	0.05	0.17	40.92	26.58	0.15	17.26	0.22	0.13	11.56	2.33	99.36	0.589	0.001	0.003	1.353	0.049	0.271	0.004	0.721	0.005	0.003		
DOZ mélange	B025sp0118	n. d.	0.18	0.19	27.27	40.97	0.20	14.43	0.09	0.15	14.19	2.56	100.25	0.967	0.004	0.004	0.959	0.058	0.354	0.005	0.642	0.002	0.003		
DOZ mélange	B025sp0119	n. d.	0.03	0.22	25.66	44.43	0.20	14.78	0.11	0.08	13.29	1.25	100.06	1.054	0.001	0.004	0.907	0.028	0.333	0.005	0.661	0.003	0.002		
DOZ mélange	B025sp0120	n. d.	0.43	0.24	28.22	37.74	0.17	14.83	0.14	0.07	14.03	4.41	100.30	0.885	0.010	0.005	0.987	0.098	0.348	0.004	0.656	0.003	0.002		
DOZ mélange	B025sp0121	n. d.	0.04	0.24	44.05	22.43	0.11	17.70	0.25	0.25	11.27	2.98	99.32	0.491	0.001	0.004	1.437	0.062	0.261	0.003	0.730	0.005	0.005		
DOZ mélange	B025sp0122	n. d.	0.13	0.16	36.88	31.31	0.17	15.04	0.12	0.34	14.42	1.27	99.84	0.711	0.003	0.003	1.249	0.027	0.347	0.004	0.644	0.003	0.007		
DOZ mélange	B025sp0123	0.01	0.18	0.11	43.31	32.23	0.11	17.86	0.24	0.14	11.11	3.15	99.45	0.735	0.008	0.003	1.150	0.091	0.241	0.003	0.759	0.005	0.001		
DOZ mélange	B025sp0124	n. d.	0.35	0.16	29.81	36.23	0.17	16.07	0.22	0.05	12.05	4.70	99.85	0.841	0.008	0.003	1.032	0.104	0.296	0.003	0.704	0.005	0.001		
DOZ mélange	B025sp0125	n. d.	0.58	0.28	24.47	40.50	0.16	14.94	0.11	0.07	13.35	5.56	100.02	0.966	0.013	0.006	0.870	0.126	0.337	0.004	0.672	0.003	0.002		
DOZ mélange	B025sp0126	0.01	0.31	0.20	29.07	36.32	0.19	15.13	0.13	0.22	13.47	5.11	100.01	0.850	0.007	0.004	1.014	0.114	0.333	0.005	0.667	0.003	0.001		
DOZ mélange	B025sp0127	0.02	0.03	0.21	43.25	23.61	0.17	17.04	0.22	0.29	12.15	2.60	99.59	0.519	0.001	0.004	1.417	0.054	0.282	0.004	0.706	0.005	0.006		
DOZ mélange	B025sp0128	n. d.	0.02	0.13	44.15	22.13	0.15	17.49	0.28	0.17	11.59	3.38	99.49	0.484	0.000	0.002	1.440	0.070	0.268	0.003	0.721	0.006	0.003		
DOZ mélange	B025sp0129	n. d.	0.06	0.18	42.75	24.95	0.15	17.18	0.20	0.18	12.00	1.84	99.48	0.549	0.001	0.003	1.041	0.039	0.279	0.003	0.713	0.004	0.004		
DOZ mélange	B025sp0130	n. d.	0.04	0.28	29.77	37.35	0.22	13.80	0.12	0.18	15.41	3.13	100.29	0.876	0.001	0.005	1.041	0.039	0.282	0.006	0.610	0.003	0.004		
DOZ mélange	B025sp0131	n. d.	0.15	0.28	30.16	35.23	0.27	12.18	0.11	0.35	17.63	3.23	99.56	0.838	0.003	0.005	1.070	0.073	0.444	0.007	0.546	0.003	0.008		
DOZ mélange	B025sp0132	0.01	0.32	0.08	13.86	53.90	0.19	15.04	0.18	0.16	11.16	5.45	100.23	1.339	0.008	0.002	0.514	0.129	0.293	0.005	0.704	0.005	0.001		
DOZ mélange	B025sp0133	n. d.	0.15	0.18	31.34	36.67	0.18	15.66	0																

Formation	Sample & spot ID	analyses in wt%. Shown are the recalculated FeO and Fe <sub>2</sub> O <sub>3</sub> values and the amended total															cations per formula unit on the basis of 3 oxygens									
		SiO <sub>2</sub>	TiO <sub>2</sub>	V <sub>2</sub> O <sub>5</sub>	Al <sub>2</sub> O <sub>3</sub>	Cr <sub>2</sub> O <sub>3</sub>	MnO	MgO	NiO	ZnO	FeO	Fe <sub>2</sub> O <sub>3</sub>	Total	Cr	Ti	V	Al	Fe <sup>3+</sup>	Fe <sup>2+</sup>	Mn	Mg	Ni	Zn			
DOZ mélange	B025sp048	n. d.	0.32	0.21	28.91	36.46	0.17	15.29	0.13	0.07	13.27	5.37	100.20	0.851	0.007	0.004	1.007	0.119	0.328	0.004	0.673	0.003	0.001	0.001		
DOZ mélange	B025sp049	0.01	0.35	0.14	29.78	36.29	0.19	16.26	0.22	0.06	11.81	5.08	100.19	0.840	0.008	0.003	1.028	0.112	0.289	0.005	0.709	0.005	0.001	0.001		
DOZ mélange	B025sp050	0.02	0.35	0.15	29.90	36.28	0.16	16.09	0.23	0.07	12.04	4.96	99.98	0.841	0.008	0.003	1.034	0.104	0.295	0.004	0.703	0.006	0.001	0.001		
DOZ mélange	B025sp051	n. d.	0.19	0.14	43.24	23.43	0.14	17.84	0.25	0.16	11.11	2.96	99.45	0.513	0.004	0.003	1.412	0.062	0.257	0.003	0.736	0.005	0.003	0.003		
DOZ mélange	B025sp052	n. d.	0.05	0.08	49.70	16.55	0.13	17.86	0.31	0.33	11.69	2.63	99.31	0.354	0.001	0.001	1.587	0.054	0.265	0.003	0.721	0.007	0.007	0.007		
DOZ mélange	B025sp053	n. d.	0.81	0.30	28.86	34.35	0.20	15.26	0.14	0.07	13.88	6.70	100.58	0.800	0.018	0.006	1.003	0.149	0.342	0.005	0.670	0.003	0.001	0.001		
DOZ mélange	B025sp054	0.01	0.79	0.30	28.81	34.28	0.21	15.15	0.16	0.09	13.87	6.62	100.28	0.801	0.017	0.006	1.004	0.147	0.343	0.005	0.668	0.004	0.002	0.002		
DOZ mélange	B025sp055	n. d.	0.44	0.16	29.21	37.86	0.15	17.22	0.21	0.05	10.32	4.24	99.87	0.875	0.010	0.003	1.006	0.093	0.252	0.004	0.750	0.005	0.001	0.001		
DOZ mélange	B025sp056	n. d.	0.05	0.28	11.87	57.93	0.34	9.91	0.02	0.15	18.56	1.11	100.23	1.499	0.001	0.006	0.458	0.027	0.508	0.009	0.483	0.001	0.004	0.004		
DOZ mélange	B025sp058	n. d.	0.34	0.10	15.00	43.06	0.31	7.31	0.21	0.51	22.58	10.87	100.29	1.124	0.008	0.002	0.584	0.270	0.624	0.009	0.360	0.006	0.012	0.012		
DOZ mélange	B025sp059	n. d.	0.36	0.17	29.46	35.73	0.24	14.58	0.19	0.06	14.21	4.73	99.76	0.839	0.008	0.003	1.032	0.106	0.363	0.006	0.645	0.005	0.001	0.001		
DOZ mélange	B025sp060	n. d.	0.05	0.13	44.69	23.11	0.12	18.55	0.22	0.13	10.25	2.37	99.62	0.501	0.001	0.002	1.444	0.049	0.235	0.003	0.757	0.005	0.003	0.003		
DOZ mélange	B025sp062	n. d.	0.15	0.15	19.83	48.55	0.19	13.58	0.10	0.13	14.21	3.14	100.04	1.189	0.003	0.003	0.724	0.073	0.368	0.005	0.627	0.003	0.003	0.003		
DOZ mélange	B025sp063	n. d.	0.30	0.24	21.53	44.03	0.28	11.73	0.08	0.19	17.26	4.08	99.73	1.087	0.007	0.005	0.793	0.096	0.451	0.008	0.546	0.002	0.004	0.004		
DOZ mélange	B025sp069	n. d.	0.06	0.24	25.29	44.49	0.21	13.79	0.06	0.19	14.70	0.96	99.98	1.064	0.001	0.005	0.902	0.022	0.372	0.005	0.622	0.001	0.004	0.004		
DOZ mélange	B025sp070	n. d.	0.30	0.21	25.37	42.51	0.21	14.77	0.15	0.11	13.44	3.10	100.17	1.009	0.007	0.004	0.898	0.070	0.337	0.005	0.661	0.004	0.002	0.002		
DOZ mélange	B025sp071	n. d.	0.27	0.14	22.61	45.44	0.14	17.16	0.22	0.02	9.31	4.83	100.16	1.075	0.006	0.003	0.798	0.109	0.233	0.004	0.766	0.005	0.000	0.000		
DOZ mélange	B025sp072	0.03	0.29	0.20	29.68	36.36	0.17	15.52	0.14	0.06	12.91	4.68	99.94	0.847	0.006	0.004	1.028	0.104	0.318	0.004	0.682	0.003	0.001	0.001		
DOZ mélange	B025sp073	0.03	0.36	0.17	28.99	37.27	0.16	15.39	0.19	0.06	13.00	4.21	99.83	0.872	0.008	0.003	1.011	0.094	0.322	0.004	0.679	0.005	0.001	0.001		
DOZ mélange	B025sp074	n. d.	0.21	0.17	37.36	29.94	0.17	16.28	0.17	0.17	12.73	2.53	99.73	0.675	0.004	0.003	1.255	0.054	0.304	0.004	0.692	0.004	0.004	0.004		
DOZ mélange	B025sp075	1.35	0.34	0.19	32.42	30.04	0.35	15.23	0.14	0.56	12.94	6.97	100.52	0.699	0.008	0.004	1.124	0.154	0.318	0.009	0.668	0.003	0.012	0.012		
DOZ mélange	B025sp076	n. d.	0.11	0.19	19.99	44.55	0.34	9.59	0.06	0.41	20.02	5.05	100.31	1.118	0.003	0.004	0.748	0.121	0.531	0.009	0.454	0.002	0.010	0.010		
DOZ mélange	B025sp077	n. d.	0.07	0.16	41.66	25.72	0.40	15.79	0.21	0.91	12.91	1.34	99.18	0.575	0.001	0.003	1.388	0.029	0.305	0.010	0.665	0.005	0.019	0.019		
DOZ mélange	B025sp078	n. d.	0.34	0.26	27.21	38.53	0.20	13.31	0.13	0.19	16.03	4.22	100.42	0.915	0.008	0.005	0.964	0.095	0.403	0.005	0.596	0.003	0.004	0.004		
DOZ mélange	B025sp079	n. d.	0.15	0.17	30.48	35.54	0.21	13.94	0.14	0.21	13.50	4.18	100.33	0.831	0.003	0.003	1.062	0.093	0.378	0.005	0.614	0.003	0.005	0.005		
DOZ mélange	B025sp080	n. d.	0.08	0.17	37.30	30.06	0.15	15.92	0.15	0.16	13.15	2.39	99.53	0.680	0.002	0.003	1.258	0.052	0.315	0.004	0.679	0.003	0.003	0.003		
DOZ mélange	B025sp081	n. d.	0.07	0.13	47.04	19.51	0.13	17.39	0.27	0.22	12.21	2.45	99.43	0.422	0.002	0.002	1.519	0.051	0.280	0.003	0.710	0.006	0.004	0.004		
DOZ mélange	B025sp082	n. d.	0.40	0.23	26.13	39.42	0.19	14.80	0.13	0.08	13.65	5.19	100.22	0.933	0.009	0.005	0.922	0.117	0.342	0.005	0.660	0.003	0.002	0.002		
DOZ mélange	B025sp085	n. d.	0.03	0.29	30.12	32.50	0.18	13.59	0.18	0.23	15.75	7.74	100.61	0.762	0.001	0.006	1.052	0.173	0.390	0.005	0.600	0.004	0.005	0.005		
DOZ mélange	B025sp087	n. d.	0.04	0.13	46.04	21.25	0.16	18.36	0.26	0.15	10.63	2.54	99.56	0.459	0.001	0.002	1.482	0.082	0.243	0.004	0.747	0.006	0.003	0.003		
DOZ mélange	B025sp088	n. d.	0.03	0.10	31.69	37.31	0.12	17.26	0.16	0.12	10.18	2.58	99.55	0.855	0.001	0.002	1.290	0.066	0.247	0.003	0.746	0.004	0.003	0.003		
DOZ mélange	B025sp089	0.06	0.14	0.17	37.61	29.45	0.84	14.12	0.20	0.59	14.59	0.91	98.68	0.677	0.003	0.003	1.290	0.020	0.355	0.021	0.642	0.005	0.013	0.013		
DOZ mélange	B025sp090	n. d.	0.19	0.13	43.22	23.23	0.11	18.03	0.23	0.18	10.90	3.48	99.71	0.507	0.004	0.002	1.408	0.072	0.252	0.003	0.742	0.005	0.004	0.004		
DOZ mélange	B025sp091	n. d.	0.12	0.17	36.90	31.10	0.16	15.06	0.12	0.34	14.40	1.47	98.85	0.706	0.003	0.003	1.250	0.032	0.346	0.004	0.645	0.003	0.007	0.007		
DOZ mélange	TD197sp008	n. d.	0.03	0.29	22.13	45.41	0.19	12.40	0.06	0.17	16.14	2.50	99.32	1.116	0.001	0.006	0.811	0.059	0.420	0.005	0.575	0.001	0.004	0.004		
DOZ mélange	TD197sp005	n. d.	0.04	0.28	25.15	41.55	0.22	13.07	0.09	0.16	15.61	3.40	99.58	1.003	0.001	0.006	0.905	0.078	0.399	0.006	0.595	0.002	0.004	0.004		
DOZ mélange	TD197sp025	n. d.	0.04	0.25	24.91	39.45	0.23	11.03	0.06	0.39	18.47	4.76	99.59	0.966	0.001	0.005	0.910	0.111	0.479	0.006	0.509	0.001	0.009	0.009		
DOZ mélange	TD197sp004	n. d.	0.05	0.24	21.45	46.13	0.24	11.82	0.04	0.21	16.77	2.16	99.12	1.143	0.001	0.005	0.793	0.051	0.440	0.006	0.552	0.001	0.005	0.005		
DOZ mélange	TD197sp016	n. d.	0.06	0.29	17.82	48.62	0.25	11.22	0.08	0.18	17.36	4.51	100.05	1.221	0.001	0.006	0.655	0.108	0.461	0.007	0.531	0.002	0.004	0.004		
DOZ mélange	TD197sp021	n. d.	0.06	0.18	30.65	38.69	0.18	15.72	0.10	0.13	12.65	1.81	100.17	0.894	0.001	0.003	1.056	0.040	0.309	0.005	0.685	0.002	0.003	0.003		
DOZ mélange	TD197sp023	n. d.	0.06	0.18	39.53	28.73	0.15	16.23	0.17	0.30	13.04	1.64	100.02	0.641	0.001	0.003	1.315	0.035	0.308	0.004	0.682	0.004	0.006	0.006		
DOZ mélange	TD197sp006	n. d.	0.08	0.26	25.46	43.38	0.22	14.28	0.08	0.13	13.86	1.70	99.45	1.038	0.002	0.005	0.945	0.139	0.351	0.006	0.644	0.002	0.003	0.003		
DOZ mélange	TD197sp007	n. d.	0.09	0.23	51.12	57.55	0.91	3.43	0.00	0.26	26.28	5.01	98.88	1.632	0.002	0.005	0.216	0.135	0.788	0.028	0.183	0.000	0.007	0.007		
DOZ mélange	TD197sp002	n. d.	0.09	0.23	30.65	37.47	0.20	14.41	0.12	0.17	14.32	1.51	99.17	0.880	0.002	0.004	1.073	0.034	0.356	0.005	0.638	0.003	0.004	0.004		
DOZ mélange	TD197sp022	n. d.	0.09	0.21	22.79	46.16	0.20	14.45	0.09	0.10	13.32	2.43	99.82	1.112	0.002	0.004	0.819	0.056	0.339	0.005	0.656	0.002	0.002	0.002		
DOZ mélange	TD197sp014	0.01	0.10	0.18	9.64	55.57	0.58	6.64	0.01	0.54	22.33	3.89	99.49	1.499	0.003	0.004	0.388	0.100	0.637	0.017	0.338	0.000	0.014	0.014		
DOZ mélange	TD197sp018	n. d.	0.10	0.21	27.52	39.85	0.20	13.39	0.09	0.23	15.46	2.46	99.50	0.951	0.002	0.004	0.980	0.056	0.390	0.005	0.603	0.002	0.005	0.005		
DOZ mélange	TD197sp011	n. d.	0.14	0.16	9.28	55.07	0.59	5.72	0.03	0.81	23.67	4.80	100.28	1.488	0.004	0.004	0.374	0.124	0.676	0.017	0.291	0.001	0.020	0.020		
DOZ mélange	TD197sp019	n. d.	0.14	0.23	27.46	40.21	0.18	14.32	0.09																	

analyses in wt%. Shown are the recalculated FeO and Fe<sub>2</sub>O<sub>3</sub> values and the amended total

Formation	Sample & spot ID	analses in wt%. Shown are the recalculated FeO and Fe <sub>2</sub> O <sub>3</sub> values and the amended total																cations per formula unit on the basis of 3 oxygens											
		SiO <sub>2</sub>	TiO <sub>2</sub>	V <sub>2</sub> O <sub>5</sub>	Al <sub>2</sub> O <sub>3</sub>	Cr <sub>2</sub> O <sub>3</sub>	MnO	MgO	NiO	ZnO	FeO	Fe <sub>2</sub> O <sub>3</sub>	Total	Cr	Ti	V	Al	Fe <sup>3+</sup>	Fe <sup>2+</sup>	Mn	Mg	Ni	Zn						
Ugar Fm.	BO117sp001	n. d.	0.06	0.27	26.57	40.58	0.18	13.32	0.11	0.17	15.72	3.36	100.33	0.966	0.001	0.005	0.944	0.076	0.396	0.005	0.598	0.003	0.004						
Ugar Fm.	BO117sp002	n. d.	0.13	0.23	31.27	33.29	0.16	14.85	0.18	0.18	13.93	5.72	99.94	0.774	0.003	0.004	1.084	0.127	0.343	0.004	0.651	0.004	0.004						
Ugar Fm.	BO117sp003	n. d.	0.06	0.22	38.28	27.79	0.18	15.71	0.15	0.25	13.45	3.26	99.95	0.628	0.001	0.004	1.290	0.070	0.322	0.004	0.669	0.004	0.005						
Ugar Fm.	BO117sp004	n. d.	0.11	0.10	48.59	17.06	0.13	18.66	0.31	0.12	10.39	3.63	98.85	0.366	0.002	0.002	1.556	0.069	0.236	0.003	0.755	0.007	0.002						
Ugar Fm.	BO117sp005	n. d.	0.05	0.27	36.14	29.91	0.19	14.63	0.16	0.23	14.84	3.05	99.48	0.685	0.001	0.005	1.235	0.067	0.360	0.005	0.632	0.004	0.005						
Ugar Fm.	BO117sp006	n. d.	0.06	0.22	31.28	35.69	0.19	14.83	0.10	0.20	13.87	3.21	99.65	0.831	0.001	0.004	1.066	0.071	0.342	0.005	0.651	0.002	0.004						
Ugar Fm.	BO117sp007	n. d.	0.08	0.18	48.28	18.14	0.12	17.13	0.24	0.23	12.62	1.56	98.59	0.394	0.002	0.003	1.563	0.032	0.290	0.003	0.701	0.005	0.005						
Ugar Fm.	BO117sp008	n. d.	0.05	0.22	40.66	26.04	0.17	16.48	0.21	0.23	12.67	2.79	99.52	0.580	0.001	0.004	1.350	0.059	0.298	0.004	0.692	0.005	0.005						
Ugar Fm.	BO117sp009	n. d.	0.05	0.24	30.37	36.06	0.21	13.61	0.15	0.19	15.43	2.99	99.30	0.851	0.001	0.005	1.069	0.067	0.385	0.005	0.606	0.004	0.004						
Ugar Fm.	BO117sp010	n. d.	0.08	0.24	37.22	28.71	0.16	15.77	0.19	0.21	13.31	3.72	99.60	0.650	0.002	0.003	1.257	0.080	0.319	0.004	0.673	0.004	0.004						
Ugar Fm.	BO117sp011	n. d.	0.07	0.15	36.47	30.93	0.19	16.17	0.19	0.15	12.61	2.84	99.76	0.700	0.001	0.003	1.230	0.065	0.302	0.003	0.680	0.004	0.003						
Ugar Fm.	BO117sp012	n. d.	0.05	0.19	44.80	22.46	0.13	16.47	0.23	0.18	13.44	1.66	99.61	0.492	0.001	0.003	1.464	0.035	0.312	0.003	0.680	0.005	0.004						
Ugar Fm.	BO117sp014	n. d.	0.07	0.20	41.45	24.57	0.17	16.24	0.20	0.16	13.20	3.17	99.42	0.547	0.001	0.004	1.376	0.067	0.311	0.004	0.681	0.004	0.003						
Ugar Fm.	BO117sp015	n. d.	0.08	0.20	38.18	27.87	0.16	15.63	0.16	0.25	13.69	3.49	98.79	0.629	0.002	0.004	1.285	0.075	0.327	0.004	0.665	0.004	0.005						
Ugar Fm.	BO117sp016	n. d.	0.04	0.20	41.57	24.44	0.13	16.91	0.18	0.23	12.00	3.19	98.89	0.544	0.001	0.004	1.379	0.067	0.283	0.003	0.709	0.004	0.005						
Ugar Fm.	BO117sp017	n. d.	0.06	0.30	23.54	42.35	0.23	12.53	0.07	0.14	16.15	3.95	99.33	1.035	0.001	0.006	0.858	0.092	0.418	0.006	0.577	0.002	0.003						
Ugar Fm.	BO117sp018	n. d.	0.04	0.19	42.58	20.90	0.15	17.61	0.21	0.21	11.66	2.36	99.17	0.455	0.001	0.003	1.488	0.049	0.268	0.003	0.722	0.005	0.004						
Ugar Fm.	BO117sp019	n. d.	0.04	0.32	22.58	45.59	0.22	13.09	0.07	0.20	15.21	2.29	99.60	1.111	0.001	0.006	0.820	0.053	0.392	0.006	0.601	0.002	0.005						
Ugar Fm.	BO117sp020	n. d.	0.03	0.25	43.29	22.19	0.16	16.14	0.19	0.35	13.45	3.26	99.32	0.491	0.001	0.005	1.429	0.069	0.315	0.004	0.673	0.004	0.007						
Ugar Fm.	BO117sp021	n. d.	0.05	0.25	33.07	33.30	0.17	14.73	0.15	0.20	14.32	3.52	99.77	0.770	0.001	0.005	1.140	0.077	0.293	0.004	0.642	0.004	0.004						
Ugar Fm.	BO117sp022	n. d.	0.07	0.17	38.62	27.70	0.13	16.51	0.20	0.16	12.32	3.38	99.25	0.623	0.002	0.004	1.295	0.072	0.283	0.003	0.700	0.004	0.003						
Ugar Fm.	BO117sp023	n. d.	0.08	0.20	38.41	27.39	0.15	15.83	0.17	0.15	13.15	3.21	98.79	0.621	0.002	0.004	1.298	0.069	0.315	0.004	0.678	0.004	0.003						
Ugar Fm.	BO117sp025	n. d.	1.90	0.19	12.93	43.77	0.27	11.87	0.16	0.09	16.93	11.17	99.24	1.127	0.004	0.004	0.497	0.274	0.461	0.008	0.574	0.004	0.002						
Ugar Fm.	BO117sp027	n. d.	0.06	0.22	41.92	24.89	0.14	16.90	0.21	0.21	12.22	2.52	99.28	0.551	0.001	0.004	1.385	0.053	0.286	0.003	0.706	0.005	0.004						
Ugar Fm.	BO117sp028	n. d.	0.05	0.23	38.45	28.05	0.17	15.98	0.18	0.19	13.20	3.17	99.67	0.631	0.001	0.004	1.290	0.068	0.314	0.004	0.678	0.004	0.004						
Ugar Fm.	BO117sp029	n. d.	0.12	0.26	29.44	36.49	0.19	13.81	0.13	0.17	15.22	3.89	99.73	0.861	0.003	0.005	1.036	0.087	0.380	0.005	0.614	0.003	0.004						
Ugar Fm.	BO117sp030	n. d.	0.02	0.31	22.42	47.08	0.21	12.92	0.09	0.13	15.39	0.70	99.27	1.152	0.000	0.006	0.818	0.016	0.398	0.005	0.596	0.002	0.003						
Ugar Fm.	BO117sp034	n. d.	1.16	0.30	23.12	37.37	0.28	10.36	0.15	0.20	20.26	6.37	99.57	0.927	0.027	0.006	0.855	0.150	0.532	0.008	0.484	0.004	0.005						
Ugar Fm.	BO117sp037	n. d.	0.03	0.34	23.80	44.93	0.22	13.52	0.09	0.19	14.98	2.27	100.38	1.079	0.001	0.007	0.853	0.082	0.381	0.006	0.612	0.002	0.004						
Ugar Fm.	BO117sp039	n. d.	0.07	0.23	30.13	36.57	0.15	15.59	0.17	0.15	12.59	4.16	99.83	0.850	0.001	0.004	1.045	0.092	0.310	0.004	0.683	0.004	0.004						
Ugar Fm.	BO117sp040	n. d.	0.05	0.36	9.71	59.83	0.33	9.59	0.03	0.17	18.66	1.18	99.90	1.571	0.001	0.008	0.380	0.300	0.518	0.009	0.475	0.001	0.004						
Ugar Fm.	BO117sp041	n. d.	0.10	0.37	15.63	50.61	0.34	8.20	0.04	0.32	21.60	2.78	100.00	1.307	0.002	0.008	0.602	0.068	0.590	0.010	0.399	0.001	0.008						
Ugar Fm.	BO117sp042	n. d.	0.07	0.28	25.36	42.39	0.21	14.03	0.12	0.15	14.25	2.85	99.77	1.015	0.002	0.006	0.905	0.065	0.361	0.005	0.633	0.003	0.003						
Ugar Fm.	BO117sp043	n. d.	0.88	0.28	25.62	37.00	0.25	13.38	0.16	0.15	16.12	6.64	100.48	0.884	0.020	0.006	0.913	0.151	0.408	0.006	0.603	0.004	0.003						
Ugar Fm.	BO117sp044	n. d.	0.12	0.20	36.13	30.44	0.17	15.52	0.14	0.18	13.76	3.44	100.09	0.691	0.002	0.004	1.222	0.074	0.330	0.004	0.664	0.003	0.004						
Ugar Fm.	BO117sp045	n. d.	0.09	0.24	38.90	25.92	0.17	15.47	0.20	0.29	13.96	4.44	99.69	0.584	0.002	0.004	1.307	0.095	0.333	0.004	0.657	0.005	0.006						
Ugar Fm.	BO117sp046	n. d.	0.12	0.10	49.41	18.19	0.14	18.99	0.23	0.09	10.15	1.44	98.88	0.388	0.003	0.002	1.573	0.029	0.229	0.003	0.764	0.005	0.002						
Ugar Fm.	BO117sp047	n. d.	0.06	0.21	45.14	20.75	0.13	17.35	0.23	0.21	12.00	3.19	99.26	0.453	0.001	0.004	1.470	0.066	0.277	0.003	0.714	0.005	0.004						
Ugar Fm.	BO117sp048	n. d.	0.14	0.25	22.08	44.29	0.28	11.74	0.11	0.20	17.37	3.94	100.40	1.085	0.003	0.005	0.806	0.092	0.450	0.007	0.542	0.003	0.005						
Ugar Fm.	BO117sp049	n. d.	0.07	0.20	30.27	36.43	0.20	13.09	0.12	0.23	16.49	3.07	100.17	0.857	0.002	0.004	1.062	0.069	0.411	0.005	0.581	0.003	0.005						
Ugar Fm.	BO117sp051	n. d.	0.05	0.24	32.70	34.55	0.15	15.37	0.20	0.18	13.34	3.04	99.76	0.797	0.001	0.005	1.124	0.066	0.325	0.004	0.668	0.003	0.004						
Ugar Fm.	BO117sp052	n. d.	0.06	0.21	40.48	26.69	0.15	16.39	0.20	0.17	13.03	2.63	100.00	0.593	0.001	0.004	1.341	0.056	0.306	0.004	0.686	0.004	0.003						
Ugar Fm.	BO117sp053	n. d.	0.06	0.17	41.80	25.04	0.15	16.99	0.20	0.15	12.02	2.56	99.14	0.555	0.001	0.003	1.382	0.054	0.282	0.004	0.710	0.005	0.003						
Ugar Fm.	BO117sp054	n. d.	0.12	0.29	17.69	48.65	0.25	11.24	0.09	0.14	17.53	4.29	100.29	1.218	0.003	0.006	0.661	0.102	0.464	0.007	0.531	0.002	0.003						
Ugar Fm.	BO117sp055	n. d.	0.04	0.19	41.57	24.64	0.17	16.08	0.16	0.18	13.48	2.97	99.48	0.548	0.001	0.004	1.380	0.063	0.317	0.004	0.675	0.004	0.004						
Ugar Fm.	BO117sp056	n. d.	0.20	0.20	13.42	51.60	0.31	9.81	0.05	0.15	18.89	5.32	99.96	1.333	0.005	0.004	0.517	0.131	0.516	0.009	0.478	0.001	0.004						
Ugar Fm.	BO117sp058	n. d.	0.09	0.23	30.39	36.88	0.20	14.71	0.12	0.17	14.39	2.66	100.14	0.859	0.009	0.005	1.055	0.059	0.354	0.005	0.646	0.003	0.004						
Ugar Fm.	BO117sp059	n. d.	0.04	0.24	24.88	43.43	0.17	13.94	0.10	0.13	14.46	2.53	99.96	1.040	0.005	0.005	0.888	0.058	0.366	0.004	0.629	0.003	0.003						
Ugar Fm.	BO117sp060	n. d.	0.05	0.29	32.99	32.71	0.22	13.65	0.10	0.32	15.77	3.33	99.43	0.764	0.001	0.006	1.148	0.074	0.389	0.005	0.601	0.002	0.007						
Ugar Fm.	BO117sp061	n. d.	0.06	0.26	14.44	53.88	0.32	9.76	0.04	0.22	19.06	2.02	100.06	1.383	0.001	0.006	0.553	0.049	0.518	0.009	0.472	0.001	0						

analyses in wt%. Shown are the recalculated FeO and Fe<sub>2</sub>O<sub>3</sub> values and the amended total

Formation	Sample & spot ID	SiO <sub>2</sub>	TiO <sub>2</sub>	V <sub>2</sub> O <sub>5</sub>	Al <sub>2</sub> O <sub>3</sub>	Cr <sub>2</sub> O <sub>3</sub>	MnO	MgO	NiO	ZnO	FeO	Fe <sub>2</sub> O <sub>3</sub>	Total	Cations per formula unit on the basis of 3 oxygens										
														Cr	Ti	V	Al	Fe <sup>3+</sup>	Fe <sup>2+</sup>	Mn	Mg	Ni	Zn	
Ugar Fm.	BO117sp0066	n. d.	0.03	0.19	45.90	20.74	0.16	16.68	0.24	0.14	12.93	1.57	98.57	0.455	0.001	0.003	1.503	0.033	0.300	0.004	0.691	0.005	0.003	0.003
Ugar Fm.	BO117sp0067	n. d.	0.09	0.24	25.02	43.57	0.19	13.89	0.10	0.15	14.55	2.22	100.01	1.043	0.002	0.005	0.893	0.050	0.368	0.005	0.627	0.002	0.003	0.003
Ugar Fm.	BO117sp0068	n. d.	0.41	0.25	30.46	36.85	0.20	14.60	0.10	0.18	14.63	2.29	100.00	0.859	0.002	0.005	1.059	0.052	0.361	0.005	0.640	0.002	0.004	0.004
Ugar Fm.	BO117sp0069	n. d.	0.11	0.21	30.73	36.95	0.17	14.66	0.11	0.18	14.18	2.39	99.53	0.864	0.002	0.004	1.072	0.051	0.351	0.004	0.644	0.003	0.004	0.004
Ugar Fm.	BO117sp0070	n. d.	0.11	0.22	35.36	30.76	0.19	15.43	0.17	0.19	13.51	3.48	99.42	0.704	0.002	0.004	1.207	0.076	0.327	0.005	0.666	0.004	0.004	0.004
Ugar Fm.	BO117sp0071	n. d.	0.06	0.29	27.09	39.82	0.21	13.35	0.09	0.18	15.62	3.23	99.95	0.949	0.001	0.006	0.963	0.073	0.394	0.005	0.600	0.002	0.004	0.004
Ugar Fm.	BO117sp0072	n. d.	0.07	0.17	39.73	26.54	0.14	16.49	0.19	0.23	12.46	3.27	99.28	0.594	0.001	0.003	1.327	0.070	0.295	0.003	0.696	0.004	0.005	0.005
Ugar Fm.	BO117sp0073	n. d.	0.10	0.18	38.01	24.00	0.17	16.05	0.25	0.17	12.88	7.73	99.55	0.542	0.002	0.003	1.290	0.166	0.308	0.004	0.683	0.006	0.004	0.004
Ugar Fm.	BO117sp0074	n. d.	0.04	0.24	23.14	45.41	0.19	13.70	0.09	0.12	14.58	2.66	100.18	1.095	0.001	0.005	0.832	0.061	0.372	0.005	0.623	0.002	0.003	0.003
Ugar Fm.	BO117sp0075	n. d.	0.11	0.25	27.10	37.58	0.21	11.76	0.09	0.30	17.75	3.24	98.98	0.910	0.002	0.005	1.000	0.075	0.455	0.006	0.537	0.002	0.007	0.007
Ugar Fm.	BO117sp0076	n. d.	0.04	0.04	37.31	29.68	0.17	15.35	0.13	0.24	13.74	2.07	98.92	0.677	0.001	0.004	1.269	0.045	0.332	0.004	0.660	0.003	0.003	0.003
Ugar Fm.	BO117sp0077	n. d.	0.08	0.21	32.45	32.68	0.20	13.80	0.13	0.27	15.60	4.45	99.87	0.761	0.002	0.004	1.128	0.099	0.385	0.005	0.606	0.003	0.006	0.006
Ugar Fm.	BO117sp0078	n. d.	0.07	0.26	37.24	29.49	0.16	15.69	0.16	0.20	13.58	3.02	99.87	0.666	0.002	0.005	1.255	0.065	0.325	0.004	0.688	0.004	0.004	0.004
Ugar Fm.	BO117sp0079	n. d.	0.06	0.28	23.23	43.23	0.27	11.24	0.08	0.22	18.00	2.81	99.42	1.065	0.001	0.006	0.854	0.066	0.469	0.007	0.522	0.002	0.005	0.005
Ugar Fm.	BO117sp0080	n. d.	0.29	0.28	22.72	43.60	0.23	12.35	0.07	0.12	16.68	3.45	99.79	1.066	0.001	0.006	0.828	0.080	0.431	0.006	0.569	0.002	0.003	0.003
Ugar Fm.	BO117sp0081	n. d.	0.07	0.21	41.46	24.61	0.17	16.85	0.23	0.18	12.23	3.42	99.43	0.546	0.001	0.004	1.371	0.072	0.287	0.004	0.704	0.005	0.004	0.004
Ugar Fm.	BO117sp0082	n. d.	0.08	0.20	40.46	25.91	0.15	16.43	0.18	0.19	12.59	2.63	98.80	0.581	0.002	0.004	1.352	0.056	0.298	0.004	0.694	0.004	0.004	0.004
Ugar Fm.	BO117sp0083	n. d.	0.06	0.27	33.42	33.86	0.18	14.31	0.15	0.20	15.02	2.18	99.66	0.784	0.001	0.005	1.154	0.048	0.368	0.005	0.625	0.004	0.004	0.004
Ugar Fm.	BO117sp0084	n. d.	0.11	0.23	29.79	36.32	0.19	14.17	0.11	0.15	14.79	3.97	99.83	0.853	0.002	0.005	1.043	0.089	0.368	0.005	0.627	0.003	0.003	0.003
Ugar Fm.	BO117sp0085	n. d.	0.04	0.36	21.09	46.78	0.23	11.77	0.05	0.21	17.19	2.38	100.10	1.152	0.001	0.007	0.774	0.066	0.448	0.006	0.546	0.001	0.005	0.005
Ugar Fm.	BO117sp0086	n. d.	0.06	0.33	19.69	47.67	0.26	11.68	0.06	0.17	17.01	2.92	99.83	1.184	0.001	0.007	0.729	0.069	0.447	0.007	0.547	0.001	0.004	0.004
Ugar Fm.	BO117sp0087	n. d.	0.08	0.19	40.39	26.26	0.15	16.54	0.17	0.20	12.61	2.84	99.43	0.586	0.002	0.004	1.343	0.060	0.297	0.003	0.695	0.004	0.004	0.004
Ugar Fm.	BO117sp0088	n. d.	0.13	0.20	38.26	27.91	0.15	15.94	0.16	0.17	13.16	2.99	99.07	0.631	0.003	0.004	1.291	0.064	0.315	0.004	0.680	0.004	0.004	0.004
Ugar Fm.	BO117sp0089	n. d.	0.04	0.17	47.83	20.14	0.10	17.44	0.19	0.42	12.10	0.67	99.11	0.436	0.001	0.003	1.542	0.014	0.277	0.002	0.711	0.004	0.004	0.004
Ugar Fm.	BO117sp0090	n. d.	0.03	0.30	24.48	43.41	0.24	13.36	0.07	0.20	15.13	2.60	99.82	1.046	0.001	0.006	0.880	0.070	0.386	0.006	0.607	0.002	0.005	0.005
Ugar Fm.	BO16sp0001	n. d.	0.03	0.34	20.65	46.86	0.27	11.92	0.07	0.19	16.96	3.31	100.60	1.150	0.001	0.007	0.756	0.077	0.441	0.006	0.562	0.002	0.004	0.004
Ugar Fm.	BO16sp0002	n. d.	0.06	0.29	18.72	50.93	0.22	12.59	0.05	0.14	15.71	1.71	100.42	1.256	0.001	0.006	0.688	0.040	0.410	0.006	0.585	0.001	0.003	0.003
Ugar Fm.	BO16sp0003	n. d.	0.03	0.32	18.50	49.75	0.24	12.08	0.09	0.18	16.24	2.66	100.08	1.236	0.001	0.007	0.685	0.060	0.427	0.006	0.566	0.002	0.004	0.004
Ugar Fm.	BO16sp0004	n. d.	0.03	0.34	18.94	47.47	0.28	11.26	0.09	0.18	17.59	4.14	100.31	1.182	0.001	0.007	0.703	0.098	0.463	0.007	0.529	0.002	0.004	0.004
Ugar Fm.	BO16sp0005	n. d.	0.02	0.26	22.22	45.35	0.23	12.16	0.07	0.23	16.55	2.70	99.79	1.112	0.000	0.005	0.812	0.063	0.429	0.006	0.562	0.002	0.005	0.005
Ugar Fm.	BO16sp0006	n. d.	0.02	0.34	19.62	48.54	0.21	11.97	0.08	0.17	16.57	2.36	99.88	1.203	0.001	0.007	0.725	0.056	0.434	0.006	0.559	0.002	0.004	0.004
Ugar Fm.	BO16sp0007	n. d.	0.02	0.30	22.19	46.66	0.22	11.51	0.08	0.14	17.83	1.38	100.33	1.143	0.000	0.006	0.811	0.032	0.462	0.006	0.532	0.002	0.003	0.003
Ugar Fm.	BO16sp0008	n. d.	0.04	0.26	23.13	46.31	0.20	13.67	0.13	0.11	14.70	1.90	100.44	1.114	0.001	0.005	0.830	0.044	0.374	0.005	0.620	0.003	0.002	0.002
Ugar Fm.	BO16sp0009	n. d.	0.03	0.32	22.15	46.30	0.24	12.60	0.09	0.16	16.15	2.43	100.46	1.126	0.001	0.006	0.803	0.056	0.415	0.006	0.578	0.002	0.004	0.004
Ugar Fm.	BO16sp0010	n. d.	0.05	0.15	41.54	26.60	0.15	17.25	0.15	0.16	11.75	1.72	99.53	0.587	0.001	0.003	1.368	0.036	0.275	0.004	0.718	0.003	0.003	0.003
Ugar Fm.	BO16sp0011	n. d.	0.04	0.26	23.13	46.31	0.20	13.67	0.13	0.11	14.70	1.90	100.44	1.114	0.001	0.005	0.830	0.044	0.374	0.005	0.620	0.003	0.002	0.002
Ugar Fm.	BO16sp0012	n. d.	0.05	0.33	16.26	53.70	0.25	12.50	0.09	0.13	15.49	1.82	100.61	1.336	0.001	0.007	0.603	0.043	0.408	0.007	0.586	0.002	0.003	0.003
Ugar Fm.	BO16sp0013	n. d.	0.04	0.32	16.13	52.93	0.26	11.74	0.07	0.13	16.49	2.14	100.25	1.329	0.001	0.007	0.604	0.051	0.438	0.007	0.566	0.002	0.003	0.003
Ugar Fm.	BO16sp0014	n. d.	0.08	0.26	25.28	43.61	0.19	13.48	0.10	0.21	15.07	1.42	99.70	1.047	0.002	0.005	0.905	0.032	0.383	0.005	0.610	0.003	0.003	0.003
Ugar Fm.	BO16sp0015	n. d.	0.01	0.33	20.35	47.33	0.23	11.88	0.07	0.16	16.88	2.89	100.13	1.168	0.000	0.007	0.749	0.068	0.441	0.006	0.563	0.002	0.004	0.004
Ugar Fm.	BO16sp0016	n. d.	0.05	0.29	15.30	54.32	0.25	11.91	0.04	0.04	16.01	1.55	99.86	1.371	0.001	0.006	0.576	0.037	0.428	0.007	0.567	0.001	0.003	0.003
Ugar Fm.	BO16sp0017	n. d.	0.02	0.31	26.10	43.20	0.24	13.06	0.10	0.18	15.72	0.46	99.39	1.039	0.000	0.006	0.936	0.010	0.400	0.006	0.592	0.002	0.004	0.004
Ugar Fm.	BO16sp0018	n. d.	0.08	0.35	19.19	48.81	0.21	11.22	0.07	0.12	17.85	2.32	100.25	1.214	0.002	0.007	0.654	0.055	0.470	0.006	0.526	0.001	0.004	0.004
Ugar Fm.	BO16sp0019	n. d.	0.07	0.26	20.26	48.90	0.24	12.66	0.07	0.12	15.54	1.46	99.59	1.206	0.002	0.005	0.745	0.034	0.406	0.006	0.589	0.002	0.003	0.003
Ugar Fm.	BO16sp0020	n. d.	0.08	0.20	30.75	36.73	0.19	15.17	0.13	0.20	13.33	3.11	99.88	0.854	0.002	0.004	1.066	0.069	0.328	0.005	0.665	0.003	0.004	0.004
Ugar Fm.	BO16sp0021	n. d.	0.04	0.21	31.00	37.15	0.18	15.51	0.18	0.13	12.95	2.79	100.12	0.859	0.001	0.004	1.069	0.061	0.317	0.005	0.676	0.004	0.003	0.003
Ugar Fm.	BO16sp0022	n. d.	0.05	0.25	23.94	44.67	0.27	12.21	0.08	0.21	16.97	1.85	100.49	1.081	0.001	0.005	0.864	0.043	0.434	0.007	0.557	0.002	0.005	0.005
Ugar Fm.	BO16sp0023	n. d.	0.25	0.20	25.42	42.81	0.16	15.56	0.15	0.08	12.28	3.35	100.27	1.010	0.006	0.004	0.895	0.075	0.307	0.004	0.692	0.004	0.002	0.002
Ugar Fm.	BO16sp0024	n. d.	0.05	0.37																				

analyses in wt%. Shown are the recalculated FeO and Fe<sub>2</sub>O<sub>3</sub> values and the amended total

Formation	Sample & spot ID	Cations per formula unit on the basis of 3 oxygens																						
		SiO <sub>2</sub>	TiO <sub>2</sub>	V <sub>2</sub> O <sub>5</sub>	Al <sub>2</sub> O <sub>3</sub>	Cr <sub>2</sub> O <sub>3</sub>	MnO	MgO	NiO	ZnO	FeO	Fe <sub>2</sub> O <sub>3</sub>	Total	Cr	Ti	V	Al	Fe <sup>2+</sup>	Fe <sup>3+</sup>	Mn	Mg	Ni	Zn	
Ugar Fm.	BO16sp032	n. d.	0.03	0.26	27.18	41.19	0.18	14.04	0.09	0.17	14.53	2.10	99.76	0.978	0.001	0.005	0.962	0.047	0.365	0.005	0.628	0.002	0.004	0.004
Ugar Fm.	BO16sp033	n. d.	0.03	0.24	28.10	40.95	0.18	14.83	0.11	0.15	13.58	1.97	100.13	0.961	0.001	0.005	0.984	0.044	0.337	0.004	0.656	0.003	0.003	0.003
Ugar Fm.	BO16sp034	n. d.	0.03	0.35	13.92	54.95	0.28	11.15	0.05	0.14	17.10	2.47	100.43	1.396	0.001	0.007	0.527	0.060	0.460	0.008	0.534	0.001	0.003	0.001
Ugar Fm.	BO16sp035	n. d.	0.03	0.34	20.27	48.72	0.25	12.08	0.05	0.20	16.63	1.74	100.30	1.199	0.001	0.007	0.744	0.041	0.433	0.007	0.580	0.001	0.005	0.001
Ugar Fm.	BO16sp036	n. d.	0.03	0.29	23.95	44.79	0.22	12.23	0.07	0.17	16.93	1.49	100.17	1.086	0.001	0.006	0.866	0.034	0.434	0.006	0.569	0.002	0.004	0.004
Ugar Fm.	BO16sp037	n. d.	0.31	0.28	16.92	46.96	0.31	10.23	0.10	0.18	18.93	5.90	100.12	1.190	0.001	0.006	0.640	0.142	0.508	0.008	0.489	0.002	0.004	0.004
Ugar Fm.	BO16sp038	n. d.	1.21	0.50	13.47	46.69	0.28	10.11	0.15	0.15	19.55	8.19	100.31	1.201	0.030	0.011	0.517	0.201	0.532	0.008	0.490	0.004	0.003	0.003
Ugar Fm.	BO16sp039	n. d.	0.16	0.33	15.68	50.06	0.23	9.91	0.07	0.16	19.35	4.42	100.37	1.275	0.004	0.007	0.595	0.107	0.521	0.006	0.476	0.002	0.004	0.004
Ugar Fm.	BO16sp040	n. d.	0.15	0.36	21.35	43.84	0.32	9.38	0.07	0.40	20.75	3.71	100.34	1.094	0.004	0.008	0.795	0.088	0.548	0.009	0.441	0.002	0.009	0.009
Ugar Fm.	BO16sp041	n. d.	0.03	0.31	16.90	50.74	0.35	9.48	0.05	0.25	19.94	2.39	100.42	1.288	0.001	0.007	0.640	0.098	0.535	0.009	0.453	0.001	0.006	0.006
Ugar Fm.	BO16sp042	n. d.	0.03	0.27	21.28	48.21	0.22	12.55	0.09	0.15	15.86	1.05	99.71	1.184	0.001	0.005	0.779	0.025	0.412	0.006	0.581	0.002	0.004	0.004
Ugar Fm.	BO16sp043	n. d.	0.05	0.30	21.39	46.35	0.29	10.63	0.06	0.20	18.97	2.13	100.37	1.146	0.001	0.006	0.789	0.050	0.496	0.008	0.495	0.001	0.005	0.005
Ugar Fm.	BO16sp044	n. d.	0.04	0.36	23.30	44.15	0.19	12.20	0.07	0.21	16.82	2.57	99.90	1.076	0.001	0.007	0.847	0.060	0.434	0.005	0.561	0.002	0.005	0.005
Ugar Fm.	BO16sp045	n. d.	0.03	0.31	22.02	46.98	0.22	13.67	0.11	0.12	14.37	2.12	99.95	1.140	0.001	0.006	0.797	0.049	0.369	0.006	0.625	0.003	0.003	0.003
Ugar Fm.	BO16sp046	n. d.	0.17	0.27	20.69	48.30	0.22	12.96	0.07	0.16	15.33	1.69	99.87	1.184	0.004	0.006	0.756	0.039	0.398	0.006	0.599	0.002	0.004	0.004
Ugar Fm.	BO16sp047	n. d.	0.03	0.28	24.20	43.21	0.20	13.50	0.09	0.21	14.89	3.35	99.97	1.041	0.001	0.006	0.869	0.077	0.379	0.005	0.613	0.002	0.005	0.005
Ugar Fm.	BO16sp048	n. d.	0.04	0.33	23.38	44.60	0.21	14.61	0.15	0.13	17.09	3.35	99.89	1.071	0.001	0.007	0.837	0.077	0.332	0.005	0.661	0.004	0.004	0.004
Ugar Fm.	BO16sp049	n. d.	0.03	0.37	23.73	43.85	0.22	11.89	0.08	0.31	17.39	2.48	100.35	1.065	0.001	0.008	0.860	0.057	0.447	0.006	0.545	0.002	0.007	0.007
Ugar Fm.	BO16sp050	n. d.	0.04	0.31	18.01	50.57	0.22	11.80	0.06	0.16	16.76	2.44	100.37	1.258	0.001	0.006	0.668	0.058	0.441	0.006	0.563	0.001	0.004	0.004
Ugar Fm.	BO16sp051	n. d.	0.12	0.28	13.38	55.38	0.24	12.23	0.08	0.06	15.49	3.22	100.48	1.400	0.003	0.006	0.504	0.077	0.414	0.006	0.583	0.002	0.001	0.001
Ugar Fm.	BO16sp052	n. d.	0.03	0.38	23.30	45.07	0.23	12.13	0.07	0.24	17.02	1.90	100.38	1.095	0.001	0.008	0.844	0.044	0.437	0.006	0.555	0.002	0.005	0.005
Ugar Fm.	BO16sp053	n. d.	0.05	0.44	13.93	54.45	0.27	10.80	0.05	0.16	17.77	2.72	100.64	0.987	0.001	0.009	0.528	0.066	0.478	0.007	0.517	0.001	0.004	0.004
Ugar Fm.	BO16sp054	n. d.	0.81	0.04	21.48	39.82	0.28	10.89	0.14	0.13	19.17	6.88	100.04	0.987	0.019	0.009	0.794	0.162	0.502	0.008	0.509	0.004	0.003	0.003
Ugar Fm.	BO16sp055	n. d.	0.03	0.29	21.55	46.83	0.21	13.39	0.08	0.13	14.80	2.87	100.18	1.138	0.001	0.006	0.781	0.066	0.381	0.006	0.614	0.002	0.004	0.004
Ugar Fm.	BO16sp056	n. d.	0.03	0.32	20.85	47.56	0.27	11.43	0.06	0.24	17.70	2.06	100.51	1.171	0.001	0.007	0.765	0.048	0.461	0.006	0.530	0.001	0.006	0.006
Ugar Fm.	BO16sp057	n. d.	0.04	0.34	24.11	45.88	0.24	12.28	0.09	0.24	16.79	0.00	100.05	1.112	0.001	0.008	0.871	0.000	0.430	0.006	0.561	0.002	0.006	0.006
Ugar Fm.	BO16sp058	n. d.	1.47	0.60	13.65	38.24	0.31	7.57	0.20	0.13	23.38	14.07	99.62	1.008	0.037	0.013	0.537	0.353	0.652	0.009	0.376	0.005	0.003	0.003
Ugar Fm.	BO16sp059	n. d.	0.03	0.35	24.22	42.17	0.26	11.72	0.08	0.22	17.71	3.65	100.47	1.023	0.001	0.007	0.876	0.084	0.455	0.007	0.536	0.002	0.006	0.006
Ugar Fm.	BO16sp060	n. d.	0.90	0.44	16.89	39.96	0.39	6.51	0.13	0.21	24.92	9.33	99.67	1.044	0.022	0.010	0.658	0.232	0.689	0.011	0.321	0.003	0.003	0.005
Ugar Fm.	BO16sp061	n. d.	0.05	0.29	22.91	45.44	0.20	12.75	0.08	0.19	15.93	2.20	100.04	1.104	0.001	0.006	0.830	0.051	0.410	0.005	0.584	0.002	0.004	0.004
Ugar Fm.	BO16sp062	n. d.	0.02	0.26	27.63	41.24	0.17	14.60	0.10	0.15	13.84	2.02	100.04	0.972	0.000	0.004	0.971	0.045	0.345	0.004	0.649	0.002	0.003	0.003
Ugar Fm.	BO16sp063	n. d.	0.03	0.41	18.79	49.30	0.26	11.50	0.04	0.18	17.39	2.58	100.48	1.224	0.001	0.009	0.696	0.061	0.457	0.007	0.538	0.001	0.004	0.004
Ugar Fm.	BO16sp064	n. d.	0.05	0.21	24.76	44.70	0.21	14.01	0.07	0.17	14.43	1.95	100.55	1.065	0.001	0.004	0.880	0.044	0.364	0.005	0.629	0.002	0.004	0.004
Ugar Fm.	BO16sp065	n. d.	0.17	0.23	25.60	43.39	0.21	14.22	0.07	0.20	14.27	2.00	100.36	1.031	0.004	0.005	0.907	0.045	0.359	0.005	0.637	0.002	0.005	0.005
Ugar Fm.	BO16sp066	n. d.	0.06	0.19	24.40	44.53	0.23	14.95	0.11	0.09	12.80	2.77	100.12	1.060	0.001	0.004	0.866	0.063	0.322	0.006	0.671	0.003	0.002	0.002
Ugar Fm.	BO16sp067	n. d.	0.02	0.27	19.45	50.04	0.21	12.63	0.08	0.12	15.68	1.80	100.30	1.231	0.001	0.006	0.714	0.042	0.408	0.005	0.586	0.002	0.003	0.003
Ugar Fm.	BO16sp068	n. d.	0.02	0.34	26.15	38.84	0.23	10.17	0.07	0.51	20.07	3.65	100.04	0.948	0.000	0.007	0.952	0.085	0.518	0.006	0.468	0.002	0.012	0.012
Ugar Fm.	BO16sp069	n. d.	0.02	0.33	20.16	47.53	0.24	11.57	0.06	0.17	17.52	3.12	100.71	1.171	0.001	0.007	0.741	0.073	0.456	0.006	0.537	0.001	0.004	0.004
Ugar Fm.	BO16sp070	n. d.	0.06	0.29	25.24	42.66	0.22	13.46	0.10	0.18	15.47	3.27	100.95	1.015	0.001	0.006	0.896	0.078	0.390	0.005	0.604	0.002	0.004	0.004
Ugar Fm.	BO16sp071	n. d.	0.01	0.45	25.03	42.84	0.20	11.79	0.06	0.28	17.75	1.64	100.06	1.038	0.000	0.009	0.904	0.038	0.455	0.005	0.538	0.002	0.006	0.006
Ugar Fm.	BO16sp072	n. d.	0.07	0.22	5.78	58.85	0.34	7.65	0.06	0.17	20.74	5.83	99.71	1.601	0.002	0.005	0.234	0.151	0.597	0.010	0.392	0.002	0.004	0.004
Ugar Fm.	BO16sp073	n. d.	0.01	0.33	22.79	45.73	0.22	12.50	0.08	0.20	16.31	2.00	100.16	1.112	0.000	0.007	0.827	0.046	0.420	0.006	0.573	0.002	0.004	0.004
Ugar Fm.	BO16sp074	n. d.	0.05	0.32	24.40	43.09	0.23	12.68	0.08	0.25	16.33	3.00	100.42	1.038	0.001	0.007	0.877	0.069	0.416	0.006	0.576	0.002	0.006	0.006
Ugar Fm.	BO16sp075	n. d.	0.03	0.35	16.51	52.14	0.25	11.43	0.08	0.18	17.12	2.55	100.64	1.306	0.001	0.007	0.617	0.061	0.453	0.007	0.540	0.002	0.004	0.004
Ugar Fm.	BO16sp076	n. d.	0.09	0.27	26.12	42.65	0.20	13.37	0.09	0.18	15.55	1.62	100.13	1.018	0.002	0.005	0.930	0.037	0.383	0.005	0.602	0.002	0.004	0.004
Ugar Fm.	BO16sp077	n. d.	0.05	0.32	8.46	58.44	0.34	7.59	0.04	0.22	21.52	3.36	100.35	1.050	0.001	0.007	0.337	0.085	0.608	0.010	0.382	0.001	0.006	0.006
Ugar Fm.	BO16sp078	n. d.	0.07	0.16	30.49	40.21	0.14	16.08	0.12	0.12	12.12	0.64	100.15	0.927	0.002	0.003	1.049	0.014	0.296	0.004	0.699	0.003	0.003	0.003
Ugar Fm.	BO16sp079	n. d.	0.04	0.32	16.85	50.20	0.35	8.50	0.08	0.22	21.30	2.20	100.04	1.287	0.001	0.007	0.644	0.054	0.578	0.010	0.411	0.002	0.005	0.005
Ugar Fm.	BO16sp080	n. d.																						

analyses in wt%. Shown are the recalculated FeO and Fe<sub>2</sub>O<sub>3</sub> values and the amended total

Formation	Sample & spot ID	analyses in wt%. Shown are the recalculated FeO and Fe <sub>2</sub> O <sub>3</sub> values and the amended total														cations per formula unit on the basis of 3 oxygens											
		SiO <sub>2</sub>	TiO <sub>2</sub>	V <sub>2</sub> O <sub>5</sub>	Al <sub>2</sub> O <sub>3</sub>	Cr <sub>2</sub> O <sub>3</sub>	MnO	MgO	NiO	ZnO	FeO	Fe <sub>2</sub> O <sub>3</sub>	Total	Cr	Ti	V	Al	Fe <sup>3+</sup>	Fe <sup>2+</sup>	Mn	Mg	Ni	Zn				
Ugar Fm.	BO17sp0088	n. d.	0.04	0.31	22.59	45.82	0.17	13.47	0.12	0.13	14.82	2.55	100.02	1.110	0.001	0.006	0.816	0.059	0.380	0.005	0.615	0.003	0.003	0.003			
Ugar Fm.	BO16sp0089	n. d.	0.02	0.47	21.41	48.39	0.20	10.47	0.08	0.16	17.39	0.00	98.59	1.227	0.000	0.010	0.809	0.000	0.466	0.006	0.500	0.002	0.004	0.004			
Ugar Fm.	BO17sp0090	n. d.	0.03	0.29	23.92	43.98	0.20	12.92	0.09	0.16	15.93	2.84	100.35	1.061	0.001	0.006	0.860	0.065	0.406	0.005	0.587	0.002	0.004	0.004			
Ugar Fm.	BO17sp0091	n. d.	0.05	0.27	22.53	45.40	0.19	13.19	0.10	0.11	15.27	3.04	100.15	1.101	0.001	0.005	0.815	0.070	0.392	0.005	0.603	0.002	0.002	0.002			
Ugar Fm.	BO17sp0092	n. d.	0.10	0.28	18.98	47.11	0.26	11.49	0.06	0.14	17.30	4.46	100.17	1.173	0.002	0.006	0.705	0.106	0.456	0.007	0.539	0.002	0.003	0.003			
Ugar Fm.	BO17sp0093	n. d.	0.28	0.30	17.00	50.56	0.24	12.22	0.08	0.17	15.96	3.11	99.91	1.265	0.007	0.006	0.634	0.074	0.422	0.006	0.576	0.002	0.004	0.004			
Ugar Fm.	BO17sp0094	n. d.	0.06	0.30	23.21	44.00	0.23	13.27	0.12	0.12	15.22	3.66	100.19	1.064	0.001	0.006	0.837	0.084	0.389	0.006	0.605	0.003	0.003	0.003			
Ugar Fm.	BO17sp0095	n. d.	0.13	0.38	18.58	49.48	0.23	11.76	0.07	0.17	16.91	2.43	100.14	1.231	0.003	0.008	0.689	0.057	0.445	0.006	0.551	0.002	0.004	0.004			
Ugar Fm.	BO17sp0096	n. d.	0.29	0.24	19.93	45.62	0.19	13.37	0.13	0.16	14.63	5.46	100.03	1.119	0.007	0.005	0.729	0.128	0.380	0.005	0.618	0.003	0.004	0.004			
Ugar Fm.	BO17sp0097	n. d.	0.31	0.22	21.16	46.21	0.20	12.96	0.09	0.09	15.49	2.98	99.71	1.133	0.007	0.005	0.774	0.070	0.402	0.005	0.599	0.002	0.002	0.002			
Ugar Fm.	BO17sp0098	n. d.	0.04	0.36	21.11	47.05	0.23	12.79	0.07	0.18	15.52	2.42	99.77	1.154	0.001	0.007	0.772	0.056	0.403	0.006	0.591	0.002	0.004	0.004			
Ugar Fm.	BO17sp0099	n. d.	0.04	0.34	15.34	48.48	0.26	10.65	0.08	0.20	17.76	6.68	99.83	1.237	0.001	0.007	0.584	0.162	0.479	0.007	0.512	0.002	0.002	0.002			
Ugar Fm.	BO17sp0100	n. d.	0.07	0.23	17.58	50.95	0.25	12.40	0.06	0.15	15.52	2.54	99.75	1.272	0.002	0.005	0.654	0.060	0.410	0.007	0.583	0.001	0.003	0.003			
Ugar Fm.	BO17sp0101	n. d.	0.05	0.30	21.88	45.17	0.23	13.05	0.10	0.14	15.16	3.52	99.60	1.105	0.001	0.006	0.798	0.082	0.392	0.006	0.602	0.002	0.003	0.003			
Ugar Fm.	BO17sp0102	n. d.	0.09	0.26	24.49	44.27	0.19	15.49	0.12	0.08	12.04	2.90	99.92	1.052	0.002	0.005	0.868	0.066	0.303	0.005	0.694	0.002	0.003	0.002			
Ugar Fm.	BO17sp0103	n. d.	0.07	0.16	23.63	43.63	0.19	14.34	0.14	0.14	13.61	4.43	100.35	1.045	0.002	0.003	0.844	0.101	0.345	0.005	0.647	0.003	0.003	0.003			
Ugar Fm.	BO17sp0104	n. d.	0.09	0.29	22.11	43.99	0.18	12.27	0.13	0.10	16.55	4.16	99.87	1.078	0.002	0.006	0.808	0.097	0.429	0.005	0.567	0.003	0.002	0.002			
Ugar Fm.	BO17sp0105	n. d.	0.17	0.22	23.66	45.23	0.19	14.64	0.10	0.13	13.30	2.51	100.15	1.082	0.004	0.004	0.844	0.057	0.336	0.005	0.660	0.002	0.003	0.002			
Ugar Fm.	BO17sp0106	n. d.	0.20	0.27	25.50	42.78	0.21	13.90	0.09	0.15	14.79	2.36	100.24	1.020	0.004	0.005	0.906	0.054	0.373	0.005	0.625	0.002	0.002	0.002			
Ugar Fm.	BO17sp0107	n. d.	0.05	0.31	21.94	47.61	0.22	14.10	0.10	0.12	13.88	2.09	100.42	1.148	0.001	0.006	0.789	0.048	0.354	0.006	0.641	0.002	0.003	0.003			
Ugar Fm.	BO17sp0108	n. d.	0.08	0.23	29.21	38.71	0.19	14.82	0.11	0.14	13.72	2.66	99.88	0.907	0.002	0.005	1.020	0.059	0.340	0.005	0.654	0.003	0.003	0.003			
Ugar Fm.	BO17sp0109	n. d.	0.02	0.08	23.01	38.65	0.20	14.93	0.10	0.15	13.43	2.87	99.66	0.907	0.002	0.005	1.016	0.064	0.333	0.005	0.661	0.002	0.002	0.002			
Ugar Fm.	BO17sp0120	n. d.	0.12	0.31	16.39	52.52	0.21	12.40	0.06	0.13	15.59	2.34	100.08	1.313	0.003	0.006	0.611	0.066	0.413	0.006	0.585	0.002	0.003	0.003			
Ugar Fm.	BO17sp0121	n. d.	0.20	0.33	24.49	41.80	0.19	14.75	0.13	0.14	13.37	5.01	100.42	0.994	0.005	0.007	0.869	0.114	0.336	0.005	0.661	0.003	0.003	0.003			
Ugar Fm.	BO17sp0122	n. d.	0.05	0.31	20.77	46.24	0.26	12.44	0.08	0.17	16.47	3.11	100.18	1.133	0.001	0.006	0.759	0.040	0.371	0.006	0.575	0.002	0.004	0.004			
Ugar Fm.	BO17sp0123	n. d.	0.30	0.24	14.63	51.42	0.24	13.34	0.07	0.05	14.01	5.89	100.19	1.288	0.007	0.005	0.547	0.192	0.418	0.007	0.630	0.002	0.001	0.001			
Ugar Fm.	BO17sp0124	n. d.	0.18	0.21	18.44	45.96	0.22	11.19	0.12	0.18	17.68	6.22	100.39	1.148	0.004	0.004	0.687	0.148	0.467	0.006	0.527	0.003	0.004	0.004			
Ugar Fm.	BO17sp0125	n. d.	0.08	0.28	24.19	43.76	0.26	12.20	0.10	0.18	17.02	2.28	100.35	1.059	0.002	0.006	0.873	0.053	0.436	0.006	0.557	0.002	0.004	0.004			
Ugar Fm.	BO17sp0126	n. d.	0.06	0.32	18.40	50.13	0.22	12.77	0.09	0.09	15.42	3.03	100.54	1.236	0.001	0.007	0.676	0.071	0.402	0.006	0.593	0.002	0.002	0.002			
Ugar Fm.	BO17sp0127	n. d.	0.12	0.29	19.45	48.40	0.23	13.04	0.07	0.07	15.07	3.28	100.01	1.191	0.003	0.006	0.714	0.077	0.382	0.006	0.605	0.002	0.002	0.002			
Ugar Fm.	BO17sp0128	n. d.	0.06	0.29	24.75	44.60	0.17	14.62	0.11	0.11	13.35	1.68	99.73	1.065	0.001	0.006	0.882	0.038	0.337	0.004	0.658	0.002	0.002	0.002			
Ugar Fm.	BO17sp0129	n. d.	0.05	0.31	20.91	46.63	0.22	12.22	0.08	0.17	16.47	3.11	100.18	1.145	0.001	0.006	0.766	0.073	0.428	0.006	0.566	0.002	0.004	0.004			
Ugar Fm.	BO17sp0130	n. d.	0.05	0.29	24.64	42.93	0.19	13.97	0.12	0.17	14.41	3.60	100.36	1.026	0.001	0.006	0.878	0.082	0.364	0.005	0.629	0.003	0.003	0.003			
Ugar Fm.	BO17sp0131	n. d.	0.08	0.25	25.35	42.39	0.20	14.13	0.11	0.14	14.16	3.10	99.90	1.013	0.002	0.005	0.903	0.070	0.358	0.005	0.636	0.003	0.003	0.003			
Ugar Fm.	BO17sp0132	n. d.	0.05	0.27	23.71	44.35	0.19	13.34	0.09	0.12	15.09	2.44	99.64	1.074	0.001	0.006	0.856	0.056	0.386	0.005	0.609	0.002	0.003	0.003			
Ugar Fm.	BO17sp0133	n. d.	0.21	0.33	10.96	52.22	0.36	7.60	0.06	0.23	21.81	6.10	99.89	1.386	0.005	0.007	0.434	0.154	0.612	0.010	0.380	0.002	0.006	0.006			
Ugar Fm.	BO17sp0134	n. d.	0.04	0.31	22.15	46.32	0.20	13.80	0.09	0.13	14.04	2.27	99.35	1.128	0.001	0.006	0.804	0.053	0.362	0.005	0.633	0.002	0.003	0.003			
Ugar Fm.	BO17sp0135	n. d.	0.08	0.26	24.96	44.01	0.18	14.27	0.10	0.14	13.95	1.94	99.90	1.052	0.002	0.005	0.889	0.044	0.353	0.005	0.643	0.002	0.003	0.003			
Ugar Fm.	BO17sp0136	n. d.	1.20	0.45	14.89	45.02	0.28	10.78	0.17	0.14	18.68	8.68	100.30	1.146	0.029	0.010	0.565	0.210	0.503	0.008	0.517	0.004	0.003	0.003			
Ugar Fm.	BO17sp0137	n. d.	0.10	0.22	25.51	41.22	0.22	14.31	0.13	0.13	13.83	4.10	99.77	0.984	0.002	0.004	0.909	0.042	0.349	0.006	0.644	0.003	0.003	0.003			
Ugar Fm.	BO17sp0138	n. d.	0.06	0.25	26.31	42.27	0.21	13.78	0.08	0.11	14.87	1.87	99.80	1.008	0.001	0.006	0.936	0.042	0.375	0.005	0.620	0.002	0.002	0.002			
Ugar Fm.	BO17sp0139	n. d.	0.10	0.26	24.61	44.09	0.15	15.08	0.10	0.08	12.71	2.59	99.57	1.051	0.002	0.005	0.825	0.076	0.320	0.004	0.678	0.002	0.003	0.003			
Ugar Fm.	BO17sp0140	n. d.	0.07	0.25	22.61	44.71	0.21	13.27	0.09	0.14	14.93	3.27	99.74	1.089	0.002	0.005	0.851	0.076	0.385	0.005	0.609	0.002	0.002	0.002			
Ugar Fm.	BO17sp0141	n. d.	0.12	0.23	22.42	46.55	0.16	14.36	0.11	0.11	13.42	2.29	99.77	1.124	0.003	0.005	0.808	0.053	0.343	0.004	0.654	0.003	0.003	0.002			
Ugar Fm.	BO17sp0142	n. d.	0.12	0.22	22.37	46.60	0.19	14.39	0.12	0.12	13.43	2.61	100.18	1.122	0.003	0.003	0.842	0.060	0.342	0.005	0.653	0.003	0.003	0.003			
Ugar Fm.	BO17sp0143	n. d.	0.04	0.32	24.93	43.62	0.18	13.50	0.06	0.15	15.06	1.77	99.61	1.050	0.001	0.006	0.895	0.040	0.383	0.005	0.612	0.001	0.003	0.003			
Ugar Fm.	BO17sp0144	n. d.	0.10	0.29	19.30	48.68	0.22	13.31	0.11	0.09	14.55	3.27	99.92	1.198	0.002	0.006	0.708	0.077	0.379	0.006	0.617	0.003	0.002	0.002			
Ugar Fm.	BO17sp0145	n. d.	0.14	0.33	16.17	50.32	0.27	10.43	0.06	0.13	18.61	3.90	100.36	1.274	0.003	0.007	0.611	0.094	0.498	0.007	0.498	0.002					

analyses in wt%. Shown are the recalculated FeO and Fe<sub>2</sub>O<sub>3</sub> values and the amended total

Formation	Sample & spot ID	analyses in wt%. Shown are the recalculated FeO and Fe <sub>2</sub> O <sub>3</sub> values and the amended total											cations per formula unit on the basis of 3 oxygens										
		SiO <sub>2</sub>	TiO <sub>2</sub>	V <sub>2</sub> O <sub>5</sub>	Al <sub>2</sub> O <sub>3</sub>	Cr <sub>2</sub> O <sub>3</sub>	MnO	MgO	NiO	ZnO	FeO	Fe <sub>2</sub> O <sub>3</sub>	Total	Cr	Ti	V	Al	Fe <sup>3+</sup>	Fe <sup>2+</sup>	Mn	Mg	Ni	Zn
Ugar Fm.	BO17sp053	n. d.	0.05	0.33	18.00	49.00	0.33	9.32	0.06	0.20	20.20	2.15	99.63	1.247	0.001	0.007	0.683	0.052	0.544	0.009	0.447	0.001	0.005
Ugar Fm.	BO17sp054	n. d.	0.14	0.28	33.39	34.71	0.20	15.45	0.10	0.25	13.20	1.50	99.22	0.801	0.003	0.005	1.149	0.033	0.322	0.005	0.672	0.002	0.005
Ugar Fm.	BO17sp055	n. d.	0.12	0.33	21.92	45.39	0.24	10.73	0.09	0.17	15.73	2.88	99.57	1.112	0.003	0.007	0.801	0.067	0.408	0.006	0.588	0.002	0.003
Ugar Fm.	BO17sp056	n. d.	0.23	0.35	13.75	55.13	0.26	10.46	0.17	0.24	18.29	1.63	100.28	1.409	0.005	0.007	0.524	0.040	0.495	0.007	0.504	0.001	0.004
Ugar Fm.	BO17sp057	n. d.	0.06	0.30	22.09	45.12	0.22	13.25	0.10	0.13	15.18	4.02	100.48	1.093	0.001	0.006	0.798	0.093	0.389	0.006	0.605	0.003	0.003
Ugar Fm.	BO17sp058	n. d.	0.13	0.36	20.87	47.15	0.28	11.24	0.05	0.20	17.96	1.75	99.99	1.167	0.003	0.007	0.770	0.041	0.470	0.007	0.524	0.001	0.005
Ugar Fm.	BO17sp059	n. d.	0.12	0.20	31.08	36.33	0.17	14.48	0.09	0.24	14.45	2.54	99.71	0.848	0.003	0.004	1.082	0.056	0.357	0.004	0.637	0.002	0.005
Ugar Fm.	BO17sp060	n. d.	0.17	0.18	31.49	35.79	0.21	14.54	0.11	0.26	14.56	2.99	100.30	0.830	0.004	0.003	1.089	0.066	0.357	0.005	0.636	0.003	0.006
Ugar Fm.	BO17sp061	n. d.	0.18	0.46	31.15	35.85	0.17	14.69	0.16	0.15	14.14	3.15	99.77	0.835	0.001	0.010	0.643	0.127	0.501	0.008	0.496	0.004	0.003
Ugar Fm.	BO17sp062	n. d.	0.06	0.25	31.15	35.85	0.17	14.69	0.16	0.15	14.14	3.15	99.77	0.835	0.001	0.010	0.643	0.127	0.501	0.008	0.496	0.004	0.003
Ugar Fm.	BO17sp063	n. d.	0.09	0.28	22.89	45.96	0.22	14.66	0.09	0.07	13.08	2.60	99.93	1.104	0.002	0.006	0.820	0.059	0.333	0.006	0.664	0.002	0.004
Ugar Fm.	BO17sp064	n. d.	0.05	0.24	33.39	32.28	0.17	15.63	0.16	0.20	12.99	4.76	99.87	0.741	0.001	0.005	1.143	0.104	0.315	0.004	0.676	0.004	0.004
Ugar Fm.	BO17sp065	n. d.	0.04	0.04	20.76	47.53	0.23	13.02	0.08	0.15	15.14	2.71	99.95	1.164	0.001	0.006	0.758	0.063	0.392	0.006	0.601	0.002	0.003
Ugar Fm.	BO17sp066	n. d.	0.15	0.29	23.52	44.14	0.22	13.19	0.09	0.13	15.42	2.76	99.56	1.068	0.003	0.006	0.849	0.064	0.395	0.006	0.602	0.002	0.003
Ugar Fm.	BO17sp067	n. d.	0.33	0.30	23.72	43.32	0.19	15.12	0.14	0.08	12.57	3.79	99.56	1.038	0.008	0.006	0.848	0.086	0.319	0.005	0.683	0.003	0.002
Ugar Fm.	BO17sp068	n. d.	0.13	0.26	28.71	38.98	0.23	13.97	0.10	0.22	14.81	2.14	99.55	0.922	0.003	0.005	1.013	0.048	0.371	0.006	0.623	0.002	0.005
Ugar Fm.	BO17sp069	n. d.	0.11	0.24	24.77	41.51	0.21	12.55	0.09	0.21	16.34	3.53	99.55	1.007	0.003	0.005	0.896	0.081	0.419	0.005	0.574	0.002	0.005
Ugar Fm.	BO17sp070	n. d.	0.27	0.31	18.44	46.84	0.24	12.31	0.11	0.12	15.91	5.00	99.56	1.169	0.007	0.006	0.686	0.119	0.420	0.006	0.579	0.003	0.003
Ugar Fm.	BO17sp071	n. d.	0.60	0.29	19.77	44.37	0.32	10.48	0.09	0.30	18.80	6.74	99.96	1.120	0.014	0.006	0.676	0.162	0.502	0.009	0.499	0.002	0.007
Ugar Fm.	BO17sp072	n. d.	0.10	0.28	23.39	45.48	0.20	14.65	0.13	0.08	13.19	2.51	100.00	1.090	0.002	0.006	0.836	0.057	0.334	0.005	0.662	0.003	0.002
Ugar Fm.	BO17sp073	n. d.	0.07	0.26	24.13	43.65	0.21	14.99	0.12	0.12	12.71	3.86	100.12	1.041	0.002	0.005	0.858	0.088	0.320	0.005	0.674	0.003	0.003
Ugar Fm.	BO17sp074	n. d.	0.49	0.26	22.37	43.67	0.25	11.69	0.10	0.20	17.84	3.44	100.31	1.069	0.011	0.005	0.817	0.080	0.462	0.006	0.539	0.002	0.005
Ugar Fm.	BO17sp075	n. d.	0.14	0.19	28.16	40.37	0.17	14.74	0.10	0.13	13.68	1.98	99.67	0.951	0.003	0.004	0.990	0.045	0.341	0.004	0.655	0.002	0.003
Ugar Fm.	BO17sp076	n. d.	0.14	0.26	20.82	47.84	0.26	11.90	0.06	0.18	17.00	1.73	100.19	1.177	0.003	0.004	0.443	0.443	0.341	0.007	0.552	0.001	0.004
Ugar Fm.	BO17sp077	n. d.	0.04	0.27	21.53	46.52	0.20	13.19	0.10	0.17	15.05	3.12	100.21	1.132	0.001	0.006	0.782	0.388	0.050	0.005	0.605	0.003	0.004
Ugar Fm.	BO17sp078	n. d.	0.06	0.29	24.14	44.62	0.19	14.83	0.10	0.11	12.98	2.61	99.93	1.066	0.001	0.006	0.860	0.059	0.328	0.005	0.655	0.002	0.002
Ugar Fm.	BO17sp079	n. d.	0.13	0.28	17.79	48.02	0.29	10.76	0.06	0.14	18.17	4.36	100.02	1.209	0.003	0.006	0.688	0.105	0.484	0.008	0.511	0.002	0.003
Ugar Fm.	BO17sp080	n. d.	0.09	0.24	22.27	45.77	0.18	14.78	0.14	0.05	12.83	3.82	100.18	1.100	0.002	0.005	0.798	0.058	0.378	0.005	0.670	0.004	0.001
Ugar Fm.	BO17sp081	n. d.	0.21	0.25	24.30	43.74	0.20	13.64	0.12	0.22	14.86	2.55	100.09	1.051	0.005	0.005	0.871	0.058	0.378	0.005	0.618	0.003	0.005
Ugar Fm.	BO17sp082	n. d.	0.12	0.29	20.23	47.25	0.21	12.99	0.09	0.17	15.19	3.51	100.05	1.159	0.003	0.006	0.740	0.082	0.394	0.006	0.601	0.002	0.004
Ugar Fm.	BO17sp083	n. d.	0.26	0.32	21.97	46.51	0.21	13.27	0.09	0.15	15.29	2.22	100.28	1.128	0.006	0.006	0.795	0.051	0.392	0.005	0.607	0.002	0.003
Ugar Fm.	BO17sp084	n. d.	0.28	0.29	23.54	45.41	0.17	14.57	0.10	0.14	13.61	2.20	100.31	1.086	0.006	0.006	0.839	0.050	0.344	0.004	0.657	0.002	0.003
Ugar Fm.	BO17sp085	n. d.	0.27	0.23	23.50	45.36	0.17	14.43	0.07	0.13	13.74	2.20	100.10	1.087	0.006	0.005	0.840	0.050	0.348	0.004	0.652	0.002	0.003
Ugar Fm.	BO17sp086	n. d.	0.10	0.21	24.37	43.30	0.20	13.93	0.09	0.13	14.33	3.22	99.86	1.040	0.002	0.004	0.873	0.074	0.364	0.005	0.631	0.002	0.003
Ugar Fm.	BO17sp087	n. d.	0.19	0.22	27.39	39.97	0.17	13.90	0.13	0.17	15.00	3.07	100.22	0.946	0.004	0.004	0.967	0.069	0.376	0.004	0.620	0.003	0.004
Ugar Fm.	BO17sp088	n. d.	0.12	0.25	28.00	40.28	0.16	15.68	0.15	0.12	12.30	2.91	99.97	0.942	0.003	0.005	0.977	0.065	0.304	0.004	0.692	0.003	0.003
Ugar Fm.	BO17sp089	n. d.	0.16	0.28	23.90	43.36	0.18	13.93	0.14	0.13	14.40	3.64	100.13	1.041	0.004	0.006	0.856	0.083	0.366	0.005	0.631	0.003	0.003
Ugar Fm.	BO17sp090	n. d.	0.30	0.37	27.11	38.13	0.18	13.68	0.15	0.19	15.39	4.66	100.18	0.905	0.007	0.007	0.960	0.105	0.387	0.005	0.612	0.004	0.004
Ugar Fm.	BO17sp091	n. d.	0.20	0.33	18.09	48.12	0.31	9.67	0.06	0.30	19.95	3.36	100.37	1.214	0.005	0.007	0.681	0.081	0.533	0.008	0.460	0.001	0.007
Ugar Fm.	TD15sp001	n. d.	0.07	0.21	24.05	45.43	0.20	14.70	0.11	0.09	13.16	2.02	100.02	1.085	0.002	0.004	0.857	0.046	0.333	0.005	0.662	0.003	0.002
Ugar Fm.	TD15sp002	n. d.	0.24	0.23	26.81	41.38	0.18	13.64	0.10	0.20	15.22	1.74	99.75	0.987	0.005	0.005	0.953	0.039	0.384	0.005	0.613	0.002	0.004
Ugar Fm.	TD15sp003	n. d.	0.17	0.30	21.30	45.35	0.20	12.34	0.15	0.09	16.65	3.61	100.32	1.110	0.007	0.007	0.778	0.084	0.431	0.005	0.589	0.004	0.002
Ugar Fm.	TD15sp004	n. d.	0.10	0.29	12.51	57.91	0.23	11.85	0.04	0.10	15.90	1.08	100.06	1.477	0.004	0.006	0.476	0.026	0.429	0.006	0.570	0.001	0.002
Ugar Fm.	TD15sp009	n. d.	0.16	0.24	16.14	51.94	0.27	10.25	0.05	0.16	18.74	2.06	100.01	1.320	0.004	0.005	0.612	0.050	0.504	0.007	0.491	0.001	0.004
Ugar Fm.	TD15sp010	n. d.	0.48	0.45	19.72	42.86	0.28	9.89	0.12	0.18	20.23	6.15	100.36	1.074	0.011	0.009	0.737	0.147	0.536	0.007	0.467	0.003	0.004
Ugar Fm.	TD																						

Formation		Sample & spot ID		analyses in wt%. Shown are the recalculated FeO and Fe <sub>2</sub> O <sub>3</sub> values and the amended total																		
				cations per formula unit on the basis of 3 oxygens												Total						
SrO <sub>2</sub>	TiO <sub>2</sub>	V <sub>2</sub> O <sub>5</sub>	Al <sub>2</sub> O <sub>3</sub>	Cr <sub>2</sub> O <sub>3</sub>	MnO	MgO	NiO	ZnO	FeO	Fe <sub>2</sub> O <sub>3</sub>	Total	Cr	Ti	V	Al	Fe <sup>3+</sup>	Fe <sup>2+</sup>	Mn	Mg	Ni	Zn	
n. d.	0.10	0.27	25.06	42.15	0.21	12.41	0.08	0.19	16.63	2.34	99.43	1.023	0.002	0.006	0.907	0.054	0.427	0.005	0.568	0.002	0.004	
n. d.	3.26	0.71	16.81	31.93	0.34	7.63	0.22	0.22	25.62	13.73	100.48	0.824	0.080	0.015	0.647	0.337	0.699	0.009	0.371	0.006	0.005	
n. d.	0.04	0.27	20.81	46.78	0.20	12.39	0.07	0.23	15.82	2.55	99.16	1.158	0.001	0.006	0.788	0.060	0.414	0.005	0.578	0.002	0.005	
n. d.	0.04	0.29	21.44	46.38	0.21	12.26	0.09	0.24	16.16	2.24	99.36	1.144	0.001	0.006	0.789	0.063	0.422	0.006	0.570	0.002	0.006	
n. d.	0.18	0.35	15.48	52.85	0.30	10.13	0.06	0.20	18.69	1.26	99.49	1.353	0.004	0.007	0.591	0.031	0.506	0.008	0.489	0.002	0.005	
n. d.	0.03	0.27	20.54	47.99	0.22	12.49	0.08	0.13	15.75	1.86	99.38	1.186	0.001	0.006	0.757	0.044	0.412	0.006	0.582	0.002	0.003	
n. d.	0.06	0.22	15.24	53.77	0.24	11.20	0.06	0.11	16.87	1.50	99.27	1.371	0.001	0.005	0.580	0.036	0.455	0.007	0.538	0.002	0.003	
n. d.	0.09	0.27	22.86	45.51	0.18	13.61	0.14	0.12	14.46	2.16	99.40	1.106	0.002	0.005	0.828	0.050	0.372	0.005	0.623	0.003	0.003	
n. d.	0.08	0.29	20.50	47.16	0.23	12.02	0.07	0.14	16.51	2.35	99.34	1.170	0.002	0.006	0.758	0.055	0.433	0.006	0.562	0.002	0.003	
n. d.	0.15	0.28	22.44	42.94	0.21	12.57	0.14	0.17	15.95	4.64	99.50	1.052	0.003	0.006	0.820	0.108	0.414	0.006	0.581	0.004	0.004	
n. d.	0.05	0.26	26.46	42.83	0.17	13.66	0.08	0.16	14.95	0.78	99.40	1.025	0.001	0.005	0.944	0.018	0.378	0.004	0.616	0.002	0.004	
n. d.	0.07	0.26	20.01	48.51	0.24	12.57	0.07	0.15	15.61	2.09	99.57	1.199	0.002	0.005	0.737	0.049	0.408	0.006	0.586	0.002	0.004	
n. d.	1.62	0.63	15.70	36.68	0.32	8.19	0.24	0.17	22.87	13.32	99.74	0.953	0.040	0.014	0.608	0.330	0.629	0.009	0.401	0.006	0.004	
n. d.	0.04	0.31	19.02	48.98	0.33	10.57	0.09	0.11	18.33	1.41	99.20	1.235	0.001	0.007	0.715	0.034	0.489	0.009	0.502	0.002	0.003	
n. d.	0.03	0.22	22.36	43.79	0.19	13.63	0.12	0.11	14.18	4.55	99.18	1.069	0.001	0.005	0.814	0.106	0.366	0.005	0.627	0.003	0.002	
n. d.	0.07	0.23	27.72	39.12	0.21	12.63	0.10	0.27	16.48	2.34	99.16	0.940	0.002	0.005	0.993	0.054	0.419	0.005	0.572	0.002	0.006	
n. d.	0.03	0.25	19.82	48.75	0.17	13.38	0.12	0.09	14.33	2.51	99.45	1.201	0.001	0.005	0.728	0.059	0.373	0.004	0.621	0.003	0.002	
n. d.	0.27	0.28	16.27	45.61	0.26	10.72	0.12	0.13	17.74	7.68	99.07	1.167	0.006	0.006	0.621	0.187	0.480	0.007	0.517	0.003	0.003	
n. d.	0.06	0.32	20.36	48.36	0.23	12.36	0.07	0.11	15.95	1.39	99.22	1.198	0.001	0.007	0.752	0.033	0.418	0.006	0.577	0.002	0.003	
n. d.	0.11	0.27	13.43	53.78	0.31	9.29	0.02	0.19	19.43	2.31	99.14	1.403	0.003	0.006	0.522	0.057	0.536	0.009	0.457	0.001	0.005	
n. d.	0.06	0.31	20.97	46.73	0.26	12.33	0.07	0.18	16.00	2.37	99.31	1.155	0.001	0.006	0.773	0.056	0.418	0.007	0.574	0.002	0.004	
n. d.	0.10	0.32	18.27	50.78	0.25	11.79	0.05	0.16	16.46	0.94	99.13	1.275	0.002	0.007	0.684	0.064	0.437	0.007	0.568	0.001	0.004	
n. d.	0.06	0.24	23.90	43.50	0.20	12.66	0.06	0.18	16.12	2.77	99.69	1.057	0.001	0.005	0.866	0.064	0.414	0.005	0.580	0.001	0.004	
n. d.	0.06	0.39	16.03	50.98	0.29	10.08	0.05	0.24	18.67	2.54	99.34	1.305	0.002	0.008	0.662	0.062	0.506	0.008	0.487	0.001	0.006	
n. d.	0.05	0.24	26.00	43.42	0.20	13.70	0.10	0.18	14.60	0.53	99.05	1.043	0.001	0.005	0.932	0.012	0.371	0.005	0.622	0.003	0.004	
n. d.	0.07	0.24	25.18	42.97	0.20	13.72	0.11	0.15	14.65	2.18	99.45	1.033	0.002	0.005	0.903	0.050	0.373	0.005	0.621	0.003	0.003	
n. d.	0.08	0.22	24.87	44.37	0.16	14.19	0.11	0.12	13.88	1.36	99.36	1.066	0.002	0.004	0.891	0.031	0.353	0.004	0.642	0.003	0.003	
n. d.	0.11	0.26	20.38	47.58	0.24	11.98	0.06	0.15	16.46	1.84	99.21	1.007	0.001	0.005	0.940	0.040	0.375	0.005	0.617	0.003	0.004	
n. d.	0.10	0.28	14.56	54.19	0.28	10.30	0.06	0.20	18.12	1.23	99.31	1.394	0.002	0.006	0.559	0.030	0.493	0.008	0.499	0.002	0.005	
n. d.	0.16	0.30	20.82	48.48	0.20	13.50	0.10	0.10	14.57	1.60	99.83	1.184	0.004	0.006	0.758	0.037	0.376	0.005	0.622	0.002	0.002	
n. d.	0.06	0.29	23.28	44.41	0.20	12.85	0.13	0.13	15.90	2.96	100.21	1.076	0.001	0.006	0.841	0.068	0.407	0.005	0.587	0.003	0.003	
n. d.	0.06	0.37	18.08	50.39	0.23	10.90	0.08	0.18	18.18	2.01	100.48	1.259	0.001	0.008	0.674	0.048	0.481	0.006	0.514	0.002	0.004	
n. d.	0.07	0.30	21.28	46.39	0.23	12.73	0.12	0.12	15.75	3.18	100.17	1.134	0.002	0.006	0.776	0.074	0.407	0.006	0.587	0.003	0.003	
n. d.	0.05	0.32	22.25	45.31	0.23	11.53	0.08	0.19	17.56	2.14	99.67	1.116	0.001	0.007	0.817	0.050	0.458	0.006	0.535	0.002	0.004	
n. d.	0.04	0.30	21.97	46.83	0.23	12.34	0.08	0.14	16.54	1.89	100.35	1.142	0.001	0.006	0.799	0.044	0.427	0.006	0.567	0.002	0.003	
n. d.	0.31	0.25	25.88	42.41	0.22	13.21	0.07	0.14	15.86	1.39	99.74	1.017	0.007	0.005	0.926	0.032	0.403	0.006	0.597	0.002	0.003	
n. d.	0.06	0.31	21.26	47.52	0.21	11.68	0.03	0.21	17.34	1.34	99.95	1.171	0.001	0.006	0.781	0.031	0.398	0.005	0.543	0.001	0.005	
n. d.	0.07	0.31	20.72	49.85	0.18	11.63	0.09	0.15	16.41	0.00	99.40	1.243	0.001	0.007	0.771	0.000	0.433	0.005	0.547	0.002	0.006	
n. d.	0.15	0.36	22.63	46.45	0.22	13.02	0.09	0.16	15.45	1.00	99.53	1.132	0.003	0.007	0.822	0.023	0.398	0.006	0.598	0.002	0.004	
n. d.	0.06	0.26	22.28	46.89	0.20	12.94	0.08	0.15	15.66	1.76	100.29	1.138	0.001	0.005	0.807	0.041	0.402	0.005	0.592	0.002	0.003	
n. d.	0.05	0.35	17.90	49.93	0.24	11.70	0.06	0.15	16.65	2.54	99.56	1.252	0.001	0.007	0.669	0.061	0.442	0.006	0.553	0.001	0.003	
n. d.	0.04	0.26	20.74	44.34	0.24	11.25	0.11	0.25	17.84	5.42	100.49	1.095	0.001	0.005	0.764	0.128	0.466	0.006	0.524	0.003	0.006	
n. d.	0.15	0.25	23.30	45.97	0.17	14.44	0.10	0.09	13.56	1.95	99.97	1.104	0.003	0.005	0.834	0.045	0.344	0.004	0.654	0.002	0.002	
n. d.	0.03	0.36	17.13	51.66	0.25	11.36	0.06	0.16	17.28	2.11	100.42	1.293	0.001	0.007	0.639	0.050	0.457	0.007	0.536	0.001	0.004	
n. d.	0.08	0.28	24.20	44.39	0.21	13.49	0.09	0.11	14.93	1.75	99.53	1.072	0.002	0.006	0.872	0.040	0.381	0.005	0.614	0.002	0.003	
n. d.	0.07	0.30	15.37	51.51	0.33	8.71	0.05	0.30	20.69	2.54	99.86	1.329	0.002	0.006	0.591	0.062	0.565	0.009	0.424	0.001	0.007	
n. d.	0.07	0.32	19.70	48.45	0.21	12.16	0.08	0.16	16.33	2.40	99.87	1.199	0.002	0.007	0.727	0.056	0.528	0.005	0.567	0.002	0.004	
n. d.	0.17	0.29	23.13	45.44	0.23	13.36	0.09	0.14	14.99	1.67	99.52	1.103	0.004	0.006	0.838	0.039	0.385	0.006	0.612	0.002	0.003	
n. d.	0.26	0.48	20.72	42.45	0.24	10.95	0.12	0.15	18.49	5.99	99.85	1.056	0.006	0.010	0.769	0.142	0.487	0.007	0.514	0.003	0.003	
n. d.	0.06	0.32	19.97	48.26	0.24	12.21	0.07	0.14	16.29	2.34	99.89	1.192	0.001	0.007	0.736	0.055	0.426	0.006	0.569	0.002	0.003	
n. d.	0.04	0.30	20.69	47.75	0.20	11.93	0.07	0.15	16.74	1.67	99.54	1.182	0.001	0.006	0.764	0.039	0.438	0.005	0.557	0.002	0.003	
n. d.	0.11	0.37	15.20	52.63	0.28	9.92	0.05	0.20	19.17	2.36	100.27	1.349	0.003	0.008	0.578	0.057	0.437	0.008	0.477	0.001	0.004	
n. d.	0.05	0.34	19.49	49.08	0.23	11.95	0.07	0.17	16.56	1.79	99.73	1.219	0.001	0.007	0.722	0.042	0.435	0.006	0.477	0.002	0.004	

analyses in wt%. Shown are the recalculated FeO and Fe<sub>2</sub>O<sub>3</sub> values and the amended total

Formation	Sample & spot ID	analyses in wt%																	Cations per formula unit on the basis of 3 oxygens										
		SiO <sub>2</sub>	TiO <sub>2</sub>	V <sub>2</sub> O <sub>5</sub>	Al <sub>2</sub> O <sub>3</sub>	Cr <sub>2</sub> O <sub>3</sub>	MnO	MgO	NiO	ZnO	FeO	Fe <sub>2</sub> O <sub>3</sub>	Total	Cr	Ti	V	Al	Fe <sup>3+</sup>	Fe <sup>2+</sup>	Mn	Mg	Ni	Zn						
Ugar Fm.	TD151sp053	n. d.	0.03	0.30	20.61	48.19	0.22	12.68	0.09	0.11	15.78	2.24	100.24	1.181	0.001	0.006	0.753	0.052	0.409	0.006	0.586	0.002	0.002						
Ugar Fm.	TD151sp054	n. d.	0.13	0.29	22.41	45.88	0.21	12.47	0.08	0.12	16.37	1.93	99.88	1.120	0.003	0.006	0.816	0.045	0.423	0.005	0.574	0.002	0.003						
Ugar Fm.	TD151sp096	n. d.	0.09	0.04	17.22	51.22	0.29	10.76	0.07	0.25	18.07	2.06	100.32	1.288	0.002	0.006	0.646	0.049	0.481	0.008	0.510	0.002	0.006						
Vranduk Fm.	BO115sp002	n. d.	0.04	0.28	29.39	37.63	0.19	13.60	0.11	0.20	15.40	2.53	99.36	0.891	0.001	0.006	1.038	0.057	0.386	0.005	0.607	0.003	0.004						
Vranduk Fm.	BO115sp003	n. d.	0.05	0.41	16.05	52.64	0.32	10.03	0.04	0.24	18.96	1.22	99.97	1.340	0.001	0.009	0.609	0.030	0.511	0.009	0.481	0.001	0.006						
Vranduk Fm.	BO115sp004	n. d.	0.06	0.20	34.31	32.91	0.16	15.41	0.13	0.22	13.31	2.52	99.23	0.757	0.001	0.004	1.177	0.055	0.324	0.004	0.688	0.003	0.005						
Vranduk Fm.	BO115sp005	n. d.	0.05	0.29	25.40	41.10	0.25	12.46	0.09	0.21	16.56	3.26	99.67	0.994	0.001	0.006	0.916	0.075	0.424	0.006	0.568	0.002	0.005						
Vranduk Fm.	BO115sp006	n. d.	0.11	0.29	26.73	39.70	0.23	12.69	0.09	0.20	16.55	3.23	99.82	0.952	0.003	0.006	0.956	0.074	0.420	0.006	0.574	0.002	0.004						
Vranduk Fm.	BO115sp007	n. d.	0.07	0.39	20.79	46.62	0.27	11.53	0.08	0.19	17.53	2.76	100.22	1.150	0.002	0.008	0.765	0.065	0.457	0.007	0.536	0.002	0.004						
Vranduk Fm.	BO115sp008	n. d.	0.16	0.26	29.41	29.90	0.25	11.46	0.20	0.33	18.55	9.34	99.86	0.717	0.004	0.005	1.052	0.213	0.470	0.007	0.518	0.005	0.007						
Vranduk Fm.	BO115sp009	n. d.	0.04	0.38	25.71	41.73	0.24	12.56	0.12	0.23	16.79	2.75	100.51	1.000	0.001	0.008	1.047	0.063	0.426	0.006	0.567	0.002	0.005						
Vranduk Fm.	BO115sp010	n. d.	0.05	0.27	29.80	37.40	0.19	13.88	0.12	0.19	15.10	2.57	99.56	0.881	0.001	0.005	1.047	0.058	0.376	0.005	0.617	0.003	0.004						
Vranduk Fm.	BO115sp011	n. d.	0.05	0.26	33.07	33.42	0.20	14.02	0.15	0.21	15.23	2.67	99.27	0.779	0.001	0.005	1.149	0.059	0.375	0.005	0.616	0.003	0.005						
Vranduk Fm.	BO115sp012	n. d.	0.11	0.28	13.00	52.32	0.29	10.61	0.08	0.15	17.48	5.37	99.69	1.350	0.003	0.006	1.212	0.132	0.477	0.008	0.516	0.002	0.004						
Vranduk Fm.	BO115sp013	n. d.	0.09	0.43	19.72	45.52	0.25	10.10	0.10	0.19	15.32	2.60	99.47	0.712	0.006	0.004	1.212	0.055	0.387	0.004	0.608	0.003	0.007						
Vranduk Fm.	BO115sp020	n. d.	0.05	0.30	26.04	41.32	0.20	13.34	0.10	0.19	17.55	2.67	99.50	1.185	0.002	0.008	0.730	0.064	0.464	0.007	0.532	0.002	0.004						
Vranduk Fm.	BO115sp021	n. d.	0.10	0.38	19.60	47.42	0.25	11.29	0.08	0.15	17.55	2.67	99.50	1.185	0.002	0.008	0.730	0.064	0.464	0.007	0.532	0.002	0.004						
Vranduk Fm.	BO115sp022	n. d.	0.06	0.30	24.27	42.15	0.23	11.97	0.06	0.20	16.92	2.58	98.75	1.035	0.001	0.006	0.889	0.060	0.439	0.006	0.554	0.002	0.005						
Vranduk Fm.	BO115sp023	n. d.	0.06	0.19	40.23	25.81	0.16	16.19	0.20	0.18	12.85	2.85	98.72	0.580	0.001	0.004	1.349	0.061	0.305	0.004	0.686	0.005	0.004						
Vranduk Fm.	BO115sp024	n. d.	0.06	0.24	28.44	38.35	0.22	13.40	0.11	0.18	15.53	2.85	99.37	0.913	0.001	0.005	1.010	0.065	0.391	0.006	0.601	0.003	0.004						
Vranduk Fm.	BO115sp025	n. d.	0.06	0.20	31.14	34.56	0.22	13.29	0.15	0.20	16.08	3.65	99.57	0.814	0.001	0.004	1.093	0.082	0.401	0.006	0.590	0.004	0.004						
Vranduk Fm.	BO115sp026	n. d.	0.04	0.35	22.83	43.69	0.22	12.03	0.07	0.19	16.75	3.00	99.17	1.075	0.001	0.007	0.838	0.070	0.436	0.006	0.558	0.002	0.004						
Vranduk Fm.	BO115sp027	n. d.	0.04	0.32	24.24	43.10	0.20	12.94	0.09	0.18	16.61	2.53	99.25	1.047	0.001	0.006	0.878	0.058	0.401	0.005	0.593	0.002	0.004						
Vranduk Fm.	BO115sp028	n. d.	0.15	0.31	17.36	48.36	0.28	11.19	0.06	0.20	17.23	4.21	99.35	1.223	0.004	0.007	0.655	0.101	0.461	0.008	0.533	0.001	0.005						
Vranduk Fm.	BO115sp029	n. d.	0.05	0.27	24.73	42.06	0.24	12.72	0.08	0.18	15.99	3.02	99.35	1.021	0.001	0.006	0.895	0.070	0.411	0.006	0.582	0.002	0.005						
Vranduk Fm.	BO115sp030	n. d.	0.04	0.32	19.10	49.18	0.28	11.69	0.07	0.21	16.84	2.20	99.93	1.223	0.001	0.007	0.709	0.052	0.443	0.007	0.548	0.002	0.005						
Vranduk Fm.	BO115sp031	n. d.	0.14	0.29	26.61	39.74	0.25	12.24	0.07	0.19	17.13	2.75	99.41	0.960	0.003	0.006	0.958	0.063	0.438	0.006	0.557	0.002	0.004						
Vranduk Fm.	BO115sp032	0.16	0.09	0.29	29.47	36.38	0.22	13.93	0.13	0.16	15.02	4.04	98.88	0.858	0.002	0.006	1.036	0.091	0.375	0.005	0.619	0.003	0.004						
Vranduk Fm.	BO115sp033	n. d.	0.06	0.31	20.95	46.00	0.24	11.98	0.07	0.17	16.72	3.32	99.62	1.135	0.001	0.006	0.771	0.078	0.437	0.006	0.557	0.002	0.004						
Vranduk Fm.	BO115sp034	n. d.	0.08	0.27	29.03	37.79	0.20	13.88	0.12	0.19	15.00	3.08	99.63	0.893	0.002	0.005	1.023	0.069	0.375	0.005	0.618	0.003	0.004						
Vranduk Fm.	BO115sp035	n. d.	1.13	0.44	19.35	37.17	0.57	6.14	0.14	0.39	25.96	9.14	100.44	0.957	0.028	0.009	0.743	0.224	0.707	0.016	0.298	0.004	0.009						
Vranduk Fm.	BO115sp036	n. d.	0.07	0.37	13.43	53.76	0.26	10.00	0.06	0.15	18.71	3.25	100.05	1.384	0.002	0.008	0.516	0.080	0.510	0.007	0.485	0.002	0.004						
Vranduk Fm.	BO115sp037	n. d.	0.14	0.28	13.10	53.95	0.31	9.99	0.06	0.20	18.60	3.53	100.15	1.391	0.003	0.006	0.504	0.037	0.507	0.009	0.485	0.002	0.005						
Vranduk Fm.	BO115sp038	n. d.	0.06	0.24	25.16	43.92	0.21	13.71	0.08	0.16	14.80	1.62	99.96	1.052	0.001	0.005	0.898	0.037	0.375	0.005	0.619	0.002	0.003						
Vranduk Fm.	BO115sp039	n. d.	0.07	0.34	28.52	38.52	0.25	12.93	0.09	0.22	16.50	2.62	100.05	0.914	0.002	0.007	1.009	0.059	0.414	0.006	0.578	0.002	0.005						
Vranduk Fm.	BO115sp040	n. d.	0.12	0.35	19.74	45.92	0.29	10.25	0.07	0.19	19.33	3.97	100.22	1.148	0.003	0.007	0.759	0.084	0.511	0.008	0.483	0.002	0.004						
Vranduk Fm.	BO115sp041	n. d.	0.04	0.32	20.54	46.78	0.23	11.94	0.07	0.16	16.59	2.74	99.44	1.160	0.001	0.007	0.759	0.065	0.435	0.006	0.568	0.002	0.004						
Vranduk Fm.	BO115sp042	n. d.	0.12	0.22	13.78	50.45	0.30	9.44	0.06	0.19	19.52	6.21	100.29	1.301	0.003	0.005	0.530	0.153	0.533	0.008	0.469	0.002	0.005						
Vranduk Fm.	BO115sp043	n. d.	0.10	0.32	11.23	56.29	0.29	9.94	0.06	0.17	18.35	3.16	99.91	1.466	0.002	0.007	0.436	0.078	0.505	0.008	0.488	0.001	0.004						
Vranduk Fm.	BO115sp044	n. d.	0.05	0.20	36.28	30.68	0.18	15.47	0.18	0.19	13.44	2.40	99.07	0.701	0.001	0.004	1.236	0.052	0.325	0.004	0.666	0.004	0.004						
Vranduk Fm.	BO115sp046	n. d.	0.06	0.32	22.69	45.58	0.21	12.75	0.08	0.14	15.83	1.94	99.59	1.112	0.001	0.006	0.826	0.045	0.409	0.006	0.587	0.002	0.003						
Vranduk Fm.	BO115sp047	n. d.	0.07	0.40	34.90	31.85	0.13	15.44	0.14	0.18	17.30	3.05	99.48	0.730	0.002	0.004	1.192	0.066	0.327	0.003	0.667	0.003	0.004						
Vranduk Fm.	BO115sp048	n. d.	0.06	0.40	13.32	52.38	0.39	8.18	0.03	0.30	21.20	3.93	100.29	1.364	0.001	0.009	0.584	0.011	0.584	0.011	0.402	0.001	0.010						
Vranduk Fm.	BO115sp049	n. d.	0.09	0.29	20.45	46.47	0.26	11.92	0.08	0.18	16.82	3.59	100.16	1.146	0.002	0.006	0.752	0.084	0.439	0.007	0.554	0.002	0.004						
Vranduk Fm.	BO115sp050	n. d.	0.07	0.39	13.34	54.00	0.30	9.31	0.04	0.18	19.66	2.57	99.86	1.399	0.002	0.008	0.516	0.063	0.539	0.008	0.465	0.001	0.004						
Vranduk Fm.	BO115sp051	n. d.	0.08	0.08	22.47	40.05	0.23	13.31	0.09	0.16	15.67	2.46	99.67	0.955	0.002	0.004	0.977	0.056	0.395	0.006	0.598	0.002	0.004						
Vranduk Fm.	BO115sp052	n. d.	0.05	0.19	35.08	32.23	0.17	15.45	0.14	0.22	13.47	2.63	99.64	0.737	0.001	0.004	1.196	0.057	0.326	0.004	0.666	0.003	0.005						
Vranduk Fm.	BO115sp053	n. d.	0.09	0.25	23.36	42.68	0.25	11.64	0.08	0.23	17.60	3.84	100.02	1.044	0.002	0.005	0.852	0.089	0.455	0.007	0.537	0.002	0.005						
Vranduk Fm.	BO115sp054	n. d.	0.05	0.27	34.15	32.80	0.20	15.00	0.14	0.18	14.05	2.83	99.72	0.754	0.001	0.005	1.171	0.062	0.342	0.005	0.650	0.003	0.005						

n. d.: not detected

Formation	Sample & spot ID	analyses in wt%. Shown are the recalculated FeO and Fe <sub>2</sub> O <sub>3</sub> values and the amended total															Total	cations per formula unit on the basis of 3 oxygens								
		SiO <sub>2</sub>	TiO <sub>2</sub>	V <sub>2</sub> O <sub>5</sub>	Al <sub>2</sub> O <sub>3</sub>	Cr <sub>2</sub> O <sub>3</sub>	MnO	MgO	NiO	ZnO	FeO	Fe <sub>2</sub> O <sub>3</sub>	Al	Fe <sup>3+</sup>	Fe <sup>2+</sup>	Mn		Mg	Ni	Zn						
Branduk Fm.	BO115sp0055	n. d.	0.06	0.20	37.76	28.91	0.15	16.00	0.19	0.19	12.92	2.83	99.22	0.682	0.004	1.274	0.081	0.309	0.004	0.004	0.004					
Branduk Fm.	BO115sp0056	n. d.	0.18	0.26	28.38	38.74	0.22	13.36	0.11	0.22	15.77	2.45	99.68	0.598	0.003	1.005	0.055	0.396	0.005	0.005	0.005					
Branduk Fm.	BO115sp0057	n. d.	0.13	0.26	12.30	55.54	0.32	10.47	0.06	0.15	17.77	3.17	100.18	0.509	0.002	0.473	0.078	0.485	0.009	0.004	0.004					
Branduk Fm.	BO115sp0058	n. d.	0.04	0.34	24.59	43.16	0.22	12.52	0.07	0.21	16.46	2.17	99.78	0.572	0.002	0.888	0.105	0.422	0.005	0.005	0.005					
Branduk Fm.	BO115sp0059	0.07	0.22	0.33	32.71	32.38	0.21	14.36	0.16	0.26	14.90	4.16	99.77	0.629	0.004	1.333	0.092	0.366	0.005	0.006	0.006					
Branduk Fm.	BO115sp0060	n. d.	0.04	0.20	42.35	23.44	0.12	16.57	0.21	0.18	12.64	3.05	98.80	0.695	0.005	1.405	0.085	0.297	0.003	0.005	0.005					
Branduk Fm.	BO115sp0061	n. d.	0.04	0.32	24.02	44.39	0.22	12.86	0.06	0.17	16.01	2.08	100.17	0.585	0.001	0.865	0.048	0.409	0.006	0.004	0.004					
Branduk Fm.	BO115sp0062	n. d.	0.05	0.24	34.51	32.88	0.16	15.17	0.14	0.19	13.88	2.43	99.64	0.656	0.003	1.181	0.053	0.337	0.004	0.004	0.004					
Branduk Fm.	BO115sp0063	n. d.	0.06	0.25	33.09	33.18	0.17	14.68	0.12	0.18	14.21	3.01	98.95	0.644	0.003	1.148	0.067	0.350	0.004	0.004	0.004					
Branduk Fm.	BO115sp0064	n. d.	0.04	0.39	17.34	49.78	0.30	9.77	0.05	0.24	19.65	2.80	100.37	0.466	0.001	0.654	0.067	0.526	0.008	0.006	0.006					
Branduk Fm.	BO115sp0065	n. d.	0.03	0.40	16.40	52.16	0.24	11.19	0.07	0.19	17.40	2.24	100.32	0.531	0.002	0.615	0.054	0.463	0.006	0.004	0.004					
Branduk Fm.	BO115sp0066	n. d.	0.09	0.24	23.90	43.13	0.23	12.65	0.08	0.17	16.10	3.06	99.67	0.580	0.002	0.866	0.071	0.414	0.006	0.004	0.004					
Branduk Fm.	BO115sp0067	n. d.	0.23	0.26	15.91	45.85	0.30	9.78	0.11	0.19	19.28	8.06	99.96	0.472	0.003	0.607	0.196	0.522	0.008	0.003	0.005					
Branduk Fm.	BO115sp0068	n. d.	0.08	0.25	31.98	34.24	0.21	13.57	0.15	0.21	15.83	2.99	99.51	0.599	0.004	1.117	0.067	0.392	0.005	0.004	0.005					
Branduk Fm.	BO115sp0069	n. d.	0.12	0.14	24.97	39.45	0.27	11.12	0.08	0.26	18.52	5.02	99.95	0.512	0.002	0.909	0.117	0.478	0.007	0.002	0.006					
Branduk Fm.	BO115sp0070	n. d.	0.10	0.19	34.29	32.70	0.14	15.87	0.17	0.15	12.68	2.98	99.27	0.686	0.004	1.173	0.065	0.308	0.004	0.004	0.003					
Branduk Fm.	BO115sp0071	n. d.	0.07	0.24	33.71	33.07	0.18	14.95	0.12	0.17	14.05	2.86	99.43	0.651	0.003	1.161	0.063	0.343	0.004	0.003	0.004					
Branduk Fm.	BO115sp0072	n. d.	0.17	0.21	28.99	37.69	0.20	13.92	0.13	0.17	15.20	3.63	100.31	0.617	0.003	1.016	0.081	0.378	0.005	0.003	0.004					
Branduk Fm.	BO115sp0073	n. d.	0.07	0.16	40.24	27.54	0.16	16.61	0.18	0.19	12.76	2.53	100.43	0.693	0.004	1.328	0.053	0.299	0.004	0.004	0.004					
Branduk Fm.	BO115sp0074	n. d.	0.04	0.26	29.50	38.45	0.18	14.23	0.12	0.14	14.47	1.90	99.29	0.633	0.003	1.038	0.043	0.361	0.005	0.003	0.003					
Branduk Fm.	BO115sp0075	n. d.	0.10	0.24	28.88	37.76	0.19	13.03	0.10	0.28	16.30	3.00	99.87	0.583	0.002	1.022	0.068	0.409	0.005	0.006	0.006					
Branduk Fm.	BO115sp0076	n. d.	0.07	0.24	11.66	55.76	0.35	8.30	0.03	0.24	20.89	2.78	100.32	0.410	0.001	0.456	0.069	0.579	0.010	0.001	0.006					
Branduk Fm.	BO115sp0077	n. d.	0.04	0.30	24.09	43.47	0.26	12.45	0.09	0.20	16.57	2.81	100.28	0.568	0.002	0.869	0.065	0.424	0.007	0.002	0.007					
Branduk Fm.	BO115sp0078	n. d.	0.06	0.21	36.43	29.90	0.17	14.33	0.14	0.33	15.24	2.61	99.42	0.620	0.003	1.246	0.057	0.370	0.004	0.003	0.005					
Branduk Fm.	BO115sp0079	n. d.	0.22	0.30	14.88	46.49	0.35	8.38	0.09	0.24	21.21	7.82	99.97	0.410	0.002	0.576	0.193	0.582	0.010	0.002	0.006					
Branduk Fm.	BO115sp0080	n. d.	0.03	0.23	37.18	29.06	0.18	15.26	0.14	0.22	13.96	2.98	99.24	0.655	0.003	1.263	0.065	0.336	0.004	0.005	0.005					
Branduk Fm.	BO115sp0081	n. d.	0.05	0.24	34.81	32.55	0.19	14.81	0.15	0.17	14.61	2.55	100.14	0.639	0.004	1.188	0.056	0.354	0.005	0.004	0.004					
Branduk Fm.	BO115sp0082	n. d.	0.06	0.23	33.72	33.75	0.17	15.15	0.15	0.19	13.77	2.45	99.63	0.657	0.003	1.158	0.054	0.335	0.004	0.004	0.004					
Branduk Fm.	BO115sp0083	n. d.	0.07	0.21	35.53	30.42	0.17	15.31	0.19	0.19	13.82	3.97	99.87	0.658	0.004	1.209	0.086	0.333	0.004	0.004	0.004					
Branduk Fm.	BO115sp0084	n. d.	0.11	0.23	29.73	37.86	0.19	14.43	0.16	0.14	14.36	2.64	99.85	0.638	0.004	1.039	0.059	0.356	0.005	0.004	0.003					
Branduk Fm.	BO115sp0085	n. d.	0.08	0.25	28.45	39.60	0.19	13.66	0.08	0.17	15.39	1.98	99.86	0.603	0.002	1.004	0.045	0.385	0.005	0.002	0.004					
Branduk Fm.	BO115sp0086	n. d.	0.08	0.33	35.67	29.69	0.18	13.91	0.15	0.33	15.94	3.50	99.77	0.609	0.004	1.224	0.077	0.388	0.004	0.003	0.004					
Branduk Fm.	BO115sp0087	n. d.	0.42	0.31	23.36	38.68	0.29	9.85	0.11	0.28	20.44	6.01	99.75	0.461	0.003	0.865	0.142	0.537	0.008	0.003	0.007					
Branduk Fm.	BO115sp0088	n. d.	0.05	0.29	30.24	37.20	0.21	14.37	0.13	0.20	14.50	2.73	99.92	0.634	0.003	1.055	0.061	0.359	0.005	0.004	0.004					
Branduk Fm.	BO115sp0089	n. d.	0.59	0.30	20.32	42.22	0.42	8.29	0.11	0.17	22.63	5.20	100.26	0.395	0.003	0.766	0.125	0.605	0.011	0.003	0.004					
Branduk Fm.	BO115sp0090	n. d.	0.08	0.26	24.95	41.03	0.18	12.92	0.12	0.19	15.81	4.06	99.60	0.589	0.003	0.900	0.094	0.405	0.005	0.003	0.004					
Branduk Fm.	BO12sp0001	n. d.	0.13	0.31	21.47	47.76	0.23	13.45	0.10	0.14	14.88	2.07	100.54	0.614	0.003	0.776	0.048	0.381	0.006	0.003	0.003					
Branduk Fm.	BO12sp0002	n. d.	0.04	0.29	22.30	43.91	0.22	13.38	0.14	0.14	14.97	5.19	100.59	0.610	0.003	0.804	0.119	0.383	0.006	0.003	0.003					
Branduk Fm.	BO12sp0003	n. d.	0.04	0.38	11.52	58.68	0.27	10.75	0.05	0.16	17.40	1.25	100.50	0.521	0.001	0.442	0.031	0.473	0.007	0.001	0.004					
Branduk Fm.	BO12sp0004	n. d.	0.08	0.33	21.20	48.47	0.20	12.68	0.06	0.17	15.70	0.53	99.41	0.588	0.002	0.777	0.012	0.408	0.005	0.002	0.004					
Branduk Fm.	BO12sp0005	n. d.	0.09	0.21	33.95	34.83	0.15	16.65	0.18	0.12	11.70	2.13	100.02	0.713	0.004	1.150	0.046	0.281	0.004	0.004	0.003					
Branduk Fm.	BO12sp0006	n. d.	0.03	0.35	19.91	50.18	0.17	12.82	0.07	0.11	15.58	1.03	100.26	0.593	0.002	0.728	0.024	0.404	0.005	0.002	0.002					
Branduk Fm.	BO12sp0007	n. d.	0.03	0.27	22.90	44.28	0.30	10.80	0.06	0.31	18.67	2.31	99.93	0.502	0.001	0.841	0.054	0.487	0.008	0.001	0.007					
Branduk Fm.	BO12sp0008	n. d.	0.06	0.20	28.01	42.09	0.16	15.63	0.10	0.14	12.32	1.21	99.93	0.689	0.002	0.977	0.027	0.305	0.004	0.002	0.003					
Branduk Fm.	BO12sp0009	n. d.	0.07	0.24	22.31	42.86	0.22	12.43	0.08	0.17	16.35	2.18	100.63	0.573	0.004	0.813	0.126	0.419	0.005	0.004	0.004					
Branduk Fm.	BO12sp0010	n. d.	0.10	0.32	20.19	48.65	0.21	12.36	0.14	0.16	17.22	5.40	100.03	0.571	0.002	0.738	0.051	0.424	0.006	0.002	0.004					
Branduk Fm.	BO12sp0011	0.03	0.26	0.15	41.25	24.70	0.11	18.89	0.22	0.05	9.41	4.45	99.52	0.781	0.005	1.349	0.093	0.218	0.003	0.001	0.001					
Branduk Fm.	BO12sp0012	n. d.	0.03	0.35	21.45	46.84	0.19	13.06	0.09	0.15	15.41	2.86	100.43	0.599	0.002	0.778	0.066	0.396	0.005	0.002	0.003					
Branduk Fm.	BO12sp0013	0.06	0.31	0.15	37.34	28.60	0.16	18.36	0.24	0.06	9.74	5.08	100.10	0.769	0.005	1.238	0.107	0.229	0.004	0.001	0.001					
Branduk Fm.	BO12sp0014	n. d.	0.10	0.25	27.99	41.32	0.18	15.02	0.13	0.11	13.32	1.57	99.99	0.665	0.003	0.980	0.035	0.331	0.004	0.003	0.003					
Branduk Fm.	BO12sp0015	n. d.	0.14	0.16	36.73	29.87	0.18	15.76	0.18	0.20	13.41	3.45	100.08	0.672	0.004	1.238	0.074	0.321	0.004	0.004	0.004					
Branduk Fm.	BO12sp0016	n. d.	0.15	0.37	22.08	46.69	0.24	12.02	0.08	0.22	17.17	1.53	100.53	0.553	0.002	0.803	0.035	0.443	0.006	0.005	0.005					
Branduk Fm.	BO12sp0018	n. d.	0.04	0.42	20.99	47.66	0.24	11.65	0.08	0.21	17.48	1.69	100.47	0.540	0.002	0.769	0.040	0.454	0.006	0.002	0.005					
Branduk Fm.	BO12sp0019	n. d.	0.07	0.31	20.26	45.72	0.34	8.71	0.07	0.29	21.69	3.17	100.63	0.412	0.001	0.759	0.075	0.576	0.009	0.002	0.007					
Branduk Fm.	BO12sp0020	n. d.	0.07	0.33	19.33	50.51	0.23	12.21	0.04	0.22	16.34	1.07	100.3													

analyses in wt%. Shown are the recalculated FeO and Fe<sub>2</sub>O<sub>3</sub> values and the amended total  
n.d.: not detected

Formation	Sample & spot ID	SiO <sub>2</sub>	TiO <sub>2</sub>	V <sub>2</sub> O <sub>5</sub>	Al <sub>2</sub> O <sub>3</sub>	Cr <sub>2</sub> O <sub>3</sub>	MnO	MgO	NiO	ZnO	FeO	Fe <sub>2</sub> O <sub>3</sub>	Total	cations per formula unit on the basis of 3 oxygens												Zn											
														Fe <sup>3+</sup>	Fe <sup>2+</sup>	Mn	Mg	Ni																			
Vranduk Fm.	BO12sp021	n. d.	1.20	0.31	22.34	38.27	0.34	10.23	0.16	0.20	20.46	6.54	100.06	0.949	0.028	0.007	0.826	0.154	0.537	0.009	0.478	0.004	0.005														
Vranduk Fm.	BO12sp022	n. d.	0.08	0.29	26.20	42.57	0.21	13.73	0.09	0.16	14.96	1.64	99.92	1.015	0.002	0.006	0.932	0.037	0.377	0.005	0.617	0.002	0.003														
Vranduk Fm.	BO12sp023	n. d.	0.09	0.25	24.23	45.76	0.19	13.17	0.08	0.15	14.14	1.30	100.35	0.993	0.002	0.005	0.863	0.029	0.357	0.005	0.638	0.003	0.006														
Vranduk Fm.	BO12sp024	n. d.	0.58	0.29	26.70	41.45	0.22	13.12	0.11	0.25	16.15	0.42	99.26	1.095	0.013	0.006	0.956	0.010	0.410	0.006	0.594	0.002	0.006														
Vranduk Fm.	BO12sp025	n. d.	0.24	0.30	25.06	36.18	0.23	12.36	0.17	0.18	16.69	8.14	99.56	0.879	0.006	0.006	0.908	0.188	0.429	0.006	0.566	0.004	0.004														
Vranduk Fm.	BO12sp026	n. d.	0.12	0.12	28.74	39.33	0.23	15.78	0.09	0.15	12.07	3.00	99.56	0.920	0.003	0.002	1.003	0.067	0.299	0.004	0.696	0.002	0.004														
Vranduk Fm.	BO12sp028	n. d.	0.05	0.39	14.55	55.23	0.29	10.60	0.02	0.21	18.05	1.01	100.41	1.404	0.001	0.008	0.552	0.025	0.485	0.008	0.508	0.001	0.005														
Vranduk Fm.	BO12sp029	n. d.	0.07	0.31	20.81	48.87	0.23	14.00	0.10	0.13	13.90	1.70	99.92	1.189	0.002	0.006	0.755	0.039	0.353	0.006	0.642	0.002	0.003														
Vranduk Fm.	BO12sp030	n. d.	0.43	0.19	34.93	30.22	0.17	15.17	0.20	0.17	13.99	3.58	99.04	0.696	0.009	0.004	1.199	0.079	0.341	0.004	0.659	0.005	0.004														
Vranduk Fm.	BO12sp031	n. d.	0.08	0.27	21.55	47.13	0.22	13.17	0.11	0.16	14.98	2.10	99.77	1.151	0.002	0.006	0.785	0.048	0.387	0.006	0.606	0.003	0.004														
Vranduk Fm.	BO12sp032	n. d.	0.70	0.31	21.95	42.21	0.28	11.80	0.12	0.24	17.61	4.76	99.98	1.038	0.016	0.006	0.805	0.111	0.458	0.007	0.547	0.003	0.005														
Vranduk Fm.	BO12sp033	n. d.	0.05	0.30	18.42	49.74	0.23	12.45	0.05	0.14	15.80	3.10	100.27	1.231	0.001	0.006	0.680	0.073	0.414	0.006	0.581	0.001	0.003														
Vranduk Fm.	BO12sp034	n. d.	0.47	0.26	16.94	39.06	0.33	7.89	0.14	0.44	22.22	12.30	100.07	1.009	0.012	0.006	0.653	0.303	0.608	0.009	0.384	0.004	0.011														
Vranduk Fm.	BO12sp035	0.03	0.45	0.15	41.18	22.98	0.11	18.28	0.26	0.06	10.26	5.17	98.93	0.508	0.010	0.003	1.358	0.109	0.240	0.002	0.762	0.006	0.001														
Vranduk Fm.	BO12sp036	n. d.	0.12	0.33	21.64	47.80	0.21	13.06	0.06	0.11	15.48	1.34	100.16	1.163	0.003	0.007	0.786	0.031	0.399	0.006	0.599	0.001	0.003														
Vranduk Fm.	BO12sp037	n. d.	0.08	0.36	13.95	55.75	0.24	11.73	0.06	0.17	16.17	1.58	100.09	1.414	0.002	0.008	0.528	0.038	0.434	0.007	0.561	0.002	0.004														
Vranduk Fm.	BO12sp038	n. d.	0.14	0.32	25.47	35.46	0.28	11.54	0.17	0.31	17.94	8.47	100.10	0.861	0.003	0.007	0.923	0.196	0.461	0.007	0.528	0.004	0.007														
Vranduk Fm.	BO12sp039	n. d.	0.07	0.27	23.93	44.37	0.21	14.22	0.12	0.14	13.87	2.92	100.12	1.063	0.002	0.005	0.855	0.067	0.352	0.005	0.642	0.003	0.003														
Vranduk Fm.	BO12sp040	n. d.	0.04	0.30	26.29	42.77	0.19	14.28	0.10	0.16	14.11	1.68	99.92	1.016	0.001	0.006	0.931	0.038	0.355	0.005	0.640	0.002	0.004														
Vranduk Fm.	BO12sp041	n. d.	0.07	0.25	8.28	62.11	0.26	10.87	0.05	0.13	16.64	1.70	100.35	1.621	0.002	0.005	0.322	0.042	0.459	0.007	0.535	0.001	0.004														
Vranduk Fm.	BO12sp042	n. d.	0.18	0.30	19.63	50.06	0.22	12.89	0.07	0.16	15.32	1.07	99.91	1.232	0.004	0.006	0.721	0.025	0.399	0.006	0.598	0.002	0.003														
Vranduk Fm.	BO12sp043	n. d.	0.03	0.32	19.61	50.28	0.26	12.56	0.05	0.16	15.86	1.35	100.48	1.035	0.001	0.007	0.718	0.032	0.412	0.007	0.581	0.001	0.004														
Vranduk Fm.	BO12sp044	n. d.	0.19	0.22	25.12	43.55	0.22	13.47	0.09	0.18	15.24	1.72	100.01	1.044	0.004	0.004	0.898	0.039	0.387	0.006	0.609	0.002	0.004														
Vranduk Fm.	BO12sp045	n. d.	0.51	0.38	27.90	36.01	0.30	10.53	0.07	0.15	20.49	3.62	99.95	0.871	0.012	0.008	1.006	0.083	0.524	0.008	0.480	0.002	0.003														
Vranduk Fm.	BO12sp046	n. d.	0.05	0.30	11.71	57.83	0.29	10.94	0.04	0.15	17.05	2.06	100.43	1.485	0.001	0.006	0.463	0.050	0.463	0.008	0.530	0.001	0.004														
Vranduk Fm.	BO12sp047	n. d.	0.44	0.12	37.17	27.86	0.13	18.09	0.27	0.03	10.10	5.41	99.72	0.623	0.009	0.002	1.239	0.115	0.239	0.003	0.762	0.006	0.001														
Vranduk Fm.	BO12sp048	n. d.	0.48	0.22	33.78	29.84	0.17	15.49	0.22	0.17	13.55	5.76	99.67	0.686	0.011	0.004	1.158	0.126	0.329	0.004	0.671	0.005	0.004														
Vranduk Fm.	BO12sp051	n. d.	0.07	0.37	12.33	58.12	0.23	10.96	0.05	0.14	17.32	1.02	100.62	1.485	0.002	0.008	0.470	0.025	0.468	0.007	0.528	0.001	0.003														
Vranduk Fm.	BO12sp052	n. d.	0.11	0.31	20.14	49.42	0.20	12.69	0.08	0.15	15.81	1.55	100.50	1.210	0.003	0.006	0.735	0.036	0.410	0.006	0.586	0.002	0.003														
Vranduk Fm.	BO12sp053	n. d.	0.05	0.42	15.59	54.19	0.26	11.33	0.06	0.15	17.14	1.16	100.33	1.366	0.001	0.009	0.586	0.028	0.457	0.007	0.538	0.001	0.003														
Vranduk Fm.	BO12sp061	n. d.	3.45	0.53	12.99	40.40	0.36	8.46	0.21	0.16	23.80	9.79	100.15	1.055	0.086	0.011	0.506	0.243	0.658	0.010	0.416	0.006	0.004														
Vranduk Fm.	BO12sp055	n. d.	0.06	0.31	13.93	56.92	0.21	12.66	0.08	0.10	14.92	1.35	100.55	1.429	0.002	0.006	0.522	0.032	0.396	0.006	0.599	0.002	0.002														
Vranduk Fm.	BO12sp056	n. d.	0.14	0.41	14.69	54.17	0.26	11.74	0.06	0.15	16.49	2.42	100.53	1.365	0.003	0.009	0.552	0.058	0.440	0.007	0.568	0.002	0.003														
Vranduk Fm.	BO12sp057	n. d.	0.12	0.38	17.55	52.18	0.22	12.60	0.09	0.13	15.52	1.41	100.19	1.295	0.003	0.008	0.650	0.033	0.408	0.006	0.590	0.002	0.003														
Vranduk Fm.	BO12sp058	n. d.	0.33	0.22	34.31	30.30	0.17	15.53	0.20	0.16	13.56	5.20	99.99	0.693	0.007	0.004	1.170	0.113	0.328	0.004	0.670	0.005	0.003														
Vranduk Fm.	BO12sp059	n. d.	0.05	0.29	23.82	45.66	0.21	13.84	0.08	0.13	14.42	1.38	99.88	1.099	0.001	0.006	0.855	0.032	0.367	0.005	0.628	0.002	0.003														
Vranduk Fm.	BO12sp060	n. d.	0.03	0.28	17.38	52.72	0.27	12.65	0.07	0.15	15.25	1.46	100.26	1.308	0.001	0.006	0.643	0.034	0.400	0.007	0.592	0.002	0.003														
Vranduk Fm.	BO12sp061	n. d.	0.16	0.29	16.45	52.96	0.25	12.14	0.05	0.16	16.03	1.71	100.21	1.325	0.004	0.006	0.614	0.041	0.424	0.007	0.572	0.001	0.004														
Vranduk Fm.	BO12sp062	n. d.	0.04	0.28	23.69	45.48	0.22	14.18	0.06	0.14	13.89	2.01	99.98	1.092	0.001	0.006	0.848	0.046	0.353	0.006	0.642	0.001	0.003														
Vranduk Fm.	BO12sp063	n. d.	0.12	0.29	19.87	50.31	0.20	13.82	0.10	0.11	14.07	1.54	100.44	1.225	0.003	0.007	0.721	0.036	0.362	0.005	0.634	0.002	0.003														
Vranduk Fm.	BO12sp064	n. d.	0.07	0.33	14.54	53.72	0.27	10.77	0.06	0.17	17.66	2.49	100.07	1.369	0.002	0.007	0.553	0.061	0.476	0.007	0.517	0.001	0.004														
Vranduk Fm.	BO12sp065	n. d.	0.08	0.29	12.01	55.65	0.31	9.44	0.03	0.22	19.37	3.15	100.55	1.441	0.002	0.006	0.464	0.078	0.531	0.009	0.461	0.001	0.005														
Vranduk Fm.	BO12sp066	n. d.	0.49	0.21	30.77	34.62	0.16	17.04	0.17	0.06	10.81	5.18	99.52	0.798	0.011	0.004	1.058	0.114	0.264	0.004	0.741	0.004	0.001														
Vranduk Fm.	BO12sp067	n. d.	0.04	0.26	19.28	49.48	0.22	13.27	0.09	0.13	14.63	2.84	100.25	1.214	0.001	0.005	0.706	0.066																			

Formation	Sample & spot ID	analyses in wt%. Shown are the recalculated FeO and Fe <sub>2</sub> O <sub>3</sub> values and the amended total																	Cations per formula unit on the basis of 3 oxygens									
		SiO <sub>2</sub>	TiO <sub>2</sub>	V <sub>2</sub> O <sub>5</sub>	Al <sub>2</sub> O <sub>3</sub>	Cr <sub>2</sub> O <sub>3</sub>	MnO	MgO	NiO	ZnO	FeO	Fe <sub>2</sub> O <sub>3</sub>	Total	Cr	Ti	V	Al	Fe <sup>3+</sup>	Fe <sup>2+</sup>	Mn	Mg	Ni	Zn					
Vranduk Fm.	BO12sp079	n. d.	3.02	0.33	16.87	40.53	0.27	10.12	0.15	0.17	21.19	6.35	99.01	1.038	0.074	0.007	0.644	0.155	0.574	0.007	0.489	0.004	0.004	0.004				
Vranduk Fm.	BO12sp080	n. d.	1.50	0.23	25.69	33.07	0.20	13.27	0.23	0.13	16.68	9.13	100.13	0.794	0.034	0.005	0.919	0.209	0.423	0.005	0.600	0.006	0.003	0.003				
Vranduk Fm.	BO12sp081	n. d.	0.19	0.30	24.09	43.20	0.25	11.87	0.06	0.30	17.46	2.29	100.00	1.051	0.001	0.006	0.874	0.033	0.449	0.006	0.544	0.002	0.007	0.007				
Vranduk Fm.	BO12sp082	n. d.	0.03	0.30	21.42	47.90	0.20	13.68	0.11	0.11	14.16	1.64	99.56	1.168	0.001	0.006	0.779	0.038	0.365	0.005	0.629	0.003	0.003	0.003				
Vranduk Fm.	BO12sp083	n. d.	0.19	0.17	10.45	56.48	0.24	10.96	0.09	0.09	16.86	4.81	100.35	1.461	0.005	0.004	0.403	0.118	0.461	0.007	0.534	0.002	0.002	0.002				
Vranduk Fm.	BO12sp084	n. d.	0.10	0.39	18.64	50.09	0.21	12.46	0.07	0.14	15.89	2.16	100.15	1.240	0.002	0.008	0.688	0.051	0.416	0.005	0.581	0.002	0.002	0.002				
Vranduk Fm.	BO12sp085	n. d.	0.60	0.29	22.70	42.29	0.24	9.95	0.11	0.16	20.32	2.37	99.02	1.057	0.014	0.006	0.846	0.056	0.537	0.006	0.469	0.003	0.004	0.004				
Vranduk Fm.	BO12sp086	0.02	0.61	0.25	27.85	36.65	0.17	15.81	0.15	0.07	12.58	6.08	100.24	0.857	0.014	0.005	0.971	0.135	0.311	0.004	0.697	0.004	0.001	0.001				
Vranduk Fm.	BO12sp087	n. d.	0.03	0.37	19.61	50.63	0.22	13.29	0.10	0.13	14.81	1.32	100.51	1.237	0.001	0.008	0.715	0.241	0.383	0.006	0.612	0.002	0.003	0.003				
Vranduk Fm.	BO12sp088	n. d.	0.01	0.33	21.69	36.39	0.28	11.37	0.18	0.18	18.49	10.27	100.19	0.898	0.024	0.007	0.799	0.031	0.483	0.008	0.529	0.005	0.004	0.004				
Vranduk Fm.	BO12sp089	n. d.	0.06	0.23	24.05	45.37	0.23	13.86	0.08	0.15	14.40	1.61	100.05	1.089	0.001	0.005	0.861	0.037	0.366	0.006	0.627	0.002	0.003	0.003				
Vranduk Fm.	BO12sp090	n. d.	0.04	0.36	10.34	58.05	0.28	10.59	0.07	0.15	17.42	3.30	100.59	1.502	0.001	0.008	0.399	0.081	0.477	0.008	0.516	0.002	0.004	0.004				
Vranduk Fm.	BO4sp001	n. d.	0.09	0.26	11.56	56.23	0.23	11.21	0.07	0.15	16.63	3.99	100.42	1.444	0.002	0.006	0.443	0.098	0.452	0.006	0.543	0.002	0.004	0.004				
Vranduk Fm.	BO4sp002	n. d.	0.09	0.21	25.32	42.78	0.17	14.11	0.07	0.17	14.19	2.69	99.79	1.023	0.002	0.004	0.903	0.061	0.359	0.004	0.636	0.002	0.004	0.004				
Vranduk Fm.	BO4sp003	n. d.	0.03	0.40	17.98	49.66	0.26	10.71	0.06	0.19	18.31	2.55	100.14	1.247	0.001	0.008	0.673	0.061	0.486	0.007	0.507	0.002	0.004	0.004				
Vranduk Fm.	BO4sp004	n. d.	0.06	0.24	28.45	38.79	0.22	13.74	0.10	0.18	15.11	2.76	99.64	0.919	0.001	0.005	1.006	0.062	0.379	0.005	0.614	0.002	0.004	0.004				
Vranduk Fm.	BO4sp005	n. d.	0.14	0.44	13.91	51.56	0.21	12.60	0.09	0.06	15.06	6.27	100.34	1.300	0.003	0.009	0.523	0.150	0.402	0.006	0.599	0.002	0.001	0.001				
Vranduk Fm.	BO4sp006	n. d.	0.25	0.34	19.34	45.87	0.28	10.99	0.08	0.17	18.23	4.68	100.24	1.143	0.006	0.007	0.719	0.111	0.481	0.008	0.516	0.002	0.004	0.004				
Vranduk Fm.	BO4sp007	n. d.	0.05	0.33	25.52	42.13	0.25	12.16	0.05	0.28	17.27	2.27	100.31	1.015	0.001	0.007	0.917	0.052	0.440	0.006	0.552	0.001	0.006	0.006				
Vranduk Fm.	BO4sp008	n. d.	0.13	0.28	24.04	44.80	0.18	14.57	0.11	0.16	13.56	2.49	100.28	1.070	0.003	0.006	0.856	0.057	0.342	0.005	0.653	0.003	0.004	0.004				
Vranduk Fm.	BO4sp009	n. d.	0.04	0.18	34.98	32.48	0.17	15.62	0.13	0.18	13.06	2.51	99.40	1.193	0.001	0.003	1.193	0.055	0.316	0.004	0.676	0.003	0.004	0.004				
Vranduk Fm.	BO4sp010	n. d.	0.06	0.26	24.95	44.30	0.18	14.71	0.11	0.14	13.27	2.01	99.99	1.055	0.001	0.005	0.886	0.046	0.334	0.005	0.660	0.003	0.003	0.003				
Vranduk Fm.	BO4sp011	n. d.	0.08	0.26	21.38	46.11	0.27	10.97	0.07	0.28	18.33	2.45	100.19	1.139	0.002	0.005	0.788	0.058	0.479	0.007	0.511	0.002	0.002	0.006				
Vranduk Fm.	BO4sp012	n. d.	0.05	0.22	23.96	43.19	0.27	11.71	0.05	0.30	17.58	2.99	100.32	1.050	0.001	0.004	0.869	0.069	0.452	0.007	0.537	0.001	0.007	0.007				
Vranduk Fm.	BO4sp013	n. d.	0.02	0.23	34.28	33.41	0.15	16.00	0.16	0.16	12.34	2.23	99.00	0.767	0.000	0.004	1.174	0.049	0.300	0.004	0.693	0.004	0.004	0.004				
Vranduk Fm.	BO4sp014	n. d.	0.05	0.29	17.50	49.66	0.27	9.44	0.03	0.24	20.09	2.54	100.11	1.261	0.001	0.006	0.663	0.061	0.540	0.007	0.452	0.001	0.006	0.006				
Vranduk Fm.	BO4sp015	n. d.	0.04	0.32	17.54	49.71	0.26	9.44	0.05	0.26	20.12	2.47	100.22	1.261	0.001	0.007	0.663	0.060	0.540	0.007	0.451	0.001	0.006	0.006				
Vranduk Fm.	BO4sp016	n. d.	0.05	0.27	27.84	39.70	0.21	13.66	0.08	0.23	15.25	2.74	100.04	0.941	0.001	0.005	0.984	0.062	0.382	0.005	0.610	0.002	0.002	0.002				
Vranduk Fm.	BO4sp017	n. d.	0.05	0.31	18.20	51.58	0.46	11.99	0.08	0.14	15.88	0.40	99.10	1.293	0.001	0.007	0.681	0.101	0.421	0.012	0.567	0.002	0.003	0.003				
Vranduk Fm.	BO4sp018	n. d.	0.18	0.22	24.91	42.35	0.21	13.05	0.08	0.21	15.53	2.34	99.08	1.027	0.004	0.004	0.901	0.054	0.398	0.005	0.597	0.002	0.005	0.005				
Vranduk Fm.	BO4sp019	n. d.	0.07	0.34	19.34	47.36	0.25	11.90	0.10	0.14	16.67	3.87	100.04	1.175	0.002	0.007	0.716	0.025	0.437	0.007	0.557	0.003	0.003	0.003				
Vranduk Fm.	BO4sp020	n. d.	0.04	0.23	30.20	38.84	0.18	14.97	0.13	0.13	13.44	1.11	99.27	0.909	0.001	0.005	1.054	0.025	0.333	0.005	0.661	0.003	0.003	0.003				
Vranduk Fm.	BO4sp021	n. d.	0.04	0.29	21.63	45.60	0.33	10.11	0.09	0.15	19.78	2.40	100.42	1.130	0.001	0.006	0.799	0.057	0.518	0.009	0.472	0.002	0.003	0.003				
Vranduk Fm.	BO4sp022	n. d.	0.05	0.26	24.29	44.26	0.22	14.22	0.10	0.10	13.95	2.70	100.15	1.059	0.001	0.005	0.867	0.061	0.353	0.006	0.641	0.002	0.002	0.002				
Vranduk Fm.	BO4sp023	n. d.	0.06	0.28	20.66	47.48	0.24	11.93	0.05	0.22	16.88	2.52	100.32	1.168	0.001	0.006	0.758	0.059	0.439	0.006	0.553	0.001	0.005	0.005				
Vranduk Fm.	BO4sp024	n. d.	0.02	0.33	19.17	50.24	0.23	12.75	0.06	0.17	15.46	1.92	100.35	1.236	0.000	0.007	0.703	0.045	0.402	0.006	0.591	0.001	0.004	0.004				
Vranduk Fm.	BO4sp025	n. d.	0.14	0.24	14.81	39.22	0.33	7.13	0.11	0.21	22.87	14.76	99.81	1.032	0.003	0.005	0.581	0.370	0.636	0.009	0.354	0.003	0.005	0.005				
Vranduk Fm.	BO4sp026	n. d.	0.05	0.27	26.24	41.93	0.21	13.93	0.11	0.15	14.60	2.42	99.91	0.999	0.001	0.005	0.932	0.055	0.368	0.005	0.626	0.003	0.003	0.003				
Vranduk Fm.	BO4sp027	n. d.	0.10	0.24	27.76	38.78	0.18	13.04	0.09	0.26	16.10	3.18	99.73	0.925	0.002	0.005	0.988	0.072	0.406	0.005	0.587	0.002	0.006	0.006				
Vranduk Fm.	BO4sp028	n. d.	0.03	0.34	28.22	39.78	0.23	13.75	0.07	0.21	15.04	1.79	99.46	0.945	0.001	0.007	0.989	0.040	0.378	0.006	0.615	0.002	0.005	0.005				
Vranduk Fm.	BO4sp029	n. d.	0.10	0.34	16.36	51.66	0.28	10.24	0.03	0.26	18.76	2.17	100.21	1.309	0.002	0.007	0.618	0.052	0.503	0.008	0.489	0.001	0.006	0.006				
Vranduk Fm.	BO4sp030	n. d.	0.03	0.20	29.32	38.14	0.27	11.88	0.09	0.39	17.97	1.71	99.96	0.909	0.001	0.004	1.042	0.039	0.453	0.007	0.534	0.001	0.009	0.009				
Vranduk Fm.	BO4sp031	n. d.	0.26	0.30	18.89	46.21	0.28	10.80	0.09	0.15	18.46	4.81	100.23	1.156	0.006	0.006	0.704	0.114	0.488	0.007	0.509	0.002	0.003	0.003				
Vranduk Fm.	BO4sp032	n. d.	0.11	0.30	10.00	58.67	0.19	13.02	0.14	0.03	13.60	3.92	99.98	1.503	0.003	0.006	0.382	0.086	0.369	0.005	0.629	0.004	0.001	0.001				
Vranduk Fm.	BO4sp033	n. d.	0.15	0.22	22.80	45.73	0.17	13.92	0.10	0.14	14.28	2.75	100.28	1.102	0.003	0.006	0.819	0.063	0.364	0.004	0.632	0.003	0.003	0.003				
Vranduk Fm.	BO4sp034	n. d.	0.03	0.34	16.94	50.97	0.25	11.07	0.06	0.21	17.71	3.03	100.61	1.278	0.001	0.007	0.633	0.072	0.470	0.007	0.523	0.002	0.005	0.005				
Vranduk Fm.	BO4sp035	n. d.	0.44	0.27	21.69	45.09	0.19	14.49	0.13	0.08	13.52	4.36	100.25	1.088	0.010	0.005	0.780	0.100	0.345	0.005	0.659	0.003	0.002	0.002				
Vranduk Fm.	BO4sp036	n. d.	0.05	0.23	30.27	37.36	0.19	14.94	0.15	0.18	13.46	2.64	99.48	0.874	0.001	0.004	1.056	0.059	0.333	0.005	0.659	0.004	0.004	0.004				
Vranduk Fm.	BO4sp037	n. d.	0.05	0.24	26.04	41.83	0.20	13.83	0.09</																			

n.d.: not detected

analyses in wt%. Shown are the recalculated FeO and Fe<sub>2</sub>O<sub>3</sub> values and the amended total

Formation	Sample & spot ID	SiO <sub>2</sub>	TiO <sub>2</sub>	V <sub>2</sub> O <sub>5</sub>	Al <sub>2</sub> O <sub>3</sub>	Cr <sub>2</sub> O <sub>3</sub>	MnO	MgO	NiO	ZnO	FeO	Fe <sub>2</sub> O <sub>3</sub>	Total	Cr	Ti	V	Al	Fe <sup>3+</sup>	Fe <sup>2+</sup>	Mn	Mg	Ni	Zn
Vranduk Fm.	BO4sp0046	n. d.	0.28	0.27	18.98	44.82	0.26	11.50	0.08	0.19	17.35	6.48	100.20	1.116	0.007	0.006	0.705	0.154	0.457	0.007	0.540	0.002	0.004
Vranduk Fm.	BO4sp0047	n. d.	0.05	0.20	28.01	39.85	0.22	14.02	0.08	0.27	14.59	2.61	99.90	0.943	0.001	0.004	0.988	0.059	0.365	0.006	0.625	0.002	0.006
Vranduk Fm.	BO4sp0048	n. d.	0.42	0.31	21.49	38.66	0.25	9.72	0.13	0.16	20.58	8.49	100.22	0.967	0.010	0.007	0.800	0.202	0.543	0.007	0.457	0.003	0.004
Vranduk Fm.	BO4sp0049	n. d.	0.10	0.24	23.93	44.35	0.21	13.57	0.09	0.14	14.90	2.56	100.10	1.065	0.002	0.005	0.859	0.059	0.379	0.005	0.616	0.002	0.003
Vranduk Fm.	BO4sp0051	n. d.	0.02	0.31	22.59	45.69	0.24	12.86	0.08	0.16	15.74	2.55	100.24	1.109	0.000	0.006	0.818	0.059	0.404	0.006	0.589	0.002	0.004
Vranduk Fm.	BO4sp0052	n. d.	0.06	0.27	6.57	61.95	0.35	8.97	0.04	0.19	19.01	2.58	99.99	1.856	0.001	0.006	0.262	0.066	0.538	0.010	0.452	0.001	0.005
Vranduk Fm.	BO4sp0053	n. d.	0.04	0.27	18.33	51.02	0.23	13.96	0.07	0.12	13.18	2.16	99.38	1.260	0.001	0.006	0.675	0.051	0.344	0.006	0.650	0.002	0.003
Vranduk Fm.	BO4sp0054	n. d.	0.21	0.22	15.18	52.81	0.27	11.20	0.09	0.19	17.26	2.97	100.33	1.336	0.005	0.005	0.573	0.072	0.462	0.007	0.534	0.002	0.003
Vranduk Fm.	BO4sp0055	n. d.	0.13	0.35	25.69	42.99	0.18	13.97	0.10	0.19	14.50	1.54	99.64	1.028	0.003	0.007	0.916	0.035	0.367	0.005	0.630	0.002	0.004
Vranduk Fm.	BO4sp0056	n. d.	0.05	0.38	14.74	51.99	0.33	10.51	0.06	0.15	18.10	3.94	100.25	1.325	0.001	0.008	0.488	0.096	0.488	0.009	0.505	0.002	0.003
Vranduk Fm.	BO4sp0057	n. d.	1.00	0.37	16.98	41.14	0.30	9.64	0.15	0.19	20.47	10.10	100.34	1.046	0.024	0.008	0.644	0.245	0.551	0.008	0.462	0.004	0.004
Vranduk Fm.	BO4sp0058	n. d.	0.02	0.33	17.01	51.23	0.26	11.16	0.04	0.18	17.51	2.61	100.36	1.286	0.001	0.007	0.637	0.062	0.465	0.007	0.528	0.001	0.004
Vranduk Fm.	BO4sp0059	n. d.	0.03	0.19	26.67	42.40	0.23	14.63	0.08	0.10	13.44	1.67	99.44	1.008	0.001	0.004	0.945	0.038	0.338	0.006	0.655	0.002	0.002
Vranduk Fm.	BO4sp0060	n. d.	0.11	0.31	15.93	52.57	0.23	12.77	0.10	0.10	14.90	3.05	100.07	1.314	0.003	0.006	0.394	0.073	0.394	0.006	0.602	0.002	0.002
Vranduk Fm.	BO4sp0061	n. d.	0.09	0.31	13.51	53.74	0.34	9.84	0.03	0.16	18.83	3.01	99.86	1.387	0.002	0.007	0.520	0.074	0.514	0.009	0.479	0.001	0.004
Vranduk Fm.	BO4sp0062	n. d.	0.56	0.31	22.57	41.62	0.27	12.86	0.09	0.12	16.10	5.50	100.00	1.014	0.013	0.006	0.820	0.127	0.415	0.007	0.590	0.002	0.003
Vranduk Fm.	BO4sp0063	n. d.	0.10	0.25	20.28	47.02	0.28	11.41	0.06	0.22	17.59	3.13	100.33	1.163	0.002	0.005	0.748	0.074	0.460	0.007	0.532	0.001	0.005
Vranduk Fm.	BO4sp0064	n. d.	0.03	0.31	20.72	48.41	0.23	13.53	0.09	0.17	14.34	2.13	99.95	1.182	0.001	0.006	0.754	0.049	0.370	0.006	0.623	0.002	0.004
Vranduk Fm.	BO4sp0065	n. d.	0.03	0.31	19.92	47.98	0.27	10.52	0.05	0.20	18.87	2.04	100.19	1.196	0.001	0.007	0.740	0.048	0.498	0.007	0.494	0.001	0.005
Vranduk Fm.	BO4sp0066	n. d.	0.06	0.25	27.92	41.72	0.19	14.16	0.09	0.19	14.51	0.74	99.83	0.986	0.001	0.005	0.984	0.017	0.363	0.005	0.631	0.002	0.004
Vranduk Fm.	BO4sp0067	n. d.	0.03	0.34	20.49	48.06	0.20	12.81	0.08	0.14	15.67	2.72	100.54	1.174	0.001	0.007	0.747	0.063	0.405	0.005	0.590	0.002	0.003
Vranduk Fm.	BO4sp0068	n. d.	0.26	0.31	22.47	43.84	0.23	13.65	0.09	0.10	14.79	4.59	100.33	1.059	0.006	0.006	0.810	0.106	0.378	0.006	0.622	0.002	0.002
Vranduk Fm.	BO4sp0069	n. d.	0.04	0.20	24.62	44.44	0.17	15.61	0.15	0.07	11.82	2.91	100.02	1.054	0.001	0.004	0.871	0.166	0.296	0.004	0.698	0.004	0.002
Vranduk Fm.	BO4sp0070	n. d.	0.31	0.30	17.73	47.74	0.25	11.04	0.10	0.14	18.08	4.90	100.59	1.194	0.007	0.006	0.661	0.117	0.478	0.007	0.521	0.003	0.003
Vranduk Fm.	BO4sp0071	n. d.	0.13	0.20	25.58	41.99	0.19	14.05	0.11	0.14	14.45	3.40	100.24	1.000	0.003	0.004	0.909	0.072	0.364	0.005	0.631	0.003	0.003
Vranduk Fm.	BO4sp0072	n. d.	0.12	0.32	21.65	46.69	0.24	11.45	0.03	0.19	17.96	1.81	100.45	1.146	0.003	0.007	0.792	0.042	0.466	0.006	0.530	0.001	0.004
Vranduk Fm.	BO4sp0073	n. d.	0.71	0.48	20.23	39.74	0.23	10.31	0.19	0.09	19.99	8.63	100.58	0.990	0.017	0.010	0.751	0.205	0.527	0.006	0.484	0.005	0.002
Vranduk Fm.	BO4sp0074	n. d.	0.03	0.32	13.28	46.74	0.25	12.43	0.06	0.13	16.32	2.94	100.50	1.142	0.001	0.006	0.775	0.068	0.422	0.007	0.572	0.002	0.003
Vranduk Fm.	BO4sp0075	n. d.	1.62	0.34	13.16	39.28	0.29	8.20	0.15	0.13	22.71	14.77	100.66	1.025	0.040	0.007	0.512	0.367	0.627	0.008	0.403	0.004	0.003
Vranduk Fm.	BO4sp0076	n. d.	0.04	0.30	23.76	43.96	0.27	11.55	0.07	0.28	17.75	2.04	100.02	1.073	0.001	0.006	0.865	0.047	0.458	0.007	0.531	0.002	0.006
Vranduk Fm.	BO4sp0077	n. d.	0.04	0.30	21.16	46.65	0.19	12.69	0.10	0.15	15.69	2.89	99.86	1.144	0.001	0.006	0.774	0.067	0.407	0.005	0.587	0.003	0.003
Vranduk Fm.	BO4sp0078	n. d.	0.05	0.34	16.50	49.90	0.28	10.72	0.06	0.22	17.99	4.11	100.17	1.261	0.001	0.007	0.622	0.099	0.481	0.008	0.511	0.001	0.005
Vranduk Fm.	BO4sp0079	n. d.	0.02	0.27	23.04	45.82	0.23	12.81	0.10	0.17	15.83	1.84	100.13	1.112	0.000	0.006	0.833	0.042	0.406	0.006	0.586	0.002	0.004
Vranduk Fm.	BO4sp0080	n. d.	0.06	0.30	15.68	51.95	0.26	9.75	0.04	0.18	19.52	2.74	100.48	1.322	0.001	0.001	0.595	0.066	0.526	0.007	0.468	0.001	0.004
Vranduk Fm.	BO4sp0081	n. d.	0.03	0.28	22.59	45.96	0.22	12.55	0.07	0.19	16.17	2.03	100.09	1.119	0.001	0.006	0.820	0.047	0.417	0.006	0.576	0.002	0.004
Vranduk Fm.	BO4sp0082	n. d.	0.03	0.24	22.27	45.85	0.20	13.94	0.13	0.18	13.95	3.38	100.17	1.108	0.001	0.005	0.803	0.078	0.357	0.005	0.635	0.003	0.004
Vranduk Fm.	BO4sp0083	n. d.	0.04	0.26	32.29	34.89	0.18	14.54	0.11	0.19	14.35	2.34	99.19	0.813	0.001	0.005	1.122	0.052	0.354	0.005	0.639	0.003	0.004
Vranduk Fm.	BO4sp0084	n. d.	0.17	0.28	19.89	43.86	0.31	10.44	0.12	0.25	18.66	5.51	100.55	1.102	0.004	0.006	0.745	0.132	0.496	0.008	0.495	0.003	0.006
Vranduk Fm.	BO4sp0085	n. d.	0.16	0.22	16.38	50.31	0.21	13.40	0.08	0.12	14.12	5.53	100.53	1.247	0.004	0.004	0.605	0.131	0.370	0.006	0.626	0.002	0.003
Vranduk Fm.	BO4sp0086	n. d.	0.12	0.20	30.70	38.34	0.17	15.55	0.09	0.19	12.88	1.69	99.94	0.888	0.003	0.004	1.061	0.037	0.316	0.004	0.679	0.002	0.004
Vranduk Fm.	BO4sp0087	n. d.	0.02	0.30	22.28	46.48	0.20	13.45	0.08	0.13	14.91	2.56	100.42	1.124	0.001	0.006	0.803	0.059	0.381	0.005	0.613	0.002	0.003
Vranduk Fm.	BO4sp0088	n. d.	2.65	0.65	14.32	31.82	0.35	6.25	0.18	0.11	26.78	17.23	100.35	0.840	0.067	0.014	0.564	0.433	0.748	0.010	0.311	0.005	0.003
Vranduk Fm.	BO4sp0089	n. d.	0.04	0.35	17.37	50.28	0.25	11.45	0.05	0.19	17.12	3.19	100.29	1.258	0.001	0.007	0.648	0.076	0.453	0.007	0.540	0.001	0.004
Vranduk Fm.	BO4sp0090	n. d.	0.05	0.29	19.80	48.83	0.22	12.84	0.09	0.13	15.34	2.47	100.06	1.201	0.001	0.006	0.726	0.058	0.399	0.006	0.595	0.002	0.003
Vranduk Fm.	BO52sp0001	n. d.	0.06	0.26	17.37	48.61	0.23	11.66	0.07	0.26	17.52	5.50	100.55	1.210	0.001	0.005	0.818	0.130	0.427	0.007	0.568	0.002	0.006
Vranduk Fm.	BO52sp0002	n. d.	0.05	0.34	22.40	45.18	0.23	11.66	0.07	0.26	17.53	2.49	100.21	1.106	0.001	0.007	0.645	0.150	0.454	0.006	0.538	0.002	0.003
Vranduk Fm.	BO52sp0003	n. d.	0.14	0.27	23.48	45.16	0.20	13.77	0.08	0.13	14.55	2.13	99.93	1.089	0.003	0.006	0.844	0.049	0.371	0.005	0.626	0.002	0.003
Vranduk Fm.	BO52sp0004	n. d.	0.08	0.27	25.06	43.55	0.17	14.95	0.13	0.09	12.95	2.67	99.92	1.036	0.002	0.005	0.889	0.060	0.326	0.004	0.670	0.003	0.002
Vranduk Fm.	BO52sp0005	n. d.	0.12	0.27	19.34	46.89	0.24	12.25	0.08	0.20	16.18	4.77	100.37	1.158	0.003	0.006	0.712	0.112	0.423	0.006	0.570	0.002	0.005
Vranduk Fm.	BO52sp0006	n. d.	0.05	0.23	26.75	42.05	0.21	14.37	0.13	0.15	14.04	2.16	100.14	0.995	0.001	0.005	0.944	0.049	0.351	0.005	0.641	0.003	0.003
Vranduk Fm.	BO52sp0007	n. d.	0.05	0.26	32.97	35.06	0.18	15.20	0.13	0.18	13.73	2.28	100.04	0.806	0.001	0.005	1.131</						

Formation	Sample & spot ID	analyses in wt%. Shown are the recalculated FeO and Fe <sub>2</sub> O <sub>3</sub> values and the amended total																cations per formula unit on the basis of 3 oxygens										
		SiO <sub>2</sub>	TiO <sub>2</sub>	V <sub>2</sub> O <sub>5</sub>	Al <sub>2</sub> O <sub>3</sub>	Cr <sub>2</sub> O <sub>3</sub>	MnO	MgO	NiO	ZnO	FeO	Fe <sub>2</sub> O <sub>3</sub>	Total	Cr	Ti	V	Al	Fe <sup>3+</sup>	Fe <sup>2+</sup>	Mn	Mg	Ni	Zn					
Vranduk Fm.	BO52spl012	n. d.	0.13	0.19	29.61	39.57	0.19	15.10	0.10	0.18	13.38	1.48	99.92	0.923	0.003	0.004	1.030	0.033	0.330	0.005	0.664	0.002	0.004					
Vranduk Fm.	BO52spl013	n. d.	0.07	0.28	20.96	48.21	0.19	14.04	0.10	0.09	13.75	2.39	100.09	1.171	0.002	0.006	0.759	0.055	0.353	0.005	0.643	0.003	0.002					
Vranduk Fm.	BO52spl014	n. d.	0.13	0.33	8.82	56.35	0.33	6.99	0.05	0.18	22.58	4.41	100.12	1.512	0.003	0.007	0.353	0.113	0.641	0.009	0.354	0.001	0.003					
Vranduk Fm.	BO52spl015	n. d.	0.07	0.21	30.84	37.43	0.18	15.53	0.14	0.13	12.89	2.64	100.11	0.866	0.002	0.004	1.064	0.058	0.315	0.005	0.677	0.003	0.004					
Vranduk Fm.	BO52spl016	n. d.	0.22	0.22	18.14	49.00	0.25	11.55	0.07	0.20	17.23	3.68	100.57	1.219	0.005	0.005	0.673	0.087	0.453	0.007	0.542	0.002	0.005					
Vranduk Fm.	BO52spl017	n. d.	0.41	0.30	20.80	41.28	0.25	10.99	0.12	0.12	18.64	7.52	100.44	1.022	0.010	0.006	0.768	0.177	0.488	0.007	0.513	0.003	0.004					
Vranduk Fm.	BO52spl018	n. d.	0.04	0.27	21.81	46.34	0.21	13.39	0.08	0.16	14.82	3.10	100.22	1.125	0.001	0.006	0.790	0.072	0.381	0.005	0.613	0.002	0.004					
Vranduk Fm.	BO52spl019	n. d.	0.10	0.22	24.29	44.09	0.29	12.90	0.11	0.27	15.82	2.19	100.06	1.063	0.002	0.004	0.873	0.050	0.403	0.007	0.586	0.003	0.006					
Vranduk Fm.	BO52spl020	n. d.	0.04	0.29	22.07	45.89	0.23	13.16	0.10	0.11	15.27	3.18	100.32	1.114	0.001	0.004	0.799	0.074	0.392	0.006	0.747	0.004	0.003					
Vranduk Fm.	BO52spl021	n. d.	0.11	0.23	29.67	39.10	0.14	17.20	0.09	0.09	10.23	3.01	99.95	0.901	0.002	0.004	1.019	0.066	0.249	0.004	0.707	0.004	0.002					
Vranduk Fm.	BO52spl022	n. d.	0.18	0.30	21.59	44.16	0.28	11.71	0.17	0.17	17.40	4.43	100.33	1.084	0.004	0.006	0.846	0.104	0.452	0.007	0.542	0.003	0.004					
Vranduk Fm.	BO52spl023	n. d.	0.07	0.28	23.87	44.80	0.15	15.45	0.14	0.08	12.11	3.32	100.27	1.064	0.002	0.006	0.846	0.075	0.304	0.004	0.692	0.003	0.002					
Vranduk Fm.	BO52spl024	n. d.	0.07	0.35	16.44	52.21	0.21	12.06	0.06	0.15	16.07	2.43	100.05	1.309	0.002	0.007	0.615	0.058	0.426	0.006	0.570	0.002	0.003					
Vranduk Fm.	BO52spl025	n. d.	0.05	0.33	24.58	43.19	0.18	13.60	0.11	0.15	14.90	2.80	99.89	1.038	0.001	0.007	0.881	0.064	0.379	0.005	0.616	0.003	0.003					
Vranduk Fm.	BO52spl026	n. d.	0.04	0.30	20.96	48.86	0.22	13.49	0.08	0.19	14.50	1.43	100.06	1.190	0.001	0.006	0.762	0.033	0.374	0.006	0.620	0.002	0.004					
Vranduk Fm.	BO52spl027	n. d.	0.28	0.29	25.31	41.09	0.18	14.15	0.13	0.12	14.48	4.33	100.36	0.978	0.006	0.006	0.899	0.098	0.365	0.005	0.635	0.003	0.003					
Vranduk Fm.	BO52spl028	n. d.	0.06	0.30	26.30	42.29	0.18	13.99	0.07	0.14	15.20	1.63	99.77	1.010	0.001	0.006	0.937	0.037	0.384	0.005	0.612	0.002	0.003					
Vranduk Fm.	BO52spl029	n. d.	0.09	0.29	15.33	52.01	0.28	9.88	0.06	0.17	19.11	2.77	99.98	1.330	0.002	0.006	0.585	0.067	0.517	0.008	0.476	0.001	0.004					
Vranduk Fm.	BO52spl030	n. d.	0.10	0.31	25.11	43.67	0.20	14.03	0.10	0.14	14.50	2.19	100.35	1.041	0.002	0.006	0.892	0.050	0.366	0.005	0.630	0.002	0.003					
Vranduk Fm.	BO52spl031	n. d.	0.08	0.21	27.87	41.80	0.16	16.26	0.15	0.08	11.38	2.01	100.00	0.974	0.002	0.004	0.969	0.045	0.281	0.004	0.715	0.004	0.002					
Vranduk Fm.	BO52spl032	n. d.	0.04	0.22	26.04	43.56	0.19	14.72	0.11	0.13	13.40	1.59	100.00	1.032	0.001	0.004	0.920	0.036	0.336	0.005	0.658	0.003	0.003					
Vranduk Fm.	BO52spl034	0.20	0.04	0.27	22.57	46.01	0.20	14.51	0.10	0.11	13.28	3.20	100.48	1.105	0.001	0.005	0.808	0.073	0.338	0.005	0.657	0.002	0.002					
Vranduk Fm.	BO52spl035	n. d.	0.10	0.23	32.86	35.21	0.15	17.51	0.21	0.10	10.09	3.20	99.66	0.802	0.002	0.004	1.116	0.069	0.243	0.004	0.751	0.005	0.002					
Vranduk Fm.	BO52spl036	n. d.	0.99	0.50	18.58	38.73	0.29	10.37	0.17	0.18	19.76	11.08	100.65	0.971	0.024	0.011	0.695	0.264	0.524	0.008	0.490	0.004	0.004					
Vranduk Fm.	BO52spl037	n. d.	0.07	0.39	16.72	49.98	0.31	9.97	0.05	0.22	19.24	3.33	100.29	1.267	0.003	0.005	0.832	0.180	0.428	0.008	0.476	0.001	0.004					
Vranduk Fm.	BO52spl038	n. d.	0.20	0.24	26.06	37.87	0.24	12.54	0.11	0.19	16.90	6.23	100.59	0.907	0.005	0.005	0.931	0.142	0.428	0.006	0.566	0.003	0.004					
Vranduk Fm.	BO52spl039	n. d.	0.20	0.34	11.22	53.96	0.33	8.09	0.04	0.27	21.30	4.64	100.39	1.418	0.005	0.007	0.440	0.116	0.592	0.009	0.401	0.001	0.007					
Vranduk Fm.	BO52spl040	n. d.	0.60	0.37	17.40	50.55	0.24	12.02	0.10	0.13	16.30	3.28	100.51	1.257	0.008	0.008	0.645	0.074	0.429	0.007	0.566	0.002	0.003					
Vranduk Fm.	BO52spl041	n. d.	0.07	0.30	26.69	36.94	0.24	12.42	0.15	0.23	17.44	5.10	100.20	0.886	0.014	0.007	0.954	0.116	0.442	0.006	0.561	0.004	0.005					
Vranduk Fm.	BO52spl042	n. d.	0.25	0.29	17.36	48.40	0.27	10.52	0.08	0.15	18.65	4.23	100.19	1.221	0.006	0.006	0.653	0.101	0.497	0.007	0.500	0.002	0.003					
Vranduk Fm.	BO52spl043	n. d.	0.21	0.26	16.07	47.97	0.24	9.08	0.12	0.10	20.62	5.54	100.20	1.229	0.005	0.006	0.614	0.135	0.559	0.006	0.438	0.003	0.002					
Vranduk Fm.	BO52spl044	n. d.	0.13	0.33	23.39	45.53	0.21	14.86	0.14	0.11	12.99	2.70	100.38	1.087	0.003	0.007	0.832	0.068	0.328	0.005	0.668	0.003	0.002					
Vranduk Fm.	BO52spl045	n. d.	0.10	0.25	26.47	42.62	0.18	16.61	0.18	0.07	10.68	3.04	100.21	0.995	0.002	0.005	0.922	0.068	0.264	0.004	0.731	0.004	0.002					
Vranduk Fm.	BO52spl046	n. d.	0.13	0.28	18.80	50.95	0.19	13.80	0.07	0.13	13.91	2.07	100.33	1.247	0.003	0.006	0.686	0.048	0.360	0.005	0.637	0.002	0.003					
Vranduk Fm.	BO52spl047	n. d.	0.04	0.29	22.67	45.57	0.22	12.31	0.07	0.20	16.75	2.58	100.70	1.106	0.001	0.006	0.820	0.060	0.430	0.006	0.563	0.002	0.005					
Vranduk Fm.	BO52spl048	n. d.	0.12	0.24	24.30	45.49	0.18	15.92	0.11	0.07	11.47	2.28	100.17	1.076	0.003	0.005	0.857	0.051	0.287	0.005	0.710	0.003	0.002					
Vranduk Fm.	BO52spl049	n. d.	0.08	0.22	27.22	41.16	0.21	14.96	0.11	0.11	13.33	2.95	100.35	0.967	0.002	0.004	0.954	0.066	0.331	0.005	0.663	0.003	0.003					
Vranduk Fm.	BO52spl050	n. d.	0.38	0.25	17.87	48.26	0.23	11.70	0.12	0.07	17.26	4.65	100.79	1.199	0.009	0.005	0.662	0.110	0.454	0.006	0.548	0.003	0.002					
Vranduk Fm.	BO52spl051	n. d.	0.07	0.25	24.48	43.61	0.18	13.73	0.11	0.16	14.78	2.95	100.32	1.044	0.002	0.005	0.874	0.067	0.374	0.005	0.620	0.003	0.004					
Vranduk Fm.	BO52spl052	n. d.	0.06	0.25	23.99	45.19	0.22	12.41	0.07	0.14	16.78	1.36	100.50	1.091	0.001	0.005	0.864	0.031	0.429	0.006	0.565	0.002	0.004					
Vranduk Fm.	BO52spl053	n. d.	0.03	0.12	26.14	39.37	0.17	14.43	0.15	0.17	13.68	5.72	99.96	0.936	0.001	0.002	0.927	0.130	0.344	0.004	0.647	0.004	0.003					
Vranduk Fm.	BO52spl054	n. d.	0.09	0.20	22.64	46.59	0.21	14.30	0.08	0.11	13.66	2.00	100.18	1.120	0.002	0.004	0.822	0.046	0.430	0.005	0.648	0.002	0.003					
Vranduk Fm.	BO52spl055	n. d.	0.23	0.29	20.54	46.14	0.25	12.57	0.08	0.11	16.16	4.19	100.57	1.129	0.005	0.006	0.750	0.098	0.418	0.007	0.580	0.002	0.003					
Vranduk Fm.	BO52spl056	n. d.	0.08	0.30	19.54	50.26	0.24	13.08	0.08	0.12	15.04	1.55	100.29	1.233	0.002	0.006	0.715	0.036	0.390	0.006	0.605	0.002	0.003					
Vranduk Fm.	BO52spl057	n. d.	0.17	0.29	27.85	38.55	0.21	14.47	0.13	0.16	14.18	4.23	100.24	0.908	0.004	0.004	0.978	0.095	0.353	0.005	0.642	0.003	0.004					
Vranduk Fm.	BO52spl058	n. d.	0.05	0.32	22.45	45.74	0.19	13.02	0.10	0.15	15.66	2.90	100.58	1.107	0.001	0.006	0.810	0.067	0.401	0.005	0.594	0.002	0.003					
Vranduk Fm.	BO52spl059	n. d.	0.31	0.30	14.33	51.21	0.31	9.69	0.07	0.19	19.48	4.51	100.40	1.313	0.007	0.006	0.548	0.110	0.529	0.008	0.468	0.002	0.005					
Vranduk Fm.	BO52spl060	n. d.	0.09	0.28	27.88	40.74	0.18	14.02	0.08	0.18	14.73	1.53	99.71	0.965	0.002	0.005	0.985	0.035	0.369	0.004	0.626	0.002	0.004					
Vranduk Fm.	BO52spl061	n. d.	0.07	0.40	21.32	47.85	0.24	13.20	0.08	0.16	15.16	1.82	100.29	1.164	0.002	0.008	0.773	0.042	0.390	0.006	0.605	0.002	0.004					
Vranduk Fm.	BO52spl062	n. d.	0.08	0.27	16.21	52.76	0.25	12.21	0.06	0.14	15.84	2.56	100.38	1.319	0.002	0.006	0.604	0.061	0.419	0.007	0.575	0.001	0.003					
Vranduk Fm.	BO52spl063	n. d.	0.06	0.31	24.13																							

**analyses in wt%. Shown are the recalculated FeO and Fe<sub>2</sub>O<sub>3</sub> values and the amended total**

Formation	Sample & spot ID	n.d.: not detected												cations per formula unit on the basis of 3 oxygens													
		SiO <sub>2</sub>	TiO <sub>2</sub>	V <sub>2</sub> O <sub>5</sub>	Al <sub>2</sub> O <sub>3</sub>	Cr <sub>2</sub> O <sub>3</sub>	MnO	MgO	NiO	ZnO	FeO	Fe <sub>2</sub> O <sub>3</sub>	Total	Cr	Ti	V	Al	Fe <sup>3+</sup>	Fe <sup>2+</sup>	Mn	Mg	Ni	Zn				
Vranduk Fm.	BO52sp068	n. d.	0.09	0.23	27.24	41.69	0.16	15.54	0.12	0.11	12.37	2.38	99.94	0.979	0.002	0.004	0.954	0.053	0.307	0.004	0.688	0.003	0.002				
Vranduk Fm.	BO52sp069	n. d.	0.05	0.35	23.37	44.87	0.18	13.23	0.08	0.15	15.42	2.53	100.23	1.083	0.001	0.007	0.841	0.058	0.394	0.005	0.602	0.002	0.003				
Vranduk Fm.	BO52sp070	n. d.	0.20	0.34	16.58	50.51	0.27	10.03	0.06	0.22	19.32	3.00	100.54	1.278	0.005	0.007	0.625	0.072	0.517	0.007	0.478	0.002	0.005				
Vranduk Fm.	BO52sp071	n. d.	0.03	0.32	21.09	46.99	0.30	12.05	0.06	0.19	16.79	2.68	100.50	1.151	0.001	0.007	0.771	0.063	0.435	0.008	0.557	0.002	0.004				
Vranduk Fm.	BO52sp072	n. d.	0.09	0.36	23.93	43.62	0.22	12.85	0.07	0.15	16.04	2.71	100.04	1.055	0.002	0.007	0.863	0.062	0.410	0.006	0.586	0.002	0.003				
Vranduk Fm.	BO52sp073	n. d.	0.21	0.28	24.39	43.93	0.21	14.11	0.09	0.11	14.41	2.75	100.49	1.048	0.005	0.006	0.868	0.063	0.364	0.005	0.635	0.002	0.002				
Vranduk Fm.	BO52sp074	n. d.	0.14	0.24	28.24	40.77	0.14	15.98	0.17	0.07	12.01	2.41	100.18	0.949	0.003	0.005	0.981	0.054	0.296	0.002	0.702	0.004	0.002				
Vranduk Fm.	BO52sp075	n. d.	0.13	0.24	22.91	44.46	0.22	13.92	0.09	0.13	14.23	3.82	100.14	1.072	0.003	0.005	0.824	0.088	0.363	0.006	0.633	0.002	0.003				
Vranduk Fm.	BO52sp076	n. d.	0.09	0.19	25.99	41.22	0.23	14.22	0.10	0.21	14.07	3.75	100.09	0.981	0.002	0.004	0.922	0.085	0.354	0.006	0.638	0.003	0.005				
Vranduk Fm.	BO52sp077	n. d.	0.06	0.33	19.89	48.40	0.24	13.11	0.09	0.12	14.98	2.94	100.16	1.187	0.001	0.007	0.727	0.069	0.389	0.006	0.606	0.002	0.003				
Vranduk Fm.	BO52sp078	n. d.	0.07	0.33	22.48	46.30	0.24	11.92	0.05	0.29	17.21	1.53	100.41	1.129	0.002	0.007	0.818	0.035	0.444	0.006	0.548	0.001	0.007				
Vranduk Fm.	BO52sp079	n. d.	0.06	0.34	24.52	42.67	0.24	12.06	0.06	0.19	17.37	2.87	100.38	1.032	0.001	0.007	0.884	0.066	0.444	0.006	0.550	0.002	0.004				
Vranduk Fm.	BO52sp080	n. d.	0.13	0.25	18.67	49.13	0.28	10.46	0.05	0.24	18.83	2.33	100.38	1.230	0.003	0.005	0.697	0.056	0.499	0.008	0.494	0.001	0.006				
Vranduk Fm.	BO52sp081	n. d.	0.03	0.38	18.91	48.55	0.25	11.22	0.06	0.22	17.67	2.92	100.22	1.210	0.001	0.008	0.703	0.069	0.466	0.007	0.527	0.001	0.005				
Vranduk Fm.	BO52sp082	n. d.	0.02	0.26	29.18	39.03	0.18	14.55	0.12	0.14	14.13	2.38	99.98	0.915	0.000	0.005	1.020	0.053	0.350	0.004	0.643	0.003	0.003				
Vranduk Fm.	BO52sp083	n. d.	0.13	0.25	11.57	56.08	0.28	10.55	0.03	0.14	17.63	3.65	100.30	1.448	0.003	0.005	0.445	0.090	0.481	0.008	0.513	0.001	0.003				
Vranduk Fm.	BO52sp084	n. d.	0.08	0.22	25.90	42.49	0.17	14.66	0.12	0.09	13.64	2.99	100.36	1.006	0.002	0.004	0.914	0.067	0.341	0.004	0.654	0.003	0.002				
Vranduk Fm.	BO52sp085	n. d.	0.04	0.31	21.76	46.62	0.21	13.35	0.07	0.15	14.94	2.83	100.28	1.132	0.001	0.006	0.788	0.065	0.384	0.006	0.611	0.002	0.003				
Vranduk Fm.	BO52sp086	n. d.	0.10	0.25	27.28	41.04	0.17	15.21	0.14	0.11	12.89	2.78	99.98	0.966	0.002	0.005	0.957	0.062	0.321	0.004	0.675	0.003	0.002				
Vranduk Fm.	BO52sp087	n. d.	0.11	0.22	27.46	39.57	0.19	15.56	0.15	0.10	12.26	4.13	99.74	0.931	0.002	0.004	0.963	0.092	0.305	0.005	0.690	0.004	0.002				
Vranduk Fm.	BO52sp088	n. d.	0.11	0.23	26.78	41.75	0.19	14.18	0.08	0.18	14.44	2.27	100.22	0.989	0.002	0.005	0.946	0.051	0.362	0.005	0.633	0.002	0.004				
Vranduk Fm.	BO52sp089	n. d.	0.10	0.31	23.78	44.64	0.22	12.12	0.06	0.20	16.89	1.05	99.36	1.091	0.002	0.006	0.867	0.024	0.437	0.006	0.568	0.001	0.005				
Vranduk Fm.	BO52sp090	n. d.	0.33	0.26	20.68	46.57	0.19	13.52	0.12	0.11	14.90	4.14	100.81	1.130	0.008	0.005	0.748	0.096	0.382	0.005	0.618	0.003	0.002				
Vranduk Fm.	BO59sp001	n. d.	0.09	0.26	23.36	44.93	0.22	13.39	0.09	0.18	15.21	2.95	100.68	1.080	0.002	0.005	0.837	0.067	0.387	0.006	0.607	0.002	0.004				
Vranduk Fm.	BO59sp002	n. d.	0.09	0.28	22.00	46.70	0.21	13.69	0.10	0.09	14.44	2.47	100.07	1.132	0.001	0.006	0.795	0.057	0.370	0.005	0.626	0.003	0.002				
Vranduk Fm.	BO59sp003	n. d.	0.04	0.21	24.99	44.37	0.15	15.08	0.11	0.15	12.79	2.45	100.34	1.051	0.001	0.004	0.883	0.055	0.320	0.004	0.674	0.003	0.003				
Vranduk Fm.	BO59sp004	n. d.	0.53	0.37	21.82	42.76	0.19	13.89	0.14	0.10	14.35	5.49	99.64	1.041	0.012	0.008	0.792	0.127	0.369	0.005	0.637	0.003	0.002				
Vranduk Fm.	BO59sp005	n. d.	0.09	0.33	21.80	46.13	0.23	12.78	0.08	0.12	15.85	2.79	100.23	1.505	0.005	0.005	0.427	0.065	0.409	0.006	0.587	0.002	0.003				
Vranduk Fm.	BO59sp006	n. d.	0.19	0.25	11.21	58.96	0.25	12.42	0.04	0.13	14.81	1.97	100.23	1.505	0.005	0.005	0.448	0.040	0.400	0.007	0.598	0.001	0.003				
Vranduk Fm.	BO59sp007	n. d.	0.05	0.43	18.00	50.06	0.23	11.70	0.07	0.15	17.04	2.89	100.61	1.244	0.001	0.009	0.667	0.068	0.448	0.006	0.548	0.002	0.003				
Vranduk Fm.	BO59sp008	n. d.	0.74	0.39	23.51	38.43	0.24	11.06	0.14	0.21	19.01	5.96	99.68	0.946	0.017	0.008	0.863	0.140	0.495	0.006	0.513	0.003	0.005				
Vranduk Fm.	BO59sp009	n. d.	0.06	0.27	23.99	44.44	0.19	14.49	0.16	0.09	13.61	3.21	100.51	1.060	0.001	0.005	0.853	0.073	0.343	0.005	0.651	0.004	0.002				
Vranduk Fm.	BO59sp010	n. d.	0.06	0.26	22.48	45.67	0.24	13.17	0.08	0.12	15.30	2.88	100.25	1.107	0.001	0.005	0.813	0.066	0.392	0.006	0.602	0.002	0.003				
Vranduk Fm.	BO59sp011	n. d.	0.10	0.29	28.56	39.82	0.18	15.45	0.13	0.13	12.66	2.43	99.74	0.932	0.002	0.006	0.997	0.054	0.314	0.004	0.682	0.003	0.003				
Vranduk Fm.	BO59sp012	n. d.	0.04	0.31	20.10	49.21	0.22	13.83	0.08	0.10	14.00	2.46	100.34	1.198	0.001	0.006	0.730	0.057	0.361	0.006	0.635	0.002	0.002				
Vranduk Fm.	BO59sp013	n. d.	0.37	0.29	21.07	43.02	0.25	10.37	0.10	0.15	19.38	4.66	99.67	1.074	0.009	0.006	0.785	0.111	0.512	0.007	0.488	0.003	0.004				
Vranduk Fm.	BO59sp014	n. d.	0.20	0.32	19.50	49.41	0.22	13.04	0.08	0.07	15.24	2.09	100.17	1.214	0.005	0.007	0.714	0.049	0.396	0.006	0.604	0.002	0.002				
Vranduk Fm.	BO59sp015	n. d.	0.06	0.29	23.20	43.66	0.22	12.47	0.07	0.17	16.27	3.19	99.59	1.066	0.001	0.006	0.845	0.074	0.420	0.006	0.574	0.002	0.004				
Vranduk Fm.	BO59sp016	n. d.	0.12	0.27	26.26	41.01	0.20	15.24	0.14	0.07	12.66	3.85	99.81	0.970	0.003	0.005	0.926	0.087	0.317	0.005	0.680	0.003	0.002				
Vranduk Fm.	BO59sp017	n. d.	0.13	0.28	17.81	51.38	0.28	11.98	0.05	0.20	16.42	1.84	100.36	1.278	0.003	0.006	0.661	0.043	0.432	0.007	0.562	0.001	0.005				
Vranduk Fm.	BO59sp018	n. d.	0.11	0.27	27.04	41.18	0.18	14.79	0.12	0.17	13.54	2.83	100.23	0.970	0.002	0.005	0.950	0.064	0.338	0.005	0.657	0.003	0.004				
Vranduk Fm.	BO59sp019	n. d.	0.24	0.27	27.62	40.42	0.22	14.54	0.13	0.16	13.90	2.08	99.58	0.957	0.005	0.005	0.975	0.047	0.348	0.006	0.649	0.003	0.004				
Vranduk Fm.	BO59sp020	0.04	0.16	0.25	23.80	41.16	0.22	12.95	0.14	0.17	15.75	5.48	100.11	0.996	0.004	0.005	0.859	0.126	0.403	0.006	0.591	0.003	0.004				
Vranduk Fm.	BO59sp021	n. d.	0.05	0.30	22.30	45.33	0.25	12.52	0.06	0.14	16.19	2.86	100.00	1.106	0.001	0.006	0.812	0.066	0.418	0.007	0.576	0.001	0.003				
Vranduk Fm.	BO59sp022	n. d.	0.06	0.29	23.54	43.96	0.23	13.13	0.06	0.16	15.51	3.23	100.16	1.062	0.001	0.006	0.848	0.074	0.396	0.006	0.598	0.002	0.004				
Vranduk Fm.	BO59sp023	n. d.	0.11	0.32																							

analyses in wt%. Shown are the recalculated FeO and Fe<sub>2</sub>O<sub>3</sub> values and the amended total cations per formula unit on the basis of 3 oxygens

Formation	Sample & spot ID	SiO <sub>2</sub>	TiO <sub>2</sub>	V <sub>2</sub> O <sub>5</sub>	Al <sub>2</sub> O <sub>3</sub>	Cr <sub>2</sub> O <sub>3</sub>	MnO	MgO	NiO	ZnO	FeO	Fe <sub>2</sub> O <sub>3</sub>	Total	Cr	Ti	V	Al	Fe <sup>3+</sup>	Fe <sup>2+</sup>	Mn	Mg	Ni	Zn
Vranduk Fm.	BO59sp036	n. d.	0.33	0.30	19.39	41.95	0.31	9.17	0.10	0.16	21.01	7.57	100.29	1.059	0.008	0.006	0.730	0.182	0.561	0.008	0.436	0.003	0.004
Vranduk Fm.	BO59sp037	n. d.	0.06	0.31	22.69	46.69	0.20	14.28	0.10	0.15	13.72	2.23	100.43	1.121	0.001	0.006	0.812	0.051	0.348	0.005	0.646	0.003	0.003
Vranduk Fm.	BO59sp038	n. d.	0.10	0.24	26.07	40.96	0.22	13.32	0.13	0.21	15.57	3.53	100.35	0.977	0.002	0.005	0.928	0.080	0.393	0.006	0.599	0.003	0.005
Vranduk Fm.	BO59sp039	n. d.	0.17	0.46	15.60	52.14	0.26	11.56	0.05	0.13	16.99	1.310	100.57	1.310	0.004	0.010	0.585	0.077	0.452	0.007	0.548	0.001	0.003
Vranduk Fm.	BO59sp040	n. d.	0.10	0.33	19.87	48.21	0.23	12.67	0.07	0.14	15.58	2.56	99.74	1.190	0.002	0.007	0.731	0.060	0.407	0.006	0.589	0.002	0.003
Vranduk Fm.	BO59sp041	n. d.	0.06	0.28	19.40	49.83	0.22	12.50	0.06	0.16	15.93	2.02	100.47	1.226	0.001	0.006	0.712	0.047	0.415	0.006	0.580	0.002	0.004
Vranduk Fm.	BO59sp042	n. d.	0.09	0.25	19.82	48.90	0.19	14.34	0.10	0.06	13.18	3.32	100.27	1.189	0.002	0.005	0.719	0.077	0.339	0.005	0.657	0.003	0.001
Vranduk Fm.	BO59sp043	n. d.	0.09	0.32	23.46	42.73	0.20	13.39	0.12	0.19	14.97	4.40	99.88	1.034	0.002	0.007	0.847	0.101	0.383	0.005	0.611	0.003	0.004
Vranduk Fm.	BO59sp044	n. d.	0.11	0.24	19.29	48.48	0.27	12.34	0.07	0.16	16.00	3.17	100.13	1.198	0.003	0.005	0.711	0.075	0.418	0.007	0.575	0.002	0.004
Vranduk Fm.	BO59sp045	n. d.	0.09	0.20	24.40	44.28	0.21	14.11	0.12	0.11	14.08	2.38	99.98	1.061	0.002	0.004	0.872	0.054	0.357	0.005	0.637	0.003	0.002
Vranduk Fm.	BO59sp046	n. d.	0.07	0.23	23.02	41.63	0.22	12.03	0.16	0.29	19.88	4.54	100.06	1.030	0.002	0.005	0.850	0.107	0.520	0.006	0.468	0.004	0.007
Vranduk Fm.	BO59sp047	n. d.	0.09	0.25	19.05	49.98	0.24	12.49	0.07	0.17	15.89	2.34	100.58	1.230	0.002	0.005	0.699	0.055	0.414	0.006	0.580	0.002	0.004
Vranduk Fm.	BO59sp048	n. d.	0.04	0.20	24.08	44.92	0.19	14.19	0.12	0.16	13.79	2.18	99.89	1.078	0.001	0.004	0.862	0.050	0.350	0.005	0.642	0.003	0.004
Vranduk Fm.	BO59sp049	n. d.	0.11	0.24	15.93	53.91	0.25	11.95	0.07	0.15	16.26	1.71	100.59	1.349	0.003	0.005	0.594	0.041	0.430	0.007	0.564	0.002	0.004
Vranduk Fm.	BO59sp050	n. d.	0.12	0.26	27.79	39.26	0.19	14.75	0.13	0.13	13.71	3.80	100.15	0.924	0.003	0.005	0.975	0.085	0.341	0.005	0.654	0.003	0.003
Vranduk Fm.	BO59sp051	n. d.	0.33	0.35	11.88	53.21	0.36	7.72	0.05	0.22	22.08	4.11	100.32	1.399	0.008	0.008	0.466	0.103	0.614	0.010	0.383	0.001	0.005
Vranduk Fm.	BO59sp052	n. d.	0.09	0.36	21.87	45.64	0.26	11.58	0.07	0.29	17.39	2.17	99.72	1.125	0.002	0.007	0.804	0.051	0.454	0.007	0.538	0.002	0.007
Vranduk Fm.	BO59sp053	n. d.	0.07	0.28	25.15	42.49	0.20	14.60	0.09	0.11	13.50	3.55	100.05	1.012	0.002	0.006	0.893	0.081	0.340	0.005	0.655	0.002	0.002
Vranduk Fm.	BO59sp054	n. d.	0.07	0.33	22.96	45.13	0.26	12.28	0.06	0.22	16.71	2.25	100.26	1.098	0.002	0.007	0.833	0.052	0.430	0.007	0.563	0.002	0.005
Vranduk Fm.	BO59sp055	n. d.	0.08	0.29	20.59	48.08	0.22	13.36	0.08	0.11	14.79	2.70	100.30	1.172	0.002	0.006	0.749	0.063	0.382	0.006	0.614	0.002	0.003
Vranduk Fm.	BO59sp056	n. d.	0.22	0.36	14.12	51.37	0.30	8.83	0.07	0.19	20.78	4.29	100.53	1.325	0.005	0.008	0.543	0.105	0.567	0.008	0.429	0.002	0.005
Vranduk Fm.	BO59sp057	n. d.	0.11	0.20	22.64	45.82	0.19	14.00	0.07	0.14	14.05	2.87	100.10	1.106	0.003	0.004	0.815	0.066	0.359	0.005	0.637	0.002	0.003
Vranduk Fm.	BO59sp058	n. d.	0.09	0.30	27.25	39.36	0.19	12.88	0.11	0.31	16.36	3.33	100.18	0.939	0.002	0.006	0.969	0.076	0.413	0.005	0.579	0.003	0.007
Vranduk Fm.	BO59sp059	n. d.	0.28	0.34	19.57	45.85	0.26	12.17	0.09	0.13	16.62	5.21	100.53	1.130	0.007	0.007	0.719	0.122	0.434	0.007	0.566	0.002	0.003
Vranduk Fm.	BO59sp060	n. d.	0.06	0.32	20.54	47.73	0.26	11.66	0.08	0.10	17.29	2.13	100.22	1.178	0.001	0.007	0.756	0.050	0.451	0.005	0.542	0.002	0.004
Vranduk Fm.	BO59sp061	n. d.	0.26	0.27	23.54	43.61	0.18	14.21	0.15	0.14	14.00	3.89	100.25	1.046	0.006	0.005	0.842	0.089	0.355	0.005	0.643	0.004	0.003
Vranduk Fm.	BO59sp062	0.57	0.23	0.31	14.94	50.75	0.22	10.49	0.09	0.18	18.20	4.46	100.45	1.297	0.006	0.007	0.589	0.109	0.492	0.006	0.505	0.002	0.004
Vranduk Fm.	BO59sp063	n. d.	0.01	0.35	21.54	46.62	0.26	12.07	0.06	0.27	16.69	2.29	100.15	1.143	0.000	0.007	0.788	0.054	0.433	0.007	0.558	0.001	0.006
Vranduk Fm.	BO59sp064	n. d.	0.10	0.24	28.89	38.73	0.17	14.75	0.14	0.14	13.78	2.92	99.88	0.909	0.002	0.005	1.011	0.065	0.342	0.004	0.653	0.003	0.003
Vranduk Fm.	BO59sp065	n. d.	0.12	0.22	25.13	43.51	0.17	15.92	0.13	0.07	11.53	3.28	100.09	1.027	0.003	0.004	0.885	0.074	0.288	0.004	0.708	0.003	0.002
Vranduk Fm.	BO59sp066	n. d.	0.22	0.26	13.64	55.08	0.25	12.46	0.10	0.10	15.17	3.14	100.42	1.389	0.005	0.006	0.513	0.075	0.405	0.007	0.593	0.003	0.002
Vranduk Fm.	BO59sp067	n. d.	0.06	0.27	25.83	41.10	0.19	14.27	0.13	0.16	14.02	4.00	100.03	0.978	0.001	0.005	0.917	0.091	0.353	0.005	0.640	0.003	0.003
Vranduk Fm.	BO59sp068	n. d.	0.16	0.39	23.06	42.42	0.24	12.49	0.12	0.20	16.47	4.75	100.29	1.031	0.004	0.008	0.836	0.110	0.423	0.006	0.572	0.003	0.005
Vranduk Fm.	BO59sp069	n. d.	0.59	0.39	17.71	44.16	0.27	10.72	0.11	0.14	18.71	7.48	100.29	1.111	0.014	0.008	0.664	0.179	0.498	0.007	0.508	0.003	0.003
Vranduk Fm.	BO59sp070	n. d.	0.06	0.24	25.93	44.31	0.20	14.18	0.05	0.21	14.18	0.49	99.84	1.055	0.001	0.005	0.921	0.011	0.357	0.005	0.637	0.001	0.005
Vranduk Fm.	BO59sp071	0.03	0.08	0.22	22.26	46.79	0.18	14.54	0.11	0.07	13.22	2.71	100.21	1.126	0.002	0.005	0.799	0.062	0.336	0.005	0.660	0.003	0.002
Vranduk Fm.	BO59sp072	n. d.	0.34	0.38	22.02	42.28	0.24	12.52	0.15	0.18	16.32	5.60	100.02	1.034	0.008	0.008	0.803	0.130	0.422	0.006	0.577	0.004	0.004
Vranduk Fm.	BO59sp073	n. d.	0.18	0.27	21.36	47.82	0.17	15.31	0.19	0.05	11.98	2.89	100.21	1.149	0.004	0.005	0.765	0.066	0.305	0.004	0.693	0.005	0.001
Vranduk Fm.	BO59sp074	n. d.	0.13	0.39	19.25	45.62	0.25	10.27	0.09	0.18	19.10	4.44	99.73	1.148	0.003	0.008	0.722	0.106	0.508	0.007	0.487	0.002	0.004
Vranduk Fm.	BO59sp075	n. d.	0.11	0.26	20.87	47.78	0.19	13.99	0.10	0.10	13.76	2.69	99.84	1.163	0.003	0.005	0.758	0.062	0.354	0.005	0.642	0.002	0.002
Vranduk Fm.	BO59sp076	n. d.	0.10	0.33	17.32	50.90	0.21	12.05	0.09	0.10	16.26	2.72	100.09	1.271	0.002	0.007	0.645	0.065	0.429	0.006	0.567	0.002	0.002
Vranduk Fm.	BO59sp077	n. d.	0.02	0.24	24.81	44.33	0.21	13.35	0.08	0.15	15.25	1.46	99.92	1.066	0.001	0.005	0.889	0.034	0.388	0.006	0.605	0.002	0.003
Vranduk Fm.	BO59sp078	n. d.	0.09	0.20	26.87	41.15	0.19	14.22	0.11	0.19	14.30	2.85	100.16	0.975	0.002	0.004	0.949	0.064	0.358	0.005	0.635	0.003	0.004
Vranduk Fm.	BO59sp079	n. d.	0.04	0.33	18.20	49.79	0.23	13.29	0.09	0.11	14.50	3.80	100.37	1.226	0.001	0.007	0.668	0.089	0.378	0.006	0.617	0.002	0.003
Vranduk Fm.	BO59sp080	n. d.	0.29	0.36	24.93	39.59	0.19	14.55	0.13	0.12	13.71	6.18	100.09	0.944	0.007	0.007	0.887	0.140	0.346	0.005	0.654	0.004	0.003
Vranduk Fm.	BO59sp081	n. d.	0.06	0.30	23.00	46.27	0.19	15.31	0.17	0.07	12.23	2.89	100.45	1.102	0.001	0.006	0.817	0.065	0.308	0.005	0.688	0.003	0.001
Vranduk Fm.	BO59sp082	n. d.	0.07	0.21	20.97	46.61	0.25	11.84	0.10	0.22	16.96	3.05	100.28	1.147	0.002	0.004	0.769	0.071	0.441	0.007	0.549	0.002	0.005
Vranduk Fm.	BO59sp083	n. d.	0.12	0.25	24.75	43.36	0.19	13.32	0.08	0.19	15.33	2.27	99.86	1.044	0.003	0.005	0.888	0.066	0.390	0.005	0.604	0.002	0.004
Vranduk Fm.	BO59sp084	n. d.	0.06	0.27	23.46	44.20	0.21	12.84	0.06	0.17	15.86	2.80	99.94	1.072	0.001	0.005	0.849	0.065	0.407	0.005	0.587	0.002	0.004
Vranduk Fm.	BO59sp085	n. d.	0.06	0.31	23.81	44.01	0.21	13.32	0.08	0.17	15.12	2.62	99.70	1.065	0.001	0.006	0.859	0.060	0.387	0.005	0.608	0.002	0.004
Vranduk Fm.	BO59sp086	n. d.	0.07	0.28	21.73	45.91	0.20	13															

Formation	Sample & spot ID	analyses in wt%. Shown are the recalculated FeO and Fe <sub>2</sub> O <sub>3</sub> values and the amended total													cations per formula unit on the basis of 3 oxygens									
		SiO <sub>2</sub>	TiO <sub>2</sub>	V <sub>2</sub> O <sub>5</sub>	Al <sub>2</sub> O <sub>3</sub>	Cr <sub>2</sub> O <sub>3</sub>	MnO	MgO	NiO	ZnO	FeO	Fe <sub>2</sub> O <sub>3</sub>	Total	Cr	Ti	V	Al	Fe <sup>3+</sup>	Fe <sup>2+</sup>	Mn	Mg	Ni	Zn	
Vranduk Fm.	BO61/sp010	n. d.	0.12	0.22	29.90	39.16	0.18	15.48	0.12	0.18	12.88	1.86	100.10	0.909	0.003	0.004	1.035	0.041	0.316	0.005	0.678	0.003	0.004	
Vranduk Fm.	BO61/sp011	n. d.	0.08	0.21	36.70	31.68	0.14	16.43	0.14	0.12	12.44	1.86	99.79	0.714	0.002	0.004	1.234	0.040	0.297	0.003	0.698	0.003	0.003	
Vranduk Fm.	BO61/sp012	n. d.	0.06	0.26	28.45	40.17	0.19	14.20	0.09	0.18	14.53	1.72	99.86	0.947	0.001	0.005	1.000	0.039	0.363	0.005	0.631	0.002	0.004	
Vranduk Fm.	BO61/sp013	n. d.	0.07	0.25	23.92	44.65	0.24	12.73	0.09	0.16	16.15	1.92	100.18	1.079	0.002	0.005	0.862	0.044	0.413	0.006	0.580	0.002	0.004	
Vranduk Fm.	BO61/sp014	n. d.	0.04	0.35	20.95	47.65	0.24	13.13	0.09	0.12	15.03	2.28	99.87	1.166	0.001	0.007	0.764	0.053	0.389	0.006	0.606	0.002	0.003	
Vranduk Fm.	BO61/sp015	n. d.	0.03	0.30	26.29	41.63	0.26	12.70	0.06	0.19	16.50	2.11	100.07	0.998	0.001	0.006	0.940	0.048	0.418	0.007	0.574	0.002	0.004	
Vranduk Fm.	BO61/sp016	n. d.	0.04	0.30	21.41	47.60	0.23	12.43	0.06	0.17	16.43	2.11	100.77	1.159	0.001	0.006	0.777	0.049	0.423	0.006	0.571	0.002	0.004	
Vranduk Fm.	BO61/sp017	n. d.	0.08	0.27	27.29	42.37	0.15	15.37	0.12	0.11	12.83	1.79	100.38	0.992	0.002	0.005	0.953	0.040	0.318	0.004	0.679	0.003	0.002	
Vranduk Fm.	BO61/sp018	n. d.	0.08	0.18	27.30	41.41	0.16	15.11	0.11	0.13	12.98	2.40	99.86	0.976	0.002	0.004	0.859	0.054	0.324	0.004	0.671	0.003	0.003	
Vranduk Fm.	BO61/sp019	n. d.	0.04	0.27	23.09	45.34	0.19	13.33	0.08	0.15	15.16	2.58	100.23	1.095	0.001	0.005	0.932	0.059	0.387	0.005	0.607	0.002	0.003	
Vranduk Fm.	BO61/sp020	n. d.	0.10	0.24	13.64	54.75	0.27	10.70	0.06	0.13	17.84	3.01	100.75	1.394	0.002	0.005	0.518	0.073	0.480	0.007	0.513	0.002	0.003	
Vranduk Fm.	BO61/sp021	n. d.	0.22	0.35	24.24	42.81	0.24	13.65	0.11	0.15	14.93	3.45	100.14	1.028	0.005	0.007	0.868	0.079	0.379	0.006	0.618	0.003	0.003	
Vranduk Fm.	BO61/sp022	n. d.	0.03	0.28	25.67	43.87	0.17	14.72	0.11	0.12	13.40	1.68	100.05	1.041	0.001	0.006	0.908	0.038	0.336	0.004	0.658	0.003	0.003	
Vranduk Fm.	BO61/sp023	n. d.	0.04	0.28	16.33	49.17	0.32	7.67	0.06	0.16	22.62	3.56	100.21	1.269	0.001	0.006	0.629	0.087	0.618	0.009	0.373	0.002	0.004	
Vranduk Fm.	BO61/sp024	n. d.	0.50	0.35	16.48	50.10	0.23	12.97	0.11	0.10	15.18	4.51	100.53	1.244	0.012	0.007	0.610	0.107	0.399	0.006	0.607	0.003	0.002	
Vranduk Fm.	BO61/sp025	n. d.	0.08	0.21	26.94	41.80	0.17	15.40	0.15	0.13	12.40	2.46	99.73	0.986	0.002	0.004	0.947	0.055	0.309	0.004	0.684	0.004	0.003	
Vranduk Fm.	BO61/sp026	n. d.	0.11	0.26	14.93	51.32	0.32	9.22	0.08	0.21	20.12	3.99	100.56	1.315	0.003	0.006	0.570	0.097	0.545	0.009	0.445	0.002	0.005	
Vranduk Fm.	BO61/sp027	n. d.	0.12	0.21	28.71	40.55	0.19	14.72	0.09	0.15	13.91	1.46	100.11	0.950	0.003	0.004	1.003	0.033	0.345	0.005	0.650	0.002	0.003	
Vranduk Fm.	BO61/sp028	n. d.	0.26	0.29	14.80	50.61	0.27	10.59	0.10	0.17	18.21	5.31	100.61	1.286	0.006	0.006	0.561	0.128	0.489	0.007	0.507	0.003	0.004	
Vranduk Fm.	BO61/sp029	n. d.	0.05	0.29	18.27	51.10	0.24	12.54	0.06	0.12	15.76	2.18	100.61	1.261	0.001	0.006	0.672	0.051	0.411	0.006	0.583	0.002	0.003	
Vranduk Fm.	BO61/sp030	n. d.	0.14	0.25	15.43	53.29	0.28	10.44	0.06	0.13	18.49	1.98	100.48	1.351	0.003	0.005	0.583	0.048	0.496	0.008	0.499	0.001	0.003	
Vranduk Fm.	BO61/sp031	n. d.	0.04	0.30	24.20	44.28	0.22	12.59	0.07	0.18	16.45	1.91	100.24	1.070	0.001	0.006	0.872	0.044	0.420	0.006	0.573	0.002	0.004	
Vranduk Fm.	BO61/sp032	n. d.	0.04	0.34	13.75	54.70	0.25	10.46	0.06	0.11	18.72	2.29	100.36	1.401	0.001	0.007	0.525	0.056	0.507	0.007	0.488	0.002	0.003	
Vranduk Fm.	BO61/sp033	n. d.	0.05	0.28	19.34	47.85	0.25	12.46	0.10	0.12	15.87	4.01	100.34	1.180	0.001	0.006	0.711	0.094	0.414	0.007	0.579	0.002	0.003	
Vranduk Fm.	BO61/sp034	n. d.	0.66	0.40	16.09	40.65	0.30	8.58	0.14	0.13	21.67	11.60	100.22	1.047	0.016	0.009	0.618	0.284	0.591	0.008	0.417	0.004	0.003	
Vranduk Fm.	BO61/sp035	n. d.	0.14	0.25	19.10	48.87	0.25	11.81	0.06	0.24	16.87	2.80	100.38	1.211	0.003	0.005	0.706	0.064	0.442	0.007	0.551	0.001	0.005	
Vranduk Fm.	BO61/sp036	n. d.	0.05	0.32	21.47	47.52	0.20	12.81	0.07	0.16	15.73	1.90	100.22	1.159	0.001	0.006	0.781	0.044	0.406	0.005	0.589	0.002	0.004	
Vranduk Fm.	BO61/sp037	n. d.	0.16	0.29	14.06	53.36	0.27	10.91	0.08	0.20	17.71	3.83	100.70	1.355	0.004	0.006	0.532	0.075	0.501	0.007	0.522	0.002	0.002	
Vranduk Fm.	BO61/sp038	n. d.	0.09	0.27	14.04	53.86	0.27	10.21	0.05	0.11	18.58	3.09	100.67	1.374	0.002	0.006	0.534	0.073	0.501	0.007	0.491	0.001	0.005	
Vranduk Fm.	BO61/sp039	n. d.	0.14	0.31	15.24	53.59	0.19	14.98	0.14	0.04	11.57	4.13	100.33	1.322	0.003	0.006	0.561	0.097	0.302	0.005	0.697	0.004	0.001	
Vranduk Fm.	BO61/sp040	n. d.	0.06	0.32	21.77	47.25	0.24	13.29	0.08	0.13	15.04	2.06	100.24	1.147	0.001	0.006	0.788	0.048	0.386	0.006	0.608	0.002	0.003	
Vranduk Fm.	BO61/sp041	n. d.	0.05	0.28	19.93	48.81	0.20	12.78	0.07	0.14	15.45	2.28	99.99	1.201	0.001	0.006	0.731	0.053	0.402	0.005	0.593	0.002	0.003	
Vranduk Fm.	BO61/sp042	n. d.	0.08	0.20	31.13	35.68	0.16	15.55	0.15	0.17	12.87	4.04	100.03	0.825	0.002	0.004	1.074	0.089	0.315	0.004	0.678	0.003	0.004	
Vranduk Fm.	BO61/sp043	n. d.	0.46	0.36	20.20	42.35	0.33	9.38	0.13	0.14	21.03	6.10	100.48	1.061	0.011	0.008	0.755	0.146	0.558	0.009	0.443	0.003	0.003	
Vranduk Fm.	BO61/sp044	n. d.	0.07	0.40	19.49	48.92	0.24	12.21	0.07	0.15	16.42	2.40	100.37	1.206	0.002	0.008	0.717	0.056	0.428	0.006	0.568	0.002	0.003	
Vranduk Fm.	BO61/sp045	n. d.	0.05	0.29	22.71	45.58	0.23	13.05	0.09	0.16	15.57	2.78	100.51	1.102	0.001	0.006	0.819	0.064	0.398	0.006	0.595	0.002	0.004	
Vranduk Fm.	BO61/sp046	n. d.	0.06	0.30	26.50	42.68	0.21	12.61	0.06	0.23	16.66	0.53	99.84	1.024	0.001	0.006	0.948	0.012	0.423	0.006	0.570	0.001	0.005	
Vranduk Fm.	BO61/sp047	n. d.	0.05	0.32	24.01	44.49	0.21	13.57	0.10	0.16	14.99	2.56	100.48	1.067	0.001	0.006	0.859	0.058	0.380	0.006	0.613	0.002	0.004	
Vranduk Fm.	BO61/sp048	n. d.	0.08	0.22	28.58	40.64	0.16	15.90	0.14	0.09	12.10	2.25	100.17	0.946	0.002	0.004	0.992	0.050	0.298	0.004	0.697	0.003	0.002	
Vranduk Fm.	BO61/sp049	n. d.	0.16	0.26	24.45	43.56	0.21	12.94	0.10	0.17	16.14	2.65	100.64	1.046	0.004	0.005	0.875	0.061	0.410	0.006	0.586	0.002	0.004	
Vranduk Fm.	BO61/sp050	n. d.	0.05	0.25	20.41	48.55	0.22	13.25	0.10	0.09	14.93	2.60	100.45	1.184	0.001	0.005	0.742	0.060	0.385	0.006	0.609	0.002	0.002	
Vranduk Fm.	BO61/sp051	n. d.	0.07	0.24	29.59	37.36	0.20	14.73	0.13	0.13	14.03	3.85	100.30	0.870	0.001	0.005	1.030	0.085	0.346	0.005	0.648	0.003	0.002	
Vranduk Fm.	BO61/sp052	n. d.	0.05	0.20	27.46	41.52	0.16	14.25	0.11	0.16	14.40	1.95	100.27	0.980	0.001	0.004	0.966	0.044	0.360	0.004	0.634	0.003	0.004	
Vranduk Fm.	BO61/sp053	n. d.	0.07	0.27	19.57	50.64	0.22	12.48	0.05	0.12	16.10	1.11	100.63	1.243	0.002	0.005	0.716	0.026	0.418	0.006	0.577	0.001	0.003	
Vranduk Fm.	BO61/sp054	n. d.	0.03	0.38	20.56	48.26	0.21	12.53	0.05	0.22	17.38	1.96	100.16	1.184	0.001	0.008	0.752	0.046	0.415	0.006	0.580	0.001	0.004	
Vranduk Fm.	BO61/sp055	n. d.	0.04	0.27	21.20	45.85	0.23	11.66	0.07	0.18	16.07	3.57	100.50	1.126	0.001	0.006	0.777	0.083	0.452	0.006	0.540	0.002	0.005	
Vranduk Fm.	BO61/sp056	n. d.	0.07	0.13	39.56	28.94	0.12	18.35	0.21	0.07	9.83	2.33	99.62	0.639	0.001	0.002	1.303	0.049	0.230	0.003	0.764	0.005	0.001	
Vranduk Fm.	BO61/sp057	n. d.	0.06	0.24	25.13	44.23	0.19	14.61	0.13	0.09	13.52	2.02	100.23	1.051	0.001	0.005	0.891	0.046	0.340	0.005	0.654	0.003	0.002	
Vranduk Fm.	BO61/sp058	n. d.	0.04	0.33	19.70	48.51	0.22	12.17	0.08	0.15	16.42	2.64	100.24	1.197	0.001	0.007	0.725	0.062	0.429	0.006	0.566	0.002	0.003	
Vranduk Fm.	BO61/sp059	n. d.	0.06	0.28	25.01	43.80	0.21	13.36	0.09	0.14	15.39	1.76	100.10	1.051	0.001	0.006	0.895	0.040	0.390	0.005	0.604	0.002	0.003	
Vranduk Fm.	BO61/sp060	n. d.	0.06	0.29	22.87																			

**analyses in wt%. Shown are the recalculated FeO and Fe<sub>2</sub>O<sub>3</sub> values and the amended total**

Formation	Sample & spot ID	n.d.: not detected		cations per formula unit on the basis of 3 oxygens																				
		SiO <sub>2</sub>	TiO <sub>2</sub>	V <sub>2</sub> O <sub>5</sub>	Al <sub>2</sub> O <sub>3</sub>	Cr <sub>2</sub> O <sub>3</sub>	MnO	MgO	NiO	ZnO	FeO	Fe <sub>2</sub> O <sub>3</sub>	Total	Cr	Ti	V	Al	Fe <sup>3+</sup>	Fe <sup>2+</sup>	Mn	Mg	Ni	Zn	
Vranduk Fm.	BO61/sp065	n. d.	0.62	0.19	30.79	34.38	0.19	14.34	0.16	0.16	15.20	4.27	100.30	0.801	0.014	0.004	1.069	0.095	0.374	0.005	0.630	0.004	0.004	0.003
Vranduk Fm.	BO61/sp067	n. d.	0.54	0.35	19.84	42.27	0.32	8.66	0.09	0.23	22.12	6.08	100.50	1.066	0.013	0.007	0.746	0.146	0.590	0.009	0.412	0.002	0.006	0.006
Vranduk Fm.	BO61/sp068	n. d.	0.83	0.37	16.89	47.62	0.25	11.58	0.13	0.15	17.58	5.12	100.52	1.192	0.020	0.008	0.630	0.122	0.465	0.007	0.546	0.003	0.004	0.004
Vranduk Fm.	BO61/sp069	n. d.	0.11	0.22	34.34	33.47	0.15	16.24	0.18	0.10	12.39	2.70	99.90	0.762	0.002	0.004	1.166	0.058	0.298	0.004	0.697	0.004	0.002	0.002
Vranduk Fm.	BO61/sp070	n. d.	0.08	0.20	29.56	39.69	0.16	15.89	0.16	0.07	12.23	2.03	100.08	0.921	0.002	0.004	1.023	0.045	0.300	0.004	0.695	0.004	0.002	0.002
Vranduk Fm.	BO61/sp071	n. d.	0.28	0.29	21.56	44.38	0.27	12.48	0.11	0.09	16.40	4.50	100.36	1.084	0.006	0.006	0.786	0.105	0.424	0.007	0.575	0.003	0.002	0.002
Vranduk Fm.	BO61/sp072	n. d.	0.22	0.38	30.05	35.52	0.19	13.09	0.13	0.22	16.80	3.87	100.47	0.835	0.007	0.007	1.053	0.086	0.418	0.005	0.580	0.003	0.002	0.005
Vranduk Fm.	BO61/sp073	n. d.	0.16	0.21	19.39	48.69	0.23	12.96	0.12	0.09	15.20	3.24	100.29	1.197	0.004	0.004	0.711	0.076	0.395	0.006	0.600	0.003	0.002	0.002
Vranduk Fm.	BO61/sp074	n. d.	0.26	0.30	21.50	43.02	0.27	10.58	0.07	0.15	19.23	4.89	100.27	1.065	0.006	0.006	0.794	0.115	0.504	0.007	0.494	0.002	0.003	0.003
Vranduk Fm.	BO61/sp075	n. d.	0.06	0.35	14.48	52.23	0.25	10.50	0.08	0.13	18.23	4.22	100.52	1.329	0.001	0.007	0.550	0.102	0.491	0.007	0.504	0.002	0.003	0.003
Vranduk Fm.	BO61/sp076	n. d.	0.51	0.34	25.29	38.97	0.23	11.95	0.14	0.20	17.95	4.79	100.37	0.941	0.012	0.005	0.911	0.110	0.459	0.006	0.544	0.003	0.005	0.005
Vranduk Fm.	BO61/sp077	n. d.	0.13	0.26	15.05	53.02	0.21	11.84	0.07	0.08	16.32	3.36	100.33	1.336	0.003	0.005	0.566	0.081	0.435	0.006	0.562	0.002	0.002	0.002
Vranduk Fm.	BO61/sp078	n. d.	0.08	0.30	20.72	49.10	0.20	13.07	0.08	0.12	15.38	1.51	100.56	1.196	0.002	0.006	0.752	0.095	0.396	0.005	0.600	0.002	0.002	0.003
Vranduk Fm.	BO61/sp079	n. d.	0.06	0.34	21.65	45.85	0.22	11.57	0.06	0.20	17.48	2.33	99.78	1.131	0.001	0.007	0.796	0.055	0.456	0.006	0.538	0.002	0.005	0.005
Vranduk Fm.	BO61/sp080	n. d.	0.06	0.32	22.78	45.79	0.20	13.77	0.12	0.11	14.55	2.78	100.49	1.102	0.001	0.007	0.818	0.064	0.370	0.005	0.625	0.003	0.002	0.002
Vranduk Fm.	BO61/sp081	n. d.	0.07	0.24	29.20	39.22	0.19	14.97	0.11	0.15	13.62	2.56	100.31	0.915	0.001	0.005	1.016	0.057	0.336	0.005	0.658	0.003	0.003	0.003
Vranduk Fm.	BO61/sp082	n. d.	0.08	0.34	8.33	57.01	0.38	7.07	0.06	0.23	22.24	4.55	100.29	1.530	0.002	0.008	0.333	0.116	0.632	0.011	0.358	0.002	0.006	0.006
Vranduk Fm.	BO61/sp083	n. d.	0.02	0.31	24.56	42.98	0.24	11.73	0.08	0.27	17.77	2.52	100.47	1.041	0.000	0.006	0.887	0.058	0.455	0.006	0.535	0.002	0.002	0.006
Vranduk Fm.	BO61/sp084	n. d.	0.05	0.24	23.83	45.63	0.21	13.72	0.07	0.07	14.83	1.88	100.54	1.093	0.001	0.005	0.851	0.043	0.376	0.006	0.620	0.002	0.002	0.002
Vranduk Fm.	BO61/sp085	n. d.	0.03	0.38	17.04	51.31	0.26	10.53	0.06	0.17	18.49	1.95	100.21	1.294	0.001	0.008	0.641	0.047	0.493	0.007	0.501	0.004	0.004	0.004
Vranduk Fm.	BO61/sp086	n. d.	0.18	0.19	31.45	37.19	0.15	15.63	0.16	0.17	12.97	2.12	100.22	0.857	0.004	0.004	1.081	0.047	0.316	0.004	0.679	0.004	0.004	0.004
Vranduk Fm.	BO61/sp087	n. d.	0.07	0.30	20.54	48.66	0.22	12.94	0.11	0.13	15.49	2.17	100.63	1.186	0.002	0.006	0.747	0.050	0.399	0.006	0.595	0.003	0.003	0.003
Vranduk Fm.	BO61/sp088	n. d.	0.08	0.26	20.12	47.09	0.21	12.36	0.11	0.16	16.21	3.91	100.42	1.157	0.002	0.005	0.737	0.091	0.421	0.006	0.572	0.003	0.004	0.004
Vranduk Fm.	BO61/sp089	n. d.	0.08	0.27	21.65	48.05	0.21	13.86	0.10	0.13	14.22	1.87	100.44	1.161	0.002	0.006	0.780	0.043	0.364	0.005	0.631	0.002	0.002	0.003
Vranduk Fm.	BO61/sp090	n. d.	0.15	0.26	15.36	52.42	0.29	11.09	0.04	0.13	17.46	3.16	100.34	1.326	0.004	0.005	0.579	0.076	0.467	0.008	0.529	0.001	0.004	0.004
Vranduk Fm.	BO61/sp091	n. d.	0.04	0.21	22.60	45.20	0.22	13.26	0.09	0.20	15.16	3.57	100.54	1.092	0.001	0.004	0.814	0.082	0.388	0.006	0.604	0.002	0.004	0.004
Vranduk Fm.	BO61/sp092	n. d.	0.11	0.23	24.97	43.17	0.23	13.40	0.10	0.15	15.32	2.51	100.18	1.035	0.003	0.005	0.893	0.057	0.389	0.006	0.606	0.002	0.002	0.003
Vranduk Fm.	BO61/sp093	n. d.	0.44	0.20	27.70	40.63	0.19	14.50	0.11	0.12	14.36	1.78	100.02	0.958	0.010	0.004	0.974	0.040	0.358	0.005	0.645	0.003	0.003	0.003
Vranduk Fm.	BO61/sp094	n. d.	0.05	0.34	20.52	47.62	0.22	12.70	0.09	0.11	15.83	2.97	100.45	1.165	0.001	0.007	0.749	0.069	0.410	0.006	0.586	0.002	0.002	0.002
Vranduk Fm.	BO61/sp095	n. d.	0.04	0.19	29.65	40.59	0.18	15.45	0.09	0.20	12.84	0.87	100.10	0.943	0.001	0.004	1.028	0.019	0.316	0.005	0.677	0.002	0.002	0.004
Vranduk Fm.	BO61/sp096	n. d.	0.29	0.37	22.93	41.85	0.23	12.90	0.13	0.16	15.85	5.24	99.93	1.018	0.007	0.007	0.832	0.121	0.408	0.006	0.591	0.003	0.004	0.004
Vranduk Fm.	BO61/sp097	n. d.	0.05	0.18	26.12	41.61	0.22	14.90	0.10	0.13	13.06	3.72	100.15	0.985	0.001	0.004	0.922	0.084	0.327	0.006	0.665	0.003	0.004	0.004
Vranduk Fm.	BO61/sp098	n. d.	0.11	0.20	25.92	43.29	0.16	15.33	0.14	0.08	12.53	2.28	100.06	1.022	0.002	0.004	0.913	0.051	0.313	0.004	0.683	0.003	0.003	0.002
Vranduk Fm.	BO61/sp099	n. d.	0.03	0.31	25.72	42.39	0.19	13.33	0.10	0.22	15.49	2.39	100.17	1.014	0.001	0.006	0.917	0.054	0.392	0.005	0.601	0.003	0.003	0.005
Vranduk Fm.	BO72/sp001	n. d.	0.06	0.28	18.17	51.18	0.27	11.30	0.06	0.22	17.51	1.49	100.53	1.275	0.001	0.006	0.675	0.035	0.461	0.007	0.531	0.002	0.005	0.005
Vranduk Fm.	BO72/sp002	n. d.	0.06	0.30	27.79	40.03	0.19	13.29	0.09	0.22	15.98	2.46	100.41	0.948	0.001	0.006	0.981	0.055	0.400	0.005	0.593	0.002	0.005	0.005
Vranduk Fm.	BO72/sp003	n. d.	0.06	0.32	10.30	57.28	0.31	9.03	0.05	0.18	19.66	3.11	100.30	1.502	0.001	0.007	0.403	0.078	0.545	0.009	0.446	0.001	0.004	0.004
Vranduk Fm.	BO72/sp004	n. d.	0.04	0.27	33.12	33.65	0.20	13.91	0.16	0.29	15.52	2.73	99.88	0.781	0.001	0.005	1.146	0.060	0.381	0.005	0.608	0.004	0.006	0.006
Vranduk Fm.	BO72/sp005	n. d.	0.04	0.35	12.10	56.73	0.33	9.86	0.07	0.18	18.92	2.40	101.09	1.456	0.001	0.008	0.467	0.059	0.514	0.009	0.477	0.002	0.004	0.004
Vranduk Fm.	BO72/sp006	n. d.	0.05	0.36	21.13	47.86	0.25	11.87	0.06	0.19	17.18	1.57	100.53	1.173	0.001	0.007	0.772	0.037	0.445	0.007	0.548	0.002	0.004	0.004
Vranduk Fm.	BO72/sp007	n. d.	0.03	0.29	9.19	61.09	0.25	11.12	0.06	0.09	16.49	1.98	100.60	1.581	0.001	0.006	0.355	0.049	0.451	0.007	0.543	0.002	0.002	0.002
Vranduk Fm.	BO72/sp008	n. d.	0.03	0.27	25.66	42.95	0.20	14.33	0.12	0.16	14.06	2.75	100.53	1.018	0.001	0.005	0.907	0.068	0.352	0.005	0.640	0.003	0.004	0.004
Vranduk Fm.	BO72/sp009	n. d.	0.03	0.35	22.80	44.51	0.26	11.64	0.09	0.20	17.71	2.94	100.53	1.086	0.001	0.007	0.829	0.068	0.457	0.007	0.535	0.002	0.005	0.005
Vranduk Fm.	BO72/sp010	n. d.	0.04	0.35	23.31	45.32	0.2																	

analyses in wt%. Shown are the recalculated FeO and Fe<sub>2</sub>O<sub>3</sub> values and the amended total

Formation	Sample & spot ID	n.d.: not detected											cations per formula unit on the basis of 3 oxygens											
		SiO <sub>2</sub>	TiO <sub>2</sub>	V <sub>2</sub> O <sub>5</sub>	Al <sub>2</sub> O <sub>3</sub>	Cr <sub>2</sub> O <sub>3</sub>	MnO	MgO	NiO	ZnO	FeO	Fe <sub>2</sub> O <sub>3</sub>	Total	Cr	Ti	V	Al	Fe <sup>3+</sup>	Fe <sup>2+</sup>	Mn	Mg	Ni	Zn	
Vranduk Fm.	BO72sp022	n. d.	0.05	0.41	16.91	52.89	0.27	10.99	0.05	0.18	17.87	0.81	100.42	1.327	0.001	0.009	0.633	0.019	0.474	0.007	0.520	0.001	0.004	0.004
Vranduk Fm.	BO72sp023	n. d.	0.02	0.36	19.39	48.55	0.27	11.03	0.09	0.19	18.07	2.42	100.39	1.207	0.001	0.008	0.719	0.057	0.475	0.007	0.517	0.002	0.004	0.004
Vranduk Fm.	BO72sp024	n. d.	0.04	0.37	12.95	54.86	0.32	9.81	0.04	0.23	19.07	3.30	100.99	1.406	0.001	0.008	0.495	0.080	0.517	0.009	0.474	0.001	0.005	0.005
Vranduk Fm.	BO72sp025	n. d.	0.05	0.35	23.55	44.89	0.22	12.56	0.08	0.16	16.52	2.10	100.50	1.085	0.001	0.007	0.849	0.048	0.460	0.006	0.572	0.002	0.004	0.004
Vranduk Fm.	BO72sp027	n. d.	0.06	0.36	20.16	47.81	0.25	11.48	0.06	0.21	17.66	2.67	100.72	1.178	0.001	0.007	0.741	0.063	0.460	0.007	0.533	0.002	0.005	0.005
Vranduk Fm.	BO72sp028	n. d.	0.07	0.36	18.66	50.63	0.23	12.14	0.07	0.16	16.48	1.91	100.71	1.249	0.002	0.007	0.687	0.045	0.430	0.006	0.565	0.002	0.004	0.004
Vranduk Fm.	BO72sp029	n. d.	0.06	0.38	17.48	50.96	0.26	10.72	0.07	0.20	18.44	2.74	101.00	1.275	0.001	0.008	0.641	0.065	0.488	0.007	0.505	0.002	0.005	0.005
Vranduk Fm.	BO72sp030	n. d.	0.05	0.25	32.15	37.12	0.19	15.79	0.17	0.14	12.79	1.72	100.37	0.851	0.001	0.005	1.099	0.037	0.310	0.005	0.682	0.004	0.003	0.003
Vranduk Fm.	BO72sp031	n. d.	0.05	0.36	28.32	39.46	0.24	13.38	0.11	0.25	15.89	2.46	100.51	0.931	0.001	0.007	0.997	0.055	0.397	0.006	0.595	0.003	0.005	0.005
Vranduk Fm.	BO72sp032	n. d.	0.04	0.27	26.04	43.77	0.22	13.77	0.11	0.18	15.11	1.43	100.94	1.036	0.001	0.007	0.919	0.032	0.378	0.006	0.614	0.003	0.004	0.004
Vranduk Fm.	BO72sp033	n. d.	0.05	0.31	23.37	44.97	0.22	12.57	0.12	0.22	16.41	2.46	100.69	1.086	0.001	0.006	0.842	0.057	0.419	0.006	0.572	0.003	0.003	0.003
Vranduk Fm.	BO72sp034	n. d.	0.04	0.32	15.27	53.96	0.29	10.42	0.06	0.26	18.42	1.74	100.77	1.366	0.001	0.007	0.576	0.042	0.493	0.008	0.497	0.002	0.006	0.006
Vranduk Fm.	BO72sp035	n. d.	0.04	0.31	21.38	48.09	0.27	11.95	0.10	0.19	17.01	1.19	100.53	1.177	0.001	0.006	0.780	0.028	0.440	0.007	0.551	0.002	0.004	0.004
Vranduk Fm.	BO72sp036	n. d.	0.03	0.39	17.69	51.49	0.26	11.39	0.08	0.16	17.41	1.74	100.64	1.283	0.001	0.007	0.702	0.071	0.450	0.007	0.535	0.002	0.004	0.004
Vranduk Fm.	BO72sp038	n. d.	0.04	0.43	16.13	54.11	0.28	11.69	0.06	0.14	16.77	1.03	100.68	1.353	0.001	0.009	0.602	0.024	0.444	0.007	0.551	0.002	0.003	0.003
Vranduk Fm.	BO72sp039	n. d.	0.05	0.23	32.45	35.91	0.17	15.16	0.12	0.15	13.90	2.42	100.60	0.824	0.001	0.004	1.111	0.063	0.338	0.004	0.666	0.003	0.003	0.003
Vranduk Fm.	BO72sp040	n. d.	0.05	0.27	32.42	35.91	0.16	14.97	0.14	0.17	14.09	2.09	100.27	0.827	0.001	0.005	1.114	0.046	0.343	0.004	0.650	0.003	0.004	0.004
Vranduk Fm.	BO72sp041	n. d.	0.04	0.24	33.72	33.66	0.17	15.27	0.16	0.22	13.58	2.74	99.80	0.773	0.001	0.005	1.155	0.060	0.330	0.004	0.661	0.004	0.004	0.005
Vranduk Fm.	BO72sp042	n. d.	0.15	0.32	25.32	42.14	0.18	14.92	0.16	0.10	13.20	3.84	100.34	0.998	0.003	0.006	0.895	0.087	0.331	0.005	0.666	0.004	0.004	0.002
Vranduk Fm.	BO72sp043	n. d.	0.04	0.28	31.41	36.11	0.16	14.24	0.16	0.19	14.95	2.57	100.10	0.840	0.001	0.005	1.090	0.057	0.368	0.004	0.625	0.004	0.004	0.004
Vranduk Fm.	BO72sp044	n. d.	0.04	0.21	39.12	28.28	0.18	15.73	0.18	0.20	13.72	2.16	99.82	0.935	0.001	0.004	1.309	0.046	0.326	0.004	0.665	0.004	0.004	0.004
Vranduk Fm.	BO72sp045	n. d.	0.10	0.28	19.19	52.73	0.32	9.09	0.04	0.24	20.36	2.08	100.43	1.351	0.003	0.006	0.580	0.051	0.562	0.009	0.439	0.001	0.006	0.006
Vranduk Fm.	BO72sp046	n. d.	0.05	0.29	25.42	43.44	0.22	12.42	0.08	0.25	16.87	1.33	100.37	1.044	0.001	0.006	0.911	0.031	0.429	0.006	0.563	0.002	0.006	0.006
Vranduk Fm.	BO72sp047	n. d.	0.13	0.24	33.90	34.86	0.15	15.39	0.13	0.18	13.69	1.45	100.11	0.797	0.003	0.004	1.156	0.032	0.331	0.004	0.664	0.003	0.004	0.004
Vranduk Fm.	BO72sp048	n. d.	0.08	0.24	29.37	38.84	0.18	14.76	0.12	0.18	13.92	2.53	100.22	0.907	0.002	0.005	1.023	0.056	0.344	0.004	0.650	0.003	0.004	0.004
Vranduk Fm.	BO72sp049	n. d.	0.05	0.28	28.99	39.08	0.18	14.71	0.15	0.14	13.94	2.70	100.23	0.914	0.001	0.006	1.011	0.060	0.345	0.005	0.649	0.004	0.003	0.003
Vranduk Fm.	BO72sp050	n. d.	0.03	0.34	24.08	44.06	0.24	11.98	0.10	0.24	17.36	2.04	100.48	1.067	0.001	0.007	0.870	0.047	0.347	0.006	0.547	0.002	0.005	0.005
Vranduk Fm.	BO72sp051	n. d.	0.07	0.32	24.48	42.96	0.26	12.34	0.10	0.23	16.88	2.91	100.55	1.036	0.002	0.006	0.880	0.067	0.431	0.007	0.561	0.003	0.005	0.005
Vranduk Fm.	BO72sp052	n. d.	0.05	0.31	12.02	56.39	0.35	8.40	0.04	0.26	21.01	2.12	100.95	1.465	0.001	0.007	0.466	0.082	0.577	0.010	0.411	0.001	0.006	0.006
Vranduk Fm.	BO72sp054	0.21	0.06	0.40	16.18	51.76	0.28	10.68	0.07	0.18	18.15	2.58	100.54	1.308	0.001	0.009	0.610	0.062	0.485	0.007	0.509	0.002	0.004	0.004
Vranduk Fm.	BO72sp055	n. d.	0.06	0.29	31.53	35.63	0.24	13.97	0.13	0.21	15.25	2.49	99.81	0.832	0.001	0.006	1.098	0.055	0.377	0.006	0.615	0.003	0.005	0.005
Vranduk Fm.	BO72sp056	n. d.	0.16	0.22	37.10	28.62	0.23	15.04	0.17	0.24	14.62	3.91	100.32	0.648	0.003	0.004	1.252	0.084	0.350	0.005	0.642	0.004	0.005	0.005
Vranduk Fm.	BO72sp057	n. d.	0.06	0.17	48.05	18.38	0.13	17.76	0.29	0.27	11.95	3.01	100.05	0.994	0.001	0.003	1.536	0.061	0.271	0.003	0.718	0.006	0.005	0.005
Vranduk Fm.	BO72sp058	n. d.	0.13	0.24	12.79	54.75	0.29	11.35	0.10	0.14	16.50	3.94	100.24	1.399	0.003	0.005	0.446	0.086	0.446	0.008	0.547	0.003	0.003	0.003
Vranduk Fm.	BO72sp059	n. d.	0.04	0.41	18.22	50.98	0.25	10.99	0.06	0.21	18.05	1.23	100.44	1.272	0.001	0.009	0.678	0.029	0.477	0.007	0.517	0.002	0.005	0.005
Vranduk Fm.	BO72sp060	n. d.	0.05	0.25	35.20	31.38	0.16	14.65	0.14	0.25	14.80	3.01	99.89	0.719	0.001	0.005	1.203	0.066	0.359	0.004	0.633	0.003	0.005	0.005
Vranduk Fm.	BO72sp061	n. d.	0.06	0.35	22.74	46.34	0.21	12.95	0.07	0.17	15.97	2.12	100.98	1.117	0.001	0.007	0.817	0.049	0.407	0.005	0.588	0.002	0.004	0.004
Vranduk Fm.	BO72sp062	n. d.	0.09	0.31	7.81	61.31	0.31	8.60	0.04	0.20	20.01	1.75	100.43	1.627	0.002	0.007	0.309	0.044	0.562	0.009	0.430	0.001	0.005	0.005
Vranduk Fm.	BO72sp063	n. d.	0.08	0.33	16.64	51.52	0.33	10.26	0.07	0.18	18.78	2.11	100.30	1.303	0.002	0.007	0.628	0.051	0.502	0.009	0.489	0.002	0.004	0.004
Vranduk Fm.	BO72sp064	n. d.	0.03	0.30	18.70	49.84	0.26	12.43	0.09	0.29	15.75	2.87	100.71	1.230	0.001	0.006	0.688	0.068	0.411	0.007	0.578	0.002	0.007	0.007
Vranduk Fm.	BO72sp065	n. d.	0.06	0.16	30.82	30.82	0.24	11.68	0.15	0.37	18.60	7.80	100.70	1.079	0.001	0.003	1.087	0.176	0.465	0.006	0.521	0.004	0.008	0.008
Vranduk Fm.	BO72sp066	0.02	0.06	0.27	22.67	47.35	0.20	13.06	0.11	0.17	15.46	0.78	100.14	1.148	0.001	0.005	0.820	0.018	0.396	0.005	0.597	0.003	0.004	0.004
Vranduk Fm.	BO72sp067	n. d.	0.07	0.11	8.85	63.39	0.22	13.16	0.05	0.09	13.29	1.36	100.61	1.621	0.002	0.002	0.337	0.033	0.360	0.006	0.634	0.001	0.002	0.002
Vranduk Fm.	BO72sp068	n. d.	0.05	0.39	13.60	54.30	0.34																	

Analyses in wt%. Shown are the recalculated FeO and Fe<sub>2</sub>O<sub>3</sub> values and the amended total

Formation	Sample & spot ID	Analyses in wt%												Cations per formula unit on the basis of 3 oxygens														
		SiO <sub>2</sub>	TiO <sub>2</sub>	V <sub>2</sub> O <sub>5</sub>	Al <sub>2</sub> O <sub>3</sub>	Cr <sub>2</sub> O <sub>3</sub>	MnO	MgO	NiO	ZnO	FeO	Fe <sub>2</sub> O <sub>3</sub>	Total	Cr	Ti	V	Al	Fe <sup>3+</sup>	Fe <sup>2+</sup>	Mn	Mg	Ni	Zn					
Vranduk Fm.	BO72sp0079	n. d.	0.04	0.37	16.08	52.60	0.26	10.60	0.06	0.19	18.31	2.02	100.53	1.328	0.001	0.008	0.605	0.049	0.489	0.007	0.504	0.001	0.004					
Vranduk Fm.	BO72sp0080	n. d.	0.09	0.37	9.05	59.15	0.31	9.20	0.05	0.17	19.32	2.70	100.42	1.556	0.002	0.008	0.355	0.068	0.489	0.009	0.466	0.001	0.004					
Vranduk Fm.	BO72sp0081	n. d.	0.17	0.18	26.92	38.04	0.23	13.10	0.14	0.18	16.21	5.70	100.87	0.903	0.004	0.004	0.953	0.129	0.407	0.006	0.586	0.003	0.004					
Vranduk Fm.	BO72sp0082	0.03	0.39	0.16	38.33	27.10	0.13	17.27	0.26	0.06	11.85	5.16	100.74	0.601	0.008	0.003	1.268	0.109	0.407	0.003	0.722	0.006	0.001					
Vranduk Fm.	BO72sp0083	n. d.	0.06	0.37	15.60	52.85	0.27	10.90	0.08	0.16	17.87	2.64	100.79	1.331	0.001	0.008	0.586	0.063	0.476	0.007	0.518	0.002	0.004					
Vranduk Fm.	BO72sp0084	n. d.	1.02	0.47	19.78	38.39	0.31	7.99	0.18	0.24	23.49	8.53	100.40	0.974	0.025	0.010	0.749	0.206	0.631	0.008	0.382	0.005	0.006					
Vranduk Fm.	BO72sp0085	n. d.	0.04	0.25	40.14	27.49	0.16	16.26	0.19	0.17	13.26	2.31	100.28	0.610	0.005	0.005	1.329	0.049	0.312	0.004	0.681	0.004	0.004					
Vranduk Fm.	BO72sp0086	n. d.	0.04	0.26	45.04	21.79	0.15	16.92	0.22	0.25	12.92	2.83	100.34	0.473	0.001	0.003	1.459	0.058	0.297	0.003	0.693	0.005	0.005					
Vranduk Fm.	BO72sp0087	n. d.	0.06	0.38	14.14	53.90	0.30	10.73	0.07	0.13	17.82	2.46	100.26	1.373	0.006	0.008	0.537	0.060	0.480	0.008	0.518	0.002	0.003					
Vranduk Fm.	BO72sp0088	n. d.	0.06	0.36	14.05	55.05	0.25	10.73	0.05	0.17	17.80	1.87	100.39	1.402	0.001	0.008	0.534	0.045	0.479	0.007	0.515	0.001	0.004					
Vranduk Fm.	BO72sp0089	n. d.	0.05	0.30	15.16	52.42	0.35	8.90	0.07	0.16	20.58	2.44	100.50	1.344	0.001	0.006	0.580	0.060	0.568	0.010	0.430	0.002	0.006					
Vranduk Fm.	BO72sp0090	n. d.	0.03	0.41	18.38	50.76	0.28	11.43	0.06	0.16	17.55	1.84	100.90	1.258	0.001	0.008	0.679	0.043	0.460	0.007	0.534	0.001	0.004					
Vranduk Fm.	BO72sp0091	n. d.	0.06	0.16	46.96	20.02	0.12	17.45	0.25	0.22	12.28	2.33	99.85	0.432	0.001	0.003	1.512	0.048	0.280	0.003	0.710	0.005	0.004					
Vranduk Fm.	BO72sp0092	n. d.	0.12	0.16	42.59	24.92	0.14	18.04	0.26	0.13	10.86	2.81	100.03	0.544	0.003	0.003	1.386	0.058	0.251	0.003	0.742	0.006	0.003					
Vranduk Fm.	BO72sp0093	n. d.	0.08	0.08	13.45	56.61	0.27	10.90	0.04	0.17	17.45	1.01	100.34	1.444	0.002	0.008	0.512	0.025	0.471	0.007	0.524	0.001	0.004					
Vranduk Fm.	BO72sp0094	n. d.	0.08	0.28	26.63	41.56	0.21	14.93	0.13	0.09	13.30	3.10	100.31	0.979	0.002	0.005	0.936	0.070	0.332	0.005	0.663	0.003	0.002					
Vranduk Fm.	BO72sp0095	n. d.	0.08	0.21	39.86	27.81	0.14	17.23	0.22	0.13	11.69	2.64	100.01	0.616	0.002	0.004	1.317	0.056	0.274	0.003	0.719	0.005	0.003					
Vranduk Fm.	BO72sp0096	n. d.	0.16	0.10	46.90	19.93	0.15	18.51	0.26	0.16	10.67	2.87	99.71	0.428	0.003	0.002	1.503	0.059	0.242	0.004	0.750	0.006	0.003					
Vranduk Fm.	BO72sp0097	n. d.	0.21	0.25	22.58	42.33	0.21	12.00	0.09	0.22	17.17	5.35	100.40	1.033	0.005	0.005	0.822	0.124	0.443	0.005	0.552	0.002	0.005					
Vranduk Fm.	BO72sp0098	0.04	0.04	0.18	46.73	20.96	0.11	18.47	0.24	0.17	10.67	2.03	99.65	0.451	0.001	0.003	1.489	0.042	0.243	0.002	0.749	0.005	0.003					
Vranduk Fm.	BO72sp0099	n. d.	0.12	0.21	43.24	23.34	0.11	17.58	0.27	0.17	11.47	2.93	99.43	0.512	0.002	0.004	1.414	0.061	0.266	0.003	0.727	0.006	0.003					
Vranduk Fm.	BO72sp0100	n. d.	0.07	0.17	43.13	21.97	0.13	17.47	0.28	0.16	11.70	4.98	100.06	0.480	0.001	0.003	1.407	0.104	0.271	0.003	0.720	0.006	0.003					
Vranduk Fm.	BO72sp0101	n. d.	0.15	0.17	43.28	23.69	0.13	17.89	0.25	0.11	11.13	2.75	99.62	0.518	0.003	0.003	1.411	0.059	0.257	0.003	0.737	0.006	0.002					
Vranduk Fm.	BO72sp0102	n. d.	0.09	0.16	45.20	21.12	0.11	17.36	0.24	0.23	11.97	2.84	99.22	0.461	0.002	0.003	1.472	0.057	0.276	0.003	0.715	0.005	0.005					
Vranduk Fm.	BO72sp0103	n. d.	0.12	0.20	44.21	20.94	0.15	16.87	0.25	0.24	12.69	4.03	99.70	0.444	0.004	0.004	1.444	0.084	0.294	0.004	0.697	0.006	0.005					
Vranduk Fm.	BO72sp0104	n. d.	0.66	0.20	34.94	29.61	0.21	14.87	0.18	0.12	15.04	4.31	100.14	0.677	0.014	0.004	1.192	0.094	0.364	0.005	0.641	0.004	0.003					
Vranduk Fm.	BO72sp0105	n. d.	0.10	0.25	34.12	33.11	0.16	14.17	0.13	0.25	15.60	2.52	100.40	0.761	0.002	0.005	1.169	0.055	0.379	0.004	0.614	0.003	0.005					
Vranduk Fm.	BO72sp0106	n. d.	0.08	0.13	49.61	17.30	0.13	19.08	0.27	0.14	9.94	2.21	98.87	0.369	0.002	0.002	1.578	0.045	0.224	0.003	0.767	0.006	0.003					
Vranduk Fm.	BO72sp0107	n. d.	0.17	0.24	33.16	33.59	0.16	14.58	0.16	0.20	14.75	2.94	99.95	0.776	0.004	0.005	1.142	0.065	0.360	0.004	0.635	0.004	0.004					
Vranduk Fm.	BO72sp0108	n. d.	0.12	0.33	20.30	47.03	0.26	12.05	0.12	0.18	16.74	3.44	100.57	1.156	0.003	0.007	0.744	0.081	0.435	0.007	0.588	0.003	0.004					
Vranduk Fm.	BO72sp0109	n. d.	0.45	0.25	32.77	32.69	0.21	14.20	0.19	0.20	15.54	3.81	100.31	0.756	0.010	0.010	1.130	0.084	0.380	0.005	0.619	0.005	0.005					
Vranduk Fm.	BO72sp0110	n. d.	0.21	0.34	26.78	37.88	0.22	12.46	0.13	0.22	17.11	4.93	100.28	0.907	0.005	0.007	0.956	0.112	0.434	0.006	0.562	0.003	0.003					
Vranduk Fm.	BO72sp0111	0.01	0.20	0.14	44.87	23.46	0.11	18.13	0.30	0.09	11.25	1.70	100.25	0.507	0.004	0.002	1.445	0.035	0.257	0.003	0.738	0.007	0.002					
Vranduk Fm.	BO72sp0112	n. d.	0.05	0.25	27.71	35.99	0.24	10.75	0.13	0.35	19.37	4.95	99.79	0.872	0.001	0.005	1.001	0.114	0.496	0.006	0.491	0.003	0.008					
Vranduk Fm.	BO72sp0113	n. d.	0.15	0.30	21.55	46.46	0.21	12.78	0.09	0.13	15.93	2.87	100.46	1.131	0.003	0.006	0.783	0.067	0.410	0.005	0.587	0.002	0.003					
Vranduk Fm.	BO72sp0114	n. d.	0.27	0.16	35.68	30.71	0.18	15.38	0.19	0.13	14.10	3.62	100.42	0.697	0.006	0.003	1.207	0.078	0.338	0.004	0.658	0.004	0.003					
Vranduk Fm.	BO72sp0115	n. d.	0.28	0.27	14.03	55.66	0.19	12.98	0.08	0.04	14.55	2.06	100.14	1.399	0.007	0.006	0.526	0.049	0.387	0.005	0.615	0.002	0.001					
Vranduk Fm.	BO72sp0116	0.11	0.08	0.13	49.33	17.62	0.12	18.77	0.31	0.21	10.51	2.51	99.69	0.375	0.002	0.002	1.566	0.051	0.237	0.003	0.753	0.007	0.004					
Vranduk Fm.	BO72sp0117	n. d.	0.52	0.39	28.19	34.66	0.24	12.14	0.17	0.20	18.12	5.78	100.41	0.826	0.012	0.008	1.002	0.131	0.457	0.006	0.546	0.004	0.004					
Vranduk Fm.	BO72sp0118	n. d.	0.08	0.27	26.98	39.22	0.21	12.62	0.12	0.20	16.68	3.74	100.21	0.938	0.002	0.005	0.962	0.085	0.422	0.005	0.569	0.003	0.007					
Vranduk Fm.	BO72sp0119	0.01	0.53	0.15	25.43	38.32	0.23	14.46	0.14	0.19	13.99	6.71	100.07	0.913	0.012	0.012	0.904	0.152	0.353	0.006	0.650	0.003	0.002					
Vranduk Fm.	BO72sp0120	n. d.	0.33	0.19	31.14	37.19	0.16	15.97	0.15	0.12	12.57	2.39	100.23	0.856	0.007	0.004	1.069	0.052	0.306	0.004	0.693	0.003	0.003					
Vranduk Fm.	BO72sp0121	n. d.	0.15	0.14	42.67	23.53	0.13	17.96	0.29	0.12	10.86	3.83	99.67	0.515	0.003	0.003	1.393	0.080	0.252	0.003	0.741	0.006	0.003					
Vranduk Fm.	BO72sp0122	n. d.	0.10	0.14	44.90	21.70	0.10	17.64	0.24	0.15	11.50	2.50	98.99	0.474	0.002	0.003	1.464	0.052	0.266	0.002	0.727	0.005	0.003					
Vranduk Fm.	BO72sp0123	n. d.	0.10	0.19	38.41	28.86	0.16	16.14	0.18	0.18	13.08	2.63	99.94	0.647	0.002	0.004	1.285	0.056	0.310	0.004	0.682	0.004						

Formation	Sample & spot ID	analyses in wt%. Shown are the recalculated FeO and Fe <sub>2</sub> O <sub>3</sub> values and the amended total																	Cations per formula unit on the basis of 3 oxygens									
		SiO <sub>2</sub>	TiO <sub>2</sub>	V <sub>2</sub> O <sub>5</sub>	Al <sub>2</sub> O <sub>3</sub>	Cr <sub>2</sub> O <sub>3</sub>	MnO	MgO	NiO	ZnO	FeO	Fe <sub>2</sub> O <sub>3</sub>	Total	Cr	Ti	V	Al	Fe <sup>3+</sup>	Fe <sup>2+</sup>	Mn	Mg	Ni	Zn					
		n. d.	n. d.	n. d.	n. d.	n. d.	n. d.	n. d.	n. d.	n. d.	n. d.	n. d.	n. d.	n. d.	n. d.	n. d.	n. d.	n. d.	n. d.	n. d.	n. d.	n. d.	n. d.	n. d.	n. d.			
Vranduk Fm.	BO73sp043	0.13	0.22	0.31	39.31	28.03	0.12	16.17	0.17	0.18	13.35	2.50	100.19	0.625	0.003	0.004	1.308	0.053	0.315	0.003	0.680	0.004	0.004	0.004				
Vranduk Fm.	BO73sp044	0.46	0.29	19.76	42.43	0.27	11.14	0.12	0.16	18.12	7.33	100.49	1.057	0.011	0.006	0.734	0.174	0.478	0.007	0.523	0.003	0.003	0.004					
Vranduk Fm.	BO73sp045	0.08	0.13	50.96	16.45	0.09	19.17	0.29	0.10	10.21	1.88	99.40	0.348	0.002	0.002	1.606	0.038	0.228	0.002	0.764	0.006	0.006	0.003					
Vranduk Fm.	BO73sp046	0.17	0.08	32.91	30.82	0.18	14.91	0.21	0.15	14.12	6.74	100.26	0.710	0.002	0.003	1.131	0.148	0.344	0.005	0.648	0.005	0.002	0.002					
Vranduk Fm.	BO73sp047	0.09	0.14	45.63	21.95	0.13	18.45	0.27	0.10	10.53	2.23	99.51	0.474	0.002	0.003	1.471	0.046	0.241	0.003	0.752	0.006	0.006	0.002					
Vranduk Fm.	BO73sp048	0.04	0.18	33.52	35.30	0.14	16.25	0.19	0.13	12.18	2.10	100.03	0.805	0.001	0.003	1.140	0.046	0.294	0.003	0.699	0.004	0.003	0.003					
Vranduk Fm.	BO73sp049	0.12	0.14	46.05	20.88	0.12	17.80	0.27	0.18	11.60	2.51	99.67	0.452	0.002	0.003	1.486	0.052	0.265	0.003	0.726	0.006	0.004	0.004					
Vranduk Fm.	BO73sp050	0.29	0.27	32.52	31.76	0.20	12.80	0.15	0.27	17.39	4.36	100.02	0.743	0.006	0.005	1.135	0.097	0.431	0.005	0.565	0.004	0.006	0.006					
Vranduk Fm.	BO73sp051	0.27	0.29	33.02	31.33	0.18	13.01	0.15	0.26	17.19	4.38	100.08	0.731	0.006	0.006	1.148	0.097	0.424	0.004	0.572	0.004	0.006	0.006					
Vranduk Fm.	BO73sp052	0.12	0.23	30.76	37.23	0.16	15.43	0.14	0.12	13.07	2.60	100.14	0.864	0.003	0.004	1.064	0.057	0.321	0.003	0.675	0.003	0.003	0.003					
Vranduk Fm.	BO73sp053	0.05	0.16	42.20	25.06	0.15	17.46	0.20	0.18	11.49	3.45	99.63	0.551	0.001	0.003	1.384	0.057	0.267	0.003	0.724	0.005	0.003	0.003					
Vranduk Fm.	BO73sp054	0.11	0.22	42.35	23.38	0.14	16.01	0.20	0.20	13.84	3.45	99.98	0.517	0.002	0.004	1.397	0.073	0.324	0.003	0.668	0.004	0.006	0.006					
Vranduk Fm.	BO73sp055	0.19	0.14	38.02	29.01	0.14	16.04	0.15	0.24	13.22	2.81	99.96	0.652	0.004	0.003	1.274	0.060	0.314	0.003	0.680	0.003	0.003	0.005					
Vranduk Fm.	BO73sp056	0.13	0.17	31.54	35.00	0.18	14.46	0.13	0.16	14.64	3.67	100.10	0.813	0.003	0.003	1.093	0.081	0.360	0.005	0.633	0.003	0.003	0.004					
Vranduk Fm.	BO73sp057	0.12	0.19	36.41	30.81	0.15	15.91	0.17	0.16	13.22	2.96	100.10	0.696	0.003	0.004	1.227	0.064	0.316	0.004	0.678	0.004	0.004	0.004					
Vranduk Fm.	BO73sp058	0.85	0.33	22.20	41.23	0.22	14.40	0.09	0.10	14.21	7.00	100.65	0.991	0.020	0.007	0.796	0.160	0.361	0.006	0.652	0.002	0.002	0.002					
Vranduk Fm.	BO73sp059	0.34	0.20	14.14	46.16	0.35	8.41	0.16	0.35	20.78	8.58	99.43	1.208	0.008	0.004	0.552	0.214	0.575	0.010	0.415	0.003	0.008	0.008					
Vranduk Fm.	BO73sp060	1.02	0.35	19.64	40.97	0.30	10.56	0.16	0.14	19.53	7.57	100.25	1.024	0.024	0.007	0.732	0.180	0.516	0.008	0.497	0.004	0.003	0.003					
Vranduk Fm.	BO73sp061	0.12	0.27	27.38	39.30	0.20	14.24	0.18	0.13	14.39	3.98	100.19	0.929	0.003	0.005	0.965	0.090	0.360	0.005	0.634	0.004	0.003	0.003					
Vranduk Fm.	BO73sp062	0.26	0.22	35.29	31.76	0.16	15.00	0.14	0.30	14.47	2.45	100.04	0.725	0.006	0.004	1.202	0.053	0.349	0.004	0.646	0.003	0.006	0.006					
Vranduk Fm.	BO73sp063	0.12	0.10	42.98	23.24	0.12	17.49	0.25	0.22	11.61	3.80	99.94	0.509	0.002	0.002	1.403	0.079	0.269	0.003	0.722	0.006	0.005	0.005					
Vranduk Fm.	BO73sp065	0.05	0.16	41.93	24.78	0.13	16.79	0.19	0.21	12.52	3.03	99.78	0.547	0.001	0.003	1.381	0.064	0.292	0.003	0.699	0.004	0.004	0.004					
Vranduk Fm.	BO73sp066	0.44	0.21	29.23	34.21	0.21	14.92	0.20	0.11	13.81	6.80	100.14	0.800	0.010	0.004	1.020	0.151	0.342	0.005	0.658	0.005	0.005	0.002					
Vranduk Fm.	BO73sp067	0.07	0.25	34.71	32.16	0.19	14.38	0.16	0.27	15.16	2.73	100.09	0.738	0.002	0.005	1.188	0.060	0.368	0.005	0.622	0.004	0.006	0.006					
Vranduk Fm.	BO73sp068	0.08	0.16	40.12	26.38	0.15	16.88	0.22	0.18	12.05	3.42	99.63	0.587	0.002	0.003	1.331	0.072	0.284	0.004	0.708	0.005	0.005	0.004					
Vranduk Fm.	BO73sp069	0.07	0.10	43.11	23.32	0.15	16.86	0.22	0.25	12.41	3.02	99.52	0.514	0.002	0.002	1.416	0.063	0.289	0.004	0.700	0.005	0.005	0.005					
Vranduk Fm.	BO73sp071	0.13	0.15	43.12	23.52	0.13	17.42	0.22	0.19	11.77	3.07	99.72	0.515	0.003	0.003	1.409	0.064	0.273	0.003	0.720	0.005	0.005	0.004					
Vranduk Fm.	BO73sp072	0.08	0.10	43.78	23.35	0.13	17.29	0.22	0.22	12.07	2.43	99.64	0.511	0.002	0.003	1.429	0.051	0.280	0.003	0.713	0.005	0.003	0.003					
Vranduk Fm.	BO73sp073	0.17	0.29	21.82	46.75	0.23	12.59	0.09	0.18	16.22	2.12	100.46	1.138	0.004	0.006	0.792	0.049	0.418	0.006	0.578	0.002	0.004	0.004					
Vranduk Fm.	BO73sp074	0.47	0.26	37.27	26.01	0.21	14.09	0.18	0.42	16.26	5.24	100.41	0.592	0.010	0.005	1.264	0.113	0.391	0.005	0.604	0.004	0.009	0.009					
Vranduk Fm.	BO73sp075	0.14	0.17	42.55	24.36	0.14	16.88	0.21	0.19	12.55	2.56	99.74	0.537	0.003	0.003	1.397	0.054	0.292	0.003	0.701	0.005	0.004	0.004					
Vranduk Fm.	BO73sp076	0.16	0.20	28.22	37.45	0.19	14.97	0.18	0.11	13.38	5.27	100.13	0.879	0.003	0.004	0.988	0.118	0.332	0.005	0.662	0.004	0.003	0.003					
Vranduk Fm.	BO73sp077	0.23	0.16	41.55	24.02	0.15	16.57	0.23	0.20	12.82	3.59	99.52	0.533	0.005	0.003	1.375	0.076	0.301	0.003	0.693	0.005	0.004	0.004					
Vranduk Fm.	BO73sp078	0.08	0.18	43.72	23.01	0.12	17.22	0.23	0.28	12.11	2.91	99.85	0.503	0.002	0.003	1.426	0.061	0.280	0.003	0.710	0.005	0.006	0.006					
Vranduk Fm.	BO73sp079	0.12	0.14	43.55	24.18	0.13	18.19	0.25	0.13	10.62	2.21	99.51	0.527	0.002	0.003	1.417	0.046	0.245	0.003	0.748	0.005	0.003	0.003					
Vranduk Fm.	BO73sp080	0.13	0.19	42.72	24.20	0.18	17.15	0.21	0.20	12.11	2.64	99.71	0.532	0.003	0.003	1.400	0.055	0.281	0.004	0.711	0.005	0.004	0.004					
Vranduk Fm.	BO73sp081	0.10	0.16	43.02	24.11	0.12	17.30	0.24	0.19	11.83	2.36	99.44	0.530	0.002	0.003	1.410	0.049	0.275	0.003	0.717	0.005	0.005	0.004					
Vranduk Fm.	BO73sp082	0.13	0.17	39.03	28.68	0.15	17.02	0.18	0.18	11.80	2.40	99.74	0.639	0.003	0.003	1.297	0.051	0.278	0.004	0.715	0.004	0.004	0.004					
Vranduk Fm.	BO73sp083	0.24	0.15	44.93	20.47	0.13	17.07	0.20	0.19	12.52	3.19	99.08	0.449	0.005	0.003	1.469	0.067	0.290	0.003	0.705	0.005	0.004	0.004					
Vranduk Fm.	BO73sp084	0.12	0.15	46.17	20.07	0.13	17.43	0.30	0.19	12.19	3.09	99.84	0.435	0.002	0.003	1.491	0.064	0.279	0.003	0.712	0.007	0.007	0.004					
Vranduk Fm.	BO73sp085	0.08	0.25	26.86	40.46	0.18	14.32	0.12	0.10	14.20	3.48	100.05	0.959	0.002	0.005	0.949	0.078	0.356	0.005	0.640	0.003	0.002	0.002					
Vranduk Fm.	BO73sp086	0.10	0.18	41.76	24.98	0.16	17.33	0.22	0.13	11.63	2.93	99.41	0.552	0.004	0.003	1.375	0.062	0.272	0.004	0.721	0.005	0.005	0.002					
Vranduk Fm.	BO73sp087	0.18	0.16	36.50	30.18	0.18	15.53	0.18	0.21	13.67	2.99	99.78	0.685	0.004	0.003	1.236	0.065	0.328	0.004	0.665	0.004	0.005	0.005					
Vranduk Fm.	BO73sp088	0.14	0.22	29.52	38.63	0.17	15.19	0.11	0.11	13.40	2.72	100.21	0.899	0.003	0.004	1.025	0.060	0.330	0.004	0.667	0.003	0.002	0.002					
Vranduk Fm.	BO73sp089	0.05	0.26	31.57	36.61	0.18	15.02	0.12	0.21	13.93	2.51	100.48	0.845	0.002	0.005	1.086	0.055	0.340	0.005	0.653	0.003	0.005	0.005					
Vranduk Fm.	BO73sp090	0.08	0.16	44.17	22.91	0.13	17.73	0.25	0.15	11.39	2.68	99.63	0.500	0.001	0.003	1.436	0.056	0.263	0.003	0.729	0.006	0.006	0.003					
Vranduk Fm.	BO73sp091	0.22	0.29	14.73	54.41	0.27	10.87	0.06	0.14	17.91	1.88	100.76	1.376	0.005	0.006	0.556	0.045	0.479	0.007	0.518	0.002	0.002	0.003					
Vranduk Fm.	BO73sp092	0.22	0.29	20.23	43.03	0.32	10.13	0.15	0.17	19.36	6.26	100.37	1.074	0.005	0.006	0.753	0.149	0.512	0.009	0.477	0.004	0.009	0.009					
Vranduk Fm.	BO73sp093	0.07	0.22	23.18	46.58	0.20	14.29	0.10	0.14	13.67	1.70	100.15	1.118	0.002	0.004	0.830	0.039	0.347	0.0									

analyses in wt%. Shown are the recalculated FeO and Fe <sub>2</sub> O <sub>3</sub> values and the amended total		Cations per formula unit on the basis of 3 oxygens																					
Formation	Sample & spot ID	SiO <sub>2</sub>	TiO <sub>2</sub>	V <sub>2</sub> O <sub>5</sub>	Al <sub>2</sub> O <sub>3</sub>	Cr <sub>2</sub> O <sub>3</sub>	MnO	MgO	NiO	ZnO	FeO	Fe <sub>2</sub> O <sub>3</sub>	Total	Cr	Ti	V	Al	Fe <sup>3+</sup>	Fe <sup>2+</sup>	Mn	Mg	Ni	Zn
Vranduk Fm.	BO75sp010	n. d.	0.14	0.27	31.53	34.94	0.21	13.49	0.09	0.22	16.22	3.13	100.25	0.816	0.003	0.005	1.098	0.070	0.401	0.005	0.594	0.002	0.005
Vranduk Fm.	BO75sp011	n. d.	0.09	0.15	41.34	25.06	0.14	17.25	0.22	0.17	11.69	3.48	99.59	0.554	0.002	0.003	1.363	0.073	0.273	0.003	0.719	0.005	0.003
Vranduk Fm.	BO75sp012	n. d.	0.15	0.23	28.89	37.72	0.20	13.11	0.12	0.34	16.17	3.07	99.99	0.894	0.003	0.005	1.021	0.069	0.405	0.005	0.586	0.003	0.008
Vranduk Fm.	BO75sp013	n. d.	0.15	0.27	22.12	45.89	0.23	11.38	0.05	0.32	17.90	1.84	100.14	1.128	0.003	0.005	1.428	0.043	0.465	0.006	0.527	0.001	0.007
Vranduk Fm.	BO75sp014	n. d.	0.20	0.34	19.70	46.77	0.29	11.15	0.07	0.21	18.17	3.90	100.79	1.157	0.005	0.007	0.727	0.092	0.475	0.008	0.520	0.002	0.005
Vranduk Fm.	BO75sp015	n. d.	0.06	0.24	41.00	25.37	0.15	16.13	0.14	0.29	13.26	2.70	99.34	0.566	0.001	0.004	1.364	0.057	0.313	0.004	0.679	0.003	0.006
Vranduk Fm.	BO75sp016	n. d.	0.22	0.28	9.77	56.44	0.37	8.15	0.04	0.23	21.02	4.06	100.60	1.489	0.005	0.006	1.484	0.102	0.587	0.011	0.405	0.001	0.006
Vranduk Fm.	BO75sp017	n. d.	0.69	0.20	36.20	25.32	0.21	14.95	0.23	0.23	14.90	7.01	99.93	0.578	0.015	0.004	1.232	0.152	0.360	0.005	0.643	0.005	0.005
Vranduk Fm.	BO75sp018	n. d.	0.06	0.26	19.23	51.13	0.22	13.11	0.08	0.16	15.04	1.47	100.76	1.251	0.001	0.005	0.701	0.034	0.389	0.006	0.604	0.002	0.004
Vranduk Fm.	BO75sp019	n. d.	0.14	0.34	13.26	55.17	0.31	9.46	0.03	0.23	19.65	2.02	100.61	1.419	0.004	0.007	0.509	0.049	0.535	0.009	0.459	0.001	0.006
Vranduk Fm.	BO75sp020	n. d.	0.09	0.12	48.10	18.19	0.10	19.24	0.33	0.14	9.53	3.37	99.21	0.389	0.002	0.002	1.534	0.069	0.216	0.002	0.776	0.007	0.003
Vranduk Fm.	BO75sp021	n. d.	0.09	0.10	47.89	18.11	0.13	18.33	0.26	0.25	10.81	3.23	99.21	0.390	0.002	0.002	1.536	0.066	0.246	0.003	0.743	0.006	0.005
Vranduk Fm.	BO75sp022	n. d.	0.08	0.21	28.04	41.93	0.19	15.18	0.08	0.15	13.16	1.33	100.35	0.980	0.002	0.004	0.978	0.030	0.326	0.005	0.689	0.002	0.003
Vranduk Fm.	BO75sp023	n. d.	0.14	0.26	19.65	49.74	0.26	12.35	0.06	0.16	16.30	1.79	100.71	1.221	0.003	0.005	1.484	0.042	0.252	0.007	0.572	0.002	0.004
Vranduk Fm.	BO75sp024	n. d.	0.08	0.14	46.02	20.60	0.13	18.11	0.28	0.22	11.01	3.03	99.63	0.445	0.002	0.003	1.484	0.062	0.252	0.003	0.738	0.006	0.005
Vranduk Fm.	BO75sp025	n. d.	0.07	0.23	7.62	62.77	0.33	9.18	0.03	0.17	19.12	1.11	100.62	1.658	0.002	0.005	0.300	0.028	0.534	0.009	0.457	0.001	0.004
Vranduk Fm.	BO75sp026	n. d.	0.07	0.33	22.81	44.91	0.26	12.15	0.11	0.22	16.91	2.72	100.50	1.092	0.002	0.007	0.827	0.063	0.435	0.007	0.557	0.003	0.005
Vranduk Fm.	BO75sp027	n. d.	0.11	0.23	25.92	41.19	0.28	13.43	0.08	0.19	15.46	3.71	100.61	0.981	0.003	0.005	0.920	0.084	0.390	0.007	0.603	0.002	0.004
Vranduk Fm.	BO75sp028	n. d.	0.03	0.13	49.39	15.95	0.10	18.28	0.28	0.25	11.13	3.82	99.37	0.341	0.001	0.002	1.575	0.078	0.252	0.002	0.737	0.006	0.005
Vranduk Fm.	BO75sp029	n. d.	0.12	0.33	19.49	49.13	0.26	11.67	0.07	0.16	17.45	2.19	100.81	1.212	0.003	0.007	0.717	0.051	0.455	0.007	0.540	0.002	0.004
Vranduk Fm.	BO75sp030	n. d.	0.08	0.29	6.87	61.64	0.35	8.47	0.06	0.15	20.18	2.88	100.97	1.637	0.002	0.006	0.272	0.073	0.567	0.010	0.424	0.002	0.004
Vranduk Fm.	BO75sp031	n. d.	0.04	0.24	33.75	35.06	0.18	15.26	0.12	0.21	13.81	1.64	100.32	0.802	0.001	0.005	1.151	0.036	0.334	0.004	0.658	0.003	0.005
Vranduk Fm.	BO75sp032	n. d.	0.02	0.18	45.94	20.85	0.15	17.46	0.22	0.25	11.91	2.41	99.39	0.453	0.000	0.003	1.489	0.050	0.274	0.003	0.715	0.005	0.005
Vranduk Fm.	BO75sp033	n. d.	0.34	0.29	30.61	37.18	0.17	14.09	0.11	0.24	15.39	1.84	100.27	0.867	0.008	0.006	1.065	0.041	0.380	0.004	0.620	0.003	0.005
Vranduk Fm.	BO75sp034	n. d.	0.17	0.30	19.99	46.25	0.30	10.52	0.08	0.25	18.97	3.63	100.45	1.151	0.004	0.006	0.742	0.086	0.499	0.008	0.493	0.002	0.006
Vranduk Fm.	BO75sp035	n. d.	0.06	0.17	50.11	16.14	0.11	18.40	0.31	0.20	11.13	2.69	99.31	0.344	0.001	0.003	1.593	0.055	0.251	0.002	0.739	0.007	0.004
Vranduk Fm.	BO75sp036	n. d.	0.11	0.22	13.13	57.94	0.26	12.26	0.06	0.13	15.55	1.54	101.20	1.456	0.003	0.005	0.492	0.037	0.413	0.007	0.581	0.002	0.003
Vranduk Fm.	BO75sp037	n. d.	0.13	0.17	9.76	60.02	0.26	11.83	0.08	0.15	20.18	2.88	100.97	1.637	0.002	0.006	0.272	0.073	0.567	0.010	0.424	0.002	0.004
Vranduk Fm.	BO75sp038	n. d.	0.14	0.30	6.97	56.23	0.43	6.75	0.04	0.18	22.52	6.72	100.27	1.523	0.004	0.007	0.282	0.173	0.645	0.013	0.345	0.001	0.005
Vranduk Fm.	BO75sp039	n. d.	0.12	0.19	22.68	41.08	0.22	11.59	0.14	0.24	17.66	6.69	100.61	1.004	0.003	0.004	0.827	0.156	0.457	0.006	0.534	0.004	0.006
Vranduk Fm.	BO75sp040	n. d.	0.08	0.18	41.54	24.10	0.15	17.30	0.28	0.11	11.67	4.40	99.83	0.531	0.002	0.002	1.366	0.092	0.272	0.004	0.719	0.006	0.003
Vranduk Fm.	BO75sp041	n. d.	0.03	0.15	14.44	53.60	0.33	9.41	0.02	0.25	19.96	2.15	100.72	1.371	0.001	0.012	0.551	0.052	0.540	0.009	0.454	0.000	0.006
Vranduk Fm.	BO75sp042	n. d.	0.08	0.04	21.00	47.73	0.24	12.15	0.08	0.16	16.70	2.02	100.46	1.169	0.001	0.007	0.767	0.047	0.433	0.006	0.561	0.002	0.004
Vranduk Fm.	BO75sp043	n. d.	0.03	0.45	15.43	52.84	0.32	9.69	0.06	0.22	19.63	2.11	100.79	1.343	0.001	0.010	0.585	0.051	0.528	0.009	0.464	0.002	0.005
Vranduk Fm.	BO75sp044	n. d.	0.27	0.30	24.01	45.22	0.20	13.57	0.08	0.13	15.07	0.99	99.83	1.090	0.006	0.006	0.863	0.023	0.384	0.005	0.616	0.002	0.003
Vranduk Fm.	BO75sp045	n. d.	0.05	0.33	20.86	47.27	0.26	11.35	0.07	0.30	17.74	2.15	100.37	1.166	0.001	0.007	0.767	0.050	0.463	0.007	0.528	0.002	0.007
Vranduk Fm.	BO75sp046	n. d.	0.08	0.15	44.72	21.24	0.14	16.83	0.27	0.21	12.65	2.94	99.23	0.466	0.002	0.003	1.463	0.061	0.294	0.003	0.686	0.006	0.004
Vranduk Fm.	BO75sp047	n. d.	0.12	0.26	24.81	44.19	0.21	13.61	0.08	0.18	14.86	1.36	99.68	1.063	0.003	0.005	0.890	0.031	0.378	0.005	0.617	0.002	0.004
Vranduk Fm.	BO75sp048	n. d.	0.19	0.18	35.54	29.30	0.17	14.75	0.19	0.37	14.56	4.50	99.75	0.671	0.004	0.003	1.215	0.098	0.353	0.004	0.637	0.004	0.008
Vranduk Fm.	BO75sp049	n. d.	0.06	0.41	16.75	51.33	0.27	10.50	0.04	0.17	18.60	2.28	100.40	1.294	0.001	0.009	0.630	0.055	0.496	0.007	0.499	0.001	0.004
Vranduk Fm.	BO75sp050	n. d.	0.04	0.40	13.85	56.17	0.27	11.55	0.05	0.17	16.55	1.48	100.54	1.422	0.001	0.008	0.523	0.036	0.443	0.007	0.551	0.001	0.004
Vranduk Fm.	BO75sp051	n. d.	0.08	0.27	23.96	41.11	0.23	12.99	0.14	0.18	15.78	5.82	100.56	0.990	0.002	0.005	0.861	0.133	0.402	0.006	0.590	0.003	0.004
Vranduk Fm.	BO75sp052	n. d.	0.04	0.11	48.70	17.65	0.09	19.00	0.32	0.13	9.88	3.00	99.93	0.378	0.001	0.002	1.555	0.061	0.224	0.002	0.767	0.007	0.003
Vranduk Fm.	BO75sp053	n. d.	0.03	0.34	20.99	47.66	0.26	11.59	0.10	0.20	17.27	1.34	99.76	1.178	0.001	0.007	0.774	0.031	0.452	0.007	0.540	0.002	0.005
Vranduk Fm.	BO75sp054	n. d.	0.19	0.31	17.86	45.94	0.36	8.79	0.10	0.37	20.98	5.23	100.12	1.171	0.005	0.007	0.679	0.127	0.566	0.010	0.422	0.003	0.009
Vranduk Fm.	BO75sp055	n. d.	0.09	0.30	9.38	61.90	0.24	12.02	0.05														

analyses in wt%. Shown are the recalculated FeO and Fe<sub>2</sub>O<sub>3</sub> values and the amended total

Formation	Sample & spot ID	Cations per formula unit on the basis of 3 oxygens															analyses in wt%. Shown are the recalculated FeO and Fe <sub>2</sub> O <sub>3</sub> values and the amended total														
		SiO <sub>2</sub>	TiO <sub>2</sub>	V <sub>2</sub> O <sub>5</sub>	Al <sub>2</sub> O <sub>3</sub>	Cr <sub>2</sub> O <sub>3</sub>	MnO	MgO	NiO	ZnO	FeO	Fe <sub>2</sub> O <sub>3</sub>	Total	Cr	Ti	V	Al	Fe <sup>3+</sup>	Fe <sup>2+</sup>	Mn	Mg	Ni	Zn								
Vranduk Fm.	BO75sp066	n. d.	1.10	0.36	25.04	37.05	11.71	0.16	0.26	18.65	5.61	100.21	0.898	0.025	0.007	0.906	0.129	0.478	0.007	0.535	0.004	0.006	0.006								
Vranduk Fm.	BO75sp067	n. d.	0.13	0.23	46.24	19.41	16.72	0.21	0.29	13.04	2.46	98.86	0.425	0.003	0.004	1.509	0.051	0.302	0.003	0.690	0.005	0.006	0.006								
Vranduk Fm.	BO75sp068	n. d.	0.04	0.23	34.57	30.58	14.85	0.21	0.16	14.35	4.72	99.89	0.702	0.001	0.005	1.184	0.103	0.348	0.004	0.643	0.005	0.004	0.004								
Vranduk Fm.	BO75sp069	n. d.	0.09	0.26	18.44	50.49	23.13	0.09	0.17	16.55	2.04	100.32	0.683	0.002	0.005	0.683	0.048	0.435	0.006	0.585	0.002	0.004	0.004								
Vranduk Fm.	BO75sp070	n. d.	0.29	0.21	7.12	62.91	10.04	0.06	0.12	17.89	1.51	100.42	1.658	0.007	0.005	0.280	0.038	0.499	0.008	0.499	0.002	0.003	0.003								
Vranduk Fm.	BO75sp071	n. d.	0.09	0.19	32.18	35.97	14.97	0.14	0.25	13.92	2.27	100.14	0.831	0.002	0.004	1.108	0.050	0.340	0.004	0.662	0.003	0.005	0.005								
Vranduk Fm.	BO75sp072	n. d.	0.10	0.23	30.37	37.20	15.81	0.17	0.13	12.13	2.77	99.06	0.868	0.002	0.004	1.057	0.061	0.299	0.004	0.695	0.004	0.003	0.003								
Vranduk Fm.	BO75sp073	n. d.	0.12	0.44	12.64	56.19	9.28	0.03	0.22	19.81	1.44	100.37	1.454	0.003	0.009	0.484	0.035	0.543	0.008	0.453	0.001	0.005	0.005								
Vranduk Fm.	BO75sp074	n. d.	0.03	0.13	48.60	15.84	0.12	0.34	0.21	11.35	4.44	99.03	0.341	0.001	0.002	1.561	0.091	0.259	0.003	0.729	0.007	0.004	0.004								
Vranduk Fm.	BO75sp075	n. d.	0.09	0.14	44.82	22.34	18.24	0.27	0.17	10.82	3.05	100.07	0.483	0.002	0.002	1.445	0.063	0.248	0.003	0.744	0.006	0.006	0.006								
Vranduk Fm.	BO75sp076	n. d.	0.06	0.30	22.86	44.91	19.19	0.06	0.19	15.93	2.76	100.02	1.092	0.001	0.006	0.829	0.064	0.410	0.005	0.585	0.002	0.004	0.004								
Vranduk Fm.	BO75sp077	n. d.	0.05	0.34	14.99	54.82	0.34	0.15	0.05	17.38	1.76	100.79	1.377	0.001	0.007	0.563	0.042	0.463	0.008	0.530	0.001	0.004	0.004								
Vranduk Fm.	BO75sp078	n. d.	0.08	0.28	15.35	54.37	0.27	0.09	0.12	15.46	1.55	99.80	1.370	0.002	0.006	0.577	0.037	0.412	0.007	0.582	0.002	0.003	0.003								
Vranduk Fm.	BO75sp079	n. d.	0.07	0.32	22.13	45.60	0.26	0.11	0.16	17.53	2.65	100.56	1.115	0.002	0.007	0.807	0.062	0.453	0.007	0.539	0.002	0.005	0.005								
Vranduk Fm.	BO75sp080	n. d.	0.09	0.17	46.96	19.44	15.66	0.26	0.20	11.86	2.71	99.49	0.420	0.002	0.003	1.514	0.056	0.271	0.003	0.720	0.006	0.004	0.004								
Vranduk Fm.	BO75sp081	n. d.	0.34	0.43	16.91	51.43	0.26	0.18	0.09	17.72	1.51	100.03	1.294	0.008	0.009	0.634	0.036	0.472	0.007	0.529	0.002	0.004	0.004								
Vranduk Fm.	BO75sp082	n. d.	0.07	0.28	27.01	39.92	13.37	0.12	0.18	15.63	3.37	100.13	0.950	0.006	0.006	0.959	0.076	0.394	0.005	0.600	0.003	0.004	0.004								
Vranduk Fm.	BO75sp083	n. d.	0.19	0.25	36.89	28.80	15.66	0.22	0.19	13.59	3.83	99.76	0.653	0.004	0.005	1.247	0.083	0.326	0.004	0.689	0.005	0.004	0.004								
Vranduk Fm.	BO75sp084	n. d.	0.12	0.32	21.88	47.16	19.13	0.09	0.19	15.46	1.99	100.50	1.144	0.003	0.007	0.791	0.046	0.397	0.005	0.599	0.002	0.004	0.004								
Vranduk Fm.	BO75sp085	n. d.	0.08	0.21	31.51	32.86	19.19	0.20	0.12	14.42	5.67	99.78	0.766	0.002	0.004	1.096	0.126	0.356	0.005	0.635	0.005	0.004	0.004								
Vranduk Fm.	BO75sp086	n. d.	0.06	0.28	25.49	42.09	0.21	0.10	0.16	15.01	3.02	100.03	1.007	0.001	0.006	0.910	0.069	0.380	0.005	0.614	0.002	0.004	0.004								
Vranduk Fm.	BO75sp087	n. d.	0.05	0.32	24.87	43.71	13.19	0.08	0.22	15.50	2.58	100.27	1.051	0.001	0.006	0.874	0.059	0.394	0.006	0.598	0.002	0.005	0.005								
Vranduk Fm.	BO75sp088	n. d.	0.09	0.20	7.86	60.96	0.33	0.54	0.05	19.88	1.88	99.95	1.626	0.002	0.004	0.312	0.048	0.561	0.010	0.429	0.001	0.004	0.004								
Vranduk Fm.	BO75sp089	n. d.	0.04	0.32	21.88	47.18	0.22	0.08	0.19	15.73	1.66	100.07	1.151	0.001	0.006	0.796	0.038	0.406	0.006	0.588	0.002	0.004	0.004								
Vranduk Fm.	BO75sp090	n. d.	0.06	0.16	46.53	19.52	14.74	0.24	0.19	12.01	2.83	99.14	0.424	0.001	0.003	1.508	0.059	0.276	0.003	0.715	0.005	0.003	0.003								
Vranduk Fm.	BO87sp001	n. d.	0.20	0.24	14.77	50.79	0.28	0.28	0.10	13.28	4.40	100.05	1.305	0.005	0.005	0.566	0.108	0.532	0.008	0.463	0.003	0.003	0.003								
Vranduk Fm.	BO87sp002	n. d.	0.04	0.29	19.94	48.03	12.49	0.10	0.15	15.84	2.97	100.07	1.183	0.001	0.006	0.733	0.070	0.413	0.006	0.580	0.002	0.003	0.003								
Vranduk Fm.	BO87sp003	n. d.	0.38	0.38	26.50	40.01	14.52	0.17	0.12	13.33	4.05	100.07	0.944	0.009	0.008	0.932	0.091	0.328	0.003	0.677	0.003	0.003	0.003								
Vranduk Fm.	BO87sp004	n. d.	0.04	0.33	17.84	50.27	0.30	0.07	0.20	18.33	2.27	100.30	1.262	0.001	0.007	0.668	0.054	0.487	0.008	0.504	0.002	0.005	0.005								
Vranduk Fm.	BO87sp005	n. d.	0.04	0.24	29.82	39.71	15.26	0.13	0.14	13.15	1.39	100.10	0.923	0.001	0.005	1.034	0.031	0.324	0.005	0.669	0.003	0.003	0.003								
Vranduk Fm.	BO87sp006	n. d.	0.96	0.08	18.99	44.31	0.23	0.10	0.10	18.82	3.17	99.16	1.111	0.023	0.010	0.747	0.076	0.499	0.006	0.519	0.003	0.002	0.002								
Vranduk Fm.	BO87sp007	n. d.	0.07	0.22	29.55	38.82	16.40	0.16	0.05	11.37	3.05	99.85	0.900	0.001	0.004	1.021	0.067	0.279	0.004	0.716	0.004	0.004	0.004								
Vranduk Fm.	BO87sp010	n. d.	0.07	0.27	28.75	40.41	14.66	0.11	0.16	13.98	1.49	100.08	0.947	0.002	0.005	1.005	0.033	0.347	0.005	0.648	0.003	0.004	0.004								
Vranduk Fm.	BO87sp011	n. d.	0.06	0.32	22.19	45.30	0.20	0.11	0.07	17.76	2.27	99.78	1.115	0.001	0.007	0.815	0.053	0.462	0.005	0.534	0.002	0.002	0.002								
Vranduk Fm.	BO87sp012	n. d.	0.08	0.24	24.91	43.56	15.27	0.15	0.09	12.53	3.31	100.30	1.032	0.002	0.005	0.880	0.075	0.314	0.004	0.682	0.004	0.004	0.004								
Vranduk Fm.	BO87sp013	n. d.	0.03	0.19	35.20	33.14	16.08	0.15	0.21	12.56	2.06	99.79	0.753	0.001	0.004	1.193	0.045	0.302	0.004	0.689	0.004	0.005	0.005								
Vranduk Fm.	BO87sp014	n. d.	0.03	0.38	18.04	50.11	11.42	0.06	0.17	17.36	2.64	100.47	1.249	0.001	0.008	0.670	0.063	0.458	0.007	0.536	0.001	0.001	0.001								
Vranduk Fm.	BO87sp015	n. d.	0.04	0.23	24.97	42.20	13.75	0.12	0.11	14.86	4.11	100.60	1.007	0.001	0.005	0.888	0.093	0.375	0.005	0.618	0.003	0.002	0.002								
Vranduk Fm.	BO87sp016	n. d.	0.05	0.35	21.18	47.09	12.82	0.09	0.14	15.70	2.67	100.30	1.149	0.001	0.007	1.021	0.062	0.405	0.005	0.590	0.002	0.003	0.003								
Vranduk Fm.	BO87sp017	n. d.	0.94	0.38	18.56	44.04	0.26	0.10	0.11	17.76	6.74	100.64	1.093	0.022	0.008	0.687	0.159	0.466	0.007	0.550	0.003	0.002	0.002								
Vranduk Fm.	BO87sp018	n. d.	0.07	0.21	28.14	40.73	14.46	0.12	0.21	14.14	2.01	100.29	0.957	0.002	0.004	0.986	0.045	0.352	0.005	0.640	0.003	0.003	0.003								
Vranduk Fm.	BO87sp021	n. d.	0.48	0.51	17.44	41.72	8.68	0.09	0.20	21.70	9.23	100.35	1.065	0.012	0.011	0.664	0.204	0.586	0.008	0.418	0.002	0.005	0.005								
Vranduk Fm.	BO87sp020	n. d.	0.11	0.40	10.84	58.01	13.35	0.09	0.06	13.45	4.01	100.55	1.470	0.003	0.008	0.410	0.037	0.361	0.006	0.638	0.002	0.001	0.001								
Vranduk Fm.	BO87sp022	n. d.	0.06	0.29	23.17	45.07	13.13	0.12	0.18	15.49	2.83	100.59	1.087	0.001	0.006	0.833	0.085	0.395	0.007	0.597	0.003	0.003	0.003								
Vranduk Fm.	BO87sp023	n. d.	0.13	0.24	24.92	44.15	12.49	0.14	0.07	13.70	5.09	100.55	1.061	0.003	0.005	0.806	0.116	0.116	0.006	0.647	0.004	0.002	0.002								
Vranduk Fm.	BO87sp024	n. d.	0.07	0.29	26.83	42.38	14.26	0.11	0.16	14.15	1.98	100.62	0.998	0.002	0.006	0.942	0.044	0.352	0.005	0.642	0.003	0.004	0.004								
Vranduk Fm.	BO87sp025	n. d.	0.05	0.26	26.44	41.55	0.20	0.11	0.17	14.82	2.78	100.25	0.987	0.001	0.005	0.937	0.063	0.372	0.005	0.621	0.003	0.003	0.003								
Vranduk Fm.	BO87sp026	n. d.	0.07	0.26	25.48	41.28	12.33	0.08	0.24	16.83	3.48	99.98	0.958	0.002	0.005	0.908	0.080	0.430	0.006	0.562	0.002	0.005	0.005								
Vranduk Fm.	BO87sp027	n. d.	0.19	0.35	26.43	40.42	0.21	0.13	0.12	14.61	3.73	100.32	0.934	0.004	0.007	0.934	0.084	0.366	0.005	0.631	0.003	0.003	0.003								
Vranduk Fm.	BO87sp029	n. d.	0.06	0.29	15.03	54.83	0.22	0.17	0.13	16.48	1.73	100.58	1.379	0.002	0.006	0.564	0.041	0.438	0.006												

analyses in wt%. Shown are the recalculated FeO and Fe<sub>2</sub>O<sub>3</sub> values and the amended total

Formation	Sample & spot ID	cations per formula unit on the basis of 3 oxygens																					
		SiO <sub>2</sub>	TiO <sub>2</sub>	V <sub>2</sub> O <sub>5</sub>	Al <sub>2</sub> O <sub>3</sub>	Cr <sub>2</sub> O <sub>3</sub>	MnO	MgO	NiO	ZnO	FeO	Fe <sub>2</sub> O <sub>3</sub>	Total	Cr	Ti	V	Al	Fe <sup>3+</sup>	Fe <sup>2+</sup>	Mn	Mg	Ni	Zn
Vranduk Fm.	BO87/sp036	n. d.	0.27	0.27	28.36	38.27	0.19	15.99	0.19	0.09	12.04	4.57	100.24	0.891	0.006	0.005	0.985	0.101	0.297	0.005	0.702	0.005	0.002
Vranduk Fm.	BO87/sp037	n. d.	0.16	0.21	26.52	42.47	0.20	15.02	0.11	0.12	13.21	2.33	100.36	1.000	0.004	0.004	0.931	0.052	0.329	0.005	0.667	0.003	0.003
Vranduk Fm.	BO87/sp038	n. d.	0.25	0.31	18.92	43.50	0.33	8.59	0.07	0.19	21.82	6.49	100.46	1.102	0.006	0.006	0.715	0.156	0.585	0.009	0.410	0.002	0.004
Vranduk Fm.	BO87/sp039	n. d.	0.06	0.27	19.24	48.98	0.32	9.89	0.06	0.30	19.67	1.65	100.43	1.227	0.001	0.006	0.719	0.039	0.521	0.009	0.467	0.002	0.007
Vranduk Fm.	BO87/sp040	n. d.	0.24	0.31	17.37	49.39	0.29	11.91	0.11	0.13	16.70	4.40	100.85	1.227	0.006	0.007	0.644	0.104	0.439	0.008	0.558	0.003	0.003
Vranduk Fm.	BO87/sp041	n. d.	0.22	0.24	27.01	39.44	0.21	12.25	0.11	0.27	17.33	3.13	100.29	1.243	0.005	0.005	0.964	0.071	0.439	0.008	0.553	0.003	0.006
Vranduk Fm.	BO87/sp042	n. d.	0.11	0.29	19.64	49.16	0.22	12.24	0.08	0.14	16.34	1.99	100.21	1.213	0.003	0.006	0.723	0.047	0.426	0.006	0.569	0.002	0.003
Vranduk Fm.	BO87/sp043	n. d.	0.38	0.15	34.85	30.11	0.16	16.46	0.20	0.12	12.22	5.15	99.80	1.181	0.004	0.003	1.181	0.111	0.294	0.004	0.705	0.005	0.002
Vranduk Fm.	BO87/sp044	n. d.	0.06	0.32	22.81	46.04	0.21	12.62	0.08	0.15	16.31	1.84	100.44	1.116	0.001	0.007	0.825	0.042	0.418	0.006	0.577	0.002	0.003
Vranduk Fm.	BO87/sp045	n. d.	0.42	0.42	9.57	37.05	0.35	6.20	0.29	0.14	23.67	22.64	100.53	1.001	0.011	0.005	0.386	0.582	0.677	0.010	0.316	0.008	0.004
Vranduk Fm.	BO87/sp046	n. d.	0.08	0.22	17.32	51.91	0.21	12.48	0.09	0.12	15.62	2.38	100.43	1.289	0.002	0.005	0.641	0.056	0.410	0.006	0.584	0.002	0.003
Vranduk Fm.	BO87/sp047	n. d.	0.14	0.28	18.14	50.48	0.19	13.61	0.11	0.08	13.99	2.98	100.00	1.245	0.003	0.006	0.667	0.070	0.365	0.005	0.633	0.003	0.002
Vranduk Fm.	BO87/sp048	n. d.	0.07	0.33	22.25	45.99	0.20	12.86	0.10	0.17	15.78	2.55	100.29	1.118	0.002	0.007	0.806	0.059	0.406	0.005	0.589	0.002	0.004
Vranduk Fm.	BO87/sp049	n. d.	0.13	0.26	21.90	46.90	0.24	12.88	0.10	0.12	15.68	1.96	100.18	1.142	0.003	0.005	0.795	0.045	0.404	0.006	0.591	0.002	0.003
Vranduk Fm.	BO87/sp050	n. d.	0.05	0.21	22.81	46.25	0.24	13.75	0.09	0.12	14.39	2.24	100.15	1.116	0.001	0.004	0.821	0.051	0.367	0.006	0.626	0.002	0.003
Vranduk Fm.	BO87/sp051	n. d.	0.07	0.27	18.34	48.39	0.25	11.86	0.13	0.15	16.62	4.40	100.47	1.202	0.002	0.006	0.679	0.104	0.437	0.007	0.555	0.003	0.004
Vranduk Fm.	BO87/sp052	n. d.	0.35	0.33	18.92	46.10	0.24	12.50	0.16	0.10	15.90	5.43	100.01	1.142	0.008	0.007	0.699	0.128	0.417	0.006	0.584	0.004	0.004
Vranduk Fm.	BO87/sp053	n. d.	0.05	0.26	22.95	42.39	0.33	9.69	0.10	0.32	20.21	3.40	99.70	1.054	0.001	0.005	0.851	0.081	0.532	0.009	0.454	0.002	0.007
Vranduk Fm.	BO87/sp054	n. d.	0.04	0.31	24.15	43.98	0.22	12.25	0.07	0.21	16.98	2.14	100.34	1.064	0.001	0.006	0.871	0.049	0.434	0.006	0.559	0.002	0.005
Vranduk Fm.	BO87/sp055	n. d.	0.05	0.23	30.74	36.75	0.16	15.50	0.14	0.12	12.90	3.28	99.87	0.852	0.001	0.004	1.063	0.072	0.317	0.004	0.678	0.003	0.003
Vranduk Fm.	BO87/sp056	n. d.	0.92	0.26	23.84	36.96	0.28	12.23	0.17	0.16	17.38	7.72	99.93	0.901	0.021	0.005	0.866	0.179	0.448	0.007	0.562	0.004	0.004
Vranduk Fm.	BO87/sp057	n. d.	0.07	0.21	26.92	40.77	0.21	14.21	0.11	0.21	14.25	3.13	100.08	0.966	0.002	0.004	0.951	0.071	0.357	0.005	0.635	0.003	0.005
Vranduk Fm.	BO87/sp058	n. d.	0.06	0.27	23.73	44.67	0.22	12.46	0.10	0.19	16.54	2.00	100.24	1.082	0.001	0.005	0.857	0.046	0.424	0.006	0.589	0.002	0.004
Vranduk Fm.	BO87/sp059	n. d.	0.06	0.28	23.71	44.41	0.24	12.44	0.09	0.19	16.41	1.97	99.79	1.080	0.001	0.006	0.860	0.046	0.422	0.006	0.570	0.002	0.004
Vranduk Fm.	BO87/sp060	n. d.	0.05	0.18	27.26	41.82	0.20	14.65	0.11	0.14	13.74	2.11	100.27	1.027	0.001	0.004	0.958	0.042	0.342	0.005	0.651	0.003	0.003
Vranduk Fm.	BO87/sp061	n. d.	0.76	0.45	20.07	41.44	0.32	9.46	0.10	0.23	21.15	6.49	100.47	1.039	0.018	0.009	0.750	0.155	0.561	0.009	0.447	0.003	0.005
Vranduk Fm.	BO87/sp062	n. d.	0.34	0.37	19.51	44.57	0.29	9.75	0.09	0.15	20.27	4.89	100.22	1.119	0.008	0.008	0.731	0.117	0.539	0.008	0.462	0.002	0.003
Vranduk Fm.	BO87/sp063	n. d.	0.07	0.30	25.33	42.17	0.22	12.50	0.17	0.19	17.36	2.29	100.11	1.019	0.002	0.008	0.912	0.039	0.444	0.006	0.550	0.003	0.004
Vranduk Fm.	BO87/sp064	n. d.	0.04	0.37	21.35	46.79	0.27	11.07	0.06	0.21	17.46	1.64	99.69	0.852	0.001	0.006	0.787	0.039	0.457	0.007	0.536	0.001	0.005
Vranduk Fm.	BO87/sp065	n. d.	0.07	0.29	20.29	49.16	0.22	12.49	0.06	0.12	16.06	1.40	100.15	1.208	0.002	0.006	0.743	0.033	0.417	0.006	0.579	0.001	0.003
Vranduk Fm.	BO87/sp066	n. d.	0.05	0.32	24.90	43.20	0.22	13.16	0.09	0.19	15.58	2.25	99.95	1.039	0.001	0.006	0.893	0.051	0.397	0.006	0.597	0.002	0.004
Vranduk Fm.	BO87/sp067	n. d.	0.07	0.39	19.48	46.62	0.27	11.07	0.10	0.19	18.01	4.07	100.28	1.160	0.002	0.008	0.723	0.036	0.474	0.007	0.519	0.003	0.004
Vranduk Fm.	BO87/sp068	n. d.	0.19	0.29	25.59	41.80	0.20	13.55	0.11	0.18	15.25	2.95	100.11	0.999	0.004	0.006	0.912	0.067	0.386	0.005	0.611	0.003	0.004
Vranduk Fm.	BO87/sp069	n. d.	0.14	0.32	30.97	33.60	0.23	13.38	0.13	0.21	16.31	5.09	100.38	0.786	0.003	0.006	1.081	0.113	0.404	0.006	0.590	0.003	0.005
Vranduk Fm.	BO87/sp070	n. d.	0.38	0.28	33.22	31.29	0.16	14.39	0.26	0.14	15.15	4.57	99.84	0.724	0.008	0.005	1.147	0.101	0.371	0.004	0.628	0.006	0.003
Vranduk Fm.	BO87/sp071	n. d.	0.16	0.28	17.05	50.53	0.24	11.99	0.06	0.09	16.30	3.26	99.97	1.265	0.004	0.006	0.637	0.078	0.432	0.006	0.566	0.002	0.002
Vranduk Fm.	BO87/sp072	n. d.	0.04	0.20	23.03	43.70	0.23	12.81	0.11	0.13	15.80	4.13	100.18	1.061	0.001	0.004	0.834	0.095	0.406	0.006	0.586	0.003	0.003
Vranduk Fm.	BO87/sp073	n. d.	0.13	0.23	22.25	44.35	0.27	11.11	0.08	0.23	18.17	2.92	99.73	1.096	0.003	0.003	0.820	0.069	0.475	0.007	0.517	0.002	0.005
Vranduk Fm.	BO87/sp074	n. d.	0.12	0.21	6.02	61.94	0.26	12.04	0.06	0.03	14.50	5.05	100.23	1.623	0.003	0.005	0.235	0.126	0.402	0.007	0.595	0.002	0.001
Vranduk Fm.	BO87/sp075	n. d.	0.05	0.30	22.69	46.40	0.19	13.90	0.10	0.11	14.23	2.13	100.11	1.119	0.001	0.006	0.816	0.049	0.363	0.005	0.632	0.003	0.002
Vranduk Fm.	BO87/sp076	n. d.	0.06	0.30	29.07	39.11	0.21	13.37	0.09	0.26	15.91	1.73	100.10	0.923	0.001	0.006	1.023	0.039	0.397	0.005	0.595	0.002	0.006
Vranduk Fm.	BO87/sp077	n. d.	0.04	0.31	22.58	45.44	0.22	12.93	0.11	0.16	15.67	2.88	100.33	1.102	0.001	0.006	0.817	0.066	0.402	0.006	0.591	0.003	0.004
Vranduk Fm.	BO87/sp078	n. d.	0.04	0.25	27.82	40.23	0.21	13.39	0.10	0.22	15.67	2.19	100.12	0.954	0.001	0.005	0.984	0.049	0.393	0.005	0.599	0.002	0.005
Vranduk Fm.	BO87/sp079	n. d.	0.27	0.23	26.21	41.33	0.15	15.01	0.13	0.13	13.12	3.23	99.81	0.979	0.006	0.004	0.926	0.073	0.329	0.004	0.670	0.003	0.003
Vranduk Fm.	BO87/sp080	n. d.	0.08	0.26	21.76	47.25	0.17	14.31	0.12	0.08	13.50	2.65	100.19	1.141	0.001	0.006	0.784	0.061	0.345	0.004	0.651	0.003	0.002
Vranduk Fm.	BO87/sp081	n. d.	0.04	0.31	21.43	46.75	0.21	12.27	0.07	0.22	16.39	2.29	99.98	1.147	0.001	0.006	0.794	0.053	0.425	0.006	0.568	0.002	0.005
Vranduk Fm.	BO87/sp082	n. d.	0.43	0.42	20.20	43.05	0.29	11.03	0.12	0.23	18.38	6.02	100.18	1.070	0.010	0.009	0.749	0.142	0.483	0.008	0.517	0.003	0.005
Vranduk Fm.	BO87/sp083	n. d.	0.06	0.28	21.57	46.79	0.21	13.02	0.10	0.14	15.35	2.57	100.09	1.141	0.001	0.006	0.784	0.060	0.396	0.005	0.598	0.002	0.003
Vranduk Fm.	BO87/sp084	n. d.	0.13	0.28	21.99	46.01	0.26	11.59	0.04	0.23	17.68	2.15	100.35	1.128	0.003	0.006	0.804	0.050	0.458	0.007	0.536	0.001	0.005
Vranduk Fm.	BO87/sp085	n. d.	0.05	0.30	21.31	47.85	0.19	14.02	0.10	0.13	13.89	2.49	100.34	1.158	0.001	0.006	0.769	0.057	0.356	0.005	0.640	0.003	0.003
Vranduk Fm.	BO87/sp086	n. d.	0.09	0.21	31.59	36.61	0.14	16.31	0.23	0.06	11.78	2.75	99.7										

Analyses in wt%. Shown are the recalculated FeO and Fe<sub>2</sub>O<sub>3</sub> values and the amended total

Formation	Sample & spot ID	n.d.: not detected		Cations per formula unit on the basis of 3 oxygens																			
		SiO <sub>2</sub>	TiO <sub>2</sub>	V <sub>2</sub> O <sub>5</sub>	Al <sub>2</sub> O <sub>3</sub>	Cr <sub>2</sub> O <sub>3</sub>	MnO	MgO	NiO	ZnO	FeO	Fe <sub>2</sub> O <sub>3</sub>	Total	Cr	Ti	V	Al	Fe <sup>3+</sup>	Fe <sup>2+</sup>	Mn	Mg	Ni	Zn
Vranduk Fm.	BO92spl001	n. d.	0.34	0.22	27.43	38.53	0.22	13.49	0.12	0.19	15.72	4.01	100.27	0.914	0.008	0.004	0.971	0.091	0.395	0.006	0.603	0.003	0.004
Vranduk Fm.	BO92spl002	n. d.	0.16	0.30	27.17	37.51	0.25	11.43	0.10	0.30	18.59	4.44	100.24	0.903	0.004	0.006	0.975	0.102	0.473	0.006	0.519	0.003	0.007
Vranduk Fm.	BO92spl003	n. d.	0.10	0.14	42.23	23.05	0.16	16.22	0.22	0.24	13.37	4.06	99.79	0.510	0.002	0.003	1.394	0.085	0.313	0.004	0.677	0.005	0.005
Vranduk Fm.	BO92spl004	n. d.	0.11	0.23	25.90	39.58	0.24	11.31	0.12	0.30	18.47	3.92	100.19	0.959	0.003	0.005	0.936	0.085	0.473	0.006	0.516	0.003	0.007
Vranduk Fm.	BO92spl005	n. d.	0.06	0.25	31.41	37.06	0.18	14.58	0.11	0.24	14.41	1.71	100.02	0.861	0.001	0.005	1.088	0.038	0.354	0.005	0.638	0.002	0.005
Vranduk Fm.	BO92spl006	n. d.	0.51	0.21	32.70	31.24	0.22	14.22	0.14	0.17	15.54	5.28	100.23	0.723	0.011	0.004	1.129	0.116	0.381	0.005	0.621	0.003	0.004
Vranduk Fm.	BO92spl007	n. d.	0.03	0.35	18.66	49.73	0.30	10.01	0.05	0.22	19.53	1.26	100.34	1.247	0.001	0.007	0.705	0.030	0.518	0.008	0.473	0.001	0.005
Vranduk Fm.	BO92spl008	n. d.	0.05	0.19	43.14	24.90	0.14	17.51	0.24	0.16	11.69	1.98	99.99	0.544	0.001	0.003	1.406	0.041	0.270	0.003	0.721	0.005	0.003
Vranduk Fm.	BO92spl009	n. d.	0.05	0.16	44.79	21.30	0.11	17.37	0.28	0.19	12.06	3.62	99.92	0.464	0.001	0.003	1.454	0.075	0.278	0.003	0.713	0.006	0.004
Vranduk Fm.	BO92spl010	n. d.	0.41	0.20	33.44	29.02	0.21	14.52	0.20	0.14	15.19	7.33	100.65	0.667	0.009	0.004	1.147	0.160	0.369	0.005	0.629	0.005	0.003
Vranduk Fm.	BO92spl011	n. d.	0.08	0.20	38.16	26.83	0.16	15.49	0.21	0.21	13.77	4.26	99.37	0.608	0.002	0.004	1.289	0.092	0.330	0.004	0.661	0.005	0.004
Vranduk Fm.	BO92spl012	n. d.	0.16	0.16	41.48	25.24	0.14	17.26	0.24	0.12	11.81	3.05	99.65	0.557	0.003	0.003	1.366	0.064	0.276	0.003	0.718	0.005	0.002
Vranduk Fm.	BO92spl013	n. d.	0.18	0.35	15.72	52.98	0.27	10.64	0.05	0.16	18.40	2.03	100.79	1.336	0.004	0.007	0.591	0.049	0.491	0.007	0.506	0.001	0.004
Vranduk Fm.	BO92spl014	n. d.	0.25	0.18	37.31	22.06	0.21	13.79	0.26	0.21	16.66	9.92	100.85	0.502	0.005	0.003	1.265	0.215	0.401	0.005	0.591	0.006	0.004
Vranduk Fm.	BO92spl015	n. d.	0.11	0.14	42.37	23.19	0.12	17.08	0.26	0.15	12.03	3.89	99.34	0.512	0.002	0.003	1.396	0.082	0.281	0.003	0.711	0.006	0.003
Vranduk Fm.	BO92spl016	n. d.	0.35	0.28	29.72	33.03	0.19	12.94	0.18	0.18	16.89	6.45	100.22	0.780	0.008	0.006	1.047	0.145	0.422	0.005	0.576	0.004	0.004
Vranduk Fm.	BO92spl017	n. d.	0.26	0.19	31.93	36.20	0.13	17.00	0.24	0.07	11.02	3.08	100.13	0.827	0.006	0.004	1.087	0.067	0.266	0.003	0.732	0.006	0.001
Vranduk Fm.	BO92spl018	n. d.	0.05	0.18	45.97	20.27	0.14	17.59	0.25	0.20	11.80	3.09	99.54	0.440	0.001	0.003	1.487	0.064	0.271	0.003	0.719	0.006	0.004
Vranduk Fm.	BO92spl019	n. d.	0.35	0.30	31.87	34.30	0.20	14.62	0.16	0.15	14.76	3.49	100.19	0.794	0.008	0.006	1.101	0.077	0.362	0.005	0.638	0.004	0.003
Vranduk Fm.	BO92spl020	n. d.	0.07	0.24	20.00	45.28	0.27	10.49	0.09	0.24	19.38	4.78	100.55	1.129	0.002	0.005	0.744	0.113	0.511	0.007	0.479	0.002	0.005
Vranduk Fm.	BO92spl021	n. d.	0.10	0.19	26.25	40.94	0.19	13.47	0.09	0.16	15.39	3.40	100.17	0.977	0.002	0.004	0.934	0.077	0.388	0.005	0.606	0.002	0.004
Vranduk Fm.	BO92spl022	n. d.	0.08	0.17	40.51	26.78	0.14	16.80	0.22	0.16	12.32	2.55	99.73	0.595	0.002	0.003	1.341	0.054	0.289	0.003	0.703	0.005	0.003
Vranduk Fm.	BO92spl023	n. d.	0.15	0.12	33.01	33.32	0.21	13.70	0.15	0.19	16.04	3.38	100.26	0.773	0.003	0.002	1.141	0.075	0.393	0.005	0.599	0.003	0.004
Vranduk Fm.	BO92spl024	n. d.	0.10	0.14	44.71	22.31	0.13	17.78	0.28	0.19	11.40	2.71	99.75	0.489	0.002	0.004	1.449	0.056	0.262	0.003	0.729	0.006	0.004
Vranduk Fm.	BO92spl025	n. d.	0.05	0.20	36.36	30.06	0.17	15.24	0.18	0.21	13.94	3.17	99.59	0.685	0.001	0.004	1.236	0.069	0.336	0.004	0.655	0.004	0.004
Vranduk Fm.	BO92spl026	n. d.	0.07	0.17	41.32	24.88	0.13	16.62	0.22	0.22	12.58	3.28	99.49	0.552	0.002	0.003	1.368	0.069	0.295	0.003	0.696	0.005	0.005
Vranduk Fm.	BO92spl027	n. d.	0.05	0.14	48.84	16.82	0.12	17.95	0.32	0.18	11.52	3.21	99.14	0.362	0.001	0.002	1.566	0.066	0.262	0.003	0.727	0.007	0.004
Vranduk Fm.	BO92spl028	n. d.	0.89	0.37	27.01	30.39	0.31	9.61	0.22	0.29	17.97	9.69	100.88	0.555	0.004	0.003	1.249	0.180	0.428	0.005	0.561	0.006	0.007
Vranduk Fm.	BO92spl029	n. d.	0.20	0.18	36.21	24.01	0.21	12.86	0.25	0.30	21.50	8.15	99.88	0.685	0.004	0.003	1.077	0.224	0.565	0.008	0.441	0.005	0.007
Vranduk Fm.	BO92spl030	n. d.	0.43	0.37	26.15	37.75	0.22	11.39	0.14	0.24	18.79	4.64	100.11	0.914	0.010	0.008	0.944	0.107	0.481	0.006	0.520	0.003	0.005
Vranduk Fm.	BO92spl031	n. d.	0.07	0.43	21.32	46.75	0.24	11.02	0.06	0.24	18.51	1.82	100.46	1.152	0.002	0.009	0.783	0.042	0.337	0.006	0.512	0.002	0.006
Vranduk Fm.	BO92spl032	n. d.	0.19	0.20	37.70	27.66	0.19	15.44	0.20	0.20	14.10	4.28	100.15	0.624	0.004	0.004	1.268	0.092	0.483	0.005	0.657	0.004	0.004
Vranduk Fm.	BO92spl033	n. d.	0.96	0.21	23.47	37.76	0.27	10.43	0.15	0.22	19.95	6.09	99.51	0.935	0.023	0.004	0.867	0.144	0.523	0.007	0.487	0.004	0.005
Vranduk Fm.	BO92spl034	n. d.	0.07	0.17	41.82	25.07	0.12	17.14	0.22	0.16	11.93	2.81	99.52	0.554	0.002	0.003	1.377	0.059	0.279	0.003	0.714	0.005	0.003
Vranduk Fm.	BO92spl035	n. d.	0.36	0.27	30.44	36.26	0.21	14.22	0.13	0.24	15.21	3.29	100.62	0.844	0.008	0.005	1.056	0.073	0.374	0.005	0.624	0.003	0.005
Vranduk Fm.	BO92spl036	n. d.	0.19	0.17	21.66	45.42	0.20	12.82	0.11	0.13	15.82	3.94	100.45	1.106	0.004	0.004	0.787	0.091	0.407	0.005	0.589	0.003	0.003
Vranduk Fm.	BO92spl037	n. d.	0.64	0.16	36.44	27.55	0.23	14.77	0.20	0.18	15.33	4.84	100.34	0.626	0.014	0.003	1.235	0.105	0.369	0.006	0.633	0.005	0.004
Vranduk Fm.	BO92spl038	n. d.	0.08	0.14	44.85	22.03	0.11	17.72	0.26	0.14	11.61	2.90	99.85	0.478	0.002	0.003	1.453	0.060	0.267	0.003	0.726	0.006	0.003
Vranduk Fm.	BO92spl039	n. d.	0.10	0.22	30.65	35.25	0.22	13.08	0.11	0.21	16.59	3.69	100.12	0.829	0.002	0.004	1.075	0.083	0.413	0.005	0.580	0.003	0.005
Vranduk Fm.	BO92spl040	n. d.	0.20	0.17	38.26	25.31	0.18	14.43	0.24	0.25	15.62	5.41	100.07	0.574	0.004	0.003	1.294	0.117	0.375	0.004	0.617	0.005	0.005
Vranduk Fm.	BO92spl041	n. d.	0.33	0.24	30.67	34.46	0.21	13.42	0.12	0.18	16.18	3.91	99.72	0.811	0.007	0.005	1.077	0.088	0.403	0.005	0.595	0.003	0.004
Vranduk Fm.	BO92spl042	n. d.	0.15	0.15	47.14	18.83	0.13	17.21	0.23	0.20	12.44	2.39	98.91	0.603	0.003	0.003	1.529	0.049	0.286	0.003	0.706	0.006	0.004
Vranduk Fm.	BO92spl043	n. d.	0.02	0.40	16.91	51.38	0.30	9.17	0.07	0.03	20.39	1.13	100.01	1.310	0.001	0.009	0.643	0.027	0.550	0.008	0.441	0.001	0.007
Vranduk Fm.	BO92spl044	n. d.	0.55	0.22	34.33	29.40	0.20	14.89	0.20	0.16	14.83	5.57	100.37	0.673	0.012	0.004	1.172	0.121	0.359	0.005	0.643	0.005	0.003
Vranduk Fm.	BO92spl045	n. d.	0.05	0.17	45.84	19.04	0.13	17.12	0.30	0.20	12.37	4.10	99.32	0.415	0.001	0.003	1.491	0.085	0.285	0.003	0.704	0.007	0.004
Vranduk Fm.	BO92spl046	n. d.	0.48	0.18	37.76	27.56	0.18	16.17	0.21	0.12	13.16	3.81	99.64	0.621	0.010	0.003	1.269	0.082	0.314	0.004	0.687	0.005	0.003
Vranduk Fm.	BO92spl047	n. d.	0.50	0.19	37.32	27.44	0.20	16.30	0.20	0.15	12.80	4.35	99.46	0.620	0.011	0.004	1.258	0.094	0.306	0.005	0.694	0.005	0.003
Vranduk Fm.	BO92spl048	n. d.	0.10	0.15	35.21	28.70	0.16	13.97	0.19	0.20	15.73	5.36	99.81	0.662	0.002	0.003	1.210	0.118	0.384	0.005	0.607	0.004	0.004
Vranduk Fm.	BO92spl049	n. d.	0.07	0.15	44.29	20.78	0.16	16.88	0.30	0.21	12.47	4.07	99.38	0.456	0.001	0.003	1.450	0.085	0.290	0.004	0.699	0.007	0.004
Vranduk Fm.	BO92spl050	n. d.	0.07	0.15	42.90	22.16	0.12	17.13	0.27	0.17	11.87	4.15	98.98	0.490	0.001	0.003	1.414	0.087	0.277	0.003	0.714	0.006	0.003
Vranduk Fm.	BO92spl051	n. d.</																					

Formation	Sample & spot ID	analyses in wt%. Shown are the recalculated FeO and Fe <sub>2</sub> O <sub>3</sub> values and the amended total											cations per formula unit on the basis of 3 oxygens										
		SiO <sub>2</sub>	TiO <sub>2</sub>	V <sub>2</sub> O <sub>5</sub>	Al <sub>2</sub> O <sub>3</sub>	Cr <sub>2</sub> O <sub>3</sub>	MnO	MgO	NiO	ZnO	FeO	Fe <sub>2</sub> O <sub>3</sub>	Total	Cr	Ti	V	Al	Fe <sup>3+</sup>	Fe <sup>2+</sup>	Mn	Mg	Ni	Zn
Vranduk Fm.	BO92sp056	n. d.	0.07	0.19	35.07	31.34	14.90	0.14	0.25	14.03	2.67	95.83	0.723	0.001	0.004	1.207	0.059	0.342	0.004	0.648	0.003	0.005	
Vranduk Fm.	BO92sp057	n. d.	0.06	0.18	37.12	28.87	15.81	0.18	0.21	13.18	3.75	99.50	0.654	0.001	0.003	1.255	0.081	0.316	0.003	0.676	0.004	0.004	
Vranduk Fm.	BO92sp058	n. d.	0.22	0.21	19.39	42.13	7.21	0.06	0.46	23.31	6.17	99.58	1.084	0.005	0.005	0.744	0.151	0.635	0.011	0.350	0.002	0.011	
Vranduk Fm.	BO92sp059	n. d.	0.13	0.23	24.80	38.66	12.44	0.15	0.15	16.61	6.56	99.93	0.937	0.003	0.005	0.896	0.151	0.426	0.003	0.588	0.004	0.003	
Vranduk Fm.	BO92sp060	n. d.	0.10	0.14	34.56	31.44	16.65	0.21	0.20	14.61	3.70	99.78	0.723	0.002	0.003	1.186	0.081	0.355	0.004	0.635	0.005	0.004	
Vranduk Fm.	BO92sp061	n. d.	0.07	0.18	43.90	21.31	16.78	0.26	0.17	12.54	3.51	98.86	0.471	0.002	0.003	1.446	0.074	0.293	0.003	0.698	0.006	0.004	
Vranduk Fm.	BO92sp062	n. d.	0.15	0.14	31.00	34.74	18.13	0.14	0.25	15.01	3.86	99.46	0.816	0.003	0.003	1.084	0.086	0.373	0.004	0.619	0.003	0.006	
Vranduk Fm.	BO92sp063	n. d.	0.75	0.30	31.40	29.91	11.64	0.16	0.27	19.24	5.77	99.67	0.711	0.017	0.006	1.113	0.131	0.484	0.006	0.521	0.004	0.006	
Vranduk Fm.	BO92sp064	n. d.	0.13	0.13	39.25	27.95	15.73	0.15	0.30	13.43	1.64	98.87	0.631	0.003	0.002	1.322	0.035	0.321	0.004	0.670	0.003	0.006	
Vranduk Fm.	BO92sp065	n. d.	0.40	0.24	24.88	39.67	13.57	0.16	0.10	15.27	5.80	100.33	0.950	0.009	0.005	0.889	0.132	0.387	0.006	0.613	0.004	0.002	
Vranduk Fm.	BO92sp066	n. d.	0.10	0.14	26.77	38.38	12.84	0.12	0.23	15.89	4.27	98.96	0.927	0.002	0.003	0.964	0.098	0.406	0.006	0.585	0.003	0.005	
Vranduk Fm.	BO92sp067	n. d.	0.37	0.28	30.28	33.02	12.85	0.17	0.19	17.01	5.41	99.78	0.781	0.008	0.006	1.068	0.122	0.426	0.005	0.573	0.004	0.004	
Vranduk Fm.	BO92sp068	n. d.	0.07	0.29	33.70	32.56	14.00	0.11	0.19	15.58	2.98	99.67	0.755	0.001	0.006	1.165	0.066	0.382	0.005	0.612	0.003	0.004	
Vranduk Fm.	BO92sp069	n. d.	0.09	0.24	19.58	47.97	10.27	0.05	0.29	18.98	2.03	99.79	1.204	0.002	0.005	0.733	0.048	0.504	0.008	0.486	0.001	0.007	
Vranduk Fm.	BO92sp070	n. d.	0.07	0.20	42.24	23.79	16.90	0.22	0.20	12.18	3.21	99.18	0.527	0.001	0.004	1.395	0.068	0.285	0.004	0.705	0.005	0.004	
Vranduk Fm.	BO92sp071	n. d.	0.10	0.20	41.57	21.52	16.44	0.27	0.20	12.59	5.70	98.74	0.481	0.002	0.004	1.386	0.121	0.298	0.004	0.693	0.006	0.004	
Vranduk Fm.	BO92sp072	n. d.	0.28	0.14	26.76	40.33	13.75	0.13	0.19	14.84	2.67	99.29	0.965	0.006	0.003	0.955	0.061	0.376	0.005	0.620	0.003	0.004	
Vranduk Fm.	BO92sp073	n. d.	0.05	0.27	23.56	46.33	13.90	0.10	0.14	14.40	1.38	100.31	1.112	0.001	0.005	0.843	0.032	0.366	0.003	0.629	0.003	0.003	
Vranduk Fm.	BO92sp074	n. d.	0.25	0.18	19.32	36.82	9.28	0.14	0.30	20.53	13.60	100.78	0.928	0.006	0.004	0.726	0.326	0.547	0.010	0.441	0.004	0.007	
Vranduk Fm.	BO92sp075	n. d.	0.27	0.25	30.56	33.23	12.47	0.15	0.25	17.57	5.13	100.10	0.785	0.006	0.005	1.077	0.115	0.439	0.006	0.555	0.004	0.005	
Vranduk Fm.	BO92sp076	n. d.	0.25	0.19	33.32	25.29	12.63	0.26	0.23	17.32	9.68	99.39	0.595	0.006	0.004	1.169	0.217	0.431	0.006	0.560	0.006	0.005	
Vranduk Fm.	BO92sp077	n. d.	0.43	0.15	30.01	33.10	14.04	0.18	0.18	15.17	6.56	100.03	0.777	0.010	0.003	1.051	0.147	0.377	0.005	0.621	0.004	0.004	
Vranduk Fm.	BO92sp078	n. d.	0.34	0.30	41.48	25.11	17.20	0.27	0.25	11.66	1.75	98.50	0.559	0.007	0.006	1.377	0.037	0.275	0.003	0.722	0.006	0.005	
Vranduk Fm.	BO92sp079	n. d.	0.07	0.17	43.20	22.26	17.11	0.26	0.17	12.09	4.06	99.55	0.489	0.001	0.003	1.416	0.085	0.281	0.004	0.709	0.006	0.003	
Vranduk Fm.	BO92sp080	n. d.	0.33	0.33	29.92	33.45	13.37	0.14	0.17	15.96	5.22	99.11	0.794	0.007	0.006	1.059	0.118	0.401	0.005	0.598	0.003	0.004	
Vranduk Fm.	BO92sp081	n. d.	0.11	0.21	33.29	30.60	14.30	0.18	0.23	14.93	5.66	99.70	0.710	0.002	0.004	1.151	0.125	0.366	0.004	0.625	0.004	0.005	
Vranduk Fm.	BO92sp082	n. d.	0.06	0.06	11.89	56.07	6.49	0.03	0.21	23.87	1.19	100.53	1.482	0.002	0.008	0.469	0.030	0.667	0.010	0.323	0.001	0.005	
Vranduk Fm.	BO92sp083	n. d.	0.10	0.12	42.70	23.91	16.67	0.21	0.17	12.61	2.41	99.07	0.530	0.002	0.002	1.410	0.051	0.296	0.004	0.696	0.005	0.004	
Vranduk Fm.	BO92sp084	n. d.	0.12	0.36	22.15	44.97	10.70	0.08	0.31	18.77	1.90	99.61	1.115	0.003	0.007	1.039	0.045	0.492	0.007	0.500	0.002	0.007	
Vranduk Fm.	BO92sp085	n. d.	0.21	0.26	29.34	37.16	13.19	0.12	0.14	16.31	2.94	99.90	0.879	0.005	0.005	1.035	0.066	0.408	0.006	0.588	0.003	0.003	
Vranduk Fm.	BO92sp086	n. d.	0.07	0.20	37.13	29.61	17.17	0.20	0.17	11.30	3.39	99.24	0.668	0.002	0.004	1.248	0.073	0.269	0.004	0.723	0.005	0.003	
Vranduk Fm.	BO92sp087	n. d.	0.06	0.23	38.41	28.66	15.87	0.16	0.21	13.37	2.45	99.56	0.646	0.001	0.004	1.290	0.052	0.319	0.004	0.674	0.004	0.004	
Vranduk Fm.	BO92sp088	n. d.	0.42	0.19	36.24	27.77	14.95	0.20	0.21	14.64	4.73	99.52	0.635	0.009	0.004	1.236	0.103	0.354	0.004	0.644	0.005	0.005	
Vranduk Fm.	BO92sp089	n. d.	0.09	0.11	46.35	20.53	18.09	0.32	0.12	10.98	2.37	98.08	0.445	0.002	0.002	1.488	0.049	0.252	0.003	0.739	0.007	0.003	
Vranduk Fm.	BO92sp090	n. d.	0.27	0.20	33.49	29.76	13.45	0.17	0.20	16.43	5.66	99.86	0.692	0.006	0.004	1.162	0.125	0.404	0.006	0.590	0.004	0.004	
Vranduk Fm.	BO92sp091	n. d.	0.04	0.26	25.90	42.53	13.20	0.09	0.17	15.65	1.84	99.89	1.019	0.001	0.005	0.926	0.042	0.397	0.005	0.596	0.002	0.004	
Vranduk Fm.	BO92sp092	n. d.	0.07	0.35	14.69	54.71	11.43	0.07	0.14	16.86	1.97	100.58	1.381	0.002	0.007	0.553	0.047	0.450	0.008	0.544	0.002	0.003	
Vranduk Fm.	BO92sp093	n. d.	0.24	0.16	24.85	41.93	12.51	0.09	0.31	16.61	3.40	100.36	1.011	0.006	0.003	0.893	0.078	0.423	0.007	0.568	0.002	0.007	
Vranduk Fm.	BO92sp094	n. d.	0.22	0.19	24.75	41.96	12.42	0.11	0.29	16.64	3.17	99.97	1.016	0.005	0.004	0.893	0.073	0.426	0.006	0.567	0.003	0.007	
Vranduk Fm.	BO92sp095	n. d.	0.05	0.36	14.59	55.47	10.99	0.05	0.17	17.47	1.04	100.48	1.405	0.001	0.008	0.551	0.025	0.468	0.008	0.525	0.001	0.004	
Vranduk Fm.	BO92sp096	n. d.	0.15	0.30	18.76	49.52	10.52	0.08	0.23	18.77	1.74	100.36	1.238	0.004	0.006	0.700	0.041	0.497	0.008	0.496	0.002	0.005	
Vranduk Fm.	BO92sp097	n. d.	0.22	0.25	36.83	30.48	15.82	0.16	0.15	13.45	2.39	99.91	0.689	0.005	0.004	1.242	0.051	0.322	0.005	0.674	0.004	0.003	
Vranduk Fm.	BO92sp098	n. d.	0.26	0.25	34.30	32.21	10.49	0.15	0.22	15.25	2.72	99.96	0.741	0.006	0.005	1.177	0.060	0.371	0.005	0.624	0.004	0.005	
Vranduk Fm.	BO92sp099	n. d.	0.06	0.22	26.75	41.48	12.43	0.08	0.19	17.08	1.89	100.41	0.992	0.001	0.004	0.954	0.043	0.432	0.006	0.560	0.002	0.004	
Vranduk Fm.	BO92sp100	n. d.	0.41	0.18	9.69	55.14	7.00	0.05	0.15	22.83	4.27	100.65	1.475	0.011	0.004	0.387	0.109	0.646	0.009	0.353	0.001	0.004	
Vranduk Fm.	BO92sp101	n. d.	0.29	0.41	13.63	53.85	9.22	0.06	0.24	20.18	2.31	100.49	1.387	0.007	0.009	0.524	0.057	0.550	0.008	0.448	0.002	0.006	
Vranduk Fm.	BO92sp102	n. d.	0.09	0.26	30.19	37.12	14.31	0.12	0.19	14.69	2.89	100.04	0.868	0.002	0.005	1.053	0.064	0.363	0.005	0.631	0.003	0.004	
Vranduk Fm.	BO92sp103	n. d.	0.26	0.31	17.92	51.04	11.14	0.05	0.25	17.80	1.16	100.17	1.278	0.006	0.006	0.669	0.028	0.471	0.006	0.526	0.001	0.006	
Vranduk Fm.	BO92sp104	n. d.	0.16	0.30	25.28	42.24	12.31	0.08	0.24	17.03	2.19	100.05	1.019	0.004	0.006	0.910	0.045	0.360	0.006	0.560	0.002	0.005	
Vranduk Fm.	BO92sp105	n. d.	0.06	0.34	4.41	65.84	8.57	0.01	0.26	19.29	0.94	100.15	1.779	0.002	0.008	0.178	0.024	0.551	0.012	0.436	0.000	0.007	
Vranduk Fm.	BO92sp106	n. d.	3.77	0.66	14.77	35.09	3.67	0.24	0.43	31.36	9.75	100.30	0.939	0.096	0.015	0.589	0.248	0.888	0.016	0.185	0.006	0.011	
Vranduk Fm.	BO92sp107	n. d.	0.14	0.27	27.68	39.38	10.25	0.15	0.24	15.21	3.34	100.34	0.931	0.003	0.005	0.976	0.075	0.381	0.005	0.612	0.004	0.005	
Vranduk Fm.	BO92sp108	n. d.	0.11	0.39	16.49	49.90	10.25</																

analyses in wt%. Shown are the recalculated FeO and Fe<sub>2</sub>O<sub>3</sub> values and the amended total

Formation	Sample & spot ID	n.d.: not detected		Cations per formula unit on the basis of 3 oxygens																				
		SiO <sub>2</sub>	TiO <sub>2</sub>	V <sub>2</sub> O <sub>5</sub>	Al <sub>2</sub> O <sub>3</sub>	Cr <sub>2</sub> O <sub>3</sub>	MnO	MgO	NiO	ZnO	FeO	Fe <sub>2</sub> O <sub>3</sub>	Total	Cr	Ti	V	Al	Fe <sup>3+</sup>	Fe <sup>2+</sup>	Mn	Mg	Ni	Zn	
Vranduk Fm.	BO95sp021	n. d.	0.05	0.14	45.77	20.91	17.71	0.13	0.28	0.15	11.65	2.92	99.70	0.453	0.001	0.003	1.479	0.060	0.267	0.003	0.724	0.006	0.003	0.003
Vranduk Fm.	BO95sp022	n. d.	0.04	0.32	19.07	50.69	11.49	0.26	0.04	0.18	17.30	0.73	100.13	1.260	0.001	0.007	0.707	0.017	0.455	0.007	0.538	0.001	0.004	0.004
Vranduk Fm.	BO95sp023	n. d.	0.20	0.29	18.91	48.83	11.74	0.24	0.06	0.17	17.00	2.67	100.12	1.214	0.005	0.006	0.701	0.063	0.447	0.006	0.590	0.002	0.004	0.004
Vranduk Fm.	BO95sp024	n. d.	0.10	0.17	48.35	17.54	17.84	0.13	0.29	0.24	11.77	3.08	99.51	0.374	0.002	0.003	1.549	0.063	0.268	0.003	0.723	0.006	0.005	0.005
Vranduk Fm.	BO95sp025	n. d.	0.02	0.48	17.31	50.51	10.67	0.29	0.05	0.23	18.21	2.23	100.00	1.273	0.000	0.010	0.651	0.063	0.486	0.008	0.507	0.001	0.005	0.005
Vranduk Fm.	BO95sp026	n. d.	0.27	0.21	23.21	36.75	10.63	0.38	0.17	0.28	19.04	9.51	100.45	0.904	0.006	0.004	0.852	0.223	0.496	0.010	0.493	0.004	0.006	0.006
Vranduk Fm.	BO95sp027	n. d.	0.28	0.21	30.37	33.09	12.39	0.25	0.16	0.29	17.68	5.73	100.45	0.974	0.006	0.004	0.862	0.129	0.442	0.006	0.551	0.004	0.006	0.006
Vranduk Fm.	BO95sp028	n. d.	0.25	0.22	32.20	35.90	15.03	0.15	0.13	0.18	14.00	1.79	99.86	0.830	0.005	0.004	1.110	0.039	0.343	0.004	0.655	0.003	0.004	0.004
Vranduk Fm.	BO95sp029	n. d.	0.03	0.14	44.26	22.79	17.26	0.15	0.23	0.24	11.97	2.45	99.51	0.949	0.001	0.002	1.444	0.051	0.277	0.003	0.712	0.005	0.005	0.005
Vranduk Fm.	BO95sp030	n. d.	0.47	0.19	34.32	31.20	17.07	0.15	0.18	0.06	11.48	4.97	100.11	0.706	0.010	0.004	1.159	0.107	0.275	0.004	0.729	0.004	0.001	0.001
Vranduk Fm.	BO95sp031	n. d.	0.09	0.26	7.19	59.23	7.92	0.38	0.06	0.17	20.75	4.16	100.21	1.589	0.002	0.006	0.288	0.106	0.589	0.011	0.401	0.002	0.004	0.004
Vranduk Fm.	BO95sp032	n. d.	0.14	0.34	22.82	45.87	12.65	0.24	0.09	0.19	16.34	1.96	100.63	1.110	0.003	0.007	0.824	0.045	0.418	0.006	0.577	0.002	0.004	0.004
Vranduk Fm.	BO95sp033	n. d.	0.21	0.24	45.76	19.20	17.63	0.15	0.30	0.15	11.86	4.03	99.53	0.417	0.004	0.004	1.482	0.083	0.273	0.003	0.722	0.007	0.003	0.003
Vranduk Fm.	BO95sp034	n. d.	0.14	0.36	16.83	51.71	11.06	0.21	0.05	0.18	17.66	1.66	99.86	1.304	0.003	0.008	0.633	0.040	0.471	0.006	0.526	0.001	0.004	0.004
Vranduk Fm.	BO95sp035	n. d.	0.06	0.24	31.75	37.24	14.88	0.16	0.12	0.26	13.99	1.31	100.01	0.862	0.001	0.005	1.096	0.029	0.343	0.004	0.649	0.003	0.006	0.006
Vranduk Fm.	BO95sp036	n. d.	0.12	0.35	23.82	44.51	12.66	0.23	0.08	0.15	16.19	1.50	99.61	1.082	0.003	0.007	0.863	0.035	0.416	0.006	0.580	0.002	0.003	0.003
Vranduk Fm.	BO95sp037	n. d.	0.14	0.13	35.85	29.38	16.46	0.15	0.22	0.16	12.09	5.23	99.81	0.665	0.003	0.002	1.211	0.113	0.290	0.004	0.703	0.005	0.003	0.003
Vranduk Fm.	BO95sp038	n. d.	0.02	0.18	41.08	24.48	16.73	0.22	0.21	0.21	12.25	4.00	99.33	0.645	0.001	0.003	1.363	0.085	0.288	0.004	0.702	0.005	0.004	0.004
Vranduk Fm.	BO95sp039	n. d.	0.07	0.35	15.81	52.73	11.30	0.23	0.07	0.11	17.19	2.32	100.18	1.330	0.002	0.007	0.595	0.056	0.459	0.006	0.537	0.002	0.003	0.003
Vranduk Fm.	BO95sp040	n. d.	0.04	0.36	16.99	52.82	11.88	0.23	0.06	0.16	16.41	1.08	100.02	1.322	0.001	0.008	0.634	0.026	0.434	0.006	0.561	0.001	0.004	0.004
Vranduk Fm.	BO95sp041	n. d.	0.06	0.33	19.92	49.80	12.82	0.23	0.08	0.12	15.43	1.27	100.07	1.223	0.001	0.007	0.730	0.030	0.401	0.006	0.594	0.001	0.004	0.004
Vranduk Fm.	BO95sp042	n. d.	0.06	0.30	18.79	50.31	11.92	0.23	0.17	0.20	16.59	1.69	100.15	1.249	0.001	0.006	0.695	0.040	0.435	0.006	0.568	0.002	0.005	0.005
Vranduk Fm.	BO95sp043	n. d.	0.31	0.35	29.04	30.72	11.55	0.28	0.18	0.27	18.61	8.55	99.85	0.737	0.007	0.007	1.039	0.195	0.472	0.007	0.522	0.004	0.006	0.006
Vranduk Fm.	BO95sp044	n. d.	0.04	0.26	33.70	33.60	14.66	0.20	0.15	0.23	14.42	2.27	99.53	0.776	0.001	0.005	1.161	0.050	0.352	0.005	0.639	0.004	0.005	0.005
Vranduk Fm.	BO95sp045	n. d.	0.04	0.29	25.91	42.67	13.28	0.19	0.12	0.17	15.47	1.55	99.72	1.023	0.001	0.006	0.927	0.035	0.393	0.005	0.600	0.003	0.004	0.004
Vranduk Fm.	BO95sp046	n. d.	0.03	0.31	16.75	52.06	11.43	0.20	0.09	0.17	17.00	2.05	100.11	1.308	0.001	0.007	0.628	0.049	0.452	0.006	0.541	0.002	0.004	0.004
Vranduk Fm.	BO95sp047	n. d.	0.17	0.18	17.62	52.04	11.85	0.25	0.05	0.16	16.70	1.53	100.54	1.294	0.004	0.004	0.654	0.036	0.439	0.007	0.556	0.001	0.004	0.004
Vranduk Fm.	BO95sp048	n. d.	0.21	0.43	10.14	58.23	8.59	0.32	0.20	0.20	20.61	1.80	100.56	1.528	0.005	0.009	0.397	0.046	0.572	0.009	0.607	0.001	0.005	0.005
Vranduk Fm.	BO95sp049	n. d.	0.06	0.31	28.56	39.47	13.18	0.20	0.10	0.24	16.20	1.95	100.27	0.933	0.001	0.006	1.007	0.044	0.405	0.005	0.588	0.002	0.005	0.005
Vranduk Fm.	BO95sp050	n. d.	0.04	0.37	18.69	49.30	10.63	0.26	0.05	0.24	18.60	2.27	100.45	1.232	0.001	0.008	0.686	0.054	0.482	0.007	0.501	0.001	0.005	0.005
Vranduk Fm.	BO95sp051	n. d.	0.07	0.33	13.87	55.38	10.30	0.29	0.10	0.16	18.32	1.37	100.13	1.418	0.002	0.001	0.530	0.033	0.496	0.008	0.497	0.001	0.004	0.004
Vranduk Fm.	BO95sp052	n. d.	0.12	0.27	21.57	46.77	11.59	0.28	0.09	0.20	17.63	2.10	100.62	1.146	0.003	0.005	0.788	0.049	0.457	0.007	0.535	0.002	0.005	0.005
Vranduk Fm.	BO95sp053	n. d.	0.07	0.32	16.61	52.61	11.22	0.25	0.06	0.21	17.33	1.48	100.15	1.324	0.002	0.007	0.623	0.035	0.461	0.007	0.532	0.001	0.005	0.005
Vranduk Fm.	BO95sp054	n. d.	0.01	0.26	28.63	38.91	12.16	0.23	0.07	0.35	17.49	1.84	99.95	0.928	0.000	0.005	1.019	0.042	0.441	0.006	0.547	0.002	0.008	0.008
Vranduk Fm.	BO95sp055	n. d.	0.03	0.18	43.29	24.74	16.54	0.15	0.21	0.19	13.20	1.55	100.07	0.543	0.001	0.003	1.417	0.032	0.306	0.004	0.684	0.005	0.004	0.004
Vranduk Fm.	BO95sp056	n. d.	0.52	0.18	35.04	30.24	16.47	0.18	0.19	0.13	12.44	4.65	100.03	0.686	0.011	0.003	1.185	0.100	0.298	0.004	0.704	0.004	0.003	0.003
Vranduk Fm.	BO95sp057	n. d.	0.03	0.18	43.77	23.44	17.11	0.12	0.21	0.17	12.21	2.07	99.32	0.515	0.001	0.003	1.433	0.043	0.284	0.003	0.708	0.005	0.003	0.003
Vranduk Fm.	BO95sp058	n. d.	0.99	0.26	23.63	36.67	11.43	0.32	0.18	0.26	18.77	8.28	100.79	0.893	0.023	0.005	0.858	0.192	0.483	0.008	0.525	0.004	0.006	0.006
Vranduk Fm.	BO95sp059	n. d.	0.17	0.23	30.99	36.73	14.57	0.19	0.08	0.20	14.55	2.58	100.33	0.853	0.004	0.005	1.073	0.057	0.357	0.005	0.638	0.003	0.004	0.004
Vranduk Fm.	BO95sp062	n. d.	0.07	0.24	21.08	49.14	14.29	0.22	0.14	0.14	13.50	1.86	100.63	1.185	0.002	0.005	0.758	0.043	0.344	0.006	0.650	0.002	0.003	0.003
Vranduk Fm.	BO95sp064	n. d.	0.12	0.27	24.40	44.09	14.04	0.19	0.13	0.12	14.37	2.64	100.37	1.054	0.003	0.005	0.869	0.060	0.363	0.005	0.632	0.003	0.003	0.003
Vranduk Fm.	BO95sp066	n. d.	0.19	0.13	16.76	52.99	14.74	0.17	0.13	0.05	12.19	3.17	100.52	1.299	0.004	0.002	0.613	0.074	0.316	0.005	0.681	0.003	0.001	0.001
Vranduk Fm.	BO95sp065	n. d.	0.08	0.35	9.17	61.77	11.36	0.25	0.11	0.11	16.16	1.16	100.45	1.598	0.002	0.007	0.354	0.029	0.429	0.004	0.554	0.001	0.003	0.003
Vranduk Fm.	BO95sp067	n. d.	0.06	0.26	20.05	49.97	13.15	0.24	0.08	0.14	14.99	1.45	100.39	1.221	0.001	0.005	0.731	0.034	0.388	0.006	0.606	0.002	0.003	0.003
Vranduk Fm.	BO95sp068	n. d.	0.04	0.37	10.97	57.73	7.73	0.32	0.06	0.15	18.99	3.08	100.55	1.505	0.001	0.008	0.399	0.077	0.524	0.009	0.468	0.002	0.004	0.004
Vranduk Fm.	BO95sp069	n. d.	0.06	0.20	33.98	33.48	15.62	0.15	0.14	0.16	13.17	2.87	99.84	0.767	0.001	0.004	1.160	0.063	0.319	0.004	0.674	0.003	0.003	0.003
Vranduk Fm.	BO95sp070	n. d.	0.04	0.47	13.80	54.55	10.70	0.26	0.06	0.18	17.75	2.37	100.19	1.393	0.001	0.010	0.526	0.058	0.480	0.007	0.515	0.001	0.004	0.004
Vranduk Fm.	BO95sp071	n. d.	0.63	0.20	31.96	32.18	15.24	0.23	0.20	0.15	13.91	5.53	100.24	0.743	0.014	0.004	1.100	0.122	0.340	0.006	0.663	0.005	0.005	0.005
Vranduk Fm.	BO95sp0																							

Analyses in wt%. Shown are the recalculated FeO and Fe<sub>2</sub>O<sub>3</sub> values and the amended total

Formation	Sample & spot ID	Analyses in wt%. Shown are the recalculated FeO and Fe <sub>2</sub> O <sub>3</sub> values and the amended total																	Cations per formula unit on the basis of 3 oxygens										
		SiO <sub>2</sub>	TiO <sub>2</sub>	V <sub>2</sub> O <sub>5</sub>	Al <sub>2</sub> O <sub>3</sub>	Cr <sub>2</sub> O <sub>3</sub>	MnO	MgO	NiO	ZnO	FeO	Fe <sub>2</sub> O <sub>3</sub>	Total	Cr	Ti	V	Al	Fe <sup>3+</sup>	Fe <sup>2+</sup>	Mn	Mg	Ni	Zn						
Vranduk Fm.	BO95sp0076	n. d.	0.12	0.23	26.70	43.02	0.17	14.36	0.08	0.14	14.07	0.75	99.63	1.022	0.003	0.005	0.946	0.017	0.354	0.004	0.643	0.002	0.003						
Vranduk Fm.	BO95sp0077	n. d.	0.06	0.34	16.33	53.24	0.25	12.07	0.06	0.14	16.19	1.98	100.66	1.328	0.001	0.007	0.607	0.047	0.427	0.007	0.567	0.002	0.003						
Vranduk Fm.	BO95sp0078	n. d.	0.03	0.30	26.35	42.00	0.21	12.89	0.07	0.16	16.09	1.31	99.42	1.010	0.001	0.006	0.945	0.030	0.409	0.005	0.585	0.002	0.004						
Vranduk Fm.	BO95sp0079	n. d.	0.22	0.24	28.66	38.08	0.25	12.75	0.09	0.25	16.79	2.52	99.82	0.906	0.005	0.005	1.017	0.057	0.423	0.006	0.572	0.002	0.005						
Vranduk Fm.	BO95sp0080	n. d.	0.06	0.29	13.94	57.06	0.25	12.69	0.08	0.14	14.83	1.30	100.64	1.432	0.002	0.006	0.522	0.031	0.394	0.007	0.600	0.002	0.003						
Vranduk Fm.	BO95sp0081	0.08	0.05	0.27	23.45	43.90	0.24	12.25	0.07	0.23	16.58	2.65	99.78	1.071	0.001	0.005	0.853	0.062	0.428	0.006	0.563	0.002	0.005						
Vranduk Fm.	BO95sp0082	n. d.	0.06	0.39	16.96	51.54	0.24	11.12	0.07	0.19	17.67	2.27	100.52	1.292	0.001	0.008	0.634	0.054	0.469	0.007	0.525	0.002	0.005						
Vranduk Fm.	BO95sp0083	n. d.	0.02	0.41	18.00	50.99	0.26	11.46	0.07	0.20	17.86	1.54	100.43	1.274	0.001	0.008	0.670	0.037	0.472	0.007	0.521	0.002	0.005						
Vranduk Fm.	BO95sp0084	n. d.	0.10	0.31	18.32	50.77	0.30	11.45	0.06	0.20	17.32	1.67	100.50	1.263	0.002	0.006	0.679	0.040	0.456	0.008	0.537	0.002	0.005						
Vranduk Fm.	BO95sp0085	n. d.	1.11	0.44	28.55	32.40	0.20	12.59	0.22	0.19	17.91	6.44	100.06	0.771	0.025	0.009	1.014	0.146	0.451	0.005	0.565	0.005	0.004						
Vranduk Fm.	BO95sp0086	n. d.	0.07	0.20	30.75	34.63	0.18	14.50	0.18	0.17	14.42	5.16	100.26	0.806	0.002	0.004	1.068	0.114	0.355	0.004	0.637	0.004	0.004						
Vranduk Fm.	BO95sp0087	n. d.	0.22	0.26	32.55	34.64	0.17	14.36	0.12	0.17	15.23	2.66	100.39	0.800	0.005	0.005	1.121	0.059	0.372	0.004	0.625	0.003	0.004						
Vranduk Fm.	BO95sp0088	n. d.	0.87	0.23	23.69	31.27	0.64	5.20	0.12	0.22	27.86	10.50	100.61	0.795	0.021	0.005	0.898	0.254	0.749	0.017	0.249	0.003	0.005						
Vranduk Fm.	BO95sp0089	n. d.	0.23	0.26	32.87	33.41	0.18	14.79	0.14	0.21	14.33	3.21	99.62	0.774	0.005	0.005	1.135	0.071	0.351	0.004	0.646	0.003	0.004						
Vranduk Fm.	BO95sp0090	n. d.	0.14	0.31	19.32	49.88	0.24	12.06	0.10	0.21	16.61	1.67	100.54	1.230	0.003	0.006	1.111	0.039	0.433	0.006	0.561	0.003	0.005						
Vranduk Fm.	TD147sp0001	n. d.	0.12	0.34	20.96	43.91	0.26	10.96	0.09	0.27	18.26	4.82	99.99	1.090	0.003	0.007	0.776	0.114	0.479	0.007	0.513	0.002	0.006						
Vranduk Fm.	TD147sp0002	n. d.	0.05	0.26	26.62	40.62	0.24	13.47	0.10	0.15	15.23	2.85	99.58	0.972	0.001	0.005	0.950	0.065	0.385	0.006	0.608	0.002	0.003						
Vranduk Fm.	TD147sp0003	n. d.	0.06	0.16	38.98	28.16	0.13	17.10	0.17	0.20	11.55	3.04	99.54	0.629	0.001	0.003	1.298	0.065	0.273	0.003	0.720	0.004	0.004						
Vranduk Fm.	TD147sp0004	n. d.	0.09	0.32	22.52	45.34	0.22	12.42	0.08	0.19	16.50	2.63	100.31	1.104	0.002	0.006	0.817	0.061	0.425	0.006	0.570	0.002	0.004						
Vranduk Fm.	TD147sp0005	n. d.	0.06	0.26	30.67	35.55	0.23	13.17	0.13	0.24	16.32	3.31	99.94	0.836	0.001	0.005	1.076	0.074	0.406	0.006	0.584	0.003	0.005						
Vranduk Fm.	TD147sp0009	n. d.	0.09	0.34	17.43	48.87	0.27	10.63	0.09	0.28	18.14	3.71	99.85	1.235	0.002	0.007	0.657	0.089	0.485	0.007	0.506	0.002	0.007						
Vranduk Fm.	TD147sp0024	n. d.	0.04	0.20	31.49	36.45	0.18	15.77	0.15	0.16	12.51	2.89	99.84	0.842	0.001	0.004	1.085	0.063	0.306	0.004	0.687	0.003	0.003						
Vranduk Fm.	TD147sp0006	n. d.	0.16	0.21	24.34	43.89	0.14	15.99	0.14	0.06	11.54	4.19	100.67	1.034	0.004	0.004	0.855	0.094	0.288	0.004	0.710	0.003	0.001						
Vranduk Fm.	TD147sp0007	n. d.	0.06	0.26	28.75	37.85	0.30	11.74	0.08	0.23	18.50	3.05	100.81	0.899	0.001	0.005	1.018	0.069	0.465	0.008	0.526	0.002	0.005						
Vranduk Fm.	TD147sp0010	n. d.	0.12	0.22	19.95	40.87	0.32	10.86	0.12	0.24	18.28	9.74	100.71	1.015	0.003	0.005	0.739	0.230	0.480	0.008	0.509	0.003	0.005						
Vranduk Fm.	TD147sp0011	n. d.	0.06	0.30	26.90	39.84	0.23	13.64	0.12	0.20	15.36	4.19	100.83	0.942	0.001	0.006	0.949	0.094	0.384	0.006	0.608	0.003	0.004						
Vranduk Fm.	TD147sp0011	n. d.	0.06	0.26	30.30	36.60	0.17	14.25	0.11	0.17	14.90	3.55	100.38	0.854	0.001	0.005	1.054	0.079	0.368	0.004	0.627	0.003	0.004						
Vranduk Fm.	TD147sp0012	n. d.	0.06	0.29	24.81	40.24	0.24	12.67	0.14	0.16	16.39	5.53	100.53	0.968	0.001	0.006	0.890	0.127	0.417	0.005	0.575	0.003	0.004						
Vranduk Fm.	TD147sp0013	n. d.	0.06	0.27	31.41	36.58	0.19	14.43	0.12	0.15	14.97	2.75	100.93	0.845	0.001	0.006	1.082	0.060	0.366	0.006	0.628	0.003	0.004						
Vranduk Fm.	TD147sp0014	n. d.	0.05	0.34	25.84	42.11	0.24	12.98	0.07	0.17	16.29	2.71	100.80	1.004	0.001	0.007	0.918	0.062	0.411	0.006	0.583	0.002	0.004						
Vranduk Fm.	TD147sp0015	n. d.	0.07	0.25	27.73	38.90	0.23	13.00	0.10	0.25	16.43	3.87	100.83	0.921	0.002	0.005	0.979	0.082	0.411	0.006	0.580	0.002	0.006						
Vranduk Fm.	TD147sp0016	n. d.	0.06	0.22	30.55	37.54	0.16	15.09	0.13	0.16	13.65	2.82	100.37	0.870	0.001	0.004	1.056	0.062	0.335	0.004	0.659	0.003	0.004						
Vranduk Fm.	TD147sp0017	n. d.	0.15	0.16	32.48	36.31	0.10	18.14	0.21	0.08	9.50	3.66	100.79	0.818	0.003	0.003	1.091	0.079	0.226	0.002	0.770	0.005	0.002						
Vranduk Fm.	TD147sp0018	n. d.	0.09	0.19	35.57	30.96	0.17	15.74	0.16	0.18	13.29	3.78	100.14	0.703	0.002	0.004	1.204	0.082	0.319	0.004	0.673	0.004	0.004						
Vranduk Fm.	TD147sp0019	n. d.	0.14	0.14	35.52	28.49	0.19	15.64	0.20	0.19	13.45	6.50	100.48	0.646	0.003	0.003	1.202	0.140	0.323	0.005	0.669	0.005	0.004						
Vranduk Fm.	TD147sp0020	n. d.	0.07	0.22	35.29	32.20	0.19	15.65	0.14	0.18	13.38	2.75	100.06	0.732	0.002	0.004	1.197	0.059	0.322	0.005	0.671	0.003	0.004						
Vranduk Fm.	TD147sp0021	n. d.	0.05	0.26	36.12	32.00	0.17	15.63	0.10	0.23	13.76	2.33	100.66	0.722	0.001	0.005	1.215	0.050	0.328	0.004	0.665	0.002	0.005						
Vranduk Fm.	TD147sp0022	n. d.	3.14	0.59	13.68	35.94	0.44	5.50	0.18	0.29	28.14	12.73	100.65	0.952	0.079	0.013	0.540	0.321	0.789	0.013	0.275	0.005	0.007						
Vranduk Fm.	TD147sp0023	n. d.	0.10	0.23	31.18	36.01	0.18	14.47	0.11	0.20	14.80	3.47	100.75	0.833	0.002	0.004	1.076	0.076	0.362	0.004	0.632	0.003	0.004						
Vranduk Fm.	TD147sp0025	n. d.	0.03	0.33	30.24	37.06	0.22	14.39	0.08	0.17	14.64	3.08	100.25	0.864	0.001	0.006	1.052	0.068	0.361	0.005	0.633	0.002	0.004						
Vranduk Fm.	TD147sp0026	n. d.	0.06	0.25	30.02	38.15	0.19	14.99	0.14	0.19	13.77	2.94	100.70	0.884	0.001	0.005	1.038	0.065	0.338	0.005	0.655	0.003	0.004						
Vranduk Fm.	TD147sp0027	n. d.	0.50	0.36	24.91	41.65	0.26	12.38	0.12	0.20	17.45	3.14	100.98	0.999	0.011	0.007	0.891	0.072	0.443	0.007	0.560	0.003	0.004						
Vranduk Fm.	TD147sp0029	n. d.	0.06	0.17	35.47	31.58	0.15	14.53	0.14	0.26	15.03	2.60	99.99	0.723	0.001	0.003	1.211	0.057	0.364	0.004	0.627	0.003	0.006						
Vranduk Fm.	TD147sp0030	n. d.	0.20	0.24	30.64	34.97	0.19	14.24	0.16	0.24	15.04	4.81	100.73	0.813	0.004	0.005	1.062	0.107	0.370	0.005	0.624	0.004	0.005						
Vranduk Fm.	TD147sp0031	n. d.	0.05	0.27	7.76	60.66	0.41	7.97	0.03	0.22	20.95	2.67	100.99	1.610	0.001	0.006	0.307	0.067	0.588	0.012	0.399	0.001	0.006						
Vranduk Fm.	TD147sp0032	n. d.	0.90	0.34	18.51	41.19	0.37	9.40	0.12	0.17	21.12	8.67	100.79	1.038	0.022	0.007	0.696	0.208	0.563	0.010	0.447	0.003	0.004						
Vranduk Fm.	TD147sp0033	n. d.	0.10	0.30	25.16	40.82	0.27	12.89	0.10	0.19	16.29	4.85	100.97	0.976	0.002	0.006	0.897	0.110	0.412	0.007	0.581	0.003	0.004						
Vranduk Fm.	TD147sp0034	n. d.	0.05	0.29	22.11	46.15	0.24	12.59	0.08	0.17	16.29	2.89	100.87	1.119	0.001	0.006	0.799	0.067	0.418	0.006	0.576	0.002	0.004						
Vranduk Fm.	TD147sp0036	n. d.	0.07	0.21	35.49	32.22	0.18	15.85	0.17	0.13	13.34	3.11	100.75	0.727	0.001	0.004	1.195	0.067	0.319	0.004	0.674	0.004	0.003						
Vranduk Fm.	TD147sp0038	n. d.	0.20	0.25	30.29	34.58	0.20	14.00	0.14	0.22	14.89	4.40	99.16	0.8															

analyses in wt%. Shown are the recalculated FeO and Fe<sub>2</sub>O<sub>3</sub> values and the amended total  
n.d.: not detected

Formation	Sample & spot ID	Cations per formula unit on the basis of 3 oxygens																						
		SiO <sub>2</sub>	TiO <sub>2</sub>	V <sub>2</sub> O <sub>5</sub>	Al <sub>2</sub> O <sub>3</sub>	Cr <sub>2</sub> O <sub>3</sub>	MnO	MgO	NiO	ZnO	FeO	Fe <sub>2</sub> O <sub>3</sub>	Total	Cr	Ti	V	Al	Fe <sup>3+</sup>	Fe <sup>2+</sup>	Mn	Mg	Ni	Zn	
Vranduk Fm.	TD147sp046	n. d.	0.07	0.23	33.22	33.57	0.17	15.05	0.16	0.18	13.73	2.93	99.32	0.777	0.001	0.005	1.146	0.065	0.336	0.004	0.656	0.004	0.004	0.004
Vranduk Fm.	TD147sp047	n. d.	0.10	0.22	37.01	28.41	0.18	15.19	0.18	0.27	14.00	3.69	99.25	0.648	0.002	0.004	1.259	0.080	0.338	0.005	0.653	0.004	0.006	0.006
Vranduk Fm.	TD147sp048	n. d.	0.13	0.31	22.23	44.17	0.28	12.76	0.09	0.22	16.50	3.91	100.13	1.079	0.003	0.006	0.810	0.091	0.427	0.007	0.566	0.002	0.005	0.005
Vranduk Fm.	TD147sp049	n. d.	0.09	0.25	25.88	41.51	0.23	13.29	0.11	0.17	14.68	2.92	99.61	0.994	0.002	0.005	0.924	0.067	0.372	0.006	0.621	0.003	0.004	0.004
Vranduk Fm.	TD147sp050	n. d.	0.07	0.28	25.81	41.03	0.18	13.86	0.11	0.15	14.58	3.57	99.63	0.982	0.002	0.006	0.921	0.081	0.369	0.005	0.626	0.003	0.003	0.003
Vranduk Fm.	TD147sp051	n. d.	0.38	0.28	23.56	42.75	0.21	13.80	0.13	0.12	14.62	3.91	99.77	1.032	0.009	0.006	0.848	0.074	0.373	0.005	0.628	0.003	0.003	0.003
Vranduk Fm.	TD147sp052	0.10	0.44	0.26	26.64	39.20	0.30	13.61	0.11	0.21	15.07	3.22	99.16	0.941	0.010	0.005	0.958	0.090	0.383	0.008	0.616	0.003	0.005	0.005
Vranduk Fm.	TD147sp053	n. d.	0.09	0.29	24.28	41.84	0.21	12.21	0.08	0.19	16.84	3.58	99.61	1.019	0.002	0.006	0.882	0.063	0.434	0.006	0.560	0.002	0.004	0.004
Vranduk Fm.	TD147sp054	n. d.	0.09	0.24	34.13	32.29	0.19	14.56	0.12	0.23	14.62	2.79	99.25	0.747	0.002	0.005	1.178	0.062	0.358	0.005	0.635	0.003	0.005	0.005
Vranduk Fm.	TD147sp056	n. d.	0.13	0.28	8.76	56.03	0.38	8.21	0.06	0.18	20.47	5.40	99.90	1.495	0.003	0.006	0.348	0.137	0.578	0.011	0.413	0.002	0.004	0.004
Vranduk Fm.	TD147sp057	n. d.	0.03	0.23	32.30	34.74	0.20	14.00	0.11	0.20	15.22	2.42	99.45	0.811	0.001	0.004	1.124	0.054	0.376	0.005	0.616	0.003	0.004	0.004
Vranduk Fm.	TD147sp058	n. d.	0.06	0.35	19.38	48.27	0.25	11.01	0.07	0.23	17.98	2.36	99.96	1.204	0.001	0.007	0.721	0.056	0.475	0.007	0.518	0.002	0.005	0.005
Vranduk Fm.	TD147sp060	n. d.	0.06	0.20	36.23	30.40	0.16	15.80	0.16	0.16	13.16	3.30	99.64	0.691	0.001	0.004	1.227	0.071	0.316	0.004	0.677	0.004	0.003	0.003
Vranduk Fm.	TD147sp061	n. d.	0.08	0.15	23.33	45.32	0.23	12.53	0.06	0.19	16.28	1.91	100.07	1.101	0.002	0.003	0.845	0.044	0.418	0.006	0.574	0.001	0.004	0.004
Vranduk Fm.	TD147sp062	n. d.	0.07	0.19	36.42	30.49	0.15	15.89	0.15	0.17	12.94	2.75	99.22	0.694	0.001	0.004	1.236	0.060	0.312	0.004	0.682	0.003	0.004	0.004
Vranduk Fm.	TD147sp063	n. d.	0.06	0.30	23.59	43.60	0.21	13.15	0.09	0.14	15.43	3.38	99.95	1.055	0.001	0.006	0.851	0.078	0.395	0.005	0.600	0.002	0.003	0.003
Vranduk Fm.	TD147sp064	n. d.	0.10	0.27	24.39	42.21	0.18	12.79	0.08	0.18	16.17	3.76	100.12	1.019	0.002	0.005	0.878	0.086	0.413	0.005	0.582	0.002	0.004	0.004
Vranduk Fm.	TD147sp065	n. d.	0.04	0.24	31.95	35.69	0.18	14.95	0.12	0.18	13.84	2.56	99.73	0.828	0.001	0.004	1.105	0.057	0.339	0.004	0.653	0.003	0.004	0.004
Vranduk Fm.	TD147sp066	n. d.	0.04	0.24	36.95	30.00	0.17	15.25	0.14	0.29	14.02	2.51	99.61	0.682	0.001	0.005	1.252	0.054	0.337	0.004	0.653	0.003	0.006	0.006
Vranduk Fm.	TD147sp067	n. d.	0.06	0.19	29.63	37.85	0.18	14.45	0.11	0.19	14.17	2.73	99.57	0.890	0.001	0.004	1.039	0.061	0.352	0.005	0.640	0.003	0.004	0.004
Vranduk Fm.	TD147sp068	n. d.	0.10	0.30	23.15	42.88	0.22	12.02	0.08	0.20	17.13	4.09	100.18	1.045	0.002	0.006	0.842	0.095	0.442	0.006	0.552	0.002	0.005	0.005
Vranduk Fm.	TD147sp069	n. d.	0.07	0.27	26.45	41.71	0.21	14.16	0.10	0.17	14.35	2.63	100.12	0.990	0.002	0.005	0.936	0.059	0.360	0.005	0.634	0.002	0.004	0.004
Vranduk Fm.	TD147sp070	n. d.	0.05	0.27	31.94	35.27	0.17	13.17	0.08	0.32	16.51	1.90	99.68	0.827	0.001	0.005	1.117	0.042	0.410	0.004	0.582	0.002	0.007	0.007
Vranduk Fm.	TD147sp071	n. d.	0.08	0.26	26.91	39.62	0.21	13.36	0.11	0.19	15.56	3.69	99.99	0.945	0.002	0.005	0.957	0.084	0.392	0.005	0.601	0.003	0.004	0.004
Vranduk Fm.	TD147sp072	n. d.	0.07	0.23	33.54	33.91	0.18	14.48	0.10	0.11	14.88	2.32	99.91	0.783	0.002	0.004	1.154	0.051	0.363	0.005	0.630	0.002	0.004	0.004
Vranduk Fm.	TD154sp069	n. d.	0.03	0.22	27.65	37.38	0.27	11.49	0.10	0.38	18.16	3.99	99.66	0.902	0.001	0.004	0.995	0.092	0.464	0.005	0.522	0.002	0.009	0.009
Vranduk Fm.	TD154sp033	n. d.	0.04	0.18	35.00	29.15	0.16	15.32	0.18	0.22	13.47	5.61	99.33	0.669	0.001	0.004	1.199	0.123	0.327	0.004	0.663	0.004	0.005	0.005
Vranduk Fm.	TD154sp032	n. d.	0.04	0.34	16.24	53.65	0.25	12.25	0.07	0.16	15.69	1.83	100.06	1.344	0.001	0.007	0.606	0.033	0.416	0.007	0.578	0.002	0.004	0.004
Vranduk Fm.	TD154sp051	n. d.	0.04	0.29	27.16	41.14	0.19	13.21	0.07	0.25	15.87	1.83	100.05	0.980	0.001	0.006	0.965	0.041	0.400	0.005	0.593	0.002	0.006	0.006
Vranduk Fm.	TD154sp005	n. d.	0.05	0.21	28.02	39.68	0.17	15.23	0.16	0.13	12.85	3.44	99.93	0.931	0.001	0.004	0.981	0.077	0.319	0.004	0.674	0.004	0.003	0.003
Vranduk Fm.	TD154sp066	n. d.	0.05	0.16	42.03	25.05	0.14	16.99	0.12	0.13	12.16	2.44	99.34	0.854	0.001	0.003	1.386	0.051	0.285	0.003	0.708	0.004	0.003	0.003
Vranduk Fm.	TD154sp070	n. d.	0.05	0.27	26.40	38.83	0.26	11.27	0.12	0.30	18.60	4.20	100.30	0.938	0.001	0.005	0.951	0.097	0.475	0.007	0.513	0.003	0.007	0.007
Vranduk Fm.	TD154sp019	n. d.	0.05	0.17	43.75	22.67	0.12	17.67	0.24	0.17	11.27	3.06	99.17	0.497	0.001	0.003	1.430	0.064	0.261	0.003	0.730	0.005	0.003	0.003
Vranduk Fm.	TD154sp021	n. d.	0.05	0.26	19.22	50.47	0.23	13.62	0.06	0.13	14.18	2.24	100.46	1.234	0.001	0.005	0.701	0.052	0.367	0.006	0.628	0.002	0.003	0.003
Vranduk Fm.	TD154sp020	n. d.	0.06	0.19	41.08	24.85	0.16	15.48	0.16	0.37	14.21	3.07	99.63	0.555	0.001	0.003	1.369	0.065	0.336	0.004	0.652	0.004	0.008	0.008
Vranduk Fm.	TD154sp002	n. d.	0.06	0.19	33.87	32.64	0.17	15.14	0.15	0.14	13.75	3.35	99.46	0.752	0.001	0.004	1.164	0.073	0.335	0.004	0.658	0.004	0.003	0.003
Vranduk Fm.	TD154sp041	n. d.	0.06	0.23	26.42	40.96	0.18	15.16	0.15	0.09	12.79	4.01	100.05	0.967	0.001	0.005	0.930	0.090	0.320	0.005	0.675	0.004	0.002	0.002
Vranduk Fm.	TD154sp034	n. d.	0.06	0.13	38.57	28.06	0.16	16.48	0.20	0.17	12.30	3.14	99.26	0.631	0.001	0.003	1.294	0.067	0.293	0.004	0.699	0.004	0.003	0.003
Vranduk Fm.	TD154sp073	0.01	0.06	0.11	51.80	14.45	0.10	19.21	0.33	0.14	10.12	2.87	99.19	0.305	0.001	0.002	1.631	0.058	0.226	0.002	0.765	0.007	0.003	0.003
Vranduk Fm.	TD154sp071	n. d.	0.07	0.23	26.48	42.22	0.21	13.09	0.08	0.17	15.98	1.53	100.04	1.009	0.001	0.005	0.944	0.035	0.404	0.005	0.590	0.002	0.004	0.004
Vranduk Fm.	TD154sp018	n. d.	0.07	0.26	26.66	42.38	0.19	14.39	0.11	0.16	14.04	1.84	100.11	1.003	0.002	0.005	0.941	0.041	0.352	0.005	0.642	0.003	0.004	0.004
Vranduk Fm.	TD154sp074	n. d.	0.07	0.18	38.79	26.52	0.14	15.95	0.17	0.17	13.21	4.10	99.31	0.598	0.001	0.003	1.304	0.088	0.315	0.003	0.678	0.004	0.004	0.004
Vranduk Fm.	TD154sp035	n. d.	0.07	0.18	39.44	26.99	0.16	16.00	0.20	0.21	13.39	3.36	100.01	0.603	0.001	0.003	1.315	0.072	0.317	0.004	0.674	0.005	0.004	0.004
Vranduk Fm.	TD154sp052	n. d.	0.07	0.17	41.61	25.60	0.14	16.37	0.16	0.25	13.02	2.01	99.40	0.569	0.002	0.003	1.379	0.043	0.306	0.003	0.686	0.004	0.005	0.005
Vranduk Fm.	TD154sp065	n. d.	0.07	0.22	31.83	36.46	0.18	15.01	0.11	0.19	13.81	2.03	99.92	0.844	0.002	0.004	1.099	0.045	0.338	0.004	0.655	0.003	0.004	0.004
Vranduk Fm.	TD154sp020	n. d.	0.08	0.34	12.11	56.59	0.34	9.39	0.03	0.18	19.49	1.90	100.45	1.468	0.002	0.007	0.468	0.047	0.534	0.009	0.458	0.001	0.004	0.004
Vranduk Fm.	TD154sp075	n. d.	0.08	0.17	42.17	24.23	0.14	16.82	0.23	0.18	12.42	3.02	99.44	0.536	0.002	0.003	1.391	0.064	0.290	0.003	0.701	0.005	0.004	0.004
Vranduk Fm.	TD154sp036	n. d.	0.08	0.22	19.05	45.30	0.28	11.40	0.13	0.23	17.07	6.02	99.76	1.133	0.002	0.004	0.710	0.143	0.452	0.007	0.537	0.003	0.005	0

Formation	Sample & spot ID	analyses in wt%. Shown are the recalculated FeO and Fe <sub>2</sub> O <sub>3</sub> values and the amended total														cations per formula unit on the basis of 3 oxygens									
		SiO <sub>2</sub>	TiO <sub>2</sub>	V <sub>2</sub> O <sub>5</sub>	Al <sub>2</sub> O <sub>3</sub>	Cr <sub>2</sub> O <sub>3</sub>	MnO	MgO	NiO	ZnO	FeO	Fe <sub>2</sub> O <sub>3</sub>	Total	Cr	Ti	V	Al	Fe <sup>3+</sup>	Fe <sup>2+</sup>	Mn	Mg	Ni	Zn		
Vranduk Fm.	TD154sp012	n. d.	0.10	0.25	32.43	33.25	14.87	0.14	0.22	13.92	4.11	99.48	0.772	0.002	0.005	1.123	0.091	0.342	0.005	0.651	0.003	0.003	0.005		
Vranduk Fm.	TD154sp057	n. d.	0.11	0.21	36.03	29.51	14.90	0.16	0.19	14.47	3.82	99.59	0.675	0.002	0.004	1.229	0.083	0.350	0.005	0.642	0.004	0.004	0.004		
Vranduk Fm.	TD154sp039	n. d.	0.11	0.41	15.19	54.40	11.87	0.06	0.12	16.29	1.55	100.26	1.369	0.003	0.006	0.570	0.037	0.434	0.007	0.563	0.002	0.003	0.004		
Vranduk Fm.	TD154sp046	n. d.	0.13	0.30	27.91	38.89	0.22	0.11	0.19	16.27	3.36	100.52	0.985	0.003	0.006	0.985	0.076	0.408	0.006	0.587	0.003	0.003	0.004		
Vranduk Fm.	TD154sp064	n. d.	0.14	0.20	32.79	35.65	15.85	0.14	0.11	12.68	1.78	99.46	0.821	0.003	0.004	1.126	0.039	0.309	0.003	0.688	0.003	0.003	0.002		
Vranduk Fm.	TD154sp065	n. d.	0.15	0.14	25.93	38.50	0.29	0.10	0.27	18.62	5.00	100.17	0.934	0.003	0.003	0.938	0.115	0.478	0.007	0.512	0.002	0.002	0.006		
Vranduk Fm.	TD154sp045	n. d.	0.17	0.15	8.92	58.49	0.21	0.08	0.04	12.68	5.63	99.82	1.505	0.004	0.003	0.342	0.138	0.345	0.006	0.652	0.002	0.001	0.001		
Vranduk Fm.	TD154sp026	n. d.	0.17	0.28	32.30	32.96	13.70	0.11	0.27	15.84	3.91	99.71	1.180	0.004	0.005	1.125	0.080	0.391	0.004	0.603	0.003	0.003	0.006		
Vranduk Fm.	TD154sp031	n. d.	0.18	0.12	16.41	46.16	9.25	0.07	0.24	20.08	7.38	100.24	1.180	0.004	0.002	0.626	0.180	0.543	0.010	0.446	0.002	0.002	0.006		
Vranduk Fm.	TD154sp024	n. d.	0.18	0.30	28.15	37.15	0.26	0.10	0.22	16.40	4.69	100.53	0.879	0.004	0.006	0.984	0.106	0.411	0.006	0.584	0.002	0.002	0.005		
Vranduk Fm.	TD154sp053	n. d.	0.19	0.21	28.01	39.26	13.28	0.11	0.17	15.88	2.40	99.69	0.934	0.004	0.004	0.994	0.054	0.400	0.005	0.596	0.003	0.003	0.004		
Vranduk Fm.	TD154sp047	n. d.	0.29	0.33	32.35	31.78	13.21	0.17	0.27	16.83	4.84	100.28	0.741	0.006	0.006	1.125	0.108	0.415	0.005	0.581	0.004	0.004	0.006		
Vranduk Fm.	TD154sp014	n. d.	0.30	0.21	29.97	33.42	12.45	0.14	0.28	17.55	5.78	100.31	0.790	0.007	0.004	1.057	0.130	0.439	0.006	0.555	0.003	0.003	0.006		
Vranduk Fm.	TD154sp020	n. d.	0.30	0.32	27.88	35.09	0.21	0.16	0.19	16.55	6.42	100.04	0.836	0.007	0.006	0.991	0.146	0.417	0.005	0.580	0.004	0.004	0.004		
Vranduk Fm.	TD154sp061	n. d.	0.32	0.30	31.92	32.45	12.80	0.15	0.21	17.41	4.34	100.12	0.761	0.007	0.006	1.116	0.097	0.432	0.006	0.566	0.004	0.004	0.004		
Vranduk Fm.	TD154sp011	n. d.	0.32	0.33	30.75	35.13	13.70	0.13	0.18	15.87	3.31	99.95	0.823	0.007	0.006	1.075	0.074	0.393	0.006	0.605	0.003	0.003	0.004		
Vranduk Fm.	TD154sp038	n. d.	0.38	0.22	8.88	47.04	6.42	0.12	0.23	23.41	13.67	100.81	1.265	0.010	0.005	0.356	0.350	0.666	0.013	0.325	0.003	0.003	0.006		
Vranduk Fm.	TD154sp049	n. d.	0.39	0.27	27.69	29.29	10.83	0.22	0.26	19.54	11.42	100.17	0.709	0.009	0.005	0.999	0.263	0.500	0.007	0.494	0.005	0.005	0.006		
Vranduk Fm.	TD154sp023	n. d.	0.39	0.23	24.68	40.40	13.61	0.11	0.11	15.33	5.63	100.72	0.965	0.009	0.004	0.879	0.128	0.388	0.006	0.613	0.003	0.003	0.002		
Vranduk Fm.	TD154sp001	n. d.	0.41	0.18	12.83	47.52	9.92	0.08	0.24	18.81	10.16	100.43	1.228	0.010	0.004	0.494	0.250	0.514	0.008	0.483	0.002	0.002	0.006		
Vranduk Fm.	TD154sp043	n. d.	0.42	0.17	37.77	26.55	15.98	0.21	0.12	13.50	5.12	100.01	0.598	0.009	0.003	1.268	0.110	0.322	0.004	0.678	0.005	0.002	0.002		
Vranduk Fm.	TD154sp068	n. d.	0.43	0.23	32.02	30.92	14.36	0.19	0.15	14.95	6.29	99.76	0.720	0.009	0.004	1.112	0.139	0.368	0.005	0.631	0.005	0.005	0.003		
Vranduk Fm.	TD154sp004	n. d.	0.44	0.19	33.52	31.98	14.74	0.16	0.16	14.69	3.72	99.79	0.738	0.010	0.004	1.154	0.082	0.358	0.005	0.641	0.004	0.004	0.003		
Vranduk Fm.	TD154sp059	n. d.	0.49	0.20	34.93	29.84	14.65	0.14	0.15	15.10	4.07	99.73	0.686	0.010	0.004	1.197	0.089	0.367	0.005	0.635	0.003	0.003	0.003		
Vranduk Fm.	TD154sp015	n. d.	0.49	0.39	21.08	40.90	12.00	0.12	0.16	17.21	7.73	100.30	1.006	0.011	0.008	0.773	0.181	0.448	0.006	0.557	0.003	0.003	0.004		
Vranduk Fm.	TD154sp003	n. d.	0.55	0.28	15.69	38.73	8.11	0.16	0.33	21.67	13.79	99.69	1.009	0.014	0.006	0.609	0.342	0.597	0.011	0.398	0.004	0.004	0.008		
Vranduk Fm.	TD154sp030	n. d.	0.59	0.23	24.91	29.32	6.67	0.19	0.36	25.39	12.36	100.61	0.735	0.014	0.005	0.931	0.295	0.673	0.015	0.315	0.005	0.005	0.008		
Vranduk Fm.	TD154sp016	n. d.	0.94	0.26	28.57	32.31	9.36	0.15	0.31	22.67	5.81	100.67	0.781	0.022	0.005	1.030	0.134	0.580	0.008	0.427	0.004	0.004	0.007		
Vranduk Fm.	TD154sp067	n. d.	1.01	0.42	25.80	34.79	10.63	0.19	0.29	20.32	6.57	100.29	0.847	0.023	0.009	0.936	0.152	0.523	0.007	0.488	0.005	0.005	0.007		
Vranduk Fm.	TD154sp063	n. d.	1.25	0.33	21.01	40.25	13.49	0.10	0.07	15.51	7.53	99.78	0.985	0.029	0.007	0.767	0.175	0.402	0.006	0.622	0.003	0.003	0.002		
Vranduk Fm.	TD154sp054	n. d.	1.31	0.19	1.80	23.33	1.27	0.31	0.35	29.14	40.72	99.66	0.690	0.037	0.005	0.080	1.102	0.912	0.040	0.069	0.009	0.010	0.010		
Vranduk Fm.	TD154sp050	n. d.	1.41	0.07	0.61	26.39	2.06	0.22	0.32	28.70	38.79	99.55	0.787	0.040	0.002	0.027	1.102	0.906	0.066	0.054	0.007	0.009	0.009		
Vranduk Fm.	TD154sp056	n. d.	1.59	0.49	15.72	40.01	7.83	0.14	0.23	23.54	10.41	100.34	1.036	0.039	0.011	0.607	0.256	0.645	0.011	0.382	0.004	0.004	0.006		
Vranduk Fm.	TD154sp055	n. d.	2.21	0.28	21.77	35.27	11.69	0.19	0.12	19.22	9.46	100.50	0.866	0.052	0.006	0.797	0.221	0.499	0.008	0.541	0.005	0.005	0.003		
Vranduk Fm.	TD154sp040	n. d.	4.62	0.66	8.29	36.08	3.78	0.25	0.18	31.03	14.64	100.07	0.997	0.122	0.015	0.342	0.385	0.907	0.016	0.197	0.007	0.007	0.005		

n. d.: not detected

Electron microprobe analyses of detrital garnet from the Dinaride Ophiolite Zone mélange and the Bosnian Flysch

Formation	Sample & spot ID	analyses in wt%						cations per formula unit on the basis of 12 oxygens												garnet end member molecules [%]						scho
		SiO <sub>2</sub>	TiO <sub>2</sub>	Al <sub>2</sub> O <sub>3</sub>	FeO	MnO	MgO	CaO	Total	Si	Ti	Al	Fe <sup>2+</sup>	Fe <sup>3+</sup>	Mn	Mg	Ca	prp	alm	grs	spc	adr				
DOZ mélange	BO22:grt001	37.91	0.01	21.60	32.75	0.90	5.09	1.45	99.71	3.013	0.001	2.024	2.177	0.000	0.060	0.603	0.123	20.35	73.45	4.15	2.04	0.00	0.02			
DOZ mélange	BO22:grt002	37.60	0.03	24.71	9.90	0.20	0.17	23.25	95.88	2.997	0.002	3.321	0.660	0.000	0.012	0.021	1.986	0.77	24.62	74.05	0.50	0.00	0.06			
DOZ mélange	BO22:grt003	37.24	n. d.	21.90	13.18	0.18	0.03	23.00	95.61	3.012	0.000	2.087	0.891	0.000	0.013	0.004	1.993	0.14	30.73	68.71	0.41	0.00	0.01			
DOZ mélange	BO22:grt004	38.01	0.07	25.24	9.50	0.04	0.01	23.50	96.37	3.011	0.003	2.457	0.629	0.000	0.003	0.001	1.995	0.05	23.93	75.76	0.11	0.00	0.15			
DOZ mélange	BO22:grt005	37.26	0.05	25.67	8.33	0.14	0.06	23.63	95.17	2.980	0.004	2.420	0.557	0.000	0.009	0.007	2.024	0.27	21.44	77.81	0.36	0.00	0.12			
DOZ mélange	BO22:grt006	37.67	0.01	21.51	31.80	1.49	4.96	1.66	99.20	3.012	0.000	2.027	2.126	0.000	0.101	0.591	0.142	19.97	71.81	4.77	3.41	0.00	0.03			
DOZ mélange	BO22:grt007	36.56	n. d.	20.92	33.04	5.39	2.11	1.52	99.57	2.978	0.000	2.009	2.217	0.034	0.372	0.257	1.133	8.62	74.44	12.49	1.70	0.01	0.01			
DOZ mélange	BO22:grt008	37.30	0.11	21.75	13.02	0.12	0.03	23.07	95.42	3.021	0.007	2.076	0.882	0.000	0.009	0.004	2.002	0.14	30.44	68.89	0.30	0.00	0.24			
DOZ mélange	BO22:grt009	37.53	0.07	23.35	11.95	0.22	0.02	23.15	96.36	2.999	0.004	2.199	0.799	0.000	0.015	0.002	1.982	0.09	28.53	70.69	0.54	0.00	0.16			
DOZ mélange	BO22:grt010	37.72	0.07	25.75	8.84	0.11	0.02	23.56	96.08	2.999	0.004	2.406	0.587	0.000	0.008	0.002	2.002	0.09	22.56	76.90	0.29	0.00	0.16			
DOZ mélange	BO22:grt011	37.20	0.04	23.18	11.90	0.21	0.02	23.17	95.88	2.990	0.004	2.196	0.800	0.000	0.014	0.002	1.995	0.08	28.45	70.87	0.51	0.00	0.09			
DOZ mélange	BO22:grt012	37.65	0.04	21.03	32.73	1.27	4.10	2.72	99.63	3.014	0.002	1.984	2.191	0.000	0.086	0.489	0.233	16.29	73.04	7.72	2.66	0.00	0.08			
DOZ mélange	BO22:grt013	37.36	0.14	22.86	11.94	0.13	0.04	23.06	95.68	3.011	0.008	2.171	0.805	0.000	0.009	0.004	1.991	0.16	28.63	70.60	0.32	0.00	0.30			
DOZ mélange	BO22:grt014	37.94	0.16	24.95	9.57	0.08	0.02	23.36	96.09	3.017	0.010	2.339	0.636	0.000	0.005	0.003	1.990	0.10	24.14	75.20	0.20	0.00	0.37			
DOZ mélange	BO22:grt015	37.18	0.10	22.50	12.21	0.04	0.03	23.03	95.09	3.012	0.006	2.149	0.827	0.000	0.002	0.004	1.999	0.14	29.19	70.36	0.08	0.00	0.22			
DOZ mélange	BO22:grt016	37.62	0.04	21.63	30.91	2.19	5.60	1.96	99.99	2.971	0.002	2.013	2.001	0.041	0.147	0.660	0.166	22.19	67.33	3.48	4.93	1.98	0.08			
DOZ mélange	BO22:grt017	36.93	n. d.	21.03	32.58	4.28	2.54	2.37	99.78	2.986	0.000	2.005	2.181	0.022	0.293	0.306	0.206	10.25	73.04	5.76	9.82	1.12	0.00			
DOZ mélange	BO22:grt018	36.93	n. d.	21.03	32.58	4.28	2.54	2.37	99.78	2.986	0.000	2.005	2.181	0.022	0.293	0.306	0.206	10.25	73.04	5.76	9.82	1.12	0.00			
DOZ mélange	BO22:grt019	37.44	0.09	20.94	27.75	2.23	1.06	9.97	99.53	3.008	0.005	1.983	1.865	0.000	0.152	0.128	0.859	4.25	62.08	28.46	5.05	0.00	0.17			
DOZ mélange	BO22:grt020	37.50	0.04	21.38	31.81	1.67	4.69	2.63	99.78	2.984	0.000	2.003	2.093	0.023	0.113	0.566	0.224	18.64	70.13	6.27	3.77	1.11	0.08			
DOZ mélange	BO22:grt021	37.61	0.12	22.18	13.25	0.06	0.02	23.13	96.45	3.015	0.008	2.096	0.888	0.000	0.004	0.006	1.987	0.08	30.81	68.70	0.14	0.00	0.26			
DOZ mélange	BO22:grt022	36.70	0.13	20.99	33.33	2.65	2.98	2.19	99.07	2.982	0.002	1.975	1.746	0.000	0.045	0.663	0.554	22.03	68.02	18.33	1.49	0.00	0.12			
DOZ mélange	BO22:grt023	37.51	n. d.	21.44	33.82	0.67	4.00	2.02	99.65	3.002	0.000	2.023	2.264	0.000	0.045	0.478	0.188	16.05	76.10	6.32	1.53	0.00	0.00			
DOZ mélange	BO22:grt024	37.25	0.04	23.84	10.97	0.05	0.05	23.47	95.69	2.986	0.002	2.252	0.735	0.000	0.004	0.006	2.016	0.20	26.64	72.95	0.13	0.00	0.08			
DOZ mélange	BO22:grt025	37.98	0.05	21.59	29.94	1.27	3.15	6.58	100.59	2.999	0.003	2.009	1.977	0.000	0.085	0.371	0.556	12.41	66.11	18.54	2.84	0.00	0.09			
DOZ mélange	BO22:grt026	36.78	0.09	20.61	27.30	7.69	0.81	6.23	99.61	2.991	0.006	1.975	1.825	0.031	0.530	0.098	0.543	3.30	60.97	16.44	17.69	1.41	0.19			
DOZ mélange	BO22:grt027	38.74	0.06	21.94	26.83	0.68	5.72	6.65	100.22	3.013	0.004	1.975	1.746	0.000	0.045	0.663	0.554	22.03	68.02	18.33	1.49	0.00	0.12			
DOZ mélange	BO22:grt028	37.60	0.04	21.41	31.09	1.40	2.82	5.70	100.08	2.997	0.002	2.011	2.073	0.000	0.095	0.335	0.477	11.20	69.52	15.93	3.22	0.00	0.10			
DOZ mélange	BO22:grt029	37.51	n. d.	21.44	33.82	0.67	4.00	2.02	99.65	3.002	0.000	2.023	2.264	0.000	0.045	0.478	0.188	16.05	76.10	6.32	1.53	0.00	0.00			
DOZ mélange	BO22:grt030	38.41	0.06	21.77	26.23	0.44	4.10	9.17	100.19	3.002	0.004	2.005	1.714	0.000	0.029	0.478	0.768	15.98	57.34	25.58	0.98	0.00	0.12			
DOZ mélange	BO22:grt031	37.56	0.08	24.02	11.21	0.17	0.03	23.16	96.23	2.996	0.005	2.258	0.747	0.000	0.012	0.004	1.979	0.11	27.25	72.04	0.43	0.00	0.17			
DOZ mélange	BO22:grt032	37.44	0.01	21.20	31.18	0.26	3.65	0.69	100.42	2.998	0.000	2.000	2.486	0.003	0.018	0.435	0.059	14.52	82.92	1.79	0.59	0.16	0.02			
DOZ mélange	BO22:grt033	37.79	0.05	21.26	31.11	1.42	2.80	5.88	100.01	3.015	0.003	2.000	2.076	0.000	0.095	0.333	0.477	11.17	69.59	15.93	3.22	0.00	0.10			
DOZ mélange	BO22:grt034	37.60	0.04	21.41	31.09	1.40	2.82	5.70	100.08	2.997	0.002	2.011	2.073	0.000	0.095	0.335	0.477	11.20	69.52	15.93	3.22	0.00	0.10			
DOZ mélange	BO22:grt035	38.12	0.01	21.15	34.23	0.72	4.02	2.26	99.53	2.978	0.001	2.000	2.255	0.042	0.049	0.481	0.195	16.14	75.70	4.40	1.64	2.11	0.02	0.02		
DOZ mélange	BO22:grt036	38.26	0.23	25.25	9.27	0.07	0.03	23.53	96.73	3.023	0.014	2.351	0.612	0.000	0.005	0.003	1.992	0.12	23.41	75.77	0.18	0.00	0.53			
DOZ mélange	BO22:grt037	37.70	0.15	25.16	9.93	0.17	0.03	23.14	96.28	2.993	0.009	2.354	0.660	0.000	0.011	0.004	1.968	0.14	24.93	74.15	0.43	0.00	0.34			
DOZ mélange	BO22:grt038	37.19	0.23	20.88	32.71	2.18	2.34	4.54	100.07	2.989	0.014	1.978	2.184	0.015	0.149	0.280	0.391	9.34	72.88	11.96	4.96	0.41	0.46			
DOZ mélange	BO22:grt039	38.22	0.09	21.52	26.15	0.43	3.49	10.18	100.16	2.998	0.005	1.990	1.711	0.005	0.029	0.408	0.855	13.59	57.03	28.15	0.96	0.10	0.17			
DOZ mélange	BO22:grt040	37.64	0.19	23.40	11.83	0.06	0.05	23.37	96.54	2.999	0.012	1.977	0.798	0.000	0.004	0.005	1.995	0.20	28.20	71.06	0.13	0.00	0.41			
DOZ mélange	BO22:grt041	38.87	0.06	21.80	23.16	0.63	6.00	9.64	100.21	2.996	0.003	1.980	1.472	0.021	0.041	0.690	0.796	23.01	49.11	25.43	1.37	0.97	0.11			
DOZ mélange	BO22:grt042	37.15	0.06	21.15	34.45	0.86	1.32	5.40	100.47	2.989	0.004	2.006	2.311	0.008	0.059	0.158	0.465	5.30	77.25	15.08	1.96	0.29	0.13			
DOZ mélange	BO22:grt043	38.34	0.10	21.77	26.74	1.06	5.58	6.47	100.07	2.990	0.006	2.001	1.736	0.008	0.070	0.649	0.540	21.68	58.01	17.50	2.35	0.26	0.20			
DOZ mélange	BO22:grt044	36.76	0.03	21.01	23.10	14.75	2.55	1.09	99.39	2.991	0.002	2.015	1.571	0.000	0.105	0.309	0.095	10.33	52.51	3.14	33.96	0.00	0.06			
DOZ mélange	BO22:grt045	37.21	0.15	21.11	34.27	0.91	4.46	1.68	99.81	2.974	0.009	1.989	2.246	0.045	0.062	0.531	0.144	17.83	75.40	3.35	2.08	0.00	0.30			
DOZ mélange	BO22:grt046	38.09	0.07	21.67	32.03	0.38	6.25	1.91	100.56	2.994	0.004	2.000	2.072	0.026	0.025	0.730	0.160	24.44	69.41	3.94	0.85	1.22	0.13			
DOZ mélange	BO22:grt047	38.18	0.04	20.96	26.41	11.87	2.50	1.95	100.11	2.998	0.001	1.988	2.348	0.013	0.109	0.374	0.168	12.47	78.31	0.93	3.63	0.63	0.04			
DOZ mélange	BO22:grt048	36.51	0.06	20.96	26.41	11.87	2.50	1.95	100.11	2.998	0.001	1.988	2.348	0.013	0.109	0.374	0.168	12.47	78.31	0.93	3.63	0.63	0.04			
DOZ mélange	BO22:grt049	37.04	0.12	20.57	26.01	10.36	2.81	2.34	99.28	3.005	0.007	1.967	1.757	0.008	0.712	0.340	0.203	11.32	58.39	6.17	23.66	0.22	0.24			
DOZ mélange	BO22:grt050	36.58	0.16	20.64	34.02	5.85	1.60	1.27	100.16	2.981	0.010	1.983	2.282	0.036	0.404	0.194	0									

Formation	analyses in wt%				cations per formula unit on the basis of 12 oxigens								garnet end member molecules [%]						adr	scho			
	SiO <sub>2</sub>	TiO <sub>2</sub>	Al <sub>2</sub> O <sub>3</sub>	FeO	MnO	MgO	CaO	Total	Si	Ti	Al	Fe <sup>2+</sup>	Fe <sup>3+</sup>	Mn	Mg	Ca	prp	alm			grs	sps	
DOZ mélange	37.46	0.13	21.07	35.15	0.45	4.85	0.71	99.88	2.992	0.008	1.983	2.331	0.017	0.031	0.577	0.061	19.27	77.80	1.00	1.02	0.86	0.25	
B023gr0025	37.46	0.22	20.71	35.15	0.45	4.85	0.71	99.88	2.992	0.008	1.983	2.331	0.017	0.031	0.577	0.061	19.27	77.80	1.00	1.02	0.86	0.25	
B023gr0026	36.60	0.02	20.71	36.57	4.09	1.52	0.62	100.16	2.990	0.001	1.988	2.469	0.029	0.283	0.185	0.054	6.18	82.57	0.31	9.46	1.44	0.45	
B023gr0027	36.60	0.09	20.94	26.04	11.60	0.92	2.49	100.09	2.982	0.005	1.996	1.732	0.029	0.794	0.245	0.216	8.21	82.03	5.62	26.62	1.34	0.18	
DOZ mélange	37.07	0.20	20.74	32.36	1.90	2.02	6.91	100.13	2.992	0.012	1.973	2.166	0.019	0.130	0.111	0.597	3.70	72.24	18.68	4.33	0.65	0.40	
B023gr0030	36.73	0.05	21.05	36.59	1.04	2.21	2.13	99.82	2.979	0.003	2.013	2.460	0.023	0.071	0.267	0.185	8.95	82.51	4.98	2.39	1.05	0.11	
DOZ mélange	37.21	0.04	21.05	35.50	2.95	2.69	1.06	100.61	2.995	0.003	1.997	2.383	0.007	0.201	0.323	0.091	10.78	79.51	2.63	6.71	0.28	0.09	
B023gr0032	37.29	0.39	20.71	31.16	1.15	3.30	5.59	99.65	2.985	0.023	1.984	2.057	0.029	0.078	0.394	0.480	13.13	68.65	13.99	2.60	0.86	0.78	
DOZ mélange	36.80	0.07	20.67	29.38	10.30	1.66	1.14	100.02	2.997	0.004	1.985	1.980	0.011	0.711	0.202	0.099	6.73	66.35	2.62	23.69	0.47	0.14	
B023gr0034	37.14	0.05	21.15	32.96	0.80	5.36	0.83	98.64	2.995	0.003	2.009	2.223	0.000	0.055	0.644	0.072	21.51	74.24	2.33	1.83	0.00	0.09	
DOZ mélange	37.26	0.28	20.39	21.65	10.16	0.25	9.90	99.93	3.005	0.017	1.938	1.444	0.017	0.694	0.029	0.855	0.98	47.90	27.12	23.03	0.00	0.57	
B023gr0036	37.85	0.02	21.70	31.71	0.66	6.68	0.85	99.51	2.986	0.001	2.018	2.086	0.006	0.044	0.786	0.072	26.30	69.84	2.05	1.48	0.29	0.44	
DOZ mélange	37.57	0.24	20.97	28.45	3.16	3.28	6.28	100.00	2.989	0.014	1.966	1.866	0.027	0.213	0.389	0.536	12.99	62.27	16.16	7.10	0.99	0.48	
B023gr0037	37.00	0.06	20.62	36.68	0.44	1.94	1.58	100.39	3.000	0.004	1.971	2.602	0.021	0.030	0.234	0.137	7.81	86.68	3.42	1.01	0.97	0.12	
DOZ mélange	37.20	0.04	21.11	36.91	1.00	2.89	3.22	100.52	2.990	0.002	2.000	2.464	0.016	0.068	0.346	0.114	11.57	82.39	2.93	2.27	0.76	0.08	
B023gr0039	38.84	0.15	22.05	26.99	0.36	10.19	0.81	99.41	2.992	0.008	2.001	1.738	0.000	0.024	1.170	0.067	38.99	57.92	2.01	0.79	0.00	0.28	
DOZ mélange	37.25	n.d.	21.23	34.10	1.78	3.78	1.69	99.84	2.988	0.000	2.007	2.270	0.017	0.121	0.452	0.145	15.13	75.96	3.98	4.05	0.87	0.00	
B023gr0046	37.05	0.14	21.23	36.23	1.47	3.03	1.16	100.41	2.979	0.008	2.012	2.424	0.012	0.104	0.363	0.100	12.17	81.25	2.53	3.36	0.41	0.28	
DOZ mélange	38.15	0.10	21.22	28.28	0.20	2.55	9.57	100.17	3.018	0.006	1.978	1.871	0.000	0.014	0.301	0.811	10.05	62.39	26.90	0.46	0.00	0.20	
B023gr0047	37.68	n.d.	21.26	35.10	0.74	4.46	0.93	100.24	3.003	0.000	1.998	2.340	0.000	0.050	0.500	0.080	17.66	78.02	3.36	1.77	0.00	0.00	
DOZ mélange	37.68	n.d.	21.26	35.10	0.74	4.46	0.93	100.24	3.003	0.000	1.998	2.340	0.000	0.050	0.500	0.080	17.66	78.02	3.36	1.77	0.00	0.00	
B023gr0049	36.76	0.05	20.89	24.42	14.12	2.94	0.53	99.71	2.978	0.004	1.982	1.870	0.000	0.068	0.588	0.487	19.48	61.93	15.53	2.26	0.00	0.80	
DOZ mélange	37.84	0.10	21.29	31.28	0.69	5.16	3.03	99.39	3.006	0.006	1.983	2.079	0.000	0.046	0.612	0.258	20.41	69.37	8.47	1.54	0.00	0.20	
B023gr0050	38.52	0.03	21.99	29.38	0.72	7.17	2.49	100.31	2.992	0.002	2.012	1.908	0.000	0.048	0.831	0.207	27.74	63.73	6.88	1.59	0.00	0.07	
DOZ mélange	38.43	0.03	21.91	25.13	0.58	6.45	6.76	99.29	2.995	0.002	2.013	1.638	0.000	0.030	0.749	0.565	25.05	54.77	18.84	1.28	0.00	0.05	
B023gr0052	35.76	0.04	20.80	28.59	1.375	0.53	0.64	99.92	2.946	0.003	2.001	1.869	0.010	0.968	0.065	0.056	2.19	60.08	0.00	32.55	0.00	0.09	
DOZ mélange	37.00	0.01	20.91	35.46	2.69	2.53	1.17	99.80	3.002	0.001	1.999	2.406	0.000	0.185	0.306	0.102	10.20	80.24	3.36	6.17	0.00	0.03	
B023gr0055	38.10	0.41	21.13	28.38	1.02	5.01	5.77	99.94	3.001	0.024	1.982	1.870	0.000	0.068	0.588	0.487	19.48	61.93	15.53	2.26	0.00	0.80	
DOZ mélange	37.74	0.06	21.33	30.00	1.50	4.86	3.90	99.42	2.998	0.004	1.997	1.993	0.000	0.101	0.385	0.124	12.87	79.71	3.16	3.35	0.79	0.13	
B023gr0056	36.87	0.08	20.62	34.03	5.62	1.88	0.93	100.16	3.001	0.005	1.978	2.305	0.011	0.388	0.228	0.085	7.58	76.76	2.16	12.91	0.43	0.17	
DOZ mélange	37.21	0.12	21.07	31.56	5.21	2.17	2.98	100.31	2.996	0.007	1.999	2.125	0.000	0.355	0.260	0.257	8.28	70.86	8.39	11.84	0.00	0.24	
B023gr0066	36.77	0.01	20.71	37.93	1.70	2.04	0.66	99.97	2.999	0.001	1.991	2.576	0.011	0.117	0.248	0.057	8.28	85.90	1.36	3.91	0.52	0.02	
DOZ mélange	37.18	0.03	20.71	37.93	1.70	2.04	0.66	99.97	2.999	0.001	1.991	2.576	0.011	0.117	0.248	0.057	8.28	85.90	1.36	3.91	0.52	0.02	
B023gr0067	37.16	0.02	20.97	29.64	0.67	1.57	9.19	99.42	2.985	0.012	1.985	1.972	0.020	0.026	0.189	0.791	6.30	65.91	25.16	5.33	0.70	0.40	
DOZ mélange	37.89	0.02	21.47	31.65	1.51	5.61	1.79	100.06	2.994	0.001	2.000	2.082	0.010	0.101	0.661	0.151	22.07	69.52	4.52	3.38	0.47	0.05	
B023gr0082	37.07	0.06	20.96	35.61	1.47	3.20	1.43	99.80	2.991	0.004	1.993	2.386	0.018	0.100	0.385	0.124	12.87	79.71	3.16	3.35	0.79	0.13	
DOZ mélange	36.87	0.08	20.62	34.03	5.62	1.88	0.93	100.16	3.001	0.005	1.978	2.305	0.011	0.388	0.228	0.085	7.58	76.76	2.16	12.91	0.43	0.17	
B023gr0064	37.33	0.07	21.33	34.54	1.85	3.21	1.69	99.88	3.006	0.004	2.006	2.327	0.000	0.126	0.385	0.146	12.91	77.95	4.78	4.23	0.00	0.14	
DOZ mélange	36.74	0.25	21.07	20.54	11.03	3.06	6.23	99.01	2.953	0.015	1.996	1.313	0.068	0.751	0.367	0.537	12.40	44.34	14.31	25.37	3.07	0.50	
B023gr0072	38.81	0.08	22.14	26.54	0.59	9.44	1.75	99.38	2.997	0.035	1.943	1.909	0.024	0.136	1.086	0.145	36.40	57.42	4.73	1.29	0.00	0.16	
DOZ mélange	37.32	0.58	20.63	28.93	2.00	3.87	5.97	99.33	2.982	0.035	1.943	1.909	0.024	0.136	1.086	0.145	36.40	57.42	4.73	1.29	0.00	0.16	
B023gr0074	36.60	0.15	20.76	34.86	4.26	1.91	1.19	99.84	2.985	0.009	1.996	2.363	0.014	0.294	0.461	0.511	15.37	63.65	14.95	4.52	0.35	1.16	
DOZ mélange	36.60	0.15	20.76	34.86	4.26	1.91	1.19	99.84	2.985	0.009	1.996	2.363	0.014	0.294	0.461	0.511	15.37	63.65	14.95	4.52	0.35	1.16	
B023gr0075	38.41	0.04	21.75	25.73	0.23	4.08	9.98	100.28	2.996	0.002	2.000	1.674	0.004	0.031	0.474	0.854	15.81	7.78	79.04	2.59	9.85	0.49	0.32
DOZ mélange	38.41	0.04	21.75	25.73	0.23	4.08	9.98	100.28	2.996	0.002	2.000	1.674	0.004	0.031	0.474	0.854	15.81	7.78	79.04	2.59	9.85	0.49	0.32
B023gr0076	37.50	0.08	21.13	28.69	0.45	2.24	9.46	99.67	2.990	0.005	1.986	1.889	0.004	0.015	0.267	0.809	8.91	63.13	25.70	1.02	1.08	0.16	
DOZ mélange	37.32	0.10	21.18	28.94	1.34	2.72	6.89	99.37	2.993	0.016	1.974	1.977	0.010	0.113	0.349	0.569	11.62	65.91	18.06	3.78	0.12	0.52	
B023gr0083	37.61	0.10	21.18	28.94	1.34	2.72	6.89	99.37	2.993	0.016	1.974	1.977	0.010	0.113	0.349	0.569	11.62	65.91	18.06	3.78	0.12	0.52	
DOZ mélange	37.80	0.03	21.25	29.70	2.29	5.63	2.64	99.39	2.998	0.002	1.987	1.955	0.015	0.154	0.666	0.225	22.21	65.19	14.64	5.13	0.71	0.20	
B023gr0084	37.49	0.30	21.05	30.53	1.67	3.40	5.32	99.88	2.993	0.018	1.980	2.038	0.000	0.113	0.404	0.455	13.42	67.60	14.64	3.75	0.00	0.59	
DOZ mélange	37.11	0.01	20.88	35.41	1.10	4.37	0.63	99.55	2.985	0.000	1.979	2.332	0.050	0.075	0.524	0.054	17.57	77.39	0.00	2.51	1.79	0.01	
B023gr0087	37.62	0.12	20.94	30.00	1.07	2.26	8.05	100.21	2.998	0.007	1.967	1.977	0.025	0.086	0.268	0.687	8.93	65.87	27.88	2.41	0.94	0.24	
DOZ mélange	36.45	0.02	20.73	39.22	1.24	0.89	1.47	100.07	2.986	0.001	2.002	2.6											

Formation	Sample & spot ID	analyses in wt%				cations per formula unit on the basis of 12 oxygens										garnet end member molecules [%]						adr	scho
		SiO <sub>2</sub>	TiO <sub>2</sub>	Al <sub>2</sub> O <sub>3</sub>	FeO	MnO	MgO	CaO	Total	Si	Ti	Al	Fe <sup>2+</sup>	Fe <sup>3+</sup>	Mn	Mg	Ca	prp	alm	grs	sps		
DOZ mélange	BO25gr003	36.89	0.09	20.99	32.28	3.41	1.03	5.49	100.23	2.981	0.006	2.000	2.155	0.026	0.233	0.124	0.475	4.14	72.21	14.46	7.82	1.18	0.19
DOZ mélange	BO25gr004	36.96	0.12	20.85	31.77	13.78	0.40	6.74	100.65	2.978	0.007	1.979	1.414	0.053	0.940	0.048	0.562	1.63	47.44	16.68	31.54	2.47	0.25
DOZ mélange	BO25gr006	37.10	0.12	20.97	34.02	2.49	3.22	2.21	100.13	2.976	0.007	1.985	2.240	0.044	0.169	0.386	0.191	12.93	75.12	3.99	5.68	2.03	0.24
DOZ mélange	BO25gr007	37.71	0.11	21.15	26.92	2.15	2.00	10.06	100.16	2.993	0.006	1.978	1.763	0.026	0.144	0.236	0.855	7.89	58.85	27.20	4.82	1.02	0.21
DOZ mélange	BO25gr008	36.50	0.07	20.49	26.53	12.58	1.52	1.88	99.67	2.985	0.004	1.975	1.768	0.046	0.871	0.185	0.165	6.20	59.19	3.09	29.16	2.21	0.15
DOZ mélange	BO25gr009	36.95	0.18	20.73	25.63	10.18	3.23	2.60	99.54	2.980	0.011	1.971	1.683	0.046	0.695	0.388	0.225	13.01	56.37	4.94	23.28	2.02	0.37
DOZ mélange	BO25gr001	38.80	0.05	21.34	25.14	3.05	6.66	4.68	99.78	3.027	0.003	1.962	1.640	0.000	0.201	0.715	0.391	25.75	54.53	12.94	6.69	0.00	0.09
DOZ mélange	BO25gr002	38.21	0.27	21.47	31.32	0.11	6.93	1.28	99.61	3.005	0.016	1.990	2.060	0.000	0.007	0.873	0.108	27.17	68.84	3.21	0.24	0.00	0.54
DOZ mélange	BO25gr003	38.30	0.09	21.73	24.65	0.73	4.32	9.88	99.70	2.997	0.005	2.004	1.613	0.000	0.048	0.504	0.828	16.82	53.87	27.53	1.61	0.00	0.18
DOZ mélange	BO25gr004	38.06	0.02	21.68	31.58	0.53	6.71	0.87	99.48	3.002	0.001	2.015	2.083	0.000	0.035	0.789	0.074	26.47	69.87	24.44	1.18	0.00	0.04
DOZ mélange	BO25gr005	38.49	0.13	21.36	23.36	1.27	4.43	10.45	99.53	3.014	0.008	1.971	1.530	0.000	0.084	0.517	0.876	17.18	50.83	28.93	2.79	0.00	0.26
DOZ mélange	BO25gr006	38.38	0.12	21.48	24.60	1.17	4.25	9.90	99.91	3.001	0.004	1.980	1.607	0.003	0.077	0.496	0.829	16.49	53.44	27.27	2.57	0.00	0.24
DOZ mélange	BO25gr007	37.98	0.07	21.36	25.79	0.76	3.39	10.11	99.47	2.999	0.004	1.988	1.698	0.006	0.051	0.399	0.856	13.29	56.56	28.11	1.70	0.20	0.14
DOZ mélange	BO25gr008	38.69	0.05	21.65	22.15	0.75	6.11	10.26	99.73	2.990	0.003	1.972	1.390	0.042	0.049	0.704	0.450	21.93	64.46	26.24	1.64	2.05	0.09
DOZ mélange	BO25gr009	37.28	0.03	21.08	32.13	1.41	2.98	4.87	99.78	2.986	0.002	1.972	1.119	0.034	0.096	0.356	0.418	11.93	70.92	12.24	3.20	1.65	0.06
DOZ mélange	BO25gr010	39.89	0.05	22.43	17.40	0.81	10.23	8.82	99.63	3.002	0.003	1.990	1.995	0.001	0.052	0.148	0.711	38.19	53.72	26.42	5.28	0.00	0.33
DOZ mélange	BO25gr011	39.55	0.21	20.88	18.48	13.28	0.74	8.50	99.75	3.027	0.013	1.984	1.246	0.000	0.907	0.988	0.734	3.00	41.82	24.33	30.43	0.00	0.42
DOZ mélange	BO25gr012	39.11	0.05	22.14	17.83	0.65	8.68	10.32	98.82	2.989	0.003	1.984	1.117	0.023	0.042	0.988	0.845	33.05	37.34	27.03	1.41	1.07	0.10
DOZ mélange	BO25gr014	37.87	0.03	21.40	25.47	1.16	5.90	6.62	98.52	2.991	0.002	1.992	1.660	0.023	0.078	0.695	0.560	23.23	55.49	17.55	2.60	1.08	0.07
DOZ mélange	BO25gr015	38.86	0.08	21.04	27.55	0.58	5.92	5.97	100.13	3.034	0.005	1.936	1.799	0.000	0.039	0.689	0.499	22.75	59.44	16.37	1.27	0.00	0.16
DOZ mélange	BO25gr016	38.14	0.09	21.50	24.04	3.00	3.00	10.38	100.21	2.998	0.005	1.981	1.578	0.003	0.199	0.352	0.874	11.73	52.57	28.86	6.64	0.00	0.18
DOZ mélange	BO25gr017	37.69	0.10	21.18	28.40	1.16	2.98	8.54	100.17	2.984	0.006	1.976	1.835	0.045	0.078	0.352	0.725	11.77	61.45	21.85	2.61	2.12	0.19
DOZ mélange	BO25gr018	39.89	0.05	22.43	17.40	0.81	10.23	8.82	99.63	3.002	0.003	1.990	1.995	0.001	0.052	0.148	0.711	38.19	53.72	26.42	5.28	0.00	0.33
DOZ mélange	BO25gr019	37.84	0.04	21.32	32.53	0.98	5.05	1.98	99.77	3.007	0.002	1.987	2.161	0.000	0.066	0.598	0.169	19.99	72.17	5.57	2.20	0.00	0.08
DOZ mélange	BO25gr020	38.64	0.21	21.44	22.84	1.58	5.27	9.96	99.98	3.000	0.012	1.982	1.470	0.014	0.004	0.610	0.829	20.29	48.89	26.59	3.46	0.38	0.40
DOZ mélange	BO25gr021	38.90	0.07	21.60	23.38	0.92	6.09	8.95	99.93	3.009	0.004	1.989	1.508	0.005	0.061	0.703	0.742	23.34	50.07	24.30	2.01	0.14	0.14
DOZ mélange	BO25gr022	37.81	0.03	21.22	30.65	1.34	5.96	1.36	99.44	3.001	0.002	1.985	2.092	0.009	0.090	0.828	0.800	27.56	44.52	26.52	1.24	0.00	0.16
DOZ mélange	BO25gr023	38.10	0.09	21.42	22.62	0.61	6.44	9.22	99.20	3.012	0.005	1.980	1.665	0.004	0.040	0.776	0.853	25.78	44.63	28.21	1.32	0.00	0.14
DOZ mélange	BO25gr030	39.33	0.07	21.52	20.85	0.57	6.76	10.32	99.48	3.031	0.004	1.955	1.344	0.000	0.337	0.776	0.853	25.78	44.63	28.21	1.32	0.00	0.14
DOZ mélange	BO25gr024	38.32	0.16	21.40	24.37	2.37	3.63	9.44	99.72	3.018	0.010	1.987	1.605	0.000	0.158	0.426	0.797	14.25	53.72	26.42	5.28	0.00	0.33
DOZ mélange	BO25gr025	38.72	0.10	21.71	21.83	0.82	4.89	12.05	100.19	2.992	0.006	1.977	1.383	0.028	0.054	0.563	0.998	18.80	46.17	31.78	1.90	1.27	0.19
DOZ mélange	BO25gr026	38.71	0.11	21.42	25.19	0.82	5.61	8.25	100.12	3.006	0.006	1.961	1.622	0.014	0.054	0.650	0.686	21.60	53.91	21.94	1.79	0.56	0.21
DOZ mélange	BO25gr027	39.15	0.09	21.84	20.79	0.57	7.22	9.71	99.37	3.012	0.002	1.980	1.827	0.000	0.037	0.828	0.800	27.56	44.52	26.52	1.24	0.00	0.16
DOZ mélange	BO25gr028	37.81	0.03	21.22	30.65	1.34	5.96	1.36	99.44	3.001	0.002	1.985	2.092	0.009	0.090	0.828	0.800	27.56	44.52	26.52	1.24	0.00	0.16
DOZ mélange	BO25gr032	38.79	0.10	21.42	22.62	0.61	6.44	9.22	99.20	3.012	0.005	1.980	1.665	0.004	0.040	0.776	0.853	25.78	44.63	28.21	1.32	0.00	0.14
DOZ mélange	BO25gr031	39.01	0.05	21.91	25.64	1.22	8.31	3.83	100.05	3.005	0.003	1.989	1.652	0.000	0.080	0.965	0.316	31.79	54.58	25.11	1.32	0.05	0.20
DOZ mélange	BO25gr032	37.27	0.08	20.88	32.22	4.15	2.68	2.45	99.74	3.011	0.005	1.988	2.177	0.000	0.284	0.323	0.212	10.77	72.64	6.97	9.47	0.00	0.16
DOZ mélange	BO25gr033	37.91	0.10	21.08	27.51	1.42	2.86	8.60	99.76	3.011	0.006	1.973	1.827	0.000	0.095	0.650	0.686	21.60	53.91	21.94	1.79	0.56	0.21
DOZ mélange	BO25gr034	37.15	0.07	20.80	30.80	0.54	3.03	2.89	99.98	2.987	0.004	1.972	2.026	0.045	0.371	0.363	0.232	12.15	60.67	5.38	12.40	2.15	0.15
DOZ mélange	BO25gr035	39.29	0.10	22.06	20.30	0.60	7.50	10.18	100.04	2.995	0.006	1.982	1.278	0.016	0.039	0.852	0.832	28.44	42.62	26.78	1.30	0.68	0.19
DOZ mélange	BO25gr036	37.95	0.23	21.16	25.45	0.30	2.75	11.48	99.37	3.006	0.014	1.975	1.685	0.000	0.020	0.325	0.975	10.80	56.02	32.05	0.67	0.00	0.46
DOZ mélange	BO25gr037	39.17	0.07	21.64	19.24	0.80	6.17	12.25	99.46	3.018	0.004	1.966	1.240	0.000	0.052	0.709	1.011	23.52	41.15	33.46	1.73	0.00	0.14
DOZ mélange	BO25gr038	39.00	0.06	22.09	19.47	0.95	6.80	11.35	99.75	2.987	0.002	1.984	1.221	0.026	0.061	0.776	0.931	25.97	40.86	29.77	2.06	1.23	0.11
DOZ mélange	BO25gr039	36.65	0.18	20.78	20.22	15.34	2.70	3.47	99.33	2.984	0.011	1.980	1.288	0.070	0.105	0.326	0.301	10.97	43.70	6.33	35.39	3.24	0.36
DOZ mélange	BO25gr040	39.11	0.06	22.15	19.68	0.66	7.07	10.94	99.68	2.993	0.003	1.988	1.250	0.009	0.043	0.807	0.897	26.94	41.74	29.40	1.43	0.38	0.11
DOZ mélange	BO25gr041	38.91	0.09	21.58	21.53	0.57	6.94	9.69	99.31	3.004	0.005	1.963	1.372	0.018	0.037	0.799	0.801	26.57	45.63	25.63	1.24	0.76	0.18
DOZ mélange	BO25gr042	40.57	0.02	23.19	15.27	0.73	14.78	4.77	99.35	2.993	0.001	2.017	0.942	0.000	0.046	1.625	0.377	54.36	31.51	12.58	1.53	0.00	0.03
DOZ mélange	BO25gr043	37.16	0.03	20.84	34.67	1.44	2.00	4.09	100.24	2.993	0.002	1.978	2.303	0.032	0.098	0.240	0.353	8.03	76.91	10.14	3.29	1.57	0.06
DOZ mélange	BO25gr044	37.80	0.17	21.07	25.54	1.47	2.47	11.01	99.58	2.999	0.010	1.970	1.684	0.011	0.099	0.292	0.936	9.71	56.04	30.35	3.28	0.29	0.34
DOZ mélange	BO25gr045	38.61	0.07	21.34	24.24	0.94	5.28	9.30	99.83	3.007	0.004	1.969	1.561	0.018	0.062	0.613	0.776	20.36	51.86	24.78	2.05	0.81	0.14
DOZ mélange	BO25gr046	37.07	0.25	21.20	14.02																		

Formation	Sample & spot ID	analyses in wt.%				cations per formula unit on the basis of 12 oxygens									garnet end member molecules [%]						adr	scho
		SiO <sub>2</sub>	TiO <sub>2</sub>	Al <sub>2</sub> O <sub>3</sub>	FeO	MnO	MgO	CaO	Total	Si	Ti	Al	Fe <sup>2+</sup>	Fe <sup>3+</sup>	Mn	Mg	Ca	prp	alm	grs		
DOZ mélange	BO25grt063	37.93	0.14	21.06	27.89	0.95	2.59	9.34	99.97	3.009	0.008	1.969	1.850	0.000	0.064	0.307	0.794	10.16	61.34	26.12	2.11	0.00
DOZ mélange	BO25grt064	38.69	0.09	21.42	24.77	1.37	3.47	10.75	100.28	3.025	0.005	1.974	1.600	0.000	0.091	0.404	0.901	13.49	53.39	29.92	2.11	0.00
DOZ mélange	BO25grt065	38.24	0.12	21.50	23.73	0.86	5.19	10.02	99.67	2.978	0.007	1.973	1.489	0.056	0.057	0.603	0.836	20.21	49.94	25.05	1.91	2.65
DOZ mélange	BO25grt066	37.76	0.12	21.07	28.23	1.64	2.59	8.64	100.05	2.997	0.007	1.971	1.853	0.021	0.110	0.306	0.735	10.20	61.75	23.26	3.67	0.87
DOZ mélange	BO25grt067	40.95	0.03	23.25	14.48	0.51	14.81	5.33	99.45	3.014	0.000	2.017	0.891	0.000	0.032	1.624	0.421	54.73	30.02	14.13	1.07	0.00
DOZ mélange	BO25grt068	38.34	0.06	21.25	24.20	1.84	4.22	9.79	99.70	3.007	0.004	1.964	1.572	0.015	0.123	0.493	0.822	16.39	52.26	26.50	4.07	0.65
DOZ mélange	BO25grt069	38.71	0.11	21.31	23.90	1.33	5.46	9.13	99.95	3.008	0.006	1.952	1.535	0.019	0.088	0.632	0.760	20.99	50.96	24.15	2.92	0.78
DOZ mélange	BO25grt070	39.17	0.01	22.26	21.04	0.73	9.05	7.32	99.59	2.985	0.001	1.999	1.312	0.028	0.047	1.029	0.588	34.45	43.95	18.58	1.58	1.41
DOZ mélange	BO25grt071	37.37	0.04	20.59	31.33	2.35	1.35	6.64	99.74	3.021	0.003	1.961	1.716	0.007	0.161	0.162	0.575	5.38	70.22	13.98	5.32	0.00
DOZ mélange	BO25grt072	38.53	n.d.	21.36	27.28	1.23	6.20	5.64	99.78	3.012	0.004	1.968	1.776	0.007	0.081	0.723	0.432	23.99	58.97	13.98	2.69	0.37
DOZ mélange	BO25grt073	38.99	0.06	21.62	20.73	1.41	7.25	9.86	99.96	3.012	0.004	1.968	1.338	0.002	0.024	0.835	0.816	27.70	44.38	26.92	0.89	0.00
DOZ mélange	BO25grt074	37.62	0.20	21.01	26.69	1.39	4.47	8.34	98.78	3.006	0.012	1.978	1.783	0.000	0.094	0.413	0.714	17.74	59.30	23.44	3.14	0.00
DOZ mélange	BO25grt075	37.81	0.06	21.31	30.62	1.57	4.48	10.06	100.06	2.996	0.003	1.990	2.019	0.011	0.105	0.495	0.380	16.50	67.35	12.07	3.52	0.44
DOZ mélange	BO25grt076	38.41	0.09	21.48	24.81	1.20	4.57	9.44	99.97	2.999	0.005	1.977	1.605	0.015	0.079	0.530	0.790	17.56	53.49	25.44	2.64	0.59
DOZ mélange	BO25grt077	36.98	0.05	21.05	36.46	1.10	2.85	10.38	99.96	3.001	0.007	1.988	1.419	0.000	0.030	0.682	0.858	22.77	47.37	28.46	1.17	0.00
DOZ mélange	BO25grt078	38.00	0.15	21.22	27.19	1.67	3.74	7.78	99.75	3.005	0.009	1.977	1.798	0.010	0.112	0.440	0.659	14.62	59.70	21.66	3.72	0.00
DOZ mélange	BO25grt084	37.29	0.14	21.07	29.88	3.02	1.48	7.29	100.22	2.989	0.009	1.991	1.990	0.014	0.205	0.177	0.626	5.91	66.47	20.00	6.86	0.47
DOZ mélange	BO25grt085	41.03	0.02	23.16	13.04	0.57	14.49	7.25	99.62	3.008	0.001	2.001	0.800	0.000	0.035	1.584	0.570	52.99	26.75	19.04	1.18	0.00
DOZ mélange	BO25grt086	38.53	0.11	21.70	22.57	1.08	6.63	8.73	99.34	2.986	0.006	1.983	1.431	0.032	0.071	0.766	0.725	25.64	47.85	22.47	2.36	1.47
DOZ mélange	BO25grt087	37.29	0.09	20.51	26.27	0.88	10.59	10.42	99.67	2.991	0.004	2.000	0.926	0.017	0.052	0.180	0.466	6.78	58.79	15.23	19.02	0.00
DOZ mélange	BO25grt088	38.38	0.07	21.59	31.32	0.84	6.18	1.87	100.37	3.010	0.004	1.996	2.055	0.000	0.066	0.722	0.157	24.15	68.69	5.15	1.87	0.00
DOZ mélange	BO25grt089	39.27	0.03	22.25	23.13	1.01	9.62	4.22	99.52	3.004	0.002	2.006	1.480	0.000	0.065	1.098	0.346	36.73	49.51	11.52	2.18	0.00
DOZ mélange	BO25grt090	37.96	0.06	21.25	28.09	1.31	3.67	7.30	99.66	3.008	0.002	1.985	1.862	0.000	0.088	0.433	0.620	14.43	61.98	20.54	2.92	0.00
DOZ mélange	BO25grt091	36.77	0.04	20.65	28.45	0.95	2.28	1.59	99.79	2.998	0.004	1.978	1.891	0.043	0.685	0.276	0.138	9.23	63.26	14.03	22.92	2.07
DOZ mélange	BO25grt092	37.69	0.20	21.03	28.87	1.08	3.65	7.25	99.77	2.998	0.012	1.965	1.880	0.035	0.072	0.432	0.616	14.42	62.78	18.55	2.41	1.44
DOZ mélange	BO25grt093	40.03	0.07	22.71	15.08	0.82	10.59	10.42	99.67	2.991	0.004	2.000	0.926	0.017	0.052	0.180	0.466	6.78	58.79	15.23	19.02	0.00
DOZ mélange	BO25grt094	36.87	0.07	20.75	31.01	5.58	4.75	99.90	1.000	0.004	1.992	2.111	0.000	0.385	1.091	0.834	39.44	30.95	27.02	1.74	0.81	
DOZ mélange	BO25grt095	39.63	0.03	22.24	18.45	0.73	9.87	8.38	99.33	3.002	0.004	1.986	1.162	0.007	0.047	1.115	0.680	37.12	38.69	22.27	1.56	0.30
DOZ mélange	BO25grt096	37.30	0.06	20.85	31.74	1.88	1.88	6.19	99.91	2.999	0.002	1.976	2.117	0.018	0.128	0.225	0.533	7.49	70.53	16.78	4.27	0.82
DOZ mélange	BO25grt097	38.56	0.07	21.59	26.67	1.08	6.08	5.76	99.86	3.009	0.004	1.986	1.741	0.000	0.071	0.708	0.482	23.57	57.98	15.96	2.37	0.00
DOZ mélange	TD19grt001	37.20	0.08	21.10	34.55	2.16	1.50	3.98	100.57	2.995	0.005	2.002	2.327	0.000	0.147	0.180	0.343	6.01	77.59	11.33	4.91	0.00
DOZ mélange	TD19grt002	37.25	0.10	20.89	25.97	1.173	0.753	4.12	100.78	3.006	0.004	1.987	1.753	0.000	0.802	0.091	0.356	3.02	58.39	11.70	26.71	0.00
DOZ mélange	TD19grt003	37.91	0.02	21.34	31.55	2.23	5.48	1.82	100.35	2.989	0.001	1.983	1.946	0.034	0.177	0.644	0.154	21.54	68.33	3.22	4.98	0.03
DOZ mélange	TD19grt004	36.71	0.02	20.87	29.14	8.96	2.66	1.14	99.50	2.992	0.001	1.988	2.046	0.034	0.617	0.322	0.099	10.80	85.22	1.57	20.67	1.88
DOZ mélange	TD19grt005	37.21	0.12	20.44	15.64	22.28	0.69	3.79	100.17	3.024	0.007	1.958	1.063	0.000	1.534	0.083	0.330	2.77	35.29	10.78	50.92	0.00
DOZ mélange	TD19grt006	38.29	0.04	21.76	27.71	2.73	8.16	0.88	99.57	2.986	0.002	2.000	1.796	0.021	0.180	0.949	0.073	31.74	59.76	1.26	6.03	1.07
DOZ mélange	TD19grt007	36.87	0.02	20.91	35.25	3.00	2.01	1.87	100.03	2.990	0.004	1.998	2.371	0.020	0.206	0.243	0.171	8.13	79.28	4.70	6.89	0.97
DOZ mélange	TD19grt008	37.06	0.10	20.87	18.03	19.92	0.55	3.88	100.20	3.012	0.006	1.999	1.225	0.000	1.371	0.066	0.320	2.21	41.06	10.56	45.95	0.00
DOZ mélange	TD19grt009	36.64	0.07	20.72	26.85	12.69	1.32	1.81	100.11	2.984	0.004	1.989	1.794	0.035	0.875	0.161	0.158	5.39	60.07	3.40	29.31	1.67
DOZ mélange	TD19grt010	37.77	0.03	21.26	33.23	2.78	4.14	1.29	100.50	3.005	0.002	1.994	2.211	0.000	0.187	0.846	0.090	28.48	64.31	0.00	4.08	0.90
DOZ mélange	TD19grt011a	37.90	0.05	21.51	30.01	1.78	7.13	1.05	99.43	2.983	0.003	1.985	1.942	0.019	0.275	0.162	0.415	5.40	71.68	13.42	9.15	0.17
DOZ mélange	TD19grt011b	37.98	0.05	21.50	30.17	1.76	7.24	1.03	99.73	2.979	0.003	1.988	1.932	0.047	0.117	0.847	0.087	28.39	64.78	0.39	3.92	2.37
DOZ mélange	TD19grt011c	37.78	0.06	21.38	30.05	1.79	7.15	1.04	99.25	2.979	0.003	1.987	1.934	0.049	0.120	0.840	0.088	28.19	64.87	0.42	4.01	2.36
DOZ mélange	TD19grt011d	37.85	0.04	21.55	30.11	1.80	7.22	1.08	99.65	2.971	0.002	1.984	1.918	0.059	0.120	0.845	0.091	28.42	64.50	0.00	4.03	2.95
DOZ mélange	TD19grt011e	37.78	0.04	21.56	30.07	1.82	7.22	1.07	99.56	2.968	0.002	1.987	1.914	0.062	0.121	0.846	0.090	28.48	64.31	0.00	4.08	2.90
DOZ mélange	TD19grt012	36.99	0.08	20.83	31.81	4.00	1.34	4.78	99.83	2.997	0.005	1.989	2.151	0.005	0.275	0.162	0.415	5.40	71.68	13.42	9.15	0.17
DOZ mélange	TD19grt013	36.40	0.11	20.82	35.89	2.11	1.35	2.90	99.58	2.973	0.007	2.004	2.415	0.036	0.146	0.165	0.254	5.53	81.15	6.53	4.90	1.66

Formation	Sample & spot ID	analyses in wt%				cations per formula unit on the basis of 12 oxgens										garnet end member molecules %						adr	scho
		SiO <sub>2</sub>	TiO <sub>2</sub>	Al <sub>2</sub> O <sub>3</sub>	FeO	MnO	MgO	CaO	Total	Si	Ti	Al	Fe <sup>2+</sup>	Fe <sup>3+</sup>	Mn	Mg	Ca	prpl	alm	grs	spss		
DOZ mélange	TD197gr020	37.82	0.00	21.46	31.22	3.63	4.43	1.86	100.42	2.998	0.000	2.070	0.000	0.244	0.524	0.158	17.47	69.08	5.21	8.13	0.06	0.00	
DOZ mélange	TD197gr021	36.49	0.24	20.31	18.48	22.62	1.33	0.72	100.19	2.979	0.015	1.954	0.058	1.564	0.162	0.063	5.43	39.11	0.00	52.36	1.38	0.49	
DOZ mélange	TD197gr022	36.75	0.02	20.95	33.52	5.43	2.25	1.00	99.91	2.984	0.001	2.005	0.024	0.373	0.272	0.087	9.12	75.45	1.63	12.51	1.21	0.00	
DOZ mélange	TD197gr023	37.14	0.03	20.87	34.42	2.63	1.80	3.08	99.97	3.008	0.002	1.992	0.000	1.180	0.217	0.267	7.25	77.80	8.80	6.02	0.07	0.00	
DOZ mélange	TD197gr024	36.71	0.11	20.42	16.52	23.52	0.91	1.82	100.01	2.999	0.007	1.966	0.020	1.628	0.110	0.159	3.67	36.92	4.10	54.19	0.85	0.23	
DOZ mélange	TD197gr025	38.67	0.02	22.10	23.40	2.26	8.44	4.67	99.56	2.980	0.001	2.007	0.030	0.148	0.970	0.386	32.53	49.60	11.41	4.95	1.48	0.03	
DOZ mélange	TD197gr026	36.87	0.07	20.98	26.06	12.57	2.29	3.15	99.99	2.997	0.004	2.004	0.013	0.863	0.277	0.099	9.25	58.63	2.57	28.86	0.94	0.15	
DOZ mélange	TD197gr027	38.04	0.05	21.18	27.63	3.59	5.83	3.44	99.76	2.995	0.003	1.966	0.035	0.239	0.684	0.290	22.82	59.49	7.73	7.98	1.81	0.10	
DOZ mélange	TD197gr028	38.48	0.29	22.08	26.53	1.19	7.72	3.20	99.48	2.990	0.007	2.023	0.000	0.078	0.895	0.267	30.16	58.14	8.40	2.63	0.00	0.56	
DOZ mélange	TD197gr029	38.16	0.14	21.80	28.57	0.83	8.55	1.03	99.07	2.980	0.018	2.007	0.014	0.055	0.896	0.066	33.32	61.99	1.81	1.83	0.67	0.27	
DOZ mélange	TD197gr031	37.96	0.01	21.47	31.71	2.26	6.02	0.74	100.17	2.991	0.001	1.994	0.019	0.151	0.707	0.063	23.61	69.14	0.95	5.04	1.11	0.02	
DOZ mélange	TD197gr032	37.23	0.08	20.87	25.18	12.85	0.79	3.17	100.17	3.026	0.005	2.000	0.000	0.885	0.096	0.276	3.22	57.65	9.14	29.80	0.00	0.17	
DOZ mélange	TD197gr033	36.64	0.05	20.94	34.47	4.77	2.01	1.12	100.00	2.978	0.003	2.006	0.031	0.328	0.244	0.097	8.17	77.55	1.53	11.02	1.57	0.11	
DOZ mélange	TD197gr034	38.14	0.00	21.71	28.33	1.91	7.16	2.65	99.90	2.975	0.000	1.996	0.020	0.126	0.833	0.231	27.98	60.31	4.70	4.24	2.74	0.00	
DOZ mélange	TD197gr035	36.17	0.04	20.58	26.72	14.52	1.07	0.40	99.80	2.972	0.021	1.993	0.053	1.011	0.131	0.035	4.99	60.49	0.00	33.87	0.11	0.70	
DOZ mélange	TD197gr036	36.41	0.08	20.67	28.39	9.24	2.42	1.86	99.27	2.965	0.005	2.003	0.057	0.637	0.294	0.162	9.90	63.21	2.40	21.47	2.83	0.16	
DOZ mélange	TD197gr037	36.66	0.10	20.69	15.03	26.29	1.07	0.25	100.08	2.998	0.006	1.994	0.028	0.821	0.130	0.022	4.33	34.24	0.58	60.66	0.00	0.20	
DOZ mélange	TD197gr038	36.49	0.12	20.17	19.08	22.46	0.95	0.69	99.96	2.994	0.007	1.951	0.046	1.561	0.116	0.061	3.87	41.70	0.00	52.07	1.66	0.24	
DOZ mélange	TD197gr039	36.87	0.05	20.67	29.77	8.55	2.42	1.21	99.54	3.000	0.003	1.982	0.011	0.589	0.294	0.106	9.78	67.11	2.88	19.63	0.49	0.10	
DOZ mélange	TD197gr040a	37.09	0.13	20.92	34.80	0.96	1.83	4.17	99.90	2.998	0.008	1.993	0.000	0.066	0.221	0.361	7.35	78.37	11.81	2.19	0.00	0.26	
DOZ mélange	TD197gr040b	37.11	0.12	20.99	35.10	0.95	1.79	4.12	100.18	2.993	0.007	1.995	0.003	0.065	0.215	0.356	7.18	78.88	11.49	2.16	0.00	0.22	
DOZ mélange	TD197gr040c	37.22	0.11	20.91	35.23	0.93	1.83	4.10	100.32	2.998	0.007	1.985	0.005	0.063	0.220	0.354	7.32	78.85	11.27	2.10	0.19	0.22	
DOZ mélange	TD197gr040d	37.11	0.12	21.14	35.44	0.85	1.86	3.92	100.44	2.985	0.007	2.004	0.011	0.058	0.223	0.338	7.46	79.38	10.51	1.94	0.44	0.24	
DOZ mélange	TD197gr041	36.02	0.10	19.83	14.22	28.55	0.35	0.46	99.52	2.985	0.002	1.937	0.082	2.004	0.043	0.040	1.45	27.32	0.00	67.07	1.04	0.21	
DOZ mélange	TD197gr042	36.85	0.13	21.07	34.77	3.73	2.75	0.80	100.11	2.978	0.008	2.007	0.020	0.255	0.331	0.070	11.11	78.10	1.06	8.56	0.86	0.27	
DOZ mélange	TD197gr043	38.55	0.02	21.87	30.32	0.71	7.08	2.28	100.68	2.990	0.004	1.999	0.015	0.047	0.819	0.173	27.35	65.34	5.06	1.56	0.52	0.13	
DOZ mélange	TD197gr044	37.04	0.07	20.89	26.25	12.63	2.20	1.21	100.24	2.996	0.000	1.992	0.015	0.865	0.265	0.105	8.85	58.77	2.76	28.88	0.71	0.03	
DOZ mélange	TD197gr045	37.37	0.04	21.27	35.34	0.92	2.90	2.48	100.32	2.996	0.002	2.010	0.000	0.062	0.347	0.213	11.59	79.20	7.03	2.09	0.00	0.08	
DOZ mélange	TD197gr046	38.60	0.06	21.73	24.69	0.44	5.71	8.39	99.62	3.004	0.003	1.993	0.000	0.029	0.663	0.700	22.09	53.59	23.22	0.96	0.00	0.11	
DOZ mélange	TD197gr047	37.63	0.01	21.00	34.34	3.26	3.35	1.01	100.60	3.012	0.000	1.981	0.000	0.221	0.400	0.086	13.30	76.47	2.82	7.35	0.01	0.03	
DOZ mélange	TD197gr048	37.97	0.05	21.41	33.79	1.77	4.56	1.15	100.70	3.006	0.003	1.998	0.000	0.119	0.538	0.098	17.99	74.77	3.13	3.97	0.00	0.09	
DOZ mélange	TD197gr049	37.36	0.06	20.83	35.47	3.77	2.16	0.94	100.59	3.016	0.002	1.982	0.000	0.258	0.260	0.868	8.68	79.94	2.46	8.61	0.08	0.12	
DOZ mélange	TD197gr050	38.98	0.05	21.82	29.65	0.76	8.03	1.16	100.45	3.016	0.002	1.990	0.000	0.050	0.926	0.096	30.97	64.14	3.10	1.66	0.00	0.11	
DOZ mélange	TD197gr051	37.50	0.04	21.26	35.09	1.31	3.27	1.53	100.00	3.013	0.003	2.013	0.000	0.089	0.392	0.132	13.18	79.37	4.34	3.00	0.00	0.08	
DOZ mélange	TD197gr052	38.36	0.09	21.55	30.22	1.65	6.78	1.52	100.17	3.001	0.005	1.987	0.000	0.109	0.791	0.127	26.31	65.79	4.03	3.64	0.00	0.17	
DOZ mélange	TD197gr053	36.77	0.05	20.81	28.91	11.02	1.39	0.42	100.38	2.995	0.003	1.998	0.005	0.760	0.169	0.037	16.65	67.80	0.84	25.37	0.22	0.11	
DOZ mélange	TD197gr055	38.10	0.10	21.25	32.95	2.02	4.75	1.00	100.62	3.013	0.006	1.981	0.000	0.135	0.560	0.123	18.68	72.70	3.82	4.51	0.00	0.19	
DOZ mélange	TD197gr056	38.90	0.06	21.67	24.87	0.58	8.29	5.11	99.48	3.002	0.004	1.971	0.014	0.038	0.954	0.423	31.71	52.92	13.09	11.25	0.77	0.12	
DOZ mélange	TD197gr057	36.75	0.15	20.66	34.01	4.82	2.00	1.13	99.52	3.002	0.009	1.989	0.000	0.334	0.244	0.059	8.12	77.42	3.03	11.11	0.00	0.30	
DOZ mélange	TD197gr058	37.56	0.01	21.15	34.05	2.24	3.72	1.37	100.10	3.008	0.001	1.996	0.000	0.152	0.444	0.117	14.83	76.15	3.83	5.07	0.06	0.02	
DOZ mélange	TD197gr059	38.03	0.04	21.41	32.54	1.16	5.97	1.07	100.21	2.996	0.002	1.988	0.014	0.077	0.701	0.090	23.39	71.04	2.21	2.57	0.69	0.07	
DOZ mélange	TD197gr060	37.47	0.02	21.38	31.52	4.83	3.64	1.53	100.39	2.991	0.001	2.012	0.003	0.327	0.433	0.131	14.47	70.22	4.14	10.91	0.18	0.04	
DOZ mélange	TD197gr061	36.89	0.07	20.88	30.11	9.21	2.00	0.87	100.02	2.997	0.004	1.999	0.000	0.634	0.242	0.075	8.08	68.25	2.33	21.14	0.00	0.14	
DOZ mélange	TD197gr062a	36.66	0.11	20.31	20.58	21.05	1.00	0.62	100.33	2.996	0.007	1.956	0.037	1.457	0.122	0.054	4.06	45.39	0.00	48.57	1.48	0.22	
DOZ mélange	TD197gr062b	36.44	0.13	20.28	20.52	21.15	1.04	0.61	100.17	2.993	0.008	1.956	0.060	1.466	0.127	0.053	4.24	43.45	0.00	49.07	1.38	0.27	
DOZ mélange	TD197gr062c	36.61	0.15	20.26	20.66	20.96	1.00	0.62	100.26	2.993	0.009	1.952	0.039	1.451	0.122	0.054	4.07	45.07	0.00	48.32	1.36	0.30	
DOZ mélange	TD197gr063	36.80	0.11	20.72	21.26	18.21	0.82	2.57	100.48	2.990	0.006	1.984	0.024	1.253	0.099	0.224	3.30	47.46	6.11	41.87	1.05	0.21	
DOZ mélange	TD197gr064	37.67	0.																				

Formation	Sample & spot ID	analyses in wt.%				cations per formula unit on the basis of 12 oxygens								garnet end member molecules %									
		SiO <sub>2</sub>	TiO <sub>2</sub>	Al <sub>2</sub> O <sub>3</sub>	FeO	MnO	MgO	CaO	Total	Si	Ti	Al	Fe <sup>2+</sup>	Fe <sup>3+</sup>	Mn	Mg	Ca	prp	alm	grs	sps	adr	schö
DOZ mélange	TD19/grt082	36.66	0.18	20.25	17.27	20.51	0.94	3.76	99.57	2.996	0.011	1.950	1.143	0.037	1.420	0.114	0.329	3.81	38.10	8.85	47.30	1.57	0.37
DOZ mélange	TD19/grt084	37.12	0.13	21.23	18.18	4.66	2.52	1.77	100.06	2.985	0.003	2.012	2.096	0.001	0.317	0.302	0.277	10.10	70.04	8.98	10.61	0.00	0.25
DOZ mélange	TD19/grt085	36.80	0.04	21.04	26.24	11.91	2.15	3.22	99.95	2.981	0.008	2.003	1.753	0.024	0.817	0.260	0.154	8.71	58.79	3.85	27.40	1.16	0.09
DOZ mélange	TD19/grt086	36.40	0.11	20.69	22.51	16.69	1.12	1.94	99.46	2.989	0.007	1.999	1.525	0.019	1.159	0.137	0.170	4.58	51.02	4.55	29.83	0.80	0.23
Ugar Fm.	BO117/grt002	36.22	0.10	20.33	25.75	16.77	1.50	1.95	98.72	2.989	0.006	1.978	1.746	0.031	0.893	0.184	0.172	6.16	68.35	4.03	38.63	1.43	0.20
Ugar Fm.	BO117/grt004	37.03	0.06	20.82	28.11	1.95	2.30	8.24	99.53	2.966	0.004	1.966	1.856	0.094	0.133	0.274	0.707	9.24	62.54	18.98	4.46	4.65	0.13
Ugar Fm.	BO117/grt005	36.71	0.08	20.68	34.80	1.21	1.71	4.42	99.67	2.979	0.002	1.979	2.309	0.053	0.083	0.207	0.384	6.96	77.45	10.10	2.78	2.95	0.16
Ugar Fm.	BO117/grt006	36.41	0.04	20.69	32.76	3.85	1.55	4.30	99.62	2.960	0.002	1.982	2.134	0.093	0.265	0.188	0.375	6.35	72.07	7.87	8.96	4.66	0.08
Ugar Fm.	BO117/grt008	36.29	0.07	20.60	30.32	1.25	1.01	9.08	98.93	2.952	0.004	1.982	1.956	0.106	0.086	0.123	0.791	4.15	66.23	21.27	5.30	1.03	0.13
Ugar Fm.	BO117/grt009	36.68	0.04	20.90	31.95	3.07	1.13	4.57	99.40	2.972	0.002	1.986	2.109	0.055	0.211	0.258	0.396	8.67	70.95	10.49	7.08	2.73	0.08
Ugar Fm.	BO117/grt012	36.64	0.04	20.65	33.49	2.90	1.16	4.79	99.75	2.981	0.002	1.980	2.225	0.054	0.200	0.141	0.471	4.72	74.62	11.24	6.70	2.64	0.08
Ugar Fm.	BO117/grt013	36.68	0.06	20.75	34.57	1.89	1.27	4.25	99.51	2.990	0.004	1.984	2.337	0.020	0.130	0.154	0.371	5.16	78.13	11.34	4.36	0.88	0.13
Ugar Fm.	BO117/grt015	36.14	0.03	20.62	33.55	2.56	1.59	4.38	98.87	2.988	0.002	1.989	2.205	0.092	0.178	0.194	0.384	6.54	74.51	8.28	6.00	4.61	0.06
Ugar Fm.	BO117/grt018	36.85	n.d.	20.53	29.81	3.65	0.92	7.26	99.22	2.986	0.008	1.971	1.988	0.043	0.252	0.111	0.642	3.73	66.51	19.13	8.43	1.97	0.25
Ugar Fm.	BO117/grt020	37.54	0.12	21.25	30.01	1.31	5.12	4.28	99.61	2.971	0.007	1.982	1.923	0.063	0.088	0.104	0.363	20.31	64.67	8.84	2.95	3.00	0.23
Ugar Fm.	BO117/grt021	36.73	n.d.	21.06	36.22	1.21	3.56	1.22	100.00	2.953	0.000	1.986	2.338	0.097	0.082	0.427	0.105	14.46	77.81	0.00	2.79	3.56	0.00
Ugar Fm.	BO16/grt003	37.09	0.11	20.70	31.97	1.32	1.76	6.28	99.23	3.004	0.007	1.976	2.162	0.004	0.090	0.163	0.755	14.08	71.90	17.78	3.01	0.02	0.22
Ugar Fm.	BO16/grt005	36.74	0.03	20.68	30.94	5.89	1.79	3.16	99.23	2.997	0.002	1.989	2.088	0.013	0.407	0.218	0.277	7.27	69.96	8.52	13.57	0.63	0.05
Ugar Fm.	BO16/grt006	37.23	0.01	20.84	32.94	3.58	3.01	2.16	99.79	3.003	0.001	1.981	2.210	0.012	0.245	0.362	0.186	12.05	73.60	5.62	8.15	0.96	0.02
Ugar Fm.	BO16/grt008	36.85	n.d.	20.85	33.61	2.41	2.76	2.42	99.08	3.000	0.000	2.001	2.288	0.000	0.166	0.334	0.211	11.15	76.28	7.03	5.53	0.00	0.01
Ugar Fm.	BO16/grt015	37.15	0.03	20.96	35.40	0.64	4.47	0.39	99.03	2.999	0.002	1.994	2.386	0.004	0.044	0.538	0.033	17.92	79.52	0.86	1.46	0.18	0.05
Ugar Fm.	BO16/grt018	37.30	0.04	20.81	15.35	18.96	3.29	3.26	99.00	3.010	0.002	1.979	1.036	0.000	0.296	0.395	0.281	13.14	34.42	9.30	43.07	0.00	0.08
Ugar Fm.	BO16/grt020	37.28	0.16	20.96	30.47	0.53	1.36	8.76	99.52	2.989	0.009	1.987	2.050	0.000	0.036	0.163	0.755	14.08	71.90	17.78	3.01	0.02	0.22
Ugar Fm.	BO16/grt023	37.41	0.02	21.20	34.24	0.91	4.15	1.64	99.59	3.000	0.001	2.004	2.296	0.000	0.062	0.496	0.141	16.57	76.65	4.68	2.07	0.00	0.03
Ugar Fm.	BO16/grt027	36.88	n.d.	20.76	34.05	1.53	3.56	1.95	98.75	2.995	0.000	1.987	2.296	0.000	0.105	0.105	0.189	14.38	76.44	4.52	3.32	1.13	0.00
Ugar Fm.	BO16/grt028	37.15	0.03	20.59	32.70	3.53	2.96	2.00	98.98	3.022	0.002	1.974	2.225	0.000	0.226	0.359	0.175	11.97	74.10	5.77	8.09	0.00	0.06
Ugar Fm.	BO16/grt045	38.36	0.07	21.37	27.46	0.31	3.88	1.83	99.39	2.993	0.004	2.002	1.826	0.000	0.021	0.460	0.674	15.44	61.23	22.48	0.71	0.00	0.13
Ugar Fm.	BO16/grt052	37.14	n.d.	20.86	33.59	1.22	3.60	2.28	98.79	3.011	0.000	1.993	1.757	0.000	0.243	0.860	0.157	28.68	58.59	4.83	7.53	0.31	0.06
Ugar Fm.	BO16/grt054	37.24	n.d.	21.18	34.88	0.98	3.74	1.59	99.66	2.995	0.000	2.007	2.343	0.000	0.067	0.436	0.198	14.55	76.05	6.59	2.80	0.00	0.01
Ugar Fm.	BO16/grt060	36.94	n.d.	20.95	33.80	3.32	2.17	2.25	99.43	3.005	0.000	2.008	2.289	0.000	0.229	0.263	0.196	8.80	76.98	6.57	7.65	0.00	0.00
Ugar Fm.	BO16/grt061	37.36	0.02	20.85	33.42	0.00	4.31	2.07	99.11	3.006	0.001	1.978	2.240	0.000	0.071	0.517	0.179	17.18	74.52	5.50	2.37	0.39	0.03
Vranduk Fm.	BO12/grt001	36.01	0.01	20.78	37.38	1.35	1.14	2.21	98.88	2.970	0.000	2.020	2.541	0.038	0.094	0.141	0.196	4.73	85.53	4.65	3.17	1.89	0.00
Vranduk Fm.	BO12/grt002	37.06	0.06	20.98	33.48	1.46	5.57	0.86	99.49	2.956	0.004	1.973	2.126	0.108	0.099	0.662	0.274	22.37	68.81	0.00	3.33	2.31	0.13
Vranduk Fm.	BO12/grt004	37.92	0.02	21.47	30.68	2.11	6.20	1.31	99.76	2.994	0.001	1.998	2.014	0.102	0.141	0.730	0.111	24.36	67.26	3.08	4.71	0.55	0.05
Vranduk Fm.	BO12/grt005	36.17	0.03	21.27	30.67	5.49	2.87	2.09	98.60	2.950	0.002	2.045	2.041	0.051	0.329	0.349	0.183	11.81	69.17	3.55	12.85	2.56	0.06
Vranduk Fm.	BO12/grt007	37.23	0.02	21.21	31.70	4.50	4.43	1.16	100.33	2.966	0.001	1.992	2.039	0.074	0.303	0.526	0.099	17.74	68.30	0.00	10.23	3.28	0.03
Vranduk Fm.	BO12/grt008	36.62	0.04	21.18	33.20	5.15	2.82	0.83	98.84	2.964	0.003	2.020	2.009	0.047	0.353	0.341	0.072	11.49	74.19	0.00	11.91	2.31	0.08
Vranduk Fm.	BO12/grt009	36.09	0.13	20.73	36.80	2.30	1.97	1.21	99.27	2.958	0.008	2.003	2.459	0.064	0.162	0.241	0.107	8.15	83.00	0.14	5.39	3.06	0.27
Vranduk Fm.	BO12/grt010	36.76	0.02	21.04	33.64	1.45	3.89	2.22	99.08	2.967	0.001	2.002	2.209	0.062	0.099	0.468	0.192	15.77	74.44	3.31	3.35	3.09	0.04
Vranduk Fm.	BO12/grt011	35.40	0.02	20.19	33.77	7.22	0.81	1.06	98.46	2.953	0.001	1.985	2.248	0.107	0.510	0.100	0.095	3.40	73.87	0.00	17.28	3.17	0.03
Vranduk Fm.	BO12/grt013	36.20	0.06	20.53	37.76	1.66	1.97	0.87	99.18	2.973	0.004	1.987	2.536	0.058	0.115	0.241	0.085	8.10	85.06	0.00	3.87	2.67	0.13
Vranduk Fm.	BO12/grt014	38.08	0.03	21.65	26.94	2.72	7.56	3.11	100.09	2.956	0.002	1.981	1.646	0.103	0.179	0.875	0.259	29.59	55.65	3.47	6.05	5.18	0.06
Vranduk Fm.	BO12/grt018	35.94	0.10	20.46	37.12	2.00	2.29	1.05	99.02	2.952	0.000	1.981	2.446	0.103	0.139	0.280	0.092	9.49	80.54	0.00	4.70	2.81	0.21
Vranduk Fm.	BO12/grt019	37.27	0.17	20.61	31.20	3.70	4.66	1.73	99.34	2.990	0.016	1.949	2.043	0.050	0.252	0.557	0.148	18.61	68.21	2.18	8.40	2.25	0.35
Vranduk Fm.	BO12/grt020	36.49	0.05	20.99	31.09	6.02	3.24	1.26	99.15	2.963	0.004	2.000	2.050	0.061	0.141	0.392	0.110	13.23	68.16	0.55	13.96	3.19	0.14
Vranduk Fm.	BO12/grt021	36.72	0.00	20.88	30.94	4.12	4.14	1.90	98.79	2.968	0.004	1.990	2.027	0.065	0.282	0.499	0.165	16.81	68.22	2.15	9.49	3.19	0.14
Vranduk Fm.	BO12/grt022	37.38	0.03	21.25	33.31	0.58	4.43	2.93	99.92	2.974	0.002	1.983	2.161	0.055	0.039	0.526	0.250	17.68	72.64	5.56	1.32	2.74	0.06
Vranduk Fm.	BO12/grt024	36.28	0.10	20.63	29.53	7.41	3.49	1.41	98.86	2.951	0.000	1.977	1.900	0.109	0.510	0.423	0.123	14.34	62.79	0.00	17.28	3.87	0.20
Vranduk Fm.	BO12/grt028	36.51	0.08	20.79	27.64	9.81	3.12	1.02	98.97	2.973	0.005	1.996	1.833	0.050	0.877	0.379	0.089	12.75	61.60	0.37	22.74	2.39	0.16
Vranduk Fm.	BO12/grt032	36.91	0.11	20.92	31.44	4.95	3.96	1.31	99.64	2.969	0.006	1.984	2.049	0.066	0.337	0.475	0.113	13.99	68.95	0.33	11.35	3.16	0.21
Vranduk Fm.	BO12/grt033	36.82	0.14	21.05	31.38	0.88	5.79	1.81	99.61	2.961	0.008	1.985	2.04										

Formation	Sample & spot ID	analyses in wt%				cations per formula unit on the basis of 12 oxygens										garnet end member molecules %					adr	scho	
		SiO <sub>2</sub>	TiO <sub>2</sub>	Al <sub>2</sub> O <sub>3</sub>	FeO	MnO	MgO	CaO	Total	Si	Ti	Al	Fe <sup>2+</sup>	Fe <sup>3+</sup>	Mn	Mg	Ca	prpl	alm	grs			sps
Vranduk Fm.	BO12gr065	36.99	0.06	20.94	31.17	4.85	3.94	1.40	99.34	2.991	0.004	1.989	2.059	0.042	0.331	0.473	0.121	15.87	69.04	1.87	11.11	1.99	0.12
Vranduk Fm.	BO12gr067	37.05	0.03	21.26	27.91	7.05	4.70	1.41	99.40	2.965	0.002	2.005	1.807	0.061	0.478	0.561	0.121	18.92	60.92	0.93	16.11	3.06	0.06
Vranduk Fm.	BO12gr068	37.35	0.04	21.05	30.89	3.22	5.31	1.13	99.10	2.991	0.002	1.987	2.043	0.026	0.218	0.634	0.097	21.20	68.28	1.88	7.30	1.26	0.07
Vranduk Fm.	BO12gr070	36.64	0.13	20.77	29.60	7.33	3.49	1.40	99.40	2.964	0.008	1.980	1.927	0.076	0.502	0.421	0.121	14.20	64.92	0.05	16.92	3.63	0.27
Vranduk Fm.	BO12gr071	36.86	0.02	20.97	33.15	1.88	3.60	2.82	99.30	2.970	0.001	1.991	2.167	0.067	0.128	0.432	0.244	14.55	72.95	4.81	4.31	3.34	0.04
Vranduk Fm.	BO12gr072	37.15	n. d.	21.03	33.11	0.50	4.44	2.88	99.24	2.979	0.000	1.988	2.168	0.053	0.034	0.530	0.247	17.80	72.76	5.61	1.14	2.69	0.00
Vranduk Fm.	BO12gr073	37.19	0.16	20.82	31.21	3.87	4.69	1.71	99.67	2.974	0.010	1.962	2.015	0.072	0.262	0.559	0.147	18.77	67.66	1.09	8.81	3.36	0.32
Vranduk Fm.	BO12gr074	36.72	0.05	20.85	31.24	5.82	3.26	1.27	99.22	2.979	0.003	1.993	2.077	0.043	0.400	0.394	0.140	13.24	69.69	1.46	13.42	2.10	0.10
Vranduk Fm.	BO12gr077	36.43	0.09	20.46	37.20	6.55	2.27	1.05	99.45	2.977	0.006	1.971	2.075	0.063	0.135	0.277	0.092	9.29	82.98	0.00	4.52	2.80	0.19
Vranduk Fm.	BO12gr078	36.69	0.05	20.90	30.36	1.99	3.59	0.93	99.12	2.976	0.003	1.988	2.015	0.045	0.450	0.434	0.080	14.56	67.67	0.37	15.12	2.17	0.11
Vranduk Fm.	BO12gr079	36.81	0.02	20.72	33.61	4.11	2.93	1.10	99.30	2.993	0.001	1.986	2.260	0.026	0.283	0.365	0.096	11.86	75.50	1.88	9.46	1.27	0.03
Vranduk Fm.	BO12gr082	36.39	0.05	20.69	34.50	3.80	2.39	1.33	99.21	2.974	0.003	1.983	2.306	0.052	0.263	0.289	0.116	9.80	77.49	1.21	8.85	2.55	0.10
Vranduk Fm.	BO12gr083	37.95	0.03	21.59	29.64	3.00	8.32	0.61	99.44	2.966	0.002	1.989	1.861	0.076	0.066	0.969	0.051	32.67	60.57	0.00	2.90	1.64	0.06
Vranduk Fm.	BO12gr084	36.21	0.02	20.70	37.70	1.25	1.17	2.24	99.32	2.975	0.001	2.004	2.549	0.042	0.087	0.143	0.198	4.82	85.65	4.48	2.91	2.09	0.05
Vranduk Fm.	BO12gr085	36.82	0.10	21.13	33.55	3.42	3.33	1.67	100.18	2.953	0.006	1.988	2.168	0.083	0.233	0.415	0.144	14.03	73.32	0.51	7.87	4.07	0.20
Vranduk Fm.	BO12gr087	36.64	0.05	20.75	34.42	3.69	2.52	1.44	99.55	2.980	0.003	1.989	2.298	0.044	0.254	0.306	0.126	10.25	77.05	1.93	8.53	2.15	0.10
Vranduk Fm.	BO12gr088	36.39	0.04	20.98	30.01	5.51	4.38	1.16	99.53	2.950	0.003	1.994	2.049	0.040	0.379	0.529	0.101	17.92	64.64	0.00	12.83	3.28	0.09
Vranduk Fm.	BO12gr089	36.59	0.07	20.88	30.58	4.96	4.23	1.24	99.58	2.967	0.004	1.996	2.011	0.062	0.341	0.511	0.107	17.22	67.75	0.37	11.48	3.05	0.14
Vranduk Fm.	BO12gr097	37.02	0.08	20.75	35.85	0.49	3.74	1.41	98.54	2.949	0.005	1.992	2.342	0.021	0.034	0.454	0.123	15.40	78.32	0.00	1.15	3.92	0.17
Vranduk Fm.	BO4gr002	37.90	0.03	21.37	31.42	4.52	4.20	1.70	101.23	2.993	0.002	1.989	2.054	0.101	0.302	0.484	0.144	16.51	89.10	0.00	3.73	10.10	0.98
Vranduk Fm.	BO4gr003	37.55	0.05	21.38	30.76	2.75	5.56	1.69	99.75	2.976	0.003	1.997	1.994	0.045	0.184	0.657	0.144	22.06	66.97	2.50	6.19	2.18	0.10
Vranduk Fm.	BO4gr004	37.27	0.04	21.15	34.72	0.69	4.16	1.87	99.99	2.980	0.002	1.993	2.279	0.042	0.047	0.496	0.160	16.62	76.46	3.19	1.57	2.08	0.07
Vranduk Fm.	BO4gr009	37.60	0.02	21.11	35.11	1.00	4.81	0.64	100.27	2.992	0.001	1.979	2.301	0.035	0.067	0.570	0.054	19.05	76.91	0.04	2.25	1.72	0.04
Vranduk Fm.	BO4gr013	37.77	0.01	21.41	31.75	2.04	4.07	3.56	100.67	2.986	0.000	1.985	2.069	0.031	0.136	0.480	0.302	16.08	69.27	8.53	4.57	1.54	0.02
Vranduk Fm.	BO4gr015	37.02	0.03	20.85	31.74	4.66	2.15	3.27	99.75	2.997	0.002	1.989	2.136	0.013	0.320	0.259	0.284	8.64	71.26	8.78	10.87	0.60	0.06
Vranduk Fm.	BO4gr017	37.10	0.09	21.48	31.69	2.02	4.01	3.56	99.99	2.954	0.005	1.998	2.043	0.067	0.136	0.476	0.304	16.10	89.10	0.00	4.60	3.27	0.17
Vranduk Fm.	BO4gr020	37.17	0.03	20.99	35.91	2.93	1.72	1.88	100.68	3.003	0.002	1.998	2.427	0.000	0.201	0.207	0.163	6.92	80.95	5.39	6.69	0.00	0.05
Vranduk Fm.	BO4gr021	36.97	0.13	21.01	31.74	2.00	4.02	3.55	99.60	2.961	0.008	1.984	2.049	0.077	0.136	0.480	0.305	16.17	69.11	6.17	4.58	3.71	0.27
Vranduk Fm.	BO4gr022	37.05	0.01	21.01	31.55	4.72	2.15	3.29	99.90	2.996	0.000	2.002	2.129	0.005	0.324	0.260	0.285	8.66	71.04	9.24	10.80	0.24	0.02
Vranduk Fm.	BO4gr025	36.78	0.03	20.84	34.20	1.75	3.62	1.87	99.13	2.977	0.002	1.988	2.261	0.054	0.120	0.437	0.162	14.66	75.91	2.65	4.02	2.70	0.06
Vranduk Fm.	BO4gr026	36.38	0.04	21.08	32.96	3.40	4.18	0.89	98.94	2.993	0.006	2.010	2.131	0.092	0.330	0.504	0.077	17.13	69.90	0.00	7.92	2.49	0.09
Vranduk Fm.	BO4gr027	37.08	0.09	20.80	34.41	1.58	3.51	1.82	98.31	2.997	0.006	1.982	2.314	0.111	0.108	0.423	0.157	14.11	77.13	4.48	3.61	0.48	0.19
Vranduk Fm.	BO72gr001	38.05	0.02	21.22	30.28	2.74	6.10	1.26	99.72	3.009	0.000	1.976	2.202	0.000	0.184	0.719	0.107	23.88	66.48	3.46	6.10	0.00	0.08
Vranduk Fm.	BO72gr004	37.54	0.04	21.23	33.50	1.74	4.69	1.14	99.93	2.995	0.001	1.996	2.223	0.012	0.117	0.558	0.098	18.63	74.21	2.63	3.92	0.58	0.03
Vranduk Fm.	BO72gr019	37.34	0.05	20.97	29.59	7.14	3.79	1.05	100.04	2.997	0.003	1.984	1.970	0.017	0.486	0.454	0.090	15.14	65.69	2.12	16.20	0.76	0.09
Vranduk Fm.	BO72gr020	37.09	0.02	21.05	30.69	4.81	4.37	1.37	99.41	2.987	0.001	1.992	2.012	0.049	0.327	0.523	0.118	17.55	67.53	1.45	10.96	2.46	0.00
Vranduk Fm.	BO72gr023	37.46	0.01	21.23	27.61	8.24	4.51	1.00	100.06	2.997	0.000	1.995	1.810	0.031	0.357	0.536	0.085	17.94	60.59	1.29	18.63	1.53	0.02
Vranduk Fm.	BO87gr001	36.55	0.03	20.74	33.98	5.19	2.10	0.94	99.56	2.985	0.002	1.996	2.280	0.030	0.359	0.255	0.083	8.55	76.70	1.20	12.01	1.46	0.07
Vranduk Fm.	BO87gr002	37.21	n. d.	21.23	28.65	7.46	3.90	1.34	99.85	2.984	0.006	2.006	1.896	0.025	0.507	0.466	0.115	15.63	63.54	2.59	16.98	1.25	0.00
Vranduk Fm.	BO87gr003	36.95	0.06	20.78	34.92	2.80	3.41	0.73	99.79	2.988	0.004	1.980	2.324	0.037	0.192	0.411	0.064	13.76	77.74	0.17	6.42	1.78	0.12
Vranduk Fm.	BO87gr004	37.06	n. d.	20.93	31.76	4.41	4.01	0.96	98.14	2.993	0.000	1.993	2.125	0.020	0.302	0.483	0.083	16.14	70.99	1.75	10.09	1.02	0.00
Vranduk Fm.	BO87gr005	36.53	n. d.	20.98	33.39	4.81	2.92	1.03	99.66	2.960	0.000	2.004	2.168	0.075	0.330	0.352	0.090	11.90	73.12	0.00	11.15	3.03	0.00
Vranduk Fm.	BO87gr006	37.76	0.45	21.12	26.65	1.04	5.25	6.84	99.11	2.982	0.026	1.966	1.742	0.018	0.069	0.618	0.578	20.65	58.17	17.76	2.32	0.22	0.88
Vranduk Fm.	BO87gr008	39.64	0.09	22.43	18.22	0.55	11.31	6.95	99.20	2.987	0.005	1.992	1.125	0.023	0.335	1.271	0.561	42.51	37.62	17.47	1.18	1.05	0.17
Vranduk Fm.	BO87gr010	37.26	0.07	21.01	30.96	1.78	3.17	5.68	100.03	2.972	0.004	1.975	1.994	0.072	0.121	0.376	0.486	12.66	67.03	12.59	4.05	3.54	0.14
Vranduk Fm.	BO87gr011	36.76	0.15	20.59	26.65	8.53	0.95	5.87	99.52</														

Formation	Sample & spot ID	analyses in wt%				cations per formula unit on the basis of 12 oxygens														garnet end member molecules %						adr	scho
		SiO <sub>2</sub>	TiO <sub>2</sub>	Al <sub>2</sub> O <sub>3</sub>	FeO	MnO	MgO	CaO	Total	Si	Ti	Al	Fe <sup>2+</sup>	Fe <sup>3+</sup>	Mn	Mg	Ca	prpl	alm	grs	sps						
Viranduk Fm.	B087grn038	36.75	0.03	20.94	33.48	1.82	3.32	2.71	99.15	2.974	0.002	1.997	2.216	0.050	0.125	0.401	0.235	13.46	74.47	5.31	4.20	2.48	0.07				
Viranduk Fm.	B087grn039	37.52	0.13	20.99	28.03	2.06	2.28	9.03	100.25	2.976	0.008	1.963	1.791	0.069	0.138	0.269	0.786	9.04	76.47	5.31	4.64	3.28	0.25				
Viranduk Fm.	B087grn040	36.61	n.d.	20.86	30.20	7.67	3.28	1.24	99.53	2.969	0.000	1.994	1.981	0.068	0.077	0.371	0.090	12.51	66.33	0.00	17.75	3.01	0.01				
Viranduk Fm.	B087grn041	36.95	0.03	20.87	32.37	5.13	2.90	1.42	99.79	2.991	0.002	1.995	1.754	0.023	0.352	0.349	0.123	11.68	72.47	2.93	11.75	1.12	0.05				
Viranduk Fm.	B087grn044	37.65	0.05	21.06	27.54	1.13	3.97	8.07	99.48	2.980	0.003	1.985	1.654	0.069	0.076	0.469	0.685	15.73	58.82	19.41	2.54	3.41	0.10				
Viranduk Fm.	B087grn045	37.41	0.09	21.29	31.54	2.45	5.19	1.53	99.53	2.980	0.006	2.000	2.074	0.028	0.165	0.616	0.131	20.66	69.52	2.82	5.54	1.27	0.19				
Viranduk Fm.	B087grn046	36.80	0.05	21.05	32.65	2.84	4.29	1.40	99.13	2.966	0.003	2.000	2.139	0.062	0.194	0.516	0.121	17.38	72.08	0.87	6.53	3.04	0.11				
Viranduk Fm.	B087grn047	37.95	0.04	21.32	27.04	1.40	5.01	6.98	99.73	2.981	0.002	1.974	1.716	0.061	0.093	0.587	0.587	19.68	57.53	16.59	3.12	2.99	0.07				
Viranduk Fm.	B087grn048	36.49	0.02	20.79	27.88	11.25	1.85	1.22	99.58	2.981	0.001	2.001	1.871	0.034	0.779	0.426	0.107	7.57	62.75	1.83	26.12	1.69	0.03				
Viranduk Fm.	B087grn049	37.24	n.d.	21.17	27.66	8.01	4.10	1.38	99.69	2.988	0.000	2.002	1.834	0.022	0.544	0.491	0.118	16.43	61.39	2.86	18.22	1.10	0.00				
Viranduk Fm.	B087grn050	36.93	n.d.	21.11	24.14	12.06	3.82	1.18	99.38	2.979	0.000	2.007	1.594	0.034	0.824	0.459	0.102	15.42	63.51	1.71	27.65	1.71	0.00				
Viranduk Fm.	B087grn052	36.72	0.03	20.91	33.25	3.48	3.61	1.46	99.47	2.965	0.002	1.990	2.167	0.078	0.238	0.435	0.127	14.66	73.08	0.31	8.02	3.88	0.06				
Viranduk Fm.	B087grn053	38.59	0.10	21.69	22.97	0.88	9.14	5.82	99.22	2.967	0.006	1.965	1.388	0.090	0.057	1.048	0.480	35.29	46.73	11.48	1.92	4.39	0.19				
Viranduk Fm.	B087grn054	36.86	0.03	21.03	32.03	6.11	2.56	1.36	99.97	2.982	0.002	2.005	2.138	0.029	0.418	0.309	0.118	10.34	71.69	2.48	14.03	1.40	0.05				
Viranduk Fm.	B087grn056	39.77	0.06	22.45	17.95	0.45	12.18	6.36	99.28	2.983	0.003	1.985	1.084	0.042	0.029	1.362	0.512	45.64	36.32	14.94	0.96	2.02	0.11				
Viranduk Fm.	B087grn057	37.97	0.06	21.17	29.70	5.69	5.00	3.51	100.19	2.998	0.003	1.970	1.735	0.028	0.380	0.589	0.297	19.63	57.85	8.42	12.68	1.30	0.12				
Viranduk Fm.	B087grn058	38.22	0.03	21.42	29.66	2.74	5.62	2.61	100.32	3.004	0.002	1.984	1.945	0.005	0.182	0.659	0.220	21.92	64.72	7.04	6.07	0.18	0.06				
Viranduk Fm.	B087grn059	37.34	0.01	21.30	31.66	2.14	5.86	0.96	99.34	2.972	0.000	1.988	2.051	0.056	0.144	0.695	0.082	23.39	68.92	0.00	4.85	2.74	0.01				
Viranduk Fm.	B087grn060	37.69	0.01	21.37	30.14	4.93	4.54	1.45	100.16	2.998	0.001	2.003	2.005	0.000	0.332	0.538	0.123	17.95	66.85	4.10	11.08	0.00	0.03				
Viranduk Fm.	B087grn061	38.06	0.08	21.61	26.68	0.89	4.80	7.56	99.78	2.988	0.005	2.000	1.736	0.016	0.059	0.561	0.636	18.77	58.06	20.36	1.98	0.67	0.16				
Viranduk Fm.	B087grn062	36.66	0.01	21.26	32.44	4.50	3.53	1.10	99.57	2.952	0.001	2.022	2.132	0.058	0.308	0.425	0.095	14.37	72.04	0.24	10.40	2.93	0.03				
Viranduk Fm.	B087grn063	36.82	0.01	20.67	31.33	5.49	3.39	1.86	99.61	2.972	0.001	1.966	2.029	0.087	0.376	0.408	0.161	13.72	68.23	1.01	12.64	4.37	0.03				
Viranduk Fm.	B087grn065	37.65	0.06	21.32	30.88	1.27	4.01	5.15	100.35	2.976	0.004	1.986	1.987	0.055	0.085	0.472	0.436	15.85	66.72	11.79	2.95	2.67	0.12				
Viranduk Fm.	B087grn066	36.87	0.01	21.05	33.59	2.24	3.59	2.11	99.47	2.970	0.000	1.989	2.204	0.059	0.153	0.431	0.183	14.51	74.20	13.15	1.52	2.95	0.02				
Viranduk Fm.	B087grn068	38.59	0.11	21.84	23.57	0.69	8.37	6.03	99.22	2.978	0.007	1.987	1.477	0.044	0.045	0.963	0.499	32.31	49.55	14.35	5.25	2.05	0.22				
Viranduk Fm.	B087grn071	37.28	0.02	21.28	29.50	2.08	7.38	1.07	98.63	2.954	0.001	1.988	1.853	0.102	0.139	0.872	0.103	14.51	67.03	0.68	15.39	2.69	0.06				
Viranduk Fm.	B087grn072	36.89	0.02	21.03	27.06	9.40	3.68	1.27	99.37	2.977	0.001	2.000	1.784	0.043	0.643	0.463	0.113	15.51	69.66	13.31	11.06	1.77	0.06				
Viranduk Fm.	B087grn073	37.22	0.11	21.20	31.99	3.07	4.74	1.46	99.34	2.969	0.003	1.983	2.079	0.055	0.208	0.520	0.549	17.33	62.20	16.51	2.23	1.64	0.09				
Viranduk Fm.	B087grn074	40.65	0.11	22.92	13.00	0.31	14.79	7.36	99.17	2.989	0.006	1.986	0.775	0.024	0.019	1.621	0.580	54.17	25.91	18.02	6.94	2.02	0.07				
Viranduk Fm.	B087grn075	36.47	n.d.	20.77	32.95	3.82	3.67	1.26	98.94	2.960	0.000	1.986	2.143	0.094	0.263	0.445	0.110	15.02	71.35	0.00	8.88	3.69	0.01				
Viranduk Fm.	B087grn076	36.70	0.03	21.02	30.23	6.67	3.84	1.18	99.26	2.973	0.002	1.997	1.993	0.054	0.468	0.421	0.103	14.15	67.03	0.68	15.39	2.69	0.06				
Viranduk Fm.	B087grn077	37.03	0.03	20.95	31.39	4.84	3.85	1.31	99.51	2.981	0.002	1.997	2.078	0.036	0.330	0.463	0.113	15.51	69.66	13.31	11.06	1.77	0.06				
Viranduk Fm.	B087grn078	37.75	0.04	20.95	28.60	0.99	4.39	6.45	99.19	2.999	0.003	1.982	1.866	0.034	0.067	0.520	0.549	17.33	62.20	16.51	2.23	1.64	0.09				
Viranduk Fm.	B087grn079	37.67	0.04	21.16	32.19	0.20	5.90	2.18	99.34	2.988	0.002	1.978	2.094	0.041	0.014	0.697	0.185	23.33	70.06	4.07	0.45	2.02	0.07				
Viranduk Fm.	B087grn080	36.88	0.02	21.04	33.05	2.91	3.22	2.33	99.45	2.977	0.001	2.002	2.189	0.042	0.199	0.388	0.202	13.03	73.53	4.63	6.67	2.10	0.03				
Viranduk Fm.	B087grn081	36.78	0.02	21.18	30.41	3.66	5.32	1.13	98.59	2.994	0.001	2.008	1.979	0.072	0.250	0.639	0.097	21.58	66.36	0.00	8.43	3.24	0.04				
Viranduk Fm.	B087grn082	37.44	n.d.	21.29	28.90	5.03	4.56	1.44	99.67	2.991	0.000	2.005	1.984	0.014	0.340	0.543	0.123	18.17	66.34	3.43	11.38	0.68	0.00				
Viranduk Fm.	B087grn083	38.06	0.04	20.94	26.58	5.55	5.07	3.64	99.89	3.010	0.003	1.952	1.734	0.024	0.372	0.597	0.309	19.84	57.59	9.02	12.35	1.11	0.09				
Viranduk Fm.	B087grn091	36.72	0.03	20.90	31.44	6.69	2.72	1.12	99.65	2.980	0.002	1.999	2.096	0.038	0.460	0.329	0.097	11.02	70.31	1.30	15.43	1.88	0.05				
Viranduk Fm.	B087grn093	39.98	0.05	22.44	17.89	0.46	12.43	6.39	99.76	2.984	0.003	1.974	1.064	0.053	0.029	1.383	0.511	46.33	35.63	14.40	0.97	2.58	0.09				
Viranduk Fm.	B087grn094	36.85	0.03	20.87	30.31	6.66	3.38	1.22	99.30	2.984	0.002	1.982	2.015	0.037	0.457	0.408	0.106	13.65	67.52	1.65	15.30	1.82	0.05				
Viranduk Fm.	B087grn095	36.99	0.01	20.83	32.17	3.84	3.06	2.71	99.67	2.984	0.001	1.981	2.121	0.050	0.263	0.368	0.234	12.32	71.05	5.33	8.80	2.48	0.03				
Viranduk Fm.	B087grn096	37.30	n.d.	21.06	30.91	5.19	3.62	1.07	99.18	3.017	0.000	2.008	2.091	0.000	0.355	0.437	0.092	14.68	70.26	31.11	11.95	0.00	0.00				
Viranduk Fm.	B087grn097	37.46	0.03	21.24	29.05	1.56	3.96	6.02	99.31	2.982	0.002	1.993	1.896	0.038	0.105	0.470	0.514	15.75	63.55	15.24	3.52	1.88	0.06				
Viranduk Fm.	B087grn099	38.01	0.05	21.41	26.95	0.79	5.34	7.24	99.80	2.975	0.004	1.976	1.696	0.068	0.052	0.623	0.607	20.93	56.97	16.89	1.75	3.37	0.21				
Viranduk Fm.	B095grn010	36.90	0.06	20.95	31.38	5.25	2.16	2.86	99.63	2.994	0.004	2.003	2.127	0.002	0.361	0.261	0.248	8.71	71.01	8.11	12.05	0.00	0.12				
Viranduk Fm.	B095grn020	37.03	0.01	20.92	34.09	0.98	3.86	1.92	98.92	2.997	0.001	1.985	2.298	0.010	0.067	0.466	0.167	15.54	76.65	5.06	2.25	0.47	0.13				
Viranduk Fm.	B095grn037	36.91	0.07	20.46	23.33	10.71	2.10	5.88	99.53	2.980	0.004	1.947	1.490	0.085	0.733	0.253	0.509	8.48	49.97	12.66	24.57	4.18	0.14				
Viranduk Fm.	B095grn043	36.87	0.07	20.65	33.98	0.52	1.86	5.36	99.30	2.990	0.004	1.974	2.289	0.037	0.036	0.350	0.466	7.50	75.81	13.62	1.20	1.73	0.14				
Viranduk Fm.	B095grn048	37.28	0.13	20.78	26.26	4.69	1.35	9.29	99.82	2.989	0.008	1.963	1.719	0.042	0.318	0.161	0.798	5.39	57.43								

**Results of U/Pb LA-ICP-SF-MS dating of detrital zircon from the Dinaride Ophiolite Zone mélangé and the Bosnian Flysch**

Formation	Sample & spot ID	Apparent ages										Conco. (%)					
		<sup>207</sup> Pb (ppm)	U (ppm)	Pb (ppm)	Th/U	<sup>206</sup> Pb/ <sup>238</sup> U	1 $\sigma$ %	Rho	<sup>207</sup> Pb/ <sup>206</sup> Pb	1 $\sigma$ %	<sup>206</sup> Pb/ <sup>238</sup> U age (Ma)		$\pm 2\sigma$ (Ma)	<sup>207</sup> Pb/ <sup>235</sup> U age (Ma)	$\pm 2\sigma$ (Ma)	<sup>207</sup> Pb/ <sup>206</sup> U age (Ma)	$\pm 2\sigma$ (Ma)
Ugar Fm.	BO16zrn007	45049	136	38	0.36	0.2602	2.0	0.92	0.0963	0.9	1491	60	1517	67	1554	16	98
Ugar Fm.	BO16zrn008	20255	645	29	0.22	0.0460	1.8	0.93	0.0529	0.7	290	11	294	12	325	16	99
Ugar Fm.	BO16zrn009	2940	119	5	0.66	0.0392	2.4	0.85	0.0548	1.5	248	12	263	15	406	33	99
Ugar Fm.	BO16zrn010	11778	180	21	1.10	0.0993	1.8	0.84	0.0612	1.2	611	22	618	27	647	25	99
Ugar Fm.	BO16zrn011	23801	737	26	0.69	0.0348	2.3	0.89	0.0635	2.4	221	10	270	18	724	51	82
Ugar Fm.	BO16zrn012	5083	36	7	1.03	0.1590	2.3	0.69	0.0736	1.2	951	44	975	51	1031	24	98
Ugar Fm.	BO16zrn013	18926	300	34	1.36	0.0890	2.4	0.97	0.0587	0.6	550	27	551	28	556	14	100
Ugar Fm.	BO16zrn014	3974	126	6	0.49	0.0438	1.8	0.85	0.0337	1.1	276	10	292	13	422	25	95
Ugar Fm.	BO16zrn015	15359	273	20	0.18	0.0763	1.9	0.90	0.0626	0.9	474	18	514	22	693	19	92
Ugar Fm.	BO16zrn016	9048	192	13	0.27	0.0672	2.0	0.91	0.0555	0.9	419	17	421	18	431	20	100
Ugar Fm.	BO16zrn020	12643	310	17	0.16	0.0566	2.3	0.88	0.0577	1.3	355	17	377	20	518	28	94
Ugar Fm.	BO16zrn021	13220	263	21	0.83	0.0754	2.2	0.83	0.0584	1.3	469	17	482	21	545	27	97
Ugar Fm.	BO16zrn022	40511	631	60	0.26	0.0966	1.7	0.94	0.0593	0.6	594	20	591	21	578	13	101
Ugar Fm.	BO16zrn023	12489	182	18	1.15	0.0864	1.9	0.90	0.0607	0.9	534	20	553	23	630	20	97
Ugar Fm.	BO16zrn024	19911	656	25	0.34	0.0360	2.9	0.90	0.0580	0.4	228	13	257	17	529	31	89
Ugar Fm.	BO16zrn025	18561	605	28	0.59	0.0430	1.8	0.95	0.0580	0.6	271	10	300	11	529	12	90
Ugar Fm.	BO16zrn026	18983	266	23	0.07	0.0922	1.7	0.93	0.0604	0.7	568	20	578	22	619	15	98
Ugar Fm.	BO16zrn027	21927	101	24	0.33	0.2345	2.3	0.94	0.0846	0.8	1358	61	1338	65	1305	16	102
Ugar Fm.	BO16zrn028	5013	48	6	0.72	0.1094	4.3	0.86	0.0703	2.6	669	57	734	73	936	52	91
Ugar Fm.	BO16zrn029	20987	258	38	1.20	0.1212	2.2	0.85	0.0644	1.5	737	32	741	39	754	31	99
Ugar Fm.	BO16zrn033	18399	646	29	0.29	0.0446	2.3	0.83	0.0551	1.4	281	13	286	16	414	32	95
Ugar Fm.	BO16zrn034	46727	176	42	0.41	0.2202	2.8	0.73	0.0945	2.6	1283	72	1374	106	1518	49	93
Ugar Fm.	BO16zrn036	5796	76	9	0.80	0.1045	2.1	0.80	0.0618	1.6	641	27	647	34	669	34	99
Ugar Fm.	BO16zrn037	16709	327	25	0.33	0.0759	1.8	0.93	0.0578	0.7	472	17	480	19	522	16	98
Ugar Fm.	BO16zrn038	51915	114	45	1.02	0.0545	2.0	0.92	0.0265	0.5	1702	79	1864	89	2050	10	91
Ugar Fm.	BO16zrn039	13062	323	15	0.21	0.0462	2.3	0.92	0.0567	0.9	291	12	313	14	479	20	93
Ugar Fm.	BO16zrn040	25327	86	29	0.25	0.3368	4.0	0.91	0.1165	1.8	1871	151	1886	167	1903	33	99
Ugar Fm.	BO16zrn041	6837	198	12	0.52	0.0545	2.0	0.87	0.0559	1.1	342	13	356	16	447	24	96
Ugar Fm.	BO16zrn042	8706	77	9	0.27	0.1036	2.9	0.90	0.0689	1.4	635	37	696	45	897	29	91
Ugar Fm.	BO16zrn046	3719	50	5	0.69	0.0967	1.8	0.75	0.0629	1.6	595	21	618	29	703	33	96
Ugar Fm.	BO16zrn047	9698	410	17	0.51	0.0380	1.8	0.78	0.0542	1.4	240	8	254	11	381	32	96
Ugar Fm.	BO16zrn048	9950	89	14	2.54	0.1298	1.9	0.69	0.0788	2.0	786	31	893	50	1166	40	88
Ugar Fm.	BO16zrn049	42183	521	56	0.25	0.1077	2.0	0.95	0.0658	0.6	660	26	692	28	800	13	95
Ugar Fm.	BO16zrn050	3262	32	5	0.43	0.1360	2.2	0.72	0.0681	2.1	822	35	836	50	872	43	98
Ugar Fm.	BO16zrn051	29606	315	48	0.1335	0.1335	1.8	0.95	0.0645	0.6	808	29	795	30	757	12	102
Ugar Fm.	BO16zrn052	2970	117	5	6.82	0.0375	3.6	0.53	0.0602	5.8	237	17	275	38	612	126	86
Ugar Fm.	BO16zrn053	12987	188	22	0.99	0.1002	1.8	0.85	0.0619	1.1	615	22	628	27	672	24	98
Ugar Fm.	BO16zrn054	1568	22	3	0.38	0.1436	2.2	0.73	0.0645	2.0	865	38	836	50	757	43	104
Ugar Fm.	BO16zrn055	2605	39	4	0.63	0.0613	1.9	0.74	0.0575	1.7	553	21	573	29	651	36	97
Ugar Fm.	BO16zrn059	7183	165	12	0.54	0.0709	2.4	0.74	0.0575	2.1	441	21	453	29	511	47	97
Ugar Fm.	BO16zrn060	38101	193	56	0.24	0.2927	2.1	0.49	0.0948	3.8	1655	71	1598	138	1523	71	104
Ugar Fm.	BO16zrn061	4209	147	8	0.78	0.0489	2.0	0.84	0.0529	1.3	308	13	310	15	322	30	99
Ugar Fm.	BO16zrn062	4746	75	8	1.21	0.0884	2.0	0.87	0.0529	1.1	546	22	557	26	601	25	98
Ugar Fm.	BO16zrn063	3703	136	7	0.51	0.0454	2.2	0.78	0.0527	1.8	286	13	290	17	318	41	99
Ugar Fm.	BO16zrn064	7912	167	11	0.24	0.0677	2.1	0.85	0.0574	1.3	422	18	436	22	507	29	97
Ugar Fm.	BO16zrn065	35985	805	41	0.68	0.0468	2.5	0.90	0.0408	1.2	295	15	371	20	876	24	80
Ugar Fm.	BO16zrn066	24538	897	26	0.38	0.0261	2.8	0.92	0.0567	1.2	166	9	189	12	480	27	88
Ugar Fm.	BO16zrn067	9119	250	16	0.36	0.0614	2.1	0.82	0.0554	1.5	384	16	390	21	428	34	98
Ugar Fm.	BO16zrn068	2147	47	3	0.80	0.0547	2.3	0.75	0.0747	2.0	343	15	454	27	1061	40	76
Ugar Fm.	BO16zrn072	10939	404	19	0.34	0.0461	2.0	0.80	0.0526	1.5	290	12	293	14	314	33	99

Formation	Sample & spot ID	<sup>207</sup> Pb (gpg)	U (ppm)	Pb (ppm)	Th/U	<sup>206</sup> Pb/ <sup>238</sup> U	1 σ %	<sup>207</sup> Pb/ <sup>235</sup> U	1 σ %	Rho	<sup>207</sup> Pb/ <sup>206</sup> Pb	1 σ %	Apparent ages				Conco. (%)				
													<sup>206</sup> Pb/ <sup>238</sup> U age ± 2σ (Ma)	<sup>207</sup> Pb/ <sup>235</sup> U age ± 2σ (Ma)	<sup>206</sup> Pb/ <sup>238</sup> U age ± 2σ (Ma)	<sup>207</sup> Pb/ <sup>235</sup> U age ± 2σ (Ma)					
Ugar Fm.	BO16zrn073	11509	250	19	0.28	0.0762	2.0	0.5885	2.4	0.84	0.0560	1.3	474	19	474	19	474	19	474	19	101
Ugar Fm.	BO16zrn075	41668	177	49	0.58	0.2512	2.2	3.3809	2.5	0.89	0.0976	1.2	1445	65	1445	65	1445	65	1445	65	96
Ugar Fm.	BO16zrn076	14000	471	19	1.44	0.0307	3.2	0.3303	4.6	0.69	0.0782	3.3	195	12	195	12	195	12	195	12	96
Ugar Fm.	BO16zrn077	39386	687	55	0.03	0.0861	2.2	0.7092	2.5	0.88	0.0597	1.2	532	24	532	24	532	24	532	24	98
Ugar Fm.	BO16zrn078	11527	169	19	0.17	0.1180	2.1	1.0015	2.3	0.92	0.0616	0.9	719	30	719	30	719	30	719	30	102
Ugar Fm.	BO16zrn079	71116	66	44	1.21	0.5097	1.8	14.2940	2.0	0.95	0.2034	0.6	2655	99	2655	99	2655	99	2655	99	96
Ugar Fm.	BO16zrn080	71112	152	15	0.35	0.0986	1.9	0.8781	6.9	0.26	0.0646	6.7	606	22	606	22	606	22	606	22	95
Ugar Fm.	BO16zrn081	7066	99	11	0.70	0.1021	1.9	0.8712	2.2	0.87	0.0619	1.1	627	24	627	24	627	24	627	24	99
Ugar Fm.	BO16zrn085	15715	288	20	0.23	0.0677	3.5	0.5475	3.7	0.97	0.0586	0.9	422	30	422	30	422	30	422	30	95
Ugar Fm.	BO16zrn086	283140	1305	322	0.35	0.2391	2.3	3.4640	2.9	0.80	0.1051	1.7	1382	65	1382	65	1382	65	1382	65	91
Ugar Fm.	BO16zrn087	3799	158	6	0.95	0.0320	3.1	0.2433	3.3	0.93	0.0551	1.2	203	13	203	13	203	13	203	13	92
Ugar Fm.	BO16zrn088	7229	156	11	0.23	0.0709	2.0	0.5803	2.4	0.81	0.0593	1.4	442	17	442	17	442	17	442	17	95
Ugar Fm.	BO16zrn089	13907	292	24	0.76	0.0747	1.9	0.5975	0.8	0.92	0.0580	0.8	464	18	464	18	464	18	464	18	98
Ugar Fm.	BO16zrn090	24125	52	20	0.70	0.3408	1.9	5.5711	2.0	0.94	0.1186	0.7	1891	71	1891	71	1891	71	1891	71	99
Ugar Fm.	BO16zrn091	6151	97	10	0.82	0.0946	1.9	0.7788	2.2	0.89	0.0597	1.0	582	23	582	23	582	23	582	23	100
Ugar Fm.	BO16zrn092	76404	2991	119	0.08	0.0372	2.1	0.3541	2.2	0.94	0.0689	0.7	236	10	236	10	236	10	236	10	77
Ugar Fm.	BO16zrn093	10944	288	10	0.13	0.0328	3.9	0.3429	6.0	0.65	0.0759	4.6	208	16	208	16	208	16	208	16	69
Ugar Fm.	BO16zrn094	1310	19	2	0.24	0.0967	2.9	0.8546	3.7	0.77	0.0641	2.4	595	34	595	34	595	34	595	34	95
Ugar Fm.	BO16zrn098	6605	118	12	1.00	0.0896	1.9	0.7256	2.3	0.84	0.0587	1.2	553	25	553	25	553	25	553	25	100
Ugar Fm.	BO16zrn100	1844	55	3	0.43	0.0416	2.4	0.3237	3.2	0.74	0.0565	2.2	262	13	262	13	262	13	262	13	92
Ugar Fm.	BO16zrn101	4336	71	7	0.61	0.0825	2.4	0.7058	3.0	0.81	0.0621	1.8	511	25	511	25	511	25	511	25	94
Ugar Fm.	BO16zrn102	6452	80	9	0.66	0.1037	1.9	0.9540	2.5	0.76	0.0667	1.6	636	24	636	24	636	24	636	24	94
Ugar Fm.	BO16zrn103	7636	117	11	0.05	0.0970	2.6	0.8274	2.9	0.91	0.0539	1.9	315	32	315	32	315	32	315	32	97
Ugar Fm.	BO16zrn104	8150	296	16	0.53	0.0500	1.9	0.3715	2.7	0.71	0.0539	1.9	407	29	407	29	407	29	407	29	98
Ugar Fm.	BO16zrn104	7680	285	13	0.28	0.0456	2.0	0.3951	2.3	0.87	0.0533	1.1	288	12	288	12	288	12	288	12	98
Ugar Fm.	BO16zrn105	9076	193	14	0.61	0.0652	3.5	0.5656	5.4	0.65	0.0629	4.1	507	29	507	29	507	29	507	29	90
Ugar Fm.	BO16zrn106	3521	59	6	1.14	0.0869	2.2	0.7341	2.8	0.80	0.0613	1.7	437	24	437	24	437	24	437	24	96
Ugar Fm.	BO16zrn107	4644	130	14	0.31	0.1084	2.3	0.8472	3.2	0.72	0.0567	2.2	663	31	663	31	663	31	663	31	106
Ugar Fm.	BO16zrn111	6591	109	12	0.90	0.0914	1.8	0.7558	2.3	0.77	0.0600	1.4	564	20	564	20	564	20	564	20	99
Ugar Fm.	BO16zrn112	14589	357	27	0.24	0.0754	2.9	0.5948	3.2	0.90	0.0572	1.4	468	27	468	27	468	27	468	27	100
Ugar Fm.	BO16zrn113	9631	359	17	0.30	0.0474	1.8	0.3429	2.0	0.88	0.0525	1.0	298	10	298	10	298	10	298	10	100
Ugar Fm.	BO16zrn114	5823	126	8	0.11	0.0704	1.8	0.5543	2.1	0.86	0.0571	1.1	438	16	438	16	438	16	438	16	98
Ugar Fm.	BO16zrn115	20799	387	29	0.03	0.0808	1.8	0.6759	2.0	0.92	0.0607	0.8	501	18	501	18	501	18	501	18	99
Ugar Fm.	BO16zrn116	32415	299	46	0.41	0.1508	1.7	1.4510	1.8	0.94	0.0698	0.6	905	31	905	31	905	31	905	31	99
Ugar Fm.	BO16zrn117	45453	99	39	0.58	0.3496	1.7	5.8789	1.8	0.94	0.1220	0.6	1933	67	1933	67	1933	67	1933	67	97
Ugar Fm.	BO16zrn118	34270	557	53	0.27	0.0881	1.8	0.8471	2.0	0.91	0.0626	0.8	604	21	604	21	604	21	604	21	97
Ugar Fm.	BO16zrn119	4949	99	9	0.49	0.0863	2.0	0.7220	2.6	0.78	0.0607	1.6	534	21	534	21	534	21	534	21	93
Ugar Fm.	BO16zrn120	20766	329	41	0.88	0.1143	2.0	1.0870	3.1	0.66	0.0690	2.3	698	28	698	28	698	28	698	28	93
Ugar Fm.	BO16zrn124	65880	148	54	0.37	0.3451	2.0	5.8425	2.2	0.93	0.1228	0.8	1911	77	1911	77	1911	77	1911	77	98
Ugar Fm.	BO16zrn125	882	33	2	1.21	0.0428	1.9	0.3308	3.6	0.53	0.0560	3.0	270	10	270	10	270	10	270	10	93
Ugar Fm.	BO16zrn126	47245	89	34	0.45	0.3444	2.2	6.0030	2.3	0.97	0.1264	0.5	1908	84	1908	84	1908	84	1908	84	97
Ugar Fm.	BO16zrn127	3421	26	8	3.84	0.1751	1.9	1.8141	2.7	0.71	0.0751	1.9	1040	39	1040	39	1040	39	1040	39	99
Ugar Fm.	BO16zrn128	7526	79	10	0.29	0.1237	2.3	1.1249	2.7	0.87	0.0659	1.3	752	35	752	35	752	35	752	35	98
Ugar Fm.	BO16zrn129	7783	293	12	0.24	0.0412	2.0	0.3051	2.3	0.87	0.0537	1.1	260	10	260	10	260	10	260	10	96
Ugar Fm.	BO16zrn130	3025	88	5	0.41	0.0537	1.8	0.4433	3.0	0.61	0.0599	2.4	337	12	337	12	337	12	337	12	91
Ugar Fm.	BO16zrn131	80955	156	74	0.82	0.4075	1.8	7.0627	1.8	0.88	0.1257	0.3	2203	78	2203	78	2203	78	2203	78	104
Ugar Fm.	BO16zrn132	2241	37	4	1.18	0.0797	2.0	0.8232	6.6	0.30	0.0749	6.3	300	20	300	20	300	20	300	20	81
Ugar Fm.	BO16zrn133	27688	946	48	0.50	0.0477	2.3	0.4405	2.7	0.86	0.0669	1.4	494	14	494	14	494	14	494	14	81
Ugar Fm.	BO16zrn137	15624	57	15	0.63	0.2257	2.0	3.1571	2.2	0.88	0.1014	1.1	1312	51	1312	51	1312	51	1312	51	91
Ugar Fm.	BO16zrn138	7241	127	12	0.33	0.0842	6.4	0.7724	7.9	0.81	0.0665	4.6	521	67	521	67	521	67	521	67	90
Ugar Fm.	BO16zrn139	13173	164	17	0.22	0.1066	1.8	0.9184	2.0	0.93	0.0625	0.7	653	24	653	24	653	24	653	24	99
Ugar Fm.	BO16zrn140	61920	1082	108	0.53	0.0955	1.7	0.7760	1.8	0.95	0.0590	0.6	588	20	588	20	588	20	588	20	101
Ugar Fm.	BO16zrn141	7830	279	13	0.34	0.0460	1.9	0.3373	2.2	0.88	0.0532	1.0	290	11	290	11	290	11	290	11	98
Ugar Fm.	BO16zrn142	10009	185	15	0.27	0.0842	1.7	0.6718	2.0	0.87	0.0578	1.0	521	18	521	18	521	18	521	18	100

Apparent ages

Formation	Sample & spot ID	<sup>207</sup> Pb (gpc)	U (ppm)	Pb (ppm)	Th/U	<sup>206</sup> Pb/ <sup>238</sup> U	1 σ %	<sup>207</sup> Pb/ <sup>235</sup> U	1 σ %	Rho	<sup>207</sup> Pb/ <sup>206</sup> Pb	1 σ %	<sup>206</sup> Pb/ <sup>238</sup> U age ± 2σ (Ma)	<sup>207</sup> Pb/ <sup>235</sup> U age ± 2σ (Ma)	<sup>207</sup> Pb/ <sup>206</sup> Pb age ± 2σ (Ma)	Conco. (%)	
Ugar Fm.	BO16zrm143	3145	44	5	0.25	0.1149	1.8	1.0111	2.4	0.78	0.0638	1.5	701	709	735	31	99
Ugar Fm.	BO16zrm144	9672	344	15	0.27	0.0451	1.7	0.3481	2.0	0.87	0.0560	1.0	284	303	34	22	94
Ugar Fm.	BO16zrm145	19613	437	33	0.68	0.0771	2.1	0.6357	3.1	0.88	0.0598	2.3	479	500	31	49	96
Ugar Fm.	BO16zrm146	8734	173	16	0.74	0.0883	1.8	0.7093	2.0	0.88	0.0583	1.0	546	544	22	21	100
Ugar Fm.	BO16zrm150	11866	93	18	1.15	0.1682	1.7	1.5637	1.9	0.93	0.0726	0.7	947	944	36	1003	98
Ugar Fm.	BO16zrm151	16692	748	31	0.54	0.0393	1.7	0.2772	1.8	0.93	0.0512	1.8	248	249	16	16	100
Ugar Fm.	BO16zrm152	3182	148	6	0.58	0.0391	1.9	0.2867	2.6	0.73	0.0532	1.8	247	256	13	337	97
Ugar Fm.	BO16zrm153	1578	21	2	1.00	0.0877	3.5	0.7574	3.9	0.89	0.0626	1.8	542	573	45	695	95
Ugar Fm.	BO16zrm154	71706	180	57	0.34	0.2978	2.6	4.6469	2.6	0.99	0.1132	0.4	1680	1851	90	1851	96
Ugar Fm.	BO16zrm155	121671	145	68	0.37	0.4213	1.7	0.4927	1.7	0.98	0.1634	0.3	2266	2387	82	2491	95
Ugar Fm.	BO16zrm156	11251	389	18	0.22	0.0480	1.8	0.3604	2.0	0.89	0.0545	0.9	302	313	13	392	97
Ugar Fm.	BO16zrm157	12789	150	16	0.05	0.1126	1.7	1.1210	4.4	0.38	0.0722	4.1	688	763	68	992	90
Ugar Fm.	BO16zrm158	196163	284	142	0.14	0.4794	2.84	10.3754	1.8	0.94	0.1570	0.6	2525	2469	91	2423	11
Ugar Fm.	BO16zrm159	11984	166	23	1.00	0.1241	1.8	1.0643	2.0	0.91	0.0622	0.8	754	736	29	681	102
Ugar Fm.	TD151zrm007	5025	168	8	1.14	0.0409	2.3	0.3011	2.7	0.86	0.0534	1.3	259	267	14	344	97
Ugar Fm.	TD151zrm008	9370	225	12	0.33	0.0526	2.2	0.4291	2.4	0.90	0.0592	1.1	330	363	18	574	91
Ugar Fm.	TD151zrm009	2358	78	4	0.88	0.0418	2.2	0.2996	1.8	0.78	0.0520	1.8	264	266	15	285	99
Ugar Fm.	TD151zrm010	2278	78	3	1.26	0.0372	2.2	0.2977	3.7	0.59	0.0581	3.0	235	265	20	534	89
Ugar Fm.	TD151zrm011	157158	200	95	1.13	0.4023	2.4	7.9334	0.4	0.99	0.1430	104	2179	2223	107	2264	7
Ugar Fm.	TD151zrm013	2393	59	4	1.10	0.0578	2.3	0.4179	2.8	0.84	0.0525	1.5	362	355	20	306	102
Ugar Fm.	TD151zrm014	1497	64	3	1.23	0.0342	2.3	0.2338	3.0	0.77	0.0495	1.9	217	213	13	172	102
Ugar Fm.	TD151zrm015	119603	78	53	1.02	0.5669	2.2	16.3379	2.2	0.99	0.2090	0.4	2895	2897	129	2898	100
Ugar Fm.	TD151zrm016	1828	25	3	1.46	0.0920	2.3	0.7457	1.8	0.78	0.0588	1.8	567	566	33	559	100
Ugar Fm.	TD151zrm020	18148	16	10	1.43	0.4918	2.3	11.5391	2.4	0.96	0.1702	0.7	2579	2568	123	2559	100
Ugar Fm.	TD151zrm021	9742	377	15	0.66	0.0371	2.2	0.2671	2.4	0.93	0.0523	0.9	235	240	12	298	98
Ugar Fm.	TD151zrm022	9478	84	12	0.64	0.1328	2.2	1.2171	2.4	0.92	0.0665	0.9	804	808	39	822	99
Ugar Fm.	TD151zrm023	10276	105	11	0.59	0.1005	2.4	0.8394	2.6	0.92	0.0606	1.0	617	619	32	624	100
Ugar Fm.	TD151zrm024	7467	131	10	0.57	0.0741	2.2	0.5743	2.4	0.92	0.0562	1.0	461	461	22	461	100
Ugar Fm.	TD151zrm025	18980	419	24	0.59	0.0639	2.2	0.5052	2.6	0.82	0.0680	1.5	338	415	22	868	82
Ugar Fm.	TD151zrm026	4752	59	7	1.16	0.0989	2.5	0.8422	3.1	0.80	0.0618	1.9	608	620	38	666	98
Ugar Fm.	TD151zrm027	22429	227	27	0.15	0.1265	2.2	1.0909	2.4	0.91	0.0625	1.0	768	749	36	693	103
Ugar Fm.	TD151zrm028	15872	559	25	1.34	0.0362	2.2	0.2766	2.5	0.90	0.0554	1.1	229	248	12	430	92
Ugar Fm.	TD151zrm029	3680	24	4	0.92	0.1664	2.3	1.6162	2.6	0.86	0.0704	1.4	992	977	51	941	102
Ugar Fm.	TD151zrm033	6024	273	9	0.45	0.0336	2.3	0.2300	2.5	0.90	0.0497	1.1	213	210	11	182	101
Ugar Fm.	TD151zrm034	6723	311	15	2.82	0.0348	2.2	0.2474	2.4	0.91	0.0515	1.0	221	224	11	263	98
Ugar Fm.	TD151zrm035	18533	258	24	0.36	0.0923	2.3	0.7558	2.4	0.95	0.0594	0.7	569	572	27	581	100
Ugar Fm.	TD151zrm036	39179	282	41	0.23	0.1509	2.3	1.4386	2.3	0.97	0.0691	0.6	906	905	42	903	100
Ugar Fm.	TD151zrm037	5292	101	8	0.96	0.0670	2.2	0.5512	2.5	0.88	0.0597	1.2	418	446	22	592	94
Ugar Fm.	TD151zrm038	3953	142	6	0.72	0.0376	2.2	0.2759	2.6	0.85	0.0533	1.4	238	247	13	340	96
Ugar Fm.	TD151zrm039	4081	110	6	1.27	0.0485	2.3	0.3592	2.7	0.83	0.0538	1.5	305	312	17	361	98
Ugar Fm.	TD151zrm040	16618	425	25	0.82	0.0537	2.2	0.4025	2.4	0.93	0.0544	0.9	337	343	16	386	98
Ugar Fm.	TD151zrm041	118588	188	74	0.41	0.3727	2.2	6.3872	2.2	0.99	0.1243	0.4	2042	2031	89	2019	101
Ugar Fm.	TD151zrm042	85989	156	59	1.00	0.3240	2.2	5.3543	2.4	0.90	0.1199	1.0	1809	1878	91	1954	96
Ugar Fm.	TD151zrm046	17915	35	13	0.96	0.3280	2.3	5.2815	2.4	0.96	0.1168	0.7	1829	1866	88	1908	98
Ugar Fm.	TD151zrm047	4657	92	7	1.30	0.0692	2.2	0.5204	2.5	0.87	0.0546	1.3	431	425	22	394	101
Ugar Fm.	TD151zrm048	35774	201	39	0.92	0.1780	2.2	1.8425	2.2	0.80	0.0751	0.5	1056	1061	47	1070	100
Ugar Fm.	TD151zrm049	2808	89	4	0.90	0.0403	2.3	0.3342	2.2	0.88	0.0601	1.7	263	293	17	606	87
Ugar Fm.	TD151zrm050	3575	137	6	1.01	0.0391	2.2	0.2801	2.6	0.95	0.0520	1.4	247	251	13	285	99
Ugar Fm.	TD151zrm051	15840	426	21	0.16	0.0627	2.2	0.3877	2.3	0.95	0.0534	0.7	331	333	16	344	99
Ugar Fm.	TD151zrm052	14641	393	20	0.16	0.0534	2.2	0.3860	2.3	0.96	0.0525	0.7	335	331	15	306	101
Ugar Fm.	TD151zrm053	14419	378	19	0.95	0.0639	2.2	0.3945	2.3	0.95	0.0531	0.7	338	338	16	332	100
Ugar Fm.	TD151zrm054	15082	396	19	0.16	0.0519	2.2	0.3839	2.4	0.93	0.0537	0.8	326	330	16	357	99
Ugar Fm.	TD151zrm055	8799	232	11	0.14	0.0520	2.3	0.3634	2.5	0.92	0.0535	1.0	327	330	16	349	99
Vranduk Fm.	BO4zrm009	36492	291	44	0.05	0.1602	1.6	1.5368	1.7	0.95	0.0696	0.5	958	945	32	915	101

Formation	Sample & spot ID	<sup>207</sup> Pb (gpc)	U (ppm)	Pb (ppm)	Th/U	<sup>206</sup> Pb/ <sup>238</sup> U	1 σ %	<sup>207</sup> Pb/ <sup>235</sup> U	1 σ %	Rho	<sup>207</sup> Pb/ <sup>206</sup> Pb	1 σ %	Apparent ages				Conco. (%)
													<sup>206</sup> Pb/ <sup>238</sup> U age ± 2σ (Ma)	<sup>207</sup> Pb/ <sup>235</sup> U age ± 2σ (Ma)	<sup>206</sup> Pb/ <sup>238</sup> U age ± 2σ (Ma)	<sup>207</sup> Pb/ <sup>235</sup> U age ± 2σ (Ma)	
Vranduk Fm.	BO4zrn010	5089	210	9	0.41	0.0399	1.8	0.2906	2.2	0.81	0.0529	1.3	252	259	323	30	97
Vranduk Fm.	BO4zrn011	8111	213	13	0.17	0.0649	1.9	0.5130	1.1	0.85	0.0573	1.1	406	420	503	25	96
Vranduk Fm.	BO4zrn012	29893	70	25	0.52	0.3299	1.8	5.2122	2.0	0.89	0.1146	0.9	1838	1855	1874	16	99
Vranduk Fm.	BO4zrn013	7707	31	12	2.89	0.2323	2.4	3.0368	3.8	0.63	0.0948	3.0	1347	1417	1524	56	95
Vranduk Fm.	BO4zrn014	11830	443	21	0.76	0.0440	1.7	0.3169	0.8	0.90	0.0523	0.8	277	280	297	18	99
Vranduk Fm.	BO4zrn015	10651	147	18	1.03	0.1066	1.7	0.8923	0.9	0.88	0.0607	0.9	653	648	629	19	101
Vranduk Fm.	BO4zrn016	2611	79	5	0.82	0.0630	1.7	0.3984	2.8	0.60	0.0545	2.2	333	340	391	50	98
Vranduk Fm.	BO4zrn020	2241	102	6	3.40	0.0398	1.9	0.2818	2.8	0.68	0.0514	2.1	252	252	257	47	100
Vranduk Fm.	BO4zrn021	9516	71	4	0.93	0.0493	1.6	0.3691	1.7	0.70	0.0543	1.7	310	319	363	37	97
Vranduk Fm.	BO4zrn022	2213	270	13	0.30	0.0470	1.8	0.3490	2.3	0.88	0.0539	1.0	296	304	366	21	97
Vranduk Fm.	BO4zrn023	2060	90	4	0.69	0.0387	1.7	0.2769	2.5	0.69	0.0519	1.8	245	248	280	41	99
Vranduk Fm.	BO4zrn025	39138	95	35	0.86	0.3187	1.6	4.9612	0.5	0.95	0.1129	0.5	1784	1813	1846	17	98
Vranduk Fm.	BO4zrn026	13417	44	15	1.32	0.2797	1.6	3.6873	1.8	0.88	0.0956	0.9	1590	1569	1540	9	98
Vranduk Fm.	BO4zrn027	6350	165	10	0.34	0.0627	1.9	0.4870	2.6	0.73	0.0563	1.8	392	403	464	39	97
Vranduk Fm.	BO4zrn028	1608	65	3	1.56	0.0386	1.8	0.2852	3.0	0.59	0.0536	2.5	244	255	353	56	96
Vranduk Fm.	BO4zrn029	2415	150	7	3.26	0.0280	1.9	0.2026	2.9	0.66	0.0526	2.2	178	187	310	49	95
Vranduk Fm.	BO4zrn034	5926	86	10	0.93	0.1035	1.8	0.8650	2.3	0.78	0.0606	1.4	635	633	626	31	100
Vranduk Fm.	BO4zrn035	20533	466	37	0.37	0.0787	1.9	0.6183	2.4	0.79	0.0570	1.5	488	489	491	32	100
Vranduk Fm.	BO4zrn036	9437	192	14	0.19	0.0784	1.7	0.6196	2.0	0.85	0.0573	1.0	487	490	503	23	99
Vranduk Fm.	BO4zrn037	49117	1641	140	0.83	0.0887	1.9	9.8900	3.1	0.92	0.1742	0.5	2221	2424	2598	8	92
Vranduk Fm.	BO4zrn038	9667	135	15	0.62	0.1070	1.7	0.9635	2.3	0.60	0.0646	2.3	655	680	763	48	96
Vranduk Fm.	BO4zrn039	5168	209	11	1.62	0.0425	1.7	0.3065	2.2	0.77	0.0523	1.4	268	271	297	31	99
Vranduk Fm.	BO4zrn041	13200	458	20	0.35	0.0448	1.8	0.3592	2.3	0.89	0.0581	1.3	283	312	534	28	91
Vranduk Fm.	BO4zrn042	142355	182	95	1.24	0.4113	3.1	9.8800	0.5	0.92	0.1742	0.5	2221	2424	2598	8	92
Vranduk Fm.	BO4zrn046	5754	259	11	1.03	0.0390	1.9	0.2913	2.5	0.78	0.0542	1.6	247	260	379	35	95
Vranduk Fm.	BO4zrn047	6004	241	11	0.58	0.0436	1.7	0.3249	1.4	0.77	0.0541	1.2	275	286	374	32	96
Vranduk Fm.	BO4zrn048	7781	333	15	0.71	0.0410	2.0	0.2928	2.2	0.86	0.0518	1.4	259	261	275	28	99
Vranduk Fm.	BO4zrn049	7244	358	16	1.20	0.0363	2.2	0.2821	2.6	0.83	0.0524	1.4	230	236	302	33	97
Vranduk Fm.	BO4zrn050	8424	181	15	0.79	0.0754	1.9	0.5871	2.2	0.86	0.0565	1.1	468	469	472	25	100
Vranduk Fm.	BO4zrn051	142768	294	110	0.34	0.3581	1.6	5.9063	0.4	0.97	0.1196	0.6	1973	1962	1951	7	101
Vranduk Fm.	BO4zrn053	18285	49	18	1.09	0.3169	1.6	4.6911	1.7	0.93	0.1074	0.6	1775	1766	1755	11	101
Vranduk Fm.	BO4zrn054	6348	304	14	1.08	0.0404	1.6	0.2842	1.9	0.85	0.0511	1.0	255	254	244	24	100
Vranduk Fm.	BO4zrn055	11520	391	20	0.52	0.0504	2.2	0.4037	3.6	0.60	0.0581	2.9	317	344	534	63	92
Vranduk Fm.	BO4zrn059	5806	371	11	0.52	0.0294	1.9	0.2073	2.2	0.84	0.0512	1.2	187	191	251	28	97
Vranduk Fm.	BO4zrn060	22419	340	34	0.32	0.0983	2.0	0.8717	2.2	0.89	0.0643	1.0	604	636	753	21	95
Vranduk Fm.	BO4zrn061	50970	47	27	0.49	0.4898	1.9	12.8036	0.6	0.96	0.1896	0.6	2570	2665	2738	9	96
Vranduk Fm.	BO4zrn062	9735	91	16	1.26	0.1384	1.1	1.2832	2.2	0.88	0.0673	1.1	835	838	846	22	100
Vranduk Fm.	BO4zrn063	22127	694	38	0.78	0.0505	2.2	0.4623	4.7	0.47	0.0664	4.1	318	386	817	86	82
Vranduk Fm.	BO4zrn064	2688	104	8	3.16	0.0446	2.0	0.3177	2.4	0.83	0.0516	1.3	281	280	269	31	100
Vranduk Fm.	BO4zrn065	7699	252	14	0.69	0.0503	1.9	0.3740	2.1	0.87	0.0539	1.0	316	323	369	23	98
Vranduk Fm.	BO4zrn066	8678	405	15	0.26	0.0360	2.0	0.2910	5.8	0.34	0.0586	5.4	228	259	552	118	88
Vranduk Fm.	BO4zrn068	110374	338	90	1.04	0.2074	2.8	4.1149	3.1	0.91	0.1439	1.3	1215	1657	2275	22	73
Vranduk Fm.	BO4zrn072	13521	105	17	0.39	0.1587	2.0	0.9971	2.2	0.90	0.0717	0.9	949	958	977	19	99
Vranduk Fm.	BO4zrn073	13928	106	20	0.92	0.1612	2.1	1.6156	2.5	0.88	0.0727	1.4	963	976	1006	29	99
Vranduk Fm.	BO4zrn074	28076	597	29	1.20	0.0390	3.0	0.4754	3.9	0.78	0.0884	2.4	247	395	1392	47	62
Vranduk Fm.	BO4zrn075	1750	89	3	1.22	0.0325	2.3	0.2421	3.3	0.70	0.0540	2.4	206	220	373	53	94
Vranduk Fm.	BO4zrn076	56532	1312	72	0.72	0.0493	2.6	0.6179	5.6	0.47	0.0909	4.9	310	489	1444	94	64
Vranduk Fm.	BO4zrn080	14534	437	25	0.41	0.0560	2.1	0.4205	2.4	0.88	0.0545	1.2	351	356	390	26	99
Vranduk Fm.	BO4zrn085	13706	222	38	3.94	0.0971	2.4	0.8179	2.9	0.81	0.0611	1.7	597	607	643	37	98
Vranduk Fm.	BO4zrn086	1841	57	3	1.14	0.0465	2.9	0.3944	4.3	0.68	0.0615	3.1	293	338	657	67	87
Vranduk Fm.	BO4zrn087	15971	339	25	0.40	0.0736	2.0	0.5968	2.2	0.88	0.0588	1.0	458	475	559	23	96
Vranduk Fm.	BO4zrn088	7240	340	14	0.62	0.0380	2.2	0.2745	2.6	0.85	0.0523	1.3	241	246	300	31	98
Vranduk Fm.	BO4zrn089	1617	72	3	0.72	0.0357	2.0	0.2607	2.8	0.73	0.0529	1.9	226	235	326	44	96
Vranduk Fm.	BO4zrn091	1514	35	3	0.67	0.0689	2.1	0.5463	2.9	0.72	0.0575	2.0	430	443	510	45	97

Formation	Sample & spot ID	<sup>207</sup> Pb (gpc)	U (ppm)	Pb (ppm)	Th/U	<sup>206</sup> Pb/ <sup>238</sup> U	1 σ %	<sup>207</sup> Pb/ <sup>235</sup> U	1 σ %	Rho	<sup>207</sup> Pb/ <sup>206</sup> Pb	1 σ %	Apparent ages				Conco. (%)		
													<sup>206</sup> Pb/ <sup>238</sup> U age ± 2σ (Ma)	<sup>207</sup> Pb/ <sup>235</sup> U age ± 2σ (Ma)	<sup>206</sup> Pb/ <sup>238</sup> U age ± 2σ (Ma)	<sup>207</sup> Pb/ <sup>235</sup> U age ± 2σ (Ma)			
Vranduk Fm.	BO4zrm094	2863	128	5	0.84	0.0378	1.9	0.2729	2.5	0.76	0.0523	1.6	239	9	245	12	300	37	98
Vranduk Fm.	BO4zrm100	6403	331	11	0.42	0.0345	2.3	0.2410	2.8	0.82	0.0506	1.6	219	10	219	12	224	37	100
Vranduk Fm.	BO4zrm101	5841	161	11	0.69	0.0593	2.6	0.4922	3.7	0.69	0.0602	2.7	371	19	406	30	611	58	91
Vranduk Fm.	BO4zrm102	18785	935	37	1.21	0.0373	2.0	0.4055	5.8	0.35	0.0789	5.4	236	10	346	40	1169	108	68
Vranduk Fm.	BO4zrm103	37554	153	6	0.43	0.0389	1.9	0.2967	3.6	0.52	0.0554	3.1	246	9	284	19	427	69	93
Vranduk Fm.	BO4zrm104	1805	119	4	0.77	0.0282	1.9	0.1984	1.8	0.73	0.0510	1.8	179	7	184	10	242	42	98
Vranduk Fm.	BO4zrm105	18481	765	30	1.33	0.0343	2.3	0.3604	2.8	0.82	0.0762	1.6	217	10	313	18	1101	32	70
Vranduk Fm.	BO4zrm106	166217	374	127	1.19	0.0303	1.9	5.8786	1.9	0.97	0.1406	0.4	1708	64	1958	75	2234	8	87
Vranduk Fm.	BO4zrm112	29761	585	54	0.68	0.0888	1.4	0.7243	1.3	0.73	0.0591	1.3	549	15	643	20	573	27	99
Vranduk Fm.	BO4zrm113	27188	680	51	0.64	0.0715	1.5	0.8862	4.0	0.36	0.0899	3.8	445	13	554	52	1424	72	69
Vranduk Fm.	BO4zrm115	40953	41	25	1.25	0.4890	1.4	12.0593	1.5	0.94	0.1789	0.5	2566	72	2609	78	2642	9	98
Vranduk Fm.	BO4zrm116	1673	28	3	0.97	0.0894	1.4	0.7325	2.2	0.55	0.0594	2.2	552	16	558	29	584	47	99
Vranduk Fm.	BO4zrm117	57113	264	66	0.87	0.2178	4.1	4.2777	5.6	0.74	0.1424	3.8	1270	105	1689	189	2257	65	75
Vranduk Fm.	BO4zrm119	1522	76	4	1.80	0.0379	2.1	0.2748	3.3	0.62	0.0526	2.6	240	10	247	16	312	59	97
Vranduk Fm.	BO4zrm120	11118	324	18	0.76	0.0601	2.1	0.3979	2.5	0.86	0.0576	1.3	315	14	340	17	516	28	93
Vranduk Fm.	BO4zrm124	3668	168	7	0.69	0.0378	1.3	0.2821	1.1	0.77	0.0541	1.1	239	6	252	9	376	25	95
Vranduk Fm.	BO4zrm125	10833	276	16	0.33	0.0557	1.3	0.5174	3.7	0.35	0.0674	3.4	349	9	423	31	850	71	82
Vranduk Fm.	BO4zrm126	8602	210	16	0.32	0.0771	1.5	0.6053	1.8	0.81	0.0569	1.1	479	14	481	18	489	24	100
Vranduk Fm.	BO4zrm132	18176	163	25	0.62	0.1450	2.1	1.3920	2.3	0.89	0.0696	1.1	873	36	886	41	917	22	99
Vranduk Fm.	BO4zrm133	1180	47	3	1.53	0.0436	1.6	0.3317	2.7	0.54	0.0552	2.3	275	8	291	16	421	51	95
Vranduk Fm.	BO4zrm142	6772	234	12	0.69	0.0504	1.6	0.3706	2.3	0.70	0.0533	1.7	317	10	320	15	342	38	99
Vranduk Fm.	BO4zrm143	14152	127	19	0.44	0.1505	1.7	1.4358	1.9	0.90	0.0692	0.8	904	31	904	34	905	17	100
Vranduk Fm.	BO4zrm144	8449	48	12	1.18	0.2202	1.6	2.4894	2.2	0.83	0.0820	1.3	1283	45	1289	55	1245	25	101
Vranduk Fm.	BO4zrm145	18702	486	29	1.53	0.0481	1.6	0.4987	2.0	0.83	0.0752	1.1	303	10	411	16	1075	22	74
Vranduk Fm.	BO12zrm007	8617	189	12	0.47	0.0590	1.5	0.4389	1.8	0.83	0.0539	1.0	370	11	369	14	368	23	100
Vranduk Fm.	BO12zrm008	18277	589	26	0.64	0.0401	1.5	0.2944	2.0	0.75	0.0532	1.3	254	7	262	10	339	30	97
Vranduk Fm.	BO12zrm009	5674	332	8	0.53	0.0237	1.6	0.1625	2.0	0.82	0.0498	1.1	151	5	153	6	183	26	99
Vranduk Fm.	BO12zrm010	9633	221	12	0.51	0.0529	1.6	0.3991	2.0	0.82	0.0547	1.2	332	11	341	14	401	26	97
Vranduk Fm.	BO12zrm011	15377	336	19	0.31	0.0576	1.7	0.4272	1.8	0.90	0.0538	0.8	361	12	361	13	364	18	100
Vranduk Fm.	BO12zrm012	15588	25	9	0.42	0.0231	1.7	5.8889	0.9	0.89	0.1305	0.9	1825	63	1960	76	2105	16	93
Vranduk Fm.	BO12zrm013	2872	158	4	0.36	0.0231	1.5	0.1639	2.1	0.72	0.0513	1.5	148	4	154	7	256	34	96
Vranduk Fm.	BO12zrm014	18268	449	42	0.05	0.0993	1.6	0.7824	3.2	0.50	0.0571	2.8	610	19	587	37	497	61	104
Vranduk Fm.	BO12zrm015	16421	516	25	0.35	0.0472	2.1	0.3590	2.3	0.88	0.0551	1.1	297	12	312	15	418	25	96
Vranduk Fm.	BO12zrm016	3724	165	5	0.98	0.0230	1.5	0.2018	2.8	0.54	0.0636	2.3	147	4	187	10	729	50	79
Vranduk Fm.	BO12zrm020	92763	366	87	0.38	0.2316	1.5	2.7480	1.9	0.82	0.0860	1.1	1343	42	1342	51	1339	21	100
Vranduk Fm.	BO12zrm021	10263	278	14	0.03	0.0664	1.7	0.4206	2.0	0.84	0.0541	1.1	353	12	357	15	377	25	99
Vranduk Fm.	BO12zrm022	3075	160	4	0.65	0.0249	1.9	0.1822	2.4	0.79	0.0531	1.5	158	6	170	8	335	34	93
Vranduk Fm.	BO12zrm023	31176	1306	47	0.12	0.0312	1.0	0.2341	2.0	0.86	0.0543	1.0	198	7	214	9	385	23	93
Vranduk Fm.	BO12zrm024	24003	816	27	0.45	0.0335	1.6	0.2496	1.7	0.90	0.0540	0.7	212	7	226	8	373	17	94
Vranduk Fm.	BO12zrm025	9119	496	13	0.32	0.0254	1.8	0.1799	2.4	0.75	0.0514	1.6	161	6	168	8	261	36	96
Vranduk Fm.	BO12zrm026	7114	100	11	1.27	0.0926	1.7	0.7768	2.3	0.74	0.0608	1.5	571	19	584	26	633	33	98
Vranduk Fm.	BO12zrm027	5278	207	8	0.38	0.0360	1.5	0.2587	1.9	0.79	0.0520	1.2	228	7	234	9	287	26	98
Vranduk Fm.	BO12zrm028	2360	136	3	0.63	0.0242	1.7	0.1701	2.6	0.66	0.0510	1.9	154	5	159	8	243	45	97
Vranduk Fm.	BO12zrm029	13596	777	18	0.19	0.0242	1.5	0.1642	1.7	0.91	0.0493	0.7	154	5	154	5	160	16	100
Vranduk Fm.	BO12zrm033	97110	234	79	0.44	0.3199	1.4	5.4270	0.5	0.94	0.1230	0.5	1789	51	1889	58	2001	9	95
Vranduk Fm.	BO12zrm034	6858	140	10	0.45	0.0684	1.6	0.5361	1.9	0.81	0.0568	1.1	427	13	436	17	485	25	98
Vranduk Fm.	BO12zrm035	5267	78	8	1.35	0.0852	4.4	0.7363	2.3	0.88	0.0627	2.3	527	47	560	56	698	50	94
Vranduk Fm.	BO12zrm036	12083	267	20	0.99	0.0612	2.9	0.5021	3.5	0.81	0.0595	2.1	383	22	413	29	586	45	93
Vranduk Fm.	BO12zrm037	52726	951	61	0.24	0.0647	2.6	0.5253	3.4	0.76	0.0589	2.2	404	21	429	29	564	48	94
Vranduk Fm.	BO12zrm038	7033	163	10	0.53	0.0569	1.8	0.4286	2.2	0.82	0.0546	1.2	357	13	362	16	397	28	98
Vranduk Fm.	BO12zrm039	1370	74	2	0.66	0.0260	1.9	0.1866	2.9	0.65	0.0521	2.2	165	6	174	10	292	50	95
Vranduk Fm.	BO12zrm040	7475	442	12	0.55	0.0268	1.5	0.1900	1.8	0.79	0.0513	1.1	171	5	177	7	256	26	97
Vranduk Fm.	BO12zrm041	6880	243	10	0.67	0.0373	1.5	0.2707	2.1	0.72	0.0526	1.4	236	7	243	10	313	32	97
Vranduk Fm.	BO12zrm042	7956	372	11	0.31	0.0279	1.8	0.1980	2.7	0.69	0.0515	1.9	177	6	183	10	265	44	97

Formation	Sample & spot ID	<sup>207</sup> Pb (gpc)	U (ppm)	Pb (ppm)	Th/U	<sup>206</sup> Pb/ <sup>238</sup> U	1 σ %	<sup>207</sup> Pb/ <sup>235</sup> U	1 σ %	Rho	<sup>207</sup> Pb/ <sup>206</sup> Pb	1 σ %	Apparent ages				Conco. (%)
													<sup>206</sup> Pb/ <sup>238</sup> U age ± 2σ (Ma)	<sup>207</sup> Pb/ <sup>235</sup> U age ± 2σ (Ma)	<sup>206</sup> Pb/ <sup>238</sup> U age ± 2σ (Ma)	<sup>207</sup> Pb/ <sup>235</sup> U age ± 2σ (Ma)	
Vranduk Fm.	BO12zrn046	8716	216	13	0.43	0.0689	1.7	0.4405	2.1	0.83	0.0542	1.2	369	13	381	26	100
Vranduk Fm.	BO12zrn047	13285	268	17	0.10	0.0665	3.1	0.6335	4.7	0.65	0.0691	3.6	415	26	498	47	83
Vranduk Fm.	BO12zrn048	2774	124	4	0.53	0.0255	2.1	0.1939	4.0	0.53	0.0552	3.4	162	7	180	14	90
Vranduk Fm.	BO12zrn049	7489	423	11	0.02	0.0283	1.5	0.1995	1.8	0.81	0.0511	1.0	180	5	185	7	97
Vranduk Fm.	BO12zrn050	5537	335	9	0.55	0.0244	1.7	0.1686	2.6	0.67	0.0501	1.9	156	5	197	45	98
Vranduk Fm.	BO12zrn051	7412	283	11	0.85	0.0366	3.4	0.2820	4.1	0.80	0.0559	2.2	232	16	252	20	92
Vranduk Fm.	BO12zrn052	4430	253	6	0.22	0.0249	1.6	0.1719	1.9	0.80	0.0501	1.2	159	5	197	27	98
Vranduk Fm.	BO12zrn053	1465	73	2	0.37	0.0235	1.9	0.1775	3.2	0.59	0.0547	2.6	150	6	401	58	90
Vranduk Fm.	BO12zrn055	14980	596	24	0.64	0.0381	2.0	0.2704	3.5	0.57	0.0514	2.9	241	10	261	66	99
Vranduk Fm.	BO12zrn059	6253	422	10	0.62	0.0216	2.9	0.1523	4.3	0.68	0.0511	3.2	138	8	244	73	96
Vranduk Fm.	BO12zrn060	6110	353	10	0.26	0.0281	2.2	0.1931	2.8	0.79	0.0499	1.7	178	8	179	10	100
Vranduk Fm.	BO12zrn061	4196	242	6	0.74	0.0251	2.2	0.1781	2.9	0.77	0.0514	1.8	160	7	166	10	96
Vranduk Fm.	BO12zrn062	7887	183	12	0.94	0.0586	2.2	0.4729	2.9	0.76	0.0585	1.9	367	16	393	23	93
Vranduk Fm.	BO12zrn063	8661	344	15	1.03	0.0379	2.6	0.2677	2.7	0.95	0.0512	0.9	240	12	241	13	100
Vranduk Fm.	BO12zrn064	1567	61	2	0.62	0.0367	3.4	0.2812	4.3	0.80	0.0556	2.6	232	16	252	22	92
Vranduk Fm.	BO12zrn065	53987	48	27	0.59	0.0503	2.4	12.6500	2.4	0.98	0.1834	0.5	2615	124	2654	9	99
Vranduk Fm.	BO12zrn066	14348	741	18	0.22	0.0243	2.3	0.1864	2.5	0.94	0.0557	0.9	155	7	174	9	89
Vranduk Fm.	BO12zrn067	2228	132	3	0.62	0.0239	2.2	0.1660	2.7	0.82	0.0503	1.5	153	7	156	8	98
Vranduk Fm.	BO12zrn072	8700	154	12	0.44	0.0752	2.6	0.6389	4.7	0.54	0.0616	4.0	468	24	502	47	93
Vranduk Fm.	BO12zrn073	6043	397	9	0.55	0.0219	3.0	0.1535	3.9	0.76	0.0508	2.5	140	8	145	11	96
Vranduk Fm.	BO12zrn074	4009	89	5	0.21	0.0609	2.6	0.4778	2.8	0.90	0.0569	1.2	381	20	397	23	96
Vranduk Fm.	BO12zrn075	4669	169	7	0.72	0.0376	2.7	0.2723	3.0	0.91	0.0525	1.2	238	13	245	15	97
Vranduk Fm.	BO12zrn076	15325	313	22	0.45	0.0699	2.3	0.5550	2.4	0.95	0.0576	0.7	435	20	448	22	94
Vranduk Fm.	BO12zrn077	6681	125	9	0.32	0.0760	2.7	0.6367	3.6	0.75	0.0608	2.3	472	25	500	36	95
Vranduk Fm.	BO12zrn078	17046	341	21	0.62	0.0542	2.3	0.4249	2.4	0.94	0.0568	0.8	340	16	360	18	95
Vranduk Fm.	BO12zrn079	1549	18	2	0.64	0.1047	2.7	0.9091	3.8	0.70	0.0630	2.7	642	34	657	50	98
Vranduk Fm.	BO12zrn080	20106	733	32	0.65	0.0404	2.2	0.2847	2.4	0.94	0.0511	0.8	256	11	254	12	100
Vranduk Fm.	BO12zrn081	13181	486	21	0.86	0.0384	2.2	0.2749	2.4	0.94	0.0520	0.8	243	11	247	12	98
Vranduk Fm.	BO12zrn085	6000	103	8	0.47	0.0761	2.2	0.6153	2.8	0.81	0.0586	1.6	473	21	487	27	97
Vranduk Fm.	BO12zrn086	3065	75	4	0.51	0.0554	2.4	0.4101	2.8	0.85	0.0537	1.5	348	17	349	20	100
Vranduk Fm.	BO12zrn087	29632	1114	46	0.47	0.0391	2.3	0.2921	2.5	0.91	0.0541	1.1	247	11	260	13	95
Vranduk Fm.	BO12zrn088	3963	90	5	0.84	0.0621	2.3	0.4074	2.7	0.85	0.0567	1.4	327	15	347	19	94
Vranduk Fm.	BO12zrn089	26490	963	44	0.10	0.0397	2.2	0.2798	2.3	0.97	0.0511	0.6	251	12	275	14	100
Vranduk Fm.	BO12zrn090	30269	1135	45	0.24	0.0410	2.4	0.3110	2.6	0.92	0.0550	1.0	259	12	275	14	94
Vranduk Fm.	BO12zrn091	114984	228	73	0.31	0.3052	2.4	5.1715	2.5	0.96	0.1229	0.7	1717	81	1848	91	93
Vranduk Fm.	BO12zrn092	4078	226	7	1.10	0.0273	2.3	0.1992	3.3	0.72	0.0530	2.3	174	8	184	12	94
Vranduk Fm.	BO12zrn093	21887	400	30	0.62	0.0736	2.3	0.5736	2.6	0.86	0.0565	1.2	458	21	460	24	99
Vranduk Fm.	BO12zrn094	6845	396	10	0.52	0.0238	2.7	0.1775	3.1	0.88	0.0541	1.6	151	8	166	10	91
Vranduk Fm.	BO12zrn098	5850	165	10	1.33	0.0605	2.3	0.3685	2.6	0.90	0.0530	1.1	317	15	319	16	100
Vranduk Fm.	BO12zrn099	9724	164	17	0.11	0.1098	2.5	1.1217	4.7	0.54	0.0741	4.0	672	34	764	72	88
Vranduk Fm.	BO12zrn101	14566	253	23	0.58	0.0890	2.4	0.6903	2.7	0.90	0.0562	1.2	550	26	533	29	103
Vranduk Fm.	BO12zrn102	1680	84	2	0.04	0.0246	2.4	0.1816	3.5	0.68	0.0535	2.5	157	7	169	12	93
Vranduk Fm.	BO12zrn103	5846	160	8	0.45	0.0508	2.3	0.3888	2.6	0.89	0.0555	1.2	319	15	333	17	96
Vranduk Fm.	BO12zrn104	16514	586	26	0.97	0.0393	2.2	0.2795	2.4	0.93	0.0516	0.9	249	11	250	12	99
Vranduk Fm.	BO12zrn105	8154	307	13	0.63	0.0406	2.2	0.2874	2.5	0.91	0.0514	1.0	256	11	256	13	100
Vranduk Fm.	BO12zrn106	3016	192	5	1.38	0.0226	2.5	0.1619	3.1	0.81	0.0520	1.8	144	7	152	9	95
Vranduk Fm.	BO12zrn107	26379	909	39	0.74	0.0391	2.2	0.3274	2.5	0.87	0.0608	1.3	247	11	288	15	86
Vranduk Fm.	BO12zrn111	8122	311	13	0.97	0.0379	2.2	0.2726	2.4	0.91	0.0522	1.0	240	11	245	12	98
Vranduk Fm.	BO12zrn112	6199	99	10	1.41	0.0869	2.3	0.7031	2.8	0.82	0.0587	1.6	537	25	541	30	99
Vranduk Fm.	BO12zrn113	32579	563	43	0.11	0.0796	2.3	0.6986	2.8	0.91	0.0637	1.2	494	25	538	30	92
Vranduk Fm.	BO12zrn114	3551	199	6	0.74	0.0300	2.4	0.2134	3.0	0.79	0.0517	1.8	196	9	196	12	97
Vranduk Fm.	BO12zrn115	4635	229	7	0.60	0.0308	2.3	0.2148	3.0	0.79	0.0505	1.8	190	9	198	12	99
Vranduk Fm.	BO12zrn116	5141	263	7	0.69	0.0238	2.5	0.1715	3.1	0.83	0.0522	1.7	152	8	161	10	94
Vranduk Fm.	BO12zrn117	13751	798	18	0.13	0.0229	2.3	0.2109	3.0	0.78	0.0667	1.9	146	7	194	12	75

Formation	Sample & spot ID	<sup>207</sup> Pb (gpc)	U (ppm)	Pb (ppm)	Th/U	<sup>206</sup> Pb/ <sup>238</sup> U	1 σ %	<sup>207</sup> Pb/ <sup>235</sup> U	1 σ %	Rho	<sup>207</sup> Pb/ <sup>206</sup> Pb	1 σ %	Apparent ages				Conco. (%)		
													<sup>206</sup> Pb/ <sup>238</sup> U age ± 2σ (Ma)	<sup>207</sup> Pb/ <sup>238</sup> U age ± 2σ (Ma)	<sup>207</sup> Pb/ <sup>235</sup> U age ± 2σ (Ma)	<sup>207</sup> Pb/ <sup>206</sup> Pb age ± 2σ (Ma)			
Vranduk Fm.	BO12zrn118	5404	236	10	0.67	0.0386	2.2	0.2720	2.6	0.85	0.0511	1.4	244	11	244	13	245	31	100
Vranduk Fm.	BO12zrn119	7833	199	11	0.64	0.0631	2.2	0.3947	2.4	0.89	0.0540	1.1	333	15	333	16	369	25	99
Vranduk Fm.	BO12zrn120	10757	400	16	0.95	0.0386	2.3	0.2719	2.4	0.95	0.0511	0.7	244	11	244	12	245	17	100
Vranduk Fm.	BO12zrn124	78999	243	55	0.40	0.2126	2.2	3.2700	2.3	0.99	0.1116	0.4	1242	55	1474	67	1825	6	84
Vranduk Fm.	BO12zrn125	5791	147	8	0.54	0.0453	2.3	0.3553	2.3	0.87	0.0568	1.3	286	13	309	16	485	28	93
Vranduk Fm.	BO12zrn126	15803	662	25	0.83	0.0345	2.3	0.2473	2.6	0.88	0.0520	1.2	219	10	224	12	284	24	97
Vranduk Fm.	BO12zrn127	11136	421	17	0.70	0.0383	2.1	0.2752	2.4	0.89	0.0521	1.1	242	10	247	12	289	24	98
Vranduk Fm.	BO12zrn128	19075	272	38	0.21	0.1453	2.2	1.3981	6.1	0.36	0.0698	5.7	874	38	888	108	922	116	98
Vranduk Fm.	BO12zrn129	5452	353	9	1.19	0.0213	2.8	0.0213	3.5	0.79	0.0491	2.1	136	8	137	10	153	50	99
Vranduk Fm.	BO12zrn130	9105	363	15	0.72	0.0397	2.3	0.2793	2.7	0.85	0.0511	1.4	251	12	250	14	245	33	100
Vranduk Fm.	BO12zrn131	2884	121	5	0.51	0.0360	2.5	0.2888	3.0	0.81	0.0581	1.8	228	11	258	16	534	39	89
Vranduk Fm.	BO12zrn132	4994	111	9	0.97	0.0752	2.1	0.6591	3.3	0.64	0.0636	2.5	467	20	514	34	727	54	91
Vranduk Fm.	BO12zrn133	2202	77	3	0.37	0.0433	2.6	0.3425	3.7	0.72	0.0573	2.5	273	14	299	22	504	56	91
Vranduk Fm.	BO12zrn137	3536	81	4	0.36	0.0532	3.5	0.4519	4.4	0.79	0.0616	2.7	334	23	379	33	660	58	88
Vranduk Fm.	BO12zrn138	5022	287	5	0.51	0.0172	2.9	0.1177	3.1	0.94	0.0496	1.1	110	6	113	7	176	25	97
Vranduk Fm.	BO12zrn140	7850	63	10	0.96	0.1461	2.1	1.3717	2.3	0.92	0.0681	0.9	879	37	877	41	872	19	100
Vranduk Fm.	BO12zrn141	3642	200	5	0.71	0.0210	2.8	0.1498	3.2	0.85	0.0517	1.7	134	7	142	9	271	39	95
Vranduk Fm.	BO12zrn142	11498	213	16	0.41	0.0719	2.1	0.5645	2.3	0.91	0.0569	1.0	448	19	454	21	489	22	99
Vranduk Fm.	BO12zrn144	3848	89	6	0.89	0.0648	2.2	0.4795	2.5	0.88	0.0537	1.2	405	17	398	20	357	26	102
Vranduk Fm.	BO12zrn146	6465	96	10	0.99	0.0881	2.2	0.7374	2.4	0.89	0.0607	1.1	544	24	561	27	628	24	97
Vranduk Fm.	BO87zrn007	23810	312	25	0.02	0.0875	1.8	0.7579	2.3	0.77	0.0628	1.5	541	19	573	26	703	31	94
Vranduk Fm.	BO87zrn008	101988	108	66	1.64	0.4232	2.1	10.0150	2.2	0.96	0.1716	0.6	2275	97	2436	108	2574	10	93
Vranduk Fm.	BO87zrn010	20427	367	29	0.36	0.0761	1.8	0.6034	2.0	0.88	0.0575	1.0	473	17	479	20	510	21	99
Vranduk Fm.	BO87zrn011	11259	232	19	0.62	0.0745	1.7	0.5707	2.1	0.88	0.0556	1.2	463	16	458	19	434	26	101
Vranduk Fm.	BO87zrn012	98786	75	42	0.57	0.4481	2.3	13.6482	2.6	0.92	0.2209	1.0	2387	112	2726	139	2987	17	88
Vranduk Fm.	BO87zrn013	72048	61	36	0.50	0.5985	2.0	12.8720	2.2	0.91	0.1836	0.9	2650	106	2670	118	2686	15	99
Vranduk Fm.	BO87zrn014	60999	84	36	0.80	0.3350	2.3	7.7394	2.5	0.94	0.1676	0.9	1862	87	2201	109	2533	14	85
Vranduk Fm.	BO87zrn015	6326	425	10	0.31	0.0234	1.8	0.1675	2.4	0.76	0.0519	1.6	149	5	157	8	281	36	95
Vranduk Fm.	BO87zrn016	10985	460	20	0.20	0.0450	1.6	0.3417	2.0	0.79	0.0550	1.3	284	9	288	12	414	28	95
Vranduk Fm.	BO87zrn020	7371	185	10	0.53	0.0496	1.7	0.3719	1.9	0.88	0.0543	0.9	312	11	321	13	385	21	97
Vranduk Fm.	BO87zrn021	14991	417	26	0.16	0.0660	5.7	0.5370	6.3	0.92	0.0590	2.5	412	47	436	55	567	54	94
Vranduk Fm.	BO87zrn022	96616	179	47	0.45	0.2364	2.0	4.9788	2.3	0.85	0.1528	1.2	1368	54	1816	84	2377	21	75
Vranduk Fm.	BO87zrn023	8599	181	5	0.12	0.0256	4.0	0.2179	4.2	0.95	0.0618	1.3	163	13	200	17	668	27	81
Vranduk Fm.	BO87zrn024	10154	388	17	0.58	0.0404	1.0	0.2902	2.0	0.87	0.0521	1.0	255	9	259	10	290	23	99
Vranduk Fm.	BO87zrn025	49180	415	40	0.44	0.0836	2.4	1.0908	4.4	0.55	0.0946	3.6	518	25	749	65	1520	69	69
Vranduk Fm.	BO87zrn026	10289	196	15	0.56	0.0713	1.8	0.5701	2.0	0.89	0.0580	0.9	444	16	458	18	529	20	97
Vranduk Fm.	BO87zrn027	8486	236	13	0.60	0.0517	1.7	0.4151	2.5	0.70	0.0562	1.8	325	11	353	18	537	39	92
Vranduk Fm.	BO87zrn028	30610	278	40	0.18	0.1472	2.2	1.3865	2.8	0.79	0.0683	1.7	885	39	883	49	878	35	100
Vranduk Fm.	BO87zrn029	31850	627	54	1.14	0.0693	2.9	0.5493	3.2	0.90	0.0575	1.4	432	25	445	28	510	30	97
Vranduk Fm.	BO87zrn033	8517	170	13	0.36	0.0722	2.0	0.5735	2.3	0.87	0.0576	1.1	450	18	460	22	514	25	98
Vranduk Fm.	BO87zrn034	229147	367	110	0.10	0.2899	1.8	6.7467	1.8	0.96	0.1688	0.5	1641	58	2079	77	2546	8	79
Vranduk Fm.	BO87zrn036	14599	364	20	0.52	0.0491	2.0	0.4134	3.6	0.57	0.0610	3.0	309	13	351	25	640	64	88
Vranduk Fm.	BO87zrn037	10757	419	17	0.49	0.0374	1.8	0.2741	2.3	0.79	0.0531	1.4	237	9	246	11	334	32	96
Vranduk Fm.	BO87zrn038	7115	98	13	0.24	0.1381	1.7	1.3682	2.6	0.76	0.0719	1.7	834	33	875	45	982	34	95
Vranduk Fm.	BO87zrn039	12205	161	14	0.37	0.0846	1.8	0.7907	2.4	0.75	0.0678	1.6	523	19	592	29	863	34	88
Vranduk Fm.	BO87zrn040	11689	325	18	0.53	0.0508	1.7	0.3803	2.0	0.88	0.0543	0.9	319	11	327	13	385	21	98
Vranduk Fm.	BO87zrn041	28076	355	48	1.40	0.0995	1.7	0.8537	2.0	0.85	0.0622	1.0	611	20	627	25	682	22	98
Vranduk Fm.	BO87zrn042	12204	207	17	0.64	0.1461	2.3	1.3964	2.5	0.92	0.0591	1.0	879	40	887	44	909	21	99
Vranduk Fm.	BO87zrn046	15305	237	23	0.66	0.0891	2.0	0.7260	2.1	0.93	0.0591	0.8	550	21	554	23	571	17	99
Vranduk Fm.	BO87zrn048	21760	365	31	0.18	0.0885	1.7	0.7276	2.4	0.74	0.0596	1.6	547	19	555	26	589	34	99
Vranduk Fm.	BO87zrn049	10396	246	16	0.64	0.0577	2.0	0.4349	2.4	0.82	0.0546	1.3	362	14	367	18	397	30	99
Vranduk Fm.	BO87zrn050	10476	185	15	0.30	0.0824	2.0	0.6493	2.4	0.83	0.0572	1.4	510	20	508	25	498	31	100
Vranduk Fm.	BO87zrn052	9777	571	14	0.42	0.0233	1.9	0.1736	3.0	0.64	0.0540	2.3	149	6	163	10	372	51	91
Vranduk Fm.	BO87zrn053	12966	146	12	0.78	0.0751	2.1	0.9939	6.2	0.34	0.0960	5.8	467	20	701	87	1548	109	67

Formation	Sample & spot ID	<sup>207</sup> Pb (gpc)	U (ppm)	Pb (ppm)	Th/U	<sup>206</sup> Pb/ <sup>238</sup> U 1 σ %	<sup>207</sup> Pb/ <sup>235</sup> U 1 σ %	Rho	<sup>207</sup> Pb/ <sup>206</sup> Pb	1 σ %	Apparent ages				Conco. (%)		
											<sup>206</sup> Pb/ <sup>238</sup> U age ± 2σ (Ma)	<sup>207</sup> Pb/ <sup>235</sup> U age ± 2σ (Ma)	<sup>206</sup> Pb/ <sup>238</sup> U age ± 2σ (Ma)	<sup>207</sup> Pb/ <sup>235</sup> U age ± 2σ (Ma)			
Vranduk Fm.	BO87zrn054	36637	540	45	0.39	0.0778	1.8	0.72	0.0725	1.7	483	17	584	29	999	35	83
Vranduk Fm.	BO87zrn055	122263	338	94	0.16	0.2716	1.1	0.86	0.1216	1.1	1549	57	1741	75	1980	20	89
Vranduk Fm.	BO87zrn059	45967	762	72	0.70	0.0859	2.7	0.94	0.0591	1.0	531	28	539	31	572	21	99
Vranduk Fm.	BO87zrn060	131445	322	21	0.37	0.0645	2.6	0.91	0.0569	1.2	403	21	416	24	488	27	97
Vranduk Fm.	BO87zrn061	120331	106	12	0.31	0.1124	2.4	0.89	0.0689	1.3	687	33	738	41	897	26	93
Vranduk Fm.	BO87zrn062	79683	221	12	0.43	0.0538	2.8	0.92	0.0530	1.1	338	17	372	19	328	24	100
Vranduk Fm.	BO87zrn063	49639	148	8	0.59	0.0630	2.7	0.76	0.0606	2.3	333	18	372	26	624	50	89
Vranduk Fm.	BO87zrn064	23444	97	4	0.64	0.0360	2.3	0.77	0.0530	1.9	228	11	237	14	328	44	96
Vranduk Fm.	BO87zrn065	9226	130	14	0.65	0.0974	2.5	0.93	0.0606	1.0	599	30	604	32	624	21	99
Vranduk Fm.	BO87zrn066	18785	112	26	0.68	0.2118	2.6	0.90	0.0803	1.3	1238	64	1226	70	1204	25	101
Vranduk Fm.	BO87zrn067	14201	389	26	0.26	0.0674	2.7	0.82	0.0570	1.9	420	23	432	29	492	42	97
Vranduk Fm.	BO87zrn068	23988	313	31	0.27	0.0995	2.4	0.96	0.0610	0.7	611	29	617	31	638	16	99
Vranduk Fm.	BO87zrn072	17177	967	27	0.46	0.0256	2.6	0.75	0.0655	2.3	163	9	211	15	791	48	77
Vranduk Fm.	BO87zrn073	42572	869	65	0.57	0.0676	2.8	0.92	0.0628	1.2	422	24	468	28	701	25	90
Vranduk Fm.	BO87zrn074	12657	245	20	0.17	0.0807	7.0	0.92	0.0723	2.9	500	70	599	91	984	59	83
Vranduk Fm.	BO87zrn076	27125	364	36	0.39	0.0936	2.8	0.89	0.0661	1.5	577	33	627	40	810	31	92
Vranduk Fm.	BO87zrn077	22268	180	35	1.23	0.1486	2.7	0.94	0.0734	1.0	893	48	932	53	1025	20	96
Vranduk Fm.	BO87zrn078	4594	132	7	0.30	0.0511	2.5	0.90	0.0573	1.2	321	16	345	19	504	27	93
Vranduk Fm.	BO87zrn079	65561	204	63	0.42	0.2924	3.0	0.93	0.1020	1.2	1654	98	1657	105	1661	22	100
Vranduk Fm.	BO87zrn080	15045	603	22	0.42	0.0348	2.7	0.92	0.0574	3.2	221	12	247	21	508	71	89
Vranduk Fm.	BO87zrn081	7768	47	9	0.33	0.1888	2.5	0.94	0.0760	0.9	1115	55	1108	59	1096	19	101
Vranduk Fm.	BO87zrn085	7652	429	14	0.48	0.0297	2.7	0.80	0.0580	3.5	189	10	217	19	531	77	87
Vranduk Fm.	BO87zrn086	49714	474	60	0.40	0.1210	2.3	0.92	0.0866	2.9	736	32	908	68	1353	57	81
Vranduk Fm.	BO87zrn087	4457	207	7	0.60	0.0335	1.7	0.85	0.0521	1.7	213	14	219	11	288	39	97
Vranduk Fm.	BO87zrn088	14276	305	30	0.87	0.0887	2.4	0.86	0.0586	1.4	548	26	549	31	584	31	100
Vranduk Fm.	BO87zrn089	3453	128	6	0.90	0.0364	2.6	0.37	0.0603	6.6	230	12	266	38	613	142	86
Vranduk Fm.	BO87zrn091	4289	283	8	1.03	0.0227	2.5	0.83	0.0529	1.6	145	7	158	9	323	37	93
Vranduk Fm.	BO87zrn092	2436	143	5	0.21	0.0298	2.3	0.84	0.0525	1.5	189	9	198	11	306	34	95
Vranduk Fm.	BO87zrn093	86166	169	80	0.81	0.4114	2.4	0.78	0.1285	1.9	2221	106	2147	131	2077	34	103
Vranduk Fm.	BO87zrn094	3899	271	7	0.54	0.0227	2.9	0.94	0.0497	1.1	145	8	147	9	183	25	98
Vranduk Fm.	BO87zrn098	19771	565	30	0.10	0.0570	2.4	0.90	0.0548	1.1	357	17	363	19	404	26	98
Vranduk Fm.	BO87zrn099	6336	92	9	0.65	0.0932	2.4	0.78	0.0631	1.9	574	28	603	38	711	41	95
Vranduk Fm.	BO87zrn100	24271	939	37	0.18	0.0392	3.7	0.92	0.0618	1.6	248	19	292	24	666	34	85
Vranduk Fm.	BO87zrn101	13310	220	22	0.72	0.0886	2.7	0.87	0.0613	1.5	547	30	567	35	649	33	96
Vranduk Fm.	BO87zrn102	10286	322	19	0.12	0.0612	2.7	0.91	0.0545	1.2	383	21	384	23	391	28	100
Vranduk Fm.	BO87zrn103	6047	86	10	1.15	0.0952	2.5	0.92	0.0622	1.1	586	29	606	32	680	22	97
Vranduk Fm.	BO87zrn104	6266	449	11	0.40	0.0251	2.6	0.90	0.0494	1.2	160	8	160	9	169	29	100
Vranduk Fm.	BO87zrn106	12870	183	18	0.50	0.0945	2.7	0.92	0.0626	1.1	582	31	606	35	694	24	96
Vranduk Fm.	BO87zrn107	12298	239	19	0.59	0.0741	2.4	0.90	0.0592	1.1	461	22	481	26	576	25	96
Vranduk Fm.	BO87zrn111	2975	202	5	0.32	0.0251	2.5	0.77	0.0520	2.1	160	8	168	11	284	47	95
Vranduk Fm.	BO87zrn112	11848	206	20	0.56	0.0890	2.8	0.85	0.0663	1.7	549	30	605	39	817	36	91
Vranduk Fm.	BO87zrn113	12518	516	22	0.60	0.0394	2.7	0.92	0.0528	1.2	249	13	256	15	319	27	97
Vranduk Fm.	BO87zrn114	19554	1067	21	0.15	0.0211	4.6	0.71	0.0802	4.5	122	11	195	25	1201	88	63
Vranduk Fm.	BO87zrn116	9058	643	14	0.34	0.0914	3.6	0.93	0.0561	1.4	136	10	147	11	169	32	93
Vranduk Fm.	BO87zrn118	30957	536	32	0.07	0.0619	3.0	0.84	0.0630	2.0	387	24	437	32	708	42	89
Vranduk Fm.	BO87zrn119	13166	215	14	0.24	0.0580	3.4	0.93	0.0616	1.4	363	25	406	30	659	29	89
Vranduk Fm.	BO87zrn120	18786	385	31	0.31	0.0803	2.8	0.86	0.0575	1.7	498	28	501	32	512	37	100
Vranduk Fm.	BO87zrn124	3889	191	7	0.78	0.0341	3.9	0.83	0.0514	2.7	216	17	220	21	257	62	98
Vranduk Fm.	BO87zrn125	3643	237	6	0.46	0.0332	2.6	0.81	0.0566	1.9	148	8	169	11	477	42	87
Vranduk Fm.	BO87zrn126	4585	203	8	0.58	0.0350	2.5	0.89	0.0519	1.3	224	11	229	13	280	29	98
Vranduk Fm.	BO87zrn127	9997	441	18	0.67	0.0367	2.6	0.89	0.0595	2.9	232	12	267	21	584	63	87
Vranduk Fm.	BO87zrn129	5389	202	9	0.49	0.0401	2.5	0.78	0.0551	1.9	253	12	270	17	416	43	94
Vranduk Fm.	BO87zrn130	6471	477	12	0.47	0.0235	2.7	0.92	0.0506	1.1	150	8	154	9	221	26	97
Vranduk Fm.	BO87zrn131	44631	2007	86	0.09	0.0386	3.0	0.65	0.0550	3.5	244	15	261	24	412	79	94

Formation	Sample & spot ID	<sup>207</sup> Pb (gpc)	U (ppm)	Pb (ppm)	Th/U	<sup>206</sup> Pb/ <sup>238</sup> U	1 σ %	<sup>207</sup> Pb/ <sup>235</sup> U	1 σ %	Rho	<sup>207</sup> Pb/ <sup>206</sup> Pb	1 σ %	Apparent ages				Conco. (%)		
													<sup>206</sup> Pb/ <sup>238</sup> U age ± 2σ (Ma)	<sup>207</sup> Pb/ <sup>238</sup> U age ± 2σ (Ma)	<sup>207</sup> Pb/ <sup>235</sup> U age ± 2σ (Ma)	<sup>207</sup> Pb/ <sup>206</sup> U age ± 2σ (Ma)			
Vranduk Fm.	BO87zm132	3083	209	5	0.32	0.0246	2.5	0.1705	2.9	0.87	0.0504	1.5	156	8	160	9	211	34	98
Vranduk Fm.	BO87zm133	16282	118	26	1.51	0.1508	2.7	1.5452	2.8	0.95	0.0743	0.9	905	48	949	53	1050	18	95
Vranduk Fm.	TD154zm007	10967	489	22	0.99	0.0389	2.2	0.2780	2.4	0.91	0.0519	1.0	246	11	249	12	279	23	99
Vranduk Fm.	TD154zm008	15059	125	20	0.39	0.1520	2.2	1.4920	2.4	0.92	0.0712	0.9	912	40	927	45	963	19	98
Vranduk Fm.	TD154zm009	11350	250	22	1.14	0.0727	2.4	0.5608	2.4	0.89	0.0560	1.1	452	19	452	22	452	25	100
Vranduk Fm.	TD154zm010	5358	437	9	0.42	0.0201	2.0	0.1377	1.6	0.78	0.0496	1.6	128	5	121	7	178	38	98
Vranduk Fm.	TD154zm011	3039	153	5	0.40	0.0341	2.7	0.2445	3.5	0.75	0.0521	2.3	216	12	222	16	288	53	97
Vranduk Fm.	TD154zm012	9246	33	9	0.41	0.2618	2.3	3.7428	2.6	0.89	0.1037	1.2	1499	70	1581	83	1691	22	95
Vranduk Fm.	TD154zm013	2137	28	3	0.91	0.1054	2.7	0.9264	2.7	0.79	0.0637	1.7	646	28	666	36	733	36	97
Vranduk Fm.	TD154zm014	1414	78	3	0.84	0.0332	2.8	0.2320	3.7	0.75	0.0506	2.5	211	12	212	16	225	57	99
Vranduk Fm.	TD154zm015	9699	223	16	0.43	0.0714	2.1	0.5551	2.4	0.89	0.0564	1.1	445	19	448	22	467	24	99
Vranduk Fm.	TD154zm020	53491	103	41	0.54	0.3554	3.1	6.7929	3.4	0.90	0.1386	1.5	1960	121	2085	144	2210	27	94
Vranduk Fm.	TD154zm021	4340	93	8	0.84	0.0731	2.0	0.5818	2.8	0.71	0.0577	2.0	455	18	466	26	518	44	98
Vranduk Fm.	TD154zm022	1361	14	3	2.23	0.1410	2.3	1.3040	3.5	0.67	0.0671	2.6	851	39	848	59	839	54	100
Vranduk Fm.	TD154zm023	6072	265	11	0.60	0.0385	2.4	0.2740	2.9	0.82	0.0516	1.7	243	12	246	14	270	38	99
Vranduk Fm.	TD154zm024	9841	217	15	0.17	0.0692	2.2	0.5672	2.6	0.85	0.0594	1.4	432	19	456	23	582	30	95
Vranduk Fm.	TD154zm025	1657	52	3	0.99	0.0477	2.2	0.3821	3.5	0.62	0.0581	2.7	300	13	329	23	533	60	91
Vranduk Fm.	TD154zm027	1174	76	3	0.33	0.0267	2.4	0.1958	3.4	0.71	0.0533	2.4	170	8	182	12	340	54	93
Vranduk Fm.	TD154zm028	3239	129	6	0.66	0.0418	2.4	0.3147	3.9	0.61	0.0546	3.1	264	13	278	22	395	70	95
Vranduk Fm.	TD154zm029	5425	238	12	1.01	0.0419	2.2	0.3039	1.6	0.80	0.0527	1.6	264	12	269	15	314	37	98
Vranduk Fm.	TD154zm033	8346	185	13	0.60	0.0738	2.9	0.5895	3.2	0.92	0.0579	1.3	459	27	471	30	526	28	98
Vranduk Fm.	TD154zm034	6112	156	10	0.34	0.0636	2.1	0.4827	2.6	0.79	0.0551	1.6	397	16	400	21	415	35	99
Vranduk Fm.	TD154zm035	19805	1017	32	0.20	0.0524	2.1	0.2451	3.4	0.62	0.0498	2.6	204	9	223	15	427	59	92
Vranduk Fm.	TD154zm036	2611	209	5	0.75	0.0234	2.2	0.1609	3.0	0.75	0.0498	2.0	149	7	151	9	187	46	98
Vranduk Fm.	TD154zm037	5316	268	9	0.49	0.0297	3.1	0.2087	3.6	0.85	0.0509	1.9	189	12	192	14	238	43	98
Vranduk Fm.	TD154zm038	4000	95	5	0.63	0.0469	3.6	0.4100	5.3	0.66	0.0634	4.0	295	21	349	37	723	85	85
Vranduk Fm.	TD154zm039	5638	270	10	0.41	0.0368	2.3	0.2587	2.5	0.91	0.0510	1.1	233	11	234	12	243	24	100
Vranduk Fm.	TD154zm040	1713	73	3	0.86	0.0418	2.2	0.3072	3.5	0.62	0.0534	2.8	264	12	272	19	344	63	97
Vranduk Fm.	TD154zm042	15202	281	23	0.66	0.0699	2.3	0.5859	2.6	0.90	0.0608	1.1	435	20	468	24	633	25	93
Vranduk Fm.	TD154zm046	1362	43	3	0.92	0.0505	2.3	0.4289	3.5	0.65	0.0516	2.7	317	14	362	25	661	57	88
Vranduk Fm.	TD154zm047	14379	308	27	0.59	0.0845	2.5	0.6771	2.7	0.92	0.0581	1.1	523	26	525	28	533	23	100
Vranduk Fm.	TD154zm048	11029	247	21	1.05	0.0716	2.4	0.5798	2.9	0.83	0.0587	1.6	446	21	464	27	556	34	96
Vranduk Fm.	TD154zm049	2574	136	5	0.56	0.0326	2.6	0.2310	3.1	0.84	0.0513	1.7	207	11	211	13	256	38	98
Vranduk Fm.	TD154zm050	3948	95	8	1.10	0.0680	2.1	0.5179	1.8	0.77	0.0553	1.8	424	18	424	23	423	39	100
Vranduk Fm.	TD154zm051	97050	128	67	0.75	0.4499	2.1	9.7619	2.2	0.97	0.1574	0.6	2395	102	2413	106	2428	10	99
Vranduk Fm.	TD154zm052	212663	547	163	0.17	0.2912	2.1	5.0941	2.2	0.97	0.1269	0.5	1648	69	1835	80	2055	10	90
Vranduk Fm.	TD154zm053	3437	228	5	0.51	0.0216	2.3	0.1656	2.0	0.75	0.0557	2.0	138	6	156	10	439	45	88
Vranduk Fm.	TD154zm054	9070	489	15	0.22	0.0311	2.3	0.2370	3.1	0.87	0.0553	1.3	197	9	216	11	423	28	91
Vranduk Fm.	TD154zm055	14985	933	26	0.18	0.0289	2.2	0.2396	2.8	0.78	0.0602	1.8	183	8	218	12	611	38	84
Vranduk Fm.	TD154zm059	64216	829	100	0.64	0.1247	1.9	1.0986	2.3	0.84	0.0639	1.3	758	29	753	35	738	26	101
Vranduk Fm.	TD154zm060	18103	588	34	0.64	0.0537	1.9	0.3945	2.3	0.91	0.0533	0.9	337	13	338	14	343	20	100
Vranduk Fm.	TD154zm061	6535	184	11	0.50	0.0567	1.9	0.4331	2.3	0.86	0.0554	1.2	355	14	365	17	430	26	97
Vranduk Fm.	TD154zm062	13402	612	25	0.50	0.0387	2.2	0.2803	2.6	0.84	0.0525	1.4	245	11	251	13	308	32	98
Vranduk Fm.	TD154zm063	8991	133	13	0.47	0.0901	2.4	0.7673	2.6	0.91	0.0618	1.1	556	26	578	30	666	23	96
Vranduk Fm.	TD154zm064	942	67	2	0.50	0.0238	2.1	0.1693	3.5	0.62	0.0515	2.7	152	6	159	11	264	62	96
Vranduk Fm.	TD154zm066	19688	309	32	0.70	0.0685	1.9	0.7922	2.0	0.93	0.0596	0.7	594	22	582	24	588	16	100
Vranduk Fm.	TD154zm067	3297	247	6	0.97	0.0230	1.9	0.1573	1.6	0.77	0.0495	1.6	147	6	148	7	172	37	99
Vranduk Fm.	TD154zm068	30810	1992	52	0.17	0.0271	1.8	0.2272	2.1	0.83	0.0609	1.2	172	6	208	9	635	25	83
Vranduk Fm.	TD154zm073	3322	238	6	0.47	0.0234	1.9	0.1635	2.4	0.76	0.0507	1.6	149	6	154	7	228	36	97
Vranduk Fm.	TD154zm074	3402	260	6	0.23	0.0223	2.1	0.1559	3.0	0.70	0.0508	2.1	142	6	147	9	232	49	96
Vranduk Fm.	TD154zm075	11651	343	21	0.33	0.0616	1.8	0.4695	2.0	0.91	0.0552	0.8	386	14	391	15	422	18	99
Vranduk Fm.	TD154zm076	2770	204	5	0.48	0.0234	2.0	0.1666	4.3	0.46	0.0516	3.8	149	6	156	14	268	88	95
Vranduk Fm.	TD154zm077	10307	175	16	0.78	0.0823	2.1	0.6956	3.3	0.62	0.0613	2.6	510	21	536	36	649	56	95
Vranduk Fm.	TD154zm078	3869	309	7	0.43	0.0222	2.2	0.1502	2.6	0.83	0.0491	1.4	141	6	142	7	153	34	100

Formation	Sample & spot ID	Apparent ages											Conco. (%)				
		<sup>207</sup> Pb (gpc)	U (ppm)	Pb (ppm)	Th/U	<sup>206</sup> Pb/ <sup>238</sup> U	1 $\sigma$ %	<sup>207</sup> Pb/ <sup>235</sup> U	1 $\sigma$ %	Rho	<sup>207</sup> Pb/ <sup>206</sup> Pb	1 $\sigma$ %		<sup>206</sup> Pb/ <sup>238</sup> U age $\pm$ 2 $\sigma$ (Ma)	<sup>207</sup> Pb/ <sup>235</sup> U age $\pm$ 2 $\sigma$ (Ma)	<sup>207</sup> Pb/ <sup>206</sup> Pb age $\pm$ 2 $\sigma$ (Ma)	Conco. (%)
Vranduk Fm.	TD154zm079	1188	214	21	1.11	0.0819	1.9	0.6770	2.1	0.91	0.0600	0.8	507	19	602	18	97
Vranduk Fm.	TD154zm080	2536	58	5	0.53	0.0760	2.1	0.6033	2.8	0.74	0.0576	1.9	472	20	513	41	99
Vranduk Fm.	TD154zm081	2730	114	5	1.04	0.0400	1.8	0.2913	2.5	0.72	0.0528	1.7	253	9	321	13	49
Vranduk Fm.	TD154zm085	14226	216	21	0.44	0.0940	1.8	0.7796	2.0	0.90	0.0602	0.9	579	21	610	19	99
Vranduk Fm.	TD154zm086	11437	520	22	0.64	0.0399	1.9	0.2874	2.5	0.76	0.0522	1.6	252	9	295	36	98
Vranduk Fm.	TD154zm087	27228	766	51	0.75	0.0630	2.1	0.4921	2.1	0.96	0.0566	1.6	394	16	478	13	97
Vranduk Fm.	TD154zm088	2009	62	4	0.53	0.0574	2.3	0.4622	3.5	0.66	0.0584	2.6	360	17	543	17	93
Vranduk Fm.	TD154zm089	4861	339	8	0.22	0.0249	2.1	0.1820	2.7	0.77	0.0531	1.7	158	7	334	39	93
Vranduk Fm.	TD154zm090	8094	174	13	0.35	0.0746	1.8	0.5836	2.0	0.90	0.0567	1.9	467	17	482	20	99
Vranduk Fm.	TD154zm091	2994	72	4	0.62	0.0365	2.1	0.4395	2.4	0.87	0.0564	1.2	354	15	470	26	96
Vranduk Fm.	TD154zm092	23757	596	38	0.32	0.0637	1.7	0.4972	2.2	0.79	0.0566	1.3	398	14	478	30	97
Vranduk Fm.	TD154zm093	8779	388	17	0.88	0.0379	1.8	0.2657	2.0	0.89	0.0509	0.9	240	9	237	22	100
Vranduk Fm.	TD154zm094	4094	276	7	0.62	0.0249	1.9	0.1858	2.8	0.67	0.0541	2.1	159	6	376	47	92
Vranduk Fm.	TD154zm098	8670	178	13	0.63	0.0675	1.9	0.5737	3.5	0.55	0.0617	2.9	421	16	663	63	91
Vranduk Fm.	TD154zm099	2845	126	5	0.82	0.0383	1.9	0.2769	2.4	0.76	0.0524	1.6	242	9	304	36	98
Vranduk Fm.	TD154zm100	8748	378	15	0.47	0.0389	1.8	0.2830	2.0	0.91	0.0528	0.8	246	9	321	18	97
Vranduk Fm.	TD154zm101	19940	516	31	0.41	0.0575	1.8	0.4465	2.0	0.90	0.0563	0.9	360	13	466	19	96
Vranduk Fm.	TD154zm102	11452	718	23	0.48	0.0315	1.9	0.2329	2.6	0.72	0.0536	1.8	200	8	355	41	94
Vranduk Fm.	TD154zm103	13022	280	23	0.49	0.0815	2.1	0.6482	2.3	0.92	0.0577	0.9	505	21	517	19	100
Vranduk Fm.	TD154zm104	3960	86	6	0.53	0.0685	1.8	0.5433	2.1	0.84	0.0576	1.2	427	15	513	25	97
Vranduk Fm.	TD154zm105	3075	86	5	0.36	0.0568	1.8	0.4265	2.4	0.76	0.0544	1.6	356	13	369	35	99
Vranduk Fm.	TD154zm106	2407	168	4	0.50	0.0243	1.9	0.1710	2.7	0.71	0.0511	1.9	155	6	246	44	96
Vranduk Fm.	TD154zm107	4694	58	7	0.69	0.1073	1.8	0.9259	2.1	0.85	0.0626	1.3	657	24	694	28	99
Vranduk Fm.	TD154zm111	40889	84	28	0.07	0.3379	2.0	5.7771	0.7	0.91	0.1240	0.7	1876	76	2015	12	97
Vranduk Fm.	TD154zm112	16367	417	29	0.30	0.0701	2.3	0.5558	2.5	0.92	0.0575	1.0	437	20	512	22	97
Vranduk Fm.	TD154zm113	5209	85	7	0.12	0.0825	2.1	0.6818	3.3	0.82	0.0599	1.5	511	22	602	33	97
Vranduk Fm.	TD154zm115	1946	101	3	0.26	0.0293	2.7	0.2084	3.8	0.71	0.0516	2.7	186	10	268	61	97
Vranduk Fm.	TD154zm116	2477	89	5	1.48	0.0465	2.3	0.3413	2.7	0.83	0.0532	1.5	293	13	338	35	98
Vranduk Fm.	TD154zm117	1939	140	4	0.58	0.0242	2.1	0.1672	2.9	0.74	0.0501	1.9	154	6	199	45	98
Vranduk Fm.	TD154zm118	2411	34	4	0.75	0.1027	2.3	0.9004	3.4	0.66	0.0636	2.5	630	28	727	54	97
Vranduk Fm.	TD154zm120	5553	133	9	0.42	0.0669	2.2	0.5250	3.1	0.71	0.0569	2.2	417	18	489	48	97
Vranduk Fm.	TD154zm124	19778	446	26	0.19	0.0697	2.7	0.4603	2.8	0.97	0.0559	0.7	374	20	449	16	97
Vranduk Fm.	TD154zm125	23296	200	29	0.30	0.1475	2.3	1.4298	2.4	0.96	0.0703	0.7	887	40	937	14	98
Vranduk Fm.	TD154zm126	6450	286	11	0.61	0.0377	2.2	0.2696	2.4	0.90	0.0519	1.1	238	10	281	25	98
Vranduk Fm.	TD154zm127	6924	509	13	0.47	0.0242	2.1	0.1667	2.4	0.87	0.0500	1.2	154	6	194	27	98
Vranduk Fm.	TD154zm128	19723	333	32	0.55	0.0915	2.1	0.7546	2.2	0.96	0.0598	0.7	564	24	598	14	99
Vranduk Fm.	TD154zm130	1076	73	2	0.16	0.0224	2.2	0.1590	3.6	0.61	0.0514	2.9	143	6	259	66	95
Vranduk Fm.	TD154zm131	172097	194	100	0.33	0.4778	2.0	11.0319	0.8	0.92	0.1675	0.8	2518	102	2532	13	100
Vranduk Fm.	TD154zm132	15497	695	22	0.52	0.0298	2.4	0.2683	3.3	0.72	0.0653	2.3	189	9	783	48	78
DOZ mélange	BO23zm007	1199	51	2	0.86	0.0397	1.9	0.3168	3.3	0.57	0.0579	2.7	251	10	527	59	90
DOZ mélange	BO23zm008	3329	100	5	0.77	0.0489	1.8	0.3739	2.5	0.72	0.0554	1.8	308	11	429	39	95
DOZ mélange	BO23zm009	3107	172	6	0.59	0.0301	1.8	0.2162	2.6	0.71	0.0520	1.8	191	7	285	41	96
DOZ mélange	BO23zm010	17373	138	25	1.06	0.1524	1.8	1.5006	2.0	0.92	0.0714	0.8	914	33	969	16	98
DOZ mélange	BO23zm011	14371	128	20	0.42	0.1521	1.8	1.5016	2.0	0.90	0.0714	0.8	913	32	975	17	98
DOZ mélange	BO23zm012	4730	248	9	0.49	0.0330	1.7	0.2378	2.2	0.80	0.0522	1.3	210	7	294	29	97
DOZ mélange	BO23zm013	361613	480	246	0.14	0.4876	1.8	11.3136	2.0	0.89	0.1683	0.9	2560	93	2541	15	100
DOZ mélange	BO23zm014	36396	86	32	1.07	0.2937	1.8	4.6354	1.9	0.96	0.1145	0.5	1660	60	1756	66	95
DOZ mélange	BO23zm015	6655	288	11	0.88	0.0374	1.7	0.2835	2.0	0.88	0.0550	0.9	237	8	1871	9	95
DOZ mélange	BO23zm016	72478	483	65	0.28	0.1338	1.8	1.4283	1.9	0.97	0.0774	0.4	809	30	901	34	90
DOZ mélange	BO23zm020	4103	111	6	0.44	0.0550	2.0	0.4431	2.5	0.79	0.0584	1.6	345	14	546	34	93
DOZ mélange	BO23zm021	2172	21	2	1.33	0.0802	2.3	1.1118	5.8	0.39	0.1006	5.3	497	23	1635	99	65
DOZ mélange	BO23zm022	5014	102	8	1.14	0.0689	1.8	0.5762	2.7	0.65	0.0606	2.0	430	15	462	44	93
DOZ mélange	BO23zm023	4109	212	7	0.18	0.0325	1.8	0.2297	2.3	0.78	0.0512	1.4	206	7	250	33	98
DOZ mélange	BO23zm024	6051	116	8	0.75	0.0594	2.5	0.5714	3.6	0.69	0.0698	2.6	372	18	923	53	81

Formation	Sample & spot ID	Apparent ages															
		<sup>207</sup> Pb (gpc)	U (ppm)	Pb (ppm)	Th/U	<sup>206</sup> Pb/ <sup>238</sup> U	1 σ %	<sup>207</sup> Pb/ <sup>235</sup> U	1 σ %	Rho	<sup>207</sup> Pb/ <sup>206</sup> Pb	1 σ %	<sup>206</sup> Pb/ <sup>238</sup> U age ± 2σ (Ma)	<sup>207</sup> Pb/ <sup>235</sup> U age ± 2σ (Ma)	<sup>207</sup> Pb/ <sup>206</sup> U age ± 2σ (Ma)	Conco. (%)	
DOZ mélange	BO23zrn025	5132	73	8	0.61	0.1027	1.7	0.9056	2.2	0.78	0.0640	630	22	741	30	741	96
DOZ mélange	BO23zrn026	7287	244	12	0.42	0.0468	1.8	0.3443	2.1	0.85	0.0534	295	11	300	26	346	98
DOZ mélange	BO23zrn027	5062	113	9	0.62	0.0714	1.7	0.5565	1.1	0.84	0.0565	445	16	449	25	473	99
DOZ mélange	BO23zrn028	24641	204	31	0.56	0.1421	1.8	1.3536	1.9	0.96	0.0691	856	31	869	32	902	99
DOZ mélange	BO23zrn033	11503	579	24	0.67	0.0390	2.4	0.2967	2.6	0.94	0.0551	247	12	284	14	417	94
DOZ mélange	BO23zrn034	6202	237	9	0.64	0.0374	1.9	0.3218	2.3	0.63	0.0374	237	9	283	17	686	84
DOZ mélange	BO23zrn035	4020	86	5	0.88	0.0446	2.2	0.5595	6.1	0.36	0.0909	281	13	451	55	1445	62
DOZ mélange	BO23zrn036	6525	305	11	0.68	0.0335	1.8	0.2477	2.2	0.84	0.0536	212	8	225	10	355	95
DOZ mélange	BO23zrn037	12213	147	16	0.76	0.1032	1.8	0.9607	2.3	0.74	0.0675	633	22	684	32	853	93
DOZ mélange	BO23zrn038	2128	97	4	0.66	0.0364	2.0	0.2767	2.6	0.74	0.0551	231	9	248	13	417	93
DOZ mélange	BO23zrn039	8302	100	13	0.98	0.1118	1.8	0.9904	2.0	0.88	0.0643	683	24	699	28	751	98
DOZ mélange	BO23zrn040	10592	103	12	0.64	0.1038	2.0	0.9978	2.2	0.92	0.0697	637	25	703	30	920	91
DOZ mélange	BO23zrn041	1258	35	2	2.18	0.0340	2.8	0.3517	4.6	0.62	0.0749	216	12	306	28	1067	71
DOZ mélange	BO23zrn042	16237	441	31	1.14	0.0600	1.8	0.4528	1.9	0.93	0.0547	376	14	379	15	401	99
DOZ mélange	BO23zrn047	8010	241	14	0.72	0.0553	1.8	0.4497	2.2	0.82	0.0589	347	12	377	17	565	92
DOZ mélange	BO23zrn048	12916	311	21	1.10	0.0583	1.8	0.5259	2.8	0.66	0.0654	366	13	429	24	786	85
DOZ mélange	BO23zrn049	18883	291	36	1.43	0.0980	1.7	0.8266	1.9	0.92	0.0612	603	21	612	23	645	99
DOZ mélange	BO23zrn050	10606	456	18	0.93	0.0364	1.7	0.2964	4.2	0.41	0.0590	231	8	264	22	569	87
DOZ mélange	BO23zrn051	14134	291	24	0.64	0.0788	1.7	0.6395	2.0	0.86	0.0588	489	17	502	20	561	92
DOZ mélange	BO23zrn052	5042	98	8	0.59	0.0790	1.7	0.6226	2.1	0.84	0.0571	490	17	491	18	497	100
DOZ mélange	BO23zrn053	3870	116	7	0.64	0.0585	1.8	0.4602	2.3	0.75	0.0570	367	13	384	18	493	95
DOZ mélange	BO23zrn054	22473	72	25	1.69	0.2491	3.0	3.8453	3.4	0.89	0.1119	1434	87	1602	109	1831	89
DOZ mélange	BO23zrn055	35151	934	65	0.73	0.0644	1.9	0.4944	2.0	0.93	0.0557	402	15	408	16	441	99
DOZ mélange	BO23zrn059	13608	437	23	0.40	0.0522	1.2	0.3896	1.5	0.82	0.0541	328	8	334	10	375	98
DOZ mélange	BO23zrn060	2881	34	4	0.46	0.1104	1.6	1.0652	2.5	0.64	0.0700	675	21	736	36	928	92
DOZ mélange	BO23zrn061	8600	391	17	0.82	0.0384	1.3	0.2797	1.7	0.77	0.0529	243	6	250	8	324	97
DOZ mélange	BO23zrn062	19694	945	35	0.51	0.0356	1.3	0.2549	1.5	0.85	0.0519	226	6	231	7	280	98
DOZ mélange	BO23zrn063	1636	66	3	0.73	0.0399	1.4	0.2993	2.4	0.57	0.0544	252	7	266	13	387	95
DOZ mélange	BO23zrn064	8506	224	16	0.85	0.0626	1.2	0.4767	1.0	0.78	0.0552	392	9	386	12	420	99
DOZ mélange	BO23zrn065	9289	363	16	0.43	0.0427	1.4	0.3151	1.4	0.66	0.0535	307	7	278	14	349	97
DOZ mélange	BO23zrn066	4988	178	10	1.03	0.0488	1.3	0.3724	2.2	0.60	0.0554	307	6	321	14	428	95
DOZ mélange	BO23zrn067	5318	240	10	0.79	0.0381	1.3	0.2734	1.7	0.75	0.0521	241	6	245	8	289	98
DOZ mélange	BO23zrn068	5713	148	10	0.38	0.0673	1.4	0.5058	1.9	0.73	0.0545	420	12	416	16	391	101
DOZ mélange	BO23zrn072	7466	120	17	2.55	0.0924	1.1	0.7760	1.8	0.64	0.0609	570	13	583	21	637	98
DOZ mélange	BO23zrn073	4269	195	8	0.75	0.0369	1.3	0.2686	1.9	0.68	0.0528	234	6	242	9	319	97
DOZ mélange	BO23zrn074	66174	183	45	0.36	0.2241	1.3	3.8679	1.7	0.76	0.1252	1304	34	1607	55	2031	81
DOZ mélange	BO23zrn075	296715	407	179	0.70	0.3732	1.7	7.6661	1.3	0.95	0.1490	2044	52	2193	59	2334	93
DOZ mélange	BO23zrn076	3480	139	7	0.82	0.0437	1.3	0.3285	2.7	0.65	0.0545	276	10	288	15	391	96
DOZ mélange	BO23zrn077	1058	39	2	1.33	0.0471	1.5	0.3665	3.6	0.40	0.0564	297	9	317	23	468	94
DOZ mélange	BO23zrn078	12436	121	12	13.69	0.0715	1.9	0.8377	4.8	0.40	0.0850	445	17	618	59	1314	85
DOZ mélange	BO23zrn079	3675	162	7	1.41	0.0368	1.3	0.3037	2.5	0.54	0.0598	233	6	269	13	597	72
DOZ mélange	BO23zrn080	3930	118	6	0.37	0.0528	1.3	0.4162	1.8	0.71	0.0572	331	8	353	13	499	94
DOZ mélange	BO23zrn081	13263	480	22	0.44	0.0458	1.3	0.3597	1.6	0.81	0.0570	289	10	312	10	492	92
DOZ mélange	BO23zrn085	9861	69	14	1.00	0.0761	1.1	1.8203	1.3	0.65	0.0761	1031	23	1031	36	1098	98
DOZ mélange	BO23zrn086	2721	115	5	0.97	0.0391	1.4	0.3060	3.2	0.43	0.0568	247	7	271	17	484	91
DOZ mélange	BO23zrn087	1539	71	3	0.64	0.0376	1.6	0.2732	2.2	0.59	0.0527	238	8	245	14	315	97
DOZ mélange	BO23zrn088	2243	79	4	0.61	0.0467	1.2	0.3641	3.3	0.37	0.0566	294	7	315	21	476	93
DOZ mélange	BO23zrn089	4266	143	9	1.15	0.0518	1.3	0.3943	2.0	0.66	0.0552	326	9	337	14	420	96
DOZ mélange	BO23zrn090	4320	191	8	0.41	0.0400	1.4	0.2880	2.2	0.63	0.0523	253	7	257	11	298	98
DOZ mélange	BO23zrn091	2644	111	5	0.63	0.0422	1.3	0.3070	2.1	0.64	0.0528	266	7	272	11	319	98
DOZ mélange	BO23zrn092	21415	20	14	1.39	0.5306	1.3	13.3346	1.7	0.78	0.1823	2744	71	2704	90	2674	101
DOZ mélange	BO23zrn093	46455	62	32	0.78	0.4599	2.3	10.7875	2.9	0.81	0.1701	2439	112	2505	143	2559	97
DOZ mélange	BO23zrn094	60790	152	49	0.46	0.3125	1.1	4.9032	1.5	0.71	0.1138	1753	37	1803	53	1861	97
DOZ mélange	BO23zrn098	38251	103	35	0.55	0.3171	1.2	4.7246	1.3	0.91	0.1081	1775	43	1772	10	1767	100

Formation	Sample & spot ID	<sup>207</sup> Pb (gpc)	U (ppm)	Pb (ppm)	Th/U	<sup>206</sup> Pb/ <sup>238</sup> U	1 σ %	<sup>207</sup> Pb/ <sup>235</sup> U	1 σ %	Rho	<sup>207</sup> Pb/ <sup>206</sup> Pb	1 σ %	Apparent ages				Conco. (%)			
													<sup>206</sup> Pb/ <sup>238</sup> U age ± 2σ (Ma)	<sup>207</sup> Pb/ <sup>235</sup> U age ± 2σ (Ma)	<sup>206</sup> Pb/ <sup>238</sup> U age ± 2σ (Ma)	<sup>207</sup> Pb/ <sup>235</sup> U age ± 2σ (Ma)				
DOZ mélange	BO23zrn099	3526	155	6	0.82	0.0381	1.3	0.2853	2.0	0.65	0.0543	1.6	241	6	241	285	10	383	35	95
DOZ mélange	BO23zrn100	11201	300	25	0.64	0.0635	1.3	0.6403	1.8	0.74	0.0556	1.2	517	14	517	502	18	436	27	103
DOZ mélange	BO23zrn101	69819	177	64	0.72	0.3304	1.1	5.1848	1.3	0.85	0.1138	0.7	1840	42	1840	1850	49	1861	13	99
DOZ mélange	BO23zrn102	11429	24	11	0.81	0.3746	1.1	6.1219	1.4	0.80	0.1185	0.8	2051	6	2051	1993	55	1934	15	103
DOZ mélange	BO23zrn103	3897	192	10	1.93	0.0393	1.2	0.2799	1.4	0.64	0.0517	1.4	248	6	248	238	9	271	32	99
DOZ mélange	BO23zrn104	2333	104	4	1.19	0.0643	2.8	0.2643	2.4	0.51	0.0523	2.4	232	7	232	238	13	298	54	97
DOZ mélange	BO23zrn106	3122	99	5	0.78	0.0470	1.3	0.3523	2.0	0.63	0.0544	1.6	296	8	296	306	12	387	36	97
DOZ mélange	BO23zrn107	166883	316	124	0.53	0.3665	1.2	6.4825	1.3	0.93	0.1283	0.5	2013	47	2013	2044	52	2075	8	99
DOZ mélange	BO23zrn111	12810	262	14	1.01	0.0491	2.5	0.3723	2.9	0.85	0.0550	1.5	309	16	309	321	19	412	34	96
DOZ mélange	BO23zrn112	12832	485	19	0.69	0.0359	2.5	0.3083	3.5	0.72	0.0623	2.4	227	11	227	273	19	685	51	83
DOZ mélange	BO23zrn113	4099	95	7	0.93	0.0706	2.4	0.5420	2.8	0.88	0.0557	1.3	440	21	440	440	25	441	30	100
DOZ mélange	BO23zrn114	7727	215	13	0.67	0.0682	2.5	0.4330	0.9	0.94	0.0540	0.9	364	18	364	365	19	371	20	100
DOZ mélange	BO23zrn115	231170	439	178	0.34	0.3806	2.5	6.4352	2.5	0.97	0.1226	0.6	2079	102	2079	2037	103	1995	10	102
DOZ mélange	BO23zrn116	30700	945	44	0.87	0.0423	2.5	0.3455	2.7	0.94	0.0592	0.9	267	14	267	301	16	575	20	89
DOZ mélange	BO23zrn117	7390	343	13	0.64	0.0361	2.5	0.2745	2.6	0.94	0.0552	0.9	228	11	228	246	13	420	19	93
DOZ mélange	BO23zrn118	10178	408	19	0.90	0.0439	2.5	0.3276	2.6	0.94	0.0541	0.9	277	14	277	288	15	375	20	96
DOZ mélange	BO23zrn119	22980	207	36	1.15	0.1581	2.5	1.5375	2.7	0.93	0.0705	1.0	946	48	946	946	52	944	21	100
DOZ mélange	BO23zrn120	5939	195	11	1.15	0.0499	2.5	0.3980	2.9	0.86	0.0578	1.5	314	16	314	340	20	523	32	92
DOZ mélange	BO23zrn124	3217	170	7	0.97	0.0354	2.7	0.2550	3.3	0.81	0.0522	1.9	224	12	224	231	15	294	43	97
DOZ mélange	BO23zrn125	7095	329	13	1.10	0.0351	2.5	0.2496	2.7	0.92	0.0515	1.0	223	11	223	226	12	263	24	98
DOZ mélange	BO23zrn126	57539	134	50	0.59	0.3488	2.4	5.4875	2.4	0.98	0.1141	0.5	1929	92	1929	1899	93	1866	9	102
DOZ mélange	BO23zrn127	178852	391	153	1.15	0.3263	2.5	5.4539	2.6	0.98	0.1212	0.5	1820	91	1820	1893	97	1974	9	96
DOZ mélange	BO23zrn128	6629	221	12	0.67	0.0502	2.5	0.3587	2.8	0.90	0.0518	1.2	316	16	316	311	17	276	27	101
DOZ mélange	BO23zrn129	6006	132	9	0.74	0.0624	2.5	0.4950	3.0	0.84	0.0575	1.6	390	19	390	408	24	511	35	96
DOZ mélange	BO23zrn130	6383	203	10	1.00	0.0437	2.5	0.3837	3.3	0.78	0.0637	2.0	276	14	276	330	21	732	43	84
DOZ mélange	BO23zrn131	9975	45	7	0.54	0.1052	3.3	1.4268	4.0	0.84	0.0984	2.2	645	43	645	900	71	1594	41	72
DOZ mélange	BO23zrn132	4730	36	6	0.87	0.1537	2.5	1.5503	2.9	0.88	0.0731	1.4	922	47	922	951	55	1018	28	97
DOZ mélange	BO23zrn133	3941	149	7	0.88	0.0426	2.9	0.3269	4.4	0.65	0.0556	3.4	269	15	269	287	25	437	75	94
DOZ mélange	BO23zrn137	11415	96	16	0.77	0.1536	2.4	1.5272	2.9	0.83	0.0721	1.6	921	45	921	941	55	990	33	98
DOZ mélange	BO23zrn138	17996	382	30	0.45	0.0788	2.5	0.6054	2.6	0.96	0.0557	0.7	489	24	489	481	25	441	15	102
DOZ mélange	BO23zrn139	6047	237	10	0.71	0.0397	2.5	0.2831	2.7	0.92	0.0517	1.1	251	13	251	253	14	272	24	99
DOZ mélange	BO23zrn140	5633	15	6	2.40	0.3125	3.0	4.8515	3.3	0.93	0.1126	1.2	1753	106	1753	1794	117	1842	22	98
DOZ mélange	BO23zrn141	3817	154	6	0.52	0.0398	2.6	0.2906	3.5	0.75	0.0529	2.3	252	13	252	259	18	324	53	97
DOZ mélange	BO23zrn142	4294	164	7	0.72	0.0433	2.7	0.3117	3.1	0.86	0.0522	1.6	273	15	273	276	17	294	36	99
DOZ mélange	BO23zrn143	9814	216	16	0.87	0.0666	2.7	0.5283	2.9	0.93	0.0575	1.1	416	22	416	431	25	511	23	97
DOZ mélange	BO23zrn144	174070	472	161	0.30	0.3368	2.6	5.1922	2.7	0.97	0.1118	0.7	1871	98	1871	1851	100	1829	13	101
DOZ mélange	BO23zrn145	4289	136	8	1.02	0.0491	2.5	0.3798	3.1	0.80	0.0561	1.9	309	15	309	327	20	457	42	95
DOZ mélange	BO23zrn146	2533	94	5	1.09	0.0453	2.6	0.3338	3.3	0.78	0.0535	2.0	285	15	285	292	19	350	46	98

**Results of detrital zircon fission track thermochronology from the Bosnian Flysch**

Sample ID	Stratigraphy	Cryst.	RhoS	[Ns]	RhoI	[Ni]	RhoD	[Nd]	P ( $\chi^2$ )	Disp.	FT age* $\pm 1\sigma$ [Ma]
BO-117	Ugar Fm.	60	138.9	[6474]	26.3	[1226]	6.60	[4859]	0	0.42	212.4 $\pm$ 13.9
TD-154	Vranduk Fm.	60	83.3	[7456]	21.0	[1880]	5.49	[2652]	0	0.24	136.9 $\pm$ 6.5

Cryst: number of dated zircon crystals.

Track densities (Rho) are as measured ( $\times 10^5$  tr/cm<sup>2</sup>); number of tracks counted (N) shown in brackets.

P ( $\chi^2$ ): probability obtaining Chi-square value for n degree of freedom (where n = no. crystals-1).

Disp.: Dispersion, according to Galbraith and Laslett (1993).

\*: Central ages calculated using dosimeter glass: CN 2 with  $z_{CN2} = 127.8 \pm 1.6$  for zircon. See text for principal age components.

**Electron microprobe analyses of detrital Cr-spinel  
from Cretaceous siliciclastic sediments in the Croatian NW Dinarides**

[analyses in wt%. bdl=below detection limit]

Formation	Sample	MgO	Al2O3	Cr2O3	FeO	V2O3	SiO2	TiO2	MnO	NiO	ZnO	total
Bistra	05-H/B-201	13.23	23.12	45.43	17.83	0.26	bdl	0.03	0.21	0.09	0.16	100.36
Bistra	05-H/B-201	14.20	26.40	42.32	16.92	0.21	bdl	0.05	0.22	0.11	0.14	100.56
Bistra	05-H/B-201	10.69	14.52	53.58	19.83	0.33	bdl	0.05	0.26	0.06	0.18	99.49
Bistra	05-H/B-201	8.66	21.01	39.38	28.95	0.29	bdl	0.68	0.29	0.12	0.16	99.55
Bistra	05-H/B-201	12.34	21.93	46.11	17.99	0.26	bdl	0.11	0.22	0.06	0.19	99.20
Bistra	05-H/B-201	13.29	17.82	50.65	17.43	0.21	bdl	0.08	0.22	0.10	0.07	99.87
Bistra	05-H/B-201	13.72	21.52	47.15	16.18	0.20	bdl	0.05	0.22	0.09	0.13	99.25
Bistra	05-H/B-201	11.58	19.93	47.23	19.92	0.26	bdl	0.03	0.24	0.06	0.20	99.44
Bistra	05-H/B-201	14.26	21.63	47.37	15.24	0.23	bdl	0.06	0.19	0.08	0.10	99.17
Bistra	05-H/B-201	14.57	27.54	41.06	16.24	0.17	bdl	0.18	0.16	0.10	0.14	100.14
Bistra	05-H/B-201	10.65	18.10	42.87	26.15	0.33	bdl	0.63	0.29	0.17	0.14	99.33
Bistra	05-H/B-201	14.17	24.47	44.28	16.05	0.18	bdl	0.15	0.18	0.10	0.15	99.73
Bistra	05-H/B-201	11.45	23.92	43.54	19.77	0.25	bdl	0.04	0.26	0.08	0.28	99.59
Bistra	05-H/B-201	9.92	20.70	43.03	24.70	0.35	bdl	0.36	0.26	0.15	0.12	99.59
Bistra	05-H/B-201	13.02	27.32	40.04	17.85	0.24	bdl	0.05	0.18	0.06	0.29	99.06
Bistra	05-H/B-201	10.00	18.51	42.29	26.78	0.31	bdl	0.54	0.26	0.13	0.19	99.01
Bistra	05-H/B-201	9.23	21.11	39.58	27.98	0.20	bdl	0.45	0.31	0.12	0.21	99.19
Bistra	05-H/B-201	17.54	41.27	25.51	14.05	0.14	bdl	0.08	0.14	0.21	0.17	99.11
Bistra	05-H/B-201	11.92	22.34	45.86	18.97	0.27	bdl	0.05	0.26	0.08	0.20	99.94
Bistra	05-H/B-201	13.55	23.50	44.81	17.25	0.17	bdl	0.09	0.21	0.10	0.13	99.80
Bistra	05-H/B-201	15.02	24.41	44.54	14.87	0.21	bdl	0.07	0.19	0.11	0.10	99.51
Bistra	05-H/B-201	13.56	27.36	39.98	17.78	0.23	bdl	0.03	0.20	0.07	0.17	99.39
Bistra	05-H/B-201	12.36	22.76	45.38	18.42	0.26	bdl	0.04	0.23	0.06	0.17	99.69
Bistra	05-H/B-201	13.26	22.74	45.70	17.01	0.23	bdl	0.04	0.26	0.09	0.16	99.48
Bistra	05-H/B-201	11.90	18.38	50.62	18.38	0.23	bdl	0.06	0.25	0.05	0.14	100.02
Bistra	05-H/B-201	11.08	19.54	42.89	24.42	0.35	bdl	0.67	0.31	0.08	0.14	99.48
Bistra	05-H/B-201	12.97	20.22	48.67	17.66	0.19	bdl	0.36	0.22	0.10	0.13	100.51
Bistra	05-H/B-201	14.18	20.61	45.58	18.15	0.25	bdl	0.45	0.21	0.10	0.08	99.62
Bistra	05-H/B-201	12.50	17.30	50.92	18.71	0.20	bdl	0.11	0.27	0.07	0.09	100.17
Bistra	05-H/B-201	12.80	25.82	41.83	18.13	0.22	bdl	0.05	0.24	0.08	0.16	99.31
Bistra	05-H/B-201	12.59	22.48	45.96	17.54	0.26	bdl	0.05	0.22	0.07	0.14	99.32
Bistra	05-H/B-201	14.08	21.62	47.42	16.25	0.18	bdl	0.04	0.23	0.10	0.09	100.02
Bistra	05-H/B-201	12.82	24.83	43.08	18.34	0.27	bdl	0.03	0.20	0.10	0.20	99.87
Bistra	05-H/B-201	11.56	18.56	46.84	21.72	0.26	bdl	0.26	0.29	0.07	0.12	99.68
Bistra	05-H/B-201	12.08	19.81	48.27	18.69	0.30	bdl	0.06	0.25	0.06	0.15	99.67
Bistra	05-H/B-201	16.15	27.23	42.40	13.29	0.18	bdl	0.10	0.14	0.13	0.09	99.72
Bistra	05-H/B-201	10.78	16.26	51.40	20.50	0.35	bdl	0.05	0.27	0.06	0.18	99.85
Bistra	05-H/B-201	10.96	17.48	50.70	20.37	0.25	bdl	0.06	0.28	0.07	0.15	100.34
Bistra	05-H/B-201	11.26	18.99	45.70	22.63	0.26	bdl	0.26	0.32	0.13	0.16	99.71
Bistra	05-H/B-201	12.44	20.67	47.79	18.27	0.27	bdl	0.05	0.23	0.04	0.18	99.95
Bistra	05-H/B-201	13.74	21.83	45.94	17.17	0.28	bdl	0.20	0.20	0.10	0.13	99.60
Bistra	05-H/B-201	12.87	22.30	45.07	18.30	0.24	bdl	0.07	0.21	0.09	0.15	99.27
Bistra	05-H/B-201	12.56	21.87	45.85	19.10	0.24	bdl	0.04	0.25	0.08	0.15	100.15
Bistra	05-H/B-201	13.49	22.30	46.73	16.53	0.28	bdl	0.03	0.21	0.09	0.12	99.77
Bistra	05-H/B-201	13.19	19.44	47.69	18.65	0.25	bdl	0.19	0.20	0.10	0.08	99.79
Bistra	05-H/B-201	12.25	20.01	48.75	18.29	0.25	bdl	0.04	0.20	0.06	0.18	100.03
Bistra	05-H/B-201	13.84	24.06	44.31	16.93	0.23	bdl	0.14	0.21	0.10	0.15	99.98
Bistra	05-H/B-201	8.75	12.62	55.65	21.77	0.17	bdl	0.17	0.25	0.03	0.17	99.59
Bistra	05-H/B-201	14.24	23.37	46.51	14.54	0.25	bdl	0.08	0.15	0.10	0.12	99.35
Bistra	05-H/B-201	12.59	20.51	48.06	18.23	0.29	bdl	0.06	0.24	0.06	0.15	100.17
Bistra	05-H/B-201	12.16	17.75	47.96	21.23	0.25	bdl	0.25	0.23	0.10	0.13	100.06
Bistra	05-H/B-201	12.50	19.64	49.42	17.55	0.27	bdl	0.03	0.27	0.06	0.18	99.93
Bistra	05-H/B-201	10.60	18.65	49.28	21.01	0.32	bdl	0.05	0.27	0.06	0.23	100.49
Bistra	05-H/B-201	13.88	25.40	42.93	16.67	0.21	bdl	0.05	0.23	0.10	0.19	99.65
Bistra	05-H/B-201	9.39	15.94	44.48	27.76	0.39	bdl	1.09	0.28	0.10	0.22	99.65
Bistra	05-H/B-201	12.06	19.68	48.96	19.05	0.34	bdl	0.02	0.28	0.06	0.18	100.62
Bistra	05-H/B-201	13.46	21.87	47.12	16.86	0.25	bdl	0.11	0.21	0.06	0.17	100.12
Bistra	05-H/B-201	11.98	18.23	49.61	19.03	0.27	bdl	0.12	0.24	0.07	0.11	99.66
Bistra	05-H/B-201	12.15	18.55	42.79	24.12	0.28	bdl	1.56	0.25	0.21	0.12	100.03
Bistra	05-H/B-201	12.42	18.83	49.70	17.73	0.31	bdl	0.11	0.28	0.04	0.25	99.67

Formation	Sample	MgO	Al2O3	Cr2O3	FeO	V2O3	SiO2	TiO2	MnO	NiO	ZnO	total
Bistra	05-H/B-201	12.73	23.22	45.23	17.94	0.24	bdl	0.06	0.24	0.08	0.23	99.98
Bistra	05-H/B-201	13.59	22.60	46.09	16.62	0.22	0.26	0.10	0.21	0.10	0.13	99.93
Bistra	05-H/B-201	12.29	19.66	48.48	18.70	0.31	bdl	0.04	0.24	0.09	0.19	99.99
Bistra	05-H/B-201	9.41	17.35	40.35	30.23	0.43	bdl	0.92	0.29	0.19	0.17	99.34
Bistra	05-H/B-201	15.07	18.28	51.87	14.38	0.10	bdl	0.23	0.18	0.13	0.07	100.30
Bistra	05-H/B-201	14.74	22.28	46.36	15.66	0.20	bdl	0.05	0.23	0.12	0.09	99.73
Bistra	05-H/B-201	9.12	16.13	39.61	31.42	0.42	bdl	2.01	0.32	0.21	0.10	99.35
Bistra	05-H/B-207	9.37	14.85	53.15	21.52	0.35	bdl	0.05	0.28	0.04	0.19	99.80
Bistra	05-H/B-207	16.04	34.35	33.65	14.88	0.18	bdl	0.05	0.18	0.18	0.14	99.66
Bistra	05-H/B-207	11.57	15.68	53.81	17.97	0.28	bdl	0.10	0.25	0.05	0.16	99.88
Bistra	05-H/B-207	8.24	9.61	58.83	21.54	0.24	bdl	0.26	0.42	0.02	0.38	99.55
Bistra	05-H/B-207	14.04	24.33	44.61	15.88	0.22	bdl	0.10	0.20	0.08	0.19	99.65
Bistra	05-H/B-207	12.07	18.58	40.55	25.84	0.26	bdl	1.31	0.20	0.15	0.05	99.01
Bistra	05-H/B-207	11.78	22.15	46.08	19.01	0.22	bdl	0.09	0.24	0.03	0.27	99.88
Bistra	05-H/B-207	9.18	11.83	57.26	20.32	0.22	bdl	0.07	0.33	0.02	0.24	99.46
Bistra	05-H/B-207	10.16	17.63	47.79	23.01	0.23	bdl	0.21	0.32	0.08	0.13	99.57
Bistra	05-H/B-207	19.86	43.18	22.57	12.56	0.11	bdl	0.32	0.11	0.24	0.05	99.05
Bistra	05-H/B-207	11.07	8.85	60.27	18.50	0.16	bdl	0.18	0.28	0.03	0.14	99.46
Bistra	05-H/B-207	15.34	34.83	32.91	15.94	0.19	bdl	0.06	0.18	0.15	0.17	99.76
Bistra	05-H/B-207	11.70	15.79	50.61	20.87	0.19	bdl	0.18	0.25	0.10	0.14	99.82
Bistra	05-H/B-207	14.07	24.36	44.27	16.10	0.24	bdl	0.08	0.18	0.11	0.11	99.52
Bistra	05-H/B-207	11.96	18.04	49.28	19.41	0.29	bdl	0.09	0.23	0.05	0.12	99.47
Bistra	05-H/B-207	14.68	26.26	41.61	16.19	0.20	bdl	0.06	0.19	0.12	0.13	99.43
Bistra	05-H/B-207	15.37	32.10	35.78	15.20	0.17	bdl	0.07	0.20	0.12	0.11	99.12
Bistra	05-H/B-207	12.94	19.91	48.14	17.36	0.22	bdl	0.04	0.22	0.09	0.11	99.02
Bistra	05-H/B-207	12.00	23.55	43.57	19.87	0.31	bdl	0.04	0.26	0.06	0.23	99.88
Bistra	05-H/B-207	15.05	27.57	36.90	18.98	0.20	0.03	0.53	0.21	0.11	0.08	99.66
Bistra	05-H/B-207	13.06	24.68	43.64	16.97	0.23	bdl	0.02	0.21	0.10	0.15	99.06
Bistra	05-H/B-207	11.55	20.40	47.94	18.77	0.21	bdl	0.09	0.26	0.05	0.14	99.41
Bistra	05-H/B-207	17.38	40.36	28.03	12.60	0.12	bdl	0.15	0.16	0.15	0.18	99.13
Bistra	05-H/B-207	12.48	20.34	48.84	17.56	0.23	bdl	0.07	0.20	0.08	0.16	99.95
Bistra	05-H/B-207	11.60	16.29	49.88	20.77	0.21	bdl	0.25	0.23	0.08	0.13	99.45
Bistra	05-H/B-207	13.37	23.54	44.13	18.21	0.19	bdl	0.07	0.20	0.10	0.13	99.95
Bistra	05-H/B-207	14.13	33.05	33.24	17.92	0.20	bdl	0.14	0.17	0.14	0.16	99.13
Bistra	05-H/B-207	13.22	27.71	40.04	17.76	0.24	bdl	0.08	0.21	0.10	0.19	99.55
Bistra	05-H/B-207	10.48	14.15	54.45	19.91	0.36	bdl	0.25	0.27	0.04	0.15	100.06
Bistra	05-H/B-207	12.24	21.38	47.22	17.97	0.24	bdl	0.06	0.24	0.07	0.14	99.56
Bistra	05-H/B-207	14.60	25.11	43.88	15.68	0.19	bdl	0.08	0.20	0.12	0.10	99.95
Bistra	05-H/B-207	15.89	23.80	42.54	16.57	0.16	bdl	0.29	0.13	0.22	0.07	99.67
Bistra	05-H/B-207	13.44	24.95	44.71	16.22	0.24	bdl	0.08	0.19	0.06	0.16	100.05
Bistra	05-H/B-207	13.84	26.18	42.62	16.32	0.19	bdl	0.07	0.18	0.09	0.21	99.71
Bistra	05-H/B-207	12.37	18.28	50.92	17.71	0.26	bdl	0.04	0.24	0.06	0.11	99.98
Bistra	05-H/B-207	13.19	26.03	41.44	17.81	0.22	bdl	0.07	0.21	0.11	0.22	99.30
Bistra	05-H/B-207	10.79	14.23	54.45	19.32	0.27	bdl	0.17	0.26	0.04	0.17	99.69
Bistra	05-H/B-207	15.65	29.98	38.42	14.65	0.15	bdl	0.08	0.15	0.12	0.15	99.34
Bistra	05-H/B-207	11.00	16.40	51.63	19.73	0.28	bdl	0.04	0.26	0.07	0.16	99.57
Bistra	05-H/B-207	11.54	21.08	46.73	19.43	0.27	bdl	0.04	0.21	0.05	0.21	99.56
Bistra	05-H/B-207	12.90	21.74	45.79	18.18	0.26	bdl	0.17	0.23	0.09	0.18	99.55
Bistra	05-H/B-207	12.31	21.02	47.85	17.99	0.19	bdl	0.08	0.21	0.06	0.20	99.91
Bistra	05-H/B-207	11.68	17.40	51.03	18.65	0.23	bdl	0.05	0.24	0.04	0.17	99.49
Bistra	05-H/B-207	13.22	21.79	46.71	17.46	0.22	bdl	0.07	0.21	0.07	0.12	99.87
Bistra	05-H/B-207	13.68	21.44	47.63	16.26	0.22	bdl	0.18	0.19	0.08	0.14	99.81
Bistra	05-H/B-207	13.44	27.15	40.60	17.61	0.21	bdl	0.05	0.18	0.10	0.18	99.52
Bistra	05-H/B-207	12.12	20.91	45.96	19.95	0.30	bdl	0.20	0.25	0.07	0.15	99.92
Bistra	05-H/B-207	10.87	17.35	49.44	21.04	0.36	bdl	0.24	0.28	0.06	0.14	99.78
Bistra	05-H/B-207	14.95	30.82	38.43	14.79	0.22	bdl	0.07	0.19	0.10	0.15	99.72
Bistra	05-H/B-207	13.19	21.67	47.47	16.86	0.24	bdl	0.07	0.18	0.08	0.12	99.88
Bistra	05-H/B-207	12.52	25.30	41.92	18.90	0.27	bdl	0.07	0.24	0.06	0.19	99.47
Bistra	05-H/B-207	12.28	22.88	42.95	20.65	0.21	bdl	0.32	0.25	0.05	0.14	99.72
Bistra	05-H/B-207	11.96	7.98	60.96	17.86	0.16	bdl	0.13	0.29	0.10	0.68	100.12
Bistra	05-H/B-207	11.15	14.47	53.42	20.66	0.21	bdl	0.11	0.27	0.06	0.09	100.43
Bistra	05-H/B-207	11.29	21.44	43.25	22.81	0.23	bdl	0.40	0.27	0.10	0.12	99.91
Bistra	05-H/B-207	13.08	21.90	46.91	17.51	0.26	bdl	0.02	0.20	0.09	0.15	100.11
Bistra	05-H/B-207	13.52	19.62	49.33	16.92	0.25	bdl	0.08	0.21	0.08	0.14	100.16

Formation	Sample	MgO	Al2O3	Cr2O3	FeO	V2O3	SiO2	TiO2	MnO	NiO	ZnO	total
Bistra	05-H/B-207	14.87	29.01	39.82	15.34	0.19	bdl	0.08	0.20	0.12	0.13	99.77
Bistra	05-H/B-207	7.84	10.84	56.33	23.50	0.23	bdl	0.17	0.37	0.03	0.27	99.57
Bistra	05-H/B-207	6.67	5.69	58.96	27.00	0.17	bdl	0.09	0.39	0.03	0.25	99.26
Bistra	05-H/B-207	14.21	30.47	38.66	15.96	0.21	bdl	0.05	0.20	0.09	0.17	100.02
Bistra	05-H/B-207	12.53	22.04	47.63	17.18	0.28	bdl	0.10	0.21	0.07	0.16	100.20
Bistra	05-H/B-207	12.77	16.97	52.66	17.03	0.23	bdl	0.15	0.22	0.07	0.09	100.20
Bistra	05-H/B-207	12.12	18.49	50.68	17.68	0.20	bdl	0.15	0.24	0.04	0.17	99.78
Bistra	05-H/B-207	13.24	22.36	44.57	18.89	0.19	bdl	0.21	0.22	0.10	0.12	99.92
Bistra	05-H/B-207	13.76	26.24	43.58	15.69	0.22	bdl	0.21	0.21	0.08	0.13	100.12
Bistra	05-H/B-207	13.78	27.15	41.70	15.95	0.24	bdl	0.09	0.17	0.09	0.16	99.34
Bistra	05-H/B-207	11.63	20.76	47.46	19.07	0.32	bdl	0.04	0.29	0.06	0.18	99.82
Bistra	05-H/B-207	16.01	37.08	31.09	14.78	0.13	bdl	0.10	0.15	0.14	0.12	99.60
Bistra	05-H/B-207	16.75	39.74	27.69	14.67	0.14	bdl	0.06	0.15	0.18	0.18	99.56
Bistra	05-H/B-207	15.59	36.02	31.68	15.67	0.19	bdl	0.06	0.14	0.14	0.23	99.72
Bistra	05-H/B-207	13.69	20.46	48.39	16.65	0.23	bdl	0.05	0.20	0.08	0.10	99.86
Bistra	05-H/B-207	14.18	29.14	38.69	16.33	0.23	bdl	0.15	0.18	0.10	0.19	99.19
Bistra	05-H/B-207	10.96	17.60	51.46	19.48	0.37	bdl	0.05	0.27	0.06	0.18	100.43
Bistra	05-H/B-207	11.40	20.60	47.74	19.27	0.24	bdl	0.07	0.27	0.09	0.19	99.86
Bistra	05-H/B-207	14.42	21.23	45.91	17.08	0.10	0.02	0.22	0.20	0.17	0.05	99.40
Bistra	05-H/B-207	12.58	20.96	46.69	18.27	0.28	bdl	0.11	0.20	0.06	0.20	99.36
Bistra	05-H/B-207	11.36	23.32	44.69	19.18	0.22	bdl	0.02	0.27	0.04	0.32	99.43
Bistra	05-H/B-207	12.02	20.43	48.95	16.93	0.32	bdl	0.19	0.21	0.04	0.17	99.26
Bistra	05-H/B-216	13.75	20.99	47.77	16.38	0.26	bdl	0.01	0.21	0.10	0.11	99.58
Bistra	05-H/B-216	13.31	23.21	44.97	16.92	0.22	bdl	0.04	0.20	0.09	0.16	99.11
Bistra	05-H/B-216	11.31	17.48	50.50	19.42	0.27	bdl	0.02	0.28	0.05	0.18	99.51
Bistra	05-H/B-216	13.08	21.20	45.87	18.09	0.21	bdl	0.05	0.23	0.10	0.15	98.97
Bistra	05-H/B-216	11.05	26.62	38.56	21.81	0.28	bdl	0.05	0.23	0.07	0.33	99.00
Bistra	05-H/B-216	12.10	21.18	44.40	20.98	0.29	bdl	0.23	0.18	0.10	0.13	99.59
Bistra	05-H/B-216	13.30	19.94	48.31	17.52	0.21	bdl	0.04	0.19	0.09	0.07	99.66
Bistra	05-H/B-216	10.61	15.48	53.27	19.67	0.25	bdl	0.01	0.28	0.04	0.15	99.77
Bistra	05-H/B-216	14.19	19.16	49.58	16.20	0.28	bdl	0.04	0.22	0.10	0.10	99.87
Bistra	05-H/B-216	13.06	20.56	47.17	17.43	0.27	bdl	0.04	0.22	0.09	0.15	98.99
Bistra	05-H/B-216	11.42	20.31	47.49	19.11	0.26	bdl	0.05	0.27	0.06	0.18	99.13
Bistra	05-H/B-216	13.85	21.39	47.11	16.41	0.20	bdl	0.10	0.19	0.08	0.12	99.45
Bistra	05-H/B-216	13.50	23.81	45.16	16.10	0.22	bdl	0.03	0.18	0.08	0.11	99.19
Bistra	05-H/B-216	13.47	22.13	46.41	16.35	0.20	bdl	0.05	0.20	0.07	0.15	99.03
Bistra	05-H/B-216	11.80	17.39	51.09	18.06	0.24	bdl	0.03	0.26	0.05	0.14	99.06
Bistra	05-H/B-216	13.00	24.23	42.89	18.28	0.25	bdl	0.03	0.17	0.09	0.17	99.12
Bistra	05-H/B-216	11.29	22.77	44.46	19.61	0.32	bdl	0.03	0.28	0.05	0.23	99.04
Bistra	05-H/B-216	13.09	21.73	46.84	16.98	0.23	bdl	0.02	0.22	0.07	0.14	99.32
Bistra	05-H/B-216	11.31	20.87	45.90	20.08	0.26	bdl	0.02	0.26	0.06	0.25	99.00
Bistra	05-H/B-216	15.71	31.75	30.43	19.61	0.17	0.01	0.77	0.18	0.21	0.06	98.89
Bistra	05-H/B-216	13.70	22.08	45.61	17.02	0.19	bdl	0.05	0.24	0.09	0.12	99.11
Bistra	05-H/B-216	12.27	21.72	45.77	18.73	0.25	bdl	0.05	0.25	0.08	0.20	99.32
Bistra	05-H/B-216	7.98	9.28	57.04	24.13	0.24	bdl	0.07	0.33	0.06	0.25	99.39
Bistra	05-H/B-216	10.39	13.26	55.33	19.46	0.42	bdl	0.05	0.27	0.03	0.22	99.43
Bistra	05-H/B-216	10.30	18.85	48.41	20.66	0.32	bdl	0.05	0.28	0.07	0.20	99.15
Bistra	05-H/B-216	11.76	24.35	41.39	20.68	0.21	bdl	0.04	0.27	0.05	0.22	98.95
Bistra	05-H/B-216	13.89	25.67	42.96	15.83	0.24	bdl	0.02	0.20	0.09	0.14	99.02
Bistra	05-H/B-216	12.62	23.14	44.63	17.90	0.25	bdl	0.02	0.22	0.08	0.15	99.01
Bistra	05-H/B-216	13.78	23.01	44.81	16.90	0.20	bdl	0.06	0.20	0.10	0.16	99.21
Bistra	05-H/B-216	13.74	14.77	48.75	20.90	0.14	bdl	0.46	0.23	0.12	0.07	99.18
Bistra	05-H/B-216	15.62	32.16	36.50	14.08	0.18	bdl	0.05	0.16	0.14	0.15	99.04
Bistra	05-H/B-216	11.10	16.55	50.69	20.42	0.29	bdl	0.12	0.28	0.07	0.11	99.61
Bistra	05-H/B-216	10.41	13.13	53.70	20.91	0.12	bdl	0.23	0.28	0.06	0.13	98.97
Bistra	05-H/B-216	13.21	24.35	44.33	16.92	0.25	bdl	0.01	0.20	0.09	0.22	99.58
Bistra	05-H/B-216	13.74	25.85	42.48	16.63	0.19	bdl	0.04	0.21	0.10	0.15	99.39
Bistra	05-H/B-216	14.62	23.01	45.57	15.40	0.19	bdl	0.07	0.20	0.14	0.08	99.26
Glog	05-H/G-102	10.63	17.77	47.80	22.47	0.23	bdl	0.17	0.24	0.08	0.21	99.60
Glog	05-H/G-102	12.13	23.95	40.44	21.58	0.18	bdl	0.20	0.21	0.10	0.19	98.97
Glog	05-H/G-102	8.52	12.49	51.11	25.93	0.15	bdl	0.12	0.34	0.07	0.27	99.01
Glog	05-H/G-102	14.34	30.76	35.16	18.26	0.15	bdl	0.12	0.18	0.14	0.24	99.34
Glog	05-H/G-102	14.95	29.29	37.76	16.40	0.13	bdl	0.13	0.21	0.13	0.18	99.17
Glog	05-H/G-102	11.97	25.00	39.36	21.98	0.17	bdl	0.14	0.26	0.11	0.24	99.21

Formation	Sample	MgO	Al2O3	Cr2O3	FeO	V2O3	SiO2	TiO2	MnO	NiO	ZnO	total
Glog	05-H/G-102	18.37	40.86	26.22	12.80	0.11	bdl	0.11	0.13	0.22	0.11	98.94
Glog	05-H/G-102	12.94	23.89	42.49	19.11	0.15	bdl	0.16	0.22	0.10	0.16	99.20
Glog	05-H/G-102	12.41	20.05	44.57	21.02	0.20	bdl	0.30	0.27	0.11	0.21	99.12
Glog	05-H/G-102	9.59	11.85	55.93	20.69	0.23	bdl	0.23	0.33	0.03	0.21	99.11
Glog	05-H/G-102	13.54	30.66	35.06	18.93	0.19	bdl	0.12	0.21	0.13	0.23	99.06
Glog	05-H/G-102	11.75	19.59	46.40	20.54	0.16	bdl	0.09	0.27	0.06	0.19	99.05
Glog	05-H/G-102	16.18	33.39	33.83	14.94	0.14	bdl	0.11	0.17	0.18	0.16	99.11
Glog	05-H/G-102	16.93	41.72	24.79	14.72	0.12	bdl	0.05	0.13	0.20	0.21	98.86
Glog	05-H/G-102	15.51	36.55	31.11	15.00	0.14	bdl	0.13	0.20	0.13	0.26	99.02
Glog	05-H/G-102	14.04	28.01	38.73	17.85	0.15	bdl	0.16	0.21	0.12	0.17	99.44
Glog	05-H/G-102	16.46	40.47	24.37	16.78	0.12	bdl	0.15	0.17	0.21	0.21	98.93
Glog	05-H/G-102	10.79	19.90	43.26	24.50	0.22	bdl	0.21	0.26	0.11	0.20	99.45
Glog	05-H/G-102	14.99	35.79	31.30	16.19	0.18	bdl	0.09	0.19	0.12	0.26	99.11
Glog	05-H/G-102	11.95	20.31	46.66	19.51	0.17	bdl	0.12	0.21	0.08	0.21	99.23
Glog	05-H/G-102	12.85	28.25	36.33	20.56	0.21	bdl	0.23	0.20	0.12	0.23	98.99
Glog	05-H/G-102	8.26	10.04	53.55	26.58	0.23	bdl	0.15	0.37	0.05	0.26	99.49
Glog	05-H/G-102	11.60	21.09	43.79	21.77	0.13	bdl	0.14	0.23	0.09	0.21	99.06
Glog	05-H/G-102	9.95	14.84	50.67	23.69	0.20	bdl	0.14	0.31	0.07	0.20	100.07
Glog	05-H/G-102	12.15	23.65	42.82	20.01	0.16	bdl	0.10	0.22	0.08	0.21	99.40
Glog	05-H/G-102	18.68	49.42	17.94	12.44	0.09	bdl	0.07	0.13	0.23	0.19	99.20
Glog	05-H/G-102	16.60	39.97	26.68	15.61	0.14	bdl	0.12	0.13	0.20	0.20	99.65
Glog	05-H/G-102	11.15	17.48	48.61	21.26	0.25	bdl	0.10	0.24	0.09	0.19	99.38
Glog	05-H/G-102	9.42	12.51	54.37	22.40	0.20	bdl	0.13	0.28	0.04	0.21	99.56
Glog	05-H/G-102	9.27	10.57	56.57	22.72	0.15	bdl	0.20	0.34	0.05	0.16	100.03
Glog	05-H/G-102	11.23	22.32	43.77	21.49	0.15	bdl	0.10	0.23	0.09	0.23	99.61
Glog	05-H/G-102	18.15	46.49	20.66	13.06	0.07	bdl	0.01	0.12	0.25	0.20	99.00
Glog	05-H/G-102	17.46	44.85	21.30	14.73	0.14	bdl	0.10	0.11	0.23	0.20	99.13
Glog	05-H/G-102	16.18	38.54	29.59	14.52	0.13	bdl	0.06	0.15	0.16	0.21	99.53
Glog	05-H/G-102	14.23	39.05	25.09	19.92	0.17	bdl	0.09	0.18	0.17	0.31	99.20
Glog	05-H/G-102	14.86	31.91	35.32	17.20	0.16	bdl	0.08	0.14	0.15	0.15	99.97
Glog	05-H/G-102	11.17	19.02	44.51	24.16	0.17	bdl	0.22	0.26	0.09	0.24	99.84
Glog	05-H/G-102	14.00	34.70	29.56	20.70	0.18	bdl	0.17	0.18	0.16	0.22	99.87
Glog	05-H/G-102	13.71	30.91	35.11	19.50	0.20	bdl	0.10	0.22	0.12	0.22	100.07
Glog	05-H/G-102	15.80	35.70	31.72	15.65	0.11	bdl	0.37	0.18	0.16	0.21	99.90
Glog	05-H/G-102	9.83	11.41	54.95	22.57	0.21	bdl	0.14	0.31	0.06	0.14	99.64
Glog	05-H/G-102	13.98	28.52	38.13	17.70	0.14	bdl	0.11	0.19	0.08	0.25	99.09
Glog	05-H/G-102	17.82	45.19	21.57	14.11	0.11	bdl	0.07	0.15	0.22	0.20	99.44
Glog	05-H/G-105/1	15.87	34.77	33.68	14.91	0.13	bdl	0.03	0.16	0.13	0.16	99.84
Glog	05-H/G-105/1	17.78	40.08	28.71	12.21	0.08	bdl	0.02	0.09	0.15	0.24	99.38
Glog	05-H/G-105/1	7.96	9.62	54.30	26.41	0.19	bdl	0.29	0.34	0.07	0.23	99.40
Glog	05-H/G-105/1	18.07	35.45	31.29	13.58	0.13	0.07	0.26	0.12	0.23	0.04	99.24
Glog	05-H/G-105/1	14.30	31.62	35.84	16.92	0.14	bdl	0.08	0.17	0.13	0.23	99.43
Glog	05-H/G-105/1	12.23	16.61	51.22	18.79	0.11	bdl	0.24	0.23	0.08	0.09	99.61
Glog	05-H/G-105/1	13.40	27.85	38.92	18.78	0.19	bdl	0.03	0.23	0.08	0.23	99.71
Glog	05-H/G-105/1	14.68	34.03	33.02	16.82	0.19	bdl	0.10	0.19	0.12	0.26	99.41
Glog	05-H/G-105/1	11.87	20.72	44.73	21.12	0.28	bdl	0.32	0.32	0.15	0.09	99.59
Glog	05-H/G-105/1	16.30	39.42	27.44	15.02	0.14	bdl	0.12	0.16	0.18	0.22	99.00
Glog	05-H/G-105/1	16.53	43.64	21.40	16.60	0.18	bdl	0.10	0.16	0.24	0.21	99.06
Glog	05-H/G-105/1	15.80	37.88	28.91	16.13	0.13	bdl	0.12	0.16	0.18	0.24	99.55
Glog	05-H/G-105/1	14.61	32.47	34.61	16.57	0.17	bdl	0.18	0.15	0.12	0.23	99.10
Glog	05-H/G-105/1	12.63	21.68	45.31	19.11	0.17	bdl	0.13	0.22	0.08	0.21	99.52
Glog	05-H/G-105/1	15.60	32.52	34.14	16.26	0.15	bdl	0.03	0.17	0.14	0.18	99.19
Glog	05-H/G-105/1	11.33	20.44	45.45	21.69	0.14	bdl	0.07	0.21	0.08	0.23	99.64
Glog	05-H/G-105/1	16.48	41.36	23.73	16.53	0.18	bdl	0.15	0.14	0.22	0.21	99.01
Glog	05-H/G-105/1	13.42	30.93	33.73	20.15	0.15	bdl	0.21	0.22	0.14	0.12	99.06
Glog	05-H/G-105/1	14.71	33.30	33.31	17.20	0.13	bdl	0.12	0.18	0.12	0.22	99.29
Glog	05-H/G-105/1	17.28	42.86	23.42	14.63	0.12	bdl	0.07	0.15	0.22	0.20	98.94
Glog	05-H/G-105/1	13.02	19.71	46.35	19.30	0.13	bdl	0.31	0.21	0.10	0.14	99.27
Glog	05-H/G-105/1	15.82	36.04	31.31	15.12	0.14	bdl	0.10	0.18	0.14	0.25	99.09
Glog	05-H/G-105/1	18.76	47.74	19.75	11.84	0.07	bdl	0.04	0.11	0.23	0.23	98.78
Glog	05-H/G-105/1	14.54	32.70	33.74	17.15	0.15	bdl	0.06	0.19	0.12	0.24	98.89
Glog	05-H/G-105/1	14.87	31.88	35.09	16.87	0.18	bdl	0.13	0.16	0.14	0.18	99.49
Glog	05-H/G-105/1	13.82	30.98	34.71	18.60	0.19	bdl	0.10	0.20	0.13	0.23	98.96
Glog	05-H/G-105/1	14.11	27.58	40.59	16.64	0.23	bdl	0.03	0.20	0.08	0.17	99.63

Formation	Sample	MgO	Al2O3	Cr2O3	FeO	V2O3	SiO2	TiO2	MnO	NiO	ZnO	total
Glog	05-H/G-105/1	15.92	41.11	23.63	17.35	0.13	bdl	0.16	0.17	0.19	0.20	98.87
Glog	05-H/G-105/1	12.72	26.23	38.88	20.16	0.15	bdl	0.19	0.22	0.12	0.28	98.96
Glog	05-H/G-105/1	11.40	22.13	44.39	20.31	0.18	bdl	0.09	0.25	0.08	0.18	99.01
Glog	05-H/G-105/1	9.07	12.11	53.08	24.21	0.28	bdl	0.19	0.33	0.08	0.20	99.54
Glog	05-H/G-105/1	11.07	16.29	52.13	19.56	0.24	bdl	0.03	0.27	0.05	0.12	99.76
Glog	05-H/G-105/1	13.42	31.51	34.36	19.04	0.20	bdl	0.10	0.20	0.11	0.25	99.19
Glog	05-H/G-105/1	13.29	22.90	44.48	18.13	0.12	bdl	0.10	0.20	0.09	0.17	99.48
Glog	05-H/G-105/1	7.37	11.33	53.72	25.96	0.28	bdl	0.16	0.36	0.05	0.30	99.52
Glog	05-H/G-105/1	9.29	12.92	51.50	24.47	0.23	bdl	0.18	0.29	0.09	0.20	99.16
Kravljak	05-H/M-52	13.70	31.22	35.52	17.70	0.28	bdl	0.03	0.21	0.08	0.27	99.03
Kravljak	05-H/M-52	12.74	21.42	47.41	17.55	0.26	0.01	0.05	0.25	0.07	0.17	99.93
Kravljak	05-H/M-52	12.11	22.03	45.79	19.01	0.28	bdl	0.08	0.21	0.06	0.19	99.76
Kravljak	05-H/M-52	12.85	23.08	45.20	17.15	0.30	bdl	0.03	0.22	0.07	0.15	99.03
Kravljak	05-H/M-52	13.32	25.17	43.97	16.32	0.26	bdl	0.03	0.21	0.08	0.12	99.49
Kravljak	05-H/M-52	14.56	25.01	43.99	15.14	0.22	bdl	0.06	0.19	0.10	0.10	99.37
Kravljak	05-H/M-52	13.18	20.35	46.95	17.87	0.20	bdl	0.13	0.19	0.12	0.11	99.09
Kravljak	05-H/M-52	13.20	21.46	47.63	16.38	0.24	bdl	0.05	0.22	0.06	0.16	99.40
Kravljak	05-H/M-52	13.13	21.09	48.25	16.68	0.25	bdl	0.06	0.19	0.08	0.17	99.90
Kravljak	05-H/M-52	11.79	21.25	45.61	20.00	0.29	bdl	0.04	0.24	0.07	0.21	99.49
Kravljak	05-H/M-52	11.73	24.05	43.31	19.43	0.22	bdl	0.04	0.23	0.06	0.20	99.27
Kravljak	05-H/M-52	10.64	17.88	50.28	19.59	0.28	bdl	0.07	0.28	0.05	0.17	99.23
Kravljak	05-H/M-52	14.07	23.16	45.54	15.92	0.22	bdl	0.03	0.21	0.09	0.12	99.36
Kravljak	05-H/M-52	9.44	20.16	45.98	22.67	0.23	bdl	0.05	0.27	0.07	0.25	99.12
Kravljak	05-H/M-52	12.46	26.15	40.71	19.25	0.27	bdl	0.11	0.22	0.08	0.22	99.47
Kravljak	05-H/M-52	13.58	21.46	47.53	16.33	0.25	bdl	0.04	0.19	0.09	0.12	99.59
Kravljak	05-H/M-52	14.22	34.08	32.92	17.03	0.22	bdl	0.13	0.23	0.13	0.22	99.19
Kravljak	05-H/M-52	10.13	13.96	51.23	23.21	0.24	bdl	0.17	0.30	0.08	0.14	99.47
Kravljak	05-H/M-52	11.94	19.15	49.00	19.01	0.24	bdl	0.05	0.26	0.06	0.17	99.88
Kravljak	05-H/M-52	12.94	22.67	45.21	17.95	0.26	bdl	0.04	0.21	0.09	0.13	99.49
Kravljak	05-H/M-52	16.00	31.18	31.66	19.12	0.16	bdl	0.81	0.17	0.21	0.06	99.38
Kravljak	05-H/M-52	13.40	24.47	43.25	17.80	0.21	bdl	0.08	0.23	0.10	0.12	99.67
Kravljak	05-H/M-52	12.50	25.53	40.90	19.44	0.27	bdl	0.42	0.21	0.08	0.25	99.60
Kravljak	05-H/M-52	11.94	17.99	49.75	19.55	0.22	bdl	0.17	0.30	0.05	0.18	100.14
Kravljak	05-H/M-52	13.27	31.58	34.86	18.43	0.27	bdl	0.05	0.22	0.09	0.33	99.09
Kravljak	05-H/M-52	11.49	16.63	52.87	18.32	0.26	bdl	0.05	0.24	0.07	0.18	100.11
Kravljak	05-H/M-52	13.35	27.71	40.94	16.67	0.21	bdl	0.13	0.21	0.09	0.20	99.50
Kravljak	05-H/M-52	17.41	28.52	37.55	14.80	0.13	0.05	0.50	0.13	0.24	0.05	99.40
Kravljak	05-H/M-52	12.29	20.79	48.39	17.85	0.27	bdl	0.03	0.24	0.06	0.16	100.07
Kravljak	05-H/M-52	9.84	15.58	52.55	21.03	0.26	bdl	0.07	0.30	0.05	0.26	99.94
Kravljak	05-H/M-52	12.65	22.22	46.30	17.59	0.27	bdl	0.05	0.23	0.08	0.14	99.53
Kravljak	05-H/M-52	8.44	16.39	49.53	23.72	0.24	bdl	0.07	0.30	0.04	0.38	99.12
Kravljak	05-H/M-52	10.58	16.19	51.93	20.27	0.29	bdl	0.08	0.25	0.04	0.22	99.83
Kravljak	05-H/M-52	13.29	23.56	44.64	17.18	0.22	bdl	0.02	0.22	0.10	0.16	99.39
Kravljak	05-H/M-52	11.99	19.85	49.12	18.28	0.27	bdl	0.04	0.25	0.04	0.17	100.01
Kravljak	05-H/M-52	12.78	17.85	51.87	16.35	0.27	bdl	0.04	0.23	0.10	0.15	99.64
Kravljak	05-H/M-52	12.57	23.78	44.13	18.47	0.26	bdl	0.03	0.22	0.07	0.16	99.67
Kravljak	05-H/M-52	11.17	16.53	52.60	18.61	0.27	bdl	0.04	0.27	0.03	0.16	99.69
Kravljak	05-H/M-52	12.36	23.63	43.71	19.07	0.25	bdl	0.05	0.23	0.06	0.20	99.57
Kravljak	05-H/M-52	13.26	19.93	49.35	16.28	0.25	bdl	0.04	0.21	0.11	0.12	99.54
Kravljak	05-H/M-52	13.30	25.32	43.11	16.81	0.20	bdl	0.06	0.19	0.09	0.18	99.26
Kravljak	05-H/M-52	11.96	21.84	46.61	18.69	0.24	bdl	0.07	0.29	0.06	0.19	99.96
Kravljak	05-H/M-52	10.69	16.87	50.51	21.10	0.27	bdl	0.05	0.24	0.07	0.17	99.97
Kravljak	05-H/M-52	12.07	22.01	46.61	18.23	0.34	bdl	0.03	0.23	0.06	0.17	99.75
Kravljak	05-H/M-52	12.54	26.59	41.09	18.48	0.26	bdl	0.03	0.20	0.06	0.17	99.43
Kravljak	05-H/M-52	12.69	21.04	47.18	18.44	0.24	bdl	0.06	0.19	0.10	0.12	100.07
Kravljak	05-H/M-52	13.81	22.64	44.19	17.57	0.17	bdl	0.23	0.25	0.12	0.05	99.04
Kravljak	05-H/M-52	8.60	16.33	50.15	23.27	0.23	bdl	0.06	0.35	0.05	0.37	99.41
Kravljak	05-H/M-52	11.87	21.06	46.29	19.38	0.23	bdl	0.03	0.24	0.07	0.21	99.37
Kravljak	05-H/M-52	10.97	20.36	47.62	19.76	0.24	bdl	0.03	0.27	0.08	0.12	99.45
Kravljak	05-H/M-52	14.87	31.16	36.14	16.14	0.18	bdl	0.07	0.19	0.10	0.20	99.05
Kravljak	05-H/M-52	9.70	21.95	43.79	22.84	0.14	bdl	0.09	0.26	0.20	0.19	99.18
Kravljak	05-H/M-52	14.30	27.60	41.27	15.72	0.16	bdl	0.04	0.18	0.10	0.17	99.54
Kravljak	05-H/M-52	12.49	22.03	46.60	18.11	0.25	bdl	0.05	0.22	0.07	0.18	100.00
Kravljak	05-H/M-52	11.91	20.48	47.47	18.83	0.27	bdl	0.06	0.21	0.07	0.18	99.48

Formation	Sample	MgO	Al2O3	Cr2O3	FeO	V2O3	SiO2	TiO2	MnO	NiO	ZnO	total
Kravljak	05-H/M-52	13.74	25.65	42.63	17.10	0.20	bdl	0.06	0.20	0.08	0.17	99.83
Kravljak	05-H/M-52	13.58	25.79	42.97	16.66	0.25	bdl	0.03	0.17	0.09	0.16	99.70
Kravljak	05-H/M-52	12.33	17.55	51.29	17.78	0.22	bdl	0.06	0.26	0.05	0.14	99.67
Kravljak	05-H/M-52	10.84	23.89	42.96	20.85	0.27	bdl	0.18	0.28	0.06	0.30	99.61
Kravljak	05-H/M-52	9.23	11.42	55.81	21.90	0.22	bdl	0.11	0.30	0.04	0.16	99.18
Kravljak	05-H/M-52	12.85	26.56	41.51	18.22	0.24	bdl	0.04	0.21	0.07	0.20	99.89
Kravljak	05-H/M-52	11.23	15.94	52.35	19.08	0.34	bdl	0.07	0.26	0.05	0.16	99.49
Kravljak	05-H/M-52	13.14	27.11	40.43	17.99	0.22	bdl	0.05	0.23	0.07	0.18	99.42
Kravljak	05-H/M-52	15.14	26.38	43.06	14.07	0.17	bdl	0.05	0.19	0.12	0.09	99.28
Kravljak	05-H/M-52	13.65	21.18	47.21	16.94	0.23	bdl	0.05	0.20	0.13	0.13	99.71
Kravljak	05-H/M-52	14.09	27.19	41.16	16.43	0.19	bdl	0.11	0.18	0.10	0.15	99.58
Kravljak	05-H/M-52	13.86	27.06	41.30	16.43	0.19	bdl	0.03	0.17	0.08	0.14	99.26
Kravljak	05-H/M-52	12.11	18.40	50.31	18.17	0.30	bdl	0.02	0.24	0.05	0.17	99.78
Kravljak	05-H/M-52	13.11	23.05	45.48	17.16	0.24	bdl	0.02	0.21	0.07	0.16	99.50
Kravljak	05-H/M-52	14.17	32.45	35.10	16.84	0.20	bdl	0.03	0.20	0.10	0.25	99.35
Kravljak	05-H/M-52	14.78	22.90	46.99	14.84	0.20	bdl	0.11	0.19	0.10	0.08	100.19
Kravljak	05-H/M-52	10.83	15.24	53.42	20.07	0.31	bdl	0.04	0.25	0.04	0.18	100.38
Kravljak	05-H/M-52	13.71	32.53	35.28	17.05	0.22	bdl	0.04	0.18	0.08	0.37	99.45
Kravljak	05-H/M-60	13.05	19.70	47.41	18.54	0.24	bdl	0.17	0.22	0.08	0.13	99.54
Kravljak	05-H/M-60	12.16	24.40	43.24	19.35	0.21	bdl	0.13	0.23	0.08	0.22	100.03
Kravljak	05-H/M-60	12.76	23.52	45.22	17.08	0.24	bdl	0.12	0.21	0.07	0.16	99.38
Kravljak	05-H/M-60	11.00	18.04	49.46	20.30	0.34	bdl	0.12	0.25	0.05	0.17	99.72
Kravljak	05-H/M-60	10.27	15.48	52.23	20.64	0.20	bdl	0.41	0.29	0.05	0.20	99.78
Kravljak	05-H/M-60	12.46	20.66	47.13	18.69	0.25	bdl	0.25	0.25	0.08	0.17	99.93
Kravljak	05-H/M-60	15.06	29.66	39.40	15.03	0.17	bdl	0.13	0.18	0.07	0.18	99.87
Kravljak	05-H/M-60	15.17	28.32	34.50	19.65	0.19	bdl	0.83	0.17	0.18	0.09	99.10
Kravljak	05-H/M-60	16.44	35.81	33.84	12.28	0.14	0.12	0.22	0.13	0.14	0.18	99.31
Kravljak	05-H/M-60	13.17	21.89	46.28	17.32	0.22	bdl	0.36	0.19	0.10	0.16	99.70
Kravljak	05-H/M-60	13.19	24.65	43.43	17.62	0.23	bdl	0.14	0.19	0.08	0.18	99.71
Kravljak	05-H/M-60	13.26	18.48	50.52	16.64	0.28	bdl	0.16	0.24	0.07	0.14	99.79
Kravljak	05-H/M-60	12.99	28.90	38.77	17.54	0.21	bdl	0.48	0.22	0.11	0.23	99.44
Kravljak	05-H/M-60	14.48	32.81	34.71	17.03	0.22	bdl	0.04	0.18	0.10	0.27	99.84
Kravljak	05-H/M-60	12.95	20.70	48.18	17.54	0.26	bdl	0.13	0.23	0.07	0.14	100.20
Kravljak	05-H/M-60	14.35	27.01	41.06	16.12	0.19	bdl	0.06	0.18	0.09	0.14	99.17
Kravljak	05-H/M-60	11.16	18.66	49.03	19.46	0.29	bdl	0.21	0.30	0.07	0.14	99.33
Kravljak	05-H/M-60	13.30	23.64	44.40	17.37	0.24	bdl	0.18	0.23	0.09	0.20	99.66
Kravljak	05-H/M-60	15.26	27.82	41.68	14.13	0.15	bdl	0.15	0.17	0.09	0.15	99.58
Kravljak	05-H/M-60	12.33	19.79	49.27	17.54	0.27	bdl	0.17	0.22	0.05	0.14	99.77
Kravljak	05-H/M-60	10.13	19.02	42.22	26.55	0.27	bdl	0.59	0.30	0.11	0.20	99.38
Kravljak	05-H/M-60	12.13	22.34	46.14	18.12	0.28	bdl	0.31	0.28	0.06	0.21	99.86
Kravljak	05-H/M-60	13.84	25.32	43.65	16.10	0.19	bdl	0.06	0.17	0.11	0.13	99.59
Kravljak	05-H/M-60	12.63	25.65	41.28	18.89	0.26	bdl	0.06	0.22	0.06	0.22	99.28
Kravljak	05-H/M-60	12.91	22.05	45.46	18.54	0.27	bdl	0.22	0.25	0.09	0.16	99.95
Kravljak	05-H/M-60	14.95	32.76	35.31	15.66	0.18	bdl	0.26	0.17	0.12	0.22	99.64
Kravljak	05-H/M-60	11.39	19.82	48.40	19.28	0.21	0.01	0.10	0.24	0.04	0.19	99.67
Kravljak	05-H/M-60	11.25	10.80	59.51	17.15	0.23	bdl	0.10	0.27	0.03	0.11	99.43
Kravljak	05-H/M-60	13.29	25.91	42.46	17.59	0.24	bdl	0.09	0.22	0.08	0.24	100.14
Kravljak	05-H/M-60	16.23	31.92	37.80	12.92	0.16	bdl	0.16	0.17	0.11	0.15	99.60
Kravljak	05-H/M-60	12.92	22.84	45.05	17.82	0.27	bdl	0.09	0.22	0.08	0.18	99.45
Kravljak	05-H/M-60	13.01	22.57	46.17	17.25	0.20	bdl	0.11	0.20	0.05	0.19	99.74
Kravljak	05-H/M-60	12.96	22.94	44.52	18.41	0.26	bdl	0.12	0.23	0.09	0.16	99.69
Kravljak	05-H/M-60	13.74	23.43	45.72	15.91	0.26	bdl	0.08	0.20	0.10	0.15	99.57
Kravljak	05-H/M-60	11.80	21.82	43.85	21.28	0.28	bdl	0.35	0.24	0.08	0.19	99.88
Kravljak	05-H/M-60	13.25	27.64	39.65	17.73	0.24	bdl	0.07	0.21	0.08	0.21	99.07
Kravljak	05-H/M-60	11.13	17.89	50.01	19.96	0.28	bdl	0.07	0.25	0.05	0.16	99.80
Kravljak	05-H/M-60	13.50	23.12	45.32	16.89	0.25	bdl	0.07	0.21	0.08	0.13	99.57
Kravljak	05-H/M-60	9.57	13.33	55.31	20.17	0.21	bdl	0.35	0.31	0.02	0.13	99.42
Kravljak	05-H/M-60	12.24	22.57	46.22	18.11	0.25	bdl	0.23	0.23	0.07	0.19	100.10
Kravljak	05-H/M-60	12.75	21.11	46.80	17.77	0.27	bdl	0.33	0.20	0.09	0.16	99.49
Kravljak	05-H/M-60	11.80	17.20	52.79	17.65	0.25	bdl	0.28	0.26	0.05	0.16	100.42
Kravljak	05-H/M-60	14.54	23.07	46.29	14.99	0.22	bdl	0.15	0.17	0.11	0.12	99.65
Kravljak	05-H/M-60	12.69	21.61	47.01	17.17	0.29	0.01	0.25	0.25	0.04	0.15	99.45
Kravljak	05-H/M-60	11.93	23.57	41.75	21.39	0.22	bdl	0.55	0.26	0.07	0.19	99.94
Kravljak	05-H/M-60	12.70	23.56	44.77	18.20	0.25	bdl	0.04	0.23	0.09	0.18	100.03

Formation	Sample	MgO	Al2O3	Cr2O3	FeO	V2O3	SiO2	TiO2	MnO	NiO	ZnO	total
Kravljak	05-H/M-60	13.01	23.80	45.14	16.67	0.18	bdl	0.15	0.18	0.07	0.20	99.40
Kravljak	05-H/M-60	11.79	20.26	48.66	18.01	0.28	bdl	0.15	0.23	0.03	0.18	99.59
Kravljak	05-H/M-60	11.24	23.68	43.65	19.97	0.22	bdl	0.34	0.25	0.04	0.23	99.62
Kravljak	05-H/M-60	13.30	25.66	42.63	17.79	0.29	bdl	0.07	0.24	0.08	0.20	100.26
Kravljak	05-H/M-60	14.61	27.29	41.64	15.58	0.18	bdl	0.23	0.17	0.12	0.16	99.98
Kravljak	05-H/M-60	12.94	23.20	45.27	17.56	0.24	bdl	0.42	0.20	0.09	0.18	100.09
Kravljak	05-H/M-60	13.98	23.45	44.93	16.67	0.19	bdl	0.21	0.21	0.09	0.10	99.83
Kravljak	05-H/M-60	12.00	18.21	50.33	18.30	0.27	bdl	0.27	0.25	0.07	0.14	99.86
Kravljak	05-H/M-60	12.96	20.15	48.72	17.41	0.23	bdl	0.11	0.23	0.06	0.14	100.00
Kravljak	05-H/M-60	10.21	16.24	48.87	23.68	0.26	bdl	0.11	0.28	0.08	0.26	99.99
Kravljak	05-H/M-60	11.85	18.24	41.47	25.94	0.35	bdl	1.02	0.30	0.11	0.10	99.38
Kravljak	05-H/M-60	12.90	23.74	44.51	17.44	0.25	bdl	0.34	0.21	0.06	0.23	99.69
Kravljak	05-H/M-60	12.41	19.45	48.76	18.47	0.23	bdl	0.18	0.24	0.06	0.11	99.92
Kravljak	05-H/M-60	11.78	19.00	49.40	18.90	0.25	bdl	0.10	0.21	0.05	0.19	99.88
Kravljak	05-H/M-60	14.05	26.96	41.28	16.90	0.23	bdl	0.24	0.19	0.12	0.18	100.15
Kravljak	05-H/M-60	12.45	18.30	50.61	17.84	0.33	bdl	0.11	0.24	0.07	0.15	100.11
Kravljak	05-H/M-60	12.90	23.22	45.92	16.90	0.15	bdl	0.11	0.23	0.09	0.18	99.71
Kravljak	05-H/M-60	13.97	23.57	44.83	16.62	0.23	bdl	0.30	0.20	0.09	0.15	99.97
Kravljak	05-H/M-60	13.51	27.70	39.52	18.17	0.27	bdl	0.21	0.21	0.10	0.19	99.88
Kravljak	05-H/M-60	16.18	36.83	30.63	14.55	0.18	bdl	0.26	0.18	0.16	0.22	99.20
Kravljak	05-H/M-60	11.51	25.36	40.87	20.07	0.25	bdl	0.32	0.33	0.07	0.35	99.14
Kravljak	05-H/M-60	13.36	20.00	46.59	18.21	0.21	bdl	0.35	0.23	0.15	0.07	99.16
Kravljak	05-H/M-60	13.00	18.41	50.39	16.93	0.24	bdl	0.14	0.23	0.07	0.15	99.56
Kravljak	05-H/M-60	13.67	24.40	44.01	16.95	0.26	bdl	0.05	0.21	0.12	0.19	99.85
Kravljak	05-H/M-60	13.27	24.76	43.51	17.68	0.26	bdl	0.13	0.20	0.08	0.19	100.06
Ostrc	05-H/O-318	11.30	12.66	55.17	19.91	0.19	bdl	0.18	0.29	0.09	0.18	99.96
Ostrc	05-H/O-318	12.08	23.24	45.39	17.62	0.23	bdl	0.04	0.24	0.13	0.12	99.09
Ostrc	05-H/O-318	12.74	19.93	49.22	17.40	0.29	bdl	0.03	0.24	0.09	0.15	100.09
Ostrc	05-H/O-318	13.49	20.68	46.76	18.47	0.25	bdl	0.05	0.22	0.11	0.12	100.14
Ostrc	05-H/O-318	12.57	18.96	49.83	17.85	0.23	bdl	0.04	0.17	0.07	0.16	99.89
Ostrc	05-H/O-318	10.63	15.87	50.56	21.74	0.25	bdl	0.22	0.28	0.07	0.12	99.73
Ostrc	05-H/O-318	9.92	17.10	51.33	20.55	0.37	bdl	0.05	0.28	0.05	0.29	99.94
Ostrc	05-H/O-318	15.10	24.68	44.96	14.82	0.15	bdl	0.07	0.19	0.09	0.11	100.17
Ostrc	05-H/O-318	13.40	22.43	46.89	16.82	0.25	bdl	0.02	0.22	0.07	0.12	100.24
Ostrc	05-H/O-318	12.80	19.28	44.01	21.87	0.35	bdl	0.76	0.25	0.15	0.14	99.62
Ostrc	05-H/O-318	9.45	20.78	40.70	26.98	0.23	bdl	0.84	0.32	0.15	0.14	99.59
Ostrc	05-H/O-318	13.79	21.71	47.74	16.36	0.24	bdl	0.04	0.22	0.09	0.13	100.33
Ostrc	05-H/O-318	15.33	25.89	44.06	14.16	0.17	bdl	0.14	0.15	0.11	0.12	100.14
Ostrc	05-H/O-318	11.36	17.01	47.94	22.12	0.23	bdl	0.25	0.26	0.09	0.11	99.37
Ostrc	05-H/O-318	11.02	16.52	51.68	19.62	0.29	bdl	0.11	0.26	0.05	0.13	99.69
Ostrc	05-H/O-318	13.28	26.09	42.08	17.72	0.23	bdl	0.04	0.22	0.09	0.21	99.96
Ostrc	05-H/O-318	9.15	16.34	42.48	29.51	0.34	bdl	0.64	0.28	0.14	0.17	99.05
Ostrc	05-H/O-318	8.38	17.95	39.81	31.76	0.28	bdl	0.25	0.31	0.10	0.19	99.03
Ostrc	05-H/O-318	12.20	20.98	47.37	18.37	0.26	bdl	0.05	0.24	0.08	0.17	99.73
Ostrc	05-H/O-318	12.32	21.17	41.28	23.61	0.30	bdl	0.37	0.22	0.12	0.15	99.54
Ostrc	05-H/O-318	15.65	34.62	34.48	14.85	0.15	bdl	0.07	0.18	0.12	0.24	100.37
Ostrc	05-H/O-318	13.38	22.39	46.85	16.50	0.24	bdl	0.03	0.22	0.08	0.13	99.82
Ostrc	05-H/O-318	16.58	31.83	35.06	15.38	0.12	bdl	0.07	0.13	0.19	0.10	99.46
Ostrc	05-H/O-318	14.92	26.62	42.04	15.79	0.12	bdl	0.10	0.17	0.11	0.16	100.03
Ostrc	05-H/O-318	12.27	22.25	46.02	18.52	0.22	bdl	0.13	0.19	0.09	0.20	99.90
Ostrc	05-H/O-318	12.49	18.03	50.95	17.67	0.23	bdl	0.05	0.23	0.09	0.15	99.89
Ostrc	05-H/O-318	13.44	23.92	44.90	17.29	0.25	bdl	0.03	0.23	0.06	0.16	100.27
Ostrc	05-H/O-318	14.63	24.22	45.30	15.60	0.19	bdl	0.03	0.20	0.11	0.11	100.39
Ostrc	05-H/O-318	11.87	18.90	49.42	18.93	0.27	bdl	0.02	0.25	0.07	0.17	99.91
Ostrc	05-H/O-318	12.88	21.27	47.08	18.10	0.25	bdl	0.04	0.23	0.08	0.15	100.08
Ostrc	05-H/O-318	13.72	22.17	46.60	16.69	0.24	bdl	0.03	0.15	0.10	0.15	99.85
Ostrc	05-H/O-318	13.67	22.54	46.17	16.86	0.23	bdl	0.04	0.18	0.09	0.13	99.91
Ostrc	05-H/O-318	10.58	21.82	39.85	26.03	0.28	bdl	0.37	0.28	0.16	0.15	99.53
Ostrc	05-H/O-318	12.21	28.10	36.44	22.12	0.29	bdl	0.13	0.24	0.13	0.28	99.94
Ostrc	05-H/O-318	9.90	15.52	39.61	30.99	0.55	bdl	2.17	0.27	0.17	0.17	99.35
Ostrc	05-H/O-318	12.65	23.36	45.34	18.11	0.21	bdl	0.05	0.25	0.07	0.19	100.22
Ostrc	05-H/O-318	12.72	21.44	47.66	17.78	0.23	bdl	0.05	0.23	0.06	0.16	100.34
Ostrc	05-H/O-318	11.67	21.31	47.37	18.72	0.24	bdl	0.04	0.26	0.04	0.17	99.81
Ostrc	05-H/O-318	10.85	17.41	50.66	20.48	0.26	bdl	0.04	0.28	0.04	0.17	100.18

Formation	Sample	MgO	Al2O3	Cr2O3	FeO	V2O3	SiO2	TiO2	MnO	NiO	ZnO	total
Ostrc	05-H/O-318	12.76	21.43	46.97	17.97	0.22	bdl	0.04	0.23	0.12	0.13	99.87
Ostrc	05-H/O-318	10.45	19.70	42.52	25.44	0.35	bdl	0.57	0.28	0.11	0.15	99.57
Ostrc	05-H/O-318	10.94	16.64	50.09	21.12	0.21	bdl	0.24	0.29	0.06	0.13	99.73
Ostrc	05-H/O-318	11.22	21.42	46.49	20.12	0.26	bdl	0.05	0.22	0.05	0.15	99.99
Ostrc	05-H/O-318	10.04	17.28	40.58	29.40	0.40	bdl	1.16	0.33	0.17	0.16	99.51
Ostrc	05-H/O-318	17.89	33.99	31.83	14.97	0.16	0.05	0.53	0.15	0.22	0.07	99.86
Ostrc	05-H/O-318	13.30	24.28	43.98	17.94	0.23	bdl	0.04	0.22	0.08	0.17	100.23
Ostrc	05-H/O-318	12.46	18.98	41.60	24.23	0.28	bdl	1.45	0.27	0.19	0.06	99.51
Ostrc	05-H/O-318	13.56	24.58	43.31	17.35	0.17	bdl	0.08	0.22	0.09	0.16	99.51
Ostrc	05-H/O-318	13.36	21.26	48.06	16.59	0.22	bdl	0.06	0.21	0.08	0.14	99.98
Ostrc	05-H/O-318	10.62	21.51	41.23	25.07	0.28	0.01	0.45	0.28	0.12	0.16	99.74
Ostrc	05-H/O-318	12.48	19.24	46.85	20.33	0.21	bdl	0.39	0.22	0.11	0.15	99.99
Ostrc	05-H/O-318	11.02	11.40	58.14	18.67	0.23	bdl	0.09	0.31	0.05	0.14	100.05
Ostrc	05-H/O-318	14.25	22.11	46.69	15.95	0.24	bdl	0.04	0.21	0.10	0.11	99.71
Ostrc	05-H/O-318	11.46	15.54	53.47	18.99	0.27	bdl	0.07	0.26	0.06	0.16	100.29
Ostrc	05-H/O-318	10.32	25.92	39.83	22.31	0.29	bdl	0.10	0.29	0.07	0.41	99.55
Ostrc	05-H/O-318	13.52	26.05	40.87	18.08	0.23	bdl	0.30	0.20	0.08	0.11	99.45
Ostrc	05-H/O-318	13.20	22.49	46.07	17.83	0.24	bdl	0.08	0.27	0.07	0.15	100.40
Ostrc	05-H/O-318	14.64	26.73	37.97	19.06	0.17	bdl	0.42	0.16	0.19	0.11	99.46
Ostrc	05-H/O-318	15.38	25.78	42.90	15.27	0.20	bdl	0.09	0.17	0.14	0.11	100.04
Ostrc	05-H/O-318	14.69	27.32	41.39	15.92	0.14	bdl	0.10	0.17	0.08	0.17	99.97
Ostrc	05-H/O-318	13.61	20.60	48.33	16.80	0.27	bdl	0.11	0.22	0.09	0.11	100.13
Ostrc	05-H/O-318	11.85	19.66	48.74	18.71	0.28	bdl	0.04	0.26	0.06	0.19	99.79
Ostrc	05-H/O-318	13.10	22.27	46.00	17.72	0.20	bdl	0.07	0.20	0.11	0.20	99.87
Ostrc	05-H/O-318	15.57	27.93	40.85	14.59	0.16	bdl	0.04	0.19	0.10	0.11	99.54
Ostrc	05-H/O-318	16.40	33.56	34.53	14.65	0.14	bdl	0.10	0.16	0.15	0.11	99.81
Ostrc	05-H/O-318	10.22	16.52	46.79	24.66	0.28	bdl	0.36	0.28	0.09	0.19	99.38
Ostrc	05-H/O-318	9.20	17.04	41.56	29.48	0.28	bdl	1.40	0.34	0.17	0.14	99.61
Ostrc	05-H/O-318	11.86	20.80	43.33	22.48	0.28	bdl	0.38	0.23	0.13	0.13	99.62
Ostrc	05-H/O-318	14.01	21.49	47.92	15.96	0.23	bdl	0.05	0.17	0.11	0.17	100.12
Ostrc	05-H/O-318	13.87	21.47	47.45	16.84	0.22	0.02	0.04	0.22	0.09	0.08	100.30
Ostrc	05-H/O-318	15.38	29.84	38.67	15.76	0.20	bdl	0.04	0.18	0.10	0.13	100.29
Ostrc	05-H/O-318	13.06	24.94	40.40	20.75	0.22	bdl	0.35	0.25	0.13	0.12	100.23
Ostrc	05-H/O-318	12.88	20.55	49.11	16.78	0.26	bdl	0.05	0.25	0.06	0.17	100.11
Ostrc	05-H/O-318	15.10	25.79	43.17	15.16	0.16	bdl	0.07	0.20	0.14	0.12	99.89
Ostrc	05-H/O-318	12.45	22.00	46.48	18.33	0.25	bdl	0.03	0.20	0.06	0.25	100.04
Ostrc	05-H/O-318	15.71	23.90	45.72	14.16	0.17	bdl	0.03	0.20	0.14	0.07	100.09
Ostrc	05-H/O-318	14.16	27.44	40.85	17.22	0.20	bdl	0.06	0.16	0.13	0.16	100.38
Ostrc	05-H/O-318	11.80	20.70	42.69	23.30	0.29	bdl	0.53	0.24	0.11	0.14	99.80
Ostrc	05-H/O-318	11.35	15.14	53.13	19.78	0.30	bdl	0.07	0.27	0.07	0.19	100.30
Ostrc	05-H/O-318	14.64	31.09	36.00	17.30	0.16	bdl	0.17	0.22	0.12	0.19	99.89
Ostrc	D-622/16	13.08	18.58	48.48	18.05	0.16	0.01	0.05	0.21	0.17	0.20	98.99
Ostrc	D-622/16	13.88	25.08	43.28	16.01	0.23	bdl	0.04	0.21	0.12	0.21	99.06
Ostrc	D-622/16	14.73	28.64	40.12	14.96	0.16	0.02	0.09	0.16	0.10	0.17	99.15
Ostrc	D-622/16	12.09	19.20	49.69	17.57	0.25	0.02	0.04	0.25	0.06	0.09	99.26
Ostrc	D-622/16	13.59	22.55	44.96	17.44	0.14	0.01	0.10	0.23	0.19	0.09	99.30
Ostrc	D-622/16	13.88	26.24	41.57	16.90	0.11	0.01	0.06	0.23	0.12	0.21	99.33
Ostrc	D-622/16	11.42	17.56	50.62	18.93	0.32	bdl	0.02	0.23	0.07	0.18	99.35
Ostrc	D-622/16	11.63	19.57	48.97	18.66	0.23	bdl	0.04	0.24	0.04	0.13	99.51
Ostrc	D-622/16	12.59	17.59	50.29	18.05	0.28	0.02	0.32	0.27	0.07	0.08	99.56
Ostrc	D-622/16	11.56	21.40	46.78	19.20	0.26	bdl	0.02	0.22	0.08	0.08	99.60
Ostrc	D-622/16	12.27	20.30	48.63	17.77	0.25	0.07	0.05	0.21	0.04	0.11	99.70
Ostrc	D-622/16	12.45	17.09	51.57	17.87	0.28	bdl	0.00	0.26	0.09	0.15	99.76
Ostrc	D-622/16	12.43	19.32	48.12	19.15	0.23	0.05	0.04	0.24	0.14	0.14	99.86
Ostrc	D-622/8	11.05	17.74	43.11	25.30	0.29	0.04	0.86	0.29	0.09	0.23	99.00
Ostrc	D-622/8	11.30	21.33	45.95	19.54	0.27	0.03	0.03	0.24	0.06	0.27	99.02
Ostrc	D-622/8	11.37	18.58	49.81	18.55	0.27	bdl	0.01	0.22	0.10	0.22	99.13
Ostrc	D-622/8	7.60	14.01	40.95	34.16	0.50	0.02	1.34	0.34	0.12	0.17	99.21
Ostrc	D-622/8	13.25	23.40	45.37	16.56	0.23	0.01	0.10	0.22	0.08	0.19	99.41
Ostrc	D-622/8	12.66	25.71	42.00	18.32	0.21	0.04	0.04	0.22	0.11	0.20	99.51
Ostrc	D-622/8	12.59	20.70	47.91	17.62	0.26	0.03	0.05	0.21	0.07	0.08	99.52
Ostrc	D-622/8	11.47	20.20	49.00	17.99	0.30	0.01	0.05	0.25	0.04	0.22	99.53
Ostrc	D-622/8	11.03	19.97	40.93	26.41	0.30	0.01	0.44	0.26	0.11	0.10	99.56
Ostrc	D-622/8	12.87	20.28	49.49	16.07	0.35	0.06	0.04	0.19	0.06	0.15	99.56

Formation	Sample	MgO	Al2O3	Cr2O3	FeO	V2O3	SiO2	TiO2	MnO	NiO	ZnO	total
Ostrc	D-622/8	9.50	9.44	59.11	20.87	0.28	0.01	0.06	0.28	0.01	0.14	99.70
Ostrc	D-622/8	11.53	18.11	50.77	18.62	0.21	bdl	0.03	0.26	0.08	0.13	99.74
Ostrc	D-622/8	12.90	23.97	44.06	17.84	0.38	bdl	0.06	0.20	0.08	0.23	99.72
Ostrc	D-622/8	9.83	17.69	43.17	27.71	0.24	bdl	0.48	0.33	0.14	0.23	99.82
Ostrc	D-622/8	11.82	17.90	50.41	19.06	0.22	0.03	0.05	0.24	0.07	0.12	99.92
Ostrc	D-622/8	10.09	20.30	42.32	25.63	0.39	0.01	0.51	0.25	0.16	0.26	99.92
Ostrc	D-622/8	13.36	24.66	42.87	18.20	0.28	bdl	0.05	0.24	0.17	0.17	100.00
Ostrc	D-622/8	12.21	18.29	51.32	17.53	0.28	0.02	0.01	0.24	0.11	0.13	100.14
Ostrc	D-634/2/2	11.72	16.18	50.86	19.46	0.22	0.01	0.09	0.22	0.13	0.12	99.01
Ostrc	D-634/2/2	12.81	21.73	46.82	16.94	0.22	0.01	0.03	0.23	0.05	0.17	99.01
Ostrc	D-634/2/2	10.55	22.53	44.18	21.04	0.26	0.03	0.03	0.30	0.02	0.10	99.04
Ostrc	D-634/2/2	14.83	29.14	39.50	15.02	0.18	bdl	0.05	0.19	0.13	0.17	99.21
Ostrc	D-634/2/2	13.08	21.60	47.30	16.66	0.16	0.03	0.01	0.23	0.09	0.11	99.27
Ostrc	D-634/2/2	12.77	20.58	49.21	16.11	0.27	bdl	0.02	0.20	0.07	0.12	99.35
Ostrc	D-634/2/2	10.72	19.67	44.65	23.31	0.24	0.04	0.36	0.20	0.04	0.14	99.37
Ostrc	D-634/2/2	11.11	18.28	50.23	19.12	0.22	0.03	0.03	0.23	0.06	0.19	99.50
Ostrc	D-634/2/2	12.58	23.58	44.54	18.27	0.22	0.01	0.06	0.20	0.05	0.18	99.69
Ostrc	D-634/2/2	11.31	21.22	46.88	19.41	0.39	0.02	0.03	0.25	0.02	0.15	99.68
Ostrc	D-634/2/2	14.07	24.46	45.09	15.59	0.13	0.01	0.04	0.17	0.14	0.11	99.81
Ostrc	D-634/2/2	9.20	13.51	54.92	21.48	0.30	0.01	0.03	0.28	0.06	0.19	99.98
Ostrc	D-634/2/2	12.46	20.17	49.19	17.54	0.21	0.01	0.02	0.21	0.04	0.19	100.04
Ostrc	D-634/2/2	13.04	21.21	46.28	18.64	0.21	0.03	0.19	0.20	0.10	0.16	100.06
Ostrc	D-634/2/2	12.81	20.93	48.36	17.59	0.26	0.01	0.03	0.21	0.13	0.10	100.43
Ostrc	D-634/3	12.14	18.84	49.77	17.60	0.24	bdl	0.06	0.17	0.04	0.13	98.99
Ostrc	D-634/3	13.39	21.69	46.50	16.68	0.25	0.02	0.05	0.21	0.10	0.11	99.00
Ostrc	D-634/3	11.05	18.68	47.08	21.27	0.30	0.02	0.21	0.18	0.10	0.14	99.03
Ostrc	D-634/3	15.06	27.21	42.92	13.28	0.14	0.03	0.05	0.14	0.12	0.18	99.13
Ostrc	D-634/3	12.53	19.26	44.73	21.31	0.38	0.02	0.37	0.20	0.17	0.11	99.08
Ostrc	D-634/3	14.12	24.11	44.53	15.67	0.20	bdl	0.06	0.18	0.20	0.16	99.23
Ostrc	D-634/3	13.55	25.46	42.61	16.86	0.23	0.03	0.06	0.22	0.12	0.17	99.31
Ostrc	D-634/3	13.47	21.09	48.46	15.75	0.18	0.02	0.01	0.14	0.10	0.11	99.33
Ostrc	D-634/3	13.99	24.02	44.10	16.63	0.22	bdl	0.08	0.20	0.08	0.07	99.39
Ostrc	D-634/3	12.46	21.36	46.83	18.09	0.23	0.03	0.02	0.20	0.05	0.14	99.41
Ostrc	D-634/3	9.56	12.66	53.69	22.30	0.33	bdl	0.36	0.30	0.06	0.16	99.42
Ostrc	D-634/3	12.97	25.93	42.48	17.30	0.26	bdl	0.06	0.21	0.09	0.14	99.44
Ostrc	D-634/3	11.62	17.94	49.11	19.89	0.23	0.04	0.26	0.26	0.11	0.14	99.60
Ostrc	D-634/3	15.58	27.41	39.24	16.38	0.16	0.06	0.42	0.15	0.10	0.13	99.63
Ostrc	D-634/3	11.28	18.97	49.54	19.04	0.28	0.02	0.05	0.20	0.13	0.12	99.63
Ostrc	D-634/3	11.66	18.53	48.54	20.04	0.25	0.02	0.15	0.23	0.05	0.18	99.65
Ostrc	D-634/3	11.86	18.31	50.75	18.03	0.30	0.03	0.02	0.23	0.07	0.11	99.71
Ostrc	D-634/3	11.83	17.77	51.58	17.83	0.25	bdl	0.04	0.22	0.01	0.21	99.74
Ostrc	D-634/3	11.44	15.92	53.37	18.35	0.24	bdl	0.03	0.23	0.09	0.16	99.83
Ostrc	D-634/3	12.59	16.06	49.09	20.65	0.29	bdl	0.69	0.22	0.15	0.09	99.83
Ostrc	D-634/3	10.61	15.32	52.86	20.32	0.25	bdl	0.03	0.27	0.05	0.13	99.84
Ostrc	D-634/3	11.76	19.84	49.14	18.58	0.28	0.01	0.05	0.23	0.09	0.21	100.19
Ostrc	DJ106/10/1/1	13.76	24.82	43.90	15.78	0.26	0.01	0.04	0.24	0.09	0.14	99.04
Ostrc	DJ106/10/1/1	12.69	21.05	48.39	16.36	0.25	bdl	0.02	0.18	0.02	0.21	99.17
Ostrc	DJ106/10/1/1	12.72	20.24	48.47	17.12	0.17	bdl	0.08	0.18	0.07	0.17	99.22
Ostrc	DJ106/10/1/1	12.33	20.56	47.72	16.88	0.26	0.99	0.02	0.17	0.13	0.15	99.21
Ostrc	DJ106/10/1/1	12.36	21.02	47.71	17.34	0.25	0.04	0.03	0.24	0.13	0.15	99.27
Ostrc	DJ106/10/1/1	13.29	23.64	45.11	16.57	0.18	0.02	0.03	0.20	0.05	0.20	99.29
Ostrc	DJ106/10/1/1	12.99	23.49	45.22	16.84	0.21	bdl	0.10	0.22	0.12	0.14	99.33
Ostrc	DJ106/10/1/1	12.09	20.35	48.45	17.87	0.18	0.01	0.03	0.17	0.12	0.18	99.45
Ostrc	DJ106/10/1/1	12.31	22.04	46.50	17.85	0.37	bdl	0.07	0.20	0.05	0.17	99.56
Ostrc	DJ106/10/1/1	11.14	16.23	52.90	18.59	0.27	bdl	0.03	0.28	0.05	0.11	99.60
Ostrc	DJ106/10/1/1	9.77	13.86	53.71	21.66	0.24	bdl	0.05	0.26	0.07	0.22	99.84
Ostrc	DJ-106/4	13.22	26.86	41.33	17.12	0.10	0.03	0.09	0.17	0.05	0.07	99.04
Ostrc	DJ-106/4	12.47	23.05	44.35	18.50	0.18	0.05	0.04	0.20	0.07	0.12	99.03
Ostrc	DJ-106/4	11.89	18.02	50.40	18.03	0.30	0.01	0.03	0.19	0.10	0.13	99.10
Ostrc	DJ-106/4	14.48	29.80	38.18	16.12	0.09	bdl	0.07	0.19	0.07	0.18	99.18
Ostrc	DJ-106/4	12.46	21.26	47.32	17.50	0.18	bdl	0.04	0.25	0.05	0.13	99.19
Ostrc	DJ-106/4	12.27	22.85	44.06	19.08	0.24	0.01	0.20	0.22	0.12	0.17	99.22
Ostrc	DJ-106/4	12.47	22.20	46.77	17.27	0.15	0.03	0.06	0.14	0.13	0.09	99.31
Ostrc	DJ-106/4	9.69	15.50	52.52	20.86	0.16	0.04	0.03	0.28	0.09	0.23	99.40

Formation	Sample	MgO	Al2O3	Cr2O3	FeO	V2O3	SiO2	TiO2	MnO	NiO	ZnO	total
Ostrc	DJ-106/4	13.40	26.07	42.14	16.94	0.24	0.01	0.20	0.19	0.11	0.15	99.45
Ostrc	DJ-106/4	11.07	17.52	50.95	18.95	0.31	0.04	0.06	0.21	0.08	0.25	99.44
Ostrc	DJ-106/4	11.78	19.98	48.67	18.32	0.26	0.04	0.04	0.21	0.08	0.09	99.47
Ostrc	DJ-106/4	12.82	15.43	50.98	19.31	0.14	bdl	0.38	0.22	0.14	0.11	99.53
Ostrc	DJ-106/4	13.84	26.38	42.19	16.34	0.25	0.03	0.02	0.20	0.15	0.16	99.56
Ostrc	DJ-106/4	11.73	17.40	51.45	18.30	0.31	bdl	0.02	0.19	0.00	0.19	99.59
Ostrc	DJ-106/4	11.74	21.00	47.07	19.16	0.28	bdl	0.02	0.29	0.07	0.15	99.78
Ostrc	DJ-106/4	11.48	18.50	49.90	19.08	0.32	bdl	0.02	0.26	0.05	0.21	99.82
Ostrc	DJ-106/4	12.36	21.11	47.10	18.64	0.29	0.01	0.12	0.20	0.10	0.14	100.07
Ostrc	DJ-106/4	15.49	26.15	43.72	14.04	0.19	0.03	0.11	0.16	0.12	0.14	100.15
Vivodina	05-H/M-26	18.26	37.02	28.90	14.10	0.12	0.07	0.44	0.14	0.28	0.07	99.39
Vivodina	05-H/M-26	11.53	16.91	51.95	19.12	0.27	bdl	0.06	0.27	0.08	0.12	100.30
Vivodina	05-H/M-26	12.34	23.08	38.77	24.21	0.15	0.07	0.85	0.19	0.20	0.09	99.95
Vivodina	05-H/M-26	12.86	18.75	49.82	18.12	0.22	bdl	0.08	0.22	0.07	0.15	100.30
Vivodina	05-H/M-26	12.95	21.02	48.01	17.25	0.26	bdl	0.10	0.22	0.08	0.13	100.03
Vivodina	05-H/M-26	10.34	18.15	40.83	28.51	0.36	bdl	0.75	0.28	0.14	0.12	99.49
Vivodina	05-H/M-26	12.97	18.80	49.00	18.56	0.26	bdl	0.45	0.26	0.02	0.09	100.40
Vivodina	05-H/M-26	10.92	17.60	50.32	19.81	0.29	bdl	0.06	0.26	0.05	0.17	99.48
Vivodina	05-H/M-26	11.85	16.27	49.80	21.08	0.24	bdl	0.36	0.25	0.10	0.12	100.07
Vivodina	05-H/M-26	14.59	26.63	43.11	14.98	0.26	bdl	0.10	0.16	0.11	0.15	100.08
Vivodina	05-H/M-26	13.50	19.99	49.33	16.53	0.24	bdl	0.20	0.21	0.09	0.12	100.20
Vivodina	05-H/M-26	13.42	22.13	46.87	16.74	0.20	bdl	0.15	0.19	0.08	0.11	99.90
Vivodina	05-H/M-26	10.04	26.96	34.82	26.68	0.19	0.03	0.56	0.29	0.12	0.13	99.82
Vivodina	05-H/M-26	12.72	25.79	42.36	17.68	0.26	bdl	0.06	0.21	0.07	0.16	99.31
Vivodina	05-H/M-26	11.11	17.08	51.12	19.68	0.36	bdl	0.13	0.25	0.07	0.13	99.92
Vivodina	05-H/M-26	14.24	20.07	50.17	14.61	0.21	bdl	0.07	0.18	0.10	0.08	99.74
Vivodina	05-H/M-26	14.20	27.08	41.56	16.45	0.21	bdl	0.05	0.19	0.09	0.16	99.99
Vivodina	05-H/M-26	10.53	20.33	44.09	23.77	0.10	0.02	0.23	0.29	0.14	0.08	99.59
Vivodina	05-H/M-26	10.90	17.00	48.36	22.54	0.22	bdl	0.21	0.24	0.08	0.13	99.69
Vivodina	05-H/M-26	5.96	18.94	37.67	34.47	0.45	bdl	0.83	0.37	0.14	0.21	99.03
Vivodina	05-H/M-26	15.61	35.09	32.29	15.74	0.17	bdl	0.05	0.17	0.15	0.19	99.46
Vivodina	05-H/M-26	14.94	26.28	42.17	15.27	0.16	bdl	0.11	0.18	0.08	0.15	99.34
Vivodina	05-H/M-26	19.21	42.48	22.77	13.75	0.14	0.04	0.34	0.11	0.27	0.05	99.17
Vivodina	05-H/M-26	10.94	19.88	48.29	20.26	0.24	bdl	0.07	0.26	0.07	0.27	100.27
Vivodina	05-H/M-26	12.01	18.17	51.03	18.33	0.28	bdl	0.12	0.25	0.06	0.15	100.39
Vivodina	05-H/M-26	16.32	35.83	27.30	19.27	0.18	0.02	0.62	0.16	0.11	0.07	99.87
Vivodina	05-H/M-26	12.10	20.93	46.95	19.25	0.22	bdl	0.09	0.23	0.08	0.17	100.02
Vivodina	05-H/M-26	18.24	41.83	22.30	15.57	0.14	0.07	0.39	0.17	0.24	0.05	99.01
Vivodina	05-H/M-26	11.53	19.09	49.30	18.68	0.29	bdl	0.10	0.21	0.05	0.17	99.42
Vivodina	05-H/M-26	10.08	12.83	52.91	23.27	0.23	bdl	0.16	0.22	0.06	0.14	99.90
Vivodina	05-H/M-26	13.88	24.23	45.11	15.30	0.23	bdl	0.08	0.18	0.09	0.13	99.23
Vivodina	05-H/M-26	17.94	37.09	27.23	15.73	0.12	0.05	0.43	0.15	0.25	0.05	99.03
Vivodina	05-H/M-26	14.96	26.57	41.71	16.02	0.20	bdl	0.05	0.18	0.14	0.11	99.93
Vivodina	05-H/M-26	13.23	20.31	48.41	17.47	0.27	bdl	0.06	0.18	0.09	0.10	100.14
Vivodina	05-H/M-26	14.91	25.17	44.33	14.61	0.17	bdl	0.11	0.18	0.12	0.09	99.69
Vivodina	05-H/M-26	12.94	21.94	47.25	17.22	0.30	bdl	0.04	0.19	0.09	0.11	100.10
Vivodina	05-H/M-26	11.71	17.46	51.36	18.77	0.26	bdl	0.09	0.28	0.07	0.18	100.17
Vivodina	05-H/M-26	13.74	22.85	47.01	16.00	0.26	bdl	0.05	0.21	0.06	0.14	100.32
Vivodina	05-H/M-26	12.41	21.52	43.30	21.28	0.28	bdl	0.29	0.24	0.12	0.10	99.54
Vivodina	05-H/M-26	10.42	18.35	47.10	23.46	0.20	bdl	0.21	0.25	0.09	0.10	100.17
Vivodina	05-H/M-26	12.56	21.74	46.77	18.04	0.26	bdl	0.05	0.20	0.09	0.15	99.86
Vivodina	05-H/M-26	12.98	21.00	48.23	16.85	0.27	bdl	0.04	0.21	0.09	0.11	99.78
Vivodina	05-H/M-26	13.05	22.27	46.16	17.86	0.24	bdl	0.16	0.20	0.08	0.14	100.16
Vivodina	05-H/M-26	13.46	24.76	43.87	16.86	0.18	bdl	0.14	0.20	0.11	0.13	99.72
Vivodina	05-H/M-26	9.13	15.30	43.42	29.53	0.48	bdl	0.85	0.31	0.16	0.20	99.37
Vivodina	05-H/M-26	10.66	18.01	43.23	26.39	0.45	bdl	0.74	0.28	0.13	0.11	100.01
Vivodina	05-H/M-26	9.05	14.95	51.68	23.38	0.24	bdl	0.10	0.33	0.04	0.21	99.98
Vivodina	05-H/M-26	12.30	18.64	50.69	17.72	0.27	bdl	0.04	0.24	0.05	0.16	100.11
Vivodina	05-H/M-26	13.78	20.89	49.34	15.81	0.26	bdl	0.05	0.20	0.08	0.12	100.52
Vivodina	05-H/M-26	9.51	7.92	60.17	20.90	0.22	bdl	0.32	0.32	0.04	0.16	99.56
Vivodina	05-H/M-26	11.89	19.53	49.18	18.66	0.23	bdl	0.12	0.25	0.05	0.19	100.11
Vivodina	05-H/M-26	8.54	17.97	44.11	27.06	0.30	bdl	0.46	0.34	0.07	0.18	99.04
Vivodina	05-H/M-26	13.90	25.59	42.42	16.97	0.22	bdl	0.05	0.22	0.08	0.15	99.59
Vivodina	05-H/M-26	12.64	21.06	48.23	17.31	0.29	bdl	0.04	0.24	0.07	0.17	100.06

Formation	Sample	MgO	Al2O3	Cr2O3	FeO	V2O3	SiO2	TiO2	MnO	NiO	ZnO	total
Vivodina	05-H/M-26	11.89	25.49	42.17	19.83	0.22	bdl	0.04	0.24	0.07	0.23	100.16
Vivodina	05-H/M-26	16.40	31.98	33.65	16.51	0.20	0.03	0.59	0.13	0.16	0.08	99.72
Vivodina	05-H/M-26	11.18	22.19	45.06	20.77	0.32	bdl	0.06	0.24	0.06	0.29	100.16
Vivodina	05-H/M-26	7.58	15.77	50.99	24.53	0.34	bdl	0.03	0.39	0.03	0.25	99.92
Vivodina	05-H/M-26	12.99	22.43	47.00	17.08	0.26	bdl	0.07	0.21	0.09	0.16	100.29
Vivodina	05-H/M-26	12.23	19.89	48.66	18.23	0.24	bdl	0.23	0.24	0.05	0.17	99.94
Vivodina	05-H/M-26	10.83	17.31	51.80	18.54	0.28	bdl	0.10	0.22	0.07	0.18	99.31
Vivodina	05-H/M-26	14.82	28.78	39.05	16.16	0.19	bdl	0.09	0.19	0.11	0.18	99.55
Vivodina	05-H/M-26	13.41	19.05	49.90	16.86	0.24	bdl	0.14	0.19	0.11	0.04	99.94
Vivodina	05-H/M-26	12.34	21.51	44.26	20.60	0.23	bdl	0.19	0.26	0.11	0.14	99.65
Vivodina	05-H/M-26	11.81	14.53	52.75	20.01	0.21	bdl	0.33	0.23	0.08	0.10	100.05
Vivodina	05-H/M-26	14.86	28.59	35.63	19.10	0.22	0.01	0.62	0.19	0.17	0.05	99.43
Vivodina	05-H/M-26	11.74	21.56	46.77	18.90	0.22	bdl	0.26	0.26	0.08	0.18	99.97
Vivodina	05-H/M-26	13.04	22.69	45.43	17.94	0.26	bdl	0.19	0.21	0.10	0.14	100.00
Vivodina	05-H/M-26	12.06	20.05	47.52	19.31	0.23	bdl	0.14	0.24	0.07	0.18	99.81
Vivodina	05-H/M-26	12.79	23.42	45.30	17.99	0.21	bdl	0.27	0.22	0.09	0.14	100.42
Vivodina	05-H/M-26	12.91	24.98	42.67	18.12	0.24	bdl	0.08	0.24	0.10	0.22	99.55
Vivodina	05-H/M-26	18.39	31.82	35.48	12.78	0.12	0.05	0.37	0.12	0.22	0.03	99.38
Vivodina	05-H/M-26	13.57	24.28	45.22	16.51	0.22	bdl	0.05	0.22	0.09	0.16	100.31
Vivodina	05-H/M-26	10.26	15.46	52.20	20.97	0.31	bdl	0.09	0.28	0.02	0.22	99.81
Vivodina	05-H/M-26	11.56	17.42	51.13	18.66	0.24	bdl	0.05	0.22	0.08	0.13	99.50
Vivodina	05-H/M-26	13.21	23.29	45.86	17.12	0.25	bdl	0.07	0.20	0.06	0.17	100.24
Vivodina	05-H/M-26	9.86	11.60	56.48	21.63	0.29	bdl	0.13	0.29	0.04	0.14	100.47
Vivodina	05-H/M-26	11.26	17.76	50.58	19.82	0.26	bdl	0.04	0.24	0.07	0.16	100.19
Vivodina	05-H/M-26	11.21	22.45	41.07	23.84	0.30	bdl	0.36	0.23	0.12	0.15	99.73
Vivodina	05-H/M-26	10.70	13.15	55.00	20.23	0.24	bdl	0.11	0.29	0.05	0.14	99.90
Vivodina	05-H/M-26	11.93	18.81	49.48	18.45	0.23	bdl	0.11	0.25	0.06	0.11	99.41
Vivodina	05-H/M-26	13.45	24.27	44.58	16.49	0.22	bdl	0.04	0.15	0.08	0.16	99.46
Vivodina	05-H/M-26	12.11	22.07	46.96	17.96	0.22	bdl	0.05	0.24	0.05	0.16	99.82
Vivodina	05-H/M-26	11.73	20.80	47.64	19.06	0.25	bdl	0.08	0.23	0.07	0.19	100.04
Vivodina	05-H/M-26	14.20	26.17	42.45	16.67	0.20	bdl	0.10	0.21	0.09	0.15	100.23
Vivodina	05-H/M-26	10.12	17.62	50.88	20.10	0.28	bdl	0.12	0.28	0.05	0.23	99.67
Vivodina	05-H/M-27	14.32	27.51	40.22	16.73	0.20	bdl	0.03	0.21	0.09	0.14	99.46
Vivodina	05-H/M-27	13.63	24.69	43.08	17.25	0.24	bdl	0.03	0.18	0.09	0.15	99.34
Vivodina	05-H/M-27	13.34	24.98	43.35	17.26	0.21	bdl	0.03	0.20	0.09	0.16	99.62
Vivodina	05-H/M-27	13.18	24.56	43.69	17.89	0.21	bdl	0.04	0.22	0.09	0.21	100.09
Vivodina	05-H/M-27	14.27	26.85	41.99	15.83	0.21	bdl	0.06	0.20	0.09	0.15	99.64
Vivodina	05-H/M-27	13.76	25.14	42.82	16.94	0.20	bdl	0.04	0.19	0.08	0.13	99.29
Vivodina	05-H/M-27	12.85	24.01	44.35	17.20	0.22	bdl	0.02	0.19	0.09	0.17	99.10
Vivodina	05-H/M-27	12.61	22.14	46.42	17.71	0.28	bdl	0.02	0.28	0.06	0.17	99.69
Vivodina	05-H/M-27	13.51	23.95	44.35	16.65	0.22	bdl	0.03	0.20	0.07	0.16	99.14
Vivodina	05-H/M-27	11.50	18.02	50.27	18.85	0.26	bdl	0.04	0.29	0.05	0.17	99.46
Vivodina	05-H/M-27	12.19	19.23	49.77	18.17	0.27	bdl	0.04	0.26	0.08	0.19	100.20
Vivodina	05-H/M-27	12.63	22.13	46.87	17.30	0.26	bdl	0.04	0.21	0.05	0.17	99.64
Vivodina	05-H/M-27	9.72	9.44	60.54	19.23	0.18	bdl	0.08	0.29	0.03	0.10	99.61
Vivodina	05-H/M-27	13.06	24.01	44.18	17.70	0.23	bdl	0.04	0.21	0.09	0.14	99.66
Vivodina	05-H/M-27	12.98	23.46	45.81	17.53	0.22	bdl	0.03	0.25	0.09	0.15	100.52
Vivodina	05-H/M-27	16.60	35.47	27.80	17.91	0.20	0.02	0.89	0.17	0.21	0.09	99.38
Vivodina	05-H/M-27	13.43	24.17	44.81	16.37	0.28	bdl	0.02	0.19	0.07	0.19	99.53
Vivodina	05-H/M-27	11.79	23.21	44.57	19.21	0.21	bdl	0.02	0.24	0.06	0.19	99.52
Vivodina	05-H/M-27	13.56	25.23	43.41	16.82	0.25	bdl	0.02	0.21	0.10	0.16	99.76
Vivodina	05-H/M-27	12.35	22.52	46.78	17.60	0.24	bdl	0.02	0.21	0.07	0.18	99.96
Vivodina	05-H/M-27	10.14	20.06	44.57	24.17	0.24	bdl	0.13	0.27	0.09	0.18	99.83
Vivodina	05-H/M-27	13.07	23.32	44.55	17.98	0.22	bdl	0.03	0.23	0.07	0.19	99.68
Vivodina	05-H/M-27	12.27	23.93	42.66	19.60	0.22	bdl	0.04	0.23	0.08	0.25	99.27
Vivodina	05-H/M-27	13.14	22.00	46.58	17.54	0.26	bdl	0.03	0.22	0.11	0.12	99.98
Vivodina	05-H/M-27	12.96	23.60	44.37	18.12	0.27	bdl	0.03	0.22	0.08	0.16	99.80
Vivodina	05-H/M-27	13.80	19.87	48.56	16.54	0.23	bdl	0.02	0.23	0.11	0.09	99.45
Vivodina	05-H/M-27	11.82	18.30	50.23	18.72	0.29	bdl	0.03	0.22	0.08	0.15	99.84
Vivodina	05-H/M-27	12.14	24.25	43.52	18.54	0.23	bdl	0.03	0.21	0.08	0.20	99.21
Vivodina	05-H/M-27	12.95	24.22	43.43	17.98	0.28	bdl	0.05	0.21	0.09	0.17	99.38
Vivodina	05-H/M-27	12.62	24.52	44.00	17.92	0.23	bdl	0.05	0.24	0.06	0.17	99.81
Vivodina	05-H/M-27	13.14	24.95	43.45	17.21	0.20	bdl	0.06	0.21	0.10	0.19	99.51
Vivodina	05-H/M-27	9.91	18.13	48.37	21.99	0.25	bdl	0.04	0.32	0.08	0.19	99.28

Formation	Sample	MgO	Al2O3	Cr2O3	FeO	V2O3	SiO2	TiO2	MnO	NiO	ZnO	total
Vivodina	05-H/M-27	11.30	15.92	52.50	19.18	0.27	bdl	0.04	0.22	0.04	0.16	99.63
Vivodina	05-H/M-27	12.42	16.91	52.02	17.42	0.28	bdl	0.03	0.21	0.06	0.11	99.46
Vivodina	05-H/M-27	13.89	23.57	45.82	15.49	0.21	bdl	0.04	0.18	0.06	0.15	99.42
Vivodina	05-H/M-27	13.71	22.37	45.70	17.03	0.23	bdl	0.07	0.24	0.11	0.12	99.56
Vivodina	05-H/M-27	12.73	22.01	46.39	18.04	0.24	bdl	0.04	0.24	0.06	0.16	99.90
Vivodina	05-H/M-27	16.11	34.50	33.79	14.14	0.14	bdl	0.07	0.16	0.11	0.22	99.23
Vivodina	05-H/M-27	11.38	19.57	48.47	19.03	0.26	bdl	0.03	0.25	0.05	0.16	99.19
Vivodina	05-H/M-27	13.61	24.14	45.01	16.59	0.22	bdl	0.03	0.20	0.09	0.13	100.02
Vivodina	05-H/M-27	12.37	21.61	46.05	18.63	0.23	bdl	0.03	0.24	0.07	0.13	99.36
Vivodina	05-H/M-27	9.52	18.40	47.07	23.59	0.18	bdl	0.21	0.34	0.04	0.37	99.72
Vivodina	05-H/M-27	12.83	18.77	50.05	17.45	0.24	bdl	0.04	0.22	0.06	0.11	99.77
Vivodina	05-H/M-27	12.14	22.73	44.93	19.41	0.23	bdl	0.03	0.23	0.09	0.19	99.97
Vivodina	05-H/M-27	14.11	30.16	37.53	16.55	0.22	bdl	0.04	0.19	0.11	0.15	99.06
Vivodina	05-H/M-27	12.12	21.79	46.33	19.08	0.26	bdl	0.09	0.27	0.05	0.18	100.17
Vivodina	05-H/M-27	13.16	26.64	41.50	17.60	0.17	bdl	0.11	0.21	0.07	0.23	99.69
Vivodina	05-H/M-27	12.38	21.16	47.01	18.44	0.23	bdl	0.03	0.23	0.09	0.16	99.73
Vivodina	05-H/M-27	10.76	18.76	48.93	20.47	0.25	bdl	0.05	0.23	0.06	0.12	99.62
Vivodina	05-H/M-27	12.14	16.82	49.22	20.70	0.23	bdl	0.30	0.19	0.08	0.08	99.76
Vivodina	05-H/M-27	12.12	19.34	49.64	18.30	0.32	bdl	0.03	0.23	0.08	0.20	100.27
Vivodina	05-H/M-27	11.10	24.05	44.47	19.68	0.24	bdl	0.05	0.25	0.05	0.20	100.08
Vivodina	05-H/M-27	13.53	28.73	38.72	17.76	0.15	bdl	0.04	0.24	0.07	0.26	99.49
Vivodina	05-H/M-27	12.44	17.93	49.64	19.16	0.25	bdl	0.16	0.23	0.08	0.12	100.00
Vivodina	05-H/M-27	14.45	25.95	43.41	15.59	0.16	bdl	0.05	0.17	0.10	0.14	100.02
Vivodina	05-H/M-27	13.07	21.22	48.41	16.71	0.21	bdl	0.04	0.21	0.09	0.11	100.07
Vivodina	05-H/M-27	12.39	23.36	44.74	19.23	0.26	bdl	0.03	0.23	0.07	0.19	100.50
Vivodina	05-H/M-27	11.54	17.20	47.90	22.35	0.24	bdl	0.12	0.27	0.11	0.14	99.88
Vivodina	05-H/M-27	14.44	26.60	42.27	15.78	0.19	bdl	0.04	0.16	0.11	0.17	99.77
Vivodina	05-H/M-27	12.65	17.07	50.27	18.96	0.23	bdl	0.24	0.22	0.08	0.11	99.83
Vivodina	05-H/M-27	11.29	15.79	51.03	20.62	0.24	bdl	0.11	0.28	0.04	0.14	99.53
Vivodina	05-H/M-27	11.14	22.07	45.04	20.74	0.21	bdl	0.10	0.25	0.07	0.20	99.84
Vivodina	05-H/M-27	14.07	24.34	44.91	15.84	0.19	bdl	0.05	0.17	0.08	0.15	99.81
Vivodina	05-H/M-27	12.44	18.93	49.69	17.69	0.27	bdl	0.02	0.22	0.10	0.13	99.50
Vivodina	05-H/M-27	11.84	19.54	47.66	19.74	0.25	bdl	0.04	0.22	0.08	0.11	99.47
Vivodina	05-H/M-27	15.01	28.27	35.34	19.44	0.17	bdl	0.58	0.20	0.11	0.05	99.18
Vivodina	05-H/M-27	9.65	15.60	51.91	22.08	0.21	bdl	0.07	0.23	0.08	0.20	100.01
Vivodina	05-H/M-27	12.08	18.95	50.26	17.68	0.28	bdl	0.06	0.24	0.08	0.15	99.77
Vivodina	05-H/M-27	12.45	23.24	43.96	19.56	0.21	bdl	0.28	0.22	0.10	0.20	100.21
Vivodina	05-H/M-27	11.79	18.67	49.51	19.03	0.27	bdl	0.06	0.24	0.08	0.18	99.83
Vivodina	05-H/M-27	12.10	20.00	47.78	18.90	0.28	bdl	0.02	0.28	0.08	0.17	99.60
Vivodina	05-H/M-27	11.17	16.90	50.97	20.15	0.29	bdl	0.04	0.24	0.07	0.15	99.98
Vivodina	05-H/M-27	13.28	20.42	48.72	16.50	0.24	bdl	0.04	0.23	0.10	0.13	99.65
Vivodina	05-H/M-27	13.62	19.45	49.92	15.61	0.24	bdl	0.06	0.22	0.07	0.12	99.32
Vivodina	05-H/M-27	13.13	22.29	46.16	17.52	0.22	bdl	0.03	0.20	0.08	0.13	99.76
Vivodina	05-H/M-27	10.92	20.66	41.83	24.75	0.29	bdl	0.34	0.26	0.14	0.11	99.31
Vivodina	05-H/M-27	13.17	22.04	46.33	17.48	0.28	bdl	0.04	0.18	0.07	0.16	99.75
Vivodina	05-H/M-27	13.20	23.56	44.58	17.70	0.22	bdl	0.05	0.19	0.08	0.17	99.75
Vivodina	05-H/M-6	13.23	21.54	46.26	18.05	0.17	bdl	0.38	0.21	0.08	0.14	100.06
Vivodina	05-H/M-6	14.66	24.15	45.52	15.41	0.20	bdl	0.06	0.20	0.08	0.11	100.40
Vivodina	05-H/M-6	11.23	16.56	51.56	19.94	0.21	bdl	0.07	0.28	0.03	0.08	99.96
Vivodina	05-H/M-6	13.86	20.64	48.08	16.35	0.26	bdl	0.06	0.19	0.14	0.08	99.67
Vivodina	05-H/M-6	12.43	21.38	46.93	18.56	0.23	bdl	0.07	0.21	0.06	0.19	100.05
Vivodina	05-H/M-6	11.42	16.77	44.84	24.17	0.41	bdl	1.31	0.34	0.21	0.17	99.64
Vivodina	05-H/M-6	15.99	33.69	32.73	16.44	0.15	bdl	0.03	0.16	0.18	0.14	99.50
Vivodina	05-H/M-6	13.22	23.08	45.29	17.91	0.23	bdl	0.12	0.22	0.10	0.17	100.35
Vivodina	05-H/M-6	10.53	16.99	51.27	20.25	0.30	bdl	0.06	0.25	0.04	0.17	99.85
Vivodina	05-H/M-6	14.28	26.52	42.03	16.16	0.23	bdl	0.09	0.19	0.08	0.20	99.78
Vivodina	05-H/M-6	14.76	25.72	43.23	15.77	0.16	bdl	0.09	0.19	0.10	0.12	100.14
Vivodina	05-H/M-6	13.46	23.76	45.37	16.96	0.23	bdl	0.05	0.23	0.08	0.20	100.34
Vivodina	05-H/M-6	18.06	43.39	23.86	13.40	0.13	bdl	0.07	0.14	0.21	0.18	99.44
Vivodina	05-H/M-6	13.02	18.11	51.91	16.72	0.23	bdl	0.06	0.23	0.06	0.08	100.43
Vivodina	05-H/M-6	12.43	20.42	47.52	19.17	0.19	bdl	0.11	0.21	0.08	0.19	100.33
Vivodina	05-H/M-6	13.95	23.66	45.20	16.78	0.25	bdl	0.08	0.21	0.08	0.16	100.36
Vivodina	05-H/M-6	13.21	21.71	46.26	17.92	0.19	bdl	0.23	0.23	0.09	0.14	99.98
Vivodina	05-H/M-6	13.10	20.79	47.53	17.61	0.26	bdl	0.05	0.23	0.07	0.12	99.76

Formation	Sample	MgO	Al2O3	Cr2O3	FeO	V2O3	SiO2	TiO2	MnO	NiO	ZnO	total
Vivodina	05-H/M-6	16.50	30.97	39.22	12.85	0.14	bdl	0.08	0.18	0.07	0.14	100.15
Vivodina	05-H/M-6	12.72	22.41	45.88	18.36	0.23	bdl	0.08	0.24	0.09	0.17	100.20
Vivodina	05-H/M-6	11.92	23.14	44.84	19.96	0.27	bdl	0.07	0.23	0.06	0.27	100.77
Vivodina	05-H/M-6	11.62	12.62	56.34	18.56	0.20	bdl	0.06	0.29	0.05	0.12	99.84
Vivodina	05-H/M-6	11.09	16.15	52.03	20.01	0.26	bdl	0.11	0.28	0.06	0.17	100.16
Vivodina	05-H/M-6	13.19	19.48	49.57	16.76	0.16	0.03	0.10	0.17	0.08	0.13	99.68
Vivodina	05-H/M-6	15.11	30.85	38.33	15.15	0.16	bdl	0.10	0.17	0.13	0.15	100.15
Vivodina	05-H/M-6	13.72	20.31	44.93	20.01	0.25	bdl	0.45	0.20	0.13	0.09	100.10
Vivodina	05-H/M-6	17.25	34.40	31.04	16.12	0.15	0.03	0.33	0.16	0.21	0.03	99.73

**WDS configuration used for the electron microprobe analyses of monazite**

Element	Crystal	Spectrometer	Line	Standard	Source of standard	Peak count time (s)	Upper and lower background count times (s)
U	PETJ	4	Mβ	UO <sub>2</sub>	synthetic; J. Hanchar (Memorial U Newfoundland)	240	120
Th	PETJ	4	Mα	ThSiO <sub>4</sub>	synthetic; J. Hanchar (Memorial U Newfoundland)	120	60
Pb	PETH	5	Mβ	Cerussite	Tsumeb, Namibia (specimen from GZG Museum)	360	180
P	PETJ	1	Kα	ScPO <sub>4</sub>	synthetic; USNM 168495	15	5
Y	PETJ	1	Lα	YAG	synthetic; FEE (Idar-Oberstein)	120	60
Ca	PETJ	1	Kα	Wollastonite	Willsboro (NY, USA)	120	60
Si	TAP	2	Kα	Wollastonite	Willsboro (NY, USA)	120	60
Sr	TAP	2	Lα	Coelestine	synthetic; P&H Developments	120	60
La	LIF	3	Lα	La glass	synthetic; P&H Developments	30	15
Ce	LIF	3	Lα	Ce glass	synthetic; P&H Developments	30	15
Nd	LIF	3	Lα	Nd glass	synthetic; P&H Developments	30	15
Pr	LIF	3	Lβ	Pr glass	synthetic; P&H Developments	60	30
Sm	LIF	3	Lα	Sm glass	synthetic; P&H Developments	30	15
Gd	LIF	3	Lβ	Gd glass	synthetic; P&H Developments	60	30
Eu	LIF	3	Lβ	Eu glass	synthetic; P&H Developments	60	30
Tb	LIF	3	Lα	Tb glass	synthetic; P&H Developments	30	15

**Results of in-situ chemical analyses and total (Th-U)Pb EPMA dating of detrital monazite from the Bosnian Flysch**

grain#	spot#	[analyses in wt%]																	spot age (Ma)	+/- (Ma)	no. total spots	no. spots rejected	grain age (Ma)	+/- (Ma)	
		P2O5	SiO2	La2O3	ThO2	PbO	Y2O3	SrO	Ce2O3	UO2	CaO	Nd2O3	Pr2O3	Sm2O3	Tb2O3	Eu2O3	Gd2O3	Total							
BO12-ST16	1	30.45	0.24	11.98	6.41	0.04	3.36	0.00	25.51	0.32	1.28	11.76	3.02	2.38	0.22	0.00	2.00	99.00	138.8	14.7					
BO12-ST16	2	29.60	0.43	13.70	7.03	0.05	1.00	0.00	27.62	0.31	1.28	11.94	3.18	2.01	0.09	0.00	1.30	99.54	159.0	13.7					
BO12-ST16	3	30.03	0.19	12.12	5.09	0.03	4.04	0.00	26.65	0.23	1.04	11.85	3.03	2.39	0.20	0.02	2.08	99.00	127.5	18.4					
BO12-ST16	4	29.62	0.43	14.44	6.62	0.05	0.87	0.00	28.54	0.31	1.21	11.92	3.15	1.98	0.06	0.00	1.22	100.42	163.1	14.5					
BO12-ST16	5	30.27	0.15	13.09	4.33	0.04	3.49	0.00	27.27	0.34	0.93	11.79	3.21	2.35	0.13	0.00	1.90	99.28	171.9	20.2					
BO12-ST16	6	29.85	0.42	14.09	6.54	0.05	1.22	0.00	28.12	0.26	1.18	12.15	3.27	2.06	0.13	0.00	1.36	100.69	160.9	15.0	6	2	155.6	9.2	
BO12-ST17	1	29.87	0.73	11.37	6.81	0.05	3.40	0.00	26.14	0.15	0.94	12.56	3.16	2.55	0.18	0.00	2.15	100.07	148.7	15.2					
BO12-ST17	2	29.86	0.42	10.71	7.71	0.05	2.31	0.00	25.99	0.26	1.47	12.80	3.19	2.97	0.18	0.00	2.40	100.33	149.1	13.0					
BO12-ST17	3	30.13	0.39	11.98	5.87	0.04	4.27	0.00	26.46	0.17	1.04	11.72	3.10	2.31	0.21	0.00	2.02	99.71	165.7	17.4					
BO12-ST17	4	29.79	0.40	12.10	6.29	0.04	3.19	0.00	26.55	0.20	1.14	12.20	3.21	2.47	0.18	0.00	2.07	99.83	147.2	16.1					
BO12-ST17	5	29.72	0.38	12.06	6.20	0.04	3.81	0.00	26.70	0.21	1.14	11.91	3.13	2.25	0.16	0.00	1.87	99.56	150.0	16.1					
BO12-ST17	6	30.25	0.40	11.64	6.24	0.04	4.39	0.00	26.14	0.16	1.11	11.74	3.09	2.32	0.19	0.00	1.99	99.70	133.5	16.2					
BO12-ST17	7	30.20	0.40	11.00	6.22	0.04	5.33	0.00	25.22	0.21	1.15	11.56	3.03	2.36	0.22	0.03	2.22	99.19	140.6	16.1	7	1	145.3	6.9	
BO12-ST18	1	30.49	0.12	12.59	4.63	0.06	2.85	0.00	27.64	0.89	1.15	11.97	3.04	2.40	0.21	0.00	1.86	99.90	178.3	14.6					
BO12-ST18	2	29.21	0.83	12.93	10.25	0.08	1.52	0.00	25.29	0.47	1.63	10.94	2.75	2.23	0.11	0.01	1.79	100.05	171.2	9.6					
BO12-ST18	3	30.27	0.13	12.72	4.63	0.04	3.32	0.00	26.85	0.42	1.04	12.08	3.13	2.45	0.25	0.00	2.14	99.46	141.4	17.9					
BO12-ST18	4	30.54	0.13	11.81	5.08	0.05	3.70	0.00	25.90	0.67	1.22	12.25	3.00	2.51	0.21	0.06	2.25	99.37	153.4	15.0					
BO12-ST18	5	29.36	0.60	13.26	7.78	0.06	1.66	0.00	26.59	0.56	1.37	11.61	2.98	2.19	0.14	0.04	1.79	99.99	155.1	11.6					
BO12-ST18	6	30.61	0.12	12.60	4.78	0.04	3.30	0.00	27.23	0.47	1.08	11.70	3.10	2.34	0.16	0.00	2.00	99.55	157.3	17.5	6	2	161.8	8.0	
BO12-ST19	1	29.17	0.73	15.88	5.28	0.03	1.10	0.00	30.39	0.11	0.67	11.00	2.99	1.63	0.10	0.00	1.02	100.08	123.9	19.2					
BO12-ST19	2	29.05	0.77	15.69	5.48	0.04	1.10	0.00	29.99	0.11	0.69	11.18	3.05	1.59	0.11	0.00	1.01	99.88	171.5	18.9					
BO12-ST19	3	27.72	1.59	15.69	8.45	0.06	0.81	0.00	29.29	0.14	0.73	10.33	2.91	1.45	0.05	0.00	0.87	100.09	164.9	12.6					
BO12-ST19	4	27.84	1.52	15.34	8.29	0.06	0.82	0.00	29.44	0.13	0.74	10.39	2.93	1.41	0.06	0.00	0.86	99.83	153.3	12.7					
BO12-ST19	5	28.05	1.51	15.27	9.00	0.06	0.90	0.00	28.91	0.16	0.79	10.32	2.84	1.46	0.07	0.00	0.92	100.26	138.4	11.6					
BO12-ST19	6	28.69	1.05	15.43	7.09	0.05	1.05	0.00	29.26	0.12	0.76	10.81	3.01	1.56	0.08	0.00	1.03	99.97	159.7	14.8					
BO12-ST19	7	29.51	0.69	16.09	4.63	0.04	1.19	0.00	30.76	0.11	0.61	11.62	3.20	1.68	0.07	0.00	1.05	101.25	185.6	22.5	7	2	154.8	8.6	
BO12-ST20	1	29.90	0.26	12.45	6.40	0.06	2.82	0.00	26.61	0.24	1.28	12.20	3.15	2.24	0.13	0.00	1.63	99.39	187.3	15.6					
BO12-ST20	2	30.23	0.27	12.70	6.86	0.05	2.41	0.00	27.45	0.20	1.38	11.70	3.12	2.04	0.16	0.00	1.62	100.17	172.0	14.8					
BO12-ST20	3	30.05	0.35	8.97	10.51	0.08	1.38	0.00	22.94	0.45	2.16	13.48	3.11	3.67	0.25	0.00	3.23	100.63	155.3	9.5					
BO12-ST20	4	28.16	1.37	10.88	10.91	0.08	0.29	0.00	26.05	0.19	1.27	13.94	3.31	2.68	0.08	0.00	1.66	100.84	155.6	9.8					
BO12-ST20	5	27.86	1.43	10.66	11.20	0.08	0.33	0.00	25.64	0.20	1.27	13.92	3.23	2.71	0.08	0.00	1.75	100.35	157.2	9.6					
BO12-ST20	6	29.38	0.84	10.07	11.13	0.08	0.88	0.00	23.87	0.31	1.75	13.83	3.25	3.30	0.14	0.00	2.46	101.27	154.0	9.4	6	1	157.1	5.9	
BO12-ST21	1	27.14	1.93	11.86	9.28	0.05	1.90	0.00	26.19	0.15	0.82	12.69	3.29	2.24	0.12	0.00	1.67	99.32	133.8	11.4					
BO12-ST21	2	27.84	1.64	11.63	8.37	0.06	2.27	0.00	26.55	0.15	0.95	12.72	3.26	2.45	0.10	0.00	1.78	99.79	166.7	12.7					
BO12-ST21	3	26.48	2.41	11.34	11.52	0.08	1.91	0.00	25.70	0.19	0.82	12.10	3.11	2.24	0.10	0.00	1.50	99.49	152.4	9.4					
BO12-ST21	4	24.36	3.67	10.33	16.90	0.10	1.74	0.00	23.20	0.24	0.84	11.72	2.88	2.13	0.08	0.00	1.51	99.69	135.5	6.5					
BO12-ST21	5	26.33	2.41	10.88	11.62	0.07	2.13	0.00	24.49	0.18	0.98	12.51	3.12	2.43	0.13	0.00	1.73	99.01	132.3	9.2					
BO12-ST21	6	27.32	2.02	11.17	10.07	0.08	2.27	0.00	25.46	0.16	1.01	12.73	3.11	2.33	0.14	0.00	1.71	99.58	184.1	10.8					
BO12-ST21	7	28.48	1.18	12.33	6.06	0.05	2.59	0.00	27.84	0.15	0.98	12.29	3.20	2.37	0.14	0.00	1.82	99.47	185.5	17.1					
BO12-ST21	8	28.17	1.25	12.09	6.32	0.04	2.52	0.00	27.58	0.14	0.88	12.54	3.20	2.30	0.16	0.00	1.85	99.04	156.5	16.4	8	2	149.7	9.1	

grain#	spot#	P2O5	SiO2	La2O3	ThO2	PbO	Y2O3	SrO	Ce2O3	UO2	CaO	Nd2O3	Pr2O3	Sm2O3	Tb2O3	Eu2O3	Gd2O3	Total	spot age (Ma)	+/- (Ma)	no. total spots	no. spots rejected	grain age (Ma)	+/- (Ma)
BO12-ST22	1	30.18	0.22	12.42	5.06	0.05	2.05	0.00	27.84	0.48	1.08	12.40	3.22	2.61	0.21	0.03	2.32	100.16	167.1	16.5				
BO12-ST22	2	30.52	0.15	12.70	4.59	0.05	3.35	0.00	27.60	0.55	1.06	12.05	3.16	2.47	0.27	0.00	2.16	100.67	179.3	17.3				
BO12-ST22	3	29.45	0.49	13.44	6.62	0.07	0.71	0.00	29.12	0.71	1.12	11.83	3.09	2.11	0.09	0.01	1.27	100.23	173.6	12.4				
BO12-ST22	4	29.98	0.21	12.78	5.06	0.05	2.43	0.00	27.15	0.43	1.05	12.10	3.17	2.54	0.24	0.00	2.29	99.48	167.0	16.9				
BO12-ST22	5	30.04	0.12	13.95	4.50	0.03	0.44	0.00	30.24	0.33	1.07	12.36	3.23	2.17	0.05	0.06	1.34	99.94	135.9	19.2				
BO12-ST22	6	30.38	0.15	13.08	4.57	0.04	2.56	0.00	28.09	0.49	1.03	11.88	3.23	2.36	0.26	0.07	1.94	100.13	155.1	17.7	6	1	169.3	8.3
BO12-ST23	1	29.83	0.23	14.19	6.28	0.05	0.26	0.00	29.11	0.17	1.25	12.51	3.14	2.06	0.04	0.00	1.12	100.22	174.9	16.2				
BO12-ST23	2	30.37	0.18	13.87	5.16	0.05	2.70	0.00	27.06	0.43	1.22	11.47	3.02	2.16	0.16	0.06	1.67	99.58	183.5	16.9				
BO12-ST23	3	30.07	0.20	14.61	4.12	0.03	0.88	0.00	29.30	0.22	0.82	12.69	3.44	2.30	0.09	0.00	1.58	100.36	147.9	22.6				
BO12-ST23	4	30.52	0.15	14.74	3.63	0.04	2.34	0.00	28.48	0.35	1.11	11.36	3.11	2.08	0.14	0.01	1.44	99.50	177.2	23.0				
BO12-ST23	5	30.26	0.17	14.87	3.43	0.03	0.67	0.00	30.63	0.17	0.70	12.71	3.31	2.15	0.10	0.00	1.35	100.56	203.5	27.6				
BO12-ST23	6	30.39	0.24	14.74	3.26	0.03	0.86	0.00	30.56	0.14	0.61	12.82	3.35	2.17	0.10	0.00	1.36	100.62	179.4	29.3				
BO12-ST23	7	30.57	0.16	13.39	4.38	0.03	2.17	0.00	28.60	0.24	0.93	12.39	3.22	2.24	0.15	0.00	1.75	100.22	135.2	20.8				
BO12-ST23	8	30.01	0.26	15.15	3.76	0.03	0.60	0.00	30.44	0.12	0.65	13.00	3.39	2.11	0.08	0.00	1.22	100.81	162.1	26.4	8	2	172.6	10.8
BO12-ST24	1	30.13	0.20	13.49	5.46	0.05	2.58	0.00	27.66	0.39	1.14	11.32	3.09	1.99	0.15	0.00	1.44	99.08	169.3	16.3				
BO12-ST24	2	30.15	0.23	12.59	6.05	0.04	1.83	0.00	28.01	0.34	1.23	12.08	3.24	2.44	0.13	0.00	1.78	100.14	118.0	15.1				
BO12-ST24	3	30.28	0.24	12.63	5.93	0.05	1.80	0.00	27.95	0.27	1.20	12.21	3.18	2.41	0.12	0.00	1.77	100.05	165.6	16.2				
BO12-ST24	4	29.81	0.24	12.55	6.10	0.05	1.91	0.00	27.39	0.34	1.25	12.25	3.20	2.45	0.19	0.00	1.72	99.44	164.4	15.4				
BO12-ST24	5	30.14	0.24	13.01	6.04	0.04	1.74	0.00	27.63	0.25	1.22	12.16	3.31	2.38	0.16	0.00	1.70	100.04	143.5	15.9				
BO12-ST24	6	29.89	0.26	12.96	6.04	0.04	1.98	0.00	27.53	0.28	1.20	12.04	3.25	2.35	0.15	0.00	1.75	99.71	147.5	15.7				
BO12-ST24	7	30.18	0.23	13.21	5.77	0.05	1.68	0.00	28.03	0.25	1.16	12.04	3.17	2.21	0.09	0.00	1.64	99.71	180.6	16.9				
BO12-ST24	8	30.18	0.28	12.24	5.88	0.04	3.05	0.00	27.19	0.26	1.12	11.97	3.21	2.42	0.19	0.00	1.99	100.03	146.2	16.5				
BO12-ST24	9	30.42	0.24	12.93	5.82	0.04	2.01	0.00	27.98	0.29	1.18	12.16	3.12	2.34	0.15	0.00	1.61	100.28	156.5	16.2	9	2	156.2	7.2
BO12-ST25	1	30.00	0.20	13.49	4.39	0.04	0.86	0.00	28.51	0.34	0.92	13.69	3.47	2.61	0.08	0.02	1.55	100.14	170.0	19.8				
BO12-ST25	2	30.43	0.18	13.30	4.01	0.04	0.95	0.00	28.67	0.36	0.94	13.68	3.47	2.66	0.02	0.04	1.58	100.34	167.8	21.1				
BO12-ST25	3	30.02	0.19	13.56	4.08	0.03	0.91	0.00	28.88	0.33	0.92	13.77	3.36	2.64	0.09	0.06	1.54	100.40	154.5	21.1				
BO12-ST25	4	30.70	0.10	13.31	3.59	0.03	3.35	0.00	27.17	0.15	0.79	12.83	3.17	2.36	0.20	0.05	2.08	99.86	167.9	27.0				
BO12-ST25	5	30.03	0.21	13.80	4.09	0.03	0.71	0.00	29.04	0.28	0.79	13.71	3.47	2.54	0.07	0.00	1.36	100.13	134.0	21.6				
BO12-ST25	6	30.49	0.08	13.01	3.09	0.02	3.40	0.00	27.65	0.15	0.67	12.63	3.12	2.47	0.24	0.06	2.37	99.47	147.2	30.6				
BO12-ST25	7	30.30	0.09	12.55	3.35	0.03	3.65	0.00	27.08	0.14	0.74	12.74	3.21	2.45	0.22	0.08	2.31	98.91	179.1	29.2				
BO12-ST25	8	30.65	0.08	12.58	3.21	0.02	3.64	0.00	27.31	0.15	0.70	12.87	3.04	2.50	0.27	0.06	2.33	99.43	140.6	29.0				
BO12-ST25	9	30.78	0.09	12.99	3.00	0.03	3.36	0.00	27.96	0.13	0.66	12.60	3.12	2.37	0.22	0.04	2.24	99.59	206.7	32.1				
BO12-ST25	10	30.07	0.21	13.33	4.41	0.03	0.84	0.00	28.64	0.33	0.93	13.76	3.43	2.61	0.10	0.00	1.53	100.24	134.9	19.7	10	1	154.4	10.0
BO12-ST26	1	30.10	0.16	13.43	4.79	0.04	3.94	0.00	26.77	0.25	0.99	11.41	3.04	2.17	0.17	0.00	1.82	99.08	168.6	20.0				
BO12-ST26	2	29.68	0.30	16.74	4.85	0.05	0.45	0.00	29.99	0.57	1.03	10.70	3.06	1.51	0.02	0.00	0.74	99.67	174.1	16.4				
BO12-ST26	3	29.90	0.28	16.59	4.58	0.05	0.43	0.00	30.19	0.57	1.00	10.86	3.09	1.64	0.03	0.05	0.80	100.04	172.0	16.8				
BO12-ST26	4	30.48	0.39	12.86	4.98	0.04	3.72	0.00	27.08	0.23	1.01	11.61	2.97	2.17	0.19	0.00	1.97	99.71	168.2	19.4				
BO12-ST26	5	29.49	0.28	16.46	4.75	0.04	0.50	0.00	30.36	0.57	1.03	10.72	3.12	1.62	0.01	0.00	0.79	99.73	155.5	16.4				
BO12-ST26	6	30.00	0.26	15.77	4.57	0.04	1.16	0.00	29.97	0.47	0.99	11.09	3.04	1.86	0.08	0.00	1.08	100.36	139.0	17.7				
BO12-ST26	7	30.35	0.29	13.37	4.83	0.05	2.63	0.00	27.79	0.36	1.01	11.62	3.08	2.05	0.14	0.00	1.68	99.24	179.5	18.4				
BO12-ST26	8	29.52	0.54	14.34	4.74	0.04	1.65	0.00	28.75	0.35	0.93	11.21	2.99	1.99	0.07	0.00	1.24	98.37	148.5	18.5	8	1	166.6	8.0
BO12-ST27	1	30.15	0.17	12.66	5.09	0.04	2.93	0.00	27.21	0.18	1.03	12.41	3.15	2.40	0.17	0.00	1.98	99.58	177.4	19.6				
BO12-ST27	2	30.23	0.19	13.89	4.70	0.05	2.57	0.00	28.09	0.25	0.95	11.72	3.05	2.13	0.16	0.00	1.62	99.60	200.0	20.3				
BO12-ST27	3	30.08	0.17	12.41	5.18	0.04	3.18	0.00	26.97	0.20	1.06	12.28	3.08	2.33	0.19	0.01	2.10	99.28	178.0	19.1				
BO12-ST27	4	29.76	0.36	15.20	5.31	0.04	0.24	0.00	30.18	0.41	0.93	11.90	3.26	1.94	0.07	0.02	0.91	100.54	135.3	16.2				
BO12-ST27	5	30.47	0.15	13.56	4.96	0.04	3.16	0.00	27.69	0.27	1.02	11.58	2.92	1.98	0.20	0.05	1.56	99.61	174.7	18.9				

grain#	spot#	P2O5	SiO2	La2O3	ThO2	PbO	Y2O3	SrO	Ce2O3	UO2	CaO	Nd2O3	Pr2O3	Sm2O3	Tb2O3	Eu2O3	Gd2O3	Total	spot age (Ma)	+/- (Ma)	no. total spots	no. spots rejected	grain age (Ma)	+/- (Ma)
BO12-ST27	6	29.83	0.36	15.62	5.16	0.04	0.14	0.00	30.16	0.42	0.91	11.81	3.25	1.94	0.01	0.02	0.87	100.55	132.9	16.5				
BO12-ST27	7	30.16	0.16	12.85	4.86	0.03	3.14	0.00	27.20	0.21	1.01	11.99	3.17	2.28	0.18	0.07	1.88	99.18	140.5	20.0				
BO12-ST27	8	30.20	0.19	12.74	5.12	0.04	2.56	0.00	27.86	0.18	1.04	12.24	3.15	2.42	0.15	0.00	2.03	99.92	163.1	19.3				
BO12-ST27	9	30.33	0.16	13.44	4.79	0.04	2.59	0.00	28.17	0.19	0.98	11.88	2.99	2.18	0.19	0.00	1.85	99.76	159.2	20.4				
BO12-ST27	10	30.33	0.16	12.72	4.76	0.04	3.21	0.00	27.32	0.22	0.99	12.04	3.02	2.27	0.16	0.00	1.83	99.05	157.9	20.1	10	2	159.7	8.9
BO12-ST28	1	30.04	0.17	11.77	5.82	0.05	4.00	0.00	25.83	0.41	1.26	11.66	3.04	2.47	0.25	0.06	2.20	99.02	160.7	15.7				
BO12-ST28	2	29.68	0.36	12.27	6.99	0.04	0.73	0.00	27.34	0.17	1.29	13.27	3.33	2.78	0.13	0.00	2.10	100.47	122.8	14.6				
BO12-ST28	3	29.47	0.36	12.15	7.19	0.05	0.92	0.00	26.88	0.18	1.34	12.97	3.12	2.81	0.12	0.00	2.24	99.81	148.4	14.3				
BO12-ST28	4	29.99	0.19	12.01	6.11	0.05	3.13	0.00	26.66	0.33	1.27	11.76	3.09	2.34	0.20	0.00	1.91	99.04	159.7	15.4				
BO12-ST28	5	30.18	0.22	12.25	6.08	0.05	2.31	0.00	26.96	0.22	1.24	12.31	3.17	2.53	0.21	0.00	2.21	99.93	172.6	16.4				
BO12-ST28	6	29.93	0.28	12.49	5.72	0.05	1.52	0.00	26.83	0.21	1.13	12.90	3.28	2.79	0.19	0.00	2.26	99.58	168.1	17.4				
BO12-ST28	7	30.09	0.50	11.70	6.90	0.04	2.82	0.00	26.39	0.20	1.11	12.40	3.21	2.63	0.21	0.00	2.34	100.54	137.3	14.7				
BO12-ST28	8	29.99	0.33	12.47	4.60	0.03	3.40	0.00	26.90	0.27	0.93	11.80	3.06	2.46	0.18	0.00	2.19	98.61	137.1	19.8				
BO12-ST28	9	29.70	0.31	12.48	6.23	0.05	0.89	0.00	27.62	0.16	1.17	13.08	3.28	2.80	0.13	0.00	2.21	100.12	175.2	16.5	9	2	156.6	8.7
BO12-ST29	1	27.57	1.45	6.87	9.52	0.11	3.18	0.00	24.50	0.18	0.81	13.57	3.66	4.03	0.24	0.00	2.76	98.45	248.9	11.8				
BO12-ST29	2	27.51	1.48	6.74	9.84	0.11	3.59	0.00	23.89	0.18	0.88	13.18	3.55	4.07	0.29	0.00	2.98	98.29	249.2	11.5	2	0	249.0	8.2
BO12-ST30	1	28.90	0.45	12.03	5.10	0.04	3.34	0.00	26.95	0.21	0.78	11.81	3.12	2.60	0.23	0.00	2.19	97.77	159.0	19.3				
BO12-ST30	2	28.83	0.41	12.66	5.33	0.04	3.43	0.00	27.44	0.23	0.86	10.87	2.95	2.26	0.18	0.00	1.94	97.43	155.7	18.3				
BO12-ST30	3	28.42	0.59	12.01	5.13	0.04	3.53	0.00	26.98	0.24	0.87	11.03	2.88	2.33	0.00	0.00	1.96	96.01	154.4	18.6				
BO12-ST30	4	30.27	0.34	10.48	3.72	0.03	3.73	0.00	27.19	0.22	0.71	13.37	3.51	3.21	0.28	0.00	2.37	99.40	150.1	24.5				
BO12-ST30	5	30.33	0.34	10.40	3.82	0.02	3.77	0.00	26.97	0.23	0.72	13.36	3.42	3.21	0.27	0.00	2.41	99.28	129.2	23.6				
BO12-ST30	6	30.09	0.33	10.58	3.62	0.03	3.73	0.00	27.28	0.21	0.70	13.48	3.44	3.18	0.23	0.00	2.41	99.34	192.6	26.0				
BO12-ST30	7	29.47	0.37	10.34	3.99	0.03	3.57	0.00	27.34	0.22	0.68	13.12	3.45	3.06	0.27	0.02	2.39	98.32	131.8	22.6	7	2	151.5	10.5
BO12-SR11	1	28.23	1.31	13.05	7.60	0.05	1.46	0.00	28.96	0.13	0.62	12.11	3.27	2.07	0.07	0.00	1.35	100.28	153.9	13.8				
BO12-SR11	2	28.22	1.25	12.93	7.44	0.05	1.45	0.00	28.88	0.15	0.63	12.07	3.27	2.08	0.10	0.00	1.35	99.87	156.2	14.1				
BO12-SR11	3	29.17	0.87	10.87	6.79	0.06	2.50	0.00	27.29	0.31	0.85	12.79	3.37	2.75	0.14	0.00	1.93	99.67	170.3	14.5				
BO12-SR11	4	28.89	0.95	10.79	6.96	0.05	2.71	0.00	27.09	0.29	0.82	12.66	3.30	2.71	0.16	0.00	1.99	99.38	162.5	14.1				
BO12-SR11	5	29.55	0.48	16.16	3.04	0.03	1.16	0.00	31.61	0.18	0.64	11.17	3.18	1.64	0.10	0.00	1.03	99.98	173.0	29.9				
BO12-SR11	6	29.63	0.66	15.04	5.11	0.04	1.40	0.00	30.08	0.21	0.80	11.30	3.10	1.75	0.11	0.00	1.21	100.43	167.6	19.0				
BO12-SR11	7	28.91	0.96	15.71	5.94	0.05	0.78	0.00	30.42	0.09	0.52	11.33	2.99	1.57	0.05	0.00	0.92	100.23	185.9	18.0				
BO12-SR11	8	29.04	0.87	16.89	5.41	0.03	0.67	0.00	30.54	0.07	0.46	11.09	3.19	1.40	0.04	0.00	0.75	100.46	136.8	19.2				
BO12-SR11	9	28.58	1.38	13.29	8.33	0.06	1.34	0.00	28.41	0.14	0.68	11.59	3.23	1.89	0.11	0.00	1.25	100.29	149.0	12.7				
BO12-SR11	10	28.66	1.36	13.42	8.12	0.06	1.36	0.00	28.52	0.15	0.67	11.72	3.21	2.00	0.08	0.00	1.24	100.59	170.9	13.1	10	2	161.2	6.9
BO12-SR28	1	28.53	1.12	13.57	4.56	0.04	2.46	0.00	29.54	0.08	0.19	12.16	3.25	2.01	0.13	0.00	1.69	99.33	185.3	23.2				
BO12-SR28	2	28.35	1.27	13.56	5.05	0.04	2.39	0.00	28.90	0.09	0.18	12.19	3.24	2.08	0.15	0.00	1.63	99.13	179.2	20.8				
BO12-SR28	3	27.02	1.88	12.69	7.37	0.05	2.48	0.00	27.17	0.12	0.21	12.03	3.14	2.12	0.07	0.00	1.65	98.01	150.0	14.4				
BO12-SR28	4	28.85	1.21	13.92	5.19	0.04	2.34	0.00	29.07	0.11	0.20	11.85	3.25	2.05	0.15	0.00	1.63	99.85	166.1	20.0	4	1	176.0	13.6
BO72-A-1	1	28.36	1.08	9.83	8.23	0.09	2.62	0.00	26.86	0.10	0.89	12.35	3.42	2.83	0.17	0.01	2.18	99.01	250.3	13.8				
BO72-A-1	2	28.19	1.19	10.31	8.90	0.11	2.43	0.00	27.22	0.11	0.94	12.00	3.38	2.74	0.18	0.00	2.06	99.75	270.1	12.9				
BO72-A-1	3	29.11	0.82	11.66	6.27	0.07	2.06	0.00	29.06	0.08	0.83	12.16	3.49	2.56	0.18	0.00	1.76	100.10	238.3	17.8				
BO72-A-1	4	29.53	0.76	11.71	5.86	0.06	2.03	0.00	29.30	0.07	0.80	12.27	3.53	2.56	0.14	0.00	1.72	100.34	250.2	19.0				
BO72-A-1	5	28.78	0.89	11.87	6.62	0.08	2.04	0.00	28.71	0.10	0.88	12.04	3.51	2.50	0.14	0.00	1.77	99.92	269.7	16.9				
BO72-A-1	6	27.83	1.22	9.45	9.03	0.09	2.57	0.00	26.46	0.10	0.94	12.43	3.39	2.80	0.19	0.01	2.21	98.73	237.1	12.6				
BO72-A-1	7	29.01	0.81	11.36	6.11	0.06	2.13	0.00	29.29	0.09	0.82	12.10	3.48	2.55	0.10	0.00	1.80	99.71	227.9	17.9				
BO72-A-1	8	27.46	1.40	9.15	9.81	0.11	2.72	0.00	26.16	0.15	0.93	12.31	3.36	2.87	0.22	0.00	2.27	98.91	252.6	11.6				
BO72-A-1	9	28.67	1.02	9.37	7.92	0.09	3.15	0.00	26.48	0.11	0.92	12.62	3.31	3.12	0.21	0.00	2.42	99.40	252.2	14.2				

grain#	spot#	P2O5	SiO2	La2O3	ThO2	PbO	Y2O3	SrO	Ce2O3	UO2	CaO	Nd2O3	Pr2O3	Sm2O3	Th2O3	Eu2O3	Gd2O3	Total	spot age (Ma)	+/- (Ma)	no. total spots	no. spots rejected	grain age (Ma)	+/- (Ma)
BO72-A-1	10	28.89	1.01	9.41	7.89	0.08	3.10	0.00	26.54	0.13	0.91	12.67	3.34	2.98	2.04	0.00	2.20	99.35	227.7	14.0	10	2	247.6	7.1
BO72-A-2	1	29.80	0.23	14.92	3.64	0.04	0.54	0.00	30.66	0.42	0.72	12.51	3.29	2.08	0.07	0.02	1.14	100.04	178.1	22.0				
BO72-A-2	2	30.50	0.11	13.87	4.09	0.05	1.79	0.00	29.43	0.39	0.95	12.13	3.23	2.08	0.15	0.00	1.51	100.28	201.7	21.0				
BO72-A-2	3	29.67	0.22	13.96	4.06	0.05	1.14	0.00	29.83	0.68	0.88	12.36	3.20	2.26	0.07	0.04	1.34	99.75	176.1	17.3				
BO72-A-2	4	30.41	0.11	13.71	4.27	0.04	2.51	0.00	28.35	0.41	0.95	12.05	3.05	2.18	0.18	0.00	1.63	99.86	183.8	19.8				
BO72-A-2	5	30.47	0.24	14.97	4.21	0.05	0.75	0.00	29.65	0.61	0.91	12.20	3.19	2.05	0.08	0.02	1.23	100.62	183.0	17.7	5	1	180.2	9.8
BO72-A-3	1	29.74	0.29	13.14	4.89	0.03	1.53	0.00	28.83	0.08	0.84	12.85	3.35	2.45	0.16	0.00	1.92	100.10	147.7	21.6				
BO72-A-3	2	29.84	0.13	13.16	3.25	0.03	0.58	0.00	30.43	0.15	0.68	14.19	3.60	2.64	0.10	0.00	1.39	100.16	164.3	30.0				
BO72-A-3	3	30.42	0.13	12.30	4.39	0.04	3.49	0.00	27.79	0.13	0.91	12.43	3.19	2.28	0.24	0.01	1.94	99.69	190.0	23.3				
BO72-A-3	4	30.04	0.15	12.44	4.45	0.04	3.35	0.00	27.71	0.13	0.89	12.44	3.17	2.16	0.22	0.05	1.94	99.18	186.6	22.9				
BO72-A-3	5	30.36	0.14	12.68	4.28	0.03	3.32	0.00	27.81	0.13	0.88	12.45	3.14	2.29	0.23	0.02	1.94	99.71	173.9	23.4	5	1	180.3	13.9
BO72-A-4	1	30.46	0.12	11.90	4.62	0.04	4.04	0.00	25.73	0.37	1.02	12.70	3.21	2.70	0.24	0.07	2.41	99.64	162.1	19.0				
BO72-A-4	2	30.44	0.13	12.62	4.52	0.03	3.39	0.00	26.90	0.31	0.98	12.43	3.15	2.44	0.20	0.00	2.06	99.61	141.1	19.8				
BO72-A-4	3	29.80	0.23	13.78	4.38	0.06	1.27	0.00	28.88	1.04	1.07	12.27	3.29	2.33	0.15	0.00	1.61	100.15	175.2	14.1				
BO72-A-4	4	29.63	0.20	14.41	3.77	0.05	0.79	0.00	30.19	0.84	0.88	12.42	3.31	2.25	0.11	0.00	1.40	100.25	187.6	16.8				
BO72-A-4	5	30.24	0.13	11.62	4.72	0.04	3.99	0.00	25.59	0.33	1.04	12.54	3.07	2.65	0.26	0.01	2.35	98.58	182.0	19.3				
BO72-A-4	6	30.08	0.21	13.96	4.50	0.05	0.84	0.00	28.87	0.85	1.07	12.61	3.36	2.30	0.11	0.00	1.48	100.29	178.6	15.1	6	1	177.4	8.7
BO72-A-5	1	29.80	0.43	10.78	5.18	0.04	4.08	0.00	25.26	0.48	0.94	12.21	3.12	3.03	0.32	0.05	2.83	98.57	130.5	16.2				
BO72-A-5	2	30.12	0.46	10.80	5.34	0.04	4.20	0.00	25.15	0.50	0.98	12.29	3.23	3.06	0.32	0.14	2.86	99.49	144.4	15.7				
BO72-A-5	3	29.35	0.51	10.90	5.92	0.06	3.85	0.00	25.43	0.56	1.03	11.98	3.16	2.89	0.30	0.02	2.83	98.77	177.9	14.5				
BO72-A-5	4	29.57	0.61	10.48	7.16	0.06	4.14	0.00	24.10	0.63	1.28	12.00	2.97	3.05	0.27	0.06	2.89	99.26	157.6	12.2				
BO72-A-5	5	29.33	0.61	10.34	7.22	0.06	4.09	0.00	23.82	0.62	1.27	11.77	3.06	2.99	0.27	0.10	2.88	98.43	160.2	12.1	5	2	155.6	9.2
BO72-A-6	1	30.04	0.14	12.75	4.87	0.04	3.23	0.00	27.18	0.29	1.04	12.18	3.17	2.25	0.24	0.00	1.97	99.38	177.8	19.3				
BO72-A-6	2	29.61	0.42	15.32	4.97	0.04	0.95	0.00	30.37	0.16	0.79	12.14	3.20	2.73	0.05	0.00	1.05	100.80	194.1	20.5				
BO72-A-6	3	30.18	0.14	13.04	5.14	0.04	3.67	0.00	26.80	0.32	1.10	11.70	2.90	2.21	0.24	0.00	1.94	99.43	155.1	17.9				
BO72-A-6	4	29.65	0.21	13.64	5.81	0.05	1.32	0.00	28.75	0.17	1.16	12.43	3.15	2.08	0.09	0.00	1.50	100.00	178.7	17.6				
BO72-A-6	5	29.64	0.18	12.89	5.33	0.05	1.71	0.00	28.15	0.32	1.13	12.98	3.24	2.31	0.14	0.00	1.63	99.70	176.6	17.5				
BO72-A-6	6	30.16	0.15	12.32	4.73	0.04	3.86	0.00	26.35	0.34	1.03	12.07	3.08	2.46	0.24	0.03	2.19	99.05	149.6	18.8				
BO72-A-6	7	30.01	0.19	13.10	5.80	0.05	1.49	0.00	28.34	0.24	1.21	12.69	3.20	2.20	0.13	0.00	1.54	100.19	176.5	17.0				
BO72-A-6	8	30.30	0.13	12.94	4.79	0.03	3.22	0.00	27.56	0.29	1.04	12.13	3.09	2.22	0.17	0.00	2.06	99.98	140.7	18.8	8	2	169.4	9.1
BO72-A-7	1	30.39	0.07	12.22	4.84	0.05	3.48	0.00	26.33	0.82	1.22	12.00	3.03	2.50	0.19	0.01	2.27	99.42	161.2	14.6				
BO72-A-7	2	30.41	0.07	12.10	4.76	0.05	3.75	0.00	26.08	0.92	1.25	11.88	3.04	2.55	0.26	0.03	2.23	99.38	138.9	13.9				
BO72-A-7	3	30.01	0.08	12.33	4.86	0.05	3.39	0.00	26.53	0.84	1.21	11.98	3.09	2.40	0.23	0.05	2.20	99.25	156.1	14.2				
BO72-A-7	4	30.10	0.09	12.72	4.75	0.04	1.81	0.00	27.83	0.60	1.13	12.49	3.18	2.55	0.23	0.00	2.17	99.71	155.6	16.2				
BO72-A-7	5	30.34	0.06	13.11	3.62	0.04	2.72	0.00	27.91	0.71	0.95	12.18	3.13	2.49	0.24	0.03	2.22	99.77	160.8	18.1	5	1	158.3	8.1
BO72-A-8	1	30.07	0.12	13.16	5.41	0.05	3.23	0.00	27.52	0.62	1.28	10.86	3.07	2.15	0.14	0.00	1.72	99.40	161.0	14.8				
BO72-A-8	2	29.71	0.11	13.30	5.17	0.05	3.27	0.00	27.40	0.74	1.21	10.60	2.95	2.13	0.19	0.03	1.70	98.55	163.1	14.5				
BO72-A-8	3	29.90	0.14	11.54	6.79	0.05	3.81	0.00	25.70	0.49	1.58	10.98	2.98	2.31	0.23	0.06	2.00	98.56	151.4	13.2				
BO72-A-8	4	30.02	0.14	12.72	6.58	0.05	2.39	0.00	27.47	0.39	1.58	11.30	3.07	2.05	0.13	0.00	1.55	99.44	153.5	14.1				
BO72-A-8	5	30.03	0.14	12.55	6.92	0.06	3.33	0.00	26.25	0.53	1.60	10.68	2.94	2.10	0.20	0.00	1.75	99.07	158.4	12.9				
BO72-A-8	6	29.54	0.39	11.73	6.07	0.07	2.81	0.00	27.12	1.31	1.37	10.97	3.05	2.31	0.18	0.00	1.67	98.59	152.7	10.5	6	0	156.1	5.8
BO72-A-9	1	29.58	0.34	12.18	4.61	0.05	2.08	0.00	28.18	0.46	0.88	13.14	3.48	2.78	0.14	0.00	1.76	99.66	178.6	18.2				
BO72-A-9	2	28.15	1.18	13.88	6.49	0.05	1.28	0.00	28.79	0.15	0.77	12.14	3.30	1.92	0.03	0.00	1.24	99.51	166.0	16.2				
BO72-A-9	3	28.43	1.10	15.15	5.31	0.04	0.89	0.00	29.71	0.08	0.56	12.04	3.20	1.82	0.03	0.00	1.03	99.41	164.7	20.1				
BO72-A-9	4	28.72	0.59	15.65	3.47	0.03	0.90	0.00	30.95	0.07	0.61	11.83	3.20	1.69	0.06	0.00	0.98	98.75	207.2	30.0				
BO72-A-9	5	29.32	0.35	17.40	1.68	0.02	0.68	0.00	33.11	0.04	0.60	11.04	3.21	1.47	0.04	0.00	0.81	99.77	199.2	60.5				

grain#	spot#	P2O5	SiO2	La2O3	ThO2	PbO	Y2O3	SrO	Ce2O3	UO2	CaO	Nd2O3	Pr2O3	Sm2O3	Tb2O3	Eu2O3	Gd2O3	Total	spot age (Ma)	+/- (Ma)	no. total spots	no. spots rejected	grain age (Ma)	+/- (Ma)
BO72-A-9	6	28.19	1.06	14.33	5.76	0.04	1.17	0.00	30.05	0.14	0.61	11.72	3.29	1.92	0.08	0.00	1.13	99.49	164.6	17.8	6	0	172.2	14.9
BO72-A-10	1	27.68	1.61	14.38	7.02	0.05	1.29	0.00	28.93	0.12	0.58	11.67	3.14	1.87	0.04	0.00	1.20	99.58	151.5	15.1				
BO72-A-10	2	27.67	1.64	14.40	7.07	0.05	1.29	0.00	28.82	0.12	0.58	11.69	3.19	1.86	0.08	0.00	1.26	99.71	163.7	15.2				
BO72-A-10	3	28.11	1.16	13.59	5.73	0.04	1.93	0.00	28.23	0.12	0.66	12.06	3.11	2.02	0.14	0.00	1.45	98.34	152.3	18.2				
BO72-A-10	4	27.69	1.67	14.13	7.35	0.06	1.19	0.00	29.20	0.12	0.57	11.50	2.98	1.90	0.10	0.00	1.27	99.71	171.8	14.5				
BO72-A-10	5	28.53	1.51	14.51	6.76	0.05	1.21	0.00	29.54	0.10	0.55	11.64	3.07	1.79	0.11	0.00	1.20	100.57	167.0	15.8	5	0	161.9	8.1
BO72-A-11	1	30.56	0.08	12.07	4.41	0.04	4.01	0.00	26.54	0.53	1.03	11.86	3.09	2.35	0.25	0.01	2.05	98.87	166.9	17.9				
BO72-A-11	2	30.65	0.08	12.59	4.59	0.04	3.85	0.00	26.57	0.43	1.06	11.87	3.02	2.38	0.21	0.00	2.08	99.42	154.3	18.2				
BO72-A-11	3	30.24	0.18	13.56	4.16	0.04	2.27	0.00	27.71	0.72	0.95	11.92	3.15	2.31	0.18	0.01	1.74	99.14	138.7	16.5				
BO72-A-11	4	30.24	0.14	13.72	3.58	0.05	1.04	0.00	29.18	0.97	0.92	12.22	3.29	2.29	0.12	0.04	1.44	99.22	166.4	16.0				
BO72-A-11	5	30.25	0.09	13.06	4.48	0.05	2.64	0.00	27.46	0.41	1.02	11.80	3.09	2.21	0.17	0.00	1.75	98.48	184.6	18.8	5	2	163.0	10.9
BO72-A-12	1	28.95	0.94	9.32	8.17	0.07	2.76	0.00	25.64	0.42	1.08	12.80	3.42	3.27	0.22	0.00	2.24	99.30	173.0	12.0				
BO72-A-12	2	28.89	0.83	9.19	7.84	0.06	3.03	0.00	25.22	0.46	1.12	12.91	3.26	3.43	0.24	0.00	2.37	98.85	157.6	12.1				
BO72-A-12	3	29.36	0.90	9.66	7.67	0.06	3.08	0.00	25.53	0.35	1.01	12.77	3.48	3.12	0.24	0.04	2.28	99.56	167.9	12.8				
BO72-A-12	4	29.36	0.95	10.07	7.33	0.06	2.81	0.00	26.34	0.30	0.88	12.80	3.39	3.06	0.22	0.00	2.20	99.76	173.8	13.6				
BO72-A-12	5	28.84	0.84	9.37	7.56	0.05	2.91	0.00	25.64	0.44	1.07	13.05	3.36	3.42	0.25	0.00	2.29	99.09	142.8	12.3	5	1	167.8	7.3
BO72-A-13	1	29.74	0.16	13.87	4.18	0.03	0.50	0.00	30.46	0.12	0.83	13.57	3.46	2.14	0.09	0.00	1.30	100.43	151.5	24.2				
BO72-A-13	2	30.37	0.18	13.64	4.32	0.04	0.56	0.00	30.05	0.10	0.87	13.45	3.53	2.23	0.09	0.00	1.36	100.79	186.5	24.0				
BO72-A-13	3	29.75	0.37	13.53	4.88	0.04	1.54	0.00	29.57	0.10	0.80	12.82	3.24	1.81	0.13	0.00	1.36	99.93	167.3	21.4				
BO72-A-13	4	30.08	0.37	13.41	4.94	0.03	1.56	0.00	29.49	0.10	0.81	12.87	3.31	1.94	0.09	0.00	1.39	100.39	157.5	21.1				
BO72-A-13	5	29.90	0.37	13.70	4.84	0.03	1.45	0.00	29.44	0.11	0.81	12.55	3.35	1.95	0.11	0.00	1.30	99.88	150.9	21.1				
BO72-A-13	6	29.51	0.42	13.78	4.88	0.04	1.32	0.00	29.41	0.07	0.75	12.61	3.21	1.82	0.08	0.00	1.26	99.17	183.7	21.5	6	0	165.9	11.1
BO72-A-14	1	30.85	0.21	11.84	5.83	0.05	4.10	0.00	26.15	0.24	1.18	11.88	3.05	2.32	0.20	0.03	2.11	100.03	162.3	16.9				
BO72-A-14	2	30.75	0.21	11.96	5.59	0.04	4.21	0.00	26.21	0.23	1.12	12.12	3.00	2.26	0.18	0.03	2.20	100.09	143.8	17.6				
BO72-A-14	3	30.39	0.19	12.06	5.74	0.05	3.95	0.00	26.33	0.26	1.17	11.67	3.00	2.18	0.18	0.01	2.01	99.20	196.3	17.2				
BO72-A-14	4	29.97	0.21	12.74	5.69	0.06	2.23	0.00	27.52	0.56	1.27	11.75	3.07	2.22	0.12	0.00	1.69	99.09	184.7	14.9				
BO72-A-14	5	30.50	0.23	12.17	5.72	0.05	3.98	0.00	26.60	0.24	1.15	11.57	3.00	2.23	0.18	0.00	1.98	99.60	171.9	17.4				
BO72-A-14	6	30.25	0.21	13.28	5.67	0.04	1.92	0.00	27.48	0.50	1.24	12.37	3.26	2.32	0.13	0.00	1.62	100.29	142.6	15.1	6	2	167.4	12.0
BO72-A-15	1	28.75	1.09	11.61	7.70	0.05	2.58	0.00	26.84	0.15	0.81	12.13	3.17	2.49	0.18	0.00	1.92	99.48	153.3	13.7				
BO72-A-15	2	28.61	1.03	14.73	6.85	0.05	1.26	0.00	29.18	0.12	0.63	11.56	3.11	1.77	0.07	0.00	1.13	100.09	174.1	15.6				
BO72-A-15	3	28.81	0.94	14.67	6.39	0.05	1.22	0.00	29.31	0.10	0.64	11.54	3.05	1.74	0.07	0.00	1.14	99.67	186.9	16.7				
BO72-A-15	4	28.93	1.10	13.77	6.90	0.05	1.46	0.00	28.84	0.12	0.58	12.07	3.17	1.81	0.06	0.00	1.26	100.11	156.7	15.4				
BO72-A-15	5	28.60	1.08	11.65	7.59	0.05	2.57	0.00	26.63	0.16	0.80	12.18	3.24	2.55	0.17	0.06	1.96	99.27	152.8	13.8	5	1	158.4	8.9
BO72-A-16	1	29.55	0.65	11.42	7.03	0.06	3.29	0.00	26.09	0.20	1.02	12.21	3.21	2.51	0.19	0.00	2.03	99.46	185.9	14.8				
BO72-A-16	2	29.33	0.75	13.17	6.68	0.04	2.11	0.00	28.00	0.15	0.84	12.09	3.21	2.06	0.13	0.00	1.58	100.15	145.7	15.5				
BO72-A-16	3	28.88	0.74	13.46	6.45	0.04	1.86	0.00	28.35	0.13	0.81	12.02	3.10	2.05	0.08	0.00	1.44	99.42	149.1	16.0				
BO72-A-16	4	29.02	0.71	11.84	7.24	0.05	2.99	0.00	26.74	0.19	1.03	11.69	3.06	2.31	0.15	0.00	1.82	98.82	150.5	14.1				
BO72-A-16	5	29.56	0.65	11.73	7.22	0.06	3.35	0.00	26.38	0.20	1.08	11.49	3.14	2.46	0.20	0.01	2.04	99.57	169.0	14.3	5	1	154.1	9.2
BO72-A-17	1	30.09	0.13	12.89	4.96	0.05	3.26	0.00	26.66	0.23	1.04	12.10	3.14	2.41	0.20	0.00	2.11	99.28	190.2	19.8				
BO72-A-17	2	30.35	0.13	12.50	5.12	0.04	3.58	0.00	26.07	0.25	1.11	12.10	3.11	2.38	0.23	0.02	2.22	99.21	171.6	19.0				
BO72-A-17	3	30.17	0.14	12.29	5.18	0.04	3.41	0.00	26.26	0.25	1.12	11.92	3.05	2.44	0.19	0.00	2.22	98.67	145.7	18.3				
BO72-A-17	4	30.17	0.13	12.86	5.07	0.04	3.33	0.00	26.76	0.23	1.11	11.84	2.96	2.30	0.18	0.00	2.18	98.16	167.5	19.0				
BO72-A-17	5	29.87	0.12	12.94	4.88	0.04	2.96	0.00	27.50	0.32	1.07	11.53	3.02	2.27	0.19	0.00	1.98	98.69	154.4	18.5	5	2	164.3	12.1
BO72-A-18	1	28.90	0.65	11.95	5.68	0.05	2.70	0.00	27.44	0.20	0.76	12.89	3.32	2.52	0.13	0.00	1.96	99.16	173.1	17.9				
BO72-A-18	2	29.32	0.64	12.08	5.66	0.04	2.71	0.00	27.76	0.20	0.77	12.76	3.31	2.51	0.14	0.00	2.02	99.91	154.2	17.6				
BO72-A-18	3	28.77	0.90	11.89	6.81	0.05	2.30	0.00	27.76	0.16	0.79	12.55	3.33	2.35	0.14	0.00	1.85	99.64	158.3	15.2				

grain#	spot#	P2O5	SiO2	La2O3	ThO2	PbO	Y2O3	SrO	Ce2O3	UO2	CaO	Nd2O3	Pr2O3	Sm2O3	Tb2O3	Eu2O3	Gd2O3	Total	spot age (Ma)	+/- (Ma)	no. total spots	no. spots rejected	grain age (Ma)	+/- (Ma)
BO72-A-18	4	28.48	0.91	12.15	6.87	0.05	2.23	0.00	27.83	0.15	0.78	12.51	3.29	2.46	0.18	0.00	1.80	99.70	162.4	15.3	5	0	163.2	8.2
BO72-A-18	5	28.83	0.75	11.63	6.10	0.05	2.66	0.00	27.63	0.22	0.79	12.94	3.30	2.53	0.18	0.00	1.95	99.56	169.3	16.6	5	0	163.2	8.2
BO72-A-19	1	29.82	0.14	12.33	5.82	0.05	2.21	0.00	26.58	0.57	1.31	12.11	3.16	2.64	0.21	0.00	2.30	99.25	160.1	14.5	5	0	163.2	8.2
BO72-A-19	2	30.33	0.11	12.76	5.73	0.04	2.27	0.00	27.01	0.43	1.30	12.31	3.19	2.55	0.20	0.00	2.25	100.47	141.7	15.5	5	0	163.2	8.2
BO72-A-19	3	29.11	0.68	13.93	6.91	0.05	0.62	0.00	28.97	0.39	1.06	12.12	3.17	2.00	0.06	0.00	1.19	100.28	157.2	13.7	5	0	163.2	8.2
BO72-A-19	4	28.27	1.25	13.10	10.64	0.07	0.46	0.00	27.13	0.42	1.35	11.74	3.09	1.83	0.07	0.00	1.02	100.45	145.2	9.4	5	0	163.2	8.2
BO72-A-19	5	28.58	1.03	13.57	9.50	0.07	0.37	0.00	27.42	0.55	1.35	11.61	3.06	1.79	0.08	0.00	0.97	99.95	152.8	10.0	5	0	163.2	8.2
BO72-A-19	6	30.22	0.14	11.96	5.87	0.04	2.29	0.00	26.44	0.36	1.32	12.57	3.12	2.64	0.18	0.00	2.28	99.46	130.4	15.5	5	0	163.2	8.2
BO72-A-19	7	30.04	0.11	12.97	5.29	0.04	3.29	0.00	26.41	0.38	1.17	11.41	3.00	2.27	0.20	0.00	2.10	98.68	159.8	16.9	8	1	151.2	5.9
BO72-A-19	8	29.97	0.13	11.87	5.69	0.05	2.29	0.00	26.61	0.49	1.29	12.57	3.13	2.79	0.21	0.00	2.46	99.55	147.7	15.2	8	1	151.2	5.9
BO72-A-20	1	29.71	0.16	13.09	4.62	0.05	2.96	0.00	27.36	0.63	1.05	11.70	3.14	2.24	0.17	0.12	1.80	98.81	177.2	16.6	7	2	158.2	9.3
BO72-A-20	2	29.40	0.36	13.94	5.26	0.04	2.29	0.00	27.81	0.43	0.98	11.74	3.17	2.13	0.15	0.13	1.67	99.51	156.7	16.6	7	2	158.2	9.3
BO72-A-20	3	30.29	0.14	13.14	5.17	0.04	1.23	0.00	27.90	0.43	1.17	12.86	3.41	2.73	0.16	0.00	2.02	100.70	155.3	16.9	7	2	158.2	9.3
BO72-A-20	4	29.60	0.10	13.28	4.82	0.04	3.16	0.00	27.25	0.43	1.09	11.59	3.10	2.07	0.15	0.02	1.52	98.22	144.7	17.5	7	2	158.2	9.3
BO72-A-20	5	29.97	0.11	12.69	4.88	0.03	1.72	0.00	27.52	0.51	1.14	12.67	3.25	2.71	0.23	0.00	2.25	99.70	117.7	16.5	7	2	158.2	9.3
BO72-A-20	6	29.96	0.10	12.94	4.77	0.04	3.43	0.00	27.06	0.48	1.09	11.65	3.04	2.25	0.19	0.00	1.84	98.85	155.6	17.4	7	2	158.2	9.3
BO72-A-20	7	29.71	0.26	13.64	4.60	0.05	2.38	0.00	27.93	0.48	0.95	11.96	3.11	2.31	0.19	0.06	1.78	99.41	190.7	17.9	7	2	158.2	9.3
BO72-A-21	1	27.87	0.85	17.25	4.84	0.05	0.39	0.00	32.05	0.05	0.52	10.63	3.09	1.24	0.02	0.00	0.60	99.44	245.5	22.8	6	0	260.0	8.5
BO72-A-21	2	28.17	0.70	17.23	3.79	0.05	0.39	0.00	32.36	0.03	0.48	10.91	3.18	1.22	0.05	0.00	0.61	99.19	303.1	29.5	6	0	260.0	8.5
BO72-A-21	3	28.36	0.80	16.74	4.56	0.06	0.42	0.00	32.45	0.05	0.52	10.77	3.10	1.22	0.06	0.00	0.59	99.68	316.4	24.6	6	0	260.0	8.5
BO72-A-21	4	29.38	0.62	13.47	5.48	0.07	1.72	0.00	30.05	0.10	0.74	11.42	3.38	2.36	0.16	0.00	1.57	100.51	280.3	20.1	6	0	260.0	8.5
BO72-A-21	5	28.68	0.71	17.01	3.94	0.05	0.41	0.00	32.82	0.03	0.48	10.79	3.14	1.25	0.03	0.00	0.59	99.93	296.0	28.5	6	0	260.0	8.5
BO72-A-21	6	28.74	0.66	16.42	4.06	0.05	0.56	0.00	32.36	0.04	0.52	10.94	3.16	1.38	0.09	0.00	0.73	99.70	284.4	27.1	6	0	260.0	8.5
BO72-A-21	7	29.11	0.73	16.73	4.03	0.05	0.49	0.00	32.30	0.04	0.41	11.12	3.24	1.32	0.06	0.00	0.72	100.36	299.1	27.4	7	2	290.4	12.7
BO72-B-1	1	28.51	0.81	11.61	6.70	0.08	1.84	0.00	28.80	0.06	0.87	11.99	3.34	2.34	0.11	0.01	1.68	98.75	267.2	16.9	6	0	260.0	8.5
BO72-B-1	2	28.94	0.73	11.77	6.35	0.08	2.00	0.00	28.89	0.07	0.85	12.23	3.37	2.49	0.12	0.00	1.87	99.75	270.3	17.8	6	0	260.0	8.5
BO72-B-1	3	29.41	0.59	10.94	5.58	0.06	2.33	0.00	28.30	0.08	0.80	12.51	3.44	2.95	0.19	0.00	2.10	99.29	260.0	19.9	6	0	260.0	8.5
BO72-B-1	4	29.70	0.23	14.61	3.53	0.04	2.34	0.00	29.74	0.07	0.65	11.19	3.15	2.18	0.16	0.00	1.70	99.30	257.4	30.4	6	0	260.0	8.5
BO72-B-1	5	29.42	0.61	10.69	5.96	0.07	2.57	0.00	27.73	0.08	0.84	12.84	3.46	3.14	0.19	0.00	2.28	99.87	257.4	18.6	6	0	260.0	8.5
BO72-B-1	6	29.65	0.53	10.20	8.49	0.12	2.48	0.00	25.82	0.81	1.67	11.51	3.28	2.83	0.25	0.01	2.09	99.75	254.5	10.7	6	0	260.0	8.5
BO72-B-2	1	28.76	0.61	12.49	4.74	0.05	1.15	0.00	30.51	0.03	0.66	12.74	3.58	2.21	0.08	0.00	1.38	99.00	252.2	23.8	6	0	260.0	8.5
BO72-B-2	2	29.08	0.63	12.88	4.93	0.06	1.13	0.00	30.65	0.04	0.73	12.65	3.47	2.18	0.08	0.00	1.41	99.90	270.3	22.7	6	0	260.0	8.5
BO72-B-2	3	29.39	0.71	12.09	5.10	0.06	1.26	0.00	30.47	0.04	0.62	13.11	3.66	2.38	0.09	0.00	1.46	100.43	262.9	22.0	6	0	260.0	8.5
BO72-B-2	4	29.17	0.45	13.90	4.03	0.06	1.07	0.00	31.04	0.04	0.73	11.93	3.40	1.94	0.10	0.00	1.19	99.03	319.9	27.6	6	0	260.0	8.5
BO72-B-2	5	28.88	0.65	13.01	4.91	0.05	1.03	0.00	31.04	0.05	0.63	12.46	3.49	2.13	0.07	0.02	1.24	99.65	246.9	22.8	6	0	260.0	8.5
BO72-B-2	6	29.42	0.60	12.98	4.41	0.05	0.99	0.00	31.15	0.05	0.57	12.89	3.60	2.05	0.09	0.00	1.23	100.08	270.6	25.1	6	1	260.4	11.5
BO72-B-3	1	29.60	0.63	13.28	4.05	0.06	1.15	0.00	30.47	0.05	0.66	12.44	3.51	2.10	0.10	0.00	1.21	99.30	324.3	25.3	6	1	260.4	11.5
BO72-B-3	2	29.69	0.57	13.26	3.63	0.04	1.11	0.00	30.95	0.04	0.50	12.73	3.68	2.15	0.12	0.00	1.27	99.73	253.4	27.5	6	1	260.4	11.5
BO72-B-3	3	29.66	0.75	13.82	4.46	0.06	0.98	0.00	30.29	0.05	0.65	12.17	3.52	1.92	0.08	0.00	1.08	99.48	290.4	22.9	6	1	260.4	11.5
BO72-B-3	4	29.48	0.66	13.32	4.37	0.06	1.19	0.00	29.77	0.06	0.69	12.34	3.59	2.08	0.08	0.00	1.28	98.97	294.8	23.2	6	1	260.4	11.5
BO72-B-3	5	29.81	0.56	12.90	4.10	0.05	1.30	0.00	29.92	0.04	0.70	12.58	3.52	2.21	0.10	0.00	1.32	99.11	294.1	24.7	5	2	293.0	13.7
BO72-B-4	1	30.61	0.09	13.90	3.37	0.03	1.04	0.00	29.03	0.24	0.90	12.86	3.42	2.42	0.09	0.00	1.44	99.45	166.5	24.1	5	2	293.0	13.7
BO72-B-4	2	30.69	0.11	12.90	4.33	0.05	3.34	0.00	26.59	0.26	1.06	11.59	3.21	2.30	0.18	0.01	1.95	98.55	207.7	20.0	5	2	293.0	13.7
BO72-B-4	3	30.64	0.12	13.79	3.75	0.04	1.14	0.00	28.71	0.24	0.94	13.12	3.36	2.41	0.08	0.00	1.43	99.76	188.0	22.3	5	2	293.0	13.7
BO72-B-4	4	30.82	0.10	13.02	4.28	0.05	3.33	0.00	26.36	0.28	1.06	11.69	3.13	2.35	0.15	0.07	1.86	98.54	217.6	19.9	5	2	293.0	13.7
BO72-B-4	5	30.93	0.11	13.76	3.70	0.03	2.12	0.00	27.83	0.24	0.95	12.28	3.23	2.33	0.14	0.00	1.75	99.40	154.2	22.6	5	2	293.0	13.7

grain#	spot#	P2O5	SiO2	La2O3	ThO2	PbO	Y2O3	SrO	Ce2O3	UO2	CaO	Nd2O3	Pr2O3	Sm2O3	Tb2O3	Eu2O3	Gd2O3	Total	spot age (Ma)	+/- (Ma)	no. total spots	no. spots rejected	grain age (Ma)	+/- (Ma)
BO72-B-5	1	31.01	0.16	11.36	5.88	0.04	3.92	0.00	24.87	0.28	1.42	11.65	3.09	2.43	0.23	0.15	2.12	98.61	150.4	15.2				
BO72-B-5	2	31.20	0.09	12.79	3.48	0.03	2.18	0.00	27.89	0.22	0.99	13.14	3.47	2.46	0.12	0.00	1.70	99.78	185.0	24.4				
BO72-B-5	3	30.63	0.16	11.66	5.18	0.04	3.09	0.00	26.25	0.16	1.22	12.71	3.21	2.52	0.18	0.05	2.13	99.17	166.2	17.9				
BO72-B-5	4	30.76	0.17	11.61	5.34	0.05	3.17	0.00	25.77	0.19	1.27	12.65	3.06	2.56	0.16	0.01	2.07	98.84	182.4	17.3				
BO72-B-5	5	30.59	0.17	11.77	5.36	0.05	3.14	0.00	25.52	0.17	1.27	12.51	3.15	2.47	0.14	0.05	1.99	98.35	190.6	17.5	5	1	180.7	11.1
BO72-B-6	1	29.51	0.94	11.21	4.43	0.04	2.99	0.00	26.56	0.33	0.67	13.44	3.44	3.09	0.23	0.03	2.40	99.30	168.6	18.6				
BO72-B-6	2	30.25	0.29	11.34	3.40	0.03	4.03	0.00	26.17	0.22	0.67	12.52	3.25	3.16	0.28	0.08	2.70	98.39	179.1	24.9				
BO72-B-6	3	30.62	0.12	13.80	1.84	0.02	3.46	0.00	29.23	0.10	0.42	12.03	3.37	2.17	0.20	0.01	1.78	99.17	183.7	46.1				
BO72-B-6	4	30.41	0.30	11.36	3.74	0.03	3.82	0.00	26.18	0.34	0.78	12.70	3.20	3.26	0.29	0.00	2.59	99.00	154.8	20.9				
BO72-B-6	5	28.74	0.97	11.30	4.48	0.04	2.94	0.00	26.85	0.33	0.34	13.43	3.38	3.14	0.27	0.00	2.29	98.50	150.3	18.1				
BO72-B-6	6	30.62	0.14	13.77	1.98	0.01	3.56	0.00	28.81	0.11	0.43	11.92	3.28	2.34	0.22	0.04	1.94	99.18	138.3	43.0				
BO72-B-6	7	30.40	0.30	12.20	3.58	0.03	3.63	0.00	26.96	0.21	0.72	12.17	3.22	2.88	0.27	0.06	2.36	98.98	160.4	23.8	7	0	161.1	12.8
BO72-B-7	1	28.56	1.04	18.43	4.51	0.04	0.37	0.00	32.13	0.06	0.28	9.38	2.94	1.01	0.02	0.00	0.48	99.25	192.0	21.8				
BO72-B-7	2	29.40	0.87	19.17	3.66	0.03	0.37	0.00	32.69	0.05	0.26	9.50	2.97	1.00	0.05	0.00	0.50	100.52	203.2	26.6				
BO72-B-7	3	29.04	0.81	20.27	3.36	0.03	0.32	0.00	32.28	0.04	0.25	9.42	2.88	0.94	0.05	0.00	0.46	100.14	187.3	29.2				
BO72-B-7	4	29.30	0.76	21.30	3.16	0.04	0.27	0.00	31.92	0.05	0.27	8.94	2.78	0.83	0.01	0.00	0.36	99.97	254.8	31.0				
BO72-B-7	5	28.91	0.82	19.42	3.36	0.03	0.35	0.00	32.62	0.03	0.23	9.48	3.00	1.00	0.01	0.00	0.49	99.75	192.0	28.9	5	1	191.7	14.1
BO72-B-8	1	29.28	0.83	15.89	5.60	0.07	1.04	0.00	30.13	0.08	0.81	10.31	3.08	1.53	0.05	0.00	0.90	99.62	263.8	18.1				
BO72-B-8	2	29.29	0.83	15.69	5.55	0.07	1.01	0.00	29.78	0.07	0.79	10.22	3.05	1.57	0.05	0.00	0.88	98.84	288.0	18.6				
BO72-B-8	3	28.97	0.99	15.45	6.37	0.08	0.94	0.00	29.49	0.09	0.86	10.13	3.10	1.54	0.07	0.00	0.91	98.99	277.0	16.1				
BO72-B-8	4	29.32	0.91	15.76	6.02	0.07	0.95	0.00	29.73	0.09	0.84	10.15	2.96	1.51	0.02	0.00	0.94	99.28	275.8	17.0				
BO72-B-8	5	29.98	0.77	16.23	5.17	0.06	0.93	0.00	30.52	0.07	0.78	10.18	3.13	1.52	0.09	0.00	0.93	100.35	265.4	19.7				
BO72-B-8	6	30.05	0.68	17.95	3.91	0.05	0.71	0.00	31.45	0.06	0.72	9.49	2.96	1.27	0.07	0.00	0.69	100.06	300.7	25.7				
BO72-B-8	7	29.75	0.73	17.29	4.30	0.05	0.79	0.00	31.25	0.06	0.75	9.58	2.92	1.35	0.02	0.00	0.74	99.58	281.4	23.3	7	1	275.1	8.6
BO72-B-9	1	29.62	0.44	14.07	5.02	0.05	0.46	0.00	28.97	0.55	1.06	12.18	3.23	2.35	0.08	0.00	1.36	99.44	168.7	14.9				
BO72-B-9	2	29.90	0.36	13.97	4.58	0.03	0.50	0.00	28.94	0.58	1.08	12.40	3.33	2.42	0.11	0.00	1.43	99.63	125.3	15.3				
BO72-B-9	3	30.66	0.08	12.88	4.03	0.04	3.30	0.00	27.16	0.38	1.06	11.78	3.17	2.45	0.19	0.03	2.21	99.43	201.4	19.5				
BO72-B-9	4	30.39	0.08	12.76	4.09	0.04	3.41	0.00	27.10	0.42	1.10	11.79	3.13	2.37	0.21	0.00	2.24	99.11	187.6	18.9				
BO72-B-9	5	29.72	0.40	14.03	4.90	0.05	0.51	0.00	29.56	0.54	1.06	12.24	3.26	2.38	0.07	0.00	1.43	100.16	191.0	15.4	5	2	181.4	11.8
BO72-B-10	1	29.43	0.60	13.09	3.92	0.04	1.14	0.00	30.91	0.05	0.62	12.46	3.52	2.12	0.07	0.00	1.31	99.29	259.4	25.8				
BO72-B-10	2	29.50	0.73	13.55	4.56	0.07	1.08	0.00	30.74	0.06	0.65	12.11	3.57	2.00	0.07	0.00	1.28	99.98	323.3	22.7				
BO72-B-10	3	28.67	0.74	12.47	4.54	0.06	1.14	0.00	30.58	0.04	0.59	12.58	3.52	2.16	0.08	0.00	1.34	98.49	309.3	22.7				
BO72-B-10	4	29.11	0.73	13.34	4.33	0.05	1.04	0.00	30.99	0.04	0.57	12.17	3.61	1.95	0.10	0.00	1.14	99.17	283.3	23.7				
BO72-B-10	5	29.44	0.64	13.56	3.98	0.05	1.12	0.00	31.18	0.05	0.60	12.28	3.49	2.07	0.09	0.00	1.23	99.77	273.7	25.3	5	2	290.0	17.4
BO72-B-11	1	30.09	0.15	12.43	4.35	0.04	3.95	0.00	26.24	0.21	1.02	11.80	3.16	2.44	0.23	0.03	2.15	98.30	200.7	20.8				
BO72-B-11	2	30.16	0.17	11.98	4.48	0.04	4.03	0.00	26.04	0.19	1.06	11.77	3.08	2.49	0.22	0.08	2.27	98.06	179.2	20.1				
BO72-B-11	3	30.26	0.20	12.96	5.07	0.04	2.64	0.00	27.04	0.17	1.17	11.91	3.08	2.27	0.21	0.01	1.96	99.00	157.9	18.0				
BO72-B-11	4	29.93	0.19	12.92	4.82	0.04	2.17	0.00	27.58	0.18	1.13	12.24	3.27	2.35	0.17	0.00	1.93	98.90	170.8	19.0				
BO72-B-11	5	30.00	0.18	12.85	4.77	0.04	2.60	0.00	27.26	0.15	1.11	11.98	3.14	2.33	0.19	0.01	1.90	98.50	166.6	19.3				
BO72-B-11	6	29.38	0.29	14.02	5.02	0.04	1.37	0.00	28.28	0.32	1.10	11.61	3.14	2.11	0.10	0.00	1.45	98.23	164.1	16.7	6	1	167.1	9.1
BO72-B-12	1	29.46	0.29	15.99	3.76	0.07	0.54	0.00	30.47	0.33	0.92	11.37	3.24	1.72	0.06	0.00	0.87	99.10	344.3	22.6				
BO72-B-12	2	29.26	0.49	16.59	5.26	0.09	0.35	0.00	30.09	0.16	0.96	10.88	3.15	1.45	0.02	0.00	0.69	99.43	348.2	19.1				
BO72-B-12	3	29.27	0.58	15.72	5.78	0.10	0.45	0.00	30.14	0.20	1.01	10.82	3.20	1.61	0.06	0.00	0.70	99.64	360.6	17.3				
BO72-B-12	4	29.12	0.41	16.36	5.03	0.08	0.35	0.00	30.14	0.16	0.97	10.67	3.15	1.46	0.03	0.00	0.71	98.64	335.7	19.8				
BO72-B-12	5	28.91	0.61	15.62	5.94	0.10	0.44	0.00	30.15	0.22	1.02	10.78	3.13	1.55	0.05	0.00	0.79	99.32	350.8	16.8	5	0	349.0	9.5
BO72-B-13	1	29.08	0.57	18.90	2.64	0.04	0.47	0.00	32.00	0.03	0.45	10.46	3.12	1.16	0.04	0.00	0.58	99.53	322.4	38.5				

grain#	spot#	P205	SiO2	La2O3	ThO2	PbO	Y2O3	SrO	Ce2O3	UO2	CaO	Nd2O3	Pr2O3	Sm2O3	Tb2O3	Eu2O3	Gd2O3	Total	spot age (Ma)	+/- (Ma)	no. total spots	no. spots rejected	grain age (Ma)	+/- (Ma)
BO72-B-13	2	28.61	0.68	17.97	3.39	0.04	0.47	0.00	30.99	0.04	0.49	10.66	3.06	1.23	0.00	0.00	0.58	98.19	283.5	29.7				
BO72-B-13	3	29.24	0.58	19.06	2.64	0.04	0.45	0.00	31.74	0.02	0.49	10.41	3.08	1.06	0.04	0.00	0.59	99.44	342.7	38.6				
BO72-B-13	4	28.66	0.63	17.77	3.19	0.04	0.51	0.00	31.47	0.03	0.45	10.66	3.08	1.23	0.06	0.00	0.64	98.45	315.9	31.9				
BO72-B-13	5	29.13	0.54	17.06	2.92	0.03	0.67	0.00	31.66	0.05	0.37	11.13	3.21	1.48	0.04	0.00	0.79	99.08	252.5	33.9	5	2	304.3	22.8
BO72-B-14	1	29.71	0.16	12.75	4.40	0.04	3.01	0.00	27.31	0.54	1.10	11.36	3.10	2.51	0.18	0.00	1.87	98.04	147.0	16.3				
BO72-B-14	2	30.10	0.19	12.25	4.47	0.04	3.46	0.00	27.01	0.32	1.05	11.88	3.21	2.61	0.16	0.03	2.04	98.82	181.5	18.7				
BO72-B-14	3	27.19	1.77	12.06	10.68	0.08	1.54	0.00	26.02	0.26	1.14	10.96	2.92	2.05	0.11	0.00	1.39	98.17	164.2	9.2				
BO72-B-14	4	29.49	0.30	12.93	4.64	0.04	3.18	0.00	27.60	0.24	0.99	11.48	3.07	2.29	0.17	0.00	1.82	98.24	178.8	18.8				
BO72-B-14	5	25.86	2.64	12.60	11.90	0.08	0.34	0.00	26.68	0.23	0.94	10.47	2.94	1.69	0.06	0.00	0.96	97.39	151.0	8.3				
BO72-B-14	6	26.14	2.47	12.69	12.18	0.08	0.37	0.00	26.80	0.24	0.91	10.77	2.95	1.68	0.06	0.00	0.96	98.31	144.6	8.1				
BO72-B-14	7	30.14	0.31	13.36	4.34	0.04	2.98	0.00	28.10	0.17	0.91	11.49	3.22	2.16	0.19	0.00	1.74	99.14	180.8	20.9	7	1	160.9	9.1
BO72-B-16	1	29.22	0.68	10.61	4.66	0.06	2.35	0.00	28.40	0.07	0.62	13.03	3.63	3.03	0.13	0.01	2.22	98.70	300.1	21.8				
BO72-B-16	2	29.25	0.73	10.16	4.92	0.07	2.42	0.00	28.44	0.07	0.65	12.95	3.74	3.09	0.16	0.00	2.27	98.91	300.4	20.8				
BO72-B-16	3	29.39	0.72	9.66	5.07	0.06	2.76	0.00	27.97	0.10	0.65	12.99	3.57	3.27	0.19	0.01	2.50	98.90	276.1	19.9				
BO72-B-16	4	29.18	0.71	10.86	4.78	0.06	1.97	0.00	28.94	0.06	0.66	12.96	3.67	2.81	0.11	0.00	2.00	98.75	262.5	21.1				
BO72-B-16	5	29.84	0.65	10.73	4.54	0.06	2.40	0.00	28.40	0.07	0.67	13.32	3.72	3.07	0.18	0.04	2.21	99.90	295.0	22.3	5	1	292.2	12.1
BO72-B-17	1	30.82	0.17	11.57	5.10	0.05	2.88	0.00	25.80	0.17	1.22	12.96	3.17	2.52	0.15	0.04	1.95	98.57	200.0	18.3				
BO72-B-17	2	30.82	0.17	11.58	5.19	0.05	2.87	0.00	26.04	0.27	1.25	12.94	3.19	2.53	0.20	0.04	2.02	99.16	189.4	17.0				
BO72-B-17	3	30.99	0.11	12.62	4.11	0.06	2.80	0.00	27.52	0.31	1.04	12.48	3.14	2.39	0.18	0.05	1.33	99.13	277.6	20.3				
BO72-B-17	4	30.69	0.16	11.51	4.95	0.03	2.73	0.00	26.46	0.24	1.19	12.92	3.21	2.46	0.14	0.00	2.19	98.86	124.4	17.4				
BO72-B-17	5	30.49	0.18	11.44	5.10	0.04	2.77	0.00	26.08	0.22	1.24	12.66	3.18	2.56	0.17	0.08	2.01	98.22	162.7	17.5	5	2	183.7	15.1
BO72-B-18	1	29.55	0.64	14.16	3.99	0.02	2.48	0.00	29.03	0.13	0.51	11.55	3.24	1.98	0.12	0.00	1.49	98.90	133.3	23.0				
BO72-B-18	2	29.82	0.76	13.83	4.02	0.04	2.46	0.00	29.33	0.18	0.45	11.56	3.20	1.99	0.14	0.00	1.58	99.36	183.8	22.1				
BO72-B-18	3	29.63	0.74	14.19	4.23	0.04	2.42	0.00	29.35	0.14	0.50	11.29	3.10	1.91	0.12	0.00	1.48	99.16	193.4	21.9				
BO72-B-18	4	29.47	0.86	13.36	4.34	0.03	3.06	0.00	28.75	0.14	0.43	11.62	3.30	2.24	0.16	0.00	1.65	99.42	170.9	21.3				
BO72-B-18	5	29.75	0.82	13.24	3.96	0.04	2.88	0.00	28.68	0.14	0.38	11.72	3.29	2.27	0.15	0.00	1.75	99.06	209.5	23.3	5	2	182.5	14.2
BO72-B-19	1	29.08	1.00	10.08	7.04	0.09	2.45	0.00	26.78	0.10	0.96	12.14	3.42	2.75	0.17	0.02	2.01	98.08	288.4	14.7				
BO72-B-19	2	29.16	0.99	9.84	7.13	0.09	2.47	0.00	26.53	0.10	0.97	12.33	3.47	2.80	0.14	0.06	2.09	98.15	271.6	14.6				
BO72-B-19	3	29.04	0.71	12.35	4.57	0.05	1.29	0.00	29.66	0.05	0.66	12.34	3.46	2.27	0.13	0.01	1.46	98.04	250.2	22.0				
BO72-B-19	4	29.68	0.66	10.03	5.87	0.08	3.32	0.00	26.58	0.12	1.18	12.09	3.28	2.95	0.21	0.08	2.35	98.46	283.6	17.2				
BO72-B-19	5	29.59	0.56	10.30	4.71	0.05	3.06	0.00	27.61	0.07	0.81	12.79	3.49	2.99	0.20	0.00	2.33	98.57	256.3	21.3	5	1	277.3	11.2
BO72-B-20	1	29.36	0.78	14.44	3.64	0.04	2.56	0.00	28.77	0.23	0.46	11.40	3.19	2.07	0.14	0.00	1.55	98.64	200.6	23.5				
BO72-B-20	2	29.54	0.79	14.50	3.76	0.03	2.53	0.00	29.11	0.21	0.47	11.29	3.10	2.10	0.14	0.00	1.53	99.08	145.1	22.5				
BO72-B-20	3	29.58	0.81	14.17	3.83	0.03	2.73	0.00	28.54	0.24	0.48	11.26	3.08	2.21	0.15	0.00	1.69	98.81	169.5	22.0				
BO72-B-20	4	29.40	0.80	13.90	3.73	0.03	2.86	0.00	28.48	0.25	0.49	11.49	3.09	2.21	0.12	0.00	1.68	98.51	168.1	22.5				
BO72-B-20	5	29.31	0.83	14.20	3.80	0.04	2.74	0.00	28.60	0.24	0.48	11.34	3.16	2.24	0.18	0.00	1.61	98.76	191.1	22.4				
BO72-B-20	6	29.40	0.56	14.48	2.23	0.03	3.69	0.00	28.73	0.43	0.55	10.88	3.06	1.92	0.20	0.02	1.58	97.76	165.3	27.1				
BO72-B-20	7	29.48	0.57	14.37	2.24	0.02	3.68	0.00	28.90	0.44	0.55	10.82	3.22	1.97	0.19	0.04	1.63	98.09	98.7	25.1				
BO72-B-20	8	29.50	0.59	14.13	2.35	0.03	3.66	0.00	28.76	0.43	0.56	10.67	3.09	1.98	0.19	0.00	1.63	97.56	194.5	26.7	8	2	171.5	12.3
BO72-B-22	1	29.99	0.14	12.29	4.58	0.05	2.90	0.00	27.19	0.46	1.16	11.95	3.16	2.31	0.14	0.00	1.82	98.13	195.8	17.0				
BO72-B-22	2	29.87	0.10	13.85	4.64	0.04	0.34	0.00	29.34	0.71	1.31	12.77	3.44	2.37	0.07	0.00	1.35	100.21	143.1	14.2				
BO72-B-22	3	30.06	0.24	11.31	4.90	0.04	3.77	0.00	25.61	0.47	1.23	12.46	3.10	2.66	0.17	0.00	2.44	98.46	149.9	15.6				
BO72-B-22	4	29.84	0.12	13.60	4.78	0.06	0.50	0.00	28.46	0.73	1.37	12.50	3.36	2.31	0.09	0.00	1.36	99.08	196.7	14.2				
BO72-B-22	5	30.25	0.20	11.15	5.00	0.04	3.92	0.00	25.40	0.49	1.23	12.42	3.25	2.60	0.18	0.01	2.21	98.35	155.2	15.2				
BO72-B-22	6	30.10	0.13	12.19	4.79	0.05	1.88	0.00	27.13	0.64	1.30	12.55	3.36	2.52	0.17	0.00	1.90	98.68	168.3	14.7	6	2	166.1	12.9
BO72-B-23	1	27.94	1.31	17.87	4.80	0.04	0.45	0.00	30.61	0.05	0.50	10.43	2.97	1.18	0.00	0.00	0.68	98.82	171.1	20.5				

grain#	spot#	P205	SiO2	La2O3	ThO2	PbO	Y2O3	SrO	Ce2O3	UO2	CaO	Nd2O3	Pr2O3	Sm2O3	Tb2O3	Eu2O3	Gd2O3	Total	spot age (Ma)	+/- (Ma)	no. total spots	no. spots rejected	grain age (Ma)	+/- (Ma)
BO72-B-23	2	30.16	0.15	13.02	3.83	0.05	2.25	0.00	27.50	1.12	1.12	11.74	3.15	2.74	0.23	0.00	1.88	98.94	164.4	13.3				
BO72-B-23	3	29.06	0.71	15.75	4.24	0.04	1.20	0.00	29.71	0.23	0.65	10.79	3.07	1.76	0.12	0.00	1.15	98.50	188.9	20.6				
BO72-B-23	4	30.26	0.13	13.90	3.70	0.06	2.13	0.00	27.65	1.08	1.10	11.57	3.21	2.51	0.16	0.00	1.77	99.23	183.0	13.9				
BO72-B-23	5	29.99	0.27	14.90	4.05	0.04	1.78	0.00	28.62	0.45	0.93	11.14	3.11	2.17	0.07	0.00	1.40	98.91	170.7	18.2	5	0	174.5	9.1
BO72-B-24	1	29.05	0.54	14.43	3.25	0.04	0.73	0.00	31.68	0.03	0.54	12.22	3.54	1.72	0.09	0.00	0.98	98.84	302.5	31.4				
BO72-B-24	2	29.43	0.44	15.92	2.10	0.03	0.60	0.00	32.99	0.03	0.55	11.49	3.42	1.66	0.05	0.00	0.80	99.51	356.0	47.8				
BO72-B-24	3	28.93	0.50	14.35	2.95	0.04	0.84	0.00	32.11	0.04	0.56	12.12	3.49	1.84	0.03	0.00	1.06	98.85	329.0	34.2				
BO72-B-24	4	29.11	0.45	15.27	2.46	0.03	0.57	0.00	32.77	0.03	0.39	12.33	3.57	1.69	0.06	0.00	0.83	99.55	287.1	40.8				
BO72-B-24	5	29.39	0.44	15.86	2.39	0.04	0.56	0.00	33.04	0.04	0.41	11.89	3.52	1.66	0.06	0.00	0.84	100.14	329.4	42.1	5	0	317.5	21.4
BO72-B-25	1	28.67	0.61	12.01	4.14	0.05	1.54	0.00	30.70	0.05	0.56	12.95	3.64	2.53	0.18	0.02	1.68	99.34	296.7	24.8				
BO72-B-25	2	28.75	0.56	11.71	3.95	0.05	1.67	0.00	30.12	0.06	0.63	12.92	3.65	2.63	0.11	0.00	1.84	98.66	274.7	25.5				
BO72-B-25	3	29.22	0.56	11.72	4.38	0.05	1.79	0.00	29.87	0.06	0.73	12.83	3.53	2.50	0.13	0.06	1.75	99.18	257.8	23.0				
BO72-B-25	4	29.09	0.66	11.86	4.47	0.06	1.49	0.00	30.58	0.05	0.62	12.68	3.55	2.46	0.09	0.00	1.62	99.28	322.7	23.2				
BO72-B-25	5	28.79	0.65	11.79	4.23	0.05	1.48	0.00	29.96	0.05	0.55	12.87	3.58	2.54	0.15	0.00	1.65	98.33	276.2	24.2				
BO72-B-25	6	28.97	0.64	11.84	4.15	0.06	1.54	0.00	30.00	0.05	0.54	13.04	3.74	2.54	0.13	0.00	1.65	98.89	304.1	24.6				
BO72-B-25	7	29.19	0.61	11.51	4.51	0.06	1.77	0.00	29.57	0.05	0.67	12.76	3.49	2.51	0.14	0.05	1.75	98.64	289.3	22.7				
BO72-B-25	8	29.16	0.64	11.95	4.54	0.06	1.62	0.00	29.88	0.05	0.69	12.60	3.52	2.43	0.14	0.04	1.64	98.94	287.7	22.6	8	2	288.2	10.9
BO72-B-26	1	29.61	0.12	13.69	4.03	0.04	2.54	0.00	27.84	0.23	1.01	11.53	3.00	2.19	0.19	0.00	1.79	97.80	181.0	21.4				
BO72-B-26	2	29.25	0.30	13.37	4.84	0.04	0.83	0.00	28.42	0.11	1.06	12.58	3.40	2.60	0.12	0.00	1.77	98.70	177.2	19.8				
BO72-B-26	3	30.04	0.12	12.69	4.25	0.03	3.88	0.00	26.56	0.26	1.07	11.50	3.12	2.36	0.17	0.05	2.00	98.13	152.4	19.6				
BO72-B-26	4	29.55	0.37	14.28	5.55	0.08	0.36	0.00	27.77	1.66	1.51	11.17	3.12	2.03	0.10	0.03	1.18	98.76	165.5	9.2				
BO72-B-26	5	30.01	0.13	12.92	4.34	0.03	2.32	0.00	26.92	0.25	1.10	12.17	3.31	2.63	0.15	0.00	2.09	98.37	144.2	19.6				
BO72-B-26	7	30.34	0.11	13.24	4.05	0.04	3.31	0.00	27.53	0.43	1.07	11.33	3.11	2.23	0.18	0.03	1.84	98.84	183.7	18.5	6	1	169.3	10.0
BO72-B-27	1	28.75	0.75	13.57	4.92	0.06	1.13	0.00	30.24	0.06	0.66	11.68	3.40	2.00	0.10	0.00	1.18	98.51	291.2	20.9				
BO72-B-27	2	28.70	0.78	13.56	5.14	0.06	1.15	0.00	30.10	0.06	0.69	11.63	3.38	2.00	0.13	0.00	1.24	98.72	275.0	20.0				
BO72-B-27	3	29.00	0.63	13.28	4.63	0.05	1.33	0.00	30.35	0.06	0.69	11.89	3.46	2.14	0.12	0.04	1.37	99.05	264.9	21.9				
BO72-B-27	4	28.81	0.59	14.04	4.14	0.06	0.91	0.00	31.46	0.05	0.65	11.56	3.38	1.84	0.05	0.00	1.09	98.64	310.6	24.5				
BO72-B-27	5	29.12	0.67	11.83	4.59	0.06	1.80	0.00	29.54	0.05	0.64	12.22	3.59	2.51	0.16	0.00	1.75	98.54	293.1	22.3				
BO72-B-27	6	28.53	0.67	12.14	4.66	0.06	1.63	0.00	29.57	0.06	0.65	12.06	3.37	2.35	0.12	0.00	1.64	97.52	273.5	22.0	6	1	279.5	11.0
BO72-B-28	1	28.43	0.75	13.42	4.51	0.06	1.03	0.00	30.46	0.07	0.66	11.90	3.43	1.96	0.07	0.01	1.13	97.90	300.3	22.4				
BO72-B-28	2	30.04	0.03	14.53	3.18	0.05	1.38	0.00	30.89	0.39	0.91	11.14	3.39	1.83	0.07	0.00	1.07	98.90	284.8	23.6				
BO72-B-28	3	28.75	0.64	13.97	3.72	0.05	1.02	0.00	30.96	0.04	0.68	12.07	3.59	2.00	0.08	0.00	1.15	98.71	300.5	27.3				
BO72-B-28	4	28.62	0.81	12.71	5.07	0.06	1.20	0.00	30.29	0.08	0.69	12.26	3.57	2.14	0.07	0.00	1.27	98.83	282.3	19.9				
BO72-B-28	5	28.82	0.64	15.17	3.49	0.05	0.68	0.00	32.18	0.05	0.52	11.35	3.33	1.57	0.04	0.00	0.91	98.79	313.9	29.1				
BO72-B-28	6	28.98	0.59	11.20	4.31	0.06	1.94	0.00	29.07	0.06	0.67	13.06	3.63	2.83	0.10	0.06	1.81	98.36	290.6	23.5	6	0	293.3	11.1
BO72-B-29	1	28.73	0.65	12.28	4.46	0.06	1.43	0.00	30.51	0.06	0.63	12.42	3.50	2.31	0.11	0.01	1.46	98.64	328.1	23.1				
BO72-B-29	2	28.44	0.64	11.99	4.52	0.05	1.60	0.00	29.70	0.06	0.68	12.63	3.50	2.40	0.10	0.04	1.52	97.88	271.7	22.3				
BO72-B-29	3	28.93	0.65	12.45	4.32	0.06	1.37	0.00	30.49	0.06	0.65	12.51	3.48	2.19	0.08	0.01	1.41	98.65	295.3	23.6				
BO72-B-29	4	29.09	0.44	13.59	3.20	0.04	1.32	0.00	31.00	0.06	0.68	12.27	3.45	2.11	0.07	0.04	1.23	98.60	298.3	31.0				
BO72-B-29	5	28.86	0.56	13.43	3.80	0.05	1.17	0.00	30.90	0.04	0.60	12.25	3.52	2.10	0.06	0.00	1.28	98.62	282.2	26.7	5	1	285.3	14.4
BO72-B-31	1	30.28	0.13	12.56	4.36	0.04	3.31	0.00	26.35	0.20	1.04	11.87	3.05	2.28	0.22	0.00	2.01	97.70	181.8	20.3				
BO72-B-31	2	30.24	0.15	14.15	4.33	0.04	3.02	0.00	27.28	0.24	1.05	11.02	2.99	1.99	0.12	0.00	1.57	98.19	193.5	20.0				
BO72-B-31	3	30.39	0.11	13.38	4.28	0.05	1.58	0.00	27.37	0.25	1.09	12.48	3.38	2.44	0.14	0.00	1.82	98.76	232.0	20.6				
BO72-B-31	4	31.08	0.14	13.58	4.32	0.05	2.97	0.00	27.05	0.18	1.04	11.24	3.01	2.06	0.20	0.00	1.80	98.73	223.4	21.2				
BO72-B-31	5	30.59	0.12	13.24	4.15	0.04	3.30	0.00	26.57	0.21	1.01	11.69	3.10	2.30	0.14	0.03	2.06	98.54	183.3	20.9	5	1	195.1	14.1
BO72-B-32	1	29.35	0.73	11.38	4.35	0.06	1.77	0.00	28.67	0.05	0.63	12.70	3.62	2.73	0.15	0.00	1.78	97.97	324.0	23.7				

grain#	spot#	P2O5	SiO2	La2O3	ThO2	PbO	Y2O3	SrO	Ce2O3	UO2	CaO	Nd2O3	Pr2O3	Sm2O3	Tb2O3	Eu2O3	Gd2O3	Total	spot age (Ma)	+/- (Ma)	no. total spots	no. spots rejected	grain age (Ma)	+/- (Ma)
BO72-B-32	2	29.51	0.81	11.37	4.69	0.06	1.87	0.00	28.55	0.07	0.72	12.69	3.66	2.72	0.13	0.04	1.83	98.73	281.6	21.7				
BO72-B-32	3	29.76	0.76	11.56	4.48	0.05	1.87	0.00	28.79	0.06	0.74	12.45	3.58	2.78	0.12	0.00	1.87	98.87	260.8	22.7				
BO72-B-32	4	29.90	0.74	11.13	4.47	0.06	1.95	0.00	29.00	0.06	0.69	12.54	3.67	2.74	0.13	0.00	1.86	98.93	278.6	22.7				
BO72-B-32	5	29.70	0.76	10.96	4.59	0.06	1.99	0.00	28.90	0.05	0.69	12.53	3.61	2.69	0.12	0.01	1.92	98.60	296.4	22.3	5	2	285.6	14.0
BO72-B-34	1	29.80	0.15	12.47	5.52	0.05	2.14	0.00	26.21	0.31	1.34	12.03	3.19	2.64	0.22	0.00	2.13	98.20	166.6	15.8				
BO72-B-34	2	30.25	0.09	13.21	5.09	0.05	3.25	0.00	26.01	0.45	1.33	11.15	2.93	2.23	0.17	0.03	1.95	98.19	169.8	15.7				
BO72-B-34	3	30.33	0.11	13.06	5.35	0.05	3.12	0.00	26.05	0.45	1.41	10.91	2.93	2.18	0.18	0.04	1.88	98.04	184.2	15.2				
BO72-B-34	4	30.33	0.14	13.14	6.04	0.05	3.20	0.00	25.71	0.49	1.56	10.54	2.78	1.97	0.19	0.04	1.68	97.84	140.4	13.2				
BO72-B-34	5	30.74	0.07	12.95	3.90	0.04	3.37	0.00	26.67	0.52	1.08	11.44	3.07	2.38	0.25	0.04	2.16	98.68	162.6	18.0				
BO72-B-34	6	30.67	0.08	12.71	4.66	0.04	3.74	0.00	26.03	0.62	1.25	11.20	2.98	2.33	0.23	0.07	2.10	98.71	157.9	15.2				
BO72-B-34	7	30.22	0.16	12.18	5.50	0.05	2.27	0.00	26.40	0.32	1.36	12.13	3.14	2.61	0.20	0.00	2.27	98.80	177.1	15.8				
BO72-B-34	8	29.05	0.58	14.20	7.30	0.06	0.63	0.00	27.21	0.57	1.52	11.10	2.99	2.04	0.08	0.00	1.22	98.55	162.0	11.3	8	2	165.5	6.9
BO72-B-35	1	30.16	0.18	13.67	3.92	0.04	2.45	0.00	27.96	0.30	1.06	11.42	3.13	2.29	0.14	0.04	1.62	98.35	183.3	20.8				
BO72-B-35	2	29.68	0.09	14.63	2.93	0.03	1.00	0.00	29.41	0.34	1.14	12.04	3.32	2.28	0.08	0.13	1.34	98.45	193.2	25.4				
BO72-B-35	3	30.18	0.11	14.72	3.64	0.04	0.88	0.00	29.21	0.33	1.13	12.08	3.25	2.26	0.05	0.14	1.28	99.30	201.3	21.8				
BO72-B-35	4	29.86	0.09	14.85	2.93	0.03	1.00	0.00	29.44	0.33	1.03	12.19	3.41	2.34	0.07	0.18	1.37	99.13	193.4	25.3				
BO72-B-35	5	29.88	0.12	15.13	3.77	0.04	1.14	0.00	28.83	0.25	1.18	11.66	3.14	2.01	0.08	0.11	1.20	98.54	222.5	22.6	5	1	192.4	12.3
BO72-B-36	1	29.01	0.77	10.35	5.01	0.06	2.25	0.00	28.70	0.05	0.61	13.05	3.63	3.03	0.16	0.04	2.21	98.93	289.0	20.9				
BO72-B-36	2	29.23	0.82	10.16	5.62	0.07	2.40	0.00	27.72	0.08	0.71	12.88	3.66	3.03	0.14	0.02	2.21	98.76	273.9	18.3				
BO72-B-36	3	28.99	0.85	10.05	5.69	0.07	2.33	0.00	27.46	0.08	0.73	12.94	3.59	2.96	0.17	0.11	2.23	98.24	287.8	18.2				
BO72-B-36	4	29.36	0.64	11.27	4.64	0.06	2.02	0.00	29.04	0.06	0.66	12.63	3.58	2.71	0.16	0.04	1.94	98.79	288.5	22.2				
BO72-B-36	5	29.15	0.68	10.94	4.82	0.06	2.08	0.00	28.56	0.06	0.63	12.74	3.55	2.80	0.15	0.00	2.03	98.27	292.9	21.3				
BO72-B-36	6	29.18	0.63	11.12	4.58	0.06	2.02	0.00	28.90	0.06	0.63	12.74	3.57	2.73	0.15	0.05	1.96	98.36	293.6	22.3	6	0	286.8	8.9
BO72-B-38	1	29.40	0.37	14.11	5.40	0.04	0.18	0.00	29.91	0.11	1.13	12.65	3.40	1.90	0.03	0.00	0.81	99.45	184.7	17.8				
BO72-B-38	2	29.56	0.38	13.93	5.68	0.05	0.21	0.00	29.47	0.10	1.19	12.66	3.27	1.88	0.01	0.00	0.81	99.19	187.3	17.2				
BO72-B-38	3	29.90	0.33	14.98	4.85	0.04	0.17	0.00	29.72	0.10	1.07	12.28	3.39	1.87	0.02	0.00	0.78	99.50	163.2	19.7				
BO72-B-38	4	29.19	0.59	11.38	5.67	0.04	3.12	0.00	26.26	0.13	0.98	12.29	3.19	2.66	0.19	0.01	2.21	97.90	148.0	16.8				
BO72-B-38	5	29.73	0.14	12.22	4.88	0.04	2.33	0.00	26.47	0.28	1.21	12.39	3.17	2.56	0.19	0.00	2.07	97.68	163.2	17.6				
BO72-B-38	6	29.05	0.49	12.18	5.25	0.05	2.55	0.00	27.50	0.10	0.98	12.31	3.14	2.46	0.16	0.00	1.90	98.13	211.9	18.8				
BO72-B-38	7	29.30	0.38	13.58	5.40	0.05	0.68	0.00	29.29	0.14	1.12	12.56	3.31	2.01	0.09	0.00	1.13	99.03	197.8	17.8	7	2	179.9	10.6
BO95-ST6	1	27.79	1.77	8.83	7.96	0.06	4.25	0.00	24.14	0.21	0.23	14.58	3.32	2.97	0.24	0.01	2.73	99.07	153.8	13.2				
BO95-ST6	2	27.42	1.60	9.11	7.02	0.05	4.08	0.00	24.57	0.18	0.22	14.57	3.26	2.81	0.19	0.00	2.57	97.64	151.2	14.8				
BO95-ST6	3	27.33	1.68	9.20	7.51	0.05	4.06	0.00	24.71	0.16	0.22	14.63	3.31	2.83	0.21	0.00	2.51	98.39	136.5	14.1				
BO95-ST6	5	29.09	1.09	10.77	5.17	0.05	4.90	0.00	24.82	0.32	0.40	12.92	3.13	3.05	0.34	0.06	2.92	99.03	177.8	18.2				
BO95-ST6	6	28.89	1.14	11.33	5.21	0.05	4.29	0.00	25.30	0.30	0.42	12.90	3.03	2.85	0.30	0.02	2.71	98.74	178.1	18.0				
BO95-ST6	7	29.11	1.04	11.14	4.76	0.04	4.61	0.00	25.61	0.30	0.37	12.94	3.05	2.91	0.32	0.03	2.89	99.12	178.2	19.4				
BO95-ST6	8	29.75	0.90	10.57	4.93	0.03	3.77	0.00	26.07	0.18	0.40	13.99	3.22	3.13	0.29	0.00	2.97	100.19	122.2	19.9				
BO95-ST6	9	29.86	0.89	10.46	4.93	0.03	3.71	0.00	26.18	0.27	0.41	14.00	3.08	3.06	0.25	0.12	2.06	99.29	111.4	18.5	8	2	152.5	11.3
BO95-ST7	1	29.91	0.10	13.61	4.37	0.03	3.13	0.00	27.63	0.27	0.94	11.46	3.01	2.13	0.18	0.00	1.77	98.55	151.6	20.9				
BO95-ST7	2	29.32	0.25	14.13	5.04	0.05	1.43	0.00	28.31	0.71	1.07	11.63	3.15	2.04	0.08	0.00	1.37	98.56	160.1	14.7				
BO95-ST7	3	30.73	0.07	13.71	4.30	0.03	3.21	0.00	27.89	0.33	0.96	11.44	3.01	2.07	0.21	0.00	1.81	99.78	144.4	20.2				
BO95-ST7	4	30.28	0.29	14.49	5.08	0.05	1.29	0.00	29.08	0.60	1.01	11.69	3.09	1.94	0.07	0.00	1.23	100.17	160.6	15.6				
BO95-ST7	5	30.70	0.08	13.48	4.23	0.03	3.16	0.00	27.75	0.31	0.95	11.63	3.06	2.04	0.17	0.00	1.76	99.34	145.4	20.6				
BO95-ST7	6	30.71	0.14	12.77	5.30	0.04	1.94	0.00	27.49	0.21	1.11	12.76	3.23	2.47	0.18	0.00	1.88	100.24	149.8	18.4	6	0	153.7	8.1
BO95-ST13	1	29.76	0.10	13.13	4.45	0.05	3.04	0.00	27.28	0.44	0.98	11.65	2.96	2.19	0.20	0.00	1.92	98.15	192.4	19.1				
BO95-ST13	2	30.24	0.24	14.59	4.60	0.06	0.50	0.00	29.99	0.64	0.96	12.16	3.28	2.08	0.08	0.00	1.17	100.58	217.2	16.8				

grain#	spot#	P2O5	SiO2	La2O3	ThO2	PbO	Y2O3	SrO	Ce2O3	UO2	CaO	Nd2O3	Pr2O3	Sm2O3	Tb2O3	Eu2O3	Gd2O3	Total	spot age (Ma)	+/- (Ma)	no. total spots	no. spots rejected	grain age (Ma)	+/- (Ma)
BO95-ST13	3	30.85	0.09	12.98	4.37	0.04	3.52	0.00	27.32	0.67	1.05	11.70	3.04	2.13	0.18	0.00	1.77	99.71	141.1	16.5				
BO95-ST13	4	29.65	0.22	15.45	3.79	0.04	0.64	0.00	30.37	0.51	0.94	11.81	3.16	1.93	0.04	0.00	1.06	99.61	184.8	20.1				
BO95-ST13	5	30.06	0.09	13.05	4.32	0.04	3.32	0.00	26.99	0.44	0.97	11.85	3.10	2.20	0.16	0.00	1.79	98.38	181.7	19.1				
BO95-ST13	6	30.68	0.24	15.03	4.44	0.05	0.51	0.00	29.54	0.61	0.92	11.96	3.25	2.04	0.05	0.00	1.07	100.39	177.7	17.0				
BO95-ST13	7	30.57	0.11	12.92	4.16	0.04	3.44	0.00	27.25	0.50	0.98	12.05	3.08	2.25	0.20	0.00	1.83	99.37	174.1	18.9	7	2	181.8	9.0
BO95-ST14	1	29.05	0.93	13.41	8.67	0.06	1.28	0.00	28.74	0.20	1.11	10.72	2.91	1.61	0.05	0.00	0.99	99.75	158.2	12.1				
BO95-ST14	2	29.38	0.81	13.52	9.70	0.06	1.34	0.00	27.48	0.15	1.45	10.72	2.92	1.57	0.10	0.00	0.98	100.17	142.7	11.0				
BO95-ST14	3	29.35	0.80	13.72	9.41	0.07	1.28	0.00	27.57	0.15	1.41	10.69	2.81	1.53	0.08	0.00	0.96	99.80	158.1	11.3				
BO95-ST14	4	29.63	0.84	14.19	8.28	0.06	1.51	0.00	27.94	0.16	1.14	10.91	2.84	1.66	0.13	0.00	1.08	100.37	164.6	12.6				
BO95-ST14	5	29.06	0.77	14.25	7.20	0.04	1.25	0.00	28.84	0.17	0.99	10.86	2.85	1.58	0.10	0.00	0.95	98.91	134.6	14.1				
BO95-ST14	6	28.74	0.78	14.09	7.31	0.05	1.24	0.00	29.05	0.18	1.00	10.73	2.90	1.55	0.06	0.00	1.00	98.74	138.3	13.9				
BO95-ST14	7	28.67	0.85	13.78	7.81	0.05	1.31	0.00	29.32	0.19	1.03	10.72	2.98	1.52	0.10	0.00	0.95	99.20	140.8	13.0				
BO95-ST14	8	28.61	0.85	14.06	7.79	0.05	1.29	0.00	28.94	0.21	1.03	10.83	2.89	1.64	0.06	0.00	0.92	99.18	152.2	13.1	8	2	148.9	6.2
BO95-1	1	28.49	0.89	11.43	7.93	0.06	2.27	0.00	26.91	0.25	1.01	12.08	3.16	2.62	0.20	0.00	1.86	99.15	157.5	13.0				
BO95-1	2	28.54	0.90	10.99	7.79	0.05	2.29	0.00	26.92	0.24	1.02	11.88	3.25	2.63	0.17	0.00	1.81	98.49	145.9	12.9				
BO95-1	3	29.08	0.72	13.15	6.35	0.05	1.91	0.00	28.37	0.12	0.83	11.87	3.02	1.94	0.11	0.00	1.46	98.97	163.2	16.4				
BO95-1	4	29.26	0.69	14.04	6.27	0.04	1.56	0.00	29.00	0.10	0.86	11.86	3.05	1.82	0.12	0.00	1.24	99.91	157.9	16.8				
BO95-1	5	29.84	0.56	13.54	5.64	0.05	1.79	0.00	28.50	0.18	0.82	12.36	3.14	2.12	0.12	0.00	1.52	100.17	172.0	17.9				
BO95-1	6	30.03	0.44	12.85	5.31	0.04	2.96	0.00	27.59	0.16	0.86	12.36	3.11	2.30	0.17	0.00	1.88	100.05	154.8	19.2				
BO95-1	7	30.84	0.21	12.42	4.56	0.04	3.97	0.00	26.58	0.23	0.90	12.50	3.11	2.53	0.22	0.06	2.18	100.36	194.3	21.5				
BO95-1	8	30.58	0.15	15.10	3.36	0.04	0.15	0.00	30.10	0.62	0.76	12.95	3.41	2.33	0.07	0.16	1.06	100.88	170.3	20.0	8	2	161.8	7.7
BO95-2	1	28.35	0.73	13.09	5.24	0.05	1.91	0.00	29.50	0.07	0.60	11.60	3.26	2.12	0.13	0.00	1.65	98.29	235.5	20.7				
BO95-2	2	29.36	0.59	13.94	4.44	0.05	1.76	0.00	30.26	0.04	0.52	11.95	3.26	2.06	0.15	0.00	1.45	99.84	278.6	25.1				
BO95-2	3	28.97	0.57	14.62	4.33	0.05	1.53	0.00	30.15	0.06	0.52	11.73	3.24	1.87	0.14	0.00	1.35	99.15	284.2	25.1				
BO95-2	4	30.18	0.54	12.42	5.00	0.05	2.21	0.00	28.76	0.09	0.78	12.52	3.33	2.80	0.15	0.00	2.00	100.82	225.6	21.5				
BO95-2	5	30.15	0.54	12.44	5.00	0.05	2.24	0.00	28.57	0.11	0.76	12.58	3.36	2.66	0.18	0.00	1.76	100.40	238.6	21.5	5	2	247.9	19.0
BO95-3	1	28.90	0.64	10.10	6.25	0.05	4.28	0.00	25.76	0.18	0.82	12.81	3.21	2.63	0.23	0.01	2.44	98.31	186.6	16.6				
BO95-3	2	28.15	1.38	8.96	9.08	0.07	4.58	0.00	24.14	0.19	0.77	12.95	3.21	2.70	0.22	0.01	2.46	98.88	173.3	11.9				
BO95-3	3	29.09	0.73	10.24	7.40	0.06	4.14	0.00	24.66	0.56	1.32	11.78	2.92	2.83	0.31	0.06	2.57	98.67	162.8	12.2				
BO95-3	4	29.26	0.58	10.73	5.84	0.05	4.30	0.00	24.88	0.60	1.22	12.01	3.08	2.95	0.30	0.09	2.57	98.45	155.0	14.3				
BO95-3	5	29.03	1.17	9.23	9.50	0.08	4.67	0.00	22.19	0.72	1.52	11.63	2.90	3.11	0.33	0.16	2.95	99.19	163.9	9.7				
BO95-3	6	29.97	0.54	10.73	5.11	0.05	3.93	0.00	25.74	0.50	1.03	12.04	3.13	2.92	0.28	0.10	2.56	98.62	161.6	16.4				
BO95-3	7	29.18	1.19	9.76	9.46	0.09	4.13	0.00	22.93	0.66	1.66	11.35	2.82	2.89	0.29	0.09	2.67	99.16	175.7	9.9	7	2	168.4	6.2
BO95-6	1	28.70	0.75	13.42	6.25	0.04	1.78	0.00	28.84	0.14	0.77	12.02	3.19	1.96	0.11	0.00	1.45	99.41	156.0	16.8				
BO95-6	2	29.92	0.39	14.99	5.68	0.05	0.97	0.00	28.50	0.22	1.49	11.43	3.04	2.00	0.11	0.00	1.44	100.24	203.4	17.7				
BO95-6	3	29.51	0.37	13.48	6.01	0.05	1.34	0.00	27.68	0.32	1.48	12.08	3.03	2.35	0.13	0.03	1.75	99.61	159.4	15.9				
BO95-6	4	29.68	0.46	14.62	6.41	0.06	0.98	0.00	27.96	0.22	1.67	11.14	3.02	1.95	0.12	0.00	1.40	99.67	198.1	15.9				
BO95-6	5	29.35	0.38	13.23	6.46	0.06	1.35	0.00	27.37	0.34	1.62	11.76	3.05	2.29	0.11	0.06	1.70	99.12	181.4	14.8				
BO95-6	6	28.59	0.89	12.97	6.98	0.05	1.83	0.00	28.34	0.13	0.80	11.88	2.99	1.99	0.12	0.00	1.45	99.03	147.8	15.0				
BO95-6	7	29.55	0.85	13.44	6.97	0.05	1.90	0.00	28.24	0.13	0.83	11.93	3.08	2.04	0.08	0.00	1.49	100.58	171.0	15.2				
BO95-6	8	29.30	0.85	12.33	6.82	0.06	2.51	0.00	27.49	0.21	0.83	11.96	3.15	2.33	0.13	0.00	1.74	99.72	187.0	14.9	9	2	179.6	8.7
BO95-6	9	29.33	0.84	12.51	6.83	0.06	2.50	0.00	27.44	0.29	0.79	11.75	3.10	2.21	0.18	0.06	1.11	99.02	197.4	14.4	2			

**Results of U/Pb LA-ICP-SF-MS dating of detrital zircon from the Bosnian Flysch**

Formation	Sample	Spot ID	<sup>207</sup> Pb (cps)	U (ppm)	Pb (ppm)	Th/U	<sup>206</sup> Pb/ <sup>238</sup> U 1 σ %	<sup>207</sup> Pb/ <sup>235</sup> U 1 σ %	Rho	<sup>207</sup> Pb/ <sup>206</sup> Pb 1 σ %	Apparent ages				Con. (%)				
											<sup>206</sup> Pb/ <sup>238</sup> U age (Ma)	<sup>207</sup> Pb/ <sup>235</sup> U age (Ma)	<sup>207</sup> Pb/ <sup>206</sup> Pb age (Ma)	± 2σ (Ma)					
Vranduk Fm.	TD-154	Z474Azrm001	2064	91	4	0.89	0.0397	2.3	0.2986	2.9	0.79	0.0546	1.8	251	12	16	395	41	95
Vranduk Fm.	TD-154	Z474Azrm002	2754	105	5	0.29	0.0482	3.2	0.3898	4.7	0.68	0.0586	3.5	304	20	32	553	75	91
Vranduk Fm.	TD-154	Z474Azrm003	565	27	1	0.31	0.0340	2.7	0.3385	6.3	0.43	0.0722	5.7	215	12	37	993	115	73
Vranduk Fm.	TD-154	Z474Azrm004	2435	112	5	0.60	0.0363	2.5	0.2753	3.7	0.69	0.0550	2.7	230	12	18	412	60	93
Vranduk Fm.	TD-154	Z474Azrm005	2314	173	5	0.27	0.0261	2.7	0.1988	4.0	0.67	0.0553	3.0	166	9	15	424	67	90
Vranduk Fm.	TD-154	Z474Azrm006	7019	151	12	0.28	0.0807	2.3	0.6644	2.8	0.83	0.0597	1.5	500	23	29	594	33	97
Vranduk Fm.	TD-154	Z474Azrm007	12465	43	14	0.54	0.2881	4.4	4.3570	6.1	0.73	0.1097	4.1	1632	145	206	1794	75	96
Vranduk Fm.	TD-154	Z474Azrm008	5917	282	16	1.46	0.0433	2.4	0.3133	2.7	0.90	0.0525	1.2	273	13	15	306	27	99
Vranduk Fm.	TD-154	Z474Azrm009	6649	50	12	1.49	0.1878	2.5	2.0200	2.9	0.87	0.0780	1.4	1110	56	65	1147	28	99
Vranduk Fm.	TD-154	Z474Azrm010	71013	157	71	0.80	0.3807	2.8	6.9594	4.1	0.67	0.1326	3.1	2080	115	175	2132	54	99
Vranduk Fm.	TD-154	Z474Azrm011	1344	60	3	0.63	0.0410	2.5	0.3080	3.5	0.71	0.0545	2.5	259	13	19	391	56	95
Vranduk Fm.	TD-154	Z474Azrm012	1429	54	3	1.76	0.0456	2.7	0.4234	7.7	0.35	0.0674	7.2	287	15	55	850	150	80
Vranduk Fm.	TD-154	Z474Azrm013	3155	86	6	0.14	0.0669	2.4	0.5539	4.6	0.52	0.0600	4.0	418	20	448	605	85	93
Vranduk Fm.	TD-154	Z474Azrm014	249	10	0	0.11	0.0296	3.8	0.3859	20.6	0.18	0.0945	20.3	188	14	137	1519	382	57
Vranduk Fm.	TD-154	Z474Azrm015	439	26	1	0.45	0.0256	2.8	0.2214	5.6	0.45	0.0628	5.0	163	13	203	700	107	80
Vranduk Fm.	TD-154	Z474Azrm016	16795	35	17	0.89	0.3820	2.8	6.7973	3.0	0.94	0.1290	1.0	2086	116	123	2085	18	100
Vranduk Fm.	TD-154	Z474Azrm017	783	51	1	0.22	0.0277	2.6	0.2198	4.3	0.60	0.0575	3.4	176	9	202	511	75	87
Vranduk Fm.	TD-154	Z474Azrm019	710	34	1	0.76	0.0286	3.0	0.3008	8.9	0.33	0.0764	8.4	182	11	267	1105	168	68
Vranduk Fm.	TD-154	Z474Azrm020	370	17	1	0.43	0.0307	2.8	0.3338	10.1	0.28	0.0789	9.7	195	11	292	1170	192	67
Vranduk Fm.	TD-154	Z474Azrm021	568	36	1	0.22	0.0247	2.5	0.2107	7.4	0.33	0.0619	7.0	157	8	194	672	149	81
Vranduk Fm.	TD-154	Z474Azrm022	4086	52	7	0.50	0.1220	2.7	1.1231	3.6	0.75	0.0668	2.4	742	40	56	831	51	97
Vranduk Fm.	TD-154	Z474Azrm023	297	9	0	0.60	0.0453	9.2	0.6569	17.6	0.52	0.1051	15.0	286	53	180	1717	276	56
Vranduk Fm.	TD-154	Z474Azrm024	614	31	1	0.27	0.0285	2.8	0.2869	6.8	0.41	0.0730	6.2	181	10	256	1015	126	71
Vranduk Fm.	TD-154	Z474Azrm025	584	35	1	0.38	0.0264	2.6	0.2201	8.5	0.30	0.0605	8.1	168	9	34	623	174	83
Vranduk Fm.	TD-154	Z474Azrm026	433	25	1	0.20	0.0270	2.9	0.2529	7.9	0.36	0.0679	7.4	172	10	36	866	153	75
Vranduk Fm.	TD-154	Z474Azrm027	4812	151	7	0.04	0.0528	2.3	0.3956	2.6	0.87	0.0544	1.3	331	15	338	387	30	98
Vranduk Fm.	TD-154	Z474Azrm028	2057	66	4	0.39	0.0573	2.5	0.4633	3.8	0.66	0.0586	2.8	359	18	29	553	62	93
Vranduk Fm.	TD-154	Z474Azrm029	3507	112	6	0.16	0.0582	2.5	0.4500	3.1	0.80	0.0561	1.9	365	18	23	456	41	97
Vranduk Fm.	TD-154	Z474Azrm030	427	14	1	0.65	0.0375	3.5	0.5956	11.1	0.32	0.1151	10.5	237	17	105	1882	189	50
Vranduk Fm.	TD-154	Z474Bzrm002	6624	58	11	1.06	0.1563	1.6	1.5063	2.1	0.74	0.0699	1.4	936	29	39	925	29	100
Vranduk Fm.	TD-154	Z474Bzrm003	5044	117	9	0.38	0.0760	1.1	1.3258	1.6	0.67	0.0559	1.2	472	10	15	448	27	101
Vranduk Fm.	TD-154	Z474Bzrm004	11225	117	18	0.47	0.1421	1.1	1.3258	1.4	0.79	0.0677	0.9	856	19	24	859	18	100
Vranduk Fm.	TD-154	Z474Bzrm005	880	68	2	0.58	0.0298	4.2	0.1910	9.3	0.44	0.0464	8.4	190	16	33	20	201	107
Vranduk Fm.	TD-154	Z474Bzrm006	5663	106	11	0.81	0.0836	1.3	0.6839	1.6	0.77	0.0593	1.1	518	13	17	579	23	98
Vranduk Fm.	TD-154	Z474Bzrm007	1812	139	4	0.71	0.0254	1.6	0.1717	2.5	0.64	0.0489	2.0	162	5	8	145	46	101
Vranduk Fm.	TD-154	Z474Bzrm008	3072	243	7	0.76	0.0294	1.6	0.1770	2.3	0.68	0.0505	1.7	162	5	10	216	39	98
Vranduk Fm.	TD-154	Z474Bzrm009	844	67	2	1.37	0.0271	1.2	0.1876	2.8	0.42	0.0503	2.5	172	4	175	207	59	99
Vranduk Fm.	TD-154	Z474Bzrm010	1269	90	3	0.43	0.0276	1.6	0.1915	3.1	0.51	0.0504	2.7	175	6	11	211	62	99
Vranduk Fm.	TD-154	Z474Bzrm011	2844	65	5	0.56	0.0758	1.6	0.5992	2.6	0.64	0.0573	2.0	471	16	25	503	44	99
Vranduk Fm.	TD-154	Z474Bzrm012	7926	263	13	0.08	0.0515	1.3	0.3868	1.6	0.80	0.0545	1.0	324	8	11	391	22	97

Apparent ages

Formation	Sample	Spot ID	<sup>207</sup> Pb (cps)	U (ppm)	Pb (ppm)	Th/U	<sup>206</sup> Pb/ <sup>238</sup> U	1 σ %	<sup>207</sup> Pb/ <sup>235</sup> U	1 σ %	Rho	<sup>207</sup> Pb/ <sup>206</sup> Pb	1 σ %	<sup>206</sup> Pb/ <sup>238</sup> U age ± 2σ (Ma)	<sup>207</sup> Pb/ <sup>235</sup> U age ± 2σ (Ma)	<sup>207</sup> Pb/ <sup>206</sup> Pb age ± 2σ (Ma)	Con. (%)	
Vranduk Fm.	TD-154	Z474Bzrm013	787	38	1	0.89	0.0231	3.5	0.2154	8.8	0.40	0.0677	8.0	147	198	859	167	74
Vranduk Fm.	TD-154	Z474Bzrm015	1504	84	4	1.00	0.0379	1.2	0.2602	2.4	0.49	0.0497	2.1	240	235	183	48	102
Vranduk Fm.	TD-154	Z474Bzrm016	1577	127	3	0.45	0.0243	1.0	0.1655	2.3	0.43	0.0493	2.0	155	156	164	47	100
Vranduk Fm.	TD-154	Z474Bzrm017	5285	87	9	0.40	0.0981	1.2	0.8128	1.6	0.73	0.0601	1.1	603	604	608	24	100
Vranduk Fm.	TD-154	Z474Bzrm018	8172	102	13	0.35	0.1200	1.8	1.0799	2.2	0.84	0.0653	1.2	731	744	783	24	98
Vranduk Fm.	TD-154	Z474Bzrm019	9107	126	5	0.15	0.0376	2.3	0.3879	3.2	0.72	0.0748	2.2	238	333	1064	44	71
Vranduk Fm.	TD-154	Z474Bzrm020	3349	289	7	0.43	0.0232	1.6	0.1556	2.5	0.65	0.0487	1.9	148	147	135	45	100
Vranduk Fm.	TD-154	Z474Bzrm021	624	50	1	0.80	0.0258	1.5	0.1687	3.0	0.50	0.0474	2.6	164	158	71	63	104
Vranduk Fm.	TD-154	Z474Bzrm022	700	45	1	0.58	0.0289	2.0	0.1989	3.2	0.61	0.0498	2.5	184	184	188	59	100
Vranduk Fm.	TD-154	Z474Bzrm023	1274	52	2	0.40	0.0400	1.4	0.2921	2.4	0.56	0.0530	2.0	253	260	328	46	97
Vranduk Fm.	TD-154	Z474Bzrm024	11664	84	19	1.32	0.1747	1.3	1.8415	1.9	0.70	0.0764	1.4	1038	1060	1106	27	98
Vranduk Fm.	TD-154	Z474Bzrm026	2863	153	6	0.46	0.0355	2.0	0.2587	2.7	0.75	0.0529	1.8	225	234	323	40	96
Vranduk Fm.	TD-154	Z474Bzrm028	2619	69	5	0.56	0.0700	1.0	0.5260	1.8	0.55	0.0545	1.5	436	429	391	34	102
Vranduk Fm.	TD-154	Z474Bzrm029	257	20	1	0.38	0.0275	1.9	0.1841	6.3	0.30	0.0485	6.0	175	172	126	141	102
Vranduk Fm.	TD-154	Z474Bzrm001	1200	94	2	0.45	0.0240	1.1	0.1644	2.8	0.39	0.0497	2.6	153	155	183	60	99

*List of samples with the geographic co-ordinates of the sampling points (Chapter 4)*

Unit	locality	Sample	Lithology	N [deg]	N [min]	E [deg]	E [min]	elev. [m]	apatite FT dating	zircon U/Pb dating	monazite (Th-U)/Pb dating
Vranduk Formation	Vranduk	BO-12	medium-grained sandstone	44	19.555	17	54.675	280			X
Vranduk Formation	Vranduk	BO-72	medium-grained sandstone	44	17.611	17	54.357	312			X
Vranduk Formation	Vranduk	BO-95	medium-grained sandstone	44	18.346	17	54.609	298			X
Vranduk Formation	Vranduk	TD-154	medium-grained sandstone	44	19.555	17	54.675	280		X	
Adriatic Carbonate Platform	Maovice	TD-375	tephra	43	53.830	16	19.595	822	X		

## **Electron microprobe total (Th-U)/Pb chemical dating of detrital monazite**

Monazite crystals were handpicked from the non-magnetic mineral fraction under the binocular microscope and verified using EDS and SE imaging. They are transparent, colourless to pale yellow, lack severe surface etch figures, and contain virtually no mineral inclusions, whereas tiny droplets of silicate melt is trapped in some of them. Grains were mounted in epoxy, polished and carbon-coated. Chemical analyses were performed using a JEOL JXA-8900RL electron microprobe at the Geoscience Center Göttingen, equipped with five wavelength-dispersive spectrometers, operated at 20 kV accelerating voltage, 80 nA probe current, and a nominal spot size of 5  $\mu\text{m}$  (20 nA and 10  $\mu\text{m}$  in case of the REE glass standards). Although advantageous for an increased count rate and better precision (e.g. Williams *et al.*, 2006), the choice of a probe current higher than 80 nA was rendered impractical in this study due to possible beam damage effects and the dimension of the monazite grains (partly <50  $\mu\text{m}$ ) being surrounded by the thermally unstable epoxy resin. Spectrometer conditions and the primary standards used for element concentration calculation are listed in Appendix 4-4. Spectral line interferences of Th  $M_\gamma$  on U  $M_\beta$ , U  $M_\zeta$  on Pb  $M_\beta$ , Ce  $L_\beta$  on Nd  $L_\alpha$ , and Ce  $L_\beta$  on Sm  $L_\alpha$  were carefully corrected. Primary standards were measured routinely after each run of c. 90 minutes to assess analysis quality. Monazite fragment #18 of the Variscan granite DVT-303 (Dunkl *et al.*, 2008) was also included in the standard batch, due to its limited chemical zoning and apparent homogeneity in (Th-U)/Pb ages, in order to monitor the consistency of sample age results.

In total, 496 spot analyses were performed on 79 grains: 123 spots on 17 grains of sample BO-12, 315 spots on 54 grains of sample BO-72 and 58 spots on 8 grains of sample BO-95. DVT-303 was analyzed in 41 spots which yielded a pooled date of  $314.9 \pm 4.7$  Ma (2 $\sigma$  s.e.), in good agreement with preliminary zircon U/Pb ages from this granite (c. 320 Ma; Dunkl *et al.*, 2008).

Net intensities were corrected using the ZAF algorithm provided by JEOL following correction for detector dead time and background subtraction. Achieved detection limits within  $\pm 3\sigma$  confidence interval were approximately 165 ppm for Th and U, and 90 ppm for Pb as quantified by Eq. 1:

$$I_{PK} - I_{BG} \geq 3\sigma \sqrt{\frac{I_{BG}}{t_{BG}}} \quad (1)$$

where

$I_{PK}$  : peak intensity [cps];

$I_{BG}$  : total (lower + upper) background intensity [cps];

$t_{BG}$  : total (lower + upper) background count time [s].

Achieved instrumental sensitivity for Pb translates to a c. 87 and 29 Ma age of "limit of dating" for a monazite having 2 and 6 wt% of ThO<sub>2</sub>, respectively, given a UO<sub>2</sub>/ThO<sub>2</sub> ratio of 0.1.

Apparent ages were calculated for each spot analysis according to Montel *et al.*, (1996), assuming a concordant isotopic system in the monazite (e.g. Cocherie *et al.*, 1998). In this study, age uncertainty calculation was based on the analytical uncertainties of the Th, U and Pb measurements:

$$\sigma(c_i) = \sqrt{c_i^2 \cdot \left( \frac{\frac{I_{PK}}{t_{PK}} + \frac{I_{BG-} + I_{BG+}}{2(t_{BG-} + t_{BG+})}}{[I_{PK} - (I_{BG-} + I_{BG+})]^2} \right)} \quad (2)$$

where

$t_{PK}$ ;  $t_{BG-}$ ;  $t_{BG+}$  : peak, lower and upper background measurement times, respectively [s];

$I_{PK}$ ;  $I_{BG-}$ ;  $I_{BG+}$  : peak, lower and upper background intensities [cps];

$c_i$  : concentration of element i in the sample.

Analytical uncertainties derived from Eq. 2 were propagated through the age equation of Montel *et al.*, (1996) to obtain age uncertainties for each spot analysis.

Spot ages  $x_j$  together with their analytical error (standard deviation,  $\sigma_j$ ) were assessed in each grain by Grubbs-test (Grubbs, 1969) to exclude outlier spot ages. Spots

passing the test were pooled together to estimate the grain weighted mean age,  $\overline{x^*}$  (with weights being inversely proportional to the square of analytical error,  $\frac{1}{\sigma_j^2}$ ):

$$\overline{x^*} = \sum_{j=1}^N \frac{1}{\sigma_j^2} \cdot \frac{1}{\sum_{j=1}^N \frac{1}{\sigma_j^2}} \cdot x_j \quad (3)$$

where  $N$  is the number of non-outlying spots within a grain.

The standard error of this mean age,  $Q$ , accounts for both the average spot analytical errors and the spread of the spot ages within that grain.  $Q$  is thus taken as the total grain age error:

$$Q = \frac{1}{N} \left[ \sum_{j=1}^N \sigma_j^2 \right] + \frac{1}{N} \left[ \sum_{j=1}^N (x_j - \overline{x^*})^2 \right] \quad (4)$$

The spread of the individual grain ages with their standard errors was visualized through a kernel density estimation, constructed as the sum of Gaussian curves centered on each grain age and its error (mean =  $\overline{x^*}$ , s.d. =  $Q$ ). This one-dimensional variable bandwidth kernel density estimation was carried out in *R* environment using the method of Sircombe and Hazelton (2004).

### **Details of age spectrum deconvolution of monazite and zircon**

The existence of several distinct age populations was tested independently with two softwares (Popshare – Dunkl and Székely, 2002; Isoplot – Ludwig, 2003) in both cases assuming a mixture of Gaussian distributions. The programs yielded estimates of the average ages ( $\mu_p$ ) for each age population, together with their spreads ( $\sigma_p$ ) and their proportion in the whole sample ( $q_p$ ). From these, the most probable age for each isolated population was determined as

$$\mu_p \pm \frac{2\sigma_p}{\sqrt{Gq_p}}$$

where G is the total number of grains, and p is the population index (i.e. the number of pre-set populations). The two softwares gave consistent results (Table 2 in Chapter 4).

**List of all calcareous nannofossil taxa cited in the text and figures of Chapter 5**

<i>Arkhangeliskiella cymbiformis</i> Vekshina 1959	Campanian – Maastrichtian
<i>Arkhangeliskiella</i> sp.	Upper Cretaceous
<i>Blackites creber</i> (Deflandre 1954) Roth 1970	Eocene
<i>Blackites</i> sp.	
<i>Braarudosphaera bigelowi</i> (Gran & Braarud 1935) Deflandre 1947	Cretaceous – recent
<i>Braarudosphaera</i> sp.	
<i>Broinsonia</i> sp.	Albian – Maastrichtian
<i>Calcidiscus leptoporus</i> (Murray & Blackman 1898) Loeblich & Tappan 1978	NN2-21
<i>Calcidiscus macintyreii</i> (Bukry & Bramlette 1969) Loeblich & Tappan 1978	NN7-19
<i>Calcidiscus premacintyreii</i> Theodoridis 1984	NN4-6
<i>Calcidiscus tropicus</i> Kamptner 1956 <i>sensu</i> Gartner 1992	NN4-10
<i>Chiasmolithus grandis</i> (Bramlette & Riedel 1954) Radomski 1968	NP11-17
<i>Chiasmolithus modestus</i> Perch-Nielsen 1971	NP16
<i>Chiasmolithus oamaruensis</i> (Deflandre 1954) Hay, Mohler & Wade 1966	NP18-22
<i>Chiasmolithus solitus</i> (Bramlette & Sullivan 1961) Locker 1968	NP10-16
<i>Chiasmolithus</i> sp.	
<i>Chiastocyclus</i> sp.	
<i>Clausiococcus fenestratus</i> (Deflandre & Fert 1954) Prins 1979	Palaeogene – NN1
<i>Coccolithus eopelagicus</i> (Bramlette & Riedel, 1954) Bramlette & Sullivan 1961	Eocene
<i>Coccolithus miopelagicus</i> Bukry 1971	?NN5-8
<i>Coccolithus pelagicus</i> (Wallich 1871) Schiller 1930	Eocene – Recent
<i>Coronocycclus nitescens</i> (Kamptner 1963) Bramlette & Wicoxon 1967	Eocene – Miocene
<i>Cribricentrum reticulatum</i> (Gartner & Smith 1967) Perch-Nielsen 1971	NP16-20
<i>Cribrosphaerella ehrenbergii</i> (Arkhangel'sky 1912) Deflandre <i>in</i> Piveteau 1952	Albian – Maastrichtian
<i>Cyclagelosphaera reinhardtii</i> (Perch-Nielsen 1968) Romein 1977	Cretaceous – Palaeocene
<i>Cyclicargolithus abisectus</i> (Müller 1970) Wise 1973	NP24-NN1
<i>Cyclicargolithus floridanus</i> (Roth & Hay <i>in</i> Hay et al. 1967) Bukry 1971	Middle Eocene – NN7
<i>Cyclicargolithus luminis</i> (Sullivan 1965) Bukry 1971	Middle Eocene – Oligocene
<i>Cyclicargolithus</i> sp.	
<i>Cyclococcolithus formosus</i> Kamptner 1963	Eocene – NP21
<i>Discoaster aster</i> Bramlette & Riedel 1954	Miocene
<i>Discoaster barbadiensis</i> Tan 1927	NP10-20
<i>Discoaster binodosus</i> Martini 1958	Lower to Middle Eocene
<i>Discoaster deflandrei</i> Bramlette & Riedel 1954	Eocene – Oligocene
<i>Discoaster distinctus</i> Martini 1958	NP12-14
<i>Discoaster exilis</i> Martini & Bramlette 1963	NN4-9
<i>Discoaster lenticularis</i> Bramlette & Sullivan 1961	NP9-10
<i>Discoaster lodoensis</i> Bramlette & Riedel 1954	NP12-14
<i>Discoaster mirus</i> Deflandre <i>in</i> Deflandre & Fert 1954	?NP13-14
<i>Discoaster multiradiatus</i> Bramlette & Riedel 1954	NP9-11
<i>Discoaster nodifer</i> (Bramlette & Riedel, 1954) Bukry 1973	NP15-22
<i>Discoaster saipanensis</i> Bramlette & Riedel 1954	NP15-20
<i>Discoaster septemradiatus</i> (Klumpp 1953) Martini 1958	NP12-14
<i>Discoaster sublodoensis</i> Bramlette & Sullivan 1961	NP14-15
<i>Discoaster tani</i> Bramlette & Riedel 1954	NP16-22
<i>Discoaster</i> sp.	
<i>Discolithina multipora</i> (Kamptner 1948) Martini, 1965	Eocene – Miocene
<i>Discolithina plana</i> (Bramlette & Sullivan, 1961) Perch-Nielsen 1971	?Palaeogene
<i>Discolithina</i> sp.	
<i>Eiffellithus eximius</i> (Sover 1966) Perch-Nielsen 1968	Turonian – Campanian
<i>Eiffellithus</i> sp.	
<i>Eiffellithus turriseiffelii</i> (Deflandre <i>in</i> Deflandre & Fert 1954) Reinhardt 1965	Upper Albian – Maastrichtian
<i>Helicosphaera ampliaptera</i> Bramlette & Wilcoxon 1967	NN2-4
<i>Helicosphaera carteri</i> (Wallich 1877) Kamptner 1954	NN1 – recent
<i>Helicosphaera compacta</i> Bramlette & Wicoxon 1967	Middle Eocene – NP24
<i>Helicosphaera euphratis</i> Haq 1966	Middle Eocene – Miocene
<i>Helicosphaera intermedia</i> Martini 1965	Middle Eocene – Miocene
<i>Helicosphaera obliqua</i> Bramlette & Wilcoxon 1967	NP24 – NN6
<i>Helicosphaera seminulum</i> Bramlette & Sullivan 1961	Lower – Middle Eocene
<i>Heliolithus kleinpellii</i> Sullivan 1964	NP6-9
<i>Isthmolithus recurvus</i> (Deflandre <i>in</i> Deflandre & Fert 1954)	NP 20-22 (marker of base NP20; Martini, 1971)
<i>Lanternithus minutus</i> Stradner 1962	NP16-22
<i>Lophodolithus nascens</i> Bramlette & Sullivan 1961	NP9-15
<i>Markalius inversus</i> (Deflandre <i>in</i> Deflandre & Fert 1954) Bramlette & Martini 1964	Cretaceous – Eocene
<i>Marthasterites</i> sp.	Upper Cretaceous
<i>Micrantholithus vesper</i> Deflandre 1954	Eocene – Miocene
<i>Microrhabdulus</i> sp.	Cenomanian – Maastrichtian
<i>Micula</i> sp.	Coniacian – Maastrichtian
<i>Nannoconus steinmanni</i> Kamptner 1931	Uppermost Jurassic – Lower Cretaceous
<i>Nannoterrina</i> sp.	NP15
<i>Neococcolithes dubius</i> (Deflandre <i>in</i> Deflandre & Fert 1954) Black 1967	NP13-16 (?17-18)
<i>Pemma papillatum</i> Martini 1959	Middle Eocene
<i>Pemma rotundum</i> Klumpp 1953	Middle Eocene
<i>Pemma</i> sp.	Middle Eocene
<i>Reticulofenestra bisecta</i> (Hay, Mohler & Wade 1966) Roth 1970	NP16-25 (or NN1)
<i>Reticulofenestra haqii</i> Backman 1978	NN2-15
<i>Reticulofenestra lockeri</i> Müller 1970	NP23 rare, NP24 – ?NN1
<i>Reticulofenestra placomorpha</i> (Kamptner 1948) Stradner <i>in</i> Stradner & Edwards 1968 [actual valid synonym: <i>R. umbilica</i> (Levin 1965) Martini & Ritzkowski 1968]	NP16-22
<i>Reticulofenestra pseudoumbilicus</i> (Gartner 1967) Gartner 1969	NN4-15 (<7µm occurs from NN5 in the Mediterranean)
<i>Rhabdolithus</i> sp.	
<i>Sphenolithus conicus</i> Bukry 1971	NP25 – NN3
<i>Sphenolithus furcatolithoides</i> Locker 1967	NP15-16
<i>Sphenolithus moriformis</i> (Brönnimann & Stradner 1960) Bramlette & Wilcoxon 1967	Lower Eocene – Miocene
<i>Sphenolithus radians</i> Deflandre <i>in</i> Deflandre & Fert 1954	Lower to Middle Eocene (rare in Upper Eocene)
<i>Sphenolithus</i> sp.	
<i>Sphenolithus</i> sp. (? <i>calyculus</i> : Bukry 1985)	<i>S. calyculus</i> : Palaeogene – NN1
<i>Sphenolithus spiniger</i> Bukry 1971	Middle Eocene

<i>Transversopontis pulcher</i> (Deflandre in Deflandre & Fert 1954) Hay, Mohler & Wade 1966	Eocene – Oligocene
<i>Transversopontis</i> sp.	
<i>Tribrachiatulus orthostylus</i> Shamrai 1963	NP11-12 (?13-14)
<i>Umbilicosphaera rotula</i> (Kamptner 1956) Varol 1982	NN2-16
<i>Uniplanarius gothicus</i> (Deflandre, 1959) Hattner & Wise, 1980	Santonian – Maastrichtian
<i>Watznaueria barnesae</i> (Black 1959) Perch-Nielsen 1968	Bajocian – Maastrichtian
<i>Zeughrabdotos embergeri</i> (Noël 1958) Perch-Nielsen 1984	Tithonian – Maastrichtian
<i>Zeughrabdotos</i> sp.	
<i>Zygrhablithus bijugatus</i> (Deflandre in Deflandre & Fert 1954) Deflandre 1959	Eocene – NP25

---

*Note:* Stratigraphic ranges of species taken from the following sources. Cretaceous: Burnett (1998) and Perch-Nielsen (1985a); Palaeogene: Perch-Nielsen (1985b) and Baldi-Beke (1977, 1984); Neogene: Fornaciari *et al.* (1996), Fornaciari & Rio (1996) and Young (1998).

*Geographic position of sampling localities for calcareous nannofossils (Chapter 5)*

Area	Sample	Locality	Latitude (N)	Longitude (E)
Istria	TD11	Dekani	45° 33' 4.3"	13° 48' 25.0"
	TD13	Izola	45° 31' 58.5"	13° 38' 24.2"
	TD15	Korte	45° 29' 14.7"	13° 40' 14.7"
	TD16	Babiči	45° 30' 55.0"	13° 46' 55.0"
	TD18	Korte	45° 29' 35.3"	13° 40' 35.3"
	MOM-3	Momjan	45° 26' 3.2"	13° 42' 18.5"
	TD22	Momjan	45° 25' 8.0"	13° 42' 8.0"
	BNE-1	Zrenj-Baredine	45° 25' 14.6"	13° 53' 32.3"
	KSG-1	Kašćerga	45° 18' 38.9"	13° 54' 46.2"
	PIC-2	Pičan	45° 12' 16.2"	14° 2' 46.2"
	TD171	Lukačići	45° 10' 53.5"	14° 0' 25.9"
	TD173	Škrbani	45° 10' 17.8"	14° 0' 54.7"
	TD177	Baštini near Draguč	45° 20' 16.2"	14° 0' 18.2"
	TD178	Baštini near Draguč	45° 20' 16.2"	14° 0' 18.2"
Northern Kvarner:	TD28	Draga Bašćanska	44° 59' 34.0"	14° 43' 0.7"
Krk Island + nearby mainland areas	TD29	Bribir (road crossing Grižane/Selce)	45° 13' 8.8"	14° 41' 31.1"
	TD30	Bribir (Štale)	45° 9' 59.9"	14° 45' 11.9"
Northern Kvarner:	TD32	Rab	44° 46' 11.9"	14° 45' 21.1"
Rab Island	TD35	Lopar	44° 50' 23.8"	14° 43' 10.9"
	TD37	Dumići	44° 48' 12.9"	14° 42' 29.9"
Pag Island	TD261	Stara Vas, 10 km SE of Pag town	44° 22' 53.5"	15° 9' 12.1"
	TD262	Stara Vas, 10 km SE of Pag town	44° 22' 53.5"	15° 9' 12.1"
	TD265	Stara Vas, 10 km SE of Pag town	44° 22' 51.2"	15° 9' 8.0"
	TD269	coastal cliffs at the SE tip of Pag Island, near Vlašići	44° 19' 5.1"	15° 13' 39.7"
	TD272	coastal cliffs at the SE tip of Pag Island, near Vlašići	44° 19' 4.8"	15° 13' 38.8"
Northern Dalmatia (Ravni-Kotari)	TD251	Šopot railway cut near Benkovac	44° 1' 24.1"	15° 35' 36.5"
	TD253	Šopot railway cut near Benkovac	44° 1' 25.5"	15° 35' 42.5"
	TD255	Šopot railway cut near Benkovac	44° 1' 25.5"	15° 35' 43.2"
	TD257	Šopot railway cut near Benkovac	44° 1' 27.1"	15° 35' 50.6"
	TD260	Zagreb-Split motorway, 3 km SSW of Islam Latinski exit	44° 10' 21.2"	15° 25' 33.5"
Central Dalmatia	TD227	Mravince, 200 m E of the limestone olistolith	43° 32' 9.3"	16° 30' 41.5"
	TD229	Mravince, marl quarry	43° 32' 16.0"	16° 31' 3.9"
	TD232	Mravince abandoned quarry near police	43° 32' 7.3"	16° 31' 26.8"
	TD233	Mravince abandoned quarry near police	43° 32' 3.6"	16° 31' 23.0"
	TD234	Mravince abandoned quarry near police	43° 32' 3.6"	16° 31' 23.0"
	TD236	Jadro creek right side, larger one out of 2 quarries	43° 32' 34.9"	16° 31' 17.0"
	TD240	Jadro valley, Vrilo Jadro	43° 32' 39.3"	16° 31' 31.6"
	TD246	Gizdići near Klis	43° 33' 27.1"	16° 30' 14.5"
	TD248	Solin, Voljak Street	43° 33' 14.9"	16° 29' 26.6"
	TD249	Solin, Voljak Street	43° 33' 14.9"	16° 29' 26.6"
	TD52	Živogošće	43° 11' 15.6"	17° 9' 43.8"
	TD55	Omiš quarry, E wall	43° 25' 33.8"	16° 42' 53.0"
	TD56	Omiš quarry, E wall	43° 25' 33.8"	16° 42' 53.0"
	TD53	Medići near Omiš	43° 24' 19.9"	16° 48' 20.4"
TD54	Mala Luka near Omiš	43° 25' 10.0"	16° 42' 59.6"	
Dalm.-Herz. Zone	TD100	Spuš	42° 31' 31.3"	19° 11' 2.0"
	TD109	Medun	42° 28' 16.1"	19° 21' 51.7"
	TD140	Crnići	43° 7' 34.1"	17° 51' 32.3"

(continued)	Sample	Locality	Latitude (N)	Longitude (E)
	TD47	Dubravka	42° 31' 1.4"	18° 25' 17.1"
	TD49	Dubravka	42° 31' 57.8"	18° 24' 56.9"
	TD38	Sutorina	42° 28' 34.1"	18° 28' 45.2"
	TD136	Sutorina	42° 28' 20.0"	18° 25' 36.9"
	TD138	Sutorina	42° 28' 20.0"	18° 25' 36.9"
	TD39	Tivat	42° 24' 54.6"	18° 43' 6.6"
	TD127	Radanovići	42° 20' 45.3"	18° 30' 37.9"
	TD134	Radanovići	42° 20' 50.1"	18° 30' 43.7"
	TD99	Stari Bar	42° 5' 19.5"	19° 8' 34.3"
	TD43	Zaljevo	42° 4' 23.0"	19° 7' 58.7"
	TD116	Ulcinj	41° 40' 51.4"	19° 0' 52.0"
	TD120	Donja Klezna - Gornja Klezna	41° 40' 46.3"	19° 0' 19.6"
	TD123	Donja Klezna - Gornja Klezna	41° 40' 46.3"	19° 0' 19.6"
	TD125	Donja Klezna - Gornja Klezna	41° 40' 42.2"	19° 0' 18.8"
	TD93	Kravari	42° 3' 51.9"	19° 21' 34.4"
	TD45	Vladimir	42° 0' 39.1"	19° 17' 15.8"

Appendix 6-1

[Table is two pages wide - note facing pages]

Detrital zircon FT-U/Pb double dating analytical results

Notes: Tect: tectonic position of the sample; D: Outer Dinaride foreland basin; S: Sava Zone. N<sub>s</sub>: spontaneous track count; ρ<sub>s</sub>: spontaneous track density (×10<sup>5</sup> tr/cm<sup>2</sup>); N<sub>i</sub>: induced track count; ρ<sub>i</sub>: induced track density (×10<sup>5</sup> tr/cm<sup>2</sup>). Peak: length of the laser ablation signal extracted for the isotope ratio calculation. p: error correlation of <sup>207</sup>Pb/<sup>235</sup>U and <sup>206</sup>Pb/<sup>238</sup>U ratios. Conco.: concordance expressed as [<sup>207</sup>Pb/<sup>235</sup>U age]/[<sup>206</sup>Pb/<sup>238</sup>U age] × 100. Peak: length of the laser ablation signal extracted for the isotope ratio calculation. N.dia: nominal pit diameter – measured diameters are c. 10% smaller at the sample surface.

FT data

sample	tect	FT mount	LA	spontaneous		induced		age	± 1σ	U	<sup>207</sup> Pb	<sup>206</sup> Pb	peak	n.dia	line	U	<sup>206</sup> Pb/ <sup>238</sup> U	± 1σ	<sup>207</sup> Pb/ <sup>235</sup> U	± 1σ	<sup>207</sup> Pb/ <sup>206</sup> Pb
		grain #	exp. #	N <sub>s</sub>	ρ <sub>s</sub>	N <sub>i</sub>	ρ <sub>i</sub>	(Ma)	(Ma)	(ppm)	(cps)	(cps)	(s)	(μm)	(μm)	(ppm)	(%)	(%)	(%)	(%)	
UST2	D	Z413A-01	no23a05	63	106.816	48	81.384	64.1	12.3	308	1457	27117	28.9	40	50	417	0.0471	0.62	0.3424	1.24	0.0529
UST2	D	Z413A-02	no23a06	129	218.718	26	44.083	239.1	51.6	167	392	7020	20.4	40	50	103	0.0476	1.32	0.3595	2.70	0.0550
UST2	D	Z413A-03	no23a07	58	65.559	29	32.779	97.4	22.2	124	1278	19281	23.6	40	46	102	0.1302	0.79	1.1821	1.46	0.0653
UST2	D	Z413A-04	no23a08	39	99.186	30	76.297	63.5	15.5	289	1374	22486	37.5	40	38	154	0.0993	0.92	0.8133	1.39	0.0602
UST2	D	Z413A-05	no23a09	72	91.556	58	73.754	60.7	10.8	279	1883	28793	27.9	40	40	172	0.1129	0.82	0.9880	1.31	0.0645
UST2	D	Z413A-06	no23a10	79	89.296	14	15.825	271.2	78.8	60	2655	27854	24.7	40	40	73	0.2540	0.95	3.3085	1.85	0.0940
UST2	D	Z413A-07	no23a11	48	54.256	27	30.519	86.7	20.9	116	717	12011	26.8	40	40	89	0.0888	0.82	0.7176	2.29	0.0589
UST2	D	Z413A-08	no23a12	87	147.508	58	98.338	73.2	12.5	372	740	14038	25.7	40	42	213	0.0427	0.98	0.3058	1.89	0.0520
UST2	D	Z413A-09	no23a13	87	98.338	30	33.91	140.8	29.9	128	280	5108	12.9	40	45	77	0.0422	1.13	0.3119	5.29	0.0540
UST2	D	Z413A-10	no23a14	125	211.936	39	66.124	155.4	28.7	250	869	16190	19.3	55	60	141	0.0451	0.45	0.3280	1.87	0.0529
UST2	D	Z413A-11	no23a15	98	124.619	50	63.581	95.5	16.7	241	2025	34881	31.1	55	55	168	0.0805	0.62	0.6282	0.75	0.0573
UST2	D	Z413A-12	no23a16	54	68.667	44	55.951	60.0	12.2	212	993	16822	17.2	40	50	144	0.0714	1.00	0.5661	1.51	0.0582
UST2	D	Z413A-13	no23b05	123	208.545	18	30.519	327.0	82.7	116	562	8842	20.4	55	70	52	0.0751	0.65	0.6396	2.69	0.0626
UST2	D	Z413A-14	no23b06	70	89.013	20	25.432	169.6	43.1	96	146	2792	37.5	40	45	50	0.0396	1.18	0.2773	3.87	0.0515
UST2	D	Z413A-15	no23b07	99	125.89	39	49.593	123.4	23.5	188	663	11403	15	40	36	100	0.0811	1.65	0.6322	1.64	0.0573
UST2	D	Z413A-16	no23b08	51	86.47	23	38.996	107.9	27.2	148	266	5033	27.9	40	48	95	0.0377	1.49	0.2655	3.04	0.0521
UST2	D	Z413A-17	no23b09	105	178.026	24	40.692	211.3	48.0	154	463	8490	30	40	42	101	0.0599	1.08	0.4374	2.27	0.0537
UST2	D	Z413A-18	no23b10	63	80.112	43	54.68	71.5	14.2	207	824	14575	12.9	40	40	143	0.0729	1.07	0.5657	2.00	0.0566
UST2	D	Z413A-19	no23b11	81	137.335	41	69.515	96.3	18.5	263	2086	34616	22.5	40	40	251	0.0983	0.74	0.7935	1.26	0.0593
UST2	D	Z413A-20	no23b12	157	266.192	33	55.951	229.4	44.1	212	3202	24923	19.3	40	50	46	0.3862	1.15	6.6467	1.73	0.1264
UST2	D	Z413A-21	no23b13	44	74.602	11	18.65	193.4	65.3	71	378	6647	27.9	40	52	121	0.0394	1.64	0.2991	2.96	0.0560
UST2	D	Z413A-22	no23b14	109	184.808	18	30.519	290.6	74.1	116	422	7275	16.1	40	55	64	0.0811	1.60	0.6318	3.45	0.0571
UST2	D	Z413A-23	no23b15	91	231.434	12	30.519	361.9	111.4	116	661	9732	22.5	40	40	53	0.1306	1.10	1.1882	1.68	0.0667
UST2	D	Z413A-25	no23b16	46	77.993	12	20.346	185.5	60.2	77	421	7642	15	55	70	58	0.0587	2.06	0.4298	2.35	0.0541
UST2	D	Z413A-25	no23c05	64	108.511	15	25.432	206.1	59.3	96	247	4532	15	40	50	55	0.0617	1.34	0.4746	2.55	0.0540
UST2	D	Z413A-26	no23c06	87	147.508	24	40.692	175.5	40.6	154	718	12107	17.2	40	42	103	0.0886	0.97	0.6948	2.50	0.0587
UST2	D	Z413A-27	no23c07	91	154.29	19	32.214	230.9	58.4	122	601	10156	17.2	40	40	89	0.0864	1.46	0.7112	2.70	0.0585
UST2	D	Z413A-28	no23c08	123	208.545	19	32.214	310.2	76.7	122	602	9820	21.4	40	37	96	0.0780	0.96	0.6518	1.92	0.0603
UST2	D	Z413A-29	no23c09	133	225.5	18	30.519	352.9	88.9	116	3160	33874	20.4	40	70	102	0.2548	0.89	3.2451	1.46	0.0921
UST2	D	Z413A-30	no23c10	92	155.985	38	64.429	117.8	22.8	244	486	9470	19.3	55	70	173	0.0265	1.24	0.1869	2.07	0.0506
CRN1	D	Z415A-01	no27a05	72	122.075	48	81.384	72.1	13.5	313	6579	89592	27.9	40	50	389	0.1660	0.58	1.6517	0.86	0.0723
CRN1	D	Z415A-02	no27a06	58	98.338	37	62.733	75.4	15.9	241	1819	31836	27.9	40	42	311	0.0742	0.81	0.5670	0.98	0.0562
CRN1	D	Z415A-03	no27a07	74	188.199	24	61.038	147.4	34.7	235	1400	21121	23.6	30	35	275	0.1337	0.58	1.2148	1.73	0.0652
CRN1	D	Z415A-04	no27a08	107	181.417	42	71.211	122.0	22.3	274	283	5195	11.8	40	45	295	0.0129	1.84	0.0962	3.03	0.0535
CRN1	D	Z415A-05	no27a09	60	67.82	18	20.346	159.2	42.9	78	101	1760	16.1	30	35	245	0.0126	2.41	0.0974	4.95	0.0566
CRN1	D	Z415A-06	no27a10	114	193.286	27	45.778	201.0	43.2	176	1116	17959	17.2	40	50	132	0.1003	0.69	0.8503	1.82	0.0611
CRN1	D	Z415A-07	no27a11	84	142.421	51	86.47	79.2	14.1	332	303	6256	22.5	40	50	355	0.0131	1.45	0.0875	2.27	0.0476
CRN1	D	Z415A-08	no27a12	68	115.293	47	79.688	69.6	13.3	306	375	5776	10.7	40	30	321	0.0134	1.62	0.1129	3.05	0.0637
CRN1	D	Z415A-09	no27a13	118	200.068	27	45.778	207.9	44.5	176	319	6001	24.7	40	40	112	0.0401	1.83	0.2779	2.51	0.0521
CRN1	D	Z415A-10	no27a14	50	127.162	18	45.778	132.9	36.6	176	627	11781	24.7	40	33	211	0.0420	1.00	0.2951	2.01	0.0522
CRN1	D	Z415A-11	no27a15	79	100.458	32	40.692	118.3	24.9	156	1019	18504	20.4	40	40	188	0.0745	1.04	0.5459	2.12	0.0540
CRN1	D	Z415A-12	no27a16	99	125.89	18	22.889	260.6	67.0	88	3448	24379	30	55	55	29	0.4063	1.07	7.4666	1.61	0.1385
CRN1	D	Z415A-14	no27b06	66	111.902	21	35.605	150.2	37.7	137	650	12358	30	55	48	154	0.0385	1.10	0.2768	1.96	0.0520
CRN1	D	Z415A-15	no27b07	42	71.211	24	40.692	84.1	21.6	156	695	13091	17.2	55	55	153	0.0413	1.09	0.2984	1.53	0.0525
CRN1	D	Z415A-16	no27b08	101	171.244	33	55.951	146.3	29.5	215	443	8159	20.4	40	30	160	0.0396	0.82	0.2904	2.66	0.0537
CRN1	D	Z415A-17	no27b09	60	101.729	26	44.083	110.6	26.1	169	1068	18088	16.1	40	32	184	0.0764	1.20	0.6182	1.53	0.0584
CRN1	D	Z415A-18	no27b10	89	150.899	72	122.075	59.5	9.5	469	370	7330	24.7	40	50	447	0.0128	0.98	0.0890	2.27	0.0500
CRN1	D	Z415A-19	no27b11	109	184.808	27	45.778	192.3	41.5	176	203	3561	17.2	40	40	67	0.0418	1.30	0.3210	4.57	0.0565
CRN1	D	Z415A-20	no27b12	69	87.742	68	86.47	48.9	8.4	332	1339	25713	21.4	55	55	310	0.0409	0.84	0.2908	1.20	0.0515
CRN1	D	Z415A-21	no27b13	65	110.207	33	55.951	94.5	20.3	215	925	17612	20.4	40	38	329	0.0424	0.69	0.3005	1.12	0.0520
CRN1	D	Z415A-22	no27b14	103	174.635	26	44.083	188.8	41.6	169	549	9876	20.4	40	40	210	0.0374	0.94	0.2857	2.47	0.0550
CRN1	D	Z415A-23	no27b15	69	116.989	38	64.429	87.2	17.7	248	331	5623	15	40	40	366	0.0123	1.09	0.0988	5.19	0.0584
CRN1	D	Z415A-24	no27b16	107	181.417	23	38.996	221.1	51.0	150	818	14443	19.3	40	45	180	0.0645	0.89	0.4972	1.87	0.0562
CRN1	D	Z415A-25	no27c05	57	96.643	36	61.038	76.1	16.3	235	1379	24060	26.8	40	38	248	0.0755	0.55	0.5928	1.61	0.0568
CRN1	D	Z415A-26	no27c06	102	172.94	58	98.338	84.5	14.0	378	181	3656	22.5	40	40	225	0.0126	2.03	0.0870	2.67	0.0489
CRN1	D	Z415A-27	no27c07	49	83.079	56	94.947	42.2	8.3	365	209	3672	27.9	55	50	272	0.0066	1.21	0.0511	3.87	0.0565
CRN1	D	Z415A-28	no27c08	79	133.944	66															

Appendix 6-1

[Table is two pages wide - note facing pages]

Detrital zircon FT-U/Pb double dating analytical results

LA-ICPMS apparent ages												
$\pm 1\sigma$ (%)	$^{208}\text{Pb}/^{232}\text{Th}$	$\pm 1\sigma$ (%)	$\rho$	$^{206}\text{Pb}/^{238}\text{U}$ $\pm 2\sigma$ age (Ma) (Ma)	$^{207}\text{Pb}/^{235}\text{U}$ $\pm 2\sigma$ age (Ma) (Ma)	$^{207}\text{Pb}/^{206}\text{Pb}$ $\pm 2\sigma$ age (Ma) (Ma)	$^{208}\text{Pb}/^{232}\text{Th}$ $\pm 2\sigma$ age (Ma) (Ma)	Conco. (%)				
1.06	0.0154	1.42	0.52	296	4	299	6	324	48	308	9	101.0
2.77	0.0157	1.95	0.19	300	8	312	15	410	124	315	12	104.0
1.25	0.0405	1.04	0.52	789	12	792	16	784	54	802	16	100.4
1.08	0.0315	0.97	0.63	610	11	604	13	610	46	627	12	99.0
1.19	0.0373	1.71	0.45	690	11	698	13	756	50	741	25	101.2
1.03	0.0774	0.91	0.93	1459	25	1483	29	1506	38	1506	27	101.6
1.87	0.0277	1.82	0.64	548	9	549	19	562	82	552	20	100.2
2.13	0.0140	2.04	0.01	269	5	271	9	282	96	282	11	100.7
5.13	0.0137	1.86	0.25	267	6	276	26	370	230	275	10	103.4
1.71	0.0142	2.18	0.46	284	3	288	9	324	78	284	12	101.4
0.98	0.0257	0.79	0.01	499	6	495	6	500	42	512	8	99.2
1.77	0.0227	2.19	0.05	445	9	456	11	538	78	453	20	102.5
1.63	0.0278	2.54	0.43	467	6	502	21	694	70	555	28	107.5
3.91	0.0132	2.96	0.12	250	6	249	17	262	180	265	16	99.6
2.36	0.0258	4.02	0.03	502	16	497	13	502	104	515	41	99.0
3.33	0.0122	2.01	0.04	239	7	239	13	288	152	245	10	100.0
2.15	0.0199	1.90	0.35	375	8	368	14	358	98	399	15	98.1
2.08	0.0229	3.95	0.19	454	9	455	15	436	92	457	36	100.2
1.16	0.0307	1.49	0.42	605	9	593	11	578	50	611	18	98.0
1.27	0.1164	2.22	0.68	2105	41	2066	30	2048	46	2226	93	98.1
2.91	0.0124	1.49	0.31	249	8	266	14	450	130	248	7	106.8
3.07	0.0249	2.92	0.46	503	16	497	27	494	136	498	29	98.8
1.58	0.0416	1.91	0.42	792	16	795	18	828	66	823	31	100.4
2.35	0.0176	2.92	0.44	368	15	363	14	374	106	352	20	98.6
2.51	0.0195	2.58	0.29	386	10	394	17	368	114	390	20	102.1
2.31	0.0270	1.49	0.38	547	10	536	21	554	102	538	16	98.0
2.60	0.0273	1.98	0.34	534	15	545	23	546	114	545	21	102.1
1.62	0.0261	2.03	0.54	484	9	510	15	614	70	520	21	105.4
1.12	0.0745	1.78	0.64	1463	23	1468	23	1468	42	1452	50	100.3
2.88	0.0091	3.35	0.48	168	4	174	7	224	132	183	12	103.6
0.69	0.0523	1.62	0.60	990	11	990	11	994	30	1030	33	100.0
0.92	0.0244	2.88	0.49	461	7	456	7	460	42	487	28	98.9
1.26	0.0388	2.01	0.87	809	9	807	19	780	54	770	30	99.8
3.41	0.0042	2.64	0.08	83	3	93	5	350	154	85	4	112.0
3.59	0.0044	7.25	0.73	81	4	94	9	472	158	88	13	116.0
1.46	0.0297	2.23	0.66	616	8	625	17	640	64	591	26	101.5
1.89	0.0040	1.51	0.56	84	2	85	4	78	90	81	2	101.2
3.30	0.0060	2.61	0.10	86	3	109	6	730	140	121	6	126.7
2.29	0.0126	2.51	0.48	253	9	249	11	290	104	253	13	98.4
2.20	0.0128	1.98	0.05	265	5	263	9	292	100	257	10	99.2
2.15	0.0224	1.28	0.22	463	9	442	15	368	96	448	11	95.5
0.91	0.1164	1.76	0.84	2198	40	2169	29	2208	32	2225	74	98.7
1.83	0.0129	1.29	0.39	243	5	248	9	284	84	258	7	102.1
1.85	0.0138	1.29	0.03	261	6	265	7	306	84	276	7	101.5
2.26	0.0121	2.56	0.61	250	4	259	12	358	102	243	12	103.6
1.45	0.0219	2.64	0.46	474	11	489	12	544	64	438	23	103.2
2.29	0.0039	1.97	0.20	82	2	87	4	194	106	79	3	106.1
3.61	0.0125	1.98	0.80	264	7	283	23	472	160	252	10	107.2
1.36	0.0131	1.15	0.15	258	4	259	5	264	64	263	6	100.4
1.30	0.0129	1.52	0.03	268	4	267	5	286	58	259	8	99.6
2.46	0.0120	1.99	0.20	237	4	255	11	412	110	241	10	107.6
4.17	0.0041	4.35	0.95	79	2	96	9	544	182	82	7	121.5
1.98	0.0194	1.28	0.11	403	7	410	13	458	88	389	10	101.7
1.41	0.0228	1.65	0.51	469	5	473	12	482	62	456	15	100.9
2.50	0.0039	3.18	0.46	81	3	85	4	142	118	79	5	104.9
3.74	0.0022	1.99	0.26	42	1	51	4	470	164	44	2	121.4
2.71	0.0037	2.12	0.58	77	2	79	5	110	128	74	3	102.6
0.71	0.0583	0.63	0.66	1182	14	1199	13	1226	26	1145	14	101.4
0.72	0.0635	0.80	0.77	1289	17	1280	16	1320	28	1244	19	99.3
2.50	0.0231	4.15	0.24	453	8	449	19	458	110	461	38	99.1
1.41	0.0189	1.18	0.57	377	9	380	11	384	62	378	9	100.8
1.81	0.0139	1.55	0.18	262	4	291	9	552	80	278	9	111.1
2.83	0.0188	2.75	0.14	372	7	385	16	456	126	376	20	103.5
3.13	0.0154	4.46	0.28	298	10	310	17	510	138	309	27	104.0
0.99	0.0342	1.91	0.66	675	10	680	13	690	42	680	26	100.7
1.73	0.0294	1.96	0.08	583	10	578	14	526	76	586	23	99.1
1.93	0.0128	1.97	0.08	270	5	266	8	240	90	256	10	98.5
2.62	0.0262	1.73	0.56	558	12	559	26	590	114	523	18	100.2
2.36	0.0129	2.00	0.14	276	5	270	11	250	108	258	10	97.8
4.67	0.0043	4.50	0.22	82	3	88	6	274	214	87	8	107.3
3.71	0.0037	3.04	0.40	81	3	83	5	106	174	75	5	102.5
2.37	0.0130	1.71	0.22	278	5	270	11	214	110	261	9	97.1

Appendix 6-1

[Table is two pages wide - note facing pages]

Detrital zircon FT-U/Pb double dating analytical results

Notes: Tect: tectonic position of the sample; D: Outer Dinaride foreland basin; S: Sava Zone.  $N_s$ : spontaneous track count;  $\rho_s$ : spontaneous track density ( $\times 10^5$  tr/cm<sup>2</sup>);  $N_i$ : induced track count;  $\rho_i$ : induced track density ( $\times 10^5$  tr/cm<sup>2</sup>). Peak: length of the laser ablation signal extracted for the isotope ratio calculation. p: error correlation of <sup>207</sup>Pb/<sup>235</sup>U and <sup>206</sup>Pb/<sup>238</sup>U ratios. Conco.: concordance expressed as  $[\frac{^{207}\text{Pb}/^{235}\text{U age}}{^{206}\text{Pb}/^{238}\text{U age}}] \times 100$ . Peak: length of the laser ablation signal extracted for the isotope ratio calculation. N.dia: nominal pit diameter – measured diameters are c. 10% smaller at the sample surface.

FT data

sample	tect	FT mount	LA	spontaneous		induced		age	$\pm 1\sigma$	U	<sup>207</sup> Pb	<sup>206</sup> Pb	peak	n.dia	line	U	<sup>206</sup> Pb/ <sup>238</sup> U	$\pm 1\sigma$	<sup>207</sup> Pb/ <sup>235</sup> U	$\pm 1\sigma$	<sup>207</sup> Pb/ <sup>206</sup> Pb
		grain #	exp. #	$N_s$	$\rho_s$	$N_i$	$\rho_i$	(Ma)	(Ma)	(ppm)	(cps)	(cps)	(s)	( $\mu\text{m}$ )		(ppm)		(%)	(%)	(%)	
CRN1	D	Z415B-19	no27e11	68	115.293	17	28.823	189.9	51.6	111	221	3843	13.9	40	36	77	0.0430	1.95	0.3337	4.80	0.0568
CRN1	D	Z415B-20	no27e12	81	137.335	31	52.56	124.7	26.4	203	362	7053	15	40	33	214	0.0288	1.16	0.1971	2.95	0.0508
CRN1	D	Z415B-28	no27f08	93	118.26	53	67.396	84.0	14.5	260	251	5441	21.4	55	62	271	0.0128	1.19	0.0811	3.35	0.0456
CRN1	D	Z415B-29	no27f09	78	99.186	65	82.655	57.5	9.7	319	1058	19930	17.2	55	55	314	0.0407	1.54	0.2958	1.07	0.0524
TD225	S	Z469A-01	no26a05	49	49.847	57	57.986	46.8	9.2	197	209	4296	12.9	40	48	231	0.0133	2.13	0.0870	3.14	0.0478
TD225	S	Z469A-03	no26a07	81	91.556	35	39.561	125.3	25.4	135	725	12789	40.7	40	40	129	0.0723	1.10	0.5614	1.77	0.0557
TD225	S	Z469A-04	no26a08	155	131.4	50	42.387	167.3	27.4	144	331	6536	19.3	40	50	114	0.0420	2.82	0.2954	4.37	0.0498
TD225	S	Z469A-05	no26a09	166	140.726	117	99.186	77.1	9.4	337	2433	43097	21.4	55	48	266	0.0747	0.77	0.5719	0.84	0.0555
TD225	S	Z469A-06	no26a10	172	109.359	114	72.482	82.0	10.0	247	193	3854	23.6	40	50	214	0.0134	1.24	0.0913	2.66	0.0493
TD225	S	Z469A-07	no26a11	58	65.559	48	54.256	65.7	12.9	185	174	3675	26.8	40	38	219	0.0126	1.27	0.0821	4.04	0.0465
TD225	S	Z469A-09	no26a13	157	133.096	120	101.729	71.1	8.7	346	3026	48674	26.8	40	50	367	0.1007	1.41	0.8430	1.35	0.0612
TD225	S	Z469A-10	no26a14	53	67.396	46	58.494	62.7	12.7	199	343	5492	27.9	40	45	43	0.0988	1.78	0.8086	3.38	0.0615
TD225	S	Z469A-13	no26b05	75	47.686	34	21.617	119.5	24.8	74	565	8467	19.3	40	45	53	0.1292	1.38	1.1825	2.87	0.0659
TD225	S	Z469A-14	no26b06	97	82.231	58	49.169	90.8	15.2	167	1515	24305	27.9	40	40	195	0.1008	1.54	0.8553	1.70	0.0616
TD225	S	Z469A-15	no26b07	81	51.501	73	46.414	60.4	9.8	158	3035	27796	25.7	40	42	89	0.2543	1.62	3.7106	2.76	0.1078
TD225	S	Z469A-16	no26b08	93	78.84	52	44.083	97.0	16.9	150	763	12475	27.9	40	42	99	0.1028	1.09	0.8600	1.94	0.0604
TD225	S	Z469A-17	no26b09	43	54.68	35	44.507	66.8	15.3	151	619	10955	19.3	40	45	120	0.0748	1.41	0.5858	3.82	0.0557
TD225	S	Z469A-18	no26b10	138	233.978	46	77.993	161.9	27.7	265	1690	29809	31.1	40	40	331	0.0742	1.43	0.5775	1.63	0.0559
TD225	S	Z469A-19	no26b11	100	84.774	81	68.667	67.1	10.1	234	394	6419	18.2	30	34	134	0.0943	1.26	0.7636	3.19	0.0605
TD225	S	Z469A-20	no26b12	162	206.002	55	69.939	159.0	25.0	238	1186	20584	18.2	40	45	236	0.0724	1.30	0.5626	1.83	0.0567
TD225	S	Z469A-21	no26b13	184	155.985	65	55.103	152.9	22.2	187	755	13647	23.6	40	58	148	0.0767	2.60	0.5504	3.15	0.0544
TD225	S	Z469A-22	no26b14	75	63.581	33	27.976	123.1	9.8	95	604	8998	30	40	38	52	0.1460	1.38	1.3010	2.17	0.0660
TD225	S	Z469A-24	no26b16	74	47.05	69	43.871	58.4	9.8	149	424	7852	16.1	40	38	131	0.0503	1.77	0.3695	3.95	0.0530
TD225	S	Z469A-25	no26c05	130	110.207	51	43.235	137.9	22.9	147	581	10430	27.9	40	40	121	0.0717	1.93	0.5436	2.47	0.0552
TD225	S	Z469A-26	no26c06	60	81.384	16	20.346	215.0	60.2	69	500	8078	20.4	40	46	65	0.1036	1.64	0.8634	1.90	0.0614
TD225	S	Z469A-27	no26c07	94	79.688	64	54.256	79.8	13.0	185	738	12828	20.4	40	43	145	0.0733	1.11	0.5948	1.41	0.0570
TD225	S	Z469A-28	no26c08	113	127.727	56	63.298	109.4	18.0	215	1382	22763	19.3	40	35	207	0.0912	1.16	0.7454	1.42	0.0602
TD225	S	Z469A-29	no26c09	115	73.118	55	34.969	113.3	18.7	119	1116	15353	25.7	40	40	78	0.1632	0.67	1.6042	1.70	0.0720
TD225	S	Z469A-30	no26c10	88	89.522	52	52.899	91.8	16.2	180	8193	62823	24.7	40	32	146	0.3565	0.53	6.3927	0.97	0.1291
TD225	S	Z469B-01	no26d05	79	100.458	56	71.211	76.7	13.5	242	673	12158	30	40	45	177	0.0590	0.82	0.4514	2.06	0.0547
TD225	S	Z469B-03	no26d07	46	51.995	22	24.867	113.4	29.5	85	265	4335	33.2	30	35	94	0.0957	1.04	0.8228	3.18	0.0604
TD225	S	Z469B-04	no26d08	85	57.647	39	26.45	118.1	23.0	90	526	8670	17.2	40	50	75	0.1023	0.95	0.8614	2.78	0.0599
TD225	S	Z469B-05	no26d09	93	59.13	29	18.438	173.1	36.9	63	654	10020	16.1	40	32	78	0.1133	0.92	0.9995	3.07	0.0644
TD225	S	Z469B-10	no26d10	88	99.469	62	70.08	77.2	12.9	238	364	6746	25.7	40	35	146	0.0414	1.07	0.3048	2.57	0.0533
TD225	S	Z469B-07	no26d11	67	56.799	35	29.671	103.9	21.8	101	548	8470	32.2	40	34	64	0.1200	0.82	1.0569	2.62	0.0639
TD225	S	Z469B-08	no26d12	69	58.494	33	27.976	113.4	24.1	95	1016	15323	16.1	40	38	116	0.1200	1.07	1.0874	2.01	0.0654
TD225	S	Z469B-09	no26d13	140	142.421	44	44.761	171.7	29.9	152	2009	26851	26.8	40	43	151	0.1627	0.74	1.6545	1.84	0.0737
TD225	S	Z469B-10	no26d14	89	75.449	90	76.297	53.9	8.1	259	141	2765	17.2	40	37	208	0.0123	2.24	0.0851	3.24	0.0503
TD225	S	Z469B-12	no26d16	78	99.186	66	83.927	64.3	10.8	285	617	10473	26.8	30	40	275	0.0853	0.77	0.6712	1.92	0.0580
TD225	S	Z469B-13	no26e05	100	63.581	42	26.704	128.9	23.8	91	394	7445	21.4	55	60	104	0.0415	1.22	0.2919	2.60	0.0521
TD225	S	Z469B-15	no26e07	86	109.359	53	67.396	88.2	15.5	229	195	3800	26.8	40	35	264	0.0133	2.31	0.0913	3.15	0.0506
TD225	S	Z469B-16	no26e08	87	98.338	49	55.386	96.4	17.3	188	798	14591	17.2	40	35	224	0.0600	1.89	0.4632	2.73	0.0539
TD225	S	Z469B-18	no26e10	108	91.556	67	56.799	87.6	13.7	193	852	14128	18.2	40	38	147	0.0880	1.28	0.7182	2.30	0.0594
TD225	S	Z469B-19	no26e11	142	160.506	32	36.17	238.3	46.8	123	1554	21841	21.4	40	28	125	0.1599	0.79	1.5477	1.72	0.0701
TD225	S	Z469B-20	no26e12	82	92.687	46	51.995	96.8	17.9	177	170	3560	24.7	40	50	244	0.0133	1.52	0.0858	2.65	0.0470
TD225	S	Z469B-21	no26e13	70	89.013	19	24.161	198.4	51.5	82	766	12300	24.7	40	38	101	0.1109	1.05	0.8856	1.90	0.0613
TD225	S	Z469B-22	no26e14	62	52.56	30	25.432	112.1	25.0	86	521	7566	22.5	40	44	60	0.1138	0.95	1.0807	2.98	0.0678
TD225	S	Z469B-23	no26e15	89	75.449	83	70.363	58.4	9.0	239	721	11554	23.6	30	33	250	0.0995	0.80	0.8510	1.51	0.0615
TD225	S	Z469B-24	no26e16	139	141.404	57	57.986	132.0	20.9	197	1058	18445	23.6	40	36	226	0.0734	0.93	0.5758	1.57	0.0565
TD225	S	Z469B-25	no26f01	38	48.321	23	29.247	89.7	23.8	99	368	6048	15	40	34	59	0.0841	1.43	0.7073	2.42	0.0602
TD254	D	Z470A-01	no28a05	134	113.598	35	29.671	137.6	26.3	152	976	17019	17.2	40	55	210	0.0733	1.35	0.5690	1.37	0.0564
TD254	D	Z470A-03	no28a07	58	39.335	40	27.128	52.5	10.9	139	1121	20133	18.2	40	56	338	0.0549	1.27	0.4100	1.62	0.0548
TD254	D	Z470A-04	no28a08	176	59.681	75	25.432	84.7	11.8	130	733	13997	22.5	55	60	194	0.0419	0.87	0.2921	1.86	0.0516
TD254	D	Z470A-05	no28a09	118	100.034	33	27.976	128.6	25.5	143	783	13470	10.7	40	46	166	0.0760	1.19	0.6059	1.49	0.0573
TD254	D	Z470A-06	no28a10	49	31.155	21	13.352	84.2	22.1	68	315	5345	17.2	40	45	55	0.0926	1.87	0.7652	4.97	0.0581
TD254	D	Z470A-07	no28a11	60	50.865	26	22.041	83.3	19.7	113	227	4113	18.2	40	60	68	0.0576	1.22	0.4418	2.24</	

Appendix 6-1

[Table is two pages wide - note facing pages]

Detrital zircon FT-U/Pb double dating analytical results

LA-ICPMS apparent ages												
$\pm 1\sigma$ (%)	$^{208}\text{Pb}/^{232}\text{Th}$	$\pm 1\sigma$ (%)	$\rho$	$^{206}\text{Pb}/^{238}\text{U}$ $\pm 2\sigma$ age (Ma) (Ma)	$^{207}\text{Pb}/^{235}\text{U}$ $\pm 2\sigma$ age (Ma) (Ma)	$^{207}\text{Pb}/^{206}\text{Pb}$ $\pm 2\sigma$ age (Ma) (Ma)	$^{208}\text{Pb}/^{232}\text{Th}$ $\pm 2\sigma$ age (Ma) (Ma)			Conco. (%)		
5.38	0.0143	3.80	0.11	272	10	292	24	484	238	287	22	107.4
2.82	0.0089	2.54	0.31	183	4	183	10	230	130	179	9	100.0
3.27	0.0039	2.60	0.24	82	2	79	5	0	54	79	4	96.3
1.93	0.0126	1.31	0.06	257	8	263	5	304	88	253	7	102.3
3.55	0.0042	2.58	0.13	85	4	85	5	86	170	85	4	100.0
1.74	0.0236	1.42	0.34	450	10	452	13	440	76	471	13	100.4
3.59	0.0147	2.96	0.57	265	15	263	20	184	168	295	17	99.2
1.22	0.0252	3.80	0.15	465	7	459	6	432	56	503	38	98.7
3.49	0.0045	2.07	0.54	86	2	89	5	160	162	91	4	103.5
4.35	0.0042	4.09	0.10	81	2	80	6	24	124	85	7	98.8
1.32	0.0333	1.86	0.54	618	17	621	12	646	56	663	24	100.5
2.43	0.0298	4.04	0.72	607	21	602	31	656	104	594	47	99.2
2.93	0.0367	3.29	0.20	783	20	792	32	802	122	728	47	101.1
1.54	0.0307	1.12	0.55	619	18	628	16	658	68	611	13	101.5
1.99	0.0886	2.14	0.70	1460	42	1574	44	1762	74	1716	70	107.8
1.66	0.0322	1.84	0.52	631	13	630	18	616	72	640	23	99.8
2.69	0.0230	2.34	0.87	465	13	468	29	440	120	460	21	100.6
1.12	0.0256	3.41	0.74	461	13	463	12	446	50	511	34	100.4
3.00	0.0280	2.13	0.34	581	14	576	28	620	128	558	23	99.1
2.04	0.0229	3.01	0.18	451	11	453	13	478	92	458	27	100.4
2.62	0.0247	3.55	0.60	476	24	445	23	386	118	493	35	93.5
1.97	0.0449	2.27	0.46	878	23	846	25	804	84	889	39	96.4
2.99	0.0292	36.90	0.70	317	11	319	22	328	136	582	423	100.6
2.69	0.0226	2.20	0.06	446	8	441	18	420	122	451	20	98.9
2.20	0.0320	2.35	0.23	635	20	632	18	652	94	636	29	99.5
1.72	0.0241	2.35	0.08	456	10	474	11	490	76	480	22	103.9
1.76	0.0294	1.75	0.08	562	13	566	12	608	76	585	20	100.7
1.16	0.0482	1.31	0.88	974	12	972	21	984	48	950	24	99.8
0.46	0.1012	0.92	0.98	1965	18	2031	17	2084	16	1948	34	103.4
1.94	0.0192	2.23	0.34	369	6	378	13	398	88	384	17	102.4
2.68	0.0290	1.36	0.61	589	12	610	29	618	116	577	15	103.6
2.34	0.0318	2.55	0.60	628	11	631	26	598	102	632	32	100.5
1.83	0.0349	2.42	0.23	692	12	704	31	754	76	693	33	101.7
1.97	0.0133	1.77	0.70	262	5	270	12	338	88	266	9	103.1
1.93	0.0374	1.60	0.89	730	11	732	27	736	82	742	23	100.3
1.79	0.0388	2.16	0.46	731	15	747	21	784	76	769	33	102.2
1.11	0.0501	0.94	0.99	972	13	991	23	1032	44	989	18	102.0
4.11	0.0039	3.24	0.09	79	4	83	5	208	192	80	5	105.1
1.56	0.0253	2.47	0.62	528	8	521	16	530	68	505	25	98.7
2.45	0.0134	1.80	0.35	262	6	260	12	290	112	270	10	99.2
3.35	0.0044	2.55	0.28	85	4	89	5	222	154	88	4	104.7
1.95	0.0195	3.32	0.70	376	14	386	18	366	88	390	26	102.7
1.54	0.0293	1.56	0.77	544	13	550	20	580	68	583	18	101.1
1.18	0.0455	2.18	0.81	956	14	950	21	930	50	900	38	99.4
2.87	0.0043	2.40	0.14	85	3	84	4	48	116	87	4	98.8
1.58	0.0333	2.52	0.56	678	14	644	18	650	68	661	33	95.0
2.90	0.0359	1.90	0.24	695	13	744	31	862	120	712	27	107.1
1.89	0.0308	1.09	0.27	612	9	625	14	654	80	613	13	102.1
1.40	0.0227	2.32	0.47	457	8	462	12	470	62	454	21	101.1
2.93	0.0263	4.24	0.10	521	14	543	20	610	128	525	44	104.2
1.78	0.0235	1.69	0.14	456	12	457	10	466	80	469	16	100.2
1.38	0.0171	1.58	0.57	344	9	349	10	404	62	342	11	101.5
1.61	0.0131	1.89	0.50	265	5	260	9	266	74	264	10	98.1
1.42	0.0253	4.26	0.46	472	11	481	11	502	62	504	42	101.9
3.67	0.0275	3.39	0.79	571	20	577	44	534	160	548	37	101.1
2.34	0.0179	3.97	0.19	361	9	372	14	384	104	359	28	103.0
0.92	0.0258	2.05	0.60	503	8	520	9	586	40	515	21	103.4
4.72	0.0137	3.12	0.05	276	10	266	21	230	218	274	17	96.4
3.47	0.0039	3.01	0.18	74	2	76	5	136	162	79	5	102.7
2.94	0.0040	1.90	0.60	79	2	83	6	182	138	80	3	105.1
3.19	0.0134	1.48	0.52	268	6	262	17	278	148	268	8	97.8
2.11	0.0128	2.01	0.32	260	6	263	10	314	96	257	10	101.2
2.12	0.0194	2.75	0.28	376	7	375	14	364	94	388	21	99.7
1.43	0.0133	1.41	0.44	265	4	270	7	320	66	268	8	101.9
3.71	0.0195	3.00	0.09	385	8	369	23	356	168	391	23	95.8
2.79	0.0040	3.26	0.35	82	3	87	5	236	128	80	5	106.1
1.61	0.0136	1.72	0.54	276	5	285	9	350	72	272	9	103.3
0.99	0.0351	0.99	0.52	690	12	686	11	666	42	698	14	99.4
1.93	0.0132	2.19	0.48	267	8	259	10	204	88	265	12	97.0
0.75	0.0189	1.09	0.77	375	5	373	7	372	34	379	8	99.5
1.03	0.1022	1.12	0.72	1945	18	1911	23	1902	38	1967	42	98.3
1.54	0.0137	1.69	0.50	268	5	271	8	304	70	275	9	101.1

Appendix 6-1

[Table is two pages wide - note facing pages]

Detrital zircon FT-U/Pb double dating analytical results

Notes: Tect: tectonic position of the sample; D: Outer Dinaride foreland basin; S: Sava Zone.  $N_s$ : spontaneous track count;  $\rho_s$ : spontaneous track density ( $\times 10^5$  tr/cm<sup>2</sup>);  $N_i$ : induced track count;  $\rho_i$ : induced track density ( $\times 10^5$  tr/cm<sup>2</sup>). Peak: length of the laser ablation signal extracted for the isotope ratio calculation. p: error correlation of <sup>207</sup>Pb/<sup>235</sup>U and <sup>206</sup>Pb/<sup>238</sup>U ratios. Conco.: concordance expressed as  $[\frac{^{207}\text{Pb}/^{235}\text{U age}}{^{206}\text{Pb}/^{238}\text{U age}}] \times 100$ . Peak: length of the laser ablation signal extracted for the isotope ratio calculation. N.dia: nominal pit diameter – measured diameters are c. 10% smaller at the sample surface.

FT data

sample	tect	FT mount	LA	spontaneous		induced		age	$\pm 1\sigma$	U	<sup>207</sup> Pb	<sup>206</sup> Pb	peak	n.dia	line	U	<sup>206</sup> Pb/ <sup>238</sup> U	$\pm 1\sigma$	<sup>207</sup> Pb/ <sup>235</sup> U	$\pm 1\sigma$	<sup>207</sup> Pb/ <sup>206</sup> Pb
		grain #	exp. #	$N_s$	$\rho_s$	$N_i$	$\rho_i$	(Ma)	(Ma)	(ppm)	(cps)	(cps)	(s)	( $\mu\text{m}$ )	( $\mu\text{m}$ )	(ppm)	(%)	(%)	(%)	(%)	(%)
TD254	D	Z470A-27	no28c07	101	128.433	13	16.531	276.2	81.6	85	1064	17855	25.7	40	45	213	0.0938	0.93	0.7665	2.28	0.0589
TD254	D	Z470A-28	no28c08	207	175.483	28	23.737	263.1	53.3	121	290	5702	25.7	40	45	132	0.0487	1.06	0.3484	2.71	0.0502
TD254	D	Z470A-29	no28c09	53	44.93	21	17.803	91.0	23.6	91	3210	24694	27.9	40	52	73	0.3811	1.09	6.7175	1.81	0.1284
TD254	D	Z470A-30	no28c10	133	84.563	62	39.42	77.5	12.0	202	768	13295	24.7	40	45	186	0.0814	0.79	0.6456	2.26	0.0570
TD254	D	Z470B-01	no28d05	159	134.791	40	33.91	142.2	25.4	174	894	15434	21.4	40	45	199	0.0795	0.99	0.6262	1.84	0.0571
TD254	D	Z470B-02	no28d06	119	201.763	45	76.297	94.9	16.8	392	394	7245	20.4	40	45	181	0.0412	2.42	0.3002	2.21	0.0536
TD254	D	Z470B-03	no28d07	83	105.544	37	47.05	80.6	16.1	242	486	9513	21.4	40	45	228	0.0431	1.02	0.3030	1.81	0.0504
TD254	D	Z470B-04	no28d08	144	162.767	75	84.774	69.1	10.0	436	281	5752	23.6	40	40	462	0.0129	1.18	0.0852	2.80	0.0482
TD254	D	Z470B-05	no28d09	91	77.145	40	33.91	81.8	15.6	174	542	9595	15	40	45	141	0.0710	1.88	0.5383	2.12	0.0557
TD254	D	Z470B-06	no28d10	52	22.041	25	10.597	74.8	18.3	54	248	4283	20.4	55	50	68	0.0410	1.48	0.3227	2.94	0.0572
TD254	D	Z470B-07	no28d11	75	50.865	68	46.117	39.8	6.7	237	739	13659	22.5	40	45	354	0.0407	1.16	0.2962	2.60	0.0534
TD254	D	Z470B-09	no28d13	113	76.636	65	44.083	62.6	9.9	227	619	11493	25.7	55	70	126	0.0605	0.83	0.4343	2.12	0.0532
TD254	D	Z470B-11	no28d15	105	89.013	58	49.169	65.2	10.8	253	207	4177	20.4	40	45	356	0.0126	2.02	0.0850	3.57	0.0490
TD254	D	Z470B-12	no28d16	89	113.174	49	62.309	65.4	11.7	320	1401	24197	27.9	40	45	326	0.0800	1.06	0.6238	1.30	0.0572
TD254	D	Z470B-13	no28e05	88	111.902	24	30.519	131.3	30.4	157	1008	16489	33.2	40	40	172	0.0902	0.85	0.7491	1.47	0.0606
TD254	D	Z470B-14	no28e06	77	48.957	44	27.976	63.0	12.0	144	508	8624	22.5	40	45	93	0.0873	1.31	0.7075	1.96	0.0584
TD254	D	Z470B-15	no28e07	121	102.577	28	23.737	154.4	32.6	122	345	6619	18.2	55	70	91	0.0425	1.28	0.3133	2.67	0.0517
TD254	D	Z470B-16	no28e08	86	97.208	39	44.083	79.3	15.4	227	1211	18612	22.5	40	35	156	0.1111	0.82	0.9927	1.60	0.0646
TD254	D	Z470B-17	no28e09	62	52.56	35	29.671	63.8	13.6	153	2078	2548	29	40	40	113	0.2066	0.74	2.3814	1.56	0.0817
TD254	D	Z470B-18	no28e10	65	82.655	39	49.593	60.0	12.2	255	754	13666	20.4	30	40	497	0.0605	1.02	0.4670	2.36	0.0548
TD254	D	Z470B-19	no28e11	59	50.017	27	22.889	78.6	18.3	118	61	1254	10.7	40	50	92	0.0125	4.98	0.0841	7.89	0.0486
TD254	D	Z470B-20	no28e12	94	119.532	15	19.074	222.8	62.2	98	86	1580	18.2	30	35	89	0.0386	2.28	0.2871	4.16	0.0538
TD254	D	Z470B-21	no28e13	100	63.581	54	34.334	66.6	11.4	176	481	9049	24.7	40	45	134	0.0612	1.69	0.4583	2.42	0.0529
TD254	D	Z470B-22	no28e14	66	41.963	31	19.71	76.6	16.8	101	251	5223	12.9	55	62	237	0.0125	1.00	0.0834	3.33	0.0479
TD254	D	Z470B-23	no28e15	75	95.371	33	41.963	81.7	17.2	216	1881	28419	22.5	40	35	216	0.1183	1.52	1.0771	1.39	0.0658
TD254	D	Z470B-24	no28e16	115	146.236	14	17.803	290.5	82.5	92	496	8711	22.5	40	50	115	0.0680	1.19	0.5383	2.43	0.0566
TD254	D	Z470B-25	no28f05	72	61.038	29	24.585	89.2	19.7	126	458	8311	16.1	40	55	142	0.0605	0.66	0.4461	1.84	0.0543
TD254	D	Z470B-26	no28f06	197	133.605	19	12.886	364.5	88.0	66	680	9377	22.5	55	57	39	0.1587	0.88	1.5343	1.87	0.0715
TD254	D	Z470B-28	no28f08	136	115.293	51	43.235	95.7	15.9	222	787	13112	32.2	40	50	145	0.0961	0.82	0.7714	2.01	0.0592
TD254	D	Z470B-29	no28f09	83	52.772	55	34.969	54.4	9.5	180	432	7473	31.1	40	57	99	0.0810	0.84	0.6282	1.68	0.0570
TD254	D	Z470B-30	no28f10	84	56.968	45	30.519	67.2	12.5	157	1164	20442	15	55	70	172	0.0809	0.82	0.6297	1.43	0.0561
TD128	D	Z471A-01	no22a05	67	85.198	29	36.877	82.7	18.5	190	990	17204	20.4	40	70	143	0.0743	1.02	0.5785	1.55	0.0564
TD128	D	Z471A-02	no22a06	74	47.05	13	8.266	201.8	60.9	43	264	5101	30	55	80	73	0.0271	1.35	0.1904	3.28	0.0507
TD128	D	Z471A-04	no22a08	91	102.86	9	10.173	354.2	124.1	53	5579	33901	22.5	40	60	47	0.4504	1.34	9.9879	1.66	0.1616
TD128	D	Z471A-05	no22a09	62	52.56	21	17.803	105.5	26.7	92	486	7738	30	40	55	47	0.1036	1.54	0.9232	2.18	0.0617
TD128	D	Z471A-06	no22a10	91	154.29	10	16.955	319.7	106.8	88	326	6300	20.4	40	60	103	0.0388	1.55	0.2743	2.68	0.0508
TD128	D	Z471A-07	no22a11	78	99.186	8	10.173	341.9	127.2	53	2496	22855	16.1	40	60	47	0.3114	0.69	4.3743	2.67	0.1074
TD128	D	Z471A-08	no22a12	139	117.837	20	16.955	245.6	59.0	88	360	6234	19.3	40	60	58	0.0691	1.16	0.5390	2.95	0.0568
TD128	D	Z471A-09	no22a13	110	124.336	67	75.732	58.9	9.2	391	293	5529	24.7	40	50	278	0.0129	0.97	0.0933	2.45	0.0523
TD128	D	Z471A-10	no22a14	67	37.866	15	8.477	158.9	45.5	44	543	8430	19.3	55	80	33	0.1024	1.01	0.8834	2.30	0.0635
TD128	D	Z471A-11	no22a15	149	101.051	30	20.346	176.4	35.5	105	711	11536	32.2	40	52	73	0.1026	0.73	0.8698	1.63	0.0608
TD128	D	Z471A-12	no22a16	50	56.516	23	25.998	77.8	19.7	134	421	7049	16.1	30	35	152	0.0726	0.99	0.5857	2.05	0.0589
TD128	D	Z471A-13	no22b05	79	80.366	18	18.311	156.0	40.9	95	950	16862	31.1	40	60	151	0.0743	0.76	0.5599	1.26	0.0556
TD128	D	Z471A-14	no22b06	59	50.017	22	18.65	95.9	24.1	96	1837	31541	27.9	55	80	185	0.0716	0.70	0.5654	1.20	0.0575
TD128	D	Z471A-15	no22b07	76	85.905	13	14.694	207.2	62.4	76	682	11079	38.6	40	60	76	0.0984	0.83	0.8149	1.79	0.0608
TD128	D	Z471A-16	no22b08	97	61.673	53	33.698	65.6	11.3	174	108	2395	16.1	40	55	131	0.0124	1.85	0.0765	5.79	0.0447
TD128	D	Z471A-17	no22b09	89	75.449	11	9.325	285.0	91.3	48	352	5209	32.2	40	65	29	0.1242	0.90	1.1489	3.34	0.0670
TD128	D	Z471A-18	no22b10	73	46.414	8	5.086	320.5	119.6	26	2220	20089	31.1	55	80	28	0.3096	0.93	4.8053	1.83	0.1095
TD128	D	Z471A-19	no22b11	81	51.501	38	24.161	76.3	15.1	125	946	15052	22.5	55	80	86	0.0754	1.17	0.6463	1.78	0.0623
TD128	D	Z471A-20	no22b12	92	38.996	46	19.498	71.6	13.0	101	328	6176	27.9	40	45	101	0.0422	1.21	0.2992	2.87	0.0528
TD128	D	Z471A-21	no22b13	197	125.254	11	6.994	614.7	191.0	36	1738	15359	25.7	40	65	37	0.2910	0.91	4.5515	2.16	0.1125
TD128	D	Z471A-22	no22b14	59	50.017	24	20.346	87.9	21.4	105	341	6513	25.7	40	50	127	0.0357	1.03	0.2502	2.23	0.0521
TD128	D	Z471A-23	no22b15	74	50.187	16	10.851	164.5	45.5	56	52	895	16.1	30	45	36	0.0413	2.41	0.3148	6.14	0.0578
TD128	D	Z471A-24	no22b16	145	92.192	27	17.167	190.6	40.2	89	608	11161	21.4	55	75	136	0.0361	1.40	0.2662	3.06	0.0544
TD128	D	Z471A-25	no22c05	70	79.123	47	53.125	53.4	10.2	274	1519	26077	22.5	40	60	227	0.0804	0.85	0.6344	1.43	0.0575
TD128	D	Z471A-26	no22c06	84	53.408	26	16.531	115.3	26.0	85	5102	43797	23.6	40	50	91	0.3387	0.72	5.3086	1.19	0.1151

Appendix 6-1

[Table is two pages wide - note facing pages]

Detrital zircon FT-U/Pb double dating analytical results

LA-ICPMS apparent ages												
$\pm 1\sigma$ (%)	$^{208}\text{Pb}/^{232}\text{Th}$	$\pm 1\sigma$ (%)	$\rho$	$^{206}\text{Pb}/^{238}\text{U}$ $\pm 2\sigma$ age (Ma) (Ma)	$^{207}\text{Pb}/^{235}\text{U}$ $\pm 2\sigma$ age (Ma) (Ma)	$^{207}\text{Pb}/^{206}\text{Pb}$ $\pm 2\sigma$ age (Ma) (Ma)	$^{208}\text{Pb}/^{232}\text{Th}$ $\pm 2\sigma$ age (Ma) (Ma)	Conco. (%)				
1.52	0.0281	1.96	0.88	578	10	578	20	560	68	561	22	100.0
2.25	0.0153	1.95	0.59	306	6	304	14	202	104	306	12	99.3
0.97	0.1059	1.23	0.89	2081	39	2075	32	2074	34	2035	48	99.7
1.96	0.0243	2.44	0.53	504	8	506	18	492	86	486	23	100.4
1.75	0.0259	2.99	0.36	493	9	494	14	494	78	517	31	100.2
2.94	0.0135	2.44	0.20	260	12	267	10	354	132	270	13	102.7
1.73	0.0135	2.55	0.36	272	5	269	9	212	80	272	14	98.9
2.61	0.0041	3.89	0.37	83	2	83	4	110	124	83	6	100.0
2.92	0.0234	4.12	0.06	442	16	437	15	440	130	467	38	98.9
3.13	0.0129	3.67	0.12	259	7	284	15	500	138	259	19	109.7
1.75	0.0130	1.40	0.84	257	6	263	12	344	78	262	7	102.3
1.59	0.0191	1.56	0.75	379	6	366	13	336	72	383	12	96.6
3.76	0.0043	3.10	0.19	81	3	83	6	144	176	87	5	102.5
0.98	0.0240	1.77	0.67	496	10	492	10	500	42	480	17	99.2
1.32	0.0270	1.00	0.46	557	9	568	13	624	56	538	11	102.0
1.82	0.0283	1.50	0.44	539	14	543	17	544	80	565	17	100.7
2.94	0.0137	2.63	0.02	268	7	277	13	272	134	275	14	103.4
1.72	0.0333	1.50	0.10	679	11	700	16	760	72	662	20	103.1
0.72	0.0601	1.61	0.40	1211	16	1237	22	1236	28	1179	37	102.1
1.80	0.0179	3.48	0.70	379	8	389	15	404	82	359	25	102.6
10.51	0.0050	5.96	0.30	80	8	82	12	130	360	101	12	102.5
4.46	0.0107	7.51	0.14	244	11	256	19	364	200	215	32	104.9
2.72	0.0195	2.67	0.16	383	13	383	15	322	124	391	21	100.0
2.84	0.0040	2.74	0.60	80	2	81	5	90	134	80	4	101.3
1.55	0.0383	1.99	0.44	721	21	742	15	800	66	760	30	102.9
2.31	0.0212	1.95	0.34	424	10	437	17	474	102	425	16	103.1
1.91	0.0198	2.82	0.07	378	5	375	12	382	86	396	22	99.2
1.28	0.0500	1.90	0.81	949	16	944	23	972	52	987	37	99.5
1.70	0.0289	1.84	0.55	592	9	581	18	572	74	576	21	98.1
1.82	0.0245	2.56	0.08	502	8	495	13	492	80	489	25	98.6
1.28	0.0248	2.69	0.46	502	8	496	11	456	56	494	26	98.8
1.27	0.0226	2.49	0.58	462	9	463	12	466	56	452	22	100.2
2.95	0.0091	2.28	0.44	173	5	177	11	224	136	184	8	102.3
0.75	0.1277	1.49	0.90	2397	54	2434	31	2472	26	2429	68	101.5
2.64	0.0307	1.90	0.02	635	19	664	21	662	114	612	23	104.6
3.34	0.0130	4.27	0.19	245	7	246	12	232	154	262	22	100.4
1.45	0.0898	1.87	0.49	1748	21	1707	44	1754	52	1739	62	97.7
2.71	0.0210	3.38	0.40	431	10	438	21	480	120	419	28	101.6
3.04	0.0040	2.68	0.48	82	2	91	4	296	140	80	4	111.0
1.73	0.0308	1.34	0.71	629	12	643	22	724	74	612	16	102.2
1.42	0.0307	0.98	0.49	629	9	635	15	630	62	611	12	101.0
2.92	0.0220	3.85	0.82	452	9	468	15	564	126	441	34	103.5
1.03	0.0217	2.00	0.58	462	7	451	9	434	46	435	17	97.6
1.09	0.0211	1.08	0.44	446	6	455	9	510	46	422	9	102.0
1.57	0.0279	1.53	0.48	605	10	605	16	630	68	556	17	100.0
5.90	0.0039	2.88	0.10	80	3	75	8	0	66	78	4	93.8
2.43	0.0354	1.56	0.40	755	13	777	36	836	102	703	22	102.9
0.94	0.0837	1.29	0.98	1739	28	1786	31	1790	34	1624	40	102.7
1.55	0.0240	1.81	0.51	469	11	506	14	684	66	478	17	107.9
2.91	0.0121	2.23	0.18	267	6	266	13	318	132	242	11	99.6
1.54	0.0813	1.10	0.79	1647	26	1740	36	1840	54	1579	34	105.6
2.54	0.0103	2.63	0.09	226	5	227	9	290	118	207	11	100.4
5.12	0.0125	6.51	0.58	261	12	278	30	520	224	252	33	106.5
2.88	0.0107	1.78	0.35	229	6	240	13	386	130	215	8	104.8
1.24	0.0226	1.41	0.51	498	8	499	11	510	54	451	13	100.2
0.57	0.0890	1.24	0.94	1880	23	1870	20	1880	20	1724	41	99.5
3.96	0.0115	2.31	0.70	245	5	250	14	284	182	231	11	102.0
1.47	0.0861	1.18	0.40	1751	34	1816	59	1786	54	1670	38	103.7
0.52	0.1254	0.92	0.46	2467	53	2600	51	2702	18	2388	42	105.4
39.34	0.0075	18.51	0.11	174	22	122	91	0	2	151	56	70.1
1.63	0.0274	1.17	0.22	591	8	606	12	656	70	545	13	102.5
5.42	0.0090	9.55	0.50	170	10	199	23	496	238	181	34	117.1
0.94	0.0300	1.52	0.87	653	8	644	14	634	40	598	18	98.6
2.08	0.0122	1.83	0.43	268	6	277	11	354	94	246	9	103.4
2.40	0.0127	2.53	0.31	265	8	288	12	424	108	255	13	108.7
2.67	0.0157	2.43	0.25	304	6	317	15	414	120	314	15	104.3
0.71	0.0857	1.82	0.96	1791	25	1763	26	1722	26	1661	58	98.4
1.82	0.0123	1.98	0.25	269	5	271	9	282	84	247	10	100.7
0.40	0.1190	0.62	0.84	2475	17	2555	13	2596	12	2273	27	103.2
0.41	0.1574	0.62	0.48	3264	21	3296	24	3262	14	2954	34	101.0
0.79	0.0127	0.61	0.52	253	4	264	4	276	36	256	3	104.3
2.24	0.0229	4.16	0.40	454	6	472	9	588	96	458	38	104.0

Appendix 6-1

[Table is two pages wide - note facing pages]

Detrital zircon FT-U/Pb double dating analytical results

Notes: Tect: tectonic position of the sample; D: Outer Dinaride foreland basin; S: Sava Zone.  $N_s$ : spontaneous track count;  $\rho_s$ : spontaneous track density ( $\times 10^5$  tr/cm<sup>2</sup>);  $N_i$ : induced track count;  $\rho_i$ : induced track density ( $\times 10^5$  tr/cm<sup>2</sup>). Peak: length of the laser ablation signal extracted for the isotope ratio calculation. p: error correlation of <sup>207</sup>Pb/<sup>235</sup>U and <sup>206</sup>Pb/<sup>238</sup>U ratios. Conco.: concordance expressed as [<sup>207</sup>Pb/<sup>235</sup>U age]/[<sup>206</sup>Pb/<sup>238</sup>U age] × 100. Peak: length of the laser ablation signal extracted for the isotope ratio calculation. N.dia: nominal pit diameter – measured diameters are c. 10% smaller at the sample surface.

FT data

sample	tect	FT mount	LA	spontaneous		induced		age	± 1σ	U	<sup>207</sup> Pb	<sup>206</sup> Pb	peak	n.dia	line	U	<sup>206</sup> Pb/ <sup>238</sup> U	± 1σ	<sup>207</sup> Pb/ <sup>235</sup> U	± 1σ	<sup>207</sup> Pb/ <sup>206</sup> Pb
		grain #	exp. #	$N_s$	$\rho_s$	$N_i$	$\rho_i$	(Ma)	(Ma)	(ppm)	(cps)	(cps)	(s)	(μm)		(ppm)	(%)	(%)	(%)	(%)	
TD128	D	Z471B-03	no22e07	173	109.995	28	17.803	218.8	44.9	92	234	4177	13.9	40	55	69	0.0434	1.56	0.3372	3.34	0.0553
TD128	D	Z471B-05	no22e09	117	132.248	24	27.128	173.2	39.0	140	346	5785	11.8	40	50	111	0.0388	1.11	0.3091	2.64	0.0592
TD128	D	Z471B-06	no22e10	156	99.186	38	24.161	146.2	26.7	125	244	4854	17.2	40	50	133	0.0276	1.69	0.1949	2.22	0.0496
TD128	D	Z471B-07	no22e11	107	136.063	22	27.976	172.8	40.7	144	144	2629	17.2	40	45	80	0.0251	2.10	0.1902	3.60	0.0541
TD128	D	Z471B-08	no22e12	164	208.545	35	44.507	166.6	31.3	230	628	12134	22.5	40	50	252	0.0376	0.76	0.2712	1.34	0.0512
TD128	D	Z471B-09	no22e13	83	105.544	24	30.519	123.4	28.7	158	2174	30028	20.4	40	50	145	0.1645	0.85	1.6077	1.39	0.0716
TD128	D	Z471B-10	no22e14	85	108.087	29	36.877	104.7	22.7	190	438	7815	21.4	40	48	164	0.0385	1.09	0.2971	1.85	0.0554
TD128	D	Z471B-12	no22e16	119	134.509	24	27.128	176.1	39.6	140	762	13675	15	55	75	191	0.0374	1.38	0.2908	3.11	0.0551
TD128	D	Z471B-13	no22f05	87	73.754	32	27.128	97.2	20.2	140	825	13481	31.1	40	60	111	0.0980	0.63	0.8256	1.79	0.0606
TD128	D	Z471B-16	no22f08	163	207.274	30	38.149	192.8	38.6	197	1040	20386	16.1	55	68	272	0.0383	0.77	0.2653	1.80	0.0505
TD128	D	Z471B-17	no22f09	134	151.464	20	22.607	236.9	57.1	117	807	15144	18.2	55	60	204	0.0381	1.13	0.2767	2.15	0.0528
TD128	D	Z471B-20	no22f12	142	160.506	48	54.256	105.7	17.8	280	1897	31587	17.2	55	65	229	0.0713	0.69	0.5913	2.62	0.0595
TD188	S	Z472B-01	my18a05	58	23.601	28	11.394	73.6	17.0	59	258	4777	14	40	57	57	0.0412	1.09	0.3007	3.33	0.0530
TD188	S	Z472B-02	my18a06	60	30.519	37	18.82	57.7	12.1	98	185	3147	12.8	30	30	88	0.0420	1.34	0.3350	3.52	0.0579
TD188	S	Z472B-03	my18a07	40	16.277	22	8.952	64.6	17.2	47	186	3628	21.7	30	30	99	0.0434	1.67	0.3015	2.63	0.0503
TD188	S	Z472B-04	my18a08	76	32.214	26	11.021	103.6	23.7	57	5191	41776	39.6	40	60	59	0.3522	0.57	5.9241	0.76	0.1220
TD188	S	Z472B-05	my18a09	39	24.797	16	10.173	86.5	25.8	53	217	4201	10.3	30	40	125	0.0399	2.61	0.2786	3.11	0.0506
TD188	S	Z472B-06	my18a10	48	19.532	11	4.476	154.0	51.6	23	474	5895	7.7	40	50	69	0.0429	1.73	0.4660	3.18	0.0789
TD188	S	Z472B-07	my18a11	76	30.926	26	10.58	103.6	23.7	55	209	4139	26.8	40	52	49	0.0426	1.45	0.2902	2.48	0.0495
TD188	S	Z472B-08	my18a12	85	43.235	42	21.363	71.9	13.7	111	384	7155	23	40	30	84	0.0425	1.00	0.3083	2.33	0.0527
TD188	S	Z472B-09	my18a13	106	53.917	54	27.467	69.7	11.8	143	593	10038	23	40	42	122	0.0415	1.29	0.3316	1.84	0.0579
TD188	S	Z472B-10	my18a14	67	28.399	17	7.206	139.2	38.0	38	81	1467	39.5	30	50	44	0.0405	1.43	0.3017	3.66	0.0541
TD188	S	Z472B-11	my18a15	28	7.912	23	6.499	43.3	12.2	34	131	2347	16.6	40	38	30	0.0390	1.13	0.2943	5.24	0.0547
TD188	S	Z472B-12	my18a16	89	36.216	34	13.835	92.8	18.8	72	240	4439	25.5	40	44	55	0.0411	1.28	0.3004	3.40	0.0529
TD188	S	Z472B-13	my18b05	120	61.038	54	27.467	78.9	13.1	143	537	10715	24.2	40	50	118	0.0417	0.82	0.2846	1.42	0.0495
TD188	S	Z472B-14	my18b06	98	62.309	46	29.247	75.6	13.6	152	1069	18096	10.2	40	45	206	0.0402	2.16	0.3237	2.54	0.0583
TD188	S	Z472B-15	my18b07	79	50.229	37	23.525	75.8	15.2	122	514	9237	31.9	40	41	102	0.0414	1.03	0.3134	2.03	0.0549
TD188	S	Z472B-16	my18b08	65	41.328	35	22.253	66.0	13.9	116	184	3614	19.2	30	20	93	0.0424	2.19	0.2937	3.84	0.0502
TD188	S	Z472B-17	my18b09	56	22.787	39	15.87	51.1	10.7	83	606	11448	21.7	40	57	126	0.0413	0.96	0.2971	2.14	0.0522
TD188	S	Z472B-18	my18b10	90	57.223	30	19.074	106.3	22.5	99	321	6140	17.8	40	73	68	0.0410	1.30	0.2907	2.68	0.0514
TD188	S	Z472B-19	my18b11	48	19.532	10	4.069	169.2	58.9	21	62	1124	28.1	30	55	31	0.0398	1.82	0.2989	5.21	0.0545
TD188	S	Z472B-20	my18b12	42	26.704	12	7.63	123.8	40.6	40	115	2019	12.8	30	50	54	0.0402	1.94	0.3109	6.30	0.0561
TD188	S	Z472B-21	my18b13	99	62.945	38	24.161	92.4	17.8	126	567	10704	17.8	40	35	115	0.0422	0.59	0.3030	1.61	0.0521
TD188	S	Z472B-22	my18b14	82	33.367	27	10.987	107.6	24.0	57	302	5756	9	40	30	64	0.0408	1.31	0.2896	2.94	0.0515
TD188	S	Z472B-23	my18b15	51	20.753	34	13.835	53.4	11.9	72	182	3658	25.5	40	38	39	0.0423	1.03	0.2847	2.58	0.0488
TD188	S	Z472B-24	my18b16	87	36.877	46	19.498	67.2	12.4	101	434	8027	38.3	40	42	87	0.0416	0.89	0.3046	1.36	0.0531
TD188	S	Z472B-25	my18c06	76	64.429	20	16.955	134.3	33.9	88	248	4679	19.1	30	32	142	0.0408	1.38	0.2935	2.16	0.0522
TD188	S	Z472B-26	my18c07	52	10.796	19	3.945	97.0	26.1	21	99	1745	19.2	40	52	22	0.0412	1.56	0.3160	4.31	0.0556
TD188	S	Z472B-27	my18c08	84	71.211	78	66.124	38.4	6.1	344	1054	20244	29.4	40	42	261	0.0409	0.65	0.2891	0.99	0.0512
TD188	S	Z472B-28	my18c09	82	23.172	35	9.89	83.1	16.9	51	161	2994	24.3	40	38	38	0.0417	1.30	0.3042	2.53	0.0529
TD188	S	Z472B-29	my18c10	64	32.553	30	15.259	75.7	16.9	79	544	10199	30.6	55	50	82	0.0417	0.68	0.3020	1.87	0.0525
TD188	S	Z472B-30	my18c11	69	29.247	26	11.021	94.1	21.8	57	214	4142	31.9	40	58	54	0.0416	0.96	0.2912	2.30	0.0508
TD188	S	Z472A-01	no21b05	83	52.772	39	24.797	75.6	14.8	129	195	3305	23.6	30	50	117	0.0436	1.64	0.3440	4.12	0.0588
TD188	S	Z472A-03	no21b07	60	24.415	34	13.835	62.7	13.5	72	83	1308	20.4	30	50	49	0.0416	1.99	0.3571	8.63	0.0629
TD188	S	Z472A-04	no21b08	117	99.186	50	42.387	83.0	14.2	221	1161	18857	41.8	30	30	308	0.0952	0.87	0.8010	1.62	0.0612
TD188	S	Z472A-08	no21b12	56	35.605	30	19.074	66.3	15.1	99	58	1044	15	30	50	39	0.0420	3.24	0.3166	9.97	0.0556
TD188	S	Z472A-12	no21b16	67	42.599	38	24.161	62.7	12.8	126	498	9073	29	40	50	141	0.0430	0.73	0.3253	2.44	0.0548
TD188	S	Z472A-13	no21c05	37	15.056	21	8.545	62.6	17.2	44	304	5245	29	55	60	35	0.0618	1.13	0.4889	2.68	0.0580
TD188	S	Z472A-15	no21c07	110	69.939	64	40.692	61.1	9.7	212	2548	38272	10.7	55	80	150	0.1052	0.65	0.9859	1.77	0.0665
TD188	S	Z472A-16	no21c08	85	54.044	42	26.704	71.9	13.7	139	592	10242	21.4	55	50	103	0.0411	1.16	0.3256	2.99	0.0577
TD188	S	Z472A-17	no21c09	99	83.927	43	36.453	81.7	15.0	190	803	13207	16.1	55	45	126	0.0431	1.12	0.3612	1.76	0.0607
TD188	S	Z472A-18	no21c10	99	62.945	26	16.531	134.6	29.8	86	13244	65948	31.1	40	35	81	0.5370	0.61	14.7777	1.21	0.2006
TD188	S	Z472A-20	no21c12	57	38.657	28	18.989	72.3	16.8	99	206	3758	19.3	40	35	59	0.0420	1.19	0.3157	3.24	0.0548
TD188	S	Z472A-22	no21c14	154	97.915	94	59.766	58.3	7.7	311	850	15829	36.5	55	30	151	0.0432	1.30	0.3189	1.66	0.0536
TD188	S	Z472A-24	no21c16	48	30.519	17	10.809	100.1	28.3	56	154	2662	19.3	40	45	41	0.0430	1.70	0.3447	3.44	0.0576
TD188	S	Z472A-25	no21d05	76	48.321	36	22.889	75.0	15.3	119	280	5189	24.7	55	60	51	0.0442	0.91	0.3255	2.26	0.0532
TD188	S	Z472A-26	no21d06	55	31.084	29	16.39	67.4	1												

Appendix 6-1

[Table is two pages wide - note facing pages]

Detrital zircon FT-U/Pb double dating analytical results

LA-ICPMS apparent ages												
$\pm 1\sigma$ (%)	$^{208}\text{Pb}/^{232}\text{Th}$	$\pm 1\sigma$ (%)	$\rho$	$^{206}\text{Pb}/^{238}\text{U}$ $\pm 2\sigma$ age (Ma) (Ma)	$^{207}\text{Pb}/^{235}\text{U}$ $\pm 2\sigma$ age (Ma) (Ma)	$^{207}\text{Pb}/^{206}\text{Pb}$ $\pm 2\sigma$ age (Ma) (Ma)	$^{208}\text{Pb}/^{232}\text{Th}$ $\pm 2\sigma$ age (Ma) (Ma)	Conco.				
2.97	0.0133	3.27	0.46	274	8	295	17	422	134	266	17	107.7
1.71	0.0117	3.29	0.90	245	5	273	13	572	74	235	15	111.4
2.39	0.0080	3.42	0.28	175	6	181	7	176	110	161	11	103.4
4.46	0.0078	4.73	0.17	160	7	177	12	372	202	157	15	110.6
1.40	0.0116	2.14	0.20	238	4	244	6	246	64	233	10	102.5
0.77	0.0499	1.15	0.87	982	15	973	17	972	32	985	22	99.1
1.59	0.0123	1.51	0.52	244	5	264	9	430	70	248	7	108.2
1.76	0.0117	2.22	0.99	237	6	259	14	416	78	235	10	109.3
1.61	0.0310	0.78	0.45	603	7	611	16	622	70	617	9	101.3
1.72	0.0117	1.94	0.32	242	4	239	8	218	80	236	9	98.8
1.57	0.0119	2.15	0.71	241	5	248	9	318	72	239	10	102.9
1.30	0.0217	1.50	0.39	444	6	472	18	584	56	434	13	106.3
2.71	0.0139	2.70	0.68	260	6	267	16	328	124	279	15	102.7
4.49	0.0131	1.98	0.63	265	7	293	18	524	198	263	10	110.6
2.57	0.0138	2.53	0.35	274	9	268	12	210	120	277	14	97.8
0.53	0.1048	0.80	0.56	1945	19	1965	10	1984	20	2014	31	101.0
4.54	0.0124	2.45	0.25	252	13	250	14	222	210	248	12	99.2
3.70	0.0173	2.12	0.05	270	9	388	21	1168	146	347	15	143.7
2.66	0.0143	1.97	0.16	269	8	259	11	168	124	287	11	96.3
2.87	0.0137	2.29	0.14	268	5	273	11	312	130	275	12	101.9
2.08	0.0147	2.28	0.15	262	7	291	9	526	90	295	13	111.1
4.04	0.0126	4.88	0.23	256	7	268	16	372	182	254	25	104.7
5.04	0.0123	2.69	0.44	247	5	262	24	400	226	248	13	106.1
3.81	0.0136	2.81	0.15	260	7	267	16	326	174	272	15	102.7
1.60	0.0139	1.48	0.06	263	4	254	6	170	74	279	8	96.6
2.08	0.0148	1.92	0.62	254	11	285	13	540	92	297	11	112.2
2.07	0.0134	2.25	0.21	261	5	277	10	408	92	269	12	106.1
3.57	0.0125	3.38	0.40	268	12	261	18	202	166	251	17	97.4
2.12	0.0127	2.42	0.25	261	5	264	10	292	98	255	12	101.1
3.03	0.0125	2.77	0.04	259	7	259	12	258	138	252	14	100.0
5.75	0.0130	5.09	0.14	252	9	266	24	390	260	262	26	105.6
7.04	0.0140	7.10	0.25	254	10	275	30	454	314	280	40	108.3
1.51	0.0138	1.55	0.35	266	3	269	8	288	70	277	9	101.1
2.89	0.0141	2.08	0.26	258	7	258	13	262	132	283	12	100.0
2.74	0.0133	2.86	0.04	267	5	254	12	138	128	267	15	95.1
1.79	0.0127	1.32	0.23	263	5	270	6	330	80	255	7	102.7
2.13	0.0126	2.85	0.34	258	7	261	10	294	98	253	14	101.2
4.55	0.0126	5.22	0.02	260	8	279	21	436	202	253	26	107.3
1.10	0.0126	1.08	0.15	258	3	258	5	250	50	254	5	100.0
2.65	0.0126	4.30	0.16	263	7	270	12	324	120	253	22	102.7
1.85	0.0125	1.29	0.21	263	4	268	9	306	84	250	6	101.9
2.29	0.0124	2.91	0.22	263	5	259	11	230	106	249	14	98.5
3.77	0.0141	2.44	0.40	275	9	300	21	556	166	283	14	109.1
6.94	0.0156	4.11	0.88	263	10	310	46	702	296	312	25	117.9
1.37	0.0288	2.62	0.53	586	10	597	15	646	60	574	30	101.9
7.99	0.0164	8.07	0.71	265	17	279	49	436	356	328	52	105.3
2.39	0.0133	1.70	0.22	272	4	286	12	400	108	266	9	105.1
2.59	0.0201	2.11	0.29	387	9	404	18	530	114	403	17	104.4
1.41	0.0351	1.22	0.68	645	8	697	18	822	60	698	17	108.1
2.85	0.0141	2.61	0.31	259	6	286	15	518	126	283	15	110.4
1.41	0.0143	2.05	0.60	272	6	313	9	628	62	286	12	115.1
0.55	0.1423	0.78	0.94	2771	28	2801	23	2830	18	2688	39	101.1
2.82	0.0131	2.94	0.51	265	6	279	16	404	126	263	15	105.3
1.52	0.0136	1.36	0.49	273	7	281	8	352	68	274	7	102.9
3.14	0.0132	4.30	0.42	271	10	301	18	512	138	265	23	111.1
2.67	0.0140	3.15	0.29	279	5	286	11	334	122	281	18	102.5
3.20	0.0133	3.33	0.20	279	8	290	16	356	144	266	18	103.9
2.92	0.0144	2.35	0.16	282	6	279	14	246	134	289	13	98.9
1.16	0.0497	1.51	0.23	1007	12	1017	14	1030	46	981	29	101.0
2.02	0.0313	1.94	0.34	618	11	635	14	714	86	622	24	102.8

Appendix 6-2

Results of detrital zircon LA-ICPMS U/Pb geochronology on non-double-dated aliquots, in conventional epoxy mounts

page 1 of 4

Notes: Tect: tectonic position of the sample; D: Outer Dinaride foreland basin; S: Sava Zone. Peak: length of the laser ablation signal extracted for the isotope ratio calculation. p: error correlation of <sup>207</sup>Pb/<sup>235</sup>U and <sup>206</sup>Pb/<sup>238</sup>U ratios. Conco.: concordance expressed as [<sup>207</sup>Pb/<sup>235</sup>U age]/[<sup>206</sup>Pb/<sup>238</sup>U age] × 100. Peak: length of the laser ablation signal extracted for the isotope ratio calculation.

LA-ICPMS apparent ages																					
tect	grain#	exp.#	peak (s)	<sup>206</sup> Pb/ <sup>238</sup> U ± 1σ (%)	<sup>207</sup> Pb/ <sup>235</sup> U ± 1σ (%)	<sup>207</sup> Pb/ <sup>206</sup> Pb ± 1σ (%)	<sup>208</sup> Pb/ <sup>232</sup> Th ± 1σ (%)	± 1σ (%)	ρ	<sup>206</sup> Pb/ <sup>238</sup> U ± 2σ (Ma)	<sup>207</sup> Pb/ <sup>235</sup> U ± 2σ (Ma)	<sup>207</sup> Pb/ <sup>206</sup> Pb ± 2σ (Ma)	<sup>208</sup> Pb/ <sup>232</sup> Th ± 2σ (Ma)	Conco. (%)							
D	TD128-001	no29a05	20.4	0.3470	1.01	5.5539	2.58	0.1219	1.18	0.0942	1.35	0.21	1920	34	1909	44	1982	42	1819	47	99.4
D	TD128-002	no29a06	16.1	0.0303	0.81	0.2191	1.78	0.0520	1.64	0.0096	1.49	0.39	193	3	201	6	286	74	192	6	104.1
D	TD128-003	no29a07	27.9	0.0367	0.65	0.2586	1.38	0.0508	1.64	0.0111	1.04	0.20	232	3	234	6	232	76	222	5	100.9
D	TD128-004	no29a08	32.2	0.0627	0.74	0.4893	1.27	0.0562	0.89	0.0219	3.48	0.73	392	6	404	8	460	40	437	30	103.1
D	TD128-005	no29a09	21.4	0.0379	0.63	0.2821	1.37	0.0533	0.98	0.0119	0.86	0.76	240	3	252	6	338	44	240	4	105.0
D	TD128-006	no29a10	20.4	0.0639	1.01	0.4844	1.43	0.0542	1.45	0.0189	0.95	0.33	399	8	401	10	380	66	379	7	100.5
D	TD128-007	no29a11	19.3	0.0450	0.77	0.3640	1.03	0.0578	0.95	0.0144	1.09	0.47	284	4	315	6	522	42	288	6	110.9
D	TD128-008	no29a12	23.6	0.0369	0.72	0.2775	1.66	0.0533	1.71	0.0121	2.88	0.15	234	3	249	7	340	78	244	14	106.4
D	TD128-009	no29a13	31.1	0.0704	0.87	0.5435	1.59	0.0555	1.18	0.0207	2.91	0.68	439	7	441	11	432	52	413	24	100.5
D	TD128-010	no29a14	35.4	0.0910	0.66	0.7554	1.37	0.0604	1.36	0.0271	1.04	0.26	561	7	571	12	616	58	540	11	101.8
D	TD128-011	no29a15	29.0	0.3247	0.80	5.1106	0.95	0.1129	0.60	0.0904	0.95	0.79	1812	19	1838	16	1846	22	1748	32	101.4
D	TD128-012	no29a16	26.8	0.0608	0.56	0.4533	1.08	0.0540	0.72	0.0179	1.86	0.79	380	4	380	7	370	32	358	13	100.0
D	TD128-013	no29b05	21.4	0.0421	1.04	0.2966	1.64	0.0516	1.82	0.0134	1.46	0.13	266	5	264	8	266	82	269	8	99.2
D	TD128-014	no29b06	39.7	0.0261	1.91	0.1810	3.17	0.0514	2.89	0.0103	4.92	0.44	166	6	169	10	258	132	207	20	101.8
D	TD128-015	no29b07	38.6	0.0357	0.38	0.2497	0.49	0.0507	0.51	0.0110	0.49	0.33	226	2	226	2	224	24	220	2	100.0
D	TD128-016	no29b08	31.1	0.0555	0.76	0.4082	1.63	0.0541	1.11	0.0165	2.60	0.81	348	5	348	10	376	50	330	17	100.0
D	TD128-017	no29b09	26.8	0.0420	1.11	0.2869	2.04	0.0516	2.00	0.0124	2.41	0.31	265	6	256	9	266	92	249	12	96.6
D	TD128-018	no29b10	25.7	0.1248	0.68	1.0742	1.43	0.0633	1.23	0.0371	1.07	0.51	758	10	741	15	718	52	737	16	97.8
D	TD128-019	no29b11	21.4	0.0420	1.22	0.2943	4.62	0.0515	5.77	0.0130	3.10	0.93	265	6	262	21	262	266	260	16	98.9
D	TD128-020	no29b12	23.6	0.0847	0.71	0.6900	1.58	0.0595	1.52	0.0255	1.95	0.31	524	7	533	13	586	66	508	20	101.7
D	TD128-021	no29b13	24.7	0.0430	1.09	0.3116	2.05	0.0533	1.88	0.0138	1.25	0.42	272	6	275	10	338	84	277	7	101.1
D	TD128-022	no29b14	21.4	0.0800	0.66	0.6280	0.92	0.0568	0.78	0.0241	2.28	0.55	496	6	495	7	484	36	481	22	99.8
D	TD128-023	no29b15	26.8	0.0421	0.99	0.3059	1.91	0.0530	1.53	0.0129	2.32	0.60	266	5	271	9	328	68	259	12	101.9
D	TD128-024	no29b16	23.6	0.0396	1.96	0.3017	4.70	0.0556	4.98	0.0121	4.38	0.06	250	10	268	22	434	222	244	21	107.2
D	TD128-025	no29c05	22.5	0.1001	0.56	0.8540	1.23	0.0610	1.18	0.0309	1.94	0.32	615	7	627	12	636	50	615	24	102.0
D	TD128-026	no29c06	34.3	0.0653	2.59	0.4888	3.92	0.0548	1.91	0.0302	2.27	0.91	408	20	404	26	402	86	601	27	99.0
D	TD128-028	no29c08	24.7	0.0726	0.47	0.5665	0.88	0.0561	0.82	0.0211	1.15	0.39	452	4	456	6	454	36	422	18	100.9
D	TD128-030	no29c10	24.7	0.0386	0.73	0.2799	1.85	0.0516	1.88	0.0116	2.19	0.16	244	3	251	8	264	86	234	9	102.9
D	TD128-031	no29c11	23.6	0.0380	1.17	0.2707	2.02	0.0519	1.81	0.0117	1.96	0.46	240	6	243	9	278	84	235	9	101.3
D	TD128-032	no29c12	16.1	0.0476	0.51	0.3659	1.73	0.0550	1.51	0.0145	1.69	0.55	300	3	317	9	412	68	290	10	105.7
D	TD128-033	no29c13	22.5	0.0250	0.73	0.1614	3.13	0.0471	2.39	0.0074	2.37	0.90	159	2	152	9	52	108	149	7	95.6
D	TD128-034	no29c14	24.7	0.0783	0.77	0.6223	1.70	0.0578	1.78	0.0243	2.79	0.12	486	7	491	13	520	78	485	27	101.0
D	TD128-035	no29c15	23.6	0.0381	0.80	0.2605	1.75	0.0495	1.96	0.0118	2.12	0.05	241	4	235	7	172	90	237	10	97.5
D	TD128-036	no29c16	21.4	0.0414	0.41	0.3013	1.51	0.0527	1.22	0.0125	0.96	0.78	261	2	267	7	312	56	251	5	102.3
D	TD128-037	no29d05	21.4	0.0867	0.61	0.7011	0.91	0.0592	0.86	0.0262	1.59	0.41	536	6	539	8	572	38	522	16	100.6
D	TD128-038	no29d06	26.8	0.0358	0.77	0.2546	2.15	0.0521	2.04	0.0112	1.79	0.32	227	3	230	9	288	92	225	8	101.3
D	TD128-039	no29d07	20.4	0.0442	1.22	0.3668	3.91	0.0610	4.00	0.0140	2.28	0.08	279	7	317	21	636	172	281	13	113.6
D	TD128-040	no29d08	15.0	0.1123	0.75	0.9734	1.82	0.0629	1.38	0.0351	1.88	0.72	686	10	690	18	704	60	697	26	100.6
D	TD128-041	no29d09	13.9	0.0338	1.54	0.2674	3.50	0.0567	3.06	0.0114	3.51	0.49	214	6	241	15	480	134	230	16	112.6
D	TD128-042	no29d10	24.7	0.0366	0.52	0.2672	1.42	0.0525	1.31	0.0112	1.08	0.39	232	2	240	6	308	60	225	5	103.4
D	TD128-043	no29d11	19.3	0.0489	0.73	0.3668	1.88	0.0541	1.64	0.0145	3.74	0.50	308	4	317	10	376	74	291	22	102.9
D	TD128-044	no29d12	15.0	0.0396	1.19	0.3447	3.39	0.0627	2.39	0.0148	2.52	0.89	250	6	301	18	698	102	296	15	120.4
D	TD128-045	no29d13	21.4	0.0674	0.84	0.5173	1.49	0.0560	1.60	0.0215	1.76	0.15	420	7	423	10	450	70	430	15	100.7
D	TD128-046	no29d14	19.3	0.0382	0.75	0.2784	2.82	0.0528	2.45	0.0122	2.12	0.59	242	4	249	12	318	112	245	10	102.9
D	TD128-047	no29d15	30.0	0.0393	0.79	0.2793	2.53	0.0520	2.38	0.0121	1.51	0.34	248	4	250	11	286	108	243	7	100.8
D	TD128-048	no29d16	26.8	0.0376	0.57	0.2597	2.02	0.0505	2.02	0.0114	2.39	0.14	238	3	234	8	218	92	229	11	98.3
D	TD128-049	no29e05	25.7	0.0383	0.46	0.2737	1.35	0.0515	1.34	0.0116	1.55	0.19	242	2	246	6	264	62	232	7	101.7
D	TD128-050	no29e06	25.7	0.0670	1.01	0.5018	2.11	0.0539	2.09	0.0150	2.68	0.26	418	8	413	14	368	94	301	16	98.8
D	TD128-051	no29e07	32.2	0.3299	0.38	5.1613	0.54	0.1136	0.28	0.0918	0.63	0.87	1838	12	1846	9	1856	10	1775	21	100.4
D	TD128-052	no29e08	31.1	0.0451	1.02	0.3335	2.13	0.0530	1.55	0.0142	1.38	0.73	284	6	292	11	328	70	285	8	102.8
D	TD128-053	no29e09	27.9	0.0330	1.15	0.2354	2.50	0.0515	2.40	0.0104	3.08	0.32	209	5	215	10	262	112	208	13	102.9
D	TD128-054	no29e10	21.4	0.3753	1.11	6.7311	2.20	0.1285	0.91	0.1062	1.73	0.57	2054	39	2077	39	2076	32	2041	67	101.1
D	TD128-055	no29e11	23.6	0.0773	1.11	0.6144	1.20	0.0562	1.10	0.0245	1.22	0.85	480	10	486	9	458	50	489	12	101.3
D	TD128-056	no29e12	24.7	0.0309	0.80	0.2193	2.60	0.0514	2.19	0.0098	1.48	0.63	196	3	201	10	256	100	197	6	102.6
D	TD128-057	no29e13	32.2	0.1075	0.96	0.9122	1.24	0.0611	1.28	0.0326	1.15	0.34	658	12	658	12	642	54	648	15	100.0
D	TD128-058	no29e14	32.2	0.0361	1.00	0.2574	2.02	0.0515	1.95	0.0113	1.53	0.32	229	4	233	8	262	90	227	7	101.7
D	TD128-059	no29e15	23.6	0.0688	0.79	0.5408	1.82	0.0562	1.84	0.0206	1.85	0.19	429	7	439	13	460	82	413	15	102.3
D	TD128-060	no29e16	24.7	0.0419	0.90	0.3033	2.49	0.0523	2.15	0.0132	2.10	0.53	264	5	269	12	298	98	265	6	101.9
D	TD128																				

Appendix 6-2

Results of detrital zircon LA-ICPMS U/Pb geochronology on non-double-dated aliquots, in conventional epoxy mounts

page 2 of 4

Notes: Tect: tectonic position of the sample; D: Outer Dinaride foreland basin; S: Sava Zone. Peak: length of the laser ablation signal extracted for the isotope ratio calculation. p: error correlation of <sup>207</sup>Pb/<sup>235</sup>U and <sup>206</sup>Pb/<sup>238</sup>U ratios. Conco.: concordance expressed as [<sup>207</sup>Pb/<sup>235</sup>U age]/[<sup>206</sup>Pb/<sup>238</sup>U age] × 100. Peak: length of the laser ablation signal extracted for the isotope ratio calculation.

LA-ICPMS apparent ages

tect	grain#	exp.#	peak (s)	<sup>206</sup> Pb/ <sup>238</sup> U ± 1σ (%)	<sup>207</sup> Pb/ <sup>235</sup> U ± 1σ (%)	<sup>207</sup> Pb/ <sup>206</sup> Pb ± 1σ (%)	<sup>208</sup> Pb/ <sup>232</sup> Th ± 1σ (%)	<sup>206</sup> Pb/ <sup>238</sup> U ± 2σ (Ma)	<sup>207</sup> Pb/ <sup>235</sup> U ± 2σ (Ma)	<sup>207</sup> Pb/ <sup>206</sup> Pb ± 2σ (Ma)	<sup>208</sup> Pb/ <sup>232</sup> Th ± 2σ (Ma)	Conco. (%)									
D	TD128-095	no30b15	21.4	0.1507	0.82	1.4778	1.16	0.0702	0.67	0.0437	2.09	0.82	905	14	921	14	934	28	864	35	101.8
D	TD128-096	no30b16	29.0	0.3756	0.65	9.0443	0.72	0.1727	0.41	0.0969	0.70	0.83	2056	23	2342	13	2582	14	1868	25	113.9
D	TD128-097	no30c05	23.6	0.0356	1.58	0.2601	4.56	0.0539	4.99	0.1110	3.35	0.11	226	7	235	19	366	224	220	15	104.0
D	TD128-98	no30c06	36.5	0.0889	0.76	0.7277	1.55	0.0591	1.34	0.0254	1.43	0.50	549	8	555	13	570	58	508	14	101.1
D	TD128-99	no30c07	17.2	0.0386	1.36	0.2615	2.74	0.0501	1.96	0.107	6.30	0.74	244	7	236	12	200	92	215	27	96.7
D	TD128-100	no30c08	32.2	0.0623	0.75	0.4750	1.15	0.0550	1.12	0.0183	1.38	0.37	390	6	395	8	412	50	366	10	101.3
D	TD128-102	no30c10	19.3	0.0117	2.36	0.0852	3.75	0.0521	4.15	0.0038	3.98	0.14	75	4	83	6	290	190	76	6	110.7
D	TD128-102R	no30c11	17.2	0.0124	1.10	0.0794	2.43	0.0467	2.25	0.0035	4.29	0.38	80	2	78	4	32	84	71	6	97.5
D	TD128-103	no30c12	32.2	0.0993	0.53	0.8440	0.81	0.0614	0.68	0.0278	1.10	0.55	610	6	621	8	652	28	553	12	101.8
D	TD128-104	no30c13	25.7	0.0490	1.80	0.3510	3.53	0.0521	3.49	0.0150	5.43	0.28	309	11	305	19	288	158	301	32	98.7
D	TD128-105	no30c14	21.4	0.0387	0.53	0.2865	1.57	0.0530	1.45	0.0113	2.51	0.39	245	3	256	7	328	66	228	11	104.5
D	TD128-106	no30c15	22.5	0.0472	0.68	0.3397	1.44	0.0519	1.25	0.0138	1.25	0.50	297	4	297	7	280	58	276	7	100.0
D	TD128-107	no30c16	26.8	0.3305	0.65	5.1943	0.96	0.1136	0.49	0.0921	2.14	0.88	1841	21	1852	16	1858	18	1780	73	100.6
D	TD128-108	no30d05	41.8	0.0982	0.44	0.8215	0.53	0.0604	0.52	0.0293	1.92	0.44	604	5	609	5	616	24	584	22	100.8
D	TD128-110	no30d06	26.8	0.0484	0.68	0.3532	1.38	0.0526	1.50	0.0145	1.17	0.06	304	4	307	7	312	68	291	7	101.0
D	TD128-112	no30d07	13.9	0.0380	1.02	0.2626	4.20	0.0505	3.30	0.0114	3.91	0.91	240	5	237	18	216	154	228	18	98.8
D	TD128-113	no30d08	25.7	0.1613	0.58	1.6021	1.08	0.0729	0.79	0.0455	0.73	0.70	964	10	971	14	1010	32	899	13	100.7
D	TD128-114	no30d09	35.4	0.0954	0.66	0.8144	1.36	0.0613	1.26	0.0279	1.19	0.39	587	7	605	12	650	54	556	13	103.1
D	TD128-115	no30d10	31.1	0.1691	0.77	1.6982	1.08	0.0726	0.79	0.0485	0.79	0.68	1007	14	1008	14	1002	34	957	15	100.1
D	TD128-116	no30d11	26.8	0.0727	0.80	0.5570	1.33	0.0551	1.09	0.0221	2.03	0.57	453	7	450	10	414	48	441	18	99.3
D	TD128-117	no30d12	24.7	0.0392	1.18	0.2812	1.82	0.0518	1.81	0.0119	1.46	0.33	248	6	252	8	276	84	239	7	101.6
D	TD128-118	no30d13	31.1	0.0368	0.76	0.2555	1.28	0.0512	1.42	0.0110	1.30	0.10	233	3	231	5	246	64	221	6	99.1
D	TD128-119	no30d14	27.9	0.0259	1.75	0.2125	5.32	0.0597	4.08	0.0119	5.13	0.79	165	6	196	19	592	178	240	24	118.8
D	TD128-120	no30d15	20.4	0.0379	0.99	0.2946	1.74	0.0564	2.09	0.0123	1.60	0.10	240	5	262	8	466	92	247	8	109.2
D	TD128-121	no30d16	16.1	0.0906	1.30	0.8032	1.86	0.0647	1.44	0.0310	2.13	0.64	559	14	599	17	762	62	617	26	107.2
D	TD128-122	no30e05	34.3	0.0723	0.54	0.5547	0.78	0.0555	0.69	0.0214	0.85	0.50	450	5	448	6	430	32	427	7	99.6
D	TD128-123	no30e06	30.0	0.0975	0.76	0.7907	1.56	0.0597	1.43	0.0284	0.89	0.41	600	9	592	14	594	62	566	10	98.7
D	TD128-124	no30e07	22.5	0.1473	0.63	1.4075	1.63	0.0696	1.09	0.0419	2.10	0.91	886	10	892	19	916	46	829	34	100.7
D	TD128-125	no30e08	26.8	0.0723	1.02	0.5707	2.56	0.0573	2.57	0.0206	3.63	0.19	450	9	458	19	504	112	412	30	101.8
D	TD128-126	no30e09	22.5	0.0539	0.96	0.3871	1.18	0.0526	1.41	0.0165	11.78	0.14	339	6	332	7	310	64	330	77	97.9
D	TD128-127	no30e10	30.0	0.0392	0.97	0.2813	1.84	0.0519	2.06	0.0116	2.56	0.02	248	5	252	8	280	94	233	12	101.6
D	TD128-128	no30e11	19.3	0.0452	1.45	0.3058	2.43	0.0488	2.64	0.0135	3.29	0.15	285	8	271	12	138	124	271	18	95.1
D	TD128-129	no30e12	18.2	0.0427	0.63	0.3056	1.59	0.0520	1.85	0.0127	1.68	0.25	270	3	271	8	284	84	256	9	100.4
D	TD128-130	no30e13	17.2	0.0545	2.35	0.4084	4.45	0.0552	4.45	0.0173	5.30	0.26	342	16	348	26	420	200	346	36	101.8
D	TD128-131	no30e14	32.2	0.1027	0.53	0.8454	1.42	0.0596	1.18	0.0298	0.93	0.60	630	6	622	13	588	52	594	11	98.7
D	TD128-132	no30e15	17.2	0.0515	1.98	0.3559	3.42	0.0500	2.90	0.0259	83.33	0.53	324	12	309	18	194	136	518	852	95.4
D	TD128-133	no30e16	21.4	0.0396	1.06	0.2812	2.54	0.0517	2.76	0.0120	4.44	0.01	250	5	252	11	268	126	241	21	100.8
D	TD128-139	no30x06	27.9	0.0461	0.82	0.3473	1.67	0.0543	1.76	0.0138	1.60	0.13	290	5	303	9	382	80	277	9	104.5
D	TD128-140	no30x07	23.6	0.0328	1.39	0.2596	5.70	0.0578	5.56	0.0110	2.59	0.02	208	6	234	24	522	244	220	11	112.5
D	TD128-141	no30x08	44.0	0.0922	0.48	0.7484	0.76	0.0590	0.60	0.0270	2.27	0.61	568	5	567	7	566	26	538	24	99.8
D	TD128-142	no30x09	17.2	0.0339	1.51	0.2553	4.25	0.0555	3.67	0.0101	4.99	0.54	215	6	231	18	430	164	203	20	107.4
D	TD128-143	no30x10	24.7	0.0378	0.54	0.2683	1.66	0.0514	1.40	0.0115	1.57	0.61	239	3	241	7	258	64	232	7	100.8
D	TD128-144	no30x11	24.7	0.0362	0.78	0.2595	1.51	0.0518	1.44	0.0108	1.93	0.35	229	4	234	6	274	66	217	8	102.2
D	TD128-145	no30x12	19.3	0.0792	0.60	0.6590	1.02	0.0608	1.04	0.0257	0.80	0.26	491	6	514	8	630	44	514	8	104.7
D	TD128-147	no30x13	20.4	0.0270	1.82	0.1788	3.43	0.0477	3.17	0.0084	3.59	0.40	172	6	167	11	82	152	170	12	97.1
D	TD128-149	no30x14	18.2	0.0376	1.54	0.2639	2.41	0.0506	2.46	0.0120	2.58	0.29	238	7	238	10	222	114	240	12	100.0
D	TD128-29R	no30x16	25.7	0.0262	1.93	0.1966	6.44	0.0536	4.87	0.0094	5.34	0.86	167	6	182	21	352	220	189	20	109.0
D	TD128-134	no30y05	20.4	0.0426	1.32	0.3105	4.05	0.0533	4.63	0.0128	3.87	0.31	269	7	275	19	340	210	258	20	102.2
D	TD128-135	no30y06	20.4	0.0381	0.67	0.2670	1.47	0.0509	1.32	0.0117	0.89	0.44	241	3	240	6	234	60	234	4	99.6
D	TD128-136	no30y07	25.7	0.0432	0.89	0.3005	2.20	0.0507	2.39	0.0126	1.86	0.02	273	5	267	10	226	110	252	9	97.8
D	TD128-137	no30y08	25.7	0.0607	0.79	0.4390	2.44	0.0526	1.99	0.0185	1.93	0.68	380	6	370	15	310	92	370	14	97.4
D	TD254-001	de03a05	33.2	0.0484	0.53	0.3447	1.43	0.0522	1.48	0.0144	1.10	0.09	305	3	301	7	292	68	288	6	98.7
D	TD254-004	de03a06	30.0	0.0487	0.51	0.3525	1.54	0.0527	1.31	0.0144	1.23	0.58	306	3	307	8	316	60	290	7	100.3
D	TD254-005	de03a07	21.4	0.0375	1.10	0.2721	1.75	0.0531	1.80	0.0111	1.80	0.27	237	5	244	8	330	82	222	8	103.0
D	TD254-006	de03a08	29.0	0.0125	0.51	0.0821	1.79	0.0471	1.83	0.0038	1.39	0.06	80	1	80	3	52	88	77	2	100.0
D	TD254-007	de03a09	26.8	0.0337	0.55	0.2438	0.98	0.0518	0.89	0.0102	1.26	0.44	214	2	221	4	274	42	205	5	103.3
D	TD254-008	de03a10	9.6	0.0473	1.60	0.3340	2.43	0.0516	2.78	0.0138	3.09	0.09	298	9	293	12	268	128	278	17	98.3
D	TD254-009	de03a11	15.0	0.0124	1.36	0.0779	2.75	0.0453	2.90	0.0038	3.34	0.13	79	2	76	4	0	30	78	5	96.2
D	TD254-010	de03a12	1																		

Notes: Tect: tectonic position of the sample; D: Outer Dinaride foreland basin; S: Sava Zone. Peak: length of the laser ablation signal extracted for the isotope ratio calculation. p: error correlation of <sup>207</sup>Pb/<sup>235</sup>U and <sup>206</sup>Pb/<sup>238</sup>U ratios. Conco.: concordance expressed as [<sup>207</sup>Pb/<sup>235</sup>U age]/[<sup>206</sup>Pb/<sup>238</sup>U age] × 100. Peak: length of the laser ablation signal extracted for the isotope ratio calculation.

LA-ICPMS apparent ages

tect	grain#	exp.#	peak (s)	<sup>206</sup> Pb/ <sup>238</sup> U ± 1 σ (%)	<sup>207</sup> Pb/ <sup>235</sup> U ± 1 σ (%)	<sup>207</sup> Pb/ <sup>206</sup> Pb ± 1 σ (%)	<sup>208</sup> Pb/ <sup>232</sup> Th ± 1 σ (%)	p	<sup>206</sup> Pb/ <sup>238</sup> U age (Ma)	<sup>207</sup> Pb/ <sup>235</sup> U age (Ma)	<sup>207</sup> Pb/ <sup>206</sup> Pb age (Ma)	<sup>208</sup> Pb/ <sup>232</sup> Th age (Ma)	Conco. (%)								
D	TD254-047	de03d09	30.0	0.0592	0.62	0.4331	1.23	0.0536	1.12	0.0176	1.04	0.42	371	4	365	8	354	52	352	7	98.4
D	TD254-048	de03d10	20.4	0.0789	1.07	0.6556	1.38	0.0597	1.69	0.0228	2.24	0.07	489	10	512	11	592	74	456	20	104.7
D	TD254-049	de03d11	23.6	0.0582	0.51	0.4354	1.21	0.0540	1.20	0.0174	1.23	0.23	364	4	367	7	370	54	348	8	100.8
D	TD254-050	de03d12	27.9	0.0783	0.74	0.6160	1.58	0.0570	1.16	0.0231	1.71	0.73	486	7	487	12	492	52	462	16	100.2
D	TD254-051	de03d13	20.4	0.0124	0.71	0.0882	1.56	0.0512	1.55	0.0038	1.47	0.24	79	1	86	3	248	72	76	2	108.9
D	TD254-052	de03d14	23.6	0.0757	0.94	0.6001	1.35	0.0571	1.05	0.0233	2.06	0.63	471	9	477	10	494	46	465	19	101.3
D	TD254-053	de03d15	18.2	0.0771	0.92	0.6046	0.82	0.0574	1.25	0.0226	2.77	0.03	479	8	480	6	504	56	452	25	100.2
D	TD254-054	de03d16	30.0	0.0403	0.59	0.2895	1.00	0.0520	0.98	0.0120	1.01	0.33	255	3	258	5	286	44	240	5	101.2
D	TD254-055	de03e05	19.3	0.0788	0.56	0.6373	1.70	0.0582	1.61	0.0227	1.83	0.32	489	5	501	13	536	70	453	16	102.5
D	TD254-056	de03e06	12.9	0.0717	0.55	0.5966	1.18	0.0587	1.13	0.0230	2.59	0.32	446	5	475	9	554	50	459	24	106.5
D	TD254-057	de03e07	31.1	0.0549	0.53	0.4123	1.26	0.0541	1.08	0.0161	1.14	0.53	344	4	351	7	374	50	322	7	102.0
D	TD254-058	de03e08	23.6	0.0762	0.51	0.6240	0.77	0.0577	0.59	0.0224	1.06	0.64	474	5	492	6	518	26	448	9	103.8
D	TD254-060	de03e09	20.4	0.0788	0.66	0.6222	1.50	0.0570	1.52	0.0219	2.80	0.19	489	6	491	12	490	66	438	24	100.4
D	TD254-061	de03e10	27.9	0.0782	0.64	0.6245	0.93	0.0571	0.82	0.0230	1.06	0.51	486	6	493	7	496	36	460	10	101.4
D	TD254-062	de03e11	23.6	0.0726	0.54	0.5642	1.40	0.0558	1.25	0.0217	2.25	0.46	452	5	454	10	444	56	433	19	100.4
D	TD254-063	de03e12	25.7	0.0557	0.75	0.4307	1.06	0.0550	0.84	0.0163	1.23	0.62	349	5	364	6	412	38	327	8	104.3
D	TD254-064	de03e13	27.9	0.0925	0.72	0.7778	1.13	0.0602	1.02	0.0271	0.90	0.46	570	8	584	10	610	44	540	10	102.5
D	TD254-065	de03e14	18.2	0.0125	0.57	0.0881	1.35	0.0496	1.57	0.0038	1.24	0.21	80	1	86	2	174	72	76	2	107.5
D	TD254-066	de03e15	24.7	0.0757	0.78	0.6142	1.29	0.0577	1.22	0.0236	2.08	0.39	470	7	486	10	516	52	472	19	103.4
D	TD254-067	de03e16	26.8	0.0405	0.67	0.3014	1.07	0.0524	1.18	0.0126	1.37	0.14	256	3	267	5	302	54	252	7	104.3
D	TD254-068	de04a05	27.9	0.0381	0.52	0.2674	1.27	0.0504	1.23	0.0109	1.40	0.28	241	2	241	5	212	58	219	6	100.0
D	TD254-069	de04a06	25.7	0.0505	1.12	0.3806	1.62	0.0547	1.28	0.0261	4.93	0.62	317	7	327	9	396	58	520	51	103.2
D	TD254-070	de04a07	24.7	0.0387	0.70	0.2749	2.15	0.0512	2.12	0.0113	1.97	0.21	245	3	247	9	250	98	227	9	100.8
D	TD254-074	de04a08	25.7	0.0599	0.81	0.4500	1.31	0.0545	1.44	0.0178	1.15	0.14	375	6	377	8	390	64	357	8	100.5
D	TD254-075	de04a09	17.2	0.0790	0.78	0.6151	1.70	0.0557	1.41	0.0234	1.70	0.57	490	7	487	13	438	62	468	16	99.4
D	TD254-076	de04a10	24.7	0.0126	0.97	0.0818	2.14	0.0471	2.04	0.0038	1.14	0.33	81	2	80	3	56	98	77	2	98.8
D	TD254-077	de04a11	26.8	0.0799	0.88	0.6385	1.15	0.0580	0.96	0.0234	2.40	0.58	496	8	501	9	526	42	468	22	101.0
D	TD254-078	de04a12	26.8	0.0597	0.87	0.4412	1.54	0.0542	1.57	0.0178	1.40	0.25	374	6	371	10	378	70	357	10	99.2
D	TD254-079	de04a13	31.1	0.0590	0.63	0.4455	1.06	0.0541	0.76	0.0179	1.11	0.71	370	5	374	7	372	36	359	8	101.1
D	TD254-080	de04a14	30.0	0.0591	0.65	0.4441	0.92	0.0542	0.96	0.0176	1.15	0.29	370	5	373	6	378	44	352	8	100.8
D	TD254-081	de04a15	22.5	0.0787	0.69	0.6116	0.90	0.0563	0.98	0.0236	1.05	0.26	489	6	485	7	464	44	471	10	99.2
D	TD254-082A	de04a16	20.4	0.0704	1.05	0.5198	3.18	0.0533	3.08	0.0217	4.45	0.26	438	9	425	22	340	78	433	38	97.0
D	TD254-082B	de04b05	30.0	0.0735	0.66	0.5867	1.90	0.0570	1.80	0.0228	4.43	0.32	457	6	469	14	490	140	455	40	102.6
D	TD254-083	de04b06	23.6	0.0517	2.28	0.3934	3.14	0.0552	2.47	0.0156	3.26	0.63	325	14	337	18	420	110	312	20	103.7
D	TD254-084	de04b07	27.9	0.0594	0.52	0.4446	0.84	0.0538	0.84	0.0176	1.13	0.26	372	4	374	5	360	38	353	8	100.5
D	TD254-085	de04b08	27.9	0.0505	0.52	0.3643	1.34	0.0522	1.33	0.0151	1.15	0.21	318	3	315	7	292	62	303	7	99.1
D	TD254-086	de04b09	24.7	0.0599	0.75	0.4597	1.60	0.0553	1.20	0.0178	1.29	0.70	375	5	384	10	424	54	356	9	102.4
D	TD254-087	de04b10	23.6	0.0599	0.68	0.4452	0.92	0.0541	1.06	0.0175	1.47	0.15	375	5	374	6	374	46	350	10	99.7
D	TD254-088	de04b11	21.4	0.0773	0.72	0.6131	1.25	0.0571	1.16	0.0232	2.06	0.41	480	7	485	10	492	52	463	19	101.0
D	TD254-089	de04b12	22.5	0.0413	1.57	0.3022	3.36	0.0520	3.50	0.0126	3.99	0.14	261	8	268	16	286	160	254	20	102.7
D	TD254-090	de04b13	24.7	0.0590	0.76	0.4561	1.41	0.0553	1.22	0.0172	1.60	0.50	369	5	382	9	422	56	345	11	103.5
D	TD254-091	de04b14	18.2	0.0769	1.10	0.6214	1.25	0.0589	1.69	0.0221	4.65	0.03	477	10	491	10	562	74	441	41	102.9
D	TD254-092	de04b15	31.1	0.0426	0.70	0.3036	1.50	0.0510	1.33	0.0127	1.34	0.46	269	4	269	7	242	62	256	7	100.0
D	TD254-093	de04b16	19.3	0.0429	1.12	0.3042	2.13	0.0512	1.72	0.0125	2.65	0.59	271	6	270	10	250	80	250	13	99.6
D	TD254-094	de04c05	11.8	0.0641	0.97	0.4845	1.77	0.0552	1.85	0.0205	1.79	0.19	401	8	401	12	418	82	410	15	100.0
D	TD254-095	de04c06	16.1	0.0330	1.10	0.3527	2.26	0.0772	1.80	0.0120	1.42	0.62	209	5	307	12	1126	72	241	7	146.9
D	TD254-096	de04c07	24.7	0.0345	0.74	0.2438	1.98	0.0516	1.88	0.0104	1.57	0.32	218	3	222	8	266	86	208	6	101.8
D	TD254-097	de04c08	25.7	0.0407	0.80	0.2894	1.58	0.0519	1.66	0.0121	1.73	0.15	257	4	258	7	278	76	243	8	100.4
D	TD254-098	de04c09	22.5	0.2967	1.00	4.4354	2.81	0.1067	1.55	0.0827	1.44	0.16	1675	29	1719	47	1742	56	1606	44	102.6
D	TD254-099	de04c10	15.0	0.0562	0.87	0.4156	1.67	0.0544	1.35	0.0173	1.65	0.59	352	6	353	10	384	60	347	11	100.3
D	TD254-100	de04c11	20.4	0.0587	0.62	0.4502	1.70	0.0562	1.68	0.0181	2.80	0.21	368	4	377	11	460	74	363	20	102.4
D	TD254-101	de04c12	24.7	0.0402	0.98	0.2790	3.36	0.0505	2.74	0.0121	2.06	0.72	254	5	250	15	218	128	242	10	98.4
D	TD254-102	de04c13	23.6	0.0709	1.08	0.5556	3.09	0.0569	2.42	0.0202	2.30	0.73	441	9	449	22	486	108	403	18	101.8
D	TD254-103	de04c14	24.7	0.0413	0.79	0.3024	2.06	0.0524	2.14	0.0127	2.35	0.57	261	4	268	10	302	80	256	12	102.7
D	TD254-104	de04c15	16.1	0.3029	0.38	5.2130	0.86	0.1231	0.57	0.0829	1.12	0.89	1706	11	1855	15	2000	20	1610	35	108.7
D	TD254-105	de04c16	24.7	0.4406	0.48	9.9059	0.89	0.1626	0.61	0.1188	1.37	0.76	2353	19	2426	16	2482	20	2269	59	103.1
D	TD254-107	de04d05	27.9	0.0398	0.66	0.2796	1.30	0.0508	1.33	0.0124	1.25	0.21	252	3	250	6	232	60	250	6	99.2
D	TD254-108	de04d06	16.1	0.0775	0.87	0.5961	1.94	0.0554	1.62	0.0234	2.48	0.56	481	8	475	15	426	72	467	23	98.8
D	TD254-109	de04d07	27.9																		

Appendix 6-2

Results of detrital zircon LA-ICPMS U/Pb geochronology on non-double-dated aliquots, in conventional epoxy mounts  
page 4 of 4

Notes: Tect: tectonic position of the sample; D: Outer Dinaride foreland basin; S: Sava Zone. Peak: length of the laser ablation signal extracted for the isotope ratio calculation. p: error correlation of  $^{207}\text{Pb}/^{235}\text{U}$  and  $^{206}\text{Pb}/^{238}\text{U}$  ratios. Conco.: concordance expressed as  $[\frac{^{207}\text{Pb}/^{235}\text{U age}}{^{206}\text{Pb}/^{238}\text{U age}}] \times 100$ . Peak: length of the laser ablation signal extracted for the isotope ratio calculation.

LA-ICPMS apparent ages																					
tect	grain#	exp.#	peak (s)	$^{206}\text{Pb}/^{238}\text{U} \pm 1\sigma$ (%)	$^{207}\text{Pb}/^{235}\text{U} \pm 1\sigma$ (%)	$^{207}\text{Pb}/^{206}\text{Pb} \pm 1\sigma$ (%)	$^{208}\text{Pb}/^{232}\text{Th} \pm 1\sigma$ (%)	p	$^{206}\text{Pb}/^{238}\text{U} \pm 2\sigma$ age (Ma)	$^{207}\text{Pb}/^{235}\text{U} \pm 2\sigma$ age (Ma)	$^{207}\text{Pb}/^{206}\text{Pb} \pm 2\sigma$ age (Ma)	$^{208}\text{Pb}/^{232}\text{Th} \pm 2\sigma$ age (Ma)	Conco. (%)								
S	TD188-001	de05f05	23.6	0.0586	1.29	0.4475	3.12	0.0554	2.24	0.0172	2.51	0.79	367	9	376	20	426	100	344	17	102.5
S	TD188-002	de05f06	23.6	0.0410	1.31	0.2974	2.91	0.0527	3.10	0.0133	2.69	0.08	259	7	264	14	316	142	266	14	101.9
S	TD188-004	de05f08	22.5	0.0414	0.78	0.2839	1.98	0.0500	2.05	0.0125	2.05	0.11	261	4	254	9	192	96	252	10	97.3
S	TD188-005	de05f09	27.9	0.0410	0.74	0.2893	2.54	0.0510	2.45	0.0125	2.26	0.27	259	4	258	12	240	114	251	11	99.6
S	TD188-006	de05f10	24.7	0.0402	0.90	0.2921	2.70	0.0528	2.58	0.0127	1.82	0.30	254	4	260	12	320	118	255	9	102.4
S	TD188-007	de05f11	26.8	0.3320	0.80	5.1803	1.10	0.1137	0.57	0.0910	0.92	0.87	1848	26	1849	19	1858	20	1761	31	100.1
S	TD188-008	de05f12	34.3	0.0412	0.89	0.3107	1.28	0.0545	1.29	0.0130	1.91	0.34	260	5	275	6	392	56	262	10	105.8
S	TD188-009	de05f13	24.7	0.0996	0.87	0.8316	1.03	0.0601	0.83	0.0294	1.01	0.63	612	10	614	10	606	36	586	12	100.3
S	TD188-010	de05f14	22.5	0.0488	1.17	0.3512	1.66	0.0531	1.74	0.0147	1.27	0.28	307	7	306	9	330	80	296	7	99.7
S	TD188-012	de05f16	35.4	0.0422	0.77	0.3032	1.46	0.0521	1.38	0.0126	1.18	0.36	266	4	269	7	288	64	252	6	101.1



# Lebenslauf von Tamás Mikes

Geboren in Budapest, am 12. August 1980  
Eltern: Zsolt Mikes und Kornélia Rózsa  
Ungarischer Staatsbürger

## AKADEMISCHER WERDEGANG

- 2004–2008     **Promotion in Geowissenschaften**, Universität Göttingen  
*Thema der Dissertation: Late Mesozoic to Cenozoic erosion and sediment dispersal in the Dinaride orogen: a sedimentary provenance approach*  
Betreuer: H. von Eynatten & I. Dunkl
- 2004     **Diplom in Geologie** (Nostrifikation), Eötvös Universität Budapest  
2003     **Diplom in Geologie (Vertiefungsrichtung Sedimentgeologie)**, Univ. Tübingen  
*Diplomarbeit: Provenance analysis of Palaeogene flysch sandstones of the Northwestern External Dinarides.* Betreuer: I. Dunkl  
*Studienarbeit: Sedimentology and palaeoseismicity recorded in Quaternary fluvial sands of the Sárrét Basin, Hungary.* Betreuer: P. Bons, M. Kázmér  
Tag der Diplomhauptprüfung: 11. November 2003; Prüfer: W. Frisch
- 2002–2003     **Geologiestudium**, Universität Tübingen  
1998–2002     **Geologiestudium**, Eötvös Universität Budapest  
1998     **Abitur**, Budapest

## HOCHSCHULLEHRER

T. Báldi, L. Csontos, F. Horváth, M. Kázmér, M. Mindszenty, Cs. Szabó, O. Sztanó (*Budapest*); T. Aigner, G. Markl, W. Frisch (*Tübingen*); H. von Eynatten, I. Dunkl (*Göttingen*); J.F. Dewey (*Davis*); D. Günther (*Zürich*); L. Nasdala (*Wien*); A.M.C. Şengör (*Istanbul*); S.M. Schmid (*Basel*); M. Wagreich (*Wien*); G. Manby (*Greenwich*); M. Williams (*Massachusetts*)

## AUSZEICHNUNGEN

- 2005     'Kriván Pál'-Plakette für junge Wissenschaftler (*Ungarische Geologische Gesellschaft*)  
2002     Studentischer Preis der *MOL Ungarischer Erdöl- und Erdgas AG*  
2002     'Studentische Exzellenz'-Preis der Naturwiss. Fakultät, Eötvös Universität, Budapest

## MITGLIEDSCHAFTEN

- Mineralogical Society of America     seit 2004  
Society for Sedimentary Geology     seit 2003  
International Association of Sedimentologists     seit 2003  
Ungarische Geologische Gesellschaft (MFT)     seit 1998